INAUGURAL – DISSERTATION

zur Erlangung der Doktorwürde

der

Naturwissenschaftlich-Mathematischen Gesamtfakultät

der

Ruprecht-Karls-Universität

Heidelberg

vorgelegt von

M.Sc. Melissa Josephine Perner

aus Worms, Deutschland

Tag der mündlichen Prüfung 23. April 2018

Evolution of Palaeoenvironment, Kerogen Composition and Thermal History in the Cenozoic of the Northern Upper Rhine Graben, SW-Germany

Gutachter:

Prof. Dr. Wolfgang Stinnesbeck

Prof. Dr. Thilo Bechstädt

Table of Contents

Abstract I

Kurzfassung II

1. Introduction 1

2. Objectives 2

3. Geological Setting 3

4. Study Area 7

5. Lithostratigraphy 9

6. Methods 12

6.1. Sampling 13

6.2. Palynofacies Analysis 13

6.3. Optical Kerogen Analysis 14

6.4. Rock-Eval Pyrolysis 14

6.5. TOC/CNS 15

6.6. Vitrinite Reflectance 15

6.7. Sporomorph Coloration Index 16

6.8. Seismic Interpretation 16

6.9. 1D Basin Modelling 17

7. Palynofacies and Kerogen analysis 17

7.1. Results 17

7.1.1. Pechelbronn Group 17

7.1.2. Rupel Clay Group 20

7.1.3. Meletta Group, Cyrena Marls Group, Bunte Niederröderner Group and Cerithium Group 23

7.1.4. Corbicula Group 28

7.1.5. Hydrobia Group 30

7.2. Interpretation of Palaeoenvironment & Hydrocarbon Generation Potential 36

7.2.1. Pechelbronn Group 36

7.2.2. Rupel Clay Group 41

7.2.3. Meletta Group, Cyrena Marls Group, Bunte Niederröderner Group and Cerithium Group 44

7.2.4. Corbicula Group 48

7.2.5. Hydrobia Group 49

8. Maturation Analysis 51

8.1. Results 51

8.2. Interpretation 61

9. Palaeothermal History and Basin Analysis 65

9.1. Input Parameters and Boundary Conditions 66

9.2. Calibration 67

9.3. 1D Simulation 67

10. Discussion 72

10.1. Palaeoenvironment Conditions 72

10.1.1. Pechelbronn Group 72

10.1.2. Rupel Clay Group 73

10.1.3. Meletta Group, Cyrena Marls Group, Bunte Niederröderner Group and Cerithium Group 74

10.1.4. Corbicula Group 75

10.1.5. Hydrobia Group 75

10.2. Hydrocarbon Potential 76

10.2.1. Pechelbronn Group 76
10.2.2. Rupel Clay Group 77
10.2.3. Meletta Group, Cyrena Marls Group, Bunte Niederröderner Group and Cerithium Group 78
10.2.4. Corbicula Group 79
10.2.5. Hydrobia Group 79
10.3. Maturation Trends and Hydrothermal Anomalies 80
10.4. Limitations of PetroMod 1D 94
11. Conclusions 95
12. Outlook 99
References 100
List of Abbreviations 115
Appendix 116
Appendix 1: Palynofacies Analysis 117
Appendix 2: Optical Kerogen Analysis 164
Appendix 3: Rock-Eval Pyrolysis 186
Appendix 4: TOC/CNS 208
Appendix 5: Vitrinite Reflectance & Sporomorph Coloration Index 210
Appendix 6: Basin Modelling 213

Abstract

The Upper Rhine Graben (URG) in SW-Germany, a classical hydrocarbon province, is part of the European Cenozoic Rift System. Rift graben development has led to a complex basin fill of fluviatile-limnic terrestrial to brackish-marine deposits, providing several hydrocarbon reservoir and source rock units. Several studies have been carried out on palaeoenvironment conditions, source rock development and the thermal history in the URG, yet the hydrocarbon potential of source rocks within the northern URG is not fully understood and investigations concerning the thermal evolution are partly contradictory. The new methodological approach that is applied in this thesis aims to investigate the impact of the rift-tectonic activity on the sedimentation history, the development of source rocks and the thermal evolution of the basin. To address this scientific interrogation, a wide set of methodologies was applied on rock material from former and recent hydrocarbon exploration wells.

Regionally small-scale differences in palaeoenvironmental conditions are observed. Besides the proximity to the graben shoulders, also the structural position largely determines the organic material composition and oxygen availability. Thereby, footwall structures tend to obtain more oxic conditions than hanging wall structures, where more anoxic conditions are often present. These differenced are tectonically induced due to variable subsidence rates on the different fault blocks and the coherently available accommodation space.

Source rocks are restricted to the pelitic units of marine transgressive intervals. Two types of source rocks are identified: (i) Transgressive marine intervals during times of high rift tectonic activity show high subsidence and therefore high terrestrial input from the uplifted graben shoulders. This led to terrestrial dominated kerogen and mainly gas-prone source rocks, which are unexpected for a transgressive interval. Even in the maximum transgressive interval (Rupel Clay Group), mainly terrestrial dominated (gas-prone) kerogen was observed due to the high rift tectonic activity, instead of mainly marine derived oil-prone kerogen as commonly expected. (ii) In contrast, marine transgressions in times of low rift tectonic activity (e.g. Hydrobia Group) and low subsidence show low terrigenous sediment input, leading to the deposition of mainly marine-brackish originated, oil-prone kerogen, as typically expected for marine intervals. Thus kerogen composition is primarily linked and majorly controlled by the intensity of rift-related tectonic activity and only in second order by sea level variations. Minor differences in the kerogen composition within these intervals are linked to the different structural positions within the rift system.

For a better understanding of the petroleum system in the northern URG the palaeothermal history was studied by integrated maturation analysis of several wells across the study area. Most wells show vertically almost uniform maturation trends based on the applied optical and geochemical methods. These trends are untypical for burial controlled maturation and clearly indicate significant secondary thermal overprint. By using one-dimensional numerical simulations, burial-controlled subsidence trends with high (90–100 mW/m^2)/low (72–75 mW/m^2) heat flows corresponding to phases of high/low rifting activity, could not be reconstructed using the obtained maturation data. Due to the absence of volcanic activity in the study area, these thermal anomalies must be related to long-lasting, very hot hydrothermal fluid

systems, well known from the URG, which were mainly concentrated along reactivated fault zones. Therefore, at least in the vicinity of fault systems, maturation in the northern URG is mainly influenced by tectonically controlled distribution of hydrothermal systems and much less by basin subsidence.
Taking into account both kerogen composition and thermal history of the graben, the best hydrocarbon potential can be expected from the highly oil-prone Hydrobia Group and the oil- to gas-prone Rupel Clay Group along the eastern graben border and within a small pull-apart basin in the northwest of the study area.
From the results of the study it can be concluded, that the development of the depositional setting, kerogen composition, thermal maturation and hydrocarbon potential is directly linked and mainly controlled by the geotectonic changes within the rift system.

Kurzfassung

Der Oberrheingraben (ORG) ist eine klassische Kohlenwasserstoffregion in SW-Deutschland und Teil des “Europäischen Känozoischen Rift Systems”. Im Zuge der Riftentwicklung kam es zur Ablagerung von fluviatil-limnisch terrestrischen und brackisch-marinen Sedimenten, von denen einige als Speicher- oder Muttergesteine für Kohlenwasserstoffe fungieren. Einige Studien beschreiben die känozoische Entwicklung der Paläoumwelt und das Kohlenwasserstoffpotenzial von Muttergesteinseinheiten sowie die thermische Geschichte des ORG, jedoch ist insbesondere das Kohlenwasserstoffpotenzial der potenziellen Muttergesteine innerhalb des nördlichen ORG noch nicht vollständig geklärt und die Studien zur thermischen Geschichte sind teils widersprüchlich. Der in dieser Thesis angewandte methodische Ansatz soll zu einem besseren Verständnis des Einflusses der Riftentwicklung auf die Sedimentations- und thermische Geschichte sowie der Muttergesteinsqualitäten beitragen. Für diese Fragestellung wurde eine große Bandbreite an Methoden an Gesteinsproben von Explorationsbohrungen angewandt. Über kurze Entfernungen wurden große Unterschiede der Paläoumwelt-Bedingungen festgestellt. Neben der Proximität zu den Grabenschultern bestimmt auch die strukturelle Lage innerhalb des Grabens maßgeblich die Zusammensetzung des organischen Materials und die Sauerstoffverhältnisse. An strukturell Liegenden Strukturen etablierten sich dabei eher oxische Verhältnisse, wohingegen Hangende Strukturen meist anoxische Verhältnisse aufweisen. Diese Unterschiede sind tektonisch bedingt und auf unterschiedliche Subsidenzraten auf den verschiedenen strukturellen Strukturen und die damit verbundenen Akkomodationsräume zurückzuführen.
Muttergesteinseinheiten sind beschränkt auf pelitische Intervalle mariner Transgressionen. Zwei Typen von Muttergesteinseinheiten lassen sich differenzieren: (i) Transgressiv-marine Intervalle, die während Phasen großer rift-tektonischer Aktivität abgelagert wurden, zeichnen sich durch hohe Subsidenz aus und enthalten demnach einen hohen terrestrischen Eintrag von den sich hebenden Grabenschultern. Dies spiegelt sich in terrestrisch dominierter Kerogenzusammensetzung und überwiegend gashöffigen Muttergesteinseinheiten wieder, welche untypisch für transgressiv-marine Intervalle sind. Dies gilt auch für größte bekannte

Transgression, welche zur Ablagerung der Rupelton Gruppe führte. Bedingt durch die hohe tektonische Aktivität während der Ablagerung ist die Kerogenzusammensetzung stark terrestrisch (gashöffig) dominiert, was nicht mit der gängigen Charakterisierung der Rupelton Gruppe als wichtigstes känzoisches Öl-Muttergestein des ORG übereinstimmt. (ii) Im Gegensatz dazu zeichnen sich transgressiv-marine Intervalle, die während tektonisch relativ inaktiven Phasen mit geringeren Subsidenzraten abgelagert wurden (z.B. Obere Hydrobien Formation), durch geringeren terrestrischen Eintrag von den Grabenschultern aus. Dies führte zur Ablagerung von ölhöffigen Sedimenten mit marin-brackischer Zusammensetzung, typisch für marine Intervalle. Es lässt sich schlussfolgern, dass die Kerogenzusammensetzung maßgeblich beeinflusst und kontrolliert wird durch die Intensität der rift-tektonischen Aktivität und nur sekundär durch Meeresspiegelschwankungen. Zusätzliche, geringe Schwankungen innerhalb der einzelnen Intervalle sind an die strukturelle Lage innerhalb des Grabens gekoppelt.

Für ein besseres Verständnis des Kohlenwasserstoffsystems im nördlichen ORG wurde an mehreren Bohrungen innerhalb des Arbeitsgebietes die thermische Geschichte untersucht. Die meisten Bohrungen wiesen dabei, basierend auf den angewandten optischen und geochemischen Analysemethoden, nahezu vertikal konstante Maturationstrends auf. Diese Trends sind untypisch für subsidenzgesteuerte organische Maturation und weisen eindeutig auf eine sekundäre thermische Überprägung hin. Auch im Rahmen einer eindimensionalen numerischen Simulation konnten basierend auf den erhobenen Matrationsdaten keine subsidenzgesteuerten Maturationstrends rekonstruiert werden, wobei den Phasen hoher/geringer tektonischer Aktivität auch erhöhte (90–100 mW/m^2)/erniedrigte (72–80 mW/m^2) Wärmeflüsse zugeordnet wurden. Da es während der Ablagerung der känozoischen Beckensedimente keinerlei vulkanische Aktivität gab, müssen die thermischen Anomalien durch langandauernde, sehr heiße hydrothermale Fluidsysteme herbeigeführt worden sein. Diese sind primär an tiefreichenden, reaktivierten Störungszonen lokalisiert und für den ORG bereits wohlbekannt. Die Maturitätsprofile im nördlichen ORG sind daher, zumindest in der näheren Umgebung von großen, tiefreichenden Störungszonen, primär von rift-induzierten, hydrothermalen Systemen beeinflusst, und nur sekundär von Beckensubsidenz.

Basierend auf den Ergebnissen der Kerogenanalyse und der thermischen Entwicklung des ORG wird das beste Kohlenwasserstoffpotenzial innerhalb der ölhöffigen Hydrobien Gruppe und der öl- bis gashöffigen Rupelton Gruppe entlang des östlichen Grabenrandes und innerhalb eines kleinen “Pull-Apart” Beckens im Nordwesten des Arbeitsgebietes erwartet.

Die Ergebnisse der Studie zeigen eindeutig, dass die Entwicklung von Paläoumweltbedingungen, der Kerogenzusammensetzung, der thermischen Maturation und das Kohlenwasserstoffpotenzial in engem Zusammenhang mit der geotektonischen Entwicklung des Riftsystems stehen und von dieser maßgeblich kontrolliert werden.

1. Introduction

The Upper Rhine Graben (URG) is a continental rift system in SW-Germany, France and Switzerland with a more than 250-year-old hydrocarbon (HC) exploration history. Oil exploration originated from the exploitation of oil seeps near Pechelbronn in the northern Alsace, France, starting in 1627. In the German part of the URG oil exploration began around 1900. Two large exploration waves are distinguished. The first large drilling campaign took place in the 1930s with the discovery of several oil accumulations. Bigger and deeper hydrocarbon fields were discovered after World War 2 during a second exploration wave. Following the first oil crisis in 1973 another pulse of exploration began. Until the mid-1980s a total of more than 5000 km of 2D seismic lines was acquired (Reinhold et al. 2016). By the early 1990s, most oil fields were abandoned and the URG considered as fully explored (Mauthe et al. 1993). Only the three fields of Eich, Landau and Rülzheim continue to produce to date. In 2003, the unexpected discovery of the Römerberg oil field near Speyer in the central part of the URG (producing from the Lower Triassic) led to a revived phase of seismic investigations, exploration (Dill et al. 2008, Gawenda 2011), and research. The Römerberg oil field is the largest oil field in the URG by far and one of the largest onshore oil fields in Germany. Since 2011, an additional 1000 km^3 of 3D seismic was acquired and one additional prospective oil field was discovered at Schwarzbach. To date, over 480 exploration wells are drilled within the German part of the URG and a total of 29 oil and gas fields have been or are under exploitation (Durst 1991, Mauthe et al. 1993, Reinhold et al. 2016). The cumulative discovered oil reserves exceed 125 MMbbl. The exploration history of the URG is summarized by Mauthe et al. (1993), Böcker (2016) and Reinhold et al. (2016).

Even though an extensive set of studies exists on the URG, the sedimentary Cenozoic graben fill in the c. 100 km long and 30-40 km wide northern segment of the URG, as defined by Schad 1964, and its geotectonic development are not fully understood. The Cenozoic palaeoenvironmental conditions known for the entire URG and the adjacent Mainz Basin are summarized in Grimm et al. (2011). Few publications specifically refer to early sny-rift sediments of the northern URG, such as Gaupp & Nickel (2001) and Nickel (1996). Stratigraphic correlations between the Cenozoic deposits of the URG and the Mainz Block (Mainz Basin) were published by Prell-Müssig (1965), Grimm (1994) and Reichenbacher (2000).
The tectono-sedimentary evolution of early syn-rift sediments in the northern graben segment was studied by Derer (2003), Derer et al. (2003) and Derer et al. (2005). New insights into the tectonic regime of the northern and central URG are furthermore described by Reinhold et al. (2016).
Recent hydrocarbon research focused mainly on the central URG: Bruss (2000), Böcker & Littke (2014), Böcker et al. (2016), Böcker & Littke (2016), and characterize the main petroleum systems, oil families, and source rocks based on geochemical methods. Geothermal investigations from the URG and models are shown in Doebl & Teichmüller (1979) and Teichmüller & Teichmüller (1979). Further data on the thermal history were published by Heling & Teichmüller (1974) and Teichmüller (1979).

The effects of hydrothermal fluid flow on the thermal history in the area of Worms in the northern URG have been numerically simulated by Lampe (2001), Lampe et al. (2001), Lampe & Person (2002).
Rückheim (1989) elucidated the migration- and accumulation history of hydrocarbons in the northern URG and related it to the diagenetic evolution of the reservoir rocks.

2. Objectives

Several hydrocarbon discoveries were made in the northern segment of the URG, such as the oil fields of Stockstadt, Kühkopf, Eich, Hofheim, Wattenheim and Schwarzbach. With the unexpected discovery of the Römerberg oil field in the central URG, new exploration activity commenced in the central and also in the northern URG (Dill et al. 2008, Gawenda 2011), resulting in seismic investigations and exploration drilling. This thesis shall allow reviewing the hydrocarbon potential of the source rocks in the northern URG on the basis of new data and new methods applied. This methodological approach combines optical and geochemical methodologies to elaborate a more precise picture of the northern URG in terms of the depositional systems, source rock development and palaeothermal history. For the estimation of the hydrocarbon potential, industrial research generally utilizes geochemical analysis, as it is provides quick results fairly cheap. Optical kerogen analysis on the contrary as described by Batten (1981, 1996) is not well established in the industry yet, because it is cost-intensive and time-consuming, even though it provides more detailed results. In order to elaborate a highly precise picture of the hydrocarbon potential in the northern URG, this thesis combines optical and geochemical methodologies.
The oil fields of Stockstadt, Kühkopf, Eich, Hofheim, Wattenheim and Schwarzbach in the northern URG were or are still producing from the Upper Eocene to Lower Oligocene Pechelbronn Group. As potential source rocks for the oil accumulations found in the northern URG the Middle Pechelbronn Formation and to even higher degree the Fish Shale Formation (Rupel Clay Group), both Lower Oligocene in age, are defined (Rückheim 1989, Hillebrand & Leythauser 1992). Shallow gas fields within the Hydrobia Group such as the gas fields Pfungstadt and Wolfskehlen might be charged from the Early Miocene Corbicula Group and Hydrobia Group (Plein 1992). On the contrary to the northern URG, where source and reservoir units depend on Cenozoic rocks alone, the hydrocarbon accumulations in the central URG are characterized by Mesozoic and Cenozoic source and reservoir rocks. The oil fields of Römerberg and Landau for example are producing from a Lower Triassic Buntsandstein reservoir (Lutz and Cleintuar 1999). Among the main oil source rocks in the Central URG is the Lower Oligocene Fish Shale Formation (Rupel Clay Group) and the Liassic black shales (Bruss 2000, Böcker 2015). The differences between the northern and the central graben segments indicate two fundamentally different petroleum systems. Therefore, existing studies from the central URG (Bruss 2000, Böcker 2016) on source rock characterization cannot be transferred to the northern URG.
The thesis shall contribute to the general understanding of the development of depositional systems, ecology and bioproductivity of the sedimentary basin fill. Thereby the focus is on the

transgressive-marine intervals, which provide potential source rock units. The study of the palaeoenvironment conditions is important in order to understand the deposition systems and their complexities in the northern URG. In a next step, conclusions on the kerogen composition and hydrocarbon generation potential can be drawn based on the composition of the organic material (OM) and geochemical studies. Both, palaeoenvironmental conditions and kerogen composition are studied within the whole Cenozoic graben filling. Special emphasis is placed on the controlling factors influencing the palaeoenvironmental conditions and kerogen composition, like tectonic activity. Therefore, potential source rock units, which were deposited during phases of high and low rift-related tectonic activities, are differentiated.

Another main objective is to improve the understanding of the hydrocarbon potential in the northern URG. Therefore, the amount of kerogen and their maturities are taken into account besides the kerogen composition of potential source rock units. Former research indicates that no simple burial controlled subsidence history, as it suggested for the central URG (Böcker 2016), is responsible for HC generation in the northern URG. Instead, hydrothermal events may play a significant role for the hydrocarbon potential (Lampe 2001). Therefore it shall be analysed, if and to what extent hydrothermal events contribute to the maturation of basin sediments and if they play a role in hydrocarbon generation.

In a last step, numerical, one-dimensional simulations shall contribute to the reconstruction of the thermal evolution in the northern URG.

At present it remains unclear if the hydrocarbons, which are found in the northern URG are derived from source rocks in the area or if they possibly migrated from an area in the central URG, known as the Heidelberg-Mannheim Basin, informally called “Heidelberger Loch”. In this area, subsidence was high during the Cenozoic leading to a deeper burial of the potential source rock units. Also it remains unclear if hydrocarbon fields can be expected to the north of the recently found oil field Schwarzbach. A palaeostructural high north of this oil field, the so called interbasin northern transfer zone or Stockstadt High (see Geological Setting) might have acted as barrier for migrating hydrocarbons from the south towards the north. Therefore, this thesis also aims to quantify the autochthonous HC potential north of this transfer zone.

3. Geological Setting

The Upper Rhine graben (URG) represents the central part of the European Cenozoic (failed) Rift system (ECRIS), a complex of rift structures in the European continent, which trends from the North Sea coast to the Mediterranean (Fig. 1a)(e.g. Ziegler 1994, Schumacher 2002, Dèzes et al. 2004, Fekiacova et al. 2007, Reinhold et al. 2016). To the south the URG is connected to the Rhone-Bresse Graben, to the North it splits into two branches: the Lower Rhine Embayment and the Hessian depression (Fig. 1a). The NNE-SSW striking URG extends to about 300 km in length and 30-40 km in width (Fig. 1b). It is located between the Rhenish Massif in the North and the Swiss Jura in the South. To the East and West, it is bound by Variscan basement and the Permian to Mesozoic deposits: The Black Forest, Odenwald Massif, the Vosges, Palatinate Forest and Mainz Basin (Walter 2007). It was initiated in the middle to late Eocene with several later rifting

events. The eastern and western flanks are thereby bordered by deep basement faults (Illies & Mueller 1970, Pflug 1982) and the graben shoulders rise up to 1 km above the valley plain (Reinhold et al. 2016).

The underlying Mesozoic succession beneath the Cenozoic graben fill indicates a SE dipping monoclinal structure due to a erosional period in late Cretaceous (Geyer & Gwinner 2011, Schumacher 2002). As a consequence, Jurassic sediments underlie the syn-rift succession in the central URG, whereas Permian Rotliegend is found beneath the Cenozoic succession in the northern URG. During the formation of the URG, distinct differences in the tectonic and stratigraphic evolution are distinguished for the northern, central and southern graben segment (Grimm et al. 2011, Schwarz 2005)(Fig. 2): the northern URG shows continuous sedimentation from middle/late Eocene until the middle Miocene, while the central and southern URG were affected by uplift since the late Oligocene, leading to the erosion of syn-rift sediments in the latter areas (Brun et al. 1992, Bartz 1974). The maximum thickness of some 4000 m of Cenozoic sediments was deposited in the Heidelberg-Mannheim Basin (Sittler 1965, 1988, Doebl & Olbrecht 1974). Results on the pre-rift settings, rifting and the tectonic framework of the Upper Rhine Graben are summarized by Pflug (1982), Ziegler (1994), Schumacher (2002) and Dèzes et al. (2004).

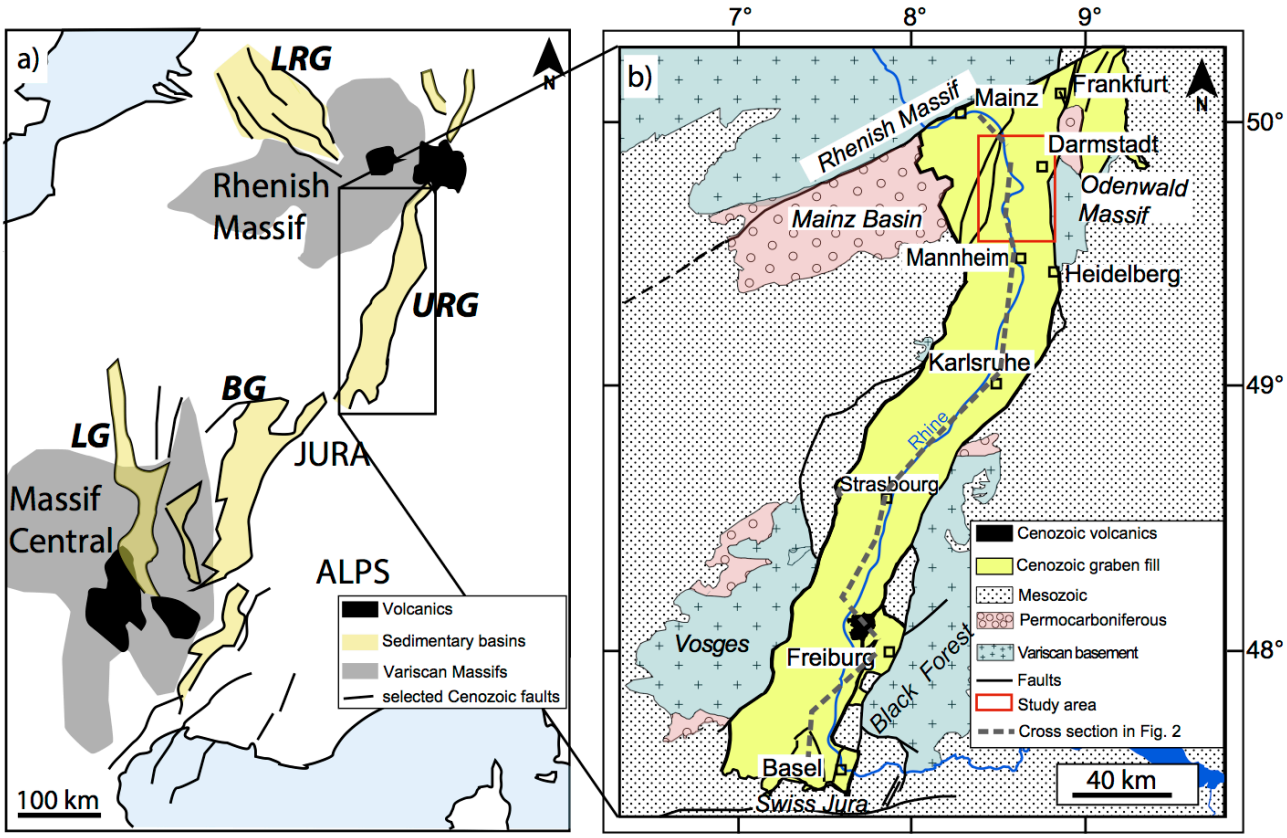

Figure 1: (a) The Upper Rhine Graben as part of the European Cenozoic Rrift System in the Alpine and Pyrenean foreland. BG: Rhone-Bresse Graben, LG: Limagne Graben, URG: Upper Rhine Graben, LRG: Lower Rhine (Roer Valley) Graben, modified from Ziegler & Dèzes (2007); (b) Geological overview of the Upper Rhine Graben. Dotted line: location of N-S Cross section given in Fig. 2.

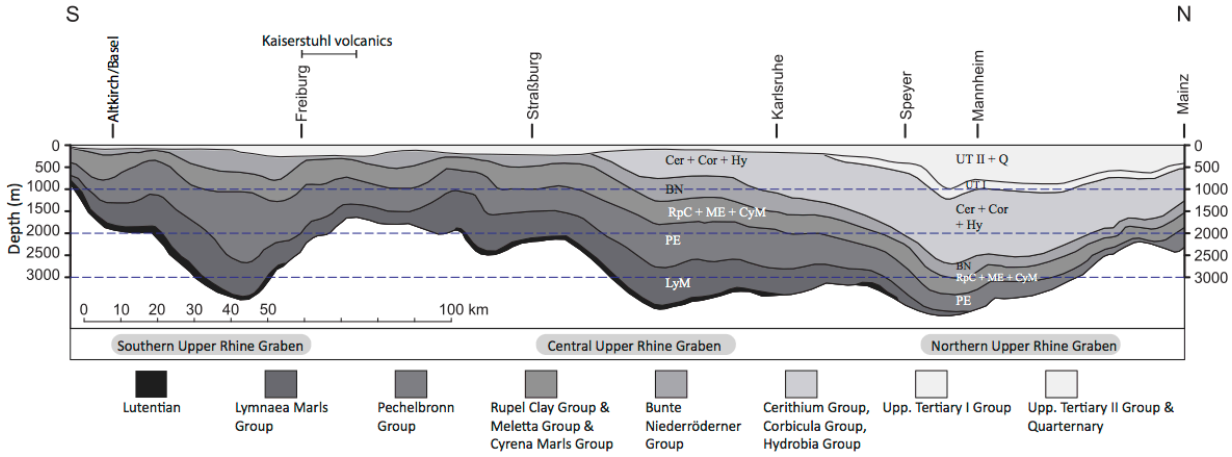

Figure 2: S-N cross section through the URG. Note that the three graben segments are differentiated based on the stratigraphic framework and tectonic evolution. See details in text. For location of cross section see Fig. 1b.

During the rift basin development two major phases of rift-related tectonic activity and subsidence rates are distinguished in the northern URG. The late Eocene to early Oligocene subsidence phase (Villemin & Coletta 1990, Schumacher 2002) occurred due to a WNW-ESE oriented extension (Meier & Eisbacher 1991, Schumacher 2002). Active tilted fault blocks and horst-graben structures throughout the graben are the result of intense syn-rift graben tectonics. Listric growth faults are oriented graben-parallel (Fig. 3a). Sediment transport during the early syn-rift phase was mainly controlled by a NE-SW oriented "interbasin northern transfer zone" (Derer 2003)(Fig. 3a). This structural palaeohigh subdivided the northern URG into a northern and a southern sub basin with opposing tilt directions during this early syn-rift phase (Late Priabonian to Early Rupelian)(Derer 2003, Derer et al. 2003). Its existence is probably influenced by pre-rift Palaeozoic basement structures (Boigk & Schoeneich 1970, Schumacher 2002). In addition to the interbasin northern transfer zone, relay ramps acted as local conduits for sediment transport during the early rifting-phase (Gaupp & Nickel 2001, Derer 2003). Sediments were majorly derived from the western graben shoulder, linked to the transfer zone mentioned above, whereas sediment input from the eastern graben shoulder was low (Perner 2014). During subsequent stages (e.g. since the Middle Rupelian), the originally strong graben morphology was diminished and gradually replaced by a relatively flat topography and the northern URG acted as one depocenter (Derer 2003). Thereby, the sub basins were merged to form the Heidelberg-Mannheim Basin, called "Heidelberger Loch" (Sittler 1965, 1967, 1988, Doebl & Olbrecht 1974), with a maximum thickness of 4000 m of Cenozoic sediments.

A second major phase of subsidence took place in the early Miocene (Aquitanian), but is mainly confined to the northern URG (Illies 1970, Ziegler 1992) (Fig. 3b). This phase was dominated by strike slip events (Grimmer et al. 2016, Reinhold et al. 2016) with minor extensional tectonics movements and concomitant normal faulting (Reinhold et al. 2016). During this subsidence phase, many of the existing Eocene-Oligocene faults were reactivated, but new faults also formed in (N)NW-(S)SE direction. A small "pull-apart basin" within the URG was formed in the northwest of the study area. A third subsidence phase took place during the Pliocene and Quaternary. This phase is characterized by a sinistral shear regime (Schumacher 2002).

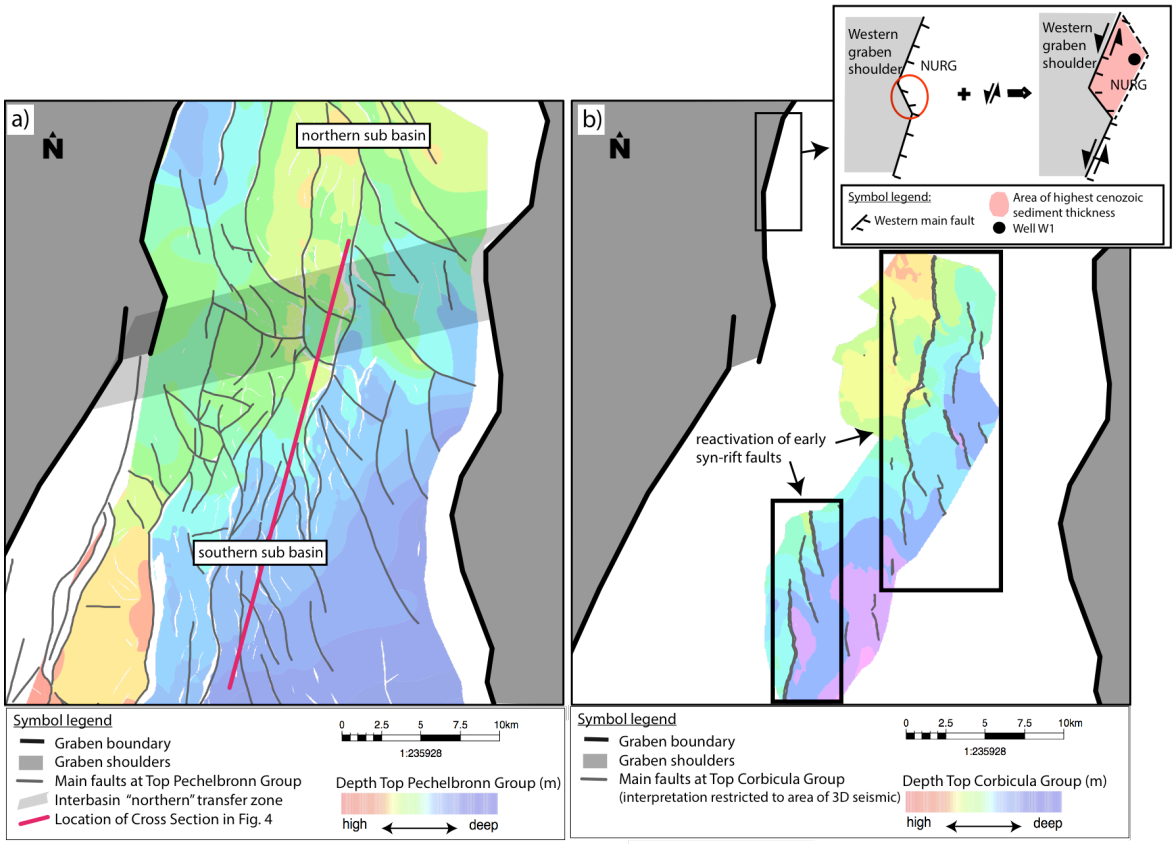

Figure 3: Early (a) and late (b) rifting phases in the northern URG. See details in text.

A cross section of the complex tectonic setting within the northern URG is shown in Fig. 4, illustrating the interbasin "northern" transfer zone and the southward dipping Cenozoic succession within the southern sub basin. In addition to the syn-rift fault systems, a pre-rift set of faults of late Palaeozoic age is mainly restricted to Rotliegend sediments. This fault system trends NW-SE (Herzynian) and can be traced sporadically through the top Pechelbronn Group in Fig 3a. Some of these faults were reactivated during early or even during later rifting stages based on seismics.

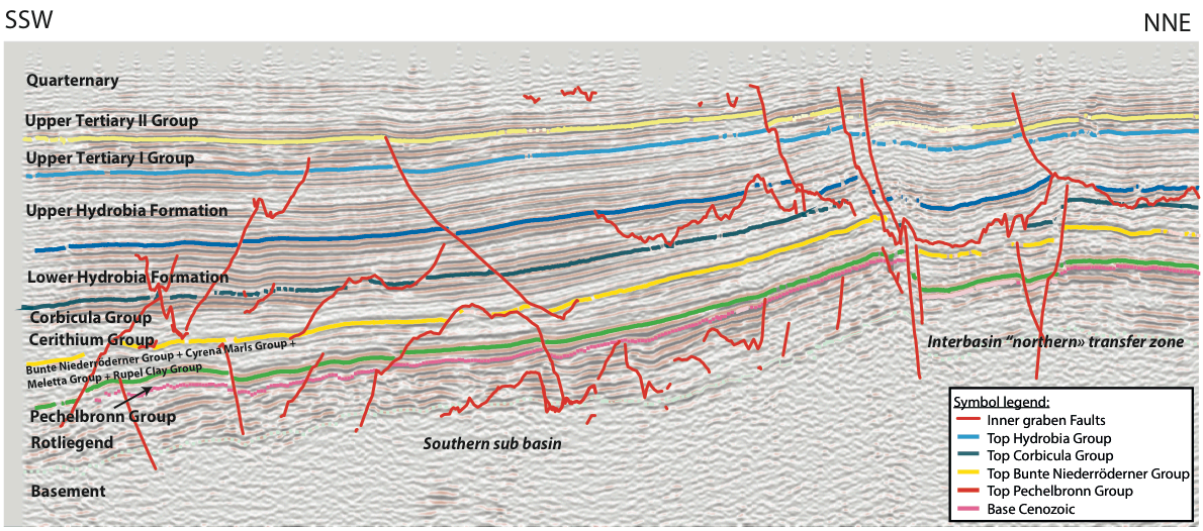

Figure 4: N-S cross-section within the 3D seismic cube in the "southern sub basin" in the northern URG. A late Palaeozoic fault system is restricted to pre-rift sediments, of which some faults were reactivated during rift development. For location of cross section see Fig. 3.

Volcanic activity took place prior and during the rifting processes of the UGR. Yet, the rifting process is not caused by volcanism, as it originated from tectonic stresses (passive rifting) and not by plume activity (active rifting)(Achauer & Masson 2002, Glahn & Granet 1992, Schwarz 2005). Two phases of volcanic activity are distinguished during syn-rift times: the first phase, in the early to middle Eocene, is identified in the entire URG; maximum activity was reached during the middle Eocene, directly prior to the initiation of rifting (Horn et al. 1972, Keller et al. 2002). The second volcanic phase is assigned to the Middle Miocene (Baranyi et al. 1976) and is restricted to the southern URG (e.g. Kaiserstuhl volcanics)(Ziegler 1992). An overview on the stratigraphic record, volcanic activity and tectonic setting in the northern URG is shown in Fig. 5.

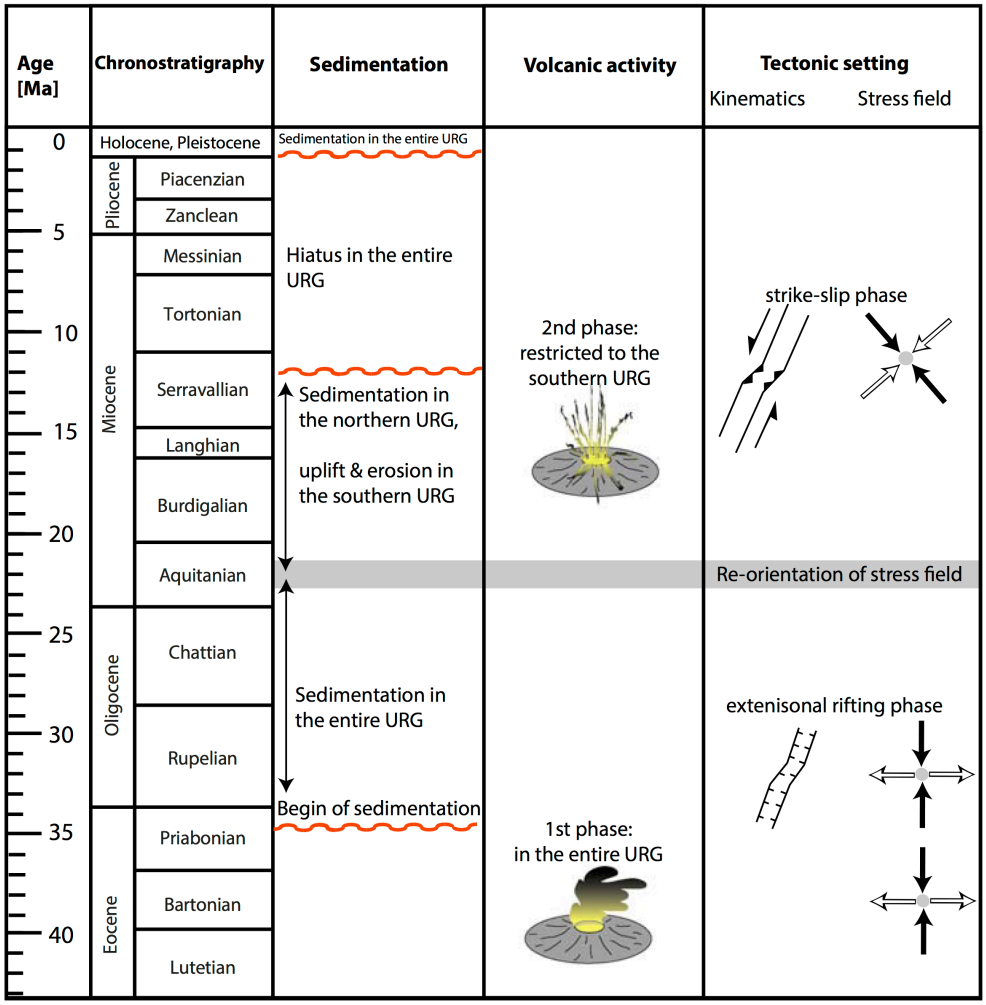

Figure 5: Sedimentation record, tectonic setting and volcanism in the Upper Rhine Graben (modified after Schwarz 2005; tectonic setting after Dèzes et al. 2014)

4. Study Area

In this study we refer to the about 100 km long and 30–40 km wide northern URG (Figs. 1, 3, 6) as defined by Schad (1964), which extends from Frankenthal/Heidelberg in the south towards the area of Frankfurt in the north. Geologically, this part of the graben is bound to the east by the

crystalline basement of the Odenwald Massif, to the west by Cenozoic rocks of the Mainz Basin, and to the north by the Palaeozoic rocks of the Rhenish Massif (Fig. 1b).

For this study, 26 hydrocarbon exploration wells and one additional deep well were investigated. Elevated heat flows, which are often found in passive and active rift-systems, allow for the development of hydrocarbon fields also in the northern URG: the location of the investigated wells and the discovered hydrocarbon reservoirs of economic importance are shown in Fig 6. While oil accumulations in the central and southern segments of the URG are derived from Jurassic and Cenozoic source rocks, hydrocarbon accumulations in the northernmost part of the URG are only sourced from Cenozoic rocks (Reinhold et al. 2016). Yet, the origin of these hydrocarbons is not fully understood and migration paths from the Heidelberg-Mannheim Basin in the central URG are considered until recently (e.g. Böcker 2016). Oil fields of economic importance are the fields Eich, Wattenheim, Stockstadt, Kühkopf and Schwarzbach, of which only the fields Eich and Schwarzbach are still producing. For all near-surface gas reservoirs in the northern URG a biogenic origin (microbial conversion of oil into gas) has been invoked (Mauthe et al. 1993, Dill et al. 2008). Böcker (2016) considers younger Micoene successions as source rocks for the existing microbial gas within the central and northern URG.

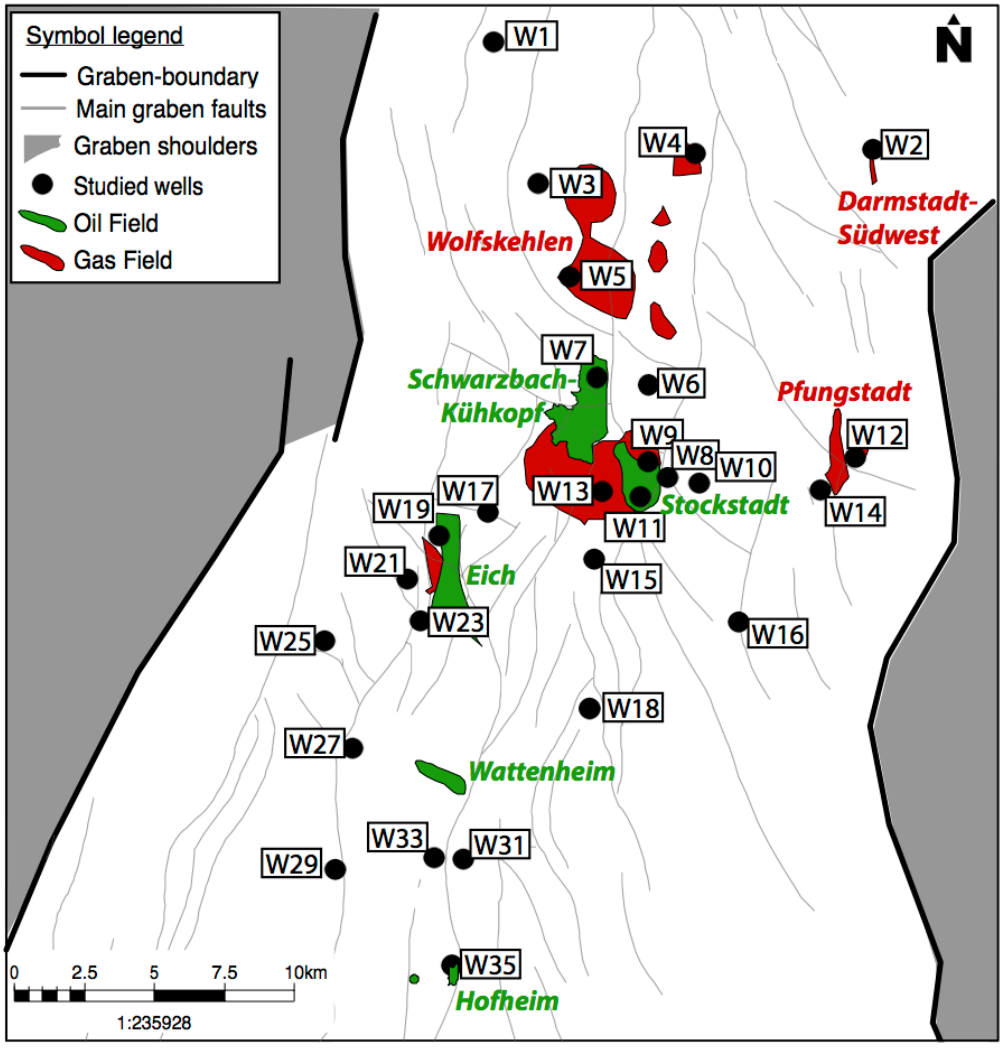

Figure 6: Studied wells and HC fields of economic importance in the study area. The different wells have been re-labeled for confidentiality purposes.

All wells studied are drilled on different fault bounded blocks within the graben. They intersect, or are located, close to deep reaching, major N-S to NNW-SSE trending faults (Fig. 6), which were active during Palaeozoic and reactivated in the Oligocene and Miocene, as indicated by seismics. Thereby the magnitude of subsidence as well as the facies of the sedimentary basin fill may vary widely between graben internal blocks (Grimmer et al. 2016).

5. Lithostratigraphy

The study area in the northern URG comprises up to 3300 m of Palaeogene to Neogene sediments. The proposed stratigraphic framework is based upon a lithostratigraphic classification established by the oil industry, which can be applied easily and reliably on all wells (Fig. 7). This classification is adapted to the modern stratigraphic terminology. The slightly more diversified stratigraphy by Grimm et al. (2011), which is based on biostratigraphy, cannot be fully applied to the seismic sections and wells, from which only cuttings and log data and no biostratigraphic data are available. These Cenozoic sediments unconformably overly the Permocarboniferous (Rotliegend) pre-rift deposits in most regions of the study area (Fig. 4) (Doebl & Olbrecht 1974).

The distribution and lateral migration of the depositional systems and the sedimentation rates are closely linked to changes in global sea level (Sissingh 1998), to the tectonic evolution, and to the structural style of the rift basin (e.g. Sissingh 1998, Schumacher 2002, Gawthorpe & Hurst 1993). The oldest syn-rift deposits known in the area are Upper Eocene to Lower Oligocene sediments of the Pechelbronn Group, lithostratigraphically subdivided into the Lower-, Middle- and Upper Pechelbronn Formation (Schnaebele 1948, Straub 1962, Plein 1992)(Fig. 7). The Lower Pechelbronn Formation is represented by a succession of massive, coarse-grained sandstones with frequent shale intercalations. Deposition took place in a fluvial environment (Reinhold et al. 2016). The first transgressive marine event occurred in the early Oligocene (early Rupelian, Ru1 transgression of Hardenbol et al. 1998), prograding from the North via the Hessische Senke (Grimm et al. 2000, Grimm & Grimm 2003). This transgression led to the deposition of the Middle Pechelbronn Formation under brackish-marine conditions, which is present almost everywhere in the URG (e.g. Doebl 1967, Gaupp & Nickel 2001). This unit consists of mudstones and fine-grained sandstones of a prograding delta / shoreface (Derer et al. 2003, Gaupp & Nickel 2001). Fine-grained calcareous sandstones characterize the Upper Pechelbronn Formation. This interval was deposited during a subsequent sea level fall in the transition zone of freshwater lakes and fluvial dominated deltas, which advanced from the west and inter-fingered with the remnant brackish/marine settings (lagoons?) of the basin center (Gaupp & Nickel 2001). In the northern URG, high thickness variations of the Pechelbronn Group, especially of the Lower Pechelbronn Formation, and to a smaller extent of the Middle and Upper Pechelbronn Formations, are controlled by syn-sedimentary tectonic activity (Reinhold et al. 2016, Perner 2014). A general, basin-wide increase in gross thickness of the Pechelbronn Group is observed from a few meters within the northernmost URG to more than 600 m in the central URG (Doebl 1967). In addition, “local” syn-rift tectonic activity forms tilted blocks with

sediment wedges and thus high small-scale thickness variations, which superimpose the general thickness increase.
The seismic reflection characteristics of the Pechelbronn Group are highly variable, but moderate to high amplitudes, low frequencies, and a low continuity are common (Derer 2003) (Fig. 4). In the northern and central URG, good to excellent reservoir properties are assigned to the Lower and Upper Pechelbronn Formations; the Middle Pechelbronn Formation shows a moderate HC generation potential (e.g. Espitalié 1979, Rückheim 1989, Böcker & Littke 2016).

The second and maximum marine transgression occurred in the late Rupelian (early Oligocene, Ru2 transgression of Hardenbol et al. 1998), leading to intermittent connections with the marine basins to the north and south (Grimm 1994, Berger 1996, Berger et al. 2005). Under these transgressive conditions the Rupel Clay Group was deposited across the entire URG. Well-stratified marine shales and shaly marlstones dominate this unit, which can be subdivided into the basal Foraminifera Marls Formation and the overlying Fish Shale Formation (Fig. 7). With the beginning of the transgression, during the deposition of the Foraminifera Marls Formation, open marine settings with optimal life conditions and high oxygen levels developed (Grimm et al. 2011). After a temporary stagnation of the sea level a further rise occurred, causing the deposition of the Fish Shale Formation (Grimm et al. 1999). The initial deterioration of life conditions (oxygen deficiency) in the entire graben resulted in generally higher bitumen contents (Doebl & Malz 1962, Grimm 1991) of the Fish Shale Formation. Normal marine conditions with water depths around 200–300 m were present, but the bottom waters were poorly oxygenated. The ongoing late Rupelian transgression led to the sedimentation of marine deposits inside the modern URG and outside its margins. The top of the Rupel Clay Group represents the most prominent seismic marker in the northern URG, characterized consistently by a high amplitude (Fig. 4). The horizon is mostly picked on a seismic peak. The Rupel Clay Group, especially the Fish Shale Formation, is a main source rock in the central and northern URG (Rückheim 1989, Bruss 2000, Böcker & Little 2014).

During the late Rupelian the potential reservoir units of the Meletta Group and the Cyrena Marls Group were deposited in the northern URG. These fine-grained sandstones and silty marlstones (Fig. 7) represent restricted marine to brackish, infrequently also terrestrial conditions, despite a further sea level rise. Sediment input was higher than accommodation gain. More proximal depositional environments developed during deposition of the Meletta Group due to high sediment influx (Grimm et al. 2005, Grimm et al. 2011). Continued fluvial sediment input characterizes the overlying Cyrena Marls Group. These two siliciclastic sandy intervals of the Meletta Group and Cyrena Marls Group represent potential reservoir units in the study area.

Subsequently, the Bunte Niederröderner Group was deposited under terrestrial, limnic-fluvial conditions in the early Chattian (Doebl 1967, Mauthe et al. 1993, Schwarz 1997, Reichenbacher 2000) (Fig. 7). The unit consists of (argillaceous) marlstones with frequent layers of carbonaceous siltstones and sandstones and accessorial anhydrite and gypsum. Locally, brackish influences occurred towards the top of the Bunte Niederröderner Group (Schwarz 1997). In seismic profiles, this formation represents another excellent seismic marker horizon (mostly

picked on seismic troughs) within the study area. The biostratigraphic top of the Bunte Niederröderner Group usually lies several 10s of meters above the seismic top of this group, which is characterized by generally moderate amplitudes (Fig. 4). In the study area, the sandy intervals of the Bunte Niederröderner Group hold reservoir potential.

The third prominent transgressive interval started in the upper Oligocene (second Chattian transgression, Hardenbol et al. 1998). The Cerithium Group are in its lower part mainly represented by shales and shaly marlstones with local limestone lenses and anhydrite concretions, indicating brackish lake environments with increased salinities (Prell-Müssig 1965, Schwarz 1997)(Fig. 7); these are followed by brackish-marine conditions, indicating an intermittent connection to the North Sea Basin (Grimm & Grimm 2003). In seismics, the Cerithium Group is characterized by very low amplitudes ("transparent") and moderate frequency (Fig. 4). For the Cerithium Group no HC generation potential has been reported from the northern or central URG.

The overlying Corbicula Group (Wirth 1954, Doebl 1958, 1961, Straub 1962) were deposited during the Aquitanian in an epicontinental sea with an algae reef-ridge, separating the lagoonal environments of the northern URG from the more open marine conditions of the Mainz Basin (Kadolsky 1988, Straub 1962, Grimm & Grimm 2003). Bituminous and laminated claystones to argillaceous marlstones (="Bändermergel" after Press-Müssing 1965) are intercalated with layers of anhydrite and dolomite (Wagner 1947, Doebl 1961, 1967)(Fig. 7). In seismic profiles, the reflectors of the Corbicula Group are traceable over long lateral distances and characterized by moderate to high amplitudes (Fig. 4). This seismic image corresponds to the ribbon-like appearance of the "Bändermergel".

During late Aquitanian to Burdigalian times, the Hydrobia Group, consisting of the Lower- and Upper Hydrobia Formation, were deposited in a limnic to brackish-marine setting, due to short-termed ingressions from the North Sea. Rapid changes in sea level and salinity characterize the rather isolated depositional setting. Partly bituminous shaly marlstones intercalate with limestone and dolomite beds, which contain partly anhydrite nodules (Wirth 1954, Doebl 1958, Doebl 1967, Straub 1956, Straub 1962)(Fig. 7). The subdivision implemented in this study relies on lithological and/or geophysical data and therefore must be considered with caution, as high thickness variations of the Corbicula- and Hydrobia Group are known from the study area, likely due to synsedimentary tectonic activity along faults (Schad 1962). The seismic reflection characteristics of the Hydrobia Group feature a rather transparent interval. Within the Hydrobia Group, the occurrence of limestone/dolomite intercalations within shaly marlstones is mirrored by moderate to high amplitudes (Fig. 4). Both, the Corbicula and Hydrobia Group, exhibit HC generation potential in the central URG (e.g. Schad 1962, Bruss 2000).

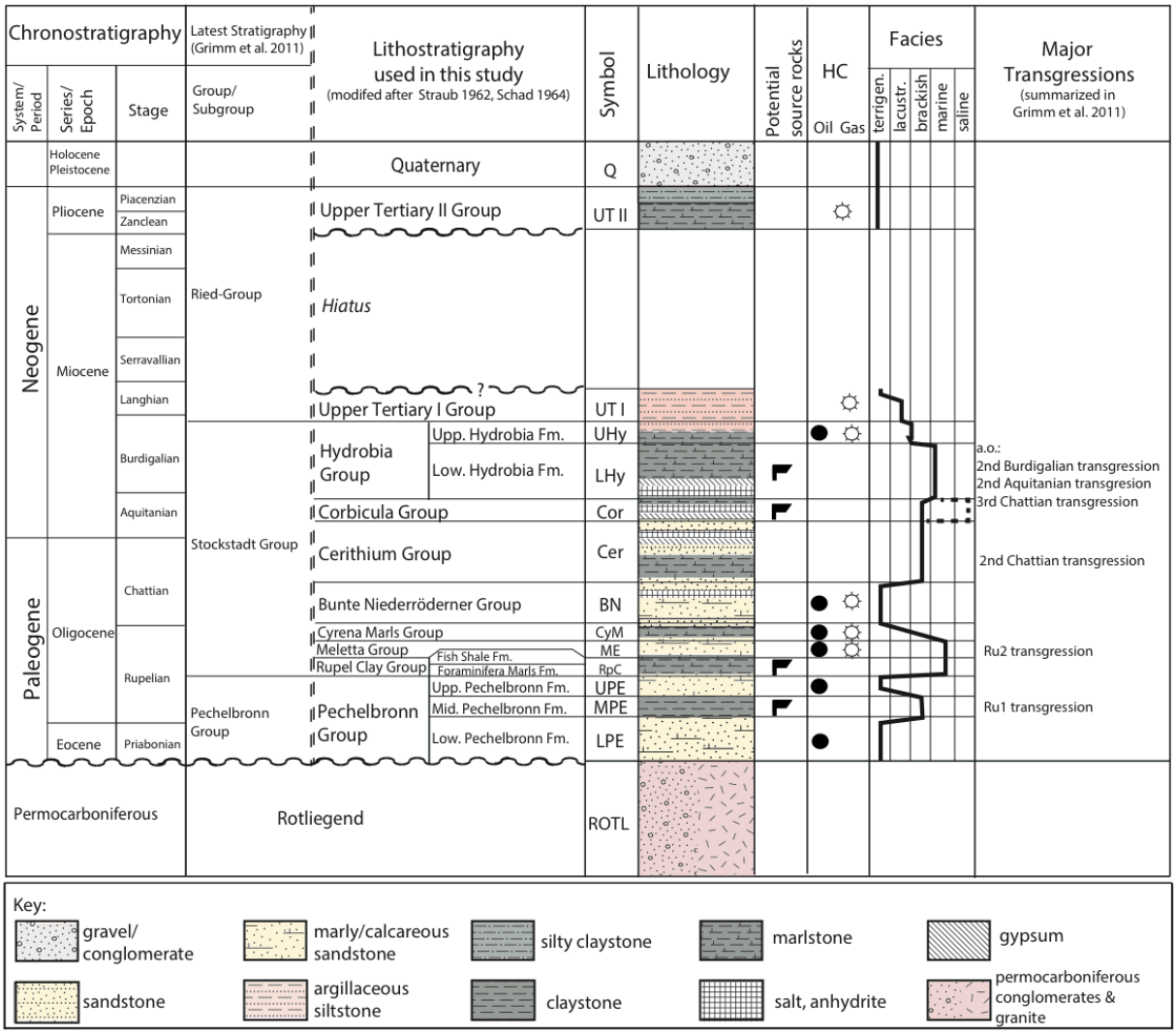

Figure 7: Lithostratigraphic chart of the northern URG including petroleum system elements and facies correlation. The stratigraphy of Grimm et al. (2011) has not been applied, because it was confined to the Mainz Basin NW of the study area and is not applicable in northern URG. Instead, lithostratigraphy is applied as defined by the oil industry (yet adapted to the modern terminology), as this lithostratigraphic subdivision is well identified in well logs and rock samples (FGDC lithology-standards 2006).

6. Methods

The study deals with three parts, palaeoenvironment, kerogen composition and thermal history. From these three parts the source rock development and hydrocarbon potential can be deduced. The study is based on 650 samples from cores and cuttings from various hydrocarbon exploration wells in the northern URG. The applied workflow is summarized in Fig. 8.

Reconstructions of the depositional system and palaeoenvironmental interpretations were carried out using palynofacies analysis. Identification of the organic matter (OM) composition and heterogeneities throughout the study area is necessary for the subsequent kerogen analysis. For kerogen analysis, optical (palynofacies analysis) and geochemical (TOC/CNS, Rock-Eval pyrolysis) methods were applied. Also for the study of the thermal history and in the context of this research most important the maturation in the northern URG, optical methods (Vitrinite Reflectance, Sporomorph Coloration Index) and geochemical methods (Rock-Eval pyrolysis)

were applied. 2D and 3D seismic data were integrated into the workflow, in order to help determine phases of rift-related tectonic activity and their influence on sediment thickness.

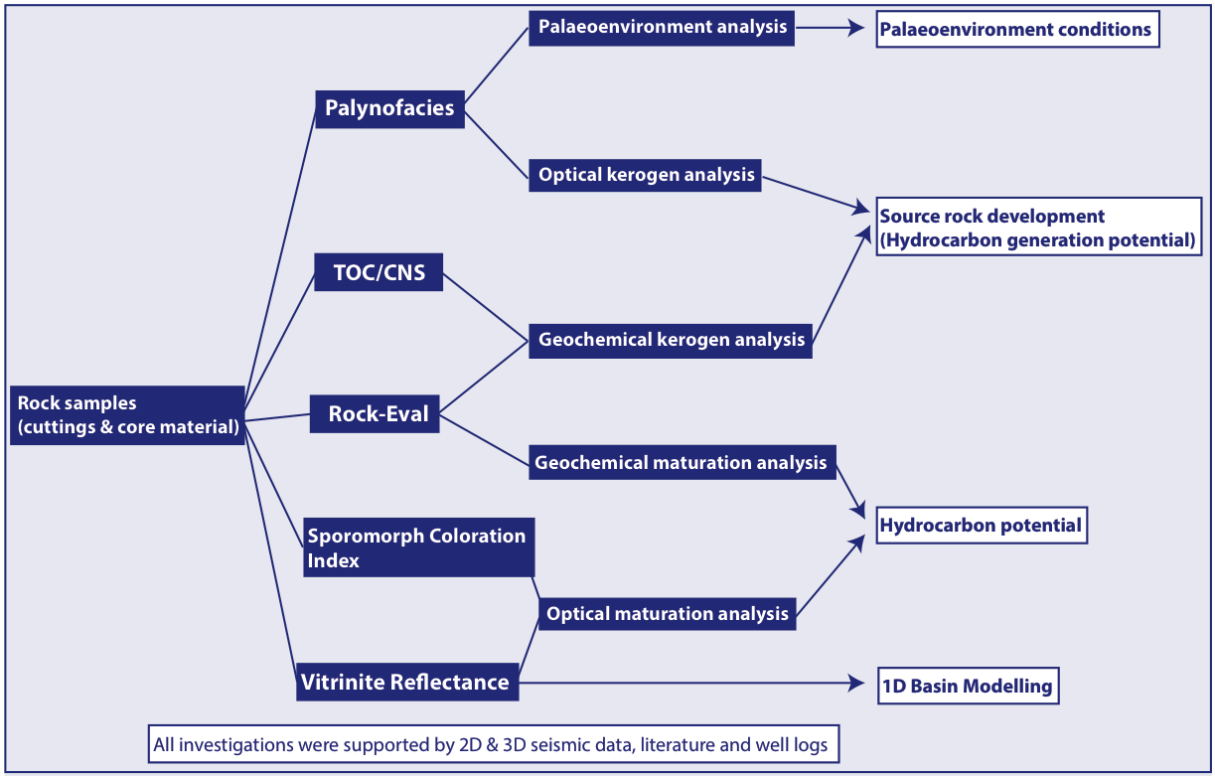

Figure 8: Workflow used in this study, combining optical (Palynofacies, Sporomorph Coloration Index, Vitrinite Reflectance) and geochemical (TOC/CNS, Rock-Eval) analysis, as well as seismic data, well logs and literature.

6.1. Sampling

The study is based on cutting and core samples from 26 exploration wells and one additional well in the northern URG. Samples were taken throughout the entire Cenozoic succession where possible. Yet, the focus is here placed on potential source rock intervals.

6.2. Palynofacies Analysis

The samples were prepared for palynofacies analysis according to standard extraction techniques (HCl, 37% HF), and sieving of the residues using 10 µm nylon sieves. Thereafter the samples were mounted on slides using epoxy without any post-acid treatment. Organic matter slides were studied by transmitted normal light and fluorescence microscopy under a Carl Zeiss Jena JENALAB POL polarizing microscope. Organic matter images were acquired using a Leica DFC 420 digital microscope camera.

All samples contained poorly to well preserved palynological assemblages consisting of continentally originated phytoclasts, sporomorphs and freshwater algae as well as marine derived phytoplankton & zooclasts (Fig. 8). Palynological samples were classified using the following groups: Phytoclasts include inertinite, vitrinite and cutinite, while sporomorphs comprise pollen and spores. The marine phytoplankton group includes dinoflagellate cysts, acritarchs, prasinophytes and leiospheres. Additionally, amorphous organic matter (AOM)

occurs, representing strongly degraded terrestrial (non-fluorescent) and brackish-marine as well as lacustrine (fluorescent) organic components. The distinct categorization of fluorescing AOM to lacustrine or brackish-marine environments is based on the co-occurrence or absence of marine phytoplankton, which is clearly attributed to brackish-marine environments. The quantitative analysis of the organic matter associations is based on counts of 200–300 specimens/particles per sample. Palynofacies raw data are attached as tables in Appendix 1.

6.3. Optical Kerogen Analysis

Integrated kerogen analysis is based on optical as well as geochemical studies. *Optical kerogen analysis* provides essential information on hydrocarbon prospectivity, based on kerogen composition and preservation following the concept of Jäger (2013). The analysis is based on the same set of slides/samples that were used for the palaeoenvironmental reconstruction. Up to 300 volumetric units of organic matter per slide were counted for the volumetric quantification of different groups of organic matter. The quantified organic matter groups are then transformed into standard kerogen types (I–IV), providing exact quantities of all four kerogen types within each sample (Jäger 2013) for the enhanced analysis of the HC generation potential (Fig. 9). Kerogen analysis data are attached as tables in Appendix 2.

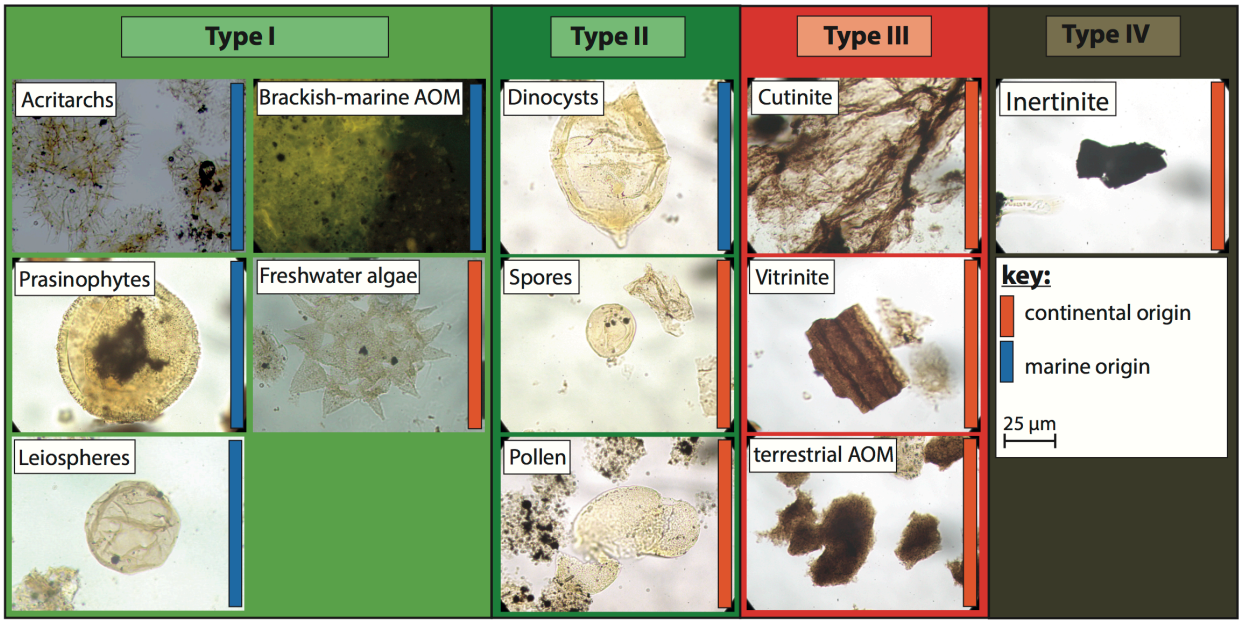

Figure 9: Classification scheme of organic matter used for palynofacies analysis and attribution to the four kerogen types I-IV. Terrestrial and marine organic components are differentiated.

6.4. Rock-Eval Pyrolysis

To verify and supplement the optically quantified relative amounts of different kerogen types, and for maturation analysis, geochemical Rock-Eval pyrolysis was carried out by Applied Petroleum Technology (APT) AS, Norway. Rock-Eval data (S1, S2, S3, HI, OI, PI, Tmax) were determined using a Bulk HAWK instrument. All procedures follow NIGOGA, 4th Edition. Jet-Rock 1 was run at every tenth samples as an external standard and checked against the acceptable

range given in NIGOGA. The programmed temperature heating started at 300°C for 3 minutes. Temperatures were subsequently increased to 650°C at a heating rate of 25 °C/min.
Two (mostly) well-defined peaks are recorded: S1 [mg HC / g rock] represents the extractable amount of HC at 300°C, which indicates the free HCs present in the samples. S2 [mg HC / g rock] represents the remaining HC potential, which is generated by cracking of the organic matter during the heating period of 300–650 °C. T_{max} is the temperature at which the maximum release of HC occurs (maximum of S2 peak). T_{max} depends on type and maturation of the kerogen, with increasing values towards higher maturities. T_{max} is about 34°C (±1 °C) lower than the temperature scale indicated by the HAWK instrument. S3 represents the amount of CO_2 [mg CO_2/g rock], which is produced during pyrolysis.
The parameters S1, S2, S3 and T_{max}, along with TOC (see below), input parameters for the calculation of the HI (Hydrogen Index, =S2/TOC*100), OI (Oxygen index, =S3/TOC*100) and PI (Production Index, =S1/(S1+S2). Detailed information on the method and measured parameters are described in Espitalié et al. (1985). Rock-Eval data are attached as tables in Appendix 3.

6.5. TOC/CNS

Total Organic Carbon/C-N-S (TOC/CNS) analysis was measured using an ELEMENTAR Variomax CNS-analyser available at the Institute of Geography of Heidelberg University. The non-metals C, H, N, S were analysed operating on a high temperature combustion (HTC) exceeding 1000 °C. With the aid of helium as a carrier gas, the generated combustion gases (oxidation products) are run through a thermal detector which is heated to over 1000 °C. Subsequently, the defined combustion gases (CO_2, H_2O, SO_2, N_2) are separated in specific adsorption columns and fed to a thermal conductivity detector and were quantified. Using the known initial weight of the analysed sample, the respective mass fraction of the elements is calculated. In terms of TOC, a "good" source rock of hydrocarbons has to contain a minimum content of organic matter (Batten 1996), assumed to be within the range of 1–2 % (Peters and Cassa 1994). The necessary minimum values are assumed to be around 0.5 % TOC for shales and 0.3 % for carbonates (Tissot and Welte 1984, Peters 1986), but the values strongly depend on the type of kerogen (I–III) present (Bordenave et al. 1993). Data from TOC/CNS analysis are attached in Appendix 4.

6.6. Vitrinite Reflectance

Optical maturation analysis is based on vitrinite reflectance (VR) and spore/pollen color analysis using the Spore Coloration Index (SCI). VR analysis was performed on 65 samples. A detailed description of the origin and diversity of vitrinite is available in Mukhopadhyay (1994). Isolated kerogen was concentrated in blocks of synthetic resin and polished at the top. Up to 50 vitrinite grains were analyzed from each block, if available. VR analysis was carried out by digital image analysis of vitrinite particles using the tool MIRONE® (Luis 2007). High-resolution digital black/white images of vitrinite grains from reflected-light microscopy are thereby used. The grey levels of the digital images were re-calculated to real VR values by specific image analysis software (Luis 2007). Image analysis was calibrated by four standards (R = 0.589; R = 0.812; R =

1.625; R = 3.225). Higher coalified, allochthon vitrinite grains, which originate from the graben shoulders and were re-deposited in the graben, were carefully eliminated from measurements.
This optical VR analysis is much more precise than the widely used VR analysis, which overestimates vitrinite reflectance in the interval of 0.5–1.7% Ro by up to 0.35%, as described by Nielsen et al. (2015). For VR analysis, wells with a continuous sample set and a preferably broad stratigraphic range were selected. The maturities that correlate to the oil-, gas- and mixed-oil-gas window of potential source rock units in regard to hydrocarbon generation are used as defined in Suárez-Ruiz et al. (2012): immature < 0.5 %Ro, oil window 0.5–1.0% Ro, mixed oil-gas window 1.0–1.2% Ro, gas window > 1.2% Ro. VR data are attached in Appendix 5.

6.7. Sporomorph Coloration Index

The Sporomorph Coloration Index (SCI) was applied to palynological slides from the studied wells as described above. Therefore, the rock samples were processed using maceration techniques with concentrated HCl and 50% HF. Isolated organic residues were washed and mounted directly on slides without any post-acid treatment. Organic matter slides were studied by transmitted normal light and fluorescence microscopy.
For the attribution of the degree of maturation, the Robertson Group SCI correlation (Fischer et al. 1981; Collins 1990) was used. SCI data are attached in Appendix 5.

6.8. Seismic Interpretation

In this study, the interpretation of 2D and 3D seismic data were integrated into the workflow, in order to (1) determine the degree of influence of syn-rift tectonic activity along large, in the seismics visible faults on sediment thickness and to (2) evaluate the structural position of the individual wells, which was needed for further interpretation.
The seismic workflow started with the loading of 3D seismic as well as 2D seismic lines into Petrel® software (Version 2015). Subsequently all seismic data were brought onto the main seismic reference level. The seismic markers mapped in the 3D seismic cube were afterwards tracked along the 2D seismic lines. In this context, additional faults were then picked along those lines. Finally, the 2D and 3D seismic interpretation was transferred from time (TWT) into depth (TVD). For this time-to-depth conversion the prestack seismic velocity field was used. The velocity field was rescaled by checkshot velocities in wells within the Stockstadt field. This resulted in mis-ties at formation tops from wells in the range of few ten of meters for the Oligocenian sediments. This was well within the vertical resolution of the 3Dseismic which amounts to some 30 m at the top of the Pechelbronn Group.
As the 2D seismic lines were acquired from different seismic surveys carried out in different years, they differ in acquisition parameters, processing order and quality. In consequence, the different stratigraphic units partly differ significantly in terms of visual appearance. Corroborating the seismic interpretations, literature data, well logs and reports as well as various industry and research related studies were available.

6.9. 1D Basin Modelling

In order to discuss the palaeothermal history, basin subsidence and accumulation history in the study area, one-dimensional simulations were performed using PetroMod1D® (Version 2011.1.1 Windows 64-bit). An introduction to the numerical basin modeling is given in e.g. Tissot & Welte (1984) and Yalcin et al. (1997). Details on the software are described in Welte & Yükler (1981). The simulation of the model is calibrated with VR data. Input parameters for one-dimensional numerical simulations are attached in Appendix 6.

7. Palynofacies and Kerogen analysis

7.1. Results

7.1.1. Pechelbronn Group

Palynofacies analysis of the Late Eocene to Early Rupelian Pechelbronn Group was carried out on 17 wells (Fig. 10). In some wells the subdivision of the Pechelbronn Group was difficult due to unclear log signatures and/or rapidly changing lithologies.

In the study area, the Lower Pechelbronn Formation is dominated by continental components. Phytoclasts (43.0–100.0 %) and moderate amounts of terrestrial AOM (0.0–34.8 %), as well as minor amounts of sporomorphs (0.0–19.2 %) are present. Freshwater algae are present only in two samples from well W10 (1.5 % and 6.3 %). A small brackish-marine fraction is present only in the latter well, consisting of small amounts of phytoplankton (0.0–3.8%) and small to moderate amounts of fluorescing AOM (0.0–33.4 %).

Similar to the Lower Pechelbronn Formation, the Middle Pechelbronn Formation is dominated by terrestrial components. Thereby phytoclasts are available in amounts of typically 44.9–100.0 %, only one sample from well W31 indicates lower amounts of 25.6 %. Sporomorphs are present in amounts up to 44.4 % in well W31, but occur mostly in the range of 0.0–26.3 %. Terrestrial AOM, which represents strongly degraded phytoclasts is available in amounts of 0.0–34.6 %. Only one sample from well W16 reaches 61.6 %. Lacustrine freshwater algae are present in only one sample from well W10 in negligible amounts (0.9 %). The marine fraction is composed of small amounts of brackish-marine AOM (0.0–22.1 %) and mostly small amounts of phytoplankton (0.0–11.1 %). Only two samples from well W16 (eastern graben margin) the amount of phytoplankton reaches amounts of 21.1 % and 23.8 %. The phytoplankton is clearly dominated by acritarcs. Dinoflagellates are less abundant (with the exception of well W15, where the amount of dinoflagellates exceeds the amount of acritarcs), leiospheres only occur sporadically.

Palynofacies composition of the Upper Pechelbronn Formation reveals clear dominance of phytoclasts, typically ranging around 64.0–88.5 % (one sample from well W16 with 33.6 %). Sporomorphs occur in amounts of 0.0–15.9 %; terrestrial AOM is present in amounts up to 15.4 % (one sample from well W35 with 25.3 %). Aquatic components occur only subordinately. Fluorescing brackish-marine AOM is present only in well W16 in amounts of 3.8 % and 39.9 %.

The phytoplankton group reaches up to 1.5 % in well W21 (solely acritarcs) and W31 (solely dinoflagellates) and 9.2 % in one sample from well W35 (mostly dinoflagellates, subordinately acritarcs and leiospheres). In wells where the subdivision of the Pechelbronn Group into Formations was not possible, similar palynofacies assemblages are observed. Also here, terrestrial derived organic material (OM) clearly dominates over the brackish-marine fraction. Distributional trends in OM composition based on palynology within the Pechelbronn Group or the different Formations cannot be reconstructed.

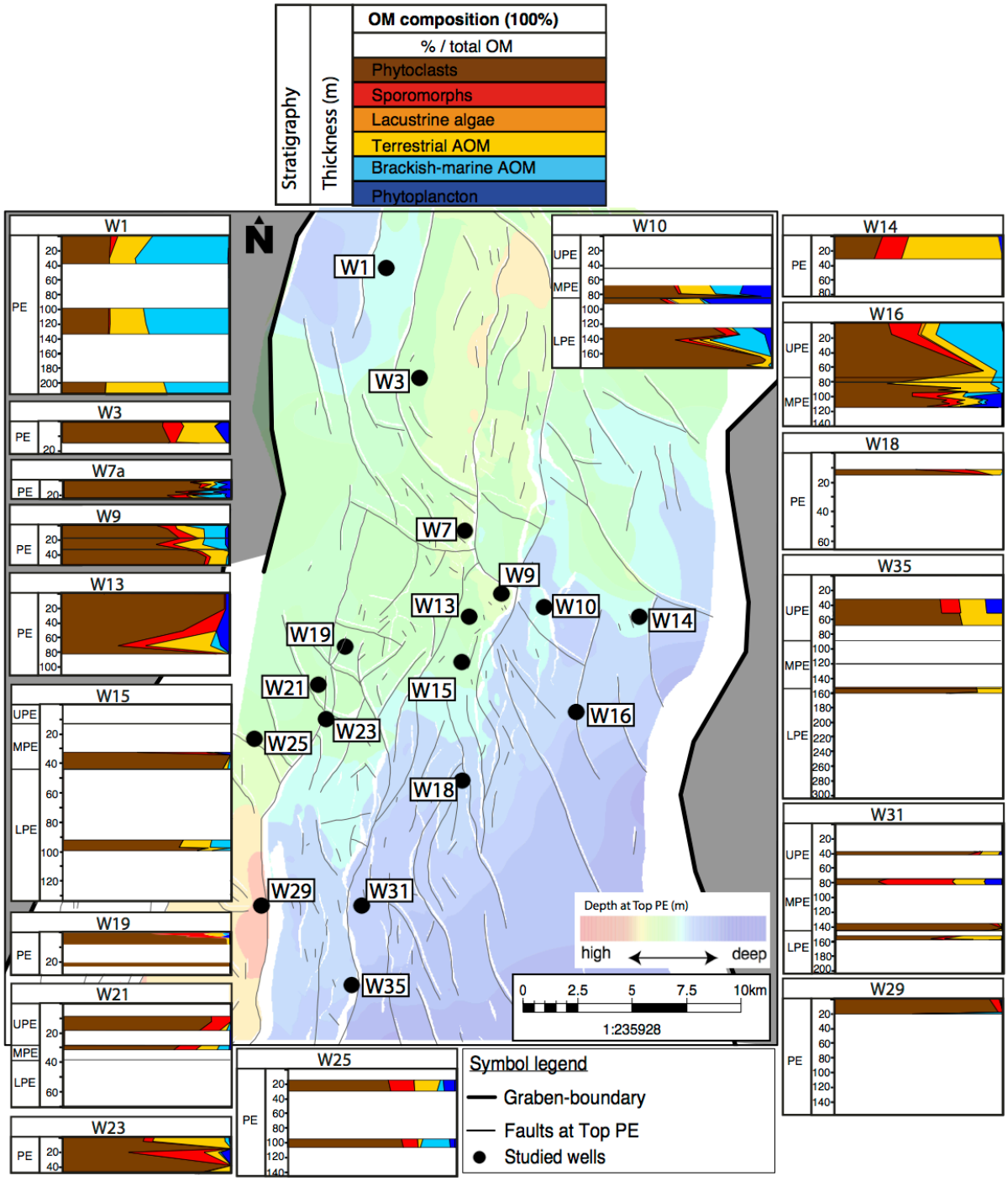

Figure 10: Palynofacies analysis of the Pechelbronn Group in the northern URG, showing the relative amounts of the main palynofacies groups for all samples within the studied wells. For each well, the thickness of the Pechelbronn Group is given.

If the OM is attributed to kerogen types, mixtures of kerogen types I–IV were found in all Pechelbronn samples (Fig. 11), although high dominance of gas-prone and barren type III/IV kerogen characterizes this unit. Amounts of oil-prone type I range from 0.0–22.1 % in most samples. Frequently amounts reach up to 54.8 %, such as in samples from W1, W29, W16, W10. Oil-prone type II kerogen is present in similar amounts of up to 32.1 %, frequently reaching 48.2 %. Gas-prone type III kerogen clearly dominates the Pechelbronn Group, usually ranging between 30–90 %, reaching up to 100% in some samples. Barren type IV kerogen occurs in highly variable amounts but usually <25 %. The highest amounts of oil-prone type I and II kerogen are present within the Middle and even more within the Upper Pechelbronn Formation in wells W1, W16, and W10.

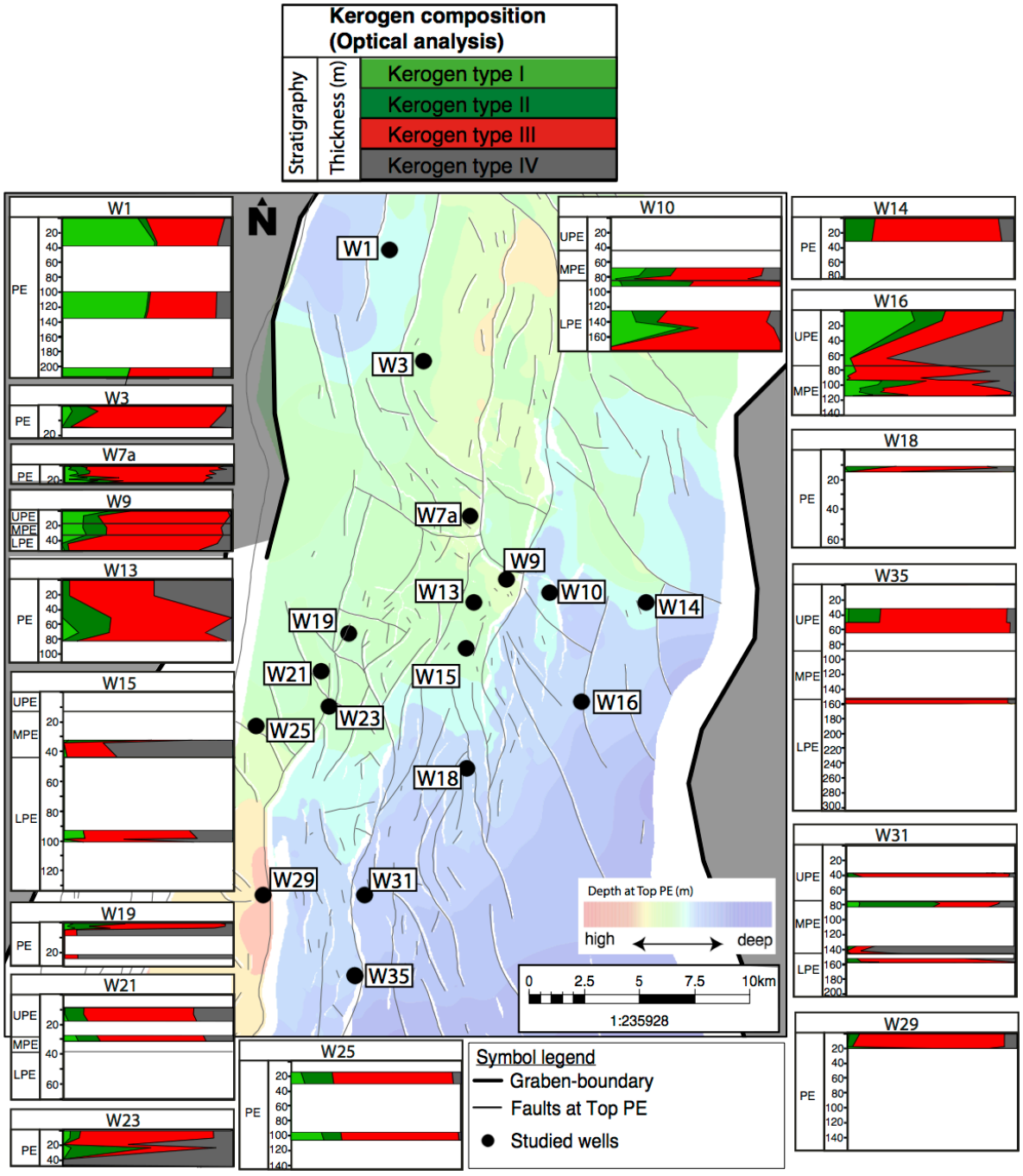

Figure 11: Optical kerogen analysis of the Pechelbronn Group in the northern URG, showing the relative amounts of the four kerogen types I-IV for all samples within the studied wells. For each well, the thickness of the Pechelbronn Group is given.

16 samples from the Pechelbronn Group (three of them from the Middle Pechelbronn Formation) were chosen for Rock-Eval pyrolysis (Fig. 12). Rock-Eval analysis shows HI values from 29–337 mg HC/g TOC. Overall low to moderate OI values were identified ranging from 5–66 mg CO_2/g TOC. Only two samples from the Middle Pechelbronn Formation from wells W10 and W16 reach OI values of 169 and 162 mg CO_2/g TOC. In the HI/OI diagram ('Pseudo van Krevelen'), most samples plot along the mixed type II-III kerogen field and lower type II kerogen pathway. Few samples, among them also the ones from the Middle Pechelbronn Formation, plot along the lower and upper type IV and III kerogen pathways. Additionally to the HI/OI diagram, the TOC/S2 graph is an effective tool for comparison of different source rocks and their established petroleum generation potentials. In the samples from the Pechelbronn Group, TOC ranges between 0.5–5.9 wt.% (0.3–0.6 wt.% for the three samples from the Middle Pechelbronn Formation). S2 values of 0.1–8.0 mg HC/g rock are reached. These values relate to relatively organic lean rocks based on TOC/S2 (Fig. 12). In this graph, most samples plot in the mixed type II-III and type III kerogen fields. Few samples indicate a purely type IV kerogen composition. The Middle Pechelbronn Formation, as also suggested by HI/OI, is purely composed of type III or type IV kerogen based on Rock-Eval pyrolysis.

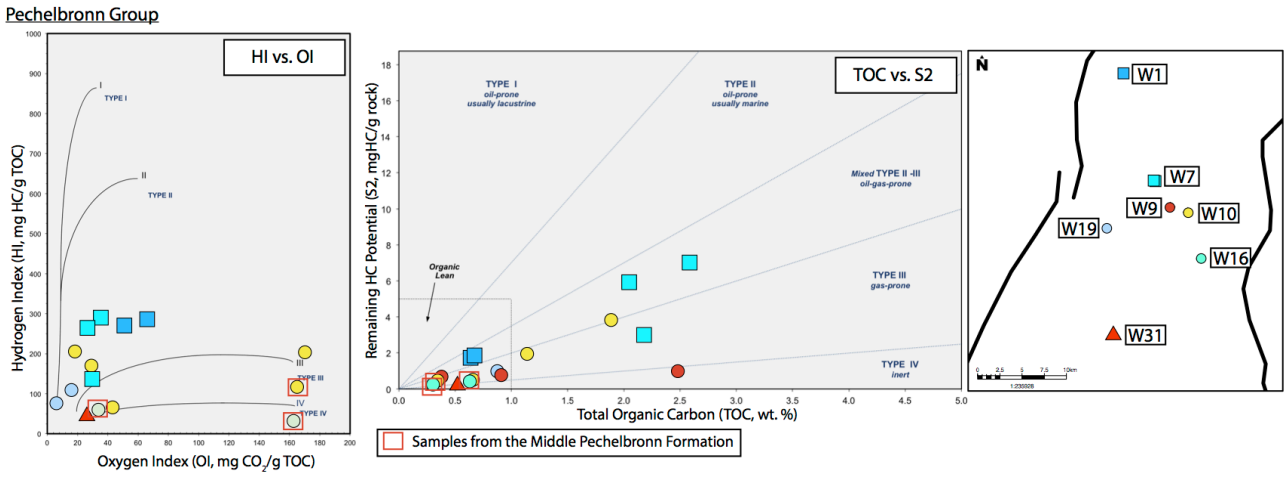

Figure 12: Rock-Eval analysis of the Pechelbronn Group

7.1.2. Rupel Clay Group

Palynofacies analysis of the Rupel Clay Group reveals dominance of terrestrial OM for both subunits, the Foraminifera Marls Formation and Fish Shale Formation) (Fig. 13).

Samples of the Foraminifera Marls Formation contain phytoclasts mostly in amounts of 10.2–37.7 %. Amounts exceeding 50 % (up to 81.9 %) of phytoclasts are present in wells located along the western graben margin and within the graben center, decreasing towards the north and east. Sporomorphs and terrestrial AOM are present in overall small amounts (2.1–14.4 % and 0.0–28.3 %), only frequently reaching up to 42.0 % (sporomorphs) and 53.3 % (terrestrial AOM). Lacustrine algae occur only in well W9 (2.4 %). The marine fraction contains brackish-marine AOM (up to 11.2 %; occasionally reaching up to 65.2 %) and phytoplancton (up to 9.3 %;

occasionally reaching up to 19.6 %). The phytoplancton group consists of mainly dinoflagellates and subordinately acritarcs and prasinophytes.

The overlying Fish Shale Formation contains phytoclasts in the range of 26.1–36.5 % on the western graben side and elevated amounts of 55.1–83.2 % on the eastern graben side. Relatively constant amounts of sporomorphs (4.8–16.5 %) are present, reaching 30.5 % only in well W16. Terrestrial AOM is present in small amounts up to 15.7 %, reaching up to 44.2 % only in wells W1 and W10. Lacustrine algae occur in negligible amounts in wells W9 and W16. The marine fraction of the Fish Shale Formation is composed of marine AOM (0.0–11.2 %, occasionally 20.7–51.9 %) and phytoplancton (0.0–9.8 %). The latter palynofacies group is dominated by dinoflagellates.

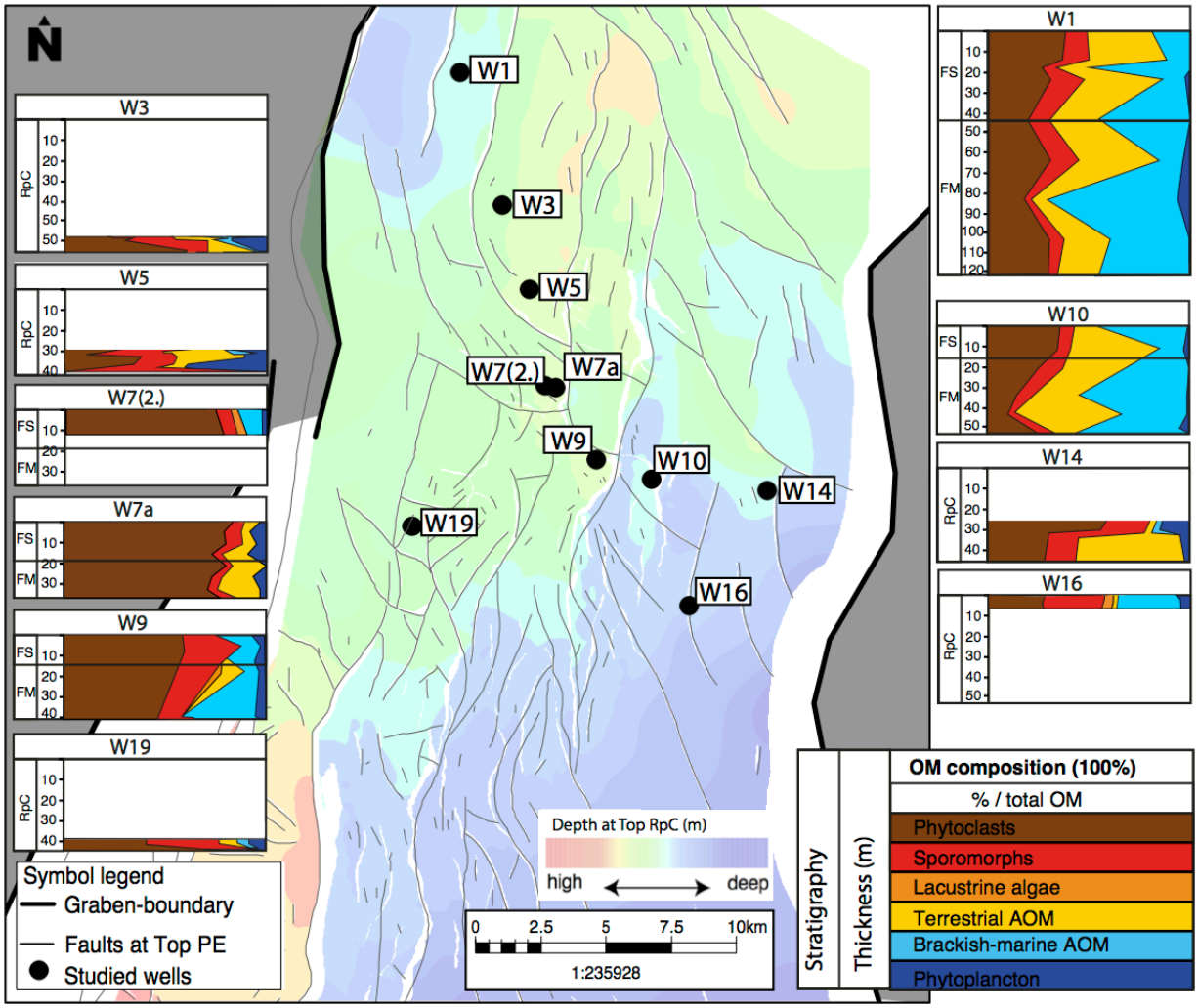

Figure 13: Palynofacies analysis of the Rupel Clay Group in the northern URG, showing the relative amounts of the main palynofacies groups for all samples within the studied wells. For each well, the thickness of the Rupel Clay Group is given.

Optical kerogen analysis of the Foraminifera Marls Formation reveals highly variable kerogen compositions (Fig. 14). Type I kerogen is present in amounts <37.2 % and in wells W1 and W10 even up to 66.4 %. Type II kerogen occurs typically in smaller amounts <17.9, but also reaches up to 50.4 % in few samples. Type III kerogen occurs in overall high amounts up to 70.7 %,

frequently even 82.1 % (W3) and 90.2 % (W7a). Small amounts of type IV kerogen (<12.8 %) are present in all samples.

For the Fish Shale Formation similar results as for the Foraminifera Marls Formation are obtained. Yet, the amounts of oil-prone type I and II kerogen are typically lower and the amount of type III and type IV higher. Amounts of type I kerogen usually range below 13.0 %, sporadically reaching up to 51.9 %. Type II kerogen is present with maximum amounts of 21.3 %. Only one sample from well W16 reaches 32.7 % of type II kerogen. Type III kerogen is present in amounts of 30.8 –81.3 %, clearly dominating the Fish Shale Formation. Type IV kerogen does not exceed 15.5 %.

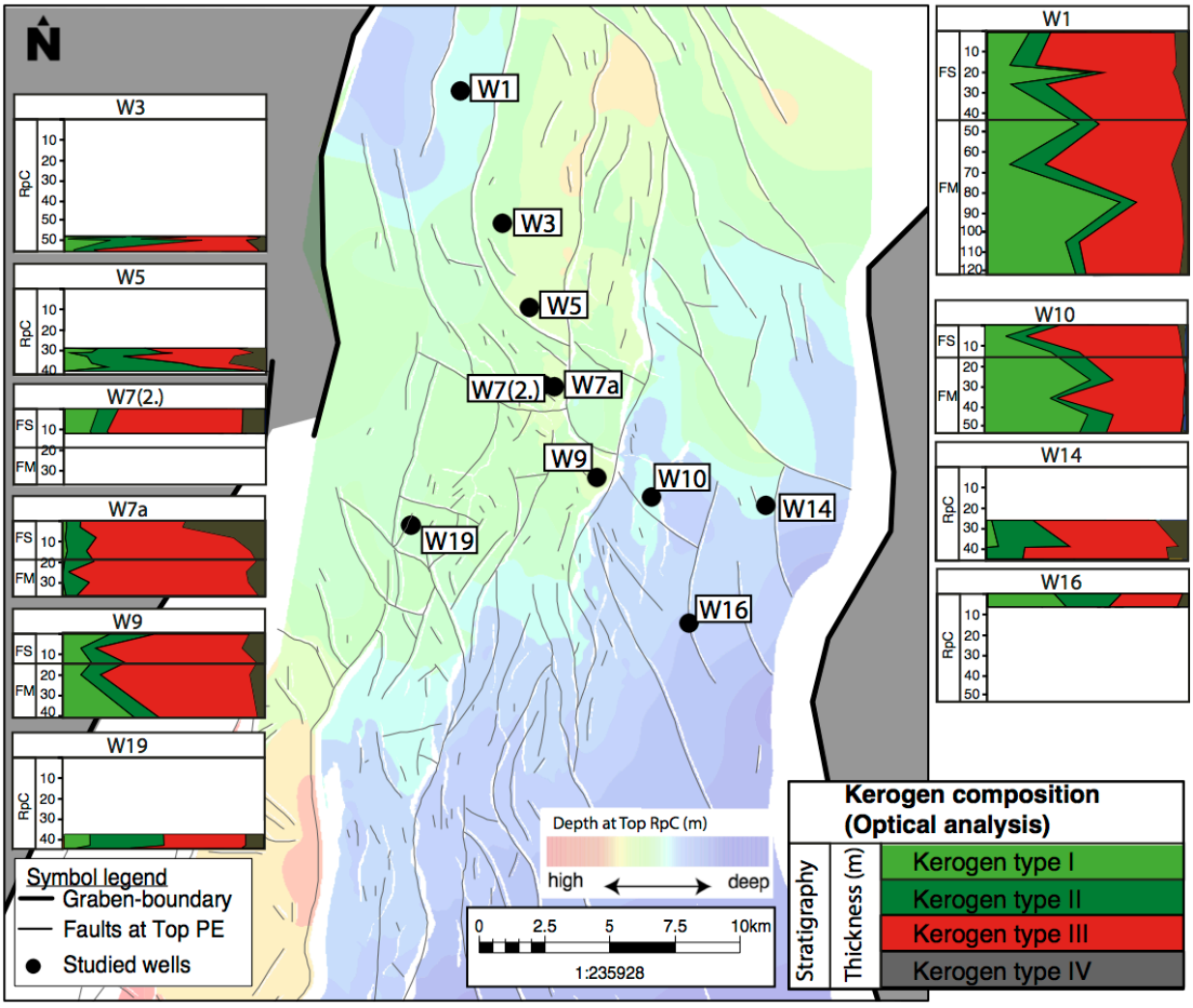

Figure 14: Optical kerogen analysis of the Rupel Clay Group in the northern URG, showing the relative amounts of the four kerogen types I-IV for all samples within the studied wells. For each well, the thickness of the Rupel Clay Group is given.

For Rock-Eval pyrolysis, 20 samples of the Foraminifera Marls Formation and 8 samples of the Fish Shale Formation were chosen. The Foraminifera Marls Formation has HI values between 32–378 mg HC/g TOC and OI values of 9.9–115 mg CO_2/g TOC (Fig. 16). In the HI/OI-diagram, one set of samples plots along the type II pathway to the field of mixed type II-III kerogen; another set plots along the type III- and IV kerogen pathways. In the TOC/S2 graph, similar kerogen compositions are shown with TOC values of 0.5–3.6 wt.% and S2 in the range of 0.2–

14.7 mg HC/g rock. Kerogen compositions of purely type II-, III- and IV kerogen as well as the dominant mixed type II/III kerogen are represented.

Rock-Eval pyrolysis of the Fish Shale Formation samples reveals HI values of 95–291 and OI values of 17–56 mg CO_2/g TOC (Fig. 15). Based on the HI/OI diagram the kerogen is dominated by the mixed type II-/III and the type III/IV. Similar results in kerogen composition are shown in the TOC/S2 graph with TOC values of 0.7–3.0 wt.% and S2 of 1.0–18.5. Type I-/III- & IV kerogen as well as the mixed type II/III kerogen field are represented.

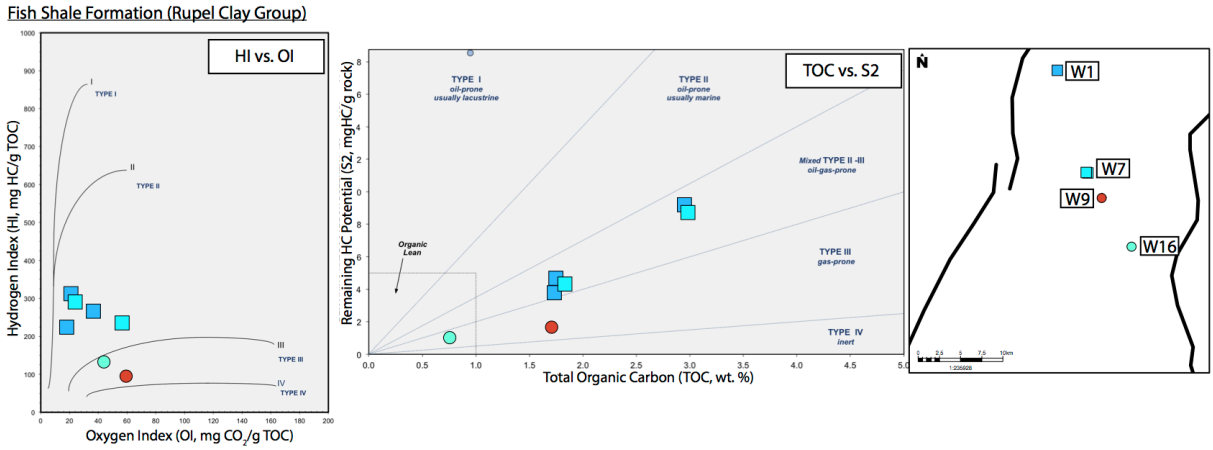

Figure 15: Rock-Eval analysis of the Fish Shale Formation (Rupel Clay Group)

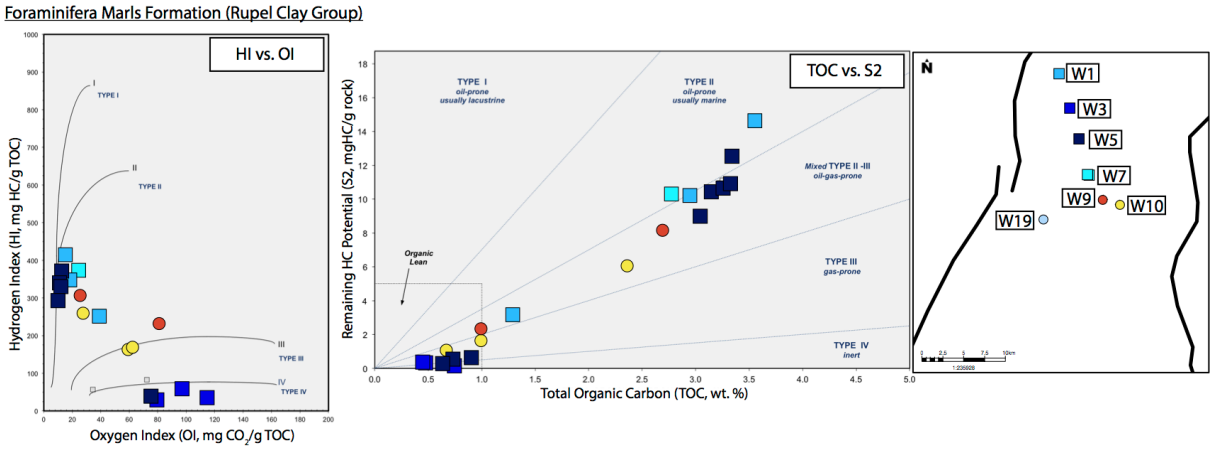

Figure 16: Rock-Eval analysis of the Foraminifera Marls Formation (Rupel Clay Group)

7.1.3. Meletta Group, Cyrena Marls Group, Bunte Niederröderner Group and Cerithium Group

Palynofacies data of the Meletta Group and Cyrena Marls Group (Fig. 17) indicate a high fluctuation in OM. The amount of phytoclasts in most samples ranges from 27.9 % (or occasionally even 9.1–96.9 %). The highest amounts occur in the lower Meletta Group, values are generally decreasing towards the top Cyrena Group. Sporomorphs occur in amounts of up to 35.5 %, terrestrial AOM is less abundant (<18.5 %). Lacustrine algae occur sporadically in amounts up to 6.6 %. The marine fraction is composed of brackish-marine AOM and

phytoplancton, with often increasing amounts towards the top Cyrena Marls Group. Brackish-marine AOM reaches amounts of 0.0–20.4 % in the eastern and southernmost wells and 34.4–69.1 % in the western and northernmost wells. Relatively constant amounts of phytoplancton up to 20.1 % are observed throughout the study area, mainly composed of dinoflagellates and subordinately acritarcs, prasinophytes and leiospheres.

Within the Bunte Niederröderner Group, high variation in the amount of phytoclasts is observed (2.3–100.0 %), mostly decreasing towards the top Bunte Niederröderner Group (Fig. 17). Relatively constant values of sporomorphs are observed, not exceeding 28.4 %. Terrestrial AOM is rare in most samples (0.0–14.2 %), and reaches exceptionally high values of 35.0–80.0 % only in few samples from the eastern wells W16 and W14, the northernmost well W1 and well W29 towards the south. Lacustrine algae are absent in most samples. But frequently reach up to 13.5 %. The brackish-marine fraction is composed of marine AOM (mostly in the range of 28.5–58.4 %, frequently absent) and phytoplancton. The latter OM group reaches 28.1 % and consists of mainly dinoflagellates and subordinately leiospheres, acritarcs and prasinophytes.

The Cerithium Group is dominated of terrestrial components in most samples; brackish-marine components dominate in the eastern and southern study area (Fig. 17). The amount of phytoclasts does usually not exceed 39.4 % and only frequently reaches values of up to 57.4 % (W1, W14). Sporomorphs are present in amounts of 8.9–37.4 %, frequently reaching values of up to 56.6 % (W14, W19). The amount of terrestrial AOM reaches maximum values of 57.8 % and often decreases towards the top Cerithium Group. Lacustrine algae occur sporadically and reach notable values of 29.7 % in well W7(2.) and 7.2–12.9 % in wells W8, W16 and W14. Brackish-marine AOM is present in moderate amounts (<37.0 %) and in few outliers (W8, W10, W14) up to 66.7 %. The amount of phytoplancton is fairly constant (up to 17.6 %) and reaches 59.9 % in only one sample from well W8. Dinoflagellates dominate over acritarcs and prasinophytes in most samples.

Optical kerogen analysis of the Meletta Group and Cyrena Marls Group (Fig. 18) reveals a type I/II dominated kerogen composition with increasing amounts of type I/II kerogen towards the top of the Cyrena Marls Group. Yet, especially wells located along the western graben shoulder indicate type III kerogen dominance. The highest amounts of type I kerogen up to 70.3 % are found in wells W10, W1, W7(2.) and W8. Type II kerogen is present in constant amounts of usually <30.0 %. The amount of type III kerogen ranges mostly between 26.0–75.0 % with frequent outliers. The amount of type IV kerogen is usually below 16.9, and reaches 38.8 %/40.9 % in only two samples from wells W7a and W14.

The Bunte Niederröderner Group contains mostly high amounts of type I and type II kerogen up to 58.4 % and 46.7 %. Extremely low amounts of oil-prone type I and II kerogen are only present in wells W29, W23, W12 and W4. Type III kerogen is present in highly variable amounts ranging from 10.3–91.1 % mostly ranging around 15.0–35.0 %.

The Cerithium Group is characterized by overall high amounts of oil-prone type I kerogen up to 65.9 % and type II kerogen up to 57.3 %. Type III kerogen rarely reaches values >40 %; type IV kerogen is present in mostly low amounts <13.4 %.

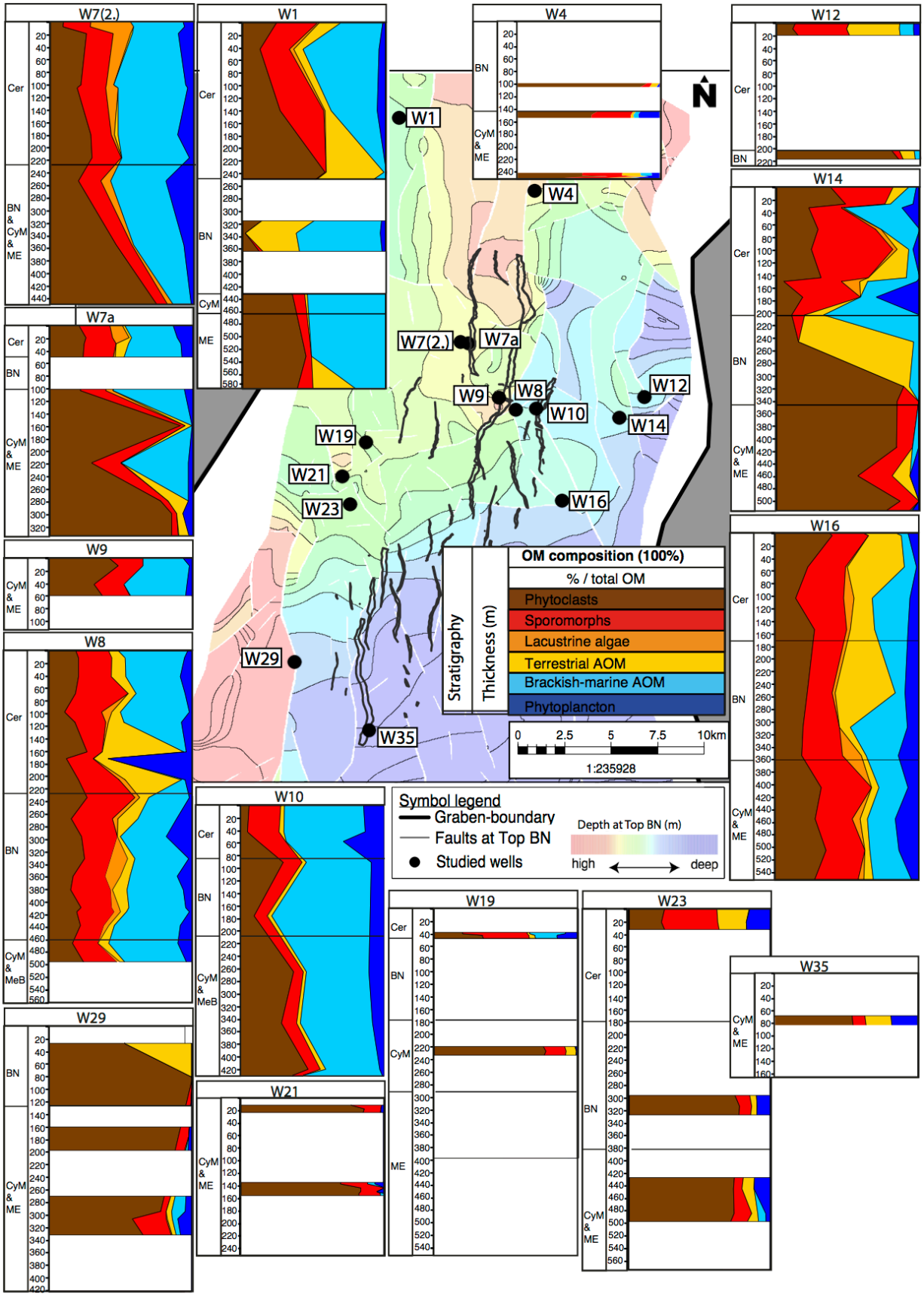

Figure 17: Palynofacies analysis of the Meletta Group, Cyrena Marls Group, Bunte Niederröderner Group and Cerithium Group in the northern URG, showing the relative amounts of the main palynofacies groups for all samples within the studied wells. For each well, the thickness of the stratigraphic interval is given.

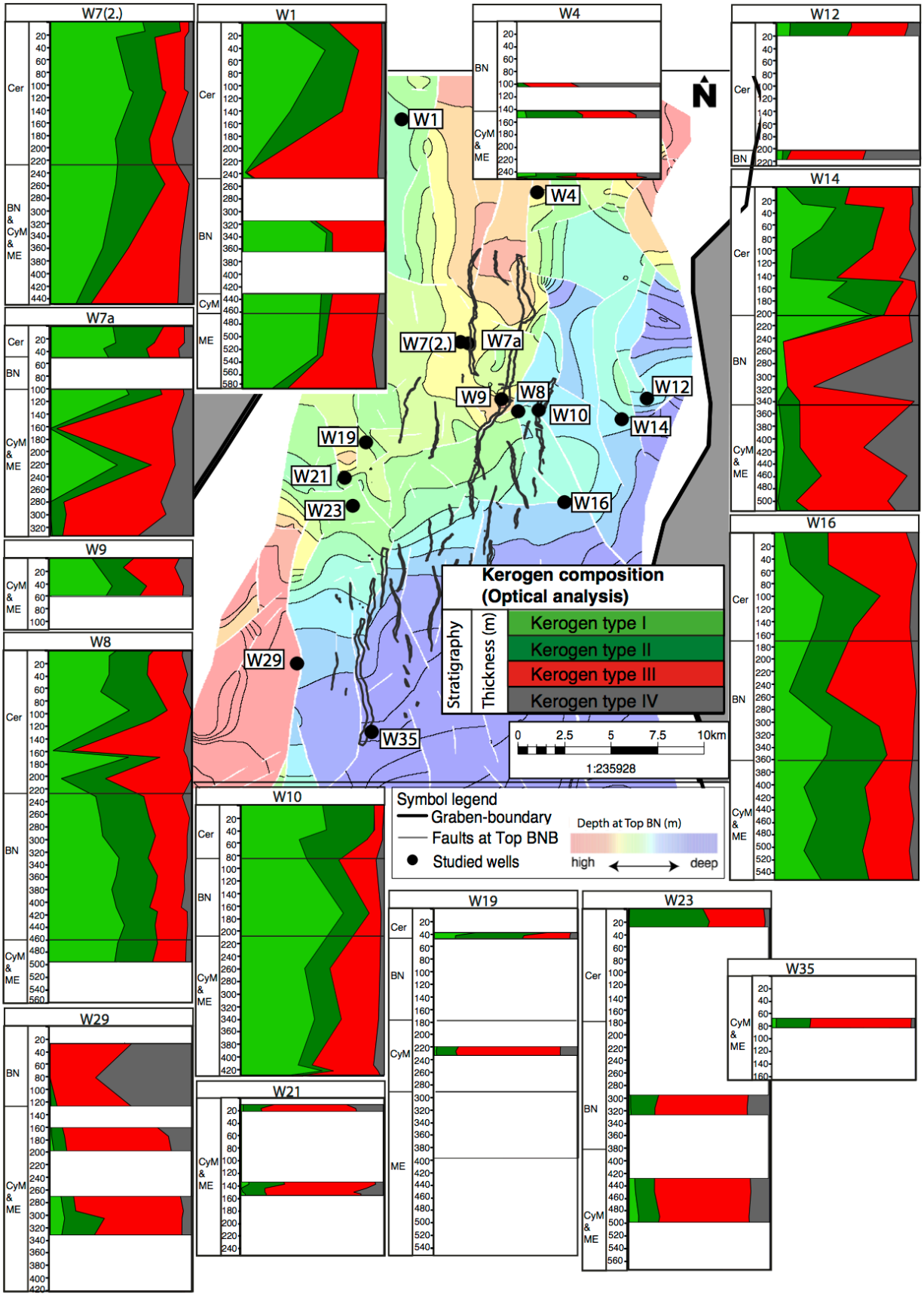

Figure 18: Optical kerogen analysis of the Meletta Group, Cyrena Marls Group, Bunte Niederröderner Group and Cerithium Group in the northern URG, showing the relative amounts of the four kerogen types I-IV for all samples within the studied wells. For each well, the thickness of the stratigraphic interval is given.

Six samples were chosen for Rock-Eval pyrolysis from the Meletta Group and Cyrena Marls Group (Fig. 20). Based on the `Pseudo Van Krevelen` diagram, HI values (55–150 mg HC/g TOC) and OI values (102–652 mg CO_2/g TOC) indicate a dominantly type III and type IV kerogen composition. Due to high S3 peaks in the three samples from well W7 extremely high OI was calculated (345–652 mg CO_2/g TOC) TOC values are generally low in the range of 0.5–0.7 wt.%. When plotted with S2 (0.3–1.1) a type III/IV kerogen is suggested.

No Rock-Eval measurements were conducted in the Bunte Niederröderner Group due to silty/sandy lithologies.

From the Cerithium Group 15 samples from 9 wells were chosen for Rock-Eval pyrolysis (Fig. 19). HI values vary from 22–362 mg HC/g TOC, OI values from 28–352 mg CO_2/g TOC, but mostly below 85 mg CO_2/g TOC. The northernmost well W1 and well W13 contain a type II/III kerogen mixture. Wells on the eastern side of the graben (W14 and W12) as well as well W7 possess purely type III/IV kerogen. For wells W8, W10 and W16 a mixed type II/III to type III composition is assumed. TOC values of the samples range between 0.2–2.2 wt.%. Plotting TOC against S2 (0.1–4.6), similar results are derived than in the HI/OI diagram. Only one sample from well W1 is assigned to a purely type II kerogen, indicating slight differences in the various Rock-Eval results.

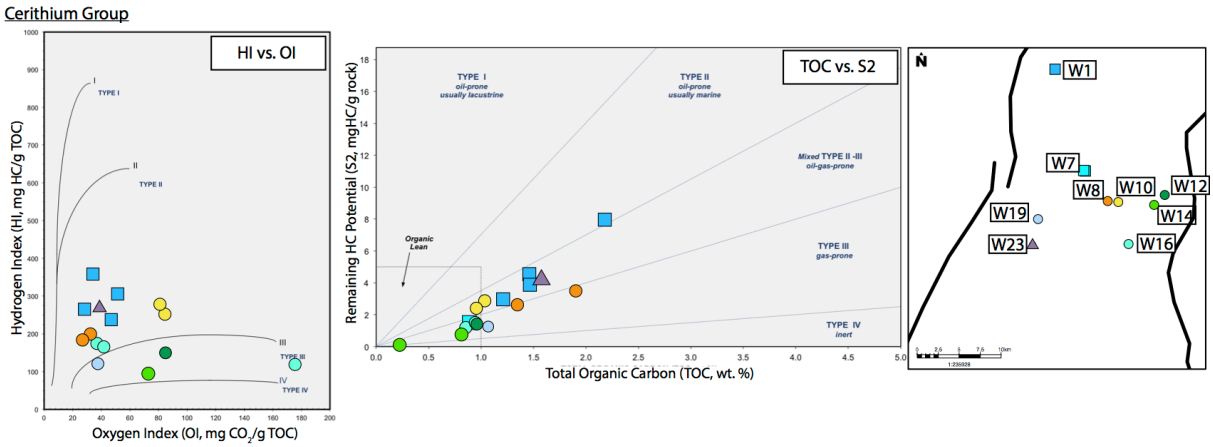

Figure 19: Rock-Eval analysis of the Cerithium Group

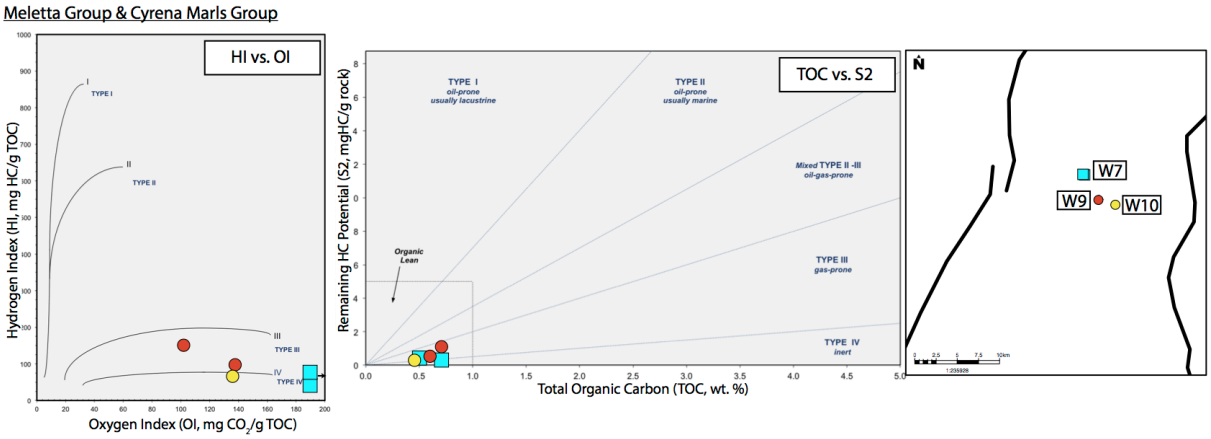

Figure 20: Rock-Eval analysis of the Meletta Group and Cyrena Marls Group

7.1.4. Corbicula Group

The Corbicula Group is characterized by strong variations in OM composition (Fig. 21). The amount of terrestrial OM is increasing, whereas the amount of brackish-marine OM is decreasing in wells W8 and W10. The overall amount of phytoclasts ranges between 5.8–34.1 %, frequently reaching up to 62.9 % (W10, W12, W14). Sporomorphs are present in small to moderate amounts (12.7–37.2 %), with the exception of two outliers of 0.0 % and 59.9 % in W14. The amount of terrestrial AOM reaches maximum values of 43.1 % and decreases towards the top Corbicula Group. One outlier in well W14 reaches 76.8 %. Lacustrine algae occur in overall negligible amounts up to 3.8 %.

The aquatic fraction is composed of brackish-marine AOM and phytoplancton. Brackish-marine AOM is present in high ranges of 0.0–58.6 % (maximum amounts within the lower section of the Corbicula Group in wells W8 and W10), phytoplancton reaches up to 21.6 %, mainly consisting of dinoflagellates and subordinately acritarcs and prasinophytes.

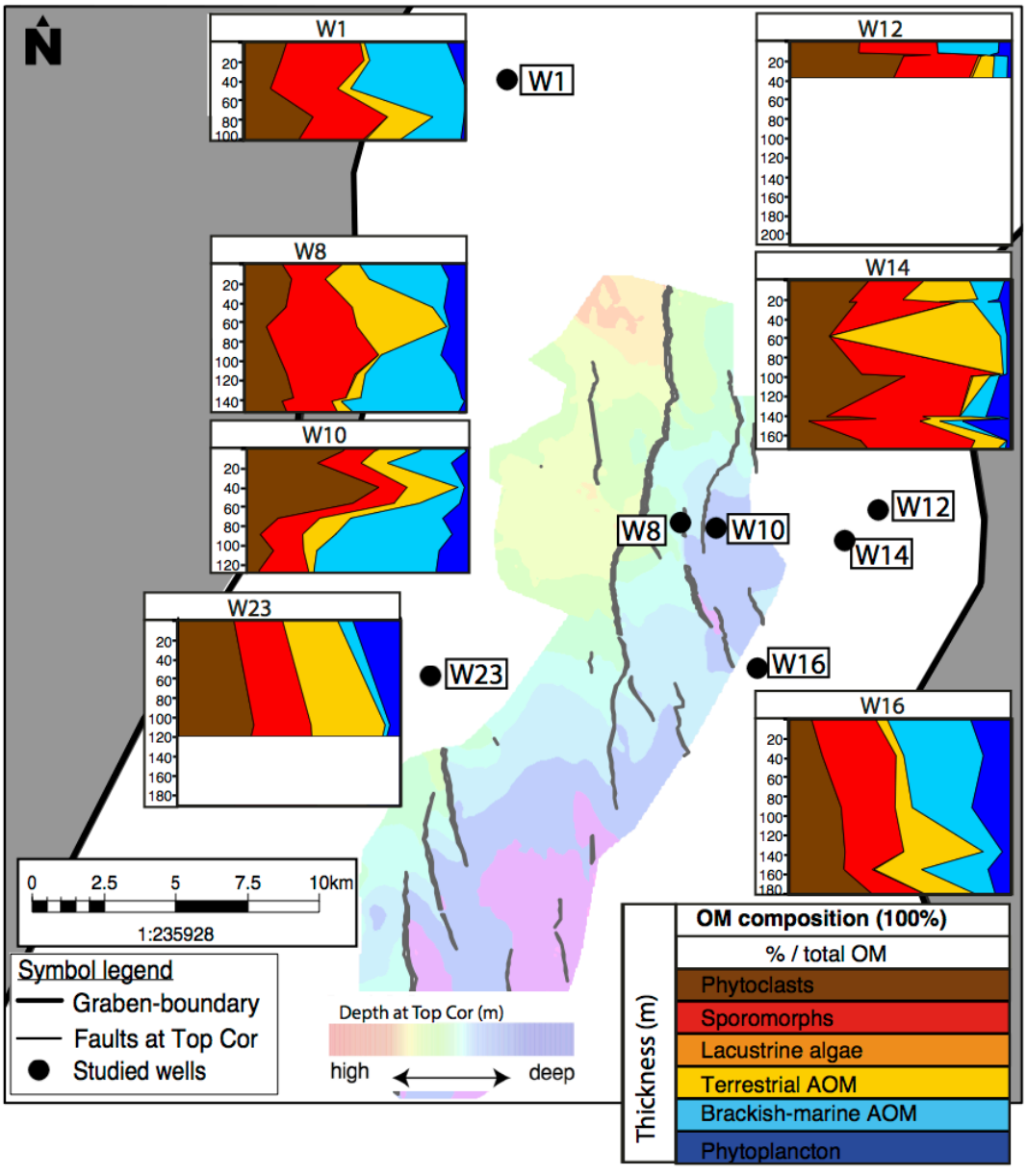

Figure 21: Palynofacies analysis of the Corbicula Group in the northern URG, showing the relative amounts of the main palynofacies groups for all samples within the studied wells. For each well, the thickness of the Corbicula Group is given.

Optical kerogen analysis of the Corbicula Group reveals high variations in kerogen composition (Fig. 22). Most wells, among which are wells W8, W10 and W14, suggest increasing amounts of type III kerogen towards the top Corbicula Group. Well W1, W23 and W16 on the contrary suggest increasing amounts of oil-prone type I and II kerogen. Type I kerogen reaches maximum amounts of 57.5 %; type II kerogen is present in amounts up to 55.2 % and even up to 70.9 % in one sample from well W14. Barren type IV kerogen is available in minor amounts <18.7 %.

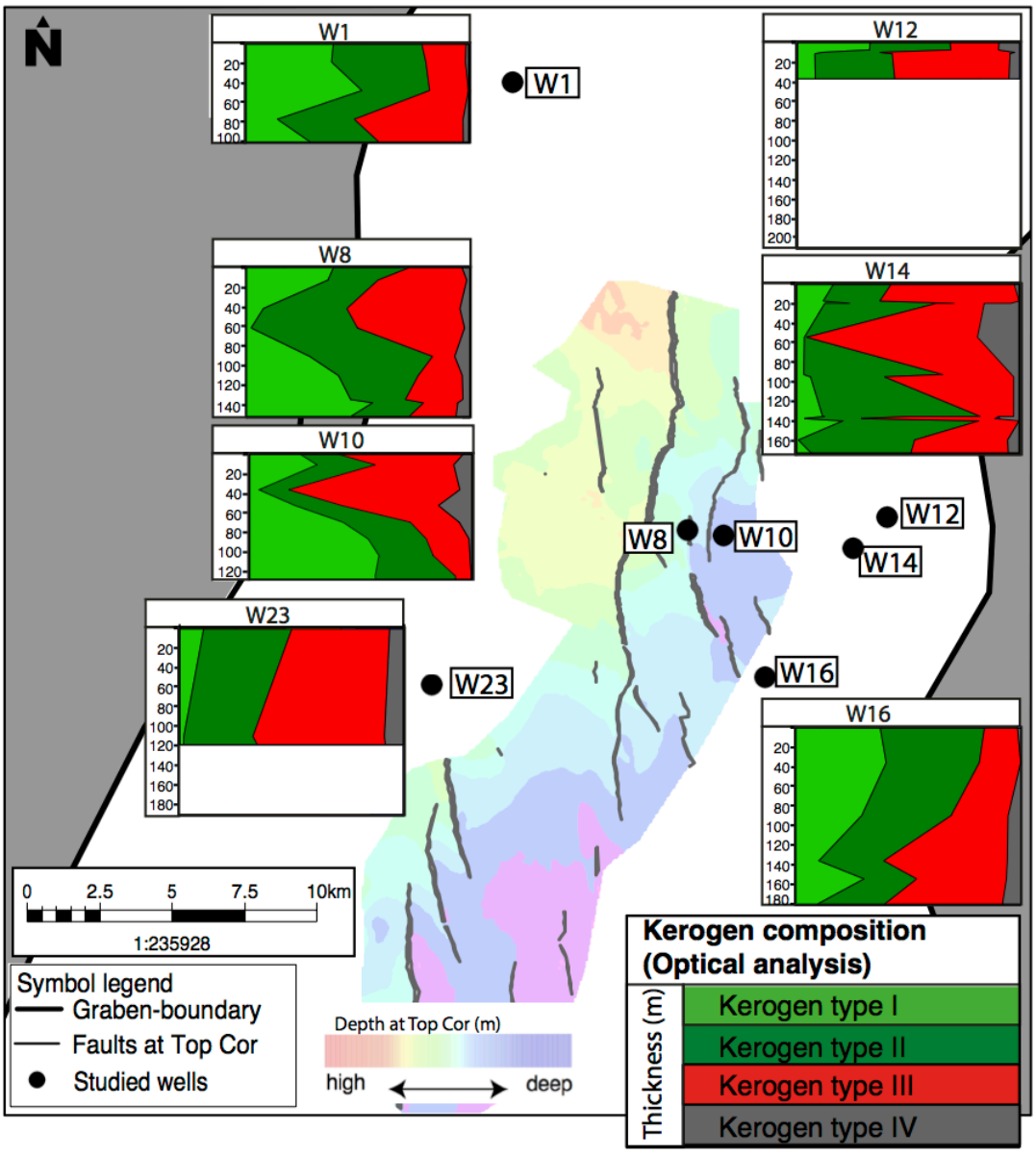

Figure 22: Optical kerogen analysis of the Corbicula Group in the northern URG, showing the relative amounts of the four kerogen types I-IV for all samples within the studied wells. For each well, the thickness of the Corbicula Group is given.

For Rock-Eval pyrolysis, 13 rock samples from the Corbicula Group from 7 wells were investigated (Fig. 23). HI values range between 125–414 mg HC/g TOC, one sample from well W14 reaches a HI value of only 8 mg HC/g TOC. OI values vary between 26–79 mg CO_2/g TOC, the above-mentioned W14 sample has an OI value of 153 mg CO_2/g TOC. When plotting the data in the `Pseudo Van Krevelen` diagram, the kerogen compositions show some spread. Mixed type

II/III kerogens characterize the northernmost well W1 and the wells W10, W16 and W8. Well W23 plots in the mixed type II/III to lower type III (/IV) field. Wells at the eastern margin of the URG (W12, W14) contain mixed type III/IV to pure type IV kerogen. TOC in the selected samples varies between 0.8–2.4 wt.%. When plotting TOC against S2 (0.1–1.5), a comparable attribution of the kerogen types as mentioned above result. Merely for samples from wells W12, W14 and W23, a purely type III kerogen composition is suggested, whereas the HI/OI diagram indicates a mixed type III/IV kerogen.

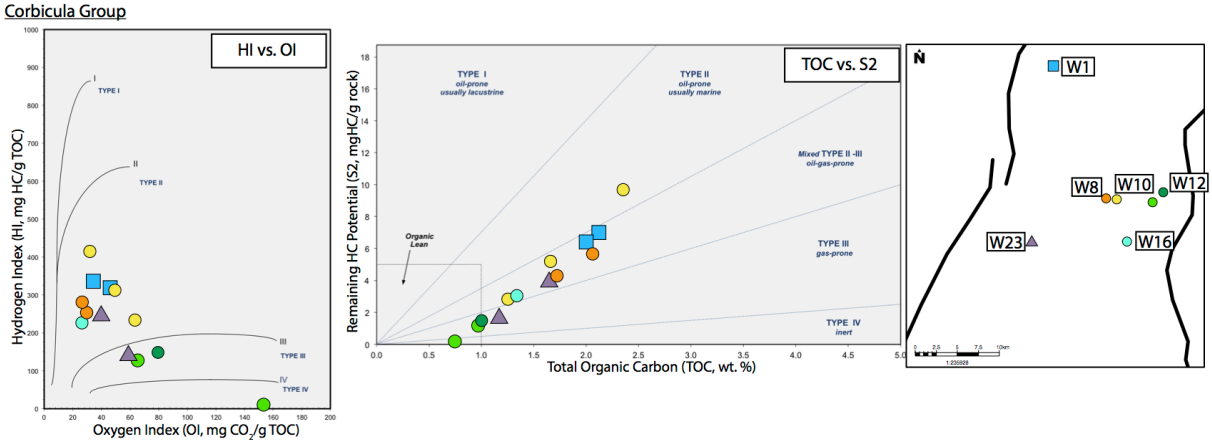

Figure 23: Rock-Eval analysis of the Corbicula Group

7.1.5. Hydrobia Group

Palynofacies analysis of the Hydrobia Group reveals increasing brackish-marine OM and thus decreasing terrestrial OM towards the top Lower Hydrobia Formation (Fig. 24). The amount of phytoclasts thereby ranges between 7.8–63.9 %, whereby the highest amounts occur within the lower section of this unit. Sporomorphs are present in small to moderate amounts (7.3–44.2 %), terrestrial AOM is absent or present in small amounts up to 23.3. Lacustrine algae occur only frequently in negligible amounts (<4.0 %). The amounts of marine AOM increases in most wells towards the top Lower Hydrobia Formation (13.0(1.1 in well W14)–67.7 %). Phytoplancton is present in small amounts up to 25.3 %, only two samples reach higher amounts of 40.2–59.3 %.

Within the Upper Hydrobia Formation, constantly low amounts of phytoclasts are found, generally not exceeding 43.0 % (Fig. 25). Few outliers from e.g. from wells W1, W2 and W14 reach values of up to 93.6. The amount of sporomorphs is fairly constant (<32.7), again with few exceptions e.g. from wells W12 and W14, reaching values of up to 62.9 %. Terrestrial AOM is often absent and reaches maximum amounts of 12.2 %. Lacustrine algae are rare, with the exception of three samples from wells W1, W10 and W8 (9.8–29.6%). The marine fraction contains high amounts of brackish-marine AOM up to 84.7 % and small amounts of phytoplancton generally below 17.9 % and rarely reaching 32.6 %. Dinoflagellates dominate over acritarcs, prasinophytes and leiospheres.

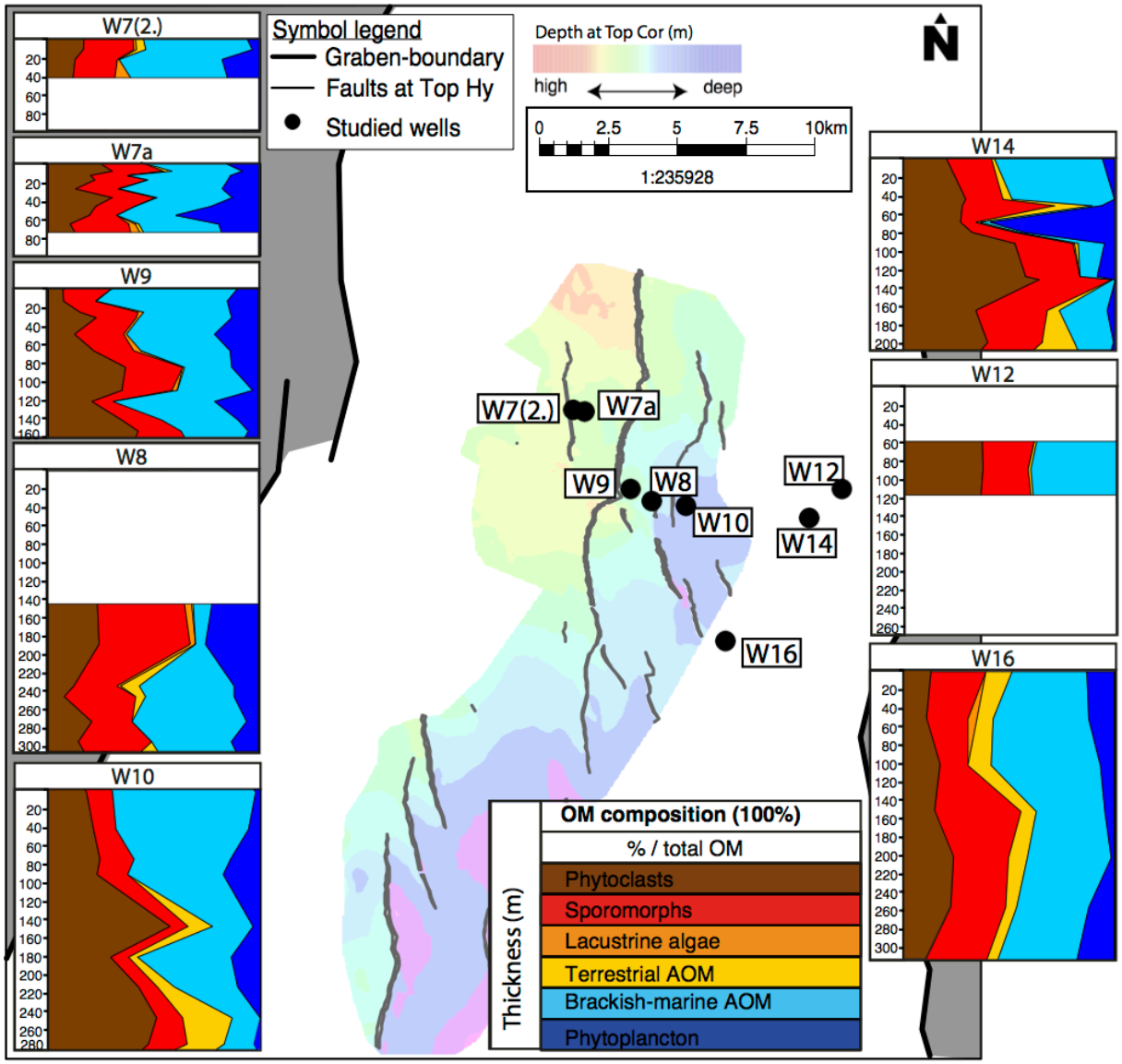

Figure 24: Palynofacies analysis of the Lower Hydrobia Formation in the northern URG, showing the relative amounts of the main palynofacies groups for all samples within the studied wells. For each well, the thickness of the Lower Hydrobia Formation is given.

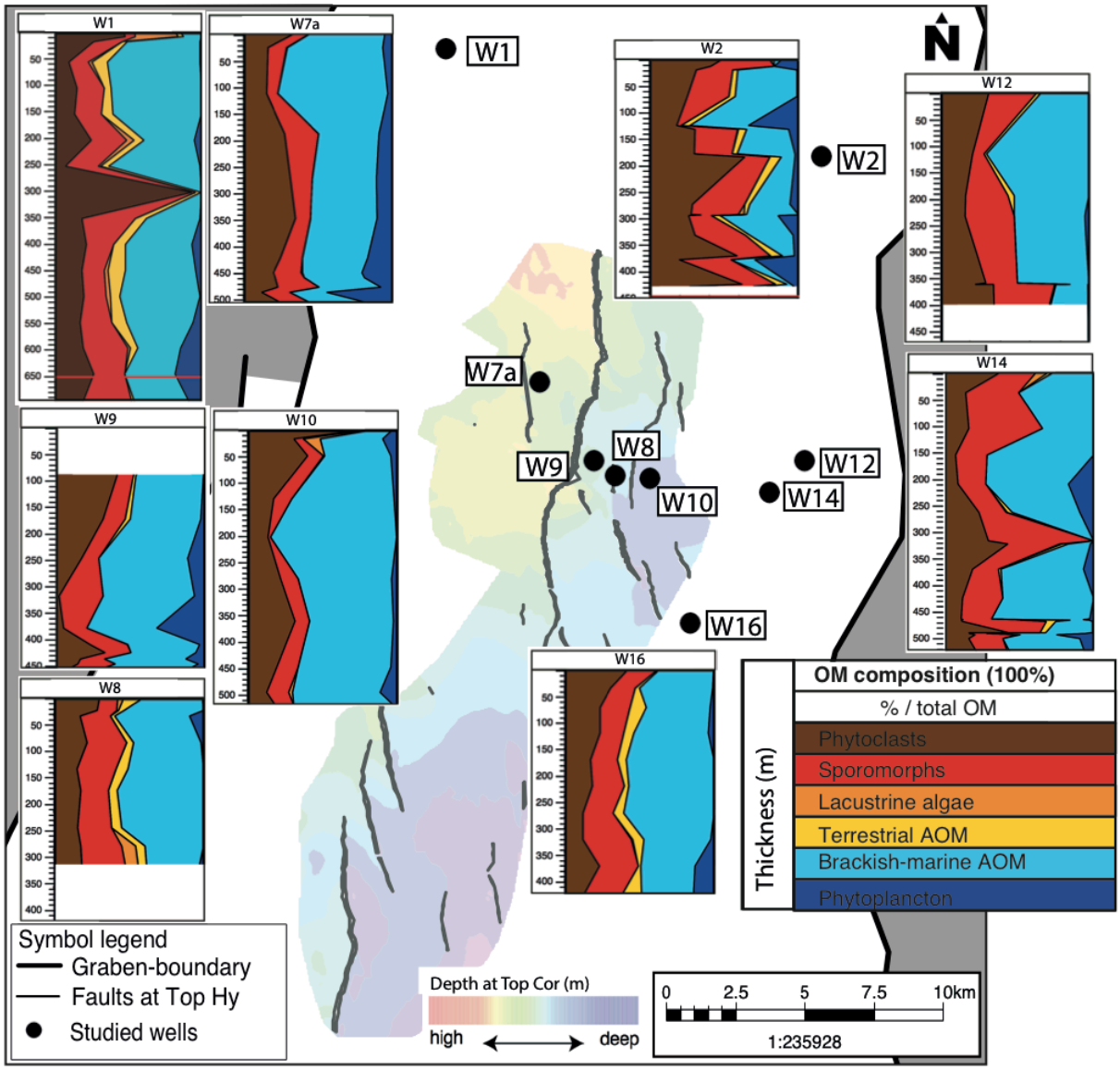

Figure 25: Palynofacies analysis of the Upper Hydrobia Formation in the northern URG, showing the relative amounts of the main palynofacies groups for all samples within the studied wells. For each well, the thickness of the Upper Hydrobia Formation is given.

Optical kerogen analysis of the Lower Hydrobia Formation results in strong dominance of oil-prone type I kerogen (<68.8 %) and type II kerogen (<68.6 %) (Fig. 26). Gas-prone type III kerogen is present in small amounts usually not exceeding 25–30 %. Only few samples from wells W10 and E14 reach higher amounts of up to 60.5 %. Type IV kerogen is present in minor amounts of up to 12.1 % with few outliers. Throughout the study area, generally increasing amounts of type I and II kerogen can be observed within the Lower Hydrobia Formation.

The kerogen composition of the Upper Hydrobia Formation is clearly dominated by oil-prone type I and type II kerogen (Fig. 27). Type I kerogen reaches maximum amounts of 85.1 %. Type II kerogen is present in amounts of up to 61.2 %. Type III kerogen occurs in rather low amounts usually <37.0 % with few outliers. Type IV kerogen is present in subordinate amounts <12.5 (<20.2 % in well W2).

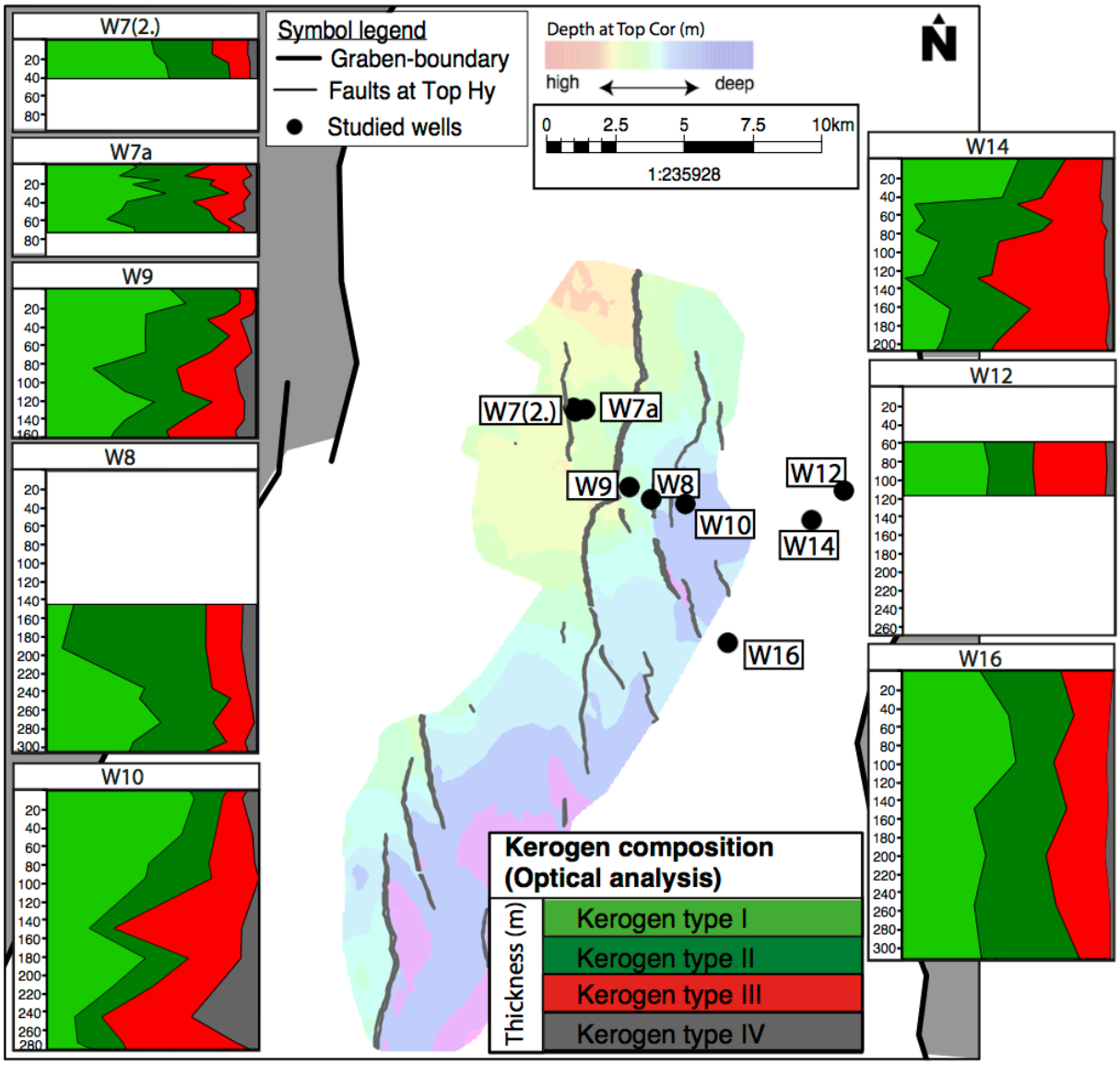

Figure 26: Optical kerogen analysis of the Lower Hydrobia Formation in the northern URG, showing the relative amounts of the four kerogen types I-IV for all samples within the studied wells. For each well, the thickness of the Lower Hydrobia Formation is given.

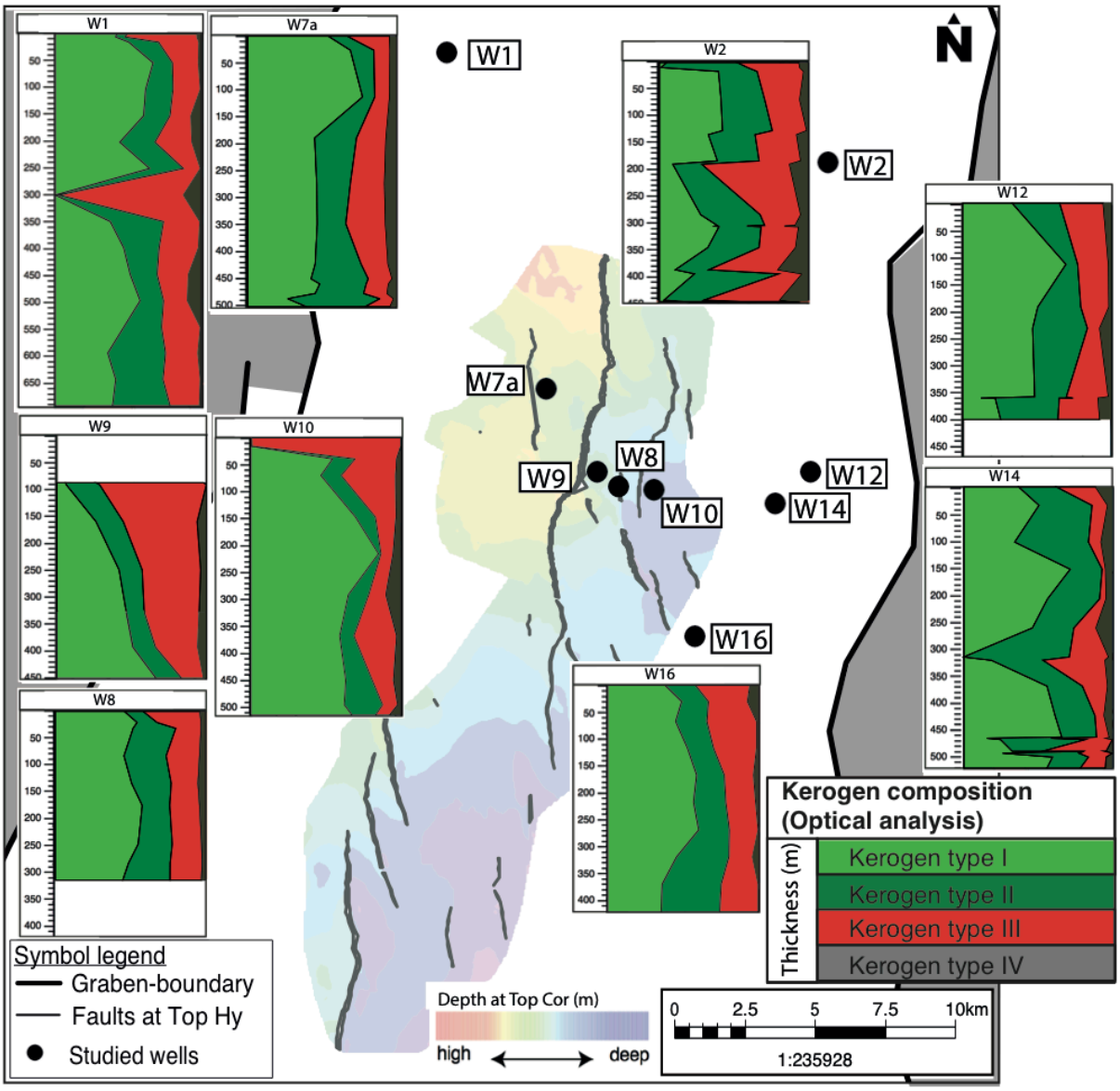

Figure 27: Optical kerogen analysis of the Upper Hydrobia Formation in the northern URG, showing the relative amounts of the four kerogen types I-IV for all samples within the studied wells. For each well, the thickness of the Upper Hydrobia Formation is given.

A total of 60 samples from the Hydrobia Group were chosen for Rock-Eval pyrolysis (29 from the Lower- and 31 from the Upper Hydrobia Formation) (Figs. 28, 29). For the Lower Hydrobia Formation HI ranges from 86–487 mg HC/g TOC and OI from 20–64 mg CO_2/g TOC; one sample from well W7 reaches exceptionally high OI values of 177 mg CO_2/g TOC. In the HI/OI diagram the data points lie mostly along the type (I/)II kerogen pathway. The highest HI values were measured for the wells W1, W7, W10 and W9. Wells located near the eastern graben margin (W2, W14, W16) tend to have higher amounts of type III and type IV kerogen. Overall TOC values are in the range of 0.8–3.3 wt.% in the Lower Hydrobia Formation. Kerogen composition retrieved from the TOC/S2 graph with S2 in the range of 0.7–15.0 stand in accordance with the results from the HI/OI plot. Samples from the wells W1, W9 and W10 contain almost pure type II kerogen. Samples from wells W2, W14 and W16 possess almost exclusively type III kerogen. Few samples from wells W8 and W12 lie in the mixed type II-III kerogen field.

The Upper Hydrobia Formation (Fig. 29) reaches HI values of 227–592 mg HC/g TOC and OI values of 17–134 mg CO_2/g TOC. As previously noted for the Lower Hydrobia Formation, samples from well W7 show again unusually high OI values (83–134 mg CO_2/g TOC). In the HI/OI diagram ('Pseudo van Krevelen') most samples from wells W12 and W9 plot along the mixed type II-III kerogen field with slightly higher amounts of type II. Samples of wells W1, W8, W17, W2, W14 and W16 plot along the upper type II kerogen pathway, one sample from W15 even along type I. Samples from well W7 show variable kerogen, ranging from strongly type III dominated to almost merely type II dominated. TOC ranges from 1.5–4.6 wt.% within the Upper Hydrobia Formation. S2 values of 4.4–25.7 are reached. In the TOC/S2 graph samples indicate type II to mixed type II/III kerogen.

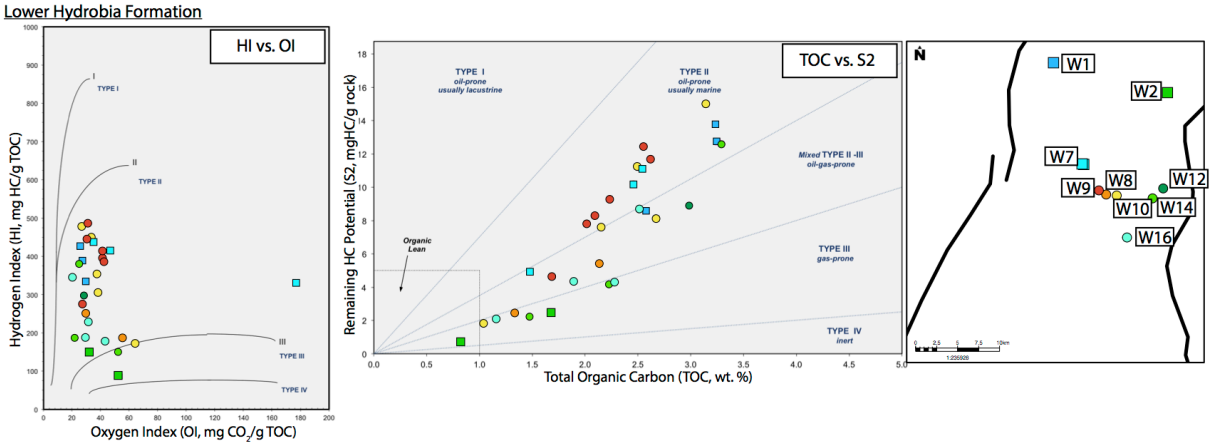

Figure 28: Rock-Eval analysis of the Lower Hydrobia Formation

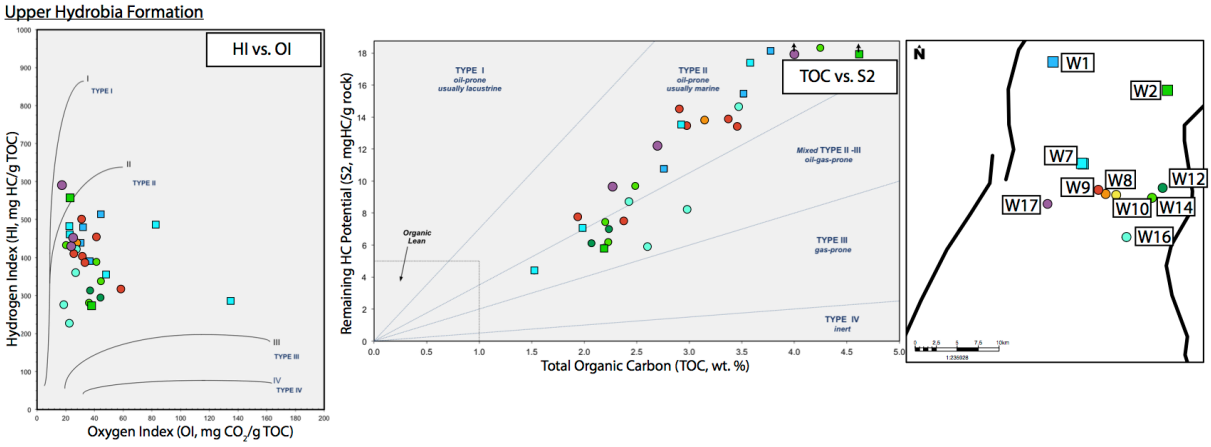

Figure 29: Rock-Eval analysis of the Upper Hydrobia Formation

7.2. Interpretation of Palaeoenvironment & Hydrocarbon Generation Potential

The extensive set of optical and geochemical data allow to analyze the changes and variations in palaeoenvironmental conditions and kerogen composition spatially as well as through time. The development of palaeoenvironment during the Cenozoic rifting period has a large impact on the type and preservation of OM and thus on the kerogen quality. In this chapter, the results are interpreted by formation on a regional scale.

Palaeoenvironmental interpretations are based on the proportions of OM components, plotted in ternary diagrams modified after Tyson (1989):

For the interpretation of the depositional system, the relative amounts of continental and brackish-marine components, namely phytoclasts, AOM (amorphous organic material, fluorescent and non-fluorescent) and palynomorphs (sporomorphs and phytoplancton) are displayed. Thereby high amounts of phytoclasts suggest proximal-oxic condition, whereas distal conditions are indicated by high amounts of AOM (distal-anoxic) and high amounts of palynomorphs (distal-oxic). The original version of this diagram after Tyson (1989) is divided into ten fields, which describe oxygen level and proximity of the depositional system. Yet, this diagram describes a typical offshore system, where closer examination of the proximity of the depositional system can be carried out. In the URG, which is a narrow rift system, relatively proximal settings are found throughout the study area, also due to multiple sediment entry points of terrestrial OM. Thus, a more rough classification of palaeoenvironmental conditions is chosen.

The interpretation of the aquatic setting does solely include brackish-marine components and is based on the relative amounts of fluorescent AOM, marine algae and dinoflagellates within the system. Thereby fluorescent AOM is an indicator for restricted marine-anoxic conditions, whereas dinoflagellate cysts indicate distal-oxic settings and acritarcs, leiospheres and prasinophytes (here summarized as “marine algae”) suggest deposition in distal-anoxic environments.

7.2.1. Pechelbronn Group

Based on a modified ternary diagram after Tyson (1989), the Lower Pechelbronn Formation was deposited in a proximal and oxic setting throughout the study area (Fig. 30). Only one sample from well W10 suggests distal-anoxic conditions. High amounts of terrestrial OM were transported via fluvial transport from the graben shoulders into the graben. Marine influence is identified in the uppermost Lower Pechelbronn Formation and marks the first marine transgression leading to the deposition of the overlying Middle Pechelbronn Formation (Fig. 10). The aquatic setting indicates restricted marine-anoxic conditions. Only two samples from a footwall well (W9) and a hanging wall well (W31) display distal-oxic settings. These oxic aquatic settings in well W9 contrast with results from the nearby hanging wall well W10 (~1.5 km apart), in which anoxic conditions are displayed (CS 1 in Fig. 33). The wells W9 and W 10 are drilled into tilted block structures, as they formed during early syn-rift development. Higher subsidence resulted in higher accommodation rates and thus higher sediment thickness on the hanging wall side (well W10). Here, the Lower Pechelbronn Formation reaches 190 m, in

contrast to only 55 m in well W9 on the footwall structure. The Stockstadt fault, which separates the two structural blocks, represents a highly active fault, which formed during Rotliegend times and was reactivated during graben development, is active to modern times (CS1 in Fig. 33). Coherent growth faults such as this fault are due to the extensional rift tectonics, causing thickness variations and distinct small-scale differences in palaeoenvironmental conditions. As this fault was active already during early sny-rift (Pechelbronn) times, the palaeoenvironmental differences in the two nearby wells W9 and W10 seem to be related to uneven distribution of terrestrial derived OM within the graben and also to variable oxygen conditions on the two blocks. The example of wells W9 and W10 nicely illustrates, how the magnitude of subsidence (leading to thickness variations) and the facies of sedimentary fill (palaeoenvironmental conditions) vary between graben internal blocks (Grimmer et al. 2016).

Oxic aquatic conditions are also represented by one sample from well W31 in the southernmost part of the study area. This well was drilled into a hanging wall structure nearby the Hofheim fault, which similar to the Stockstadt fault was active prior to rifting and was reactivated during graben formation (CS 2 in Fig. 33). Oxic conditions, which are interpreted from the dominance of dinoflagellates within the brackish-marine fraction, are possibly associated with fault related differences in oxygen levels.

The Middle Pechelbronn Formation was deposited during the first Rupelian transgression (Hardenbol et al. 1998), prograding from the north. Deposition in the study area took place under mostly proximal-oxic conditions, while overall terrestrial influx from the graben shoulders was extremely high (Fig. 31). Distal aquatic conditions characterize most parts of the study area. Oxygen ratios range from oxic in wells W10 and W15 to anoxic conditions in wells W16 and W31 within shot distances. Towards and along the interbasin northern transfer zone (Derer 2003), samples indicate restricted-marine environments. Affected samples belong to the wells W9, W21 and W16. These restricted marine environments are interpreted from high amounts of fluorescent AOM.

Similar to the Lower Pechelbronn Formation, distinct small-scale thickness variations are observed for the Middle Pechelbronn Formation throughout the study area. This indicates ongoing synsedimentary tectonic activity along large faults zones, leading to inhomogeneous palaeoenvironmental settings. Wells W9 and W10, which are located on a footwall and a hanging wall structure along the Stockstadt fault, again display strong differences within the aquatic setting. The restricted marine conditions from well W9 stand in contrast to the distal-oxic conditions in well W10. The latter are defined by high amounts of dinoflagellate cysts and are most probably fault-related.

Palynofacies analysis of the Upper Pechelbronn Formation suggests deposition took place in a proximal-oxic setting. Figure 32 illustrates the extremely high input of terrestrial OM within the entire study area. The aquatic system is characterized by rapidly changing and laterally highly variable palaeoenvironmental conditions, ranging from restricted marine to distal-oxic and -anoxic.

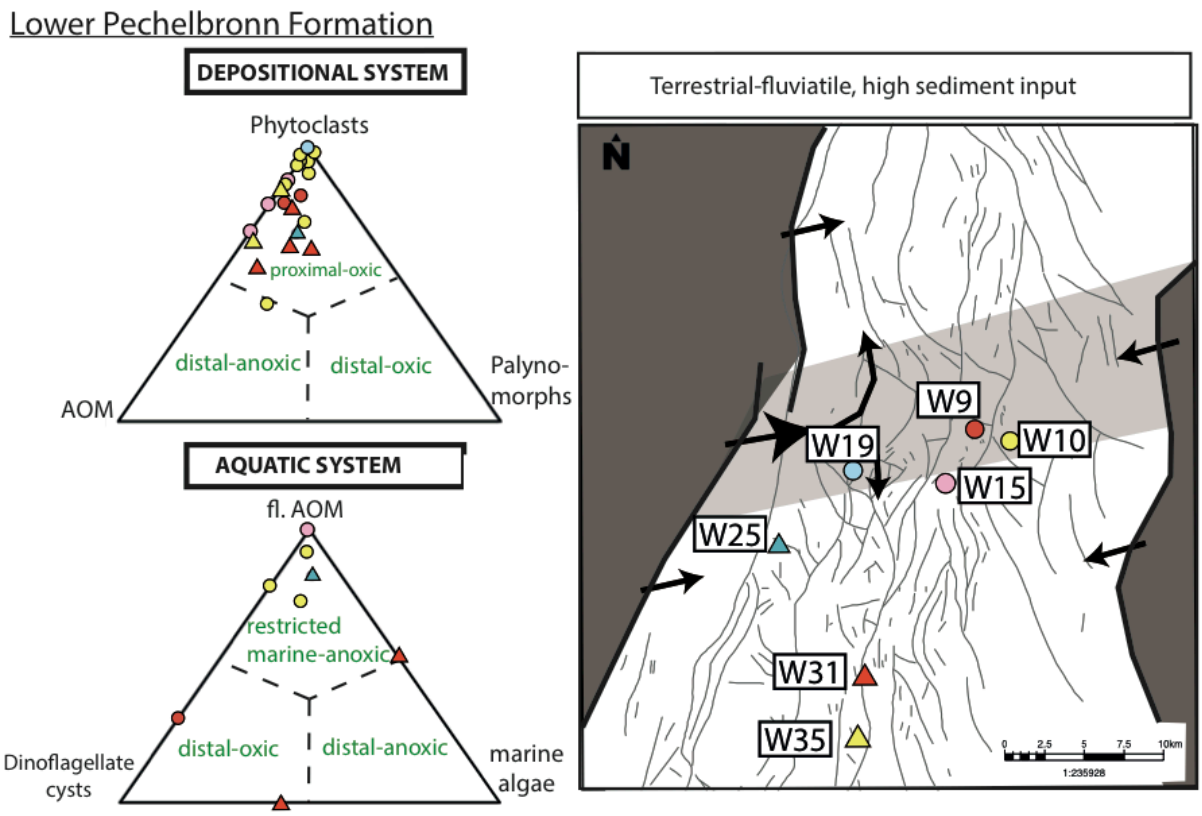

Figure 30: Palynofacies interpretations illustrated as ternary diagrams (modified after Tyson 1989) of the Lower Pechelbronn Formation

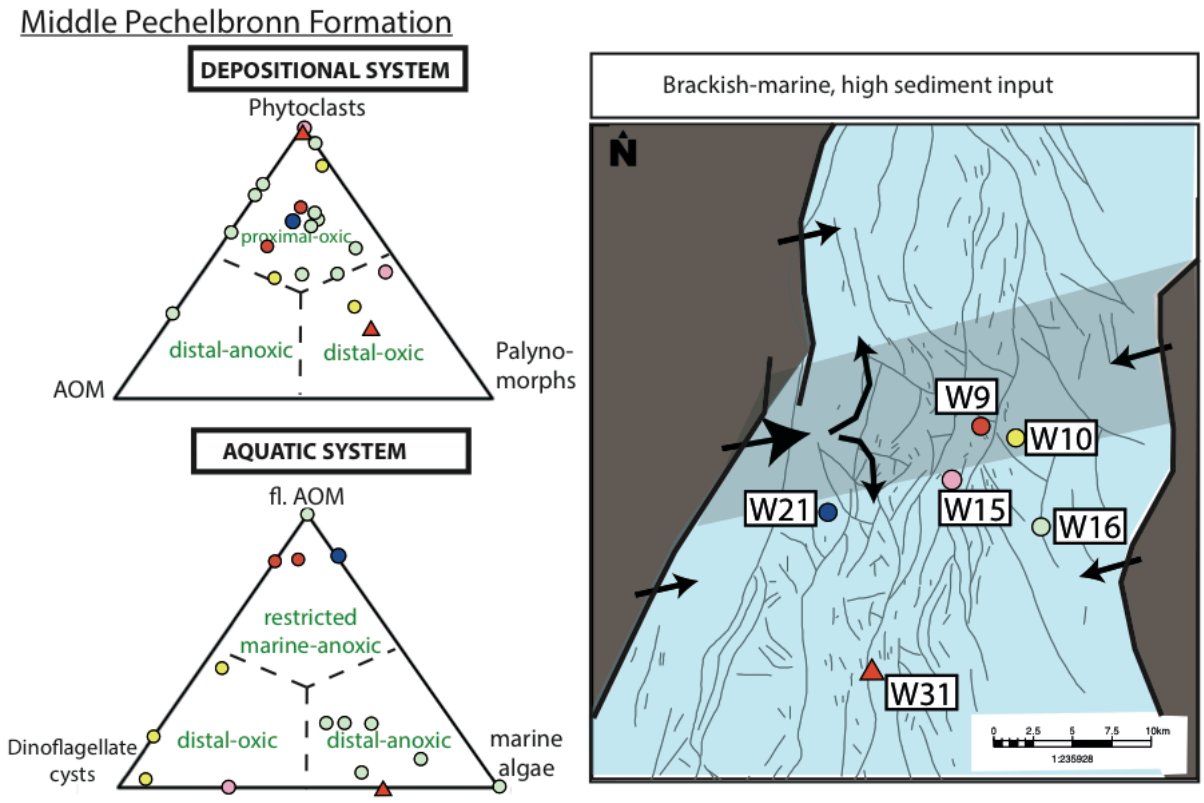

Figure 31: Palynofacies interpretations illustrated as ternary diagrams (modified after Tyson 1989) of the Middle Pechelbronn Formation

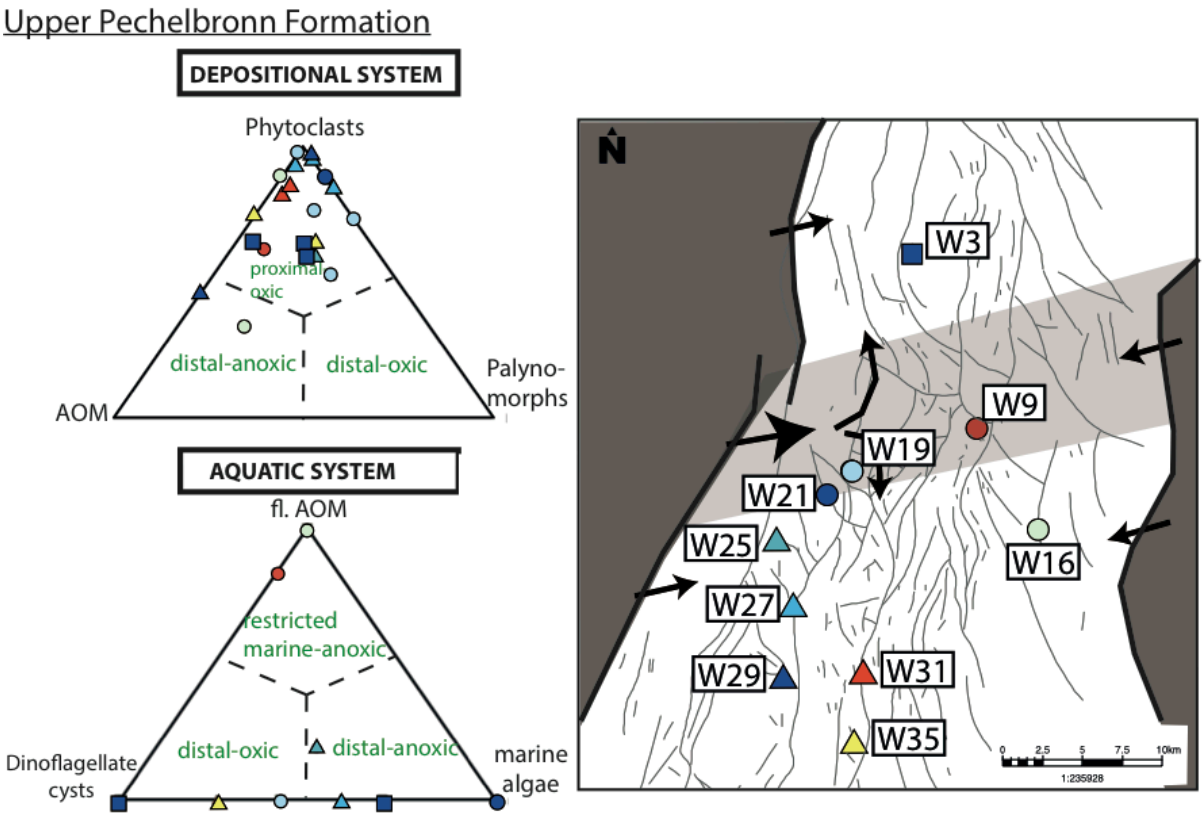

Figure 32: Palynofacies interpretations illustrated as ternary diagrams (modified after Tyson 1989) of the Lower- Middle- and Upper Pechelbronn Formation

Small-scale depositional changes in the Pechelbronn Group are also highlighted by the heterogeneous kerogen compositions (Fig. 11). In most samples all four kerogen types occur, which correlates to the above-mentioned manifold palynofacies composition. Based on optical kerogen analysis the Middle Pechelbronn Formation contains lower amounts of oil-prone type I/II kerogen and higher amounts of type III kerogen than the Lower and Upper Pechelbronn Formation. These results are unusual for a transgressive-marine interval, in which this relationship should be inverse (Tyson 1995).

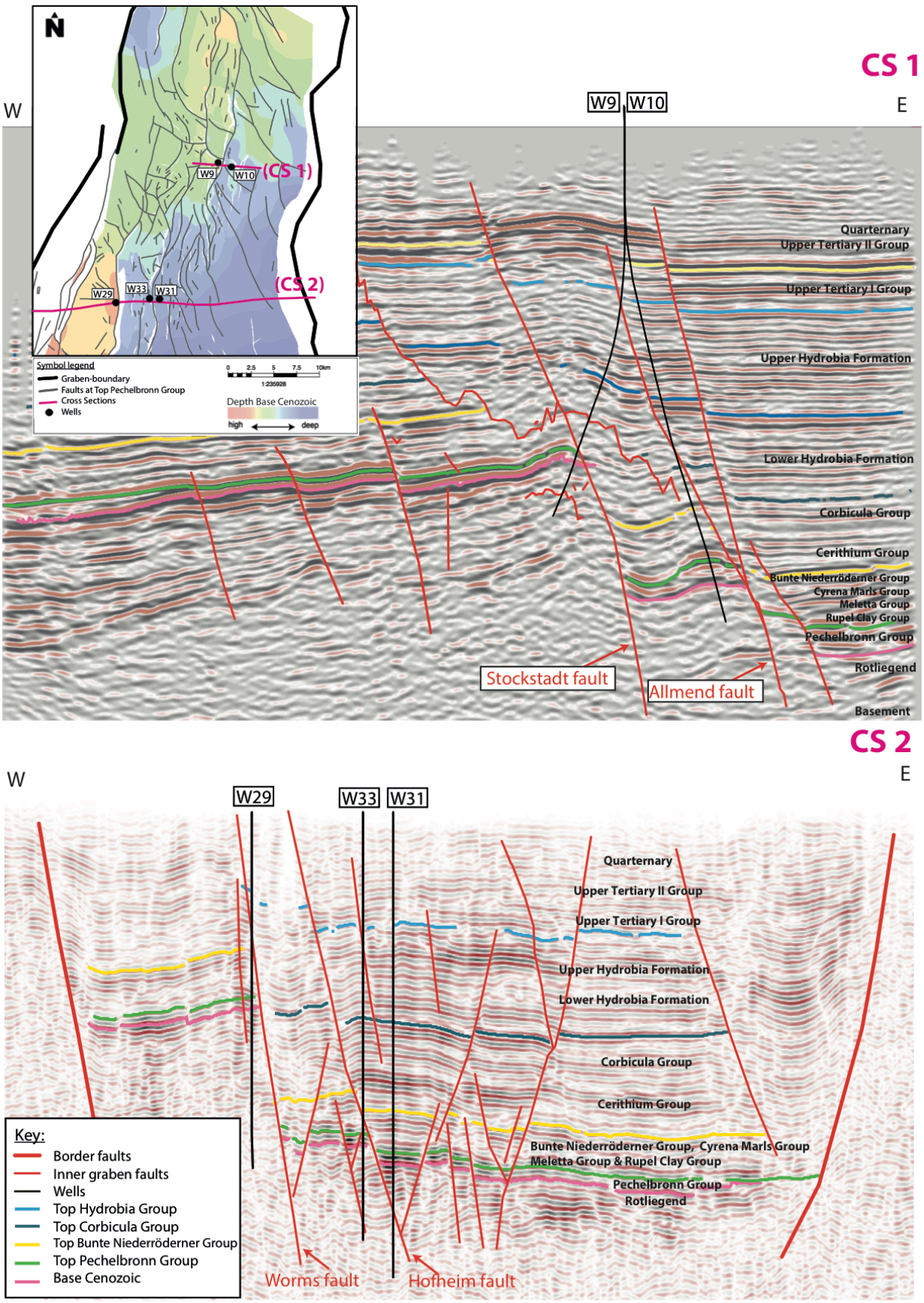

Figure 33: Cross sections through the study area and location of selected investigated wells: ***CS1*** from 3D seismic (Rhein Petroleum), crossing wells W9 and W10. ***CS 2*** is the DEKORP 9N Seismic line, crossing wells W29, W33 and W31. Seismic lines at different scales. Note the higher thickness in the east due to tilted half-graben development tilting to the East (e.g. Grimmer et al. 2016)

Geochemical Rock-Eval data from the Pechelbronn samples also indicate a strong dominance of type III and IV kerogen, especially in especially the Middle Pechelbronn Formation (Fig. 12). Only the samples from wells W9, W7 and W1 suggest a mixture of type II and III kerogen based on both Rock-Eval plots ('Pseudo Van Krevelen' diagram and TOC/S2 graph). Inconsistencies in kerogen attribution based on these two diagram types constructed from the Rock-Eval data are found i.e. in well W19. Based on HI/OI the kerogen is attributed to a type II or mixed type II/III kerogen composition. However based on TOC/S2 the kerogen is solely type III. Also in well W10 one sample is clearly attributed to the type IV kerogen based on HI/OI, which cannot be verified based on TOC/S2. These inconsistencies need to be critically evaluated when interpreting Rock-Eval data. Thus in order to obtain reliable results and for crosscheck purposes, additional optical kerogen analysis was applied. Differences and slight variations between the geochemical (Rock-Eval) and optical (Palynofacies) kerogen analysis are most probably related to the different methods analysing the complex kerogen types. In optical analysis the mixture of all four kerogen types is quantified precisely for each sample, whereas Rock-Eval measures the average composition of the kerogen mixtures.

The integrated kerogen analysis of the Pechelbronn Group indicates an overall organic poor interval in the northern URG, which is dominated by type III/IV kerogen with smaller contents of type I/II. High tectonic activity during the first major extensional phase of graben formation resulted in these exceptionally high amounts of terrestrial originated, gas-prone OM (type III/IV) kerogen, which diluted the aquatic/brackish-marine (and in parts terrestrial), oil-prone type I/II kerogen fraction.

From the integrated kerogen analysis a moderate to good gas generation potential and a low oil generation potential can be concluded. Despite TOC values of <2.5 wt.%, the irregular occurrence and reduced thickness of sampled potential source rocks (organic rich claystones) minimize the source rock potential of the Lower and Upper Pechelbronn Formation. These formations are strongly dominated by coarse-grained siliciclastic intervals. Yet the Middle Pechelbronn Formation, which is dominated by fine clastic, potential source rocks, contains much lower TOC <1.0 wt.%, which strongly minimizes the source rock potential.

7.2.2. Rupel Clay Group

In the late Rupelian (early Oligocene), a second transgression took place reaching maximum marine distribution (Hardenbol et al. 1998). This transgression is widespread in the entire URG and beyond and corresponds to the marine Rupel Clay Group. Despite the relatively consistent thickness of 52–57 m throughout the study area and homogeneous, argillaceous to marl lithologies, palynofacies analysis provides evidence of palaeoenvironmental variations (Figs. 34, 35).

Based on a modified ternary diagram after Tyson (1989), a proximal-oxic setting is present during the deposition of the Foraminifera Marls Formation and Fish Shale Formation in wells W9 and W7a/W7(2.) (and to a limited extend also in W3 and W14 for the Foraminifera Marls Formation). This emphasizes the proximity to the western graben shoulder and possibly also the close vicinity to the interbasin transfer zone. This "palaeohigh", which acted as a structural high

during Pechelbronn times, may have remained an erosive area and acted as an additional sediment source during Rupel Clay Group times (Derer 2003). Here, highest sediment input rates were located based on the ternary diagrams (Figs. 34, 35). Distal conditions with variable oxygen availability established towards the north, east and south of the study area.

The aquatic system within the Foraminifera Marls Formation is heterogeneous in terms of palaeoenvironment conditions (Fig. 35). Restricted marine conditions are present in wells W1, W9 and W10. A more distal setting, as would be expected for transgressional sediments, is mostly restricted areas located north of wells W7a/W7(2.) and from the easternmost well W14. The more distal facies towards the north of the study area is in line with the basinal setting induced by the Rupel transgression, which advanced from the north. During the deposition of the Fish Shale Formation, restricted marine conditions within the aquatic system remained unchanged in wells W1, W9 and W10. Distal conditions with variable oxygen levels established in the remaining study area.
Synsedimentary extensional tectonic activity seems to have been low during times of Rupel Clay Group deposition, as can be inferred from the relatively constant thickness distribution, but input from the graben shoulders of terrestrial OM remained unexpectedly high. This clearly proves that the uplifted graben shoulders were still an important topographical feature, providing the ongoing input of OM into the graben system. This input must have been evenly transported and distributed within the water body by currents. Variations in the composition of OM are most probably related to various sediment transport routes, which are linked to the location of fault zones, and to current directions.

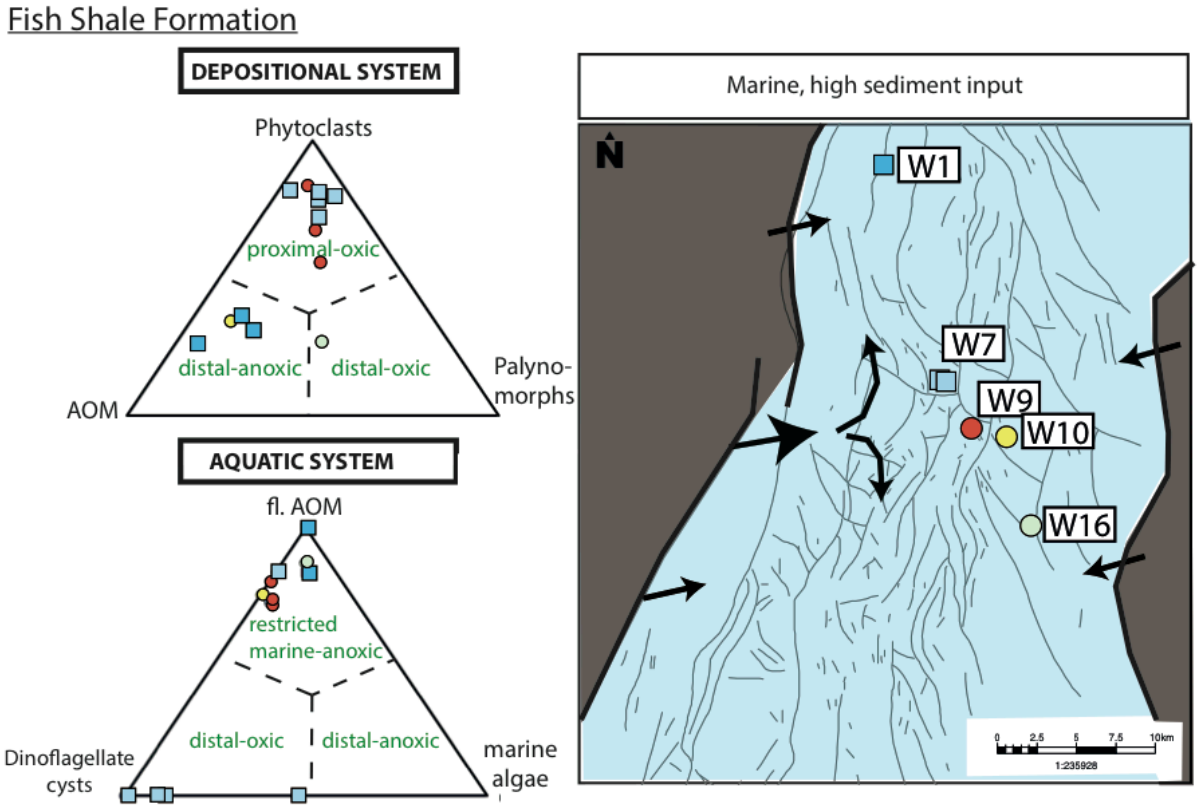

Figure 34: Palynofacies interpretations illustrated as ternary diagrams (modified after Tyson 1989) of the Fish Shale Formation (Rupel Clay).

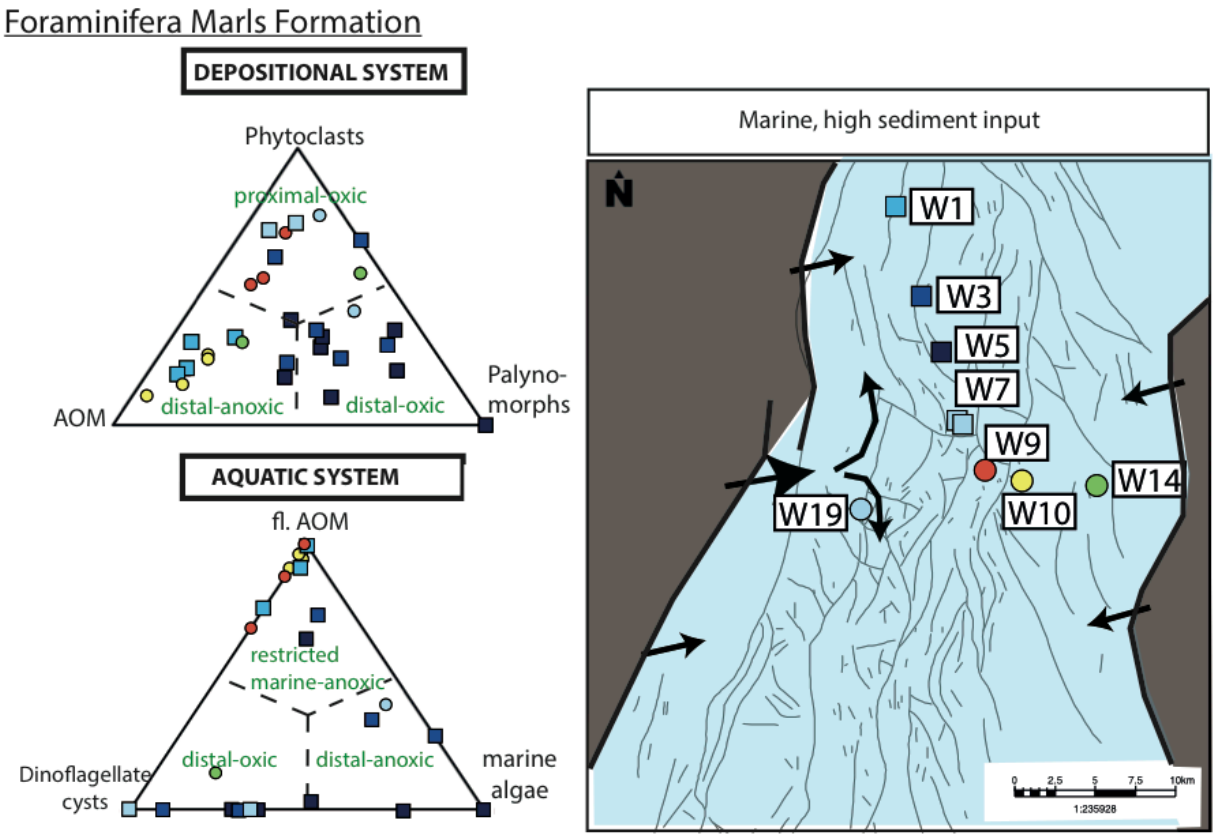

Figure 35: Palynofacies interpretations illustrated as ternary diagrams (modified after Tyson 1989) of the Foraminifera Marls Formation (Rupel Clay Group).

Similar to the Middle Pechelbronn Formation, which were affected by the first transgression, high amounts of type III/type IV kerogen are identified by optical analysis in the Foraminifera Marls- and the Fish Shale Formation (Fig. 14). Both intervals indicate a moderate oil- and a better gas generation potential. These exceptionally high amounts of terrestrially originated, gas-prone OM (type III/IV kerogen) are related to input from the subaerial graben as mentioned above (see palynofacies). Because of the homogenous sediment thickness and lithological properties of the Rupel Clay Group these differences in kerogen types are rather unexpected. They illustrate the importance of optical kerogen methodologies for a differentiation of presumably homogeneous sediments.

Geochemical analysis indicates similar kerogen composition as shown by the optical kerogen analysis, and high variations in terms of a source rock potential. In the Foraminifera Marls Formation, the lowest TOC values (0.45–0.87 wt.%) were found in samples from the W5 and W3 wells (Fig. 16). These plot along the type IV kerogen pathway in the HI/OI diagram, corroborating a very low hydrocarbon generation potential to the north of the study area. Only the northernmost well W1 indicates high amounts of oil-prone type I/II kerogen with good TOC <3.55 %. All other wells show favorable TOC values in the range of 0.66–3.32 wt.% and higher amounts of type II kerogen, indicating a better potential for HC generation. Results from Rock-Eval pyrolysis of the Fish Shale Formation indicate kerogen compositions and OM contents, which partially resemble those of the Foraminifera Marls Formation (Fig. 15). In wells W1 and W7, type II/III kerogen type is comparable to that of the Foraminifera Marls Formation. One Fish

Shale Formation sample of well W16 indicates predominantly type III kerogen based on HI/OI. The Fish Shale Formation samples in well W9 contain type III/IV kerogen mixtures. An additional sample from well W9 is not displayed in Fig. 15 due to extremely high S2 and low TOC values. Pyrograms of this sample verify the unclear Rock-Eval measurement.

Taking into account both optical and geochemical kerogen analysis, a moderate oil- (type I/II kerogen) and slightly better gas (type III kerogen) generation potential can be assumed for the Rupel Clay Group in the northern URG. Somewhat more detailed and precise information on quantities of individual kerogen types is obtainable from the optical analysis compared to geochemical Rock-Eval pyrolysis.

7.2.3. Meletta Group, Cyrena Marls Group, Bunte Niederröderner Group and Cerithium Group

Palynofacies analysis of the Meletta Group and Cyrena Marls Group suggests that deposition of these lithostratigraphic units took place in a mostly proximal-oxic setting with high input of terrestrial OM (Fig. 36). Only wells located in the graben center partly indicate more distal (to anoxic) settings. The aquatic system was characterized by heterogeneous conditions throughout the study area. Wells located in the graben center but also near the eastern graben border indicate rather anoxic conditions in a restricted marine setting. Wells located towards the western graben border are also anoxic but in a more distal setting. Frequently oxic conditions were established in wells W21, W14 and W16. Different to previously deposited Cenozoic basin sediments, the terrestrial OM input from the graben shoulders was low during the deposition of the Meletta Group and Cyrena Marls Group. This resulted most likely from low rift-tectonic dynamics and low currents within the basin.

The Bunte Niederröderner Group was deposited in a quite distal setting under anoxic-oxic conditions (Fig. 37). Input of terrestrial OM into the graben system was limited. The aquatic system represents a restricted marine-anoxic setting. Low amounts of dinoflagellate cysts suggest a more marine rather than lacustrine setting.

The Cerithium Group was deposited in a distal setting comparable to the Bunte Niederröderner Group with variable oxygen ratios and high variations in the amount of terrestrial OM (Fig. 38). The aquatic system was characterized by similarly restricted marine-anoxic conditions as shown by most samples.

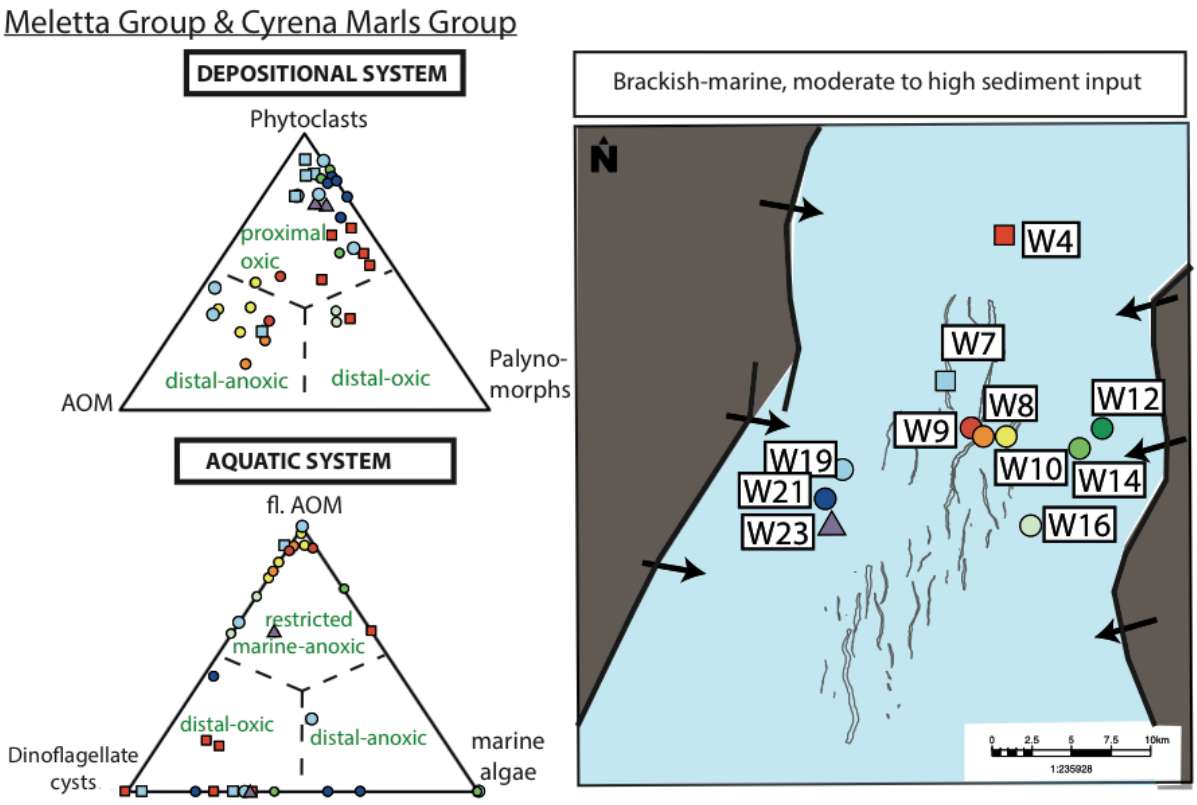

Figure 36: Palynofacies interpretations illustrated as ternary diagrams (modified after Tyson 1989) of the Meletta Group and Cyrena Marls Group

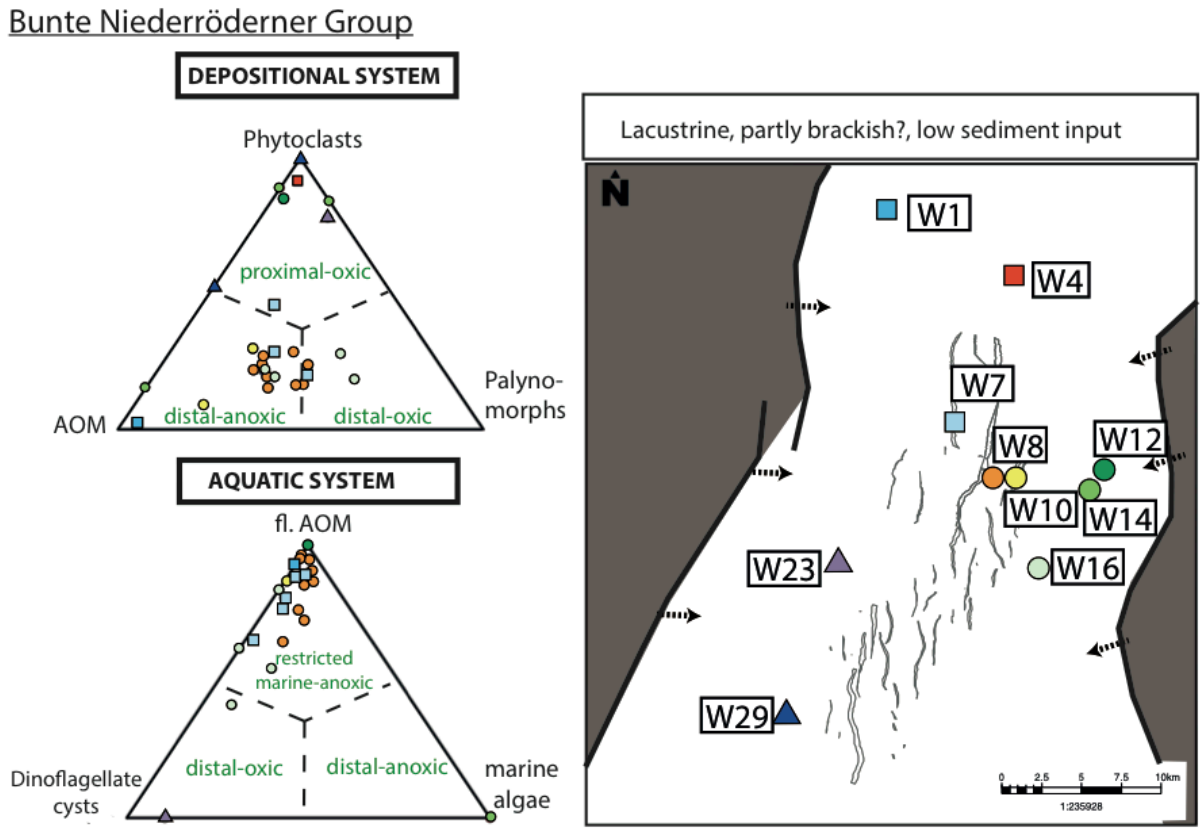

Figure 37: Palynofacies interpretations illustrated as ternary diagrams (modified after Tyson 1989) of the Bunte Niederröderner Group

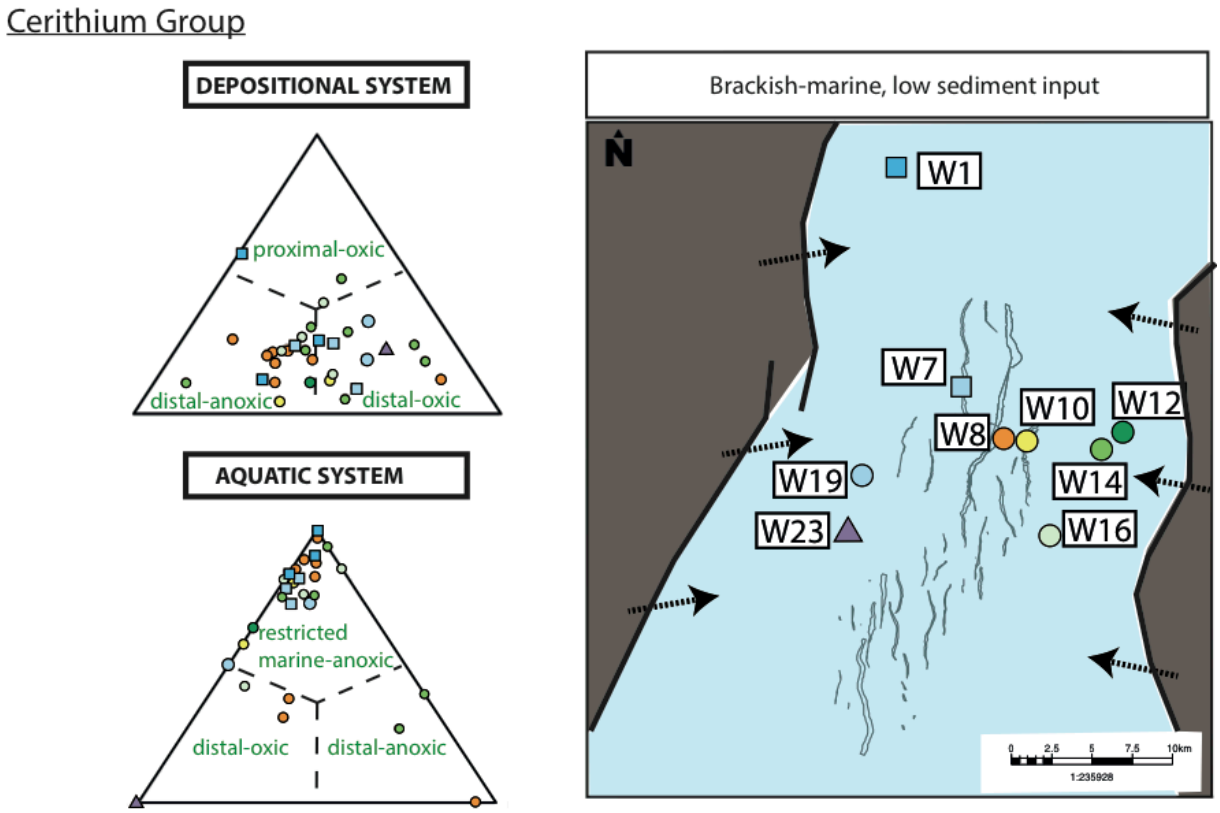

Figure 38: Palynofacies interpretations illustrated as ternary diagrams (modified after Tyson 1989) of the Cerithium Group

Optical kerogen analysis of the Meletta Group and Cyrena Marls Group indicate moderate to high amounts of oil-prone type I/II and low to moderate amounts of gas-prone and barren type III/IV kerogen (Fig. 18). The contents of type I/II kerogen are generally increasing from the base of the Meletta Group towards the top of the Cyrena Marls Group. As a result, an overall good oil and poor gas generation potential is assumed. In some contrast, based on HI/OI as well as TOC/S2 geochemical analysis, a purely type III and type IV kerogen composition is assumed (Fig. 20). Sediments therefore hold a minor gas generation potential, if at all. These results differ from the existing concept of a brackish marine depositional environment with very high sediment input from the graben shoulders (Grimm et al. 2011).

Samples from well W7 differ from the more southern wells W9 and W10 by their high S3 peak (CO_2 yield during thermal breakdown of kerogen), leading to correspondingly high OI values. These elevated S3 peaks may be an indication that calcareous lithologies are prevalent in the Cyrena Marls Group and Meletta Group in well W7 (Tissot & Welte 1984), which is confirmed by the rock samples and well log interpretation.

For the Meletta Group and Cyrena Marls Group, optical kerogen analysis shows more credible results than Rock-Eval analysis. Palynofacies data clearly prove high amounts of oil-prone kerogen, which are in accordance with the brackish-marine setting described e.g. by Grimm et al. (2011). Such indications for a brackish-marine are not observed by geochemical analysis.

This kerogen classification suggests at first sight moderate oil and better gas generation potential. Yet, low TOC values and a high content of silica and carbonate in the Meletta Group and Cyrena Marls Group suggest an overall low HC generation potential.

The Bunte Niederröderner Group shows highly variable and heterogeneous kerogen compositions based on optical kerogen analysis, ranging from purely type III/IV kerogen to dominating type I/II kerogen (Fig. 18). Because sandstones and marly sandstones are the dominant lithologies in this interval, but only the most argillaceous samples were analyzed, no significant hydrocarbon generation potential can be assumed from the Bunte Niederröderner Group. Mostly low TOC values substantiate this allegation. The reservoir potential of this unit seems strongly limited due to the predominance of argillaceous sandstones, suggesting reduced porosity and permeability.

Optical kerogen analysis of the Cerithium Group suggests high amounts of oil-prone type I/II kerogen and low to negligible amounts of gas-prone and barren type III and type IV kerogen (Fig. 18). These results reflect a low tectonic activity with low terrestrial OM input from the graben shoulders in most graben areas, leading to an excellent oil but low gas generation potential throughout the study area. Only in well W1, high subsidence rates were detected during deposition of the Cerithium Group and are interpreted to result from the location of this well within a local pull-apart basin. This site was thus affected by sinistral shear movements along the western graben fault (Fig. 3). Similar kerogen compositions are also found in well W1, containing high amounts of type I and II kerogen in the upper part, and dominance of type III kerogen in the lower part of the Cerithium Group.

Based on Rock-Eval pyrolysis, the Cerithium Group contains a mostly type II/III kerogen mixture (Fig. 19). The lowest HC generation potential and correspondingly highest amounts of barren type IV kerogen characterize the easternmost wells W14 and W12 as well as the well W7. The other wells display rather mixed type II/III kerogen, with the exception of the northernmost well W1, which shows the highest amounts of oil-prone type II kerogen. One sample from this well was chosen for additional purification and Rock-Eval measurements, because of a possible contamination. The apparently high content of type II kerogen (HI= S2/TOC*100) might be affected by a precursor to the S2 peak, which could be explained by the presence of an organic mud additive that would distort the measurement results. Yet after purification of the sample, only negligible differences were found between the newly measured Rock-Eval results and the earlier data. An explanation for the unusual S2 peak would be the presence of pyrobitumen, which influences the measured S2 value and might lead to the same results.

In wells W7 and W14 two data points do not plot inside the HI/OI diagram due to high S3 values (3.15), resulting in an elevated OI, but this may have been a result of lime lithologies. As described by Schwarz (1997), thin limestone beds are known to occur in the poorly stratified shales and shaly marlstones of the Cerithium Group. This lithological description is confirmed by log data in the northern URG.

Taking into account the rather low to moderate TOC values of the Cerithium Group, ranging around 0.2–1.0 wt.% and only in few samples reaching up to 2.2 wt.%, and the high amounts of type III (and II) kerogen (obtained from both optical and geochemical kerogen classification), an only very minor hydrocarbon generation potential is assumed for the Cerithium Group, favoring the generation of gas rather than oil.

7.2.4. Corbicula Group

In the northern URG the Corbicula Group was deposited in majorly distal settings with variable oxygen ratios (Fig. 39): Distal-oxic conditions characterize wells located along the eastern side of the graben, whereas distal-anoxic settings prevail in most of the remaining study area. The more oxic conditions in the eastern part of the study area might be related to a shift of the graben axis towards the east in the northern URG (Doebl 1967) and the thereby induced different basinal settings, characterized by higher accommodation space and higher water depths. Proximal-oxic settings are suggested for few samples from wells W10, W14 and W12, suggesting ongoing terrestrial OM from the graben shoulders during time of deposition of the Corbicula Group.
The aquatic system is characterized by more or less restricted marine-anoxic conditions. Distal oxic to anoxic environments were sporadically established in the area of wells W8 (graben center), W14 and W16 (eastern graben side).

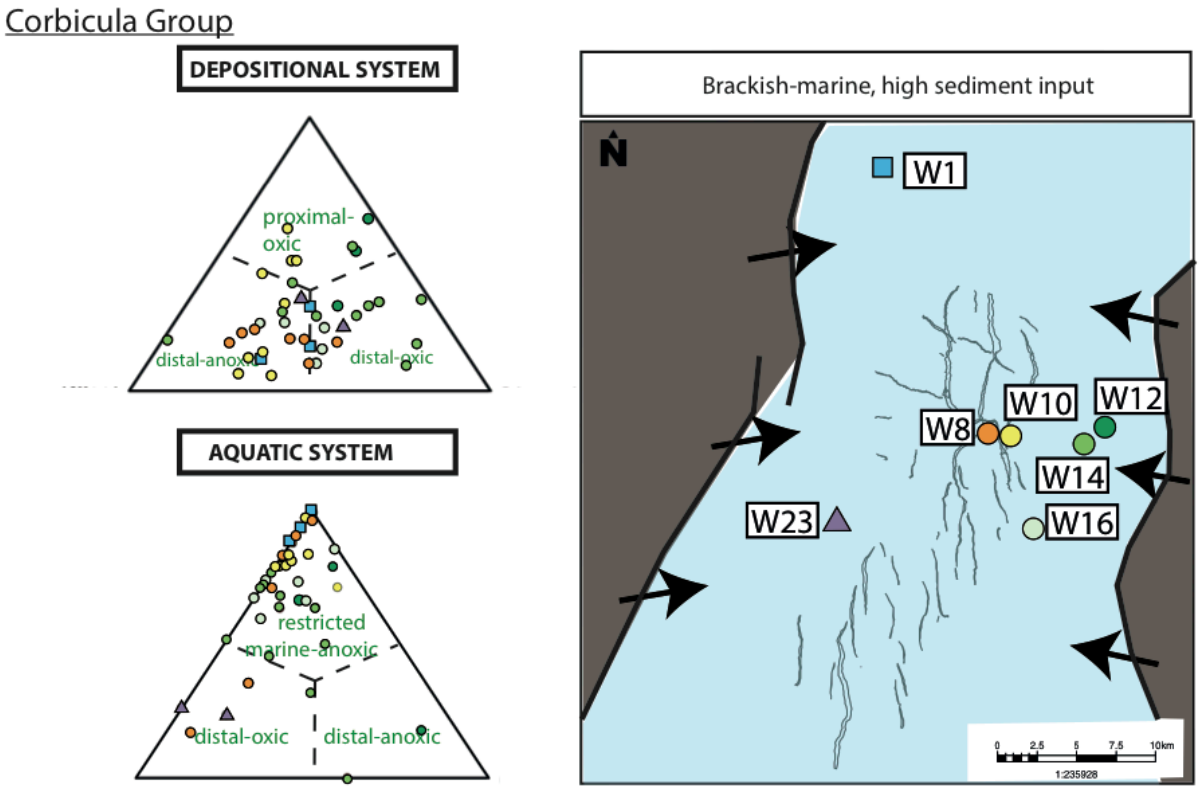

Figure 39: Palynofacies interpretations illustrated as ternary diagrams (modified after Tyson 1989) of the Corbicula Group

Optical kerogen analysis of the Corbicula Group reveals moderate to high amounts of type I, II and III kerogen (Fig. 22). Barren type IV kerogen content is low. Compared with the underlying Cerithium Group, the Corbicula Group shows much higher amounts of terrestrial type III kerogen. Results from Rock-Eval pyrolysis suggest a mainly mixed oil/gas generation potential for most studied wells (Fig. 23). The high variations and rapid changes in kerogen composition, seen in the results of both methods, are strongly related to the second main phase of rifting and subsidence in the northern URG. The higher sediment and (terrestrial) OM input and the changes in OM composition are therefore the result of strong and intermittent erosion of the

graben borderlands. In addition, sediment transport routes along fault zones may have played distributional role.

Lithologically the Corbicula Group is composed of the bituminous "Bändermergel". TOC values of between 0.8–2.4 wt.%, are representative for the entire unit and indicate good source rock potential. Based on the integrated kerogen analysis, good source rock qualities are evident, with a good gas- and a moderate oil generation potential.

7.2.5. Hydrobia Group

A mostly distal setting with variable oxygen ratios characterizes the Lower- and Upper Hydrobia Formation in the study area (Figs. 40, 41). Proximal-oxic conditions are suggested only for a few samples in the Lower- (W14 and W10) and in the Upper Hydrobia Formation (W14, W2, W1). This indicates a low to moderate input of terrestrial OM from the graben shoulders. Wells located near to the graben margins (W1, W14, W12, W2) thereby contain higher amounts of terrestrial OM. The aquatic setting was restricted marine and anoxic. The highest availability of oxygen is found along the eastern graben border and in the northernmost wells W2 and W1.

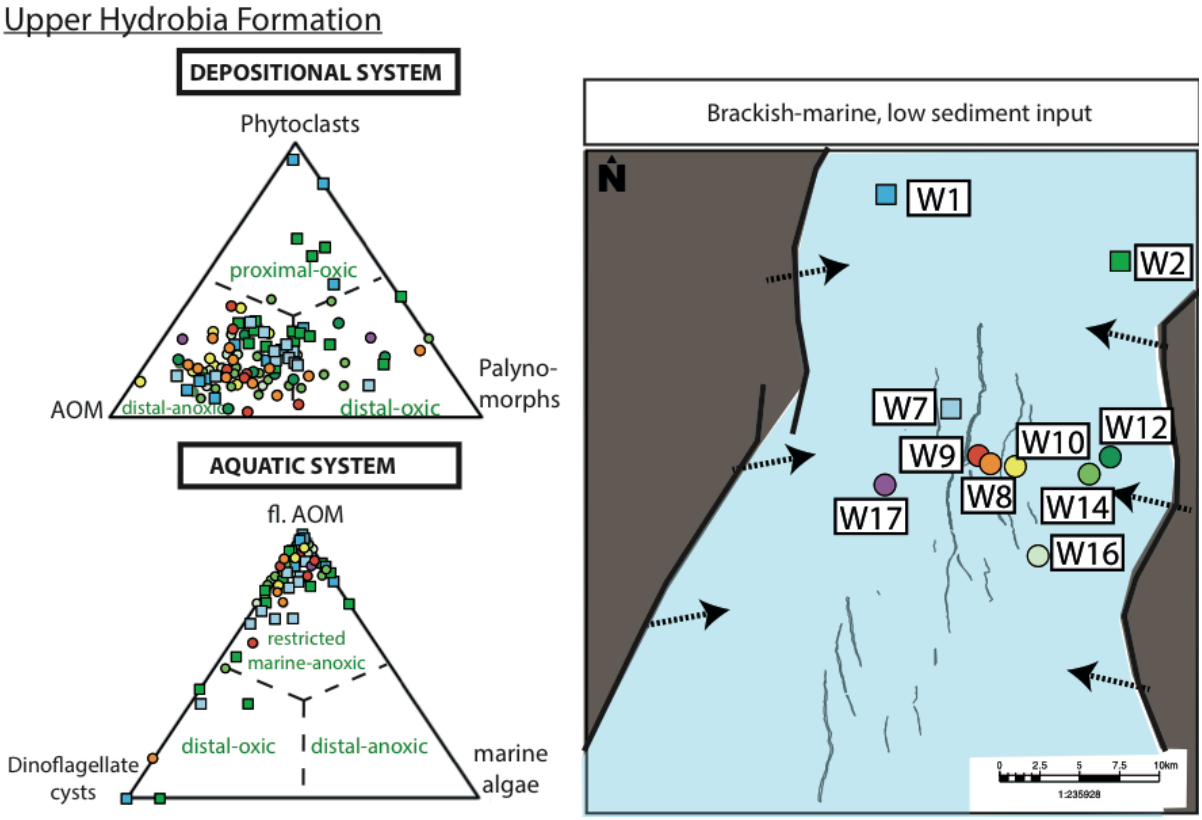

Figure 40: Palynofacies interpretations illustrated as ternary diagrams (modified after Tyson 1989) of the Upper Hydrobia Formation

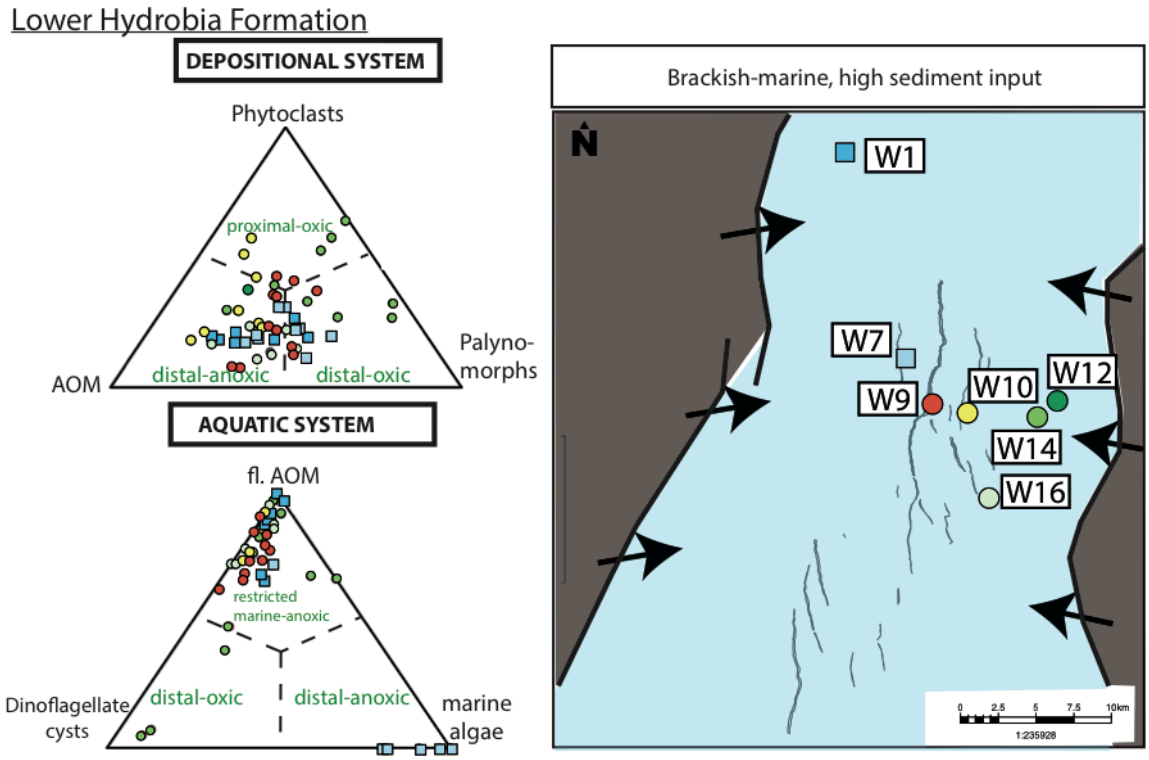

Figure 41: Palynofacies interpretations illustrated as ternary diagrams (modified after Tyson 1989) of the Lower Hydrobia Formation

Based on optical kerogen analysis of the Lower Hydrobia Formation, kerogen composition is dominated by gas-prone type III, revealing a good gas generation potential (Fig. 26). Corresponding results are retrieved from Rock-Eval pyrolysis, although some samples indicate high amounts of type II kerogen (Fig. 28). The overall high amounts of type III kerogen are most probably related to the terrestrial sediment and OM input from the graben shoulders during the second major phase of rifting, taking place during the deposition of the Corbicula Group (see above) and the Lower Hydrobia Formation. Samples from well W7 show high variations in calculated OI values, most probably related to the higher content of calcareous lithologies.

Based on optical as well as geochemical analysis, the Lower Hydrobia Formation offers good to very good oil and a poor to moderate gas generation potential in the northern URG. This is due to high amounts of oil-prone type I/II and small amounts of gas-prone type III/IV kerogen. Under the consideration that TOC values reach up to 3.3 wt.%, the Lower Hydrobia Formation offer a very good source rock potential. Based on the interpretation of well logs as well as lithologies previously described by Derer (2003) and other authors, the occurrence of potential source rocks (organic rich claystones) is nevertheless restricted in the Lower Hydrobia Formation, because favorable lithologies (organic rich clay- and marlstones) intercalate with thin layers of dolomite.

Based on optical kerogen analysis, the Upper Hydrobia Formation is dominated by oil-prone type I and II kerogen, with slightly increasing contents towards the top of the Upper Hydrobia Formation (Fig. 27). In the uppermost sample, an increase in type III kerogen is observed. The results reflect an interval of relative tectonic inactivity resulting in dominating oil-prone type I/II kerogen composition. Only few outlier samples from wells marginal to the graben boundary

indicate higher amounts of type III kerogen. This indicates some sediment transport from the shoulders into the marginal graben. Optical kerogen analysis reveals minor to moderate gas generation potential and moderate to excellent oil generation potential.
Similar to optical kerogen analysis, Rock-Eval pyrolysis also indicates mostly type II kerogen (Fig. 29). A mixed type II/III kerogen composition is less abundant. Similar to the results from the Lower Hydrobia Formation, HI/OI values plot in a relatively narrow range near to the type II pathway. Only two samples from well W7 have higher OI values, plotting towards higher gas-prone type III kerogen contents. Increased amounts of type III kerogen are sporadically identified in wells along the eastern graben margin; this is most probably due to terrestrial OM input from the eastern graben. This sediment influx is not correlated to rift-related tectonic activity but seems to result from erosion of the uplifted graben shoulders. Wells located near the graben shoulders are therefore more affected by terrestrial OM input than distant ones. Similar results are obtained from the TOC/S2 graph.
Based on integrated kerogen analysis, oil generation potential is even better in the Upper Hydrobia Formation, with TOC values of up to 4.6 wt.%. Exceedingly high amounts of oil-prone type I/II kerogen and only very minor amounts of gas-prone type III and of barren type IV kerogen characterize this unit; the values even exceed the high amounts of type I/II kerogen detected in the Lower Hydrobia Formation. No lithological differences are identified between both sub-units based on rock samples and well logs. The cause of the different kerogen compositions might thus be an increased rift activity during deposition of the Lower Hydrobia Formation.

8. Maturation Analysis

8.1. Results

The focus of the research was on wells with a dense (continuous) stratigraphic sampling. The implementation of optical and geochemical maturation analysis provides an extensive and reliable data set and allows more robust conclusions.

Well W1

Besides one sample from the Upper Tertiary II, that indicates immature conditions (0.15 %Ro), VR values of 0.54–0.76 %Ro are measured which correspond to the basal to middle oil-window (Fig. 42). Increasing VR values are identified down to the Bunte Niederröderner Group. Thereafter values slightly decrease within the Cyrena Marls Group and increase again below down to the Pechelbronn Group.
Based on SCI (1.50–4.00), a steep organic maturation trend can be assumed from an immature stage to the middle oil-window, corresponding lithostratigraphically to an interval from the Upper Tertiary II to the Bunte Niederröderner Group.
T_{max} is in the range of 415–441 °C. There is a distinct spread of values from samples from the Cerithium Group, Rupel Clay Group and Pechelbronn Group, ranging from 328–351 °C. Thus this

data must be questioned. PI (Production Index) indicates a downward increasing trend within the Cenozoic succession with values in the range of 0.08–0.32.

Well W2

In well W2, VR values range between 0.42–0.78 %Ro and increase with depth, corresponding to the immature to basal oil-window stages of organic maturation (Fig. 43).
Based on SCI, a similar trend is observed with values of 1.50–2.50, but this development corresponds to mostly immature levels.
Geochemical results indicate T_{max} in the range of 414–446 °C and PI between 0.03–0.17.

Well W7 and subsidiary wells W7(2.) and W7a

VR data from wells W7/7(2.)/7a range between 0.24–0.64 %Ro. This indicates maturities between immature to the basal oil-window (Fig. 44). Similar to well W10, the Upper Tertiary II shows strongly immature values (0.24–0.29 %Ro), whereas no clear trend in the maturation level is observed blow the Upper Hydrobia Formation (0.46–0.64).
Data retrieved from SCI analysis provide a similar picture. Maturation values of 2.00–4.00 (high value in one sample only) correspond to immature to basal oil-window. Yet, SCI samples from the Upper Tertiary II are significantly higher than the underlying Upper Tertiary I, and correspond to the basal oil-window (2.50–2.75).
Geochemical data retrieved from Rock-Eval pyrolysis display maturities ranging from immature to the barely basal oil-window (T_{max} of 424–437 °C). PI shows a distinctly downward increasing trend with values from 0.01–0.18, indicating that hydrocarbon generation may have occurred in the deeper stratigraphic intervals.

Well W8:

In well W8, VR data range from 0.29–0.66 %Ro, indicating maturation stages from immature to the basal oil-window (Fig. 45). Similar to well W10, the Upper Tertiary II shows strongly immature VR values of 0.29 %Ro. But, also the Upper Tertiary I (pre-hiatus) indicates still immature values of 0.32 %Ro. From the Upper Hydrobia Formation downwards, almost constant values of 0.50–0.66 %Ro were measured.
Data retrieved from SCI analysis provide a similar picture to VR data. The relatively uniform vertical trend of maturation of 1.75–3.00, without a regular increase with depth, corresponds to the immature field to basal oil-window.
Rock-Eval pyrolysis data display maturities from immature to barely basal oil-window, based on T_{max} (414–437 °C) and, if at all, minor hydrocarbon generation potential based on PI (0.04–0.12).

Well W9

In well W9, VR values reach 0.29–0.64 %Ro (immature to basal oil-window) (Fig. 46). A steep, vertically nearly uniform trend of maturation is reconstructed based on these VR data. Slightly elevated values compared to the general trend are present in the Upper Tertiary II (post hiatus) and the Upper Hydrobia Formation. The samples near the Stockstadt fault (crossed at 1360 m depth, see CS1 in Fig. 33) are distinctly higher, but decrease again below.

SCI data reveal maturation values of 1.75–3.25, which is still in an immature to basal oil-window stage. An almost vertically uniform trend of organic maturation is detected.
Geochemical parameters correspond well with the optical analyses. T_{max} values provide a vertically relatively constant maturation trend from the immature to the basal oil-window stage (425–437 °C). PI shows a downward increasing trend from 0.02–0.24, indicating that hydrocarbon generation may have occurred.

Well W10:
In well W10, VR values from 0.20–0.74 %Ro are recorded, indicating thermal conditions from immature up to the middle oil-window (Fig. 47). Values in the Upper Tertiary II (post hiatus) range from 0.20–0.27 %Ro. Below, from the Upper Tertiary I to the lowermost Pechelbronn Group, values reach up to 0.74 %Ro. A slight regressive trend might be present from the lower Upper Hydrobia Formation downwards. The stratigraphically lowest sample (Lower Pechelbronn Formation) gave an astonishing low value of 0.32 %Ro.
SCI data also indicate conditions from immature to the middle oil-window with values of 1.25–3.75. Here, despite some outliers in especially the upper part of the well, an almost uniform vertical trend of organic maturation becomes apparent. But again, the stratigraphical lowest sample cluster around 1.50 only.
Geochemical parameters mostly corroborate the optical data. The T_{max} values comply with conditions from immature to (just) the basal oil-window: values are in the range of 422–445 °C with few exceptions in the Pechelbronn Group (326–336 °C). Based on the PI, no hydrocarbon generation has taken place in the W10 well. Similar to T_{max} , samples from the Pechelbronn Group show abnormally PI values of up to 0.33.

Wells W12 & W14
VR data range from immature to the basal oil-window with values between 0.49–0.72 %Ro (W14) and 0.30–0.73 %Ro (W12)(Figs. 48, 49). The maturation trend is almost vertically uniform, except for samples from the Upper Tertiary I in both wells, which indicate a lower maturation level.
SCI measurements correlate well with VR data, with values of 2.00–4.00 (W14) and 2.00–3.25 (W12).
Based on Rock Eval pyrolysis, T_{max} ranges between 423 and 437 °C (W14) and 428–437 °C (W12). Two samples of the Corbicula Group and Cerithium Group (330–369°C) in well W14 reveal questionable results. Their PI ranges between 0.04–0.13 (W14) and 0.05–0.15 (W12), and indicates potential hydrocarbon generation in the Corbicula Group. The credibility of the T_{max} values of two samples from the Corbicula Group and Cerithium Group (330–369°C) in well W14 need to be questioned; also the PI results of these samples are to be scrutinized.

Well W16
In well W16, VR values from 0.18–0.82 %Ro are recorded, indicating maturities ranging from immature to the middle oil-window (Fig. 50). VR values increase from the Upper Tertiary II

down to the Bunte Niederröderner Group, but again decrease downsection to the Pechelbronn Group.

SCI data also reveal maturities from immature conditions to the middle oil-window with steadily increasing values in the range of 1.25–3.75. The Pechelbronn Group shows distinctly higher values from 3.5 to 5.5.

T_{max} indicates a maturation level from immature to the basal oil-window (422–442°C). Extremely low and questionable T_{max} values were measured in one sample from the Pechelbronn Group (307°C). Based on PI, HC generation occurred from the Lower Hydrobia Formation downsection.

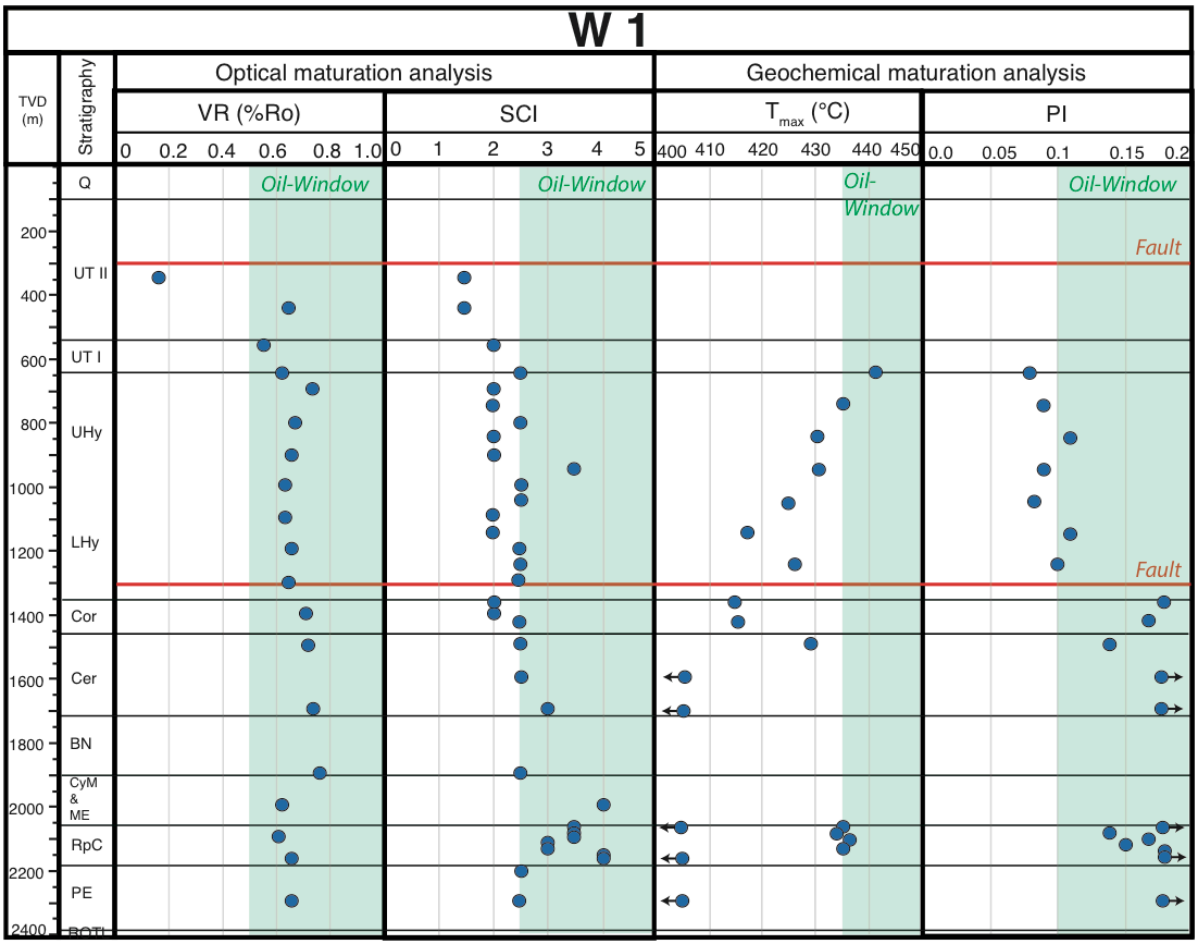

Figure 42: Maturation analysis in well W1, showing the results from Vitrinite Reflectance (VR), Sporomorph Coloration Index (SCI) and Rock-Eval (T_{max}, PI). Red lines represent major faults.

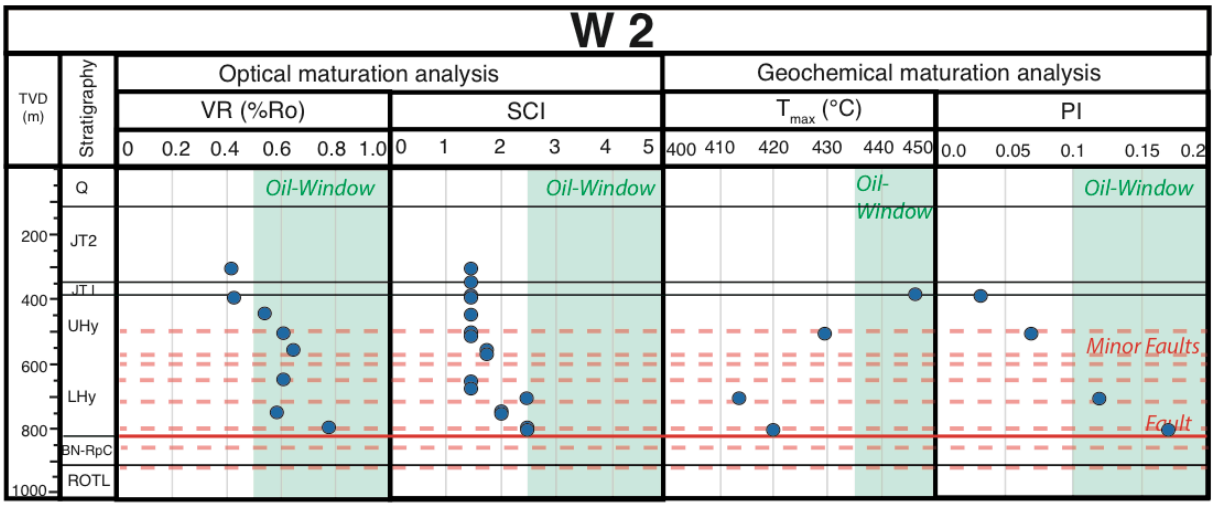

Figure 43: Maturation analysis in well W2, showing the results from Vitrinite Reflectance (VR), Sporomorph Coloration Index (SCI) and Rock-Eval (T_{max}, PI). Red line represents a major fault; dotted lines represent minor faults as indicated by well reports.

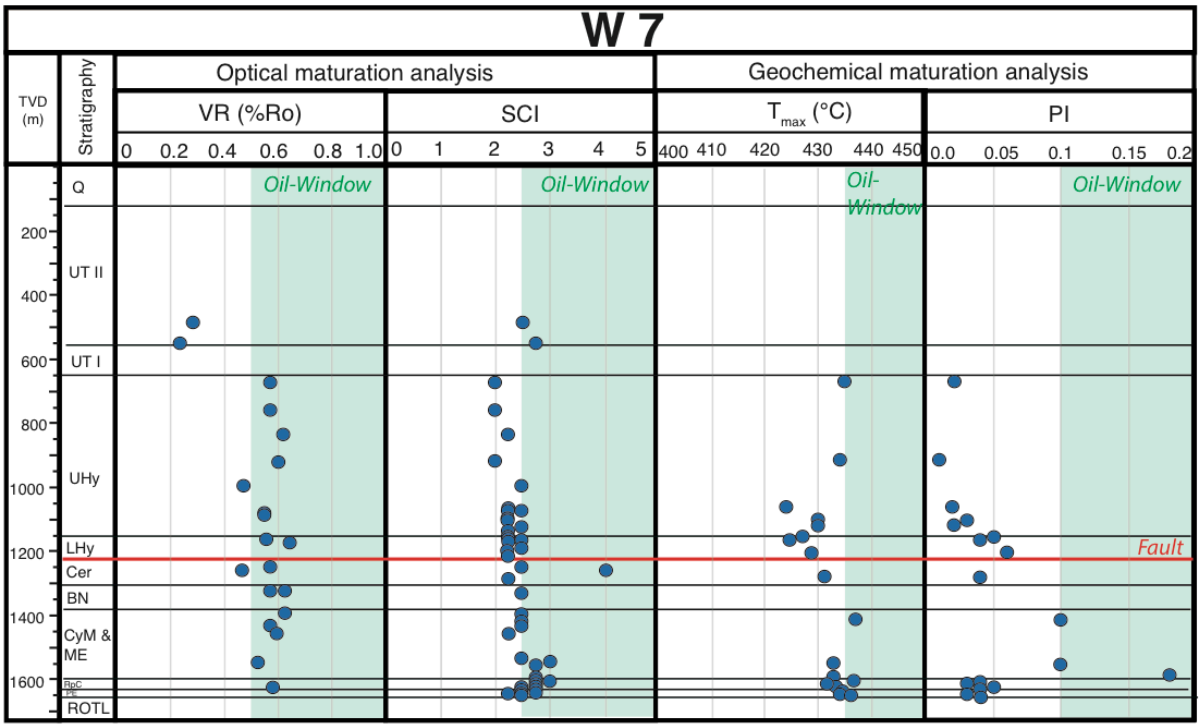

Figure 44: Maturation analysis in wells W7, W7a and W7(2.), showing the results from Vitrinite Reflectance (VR), Sporomorph Coloration Index (SCI) and Rock-Eval (T_{max}, PI). Red line represents the Stockstadt fault.

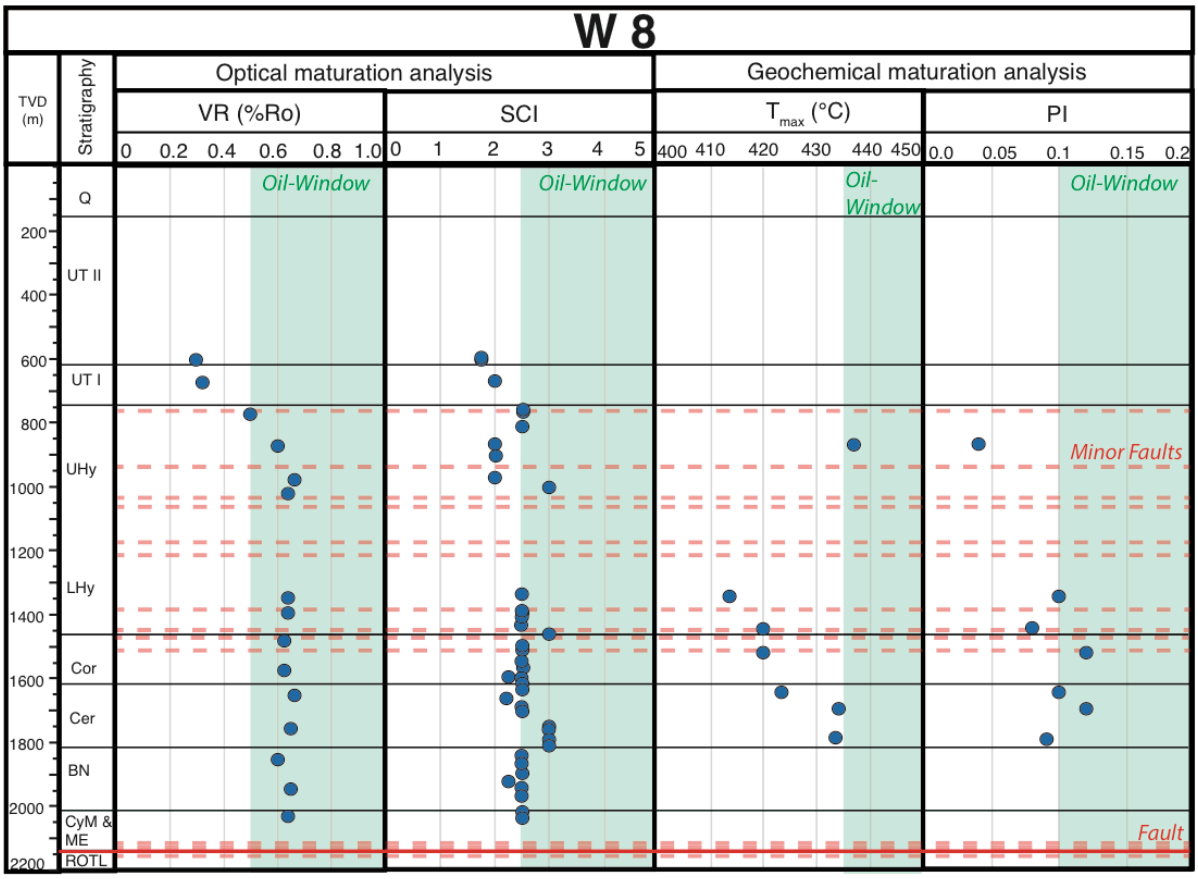

Figure 45: Maturation analysis in well W8, showing the results from Vitrinite Reflectance (VR), Sporomorph Coloration Index (SCI) and Rock-Eval (T_{max}, PI). Red line represents the Stockstadt fault; dotted lines indicate minor faults as suggested by well reports.

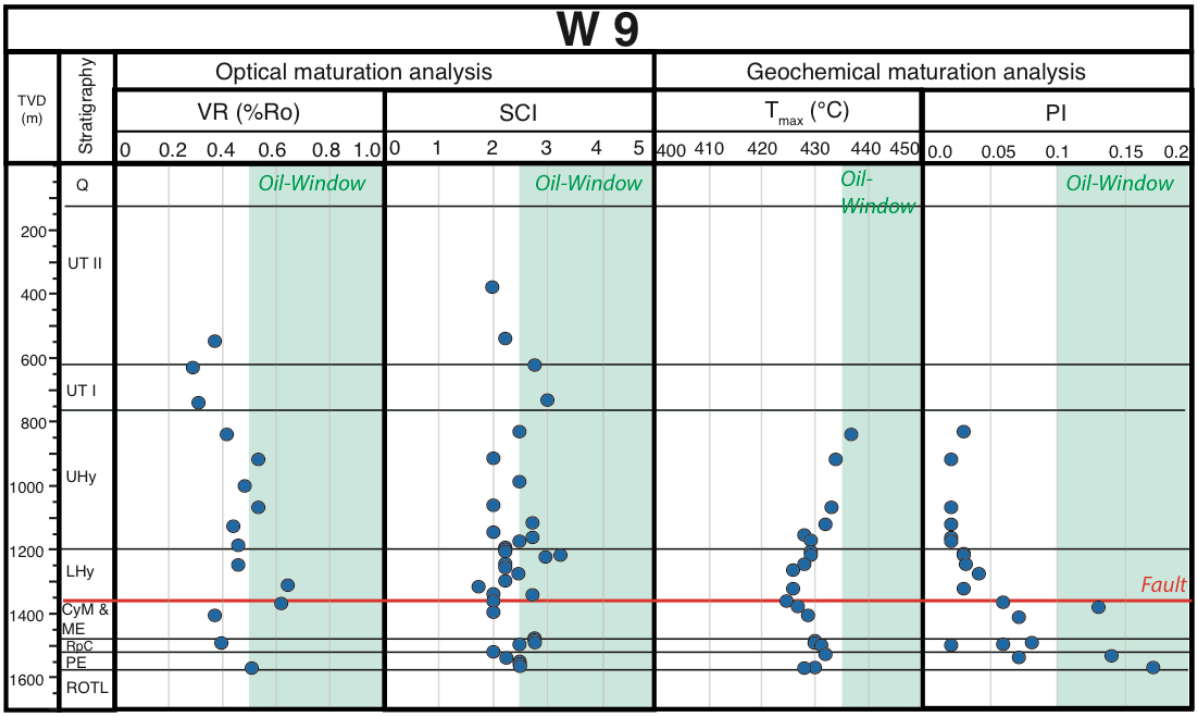

Figure 46: Maturation analysis in well W9, showing the results from Vitrinite Reflectance (VR), Sporomorph Coloration Index (SCI) and Rock-Eval (T_{max}, PI). Red line represents the Stockstadt fault (see Fig. 33 CS1).

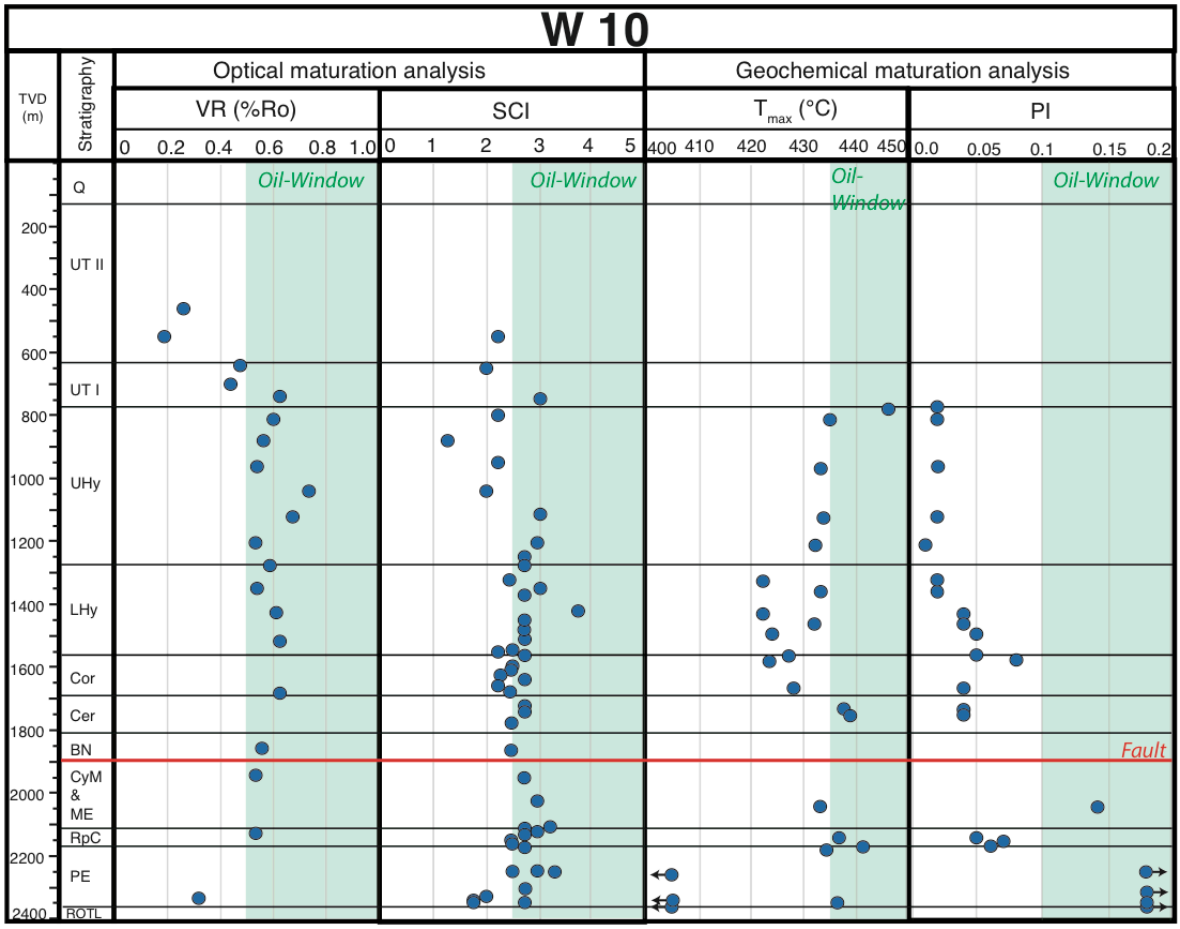

Figure 47: Maturation analysis in well W10, showing the results from Vitrinite Reflectance (VR), Sporomorph Coloration Index (SCI) and Rock-Eval (T_{max}, PI). Red line represents the Allmend fault (see Fig. 33 CS1)

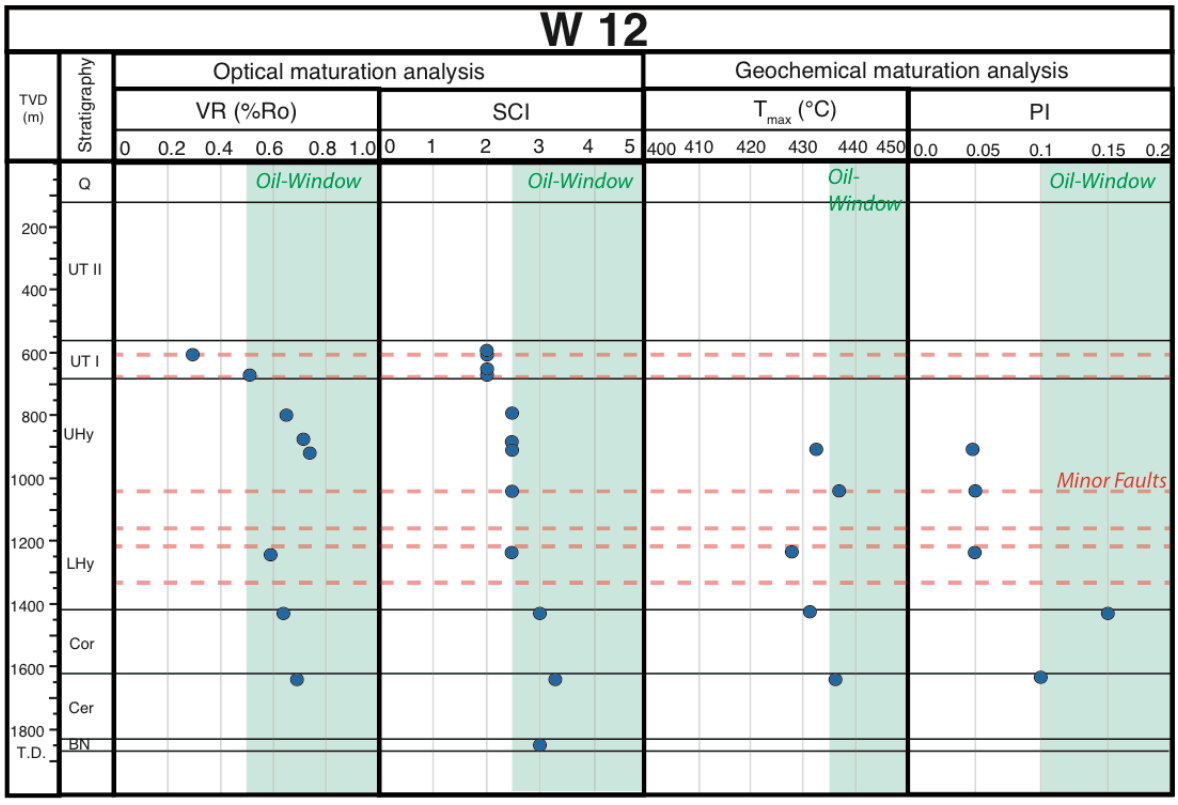

Figure 48: Maturation analysis in well W12, showing the results from Vitrinite Reflectance (VR), Sporomorph Coloration Index (SCI) and Rock-Eval (T_{max}, PI). Red dotted lines represent minor faults as indicated by well reports.

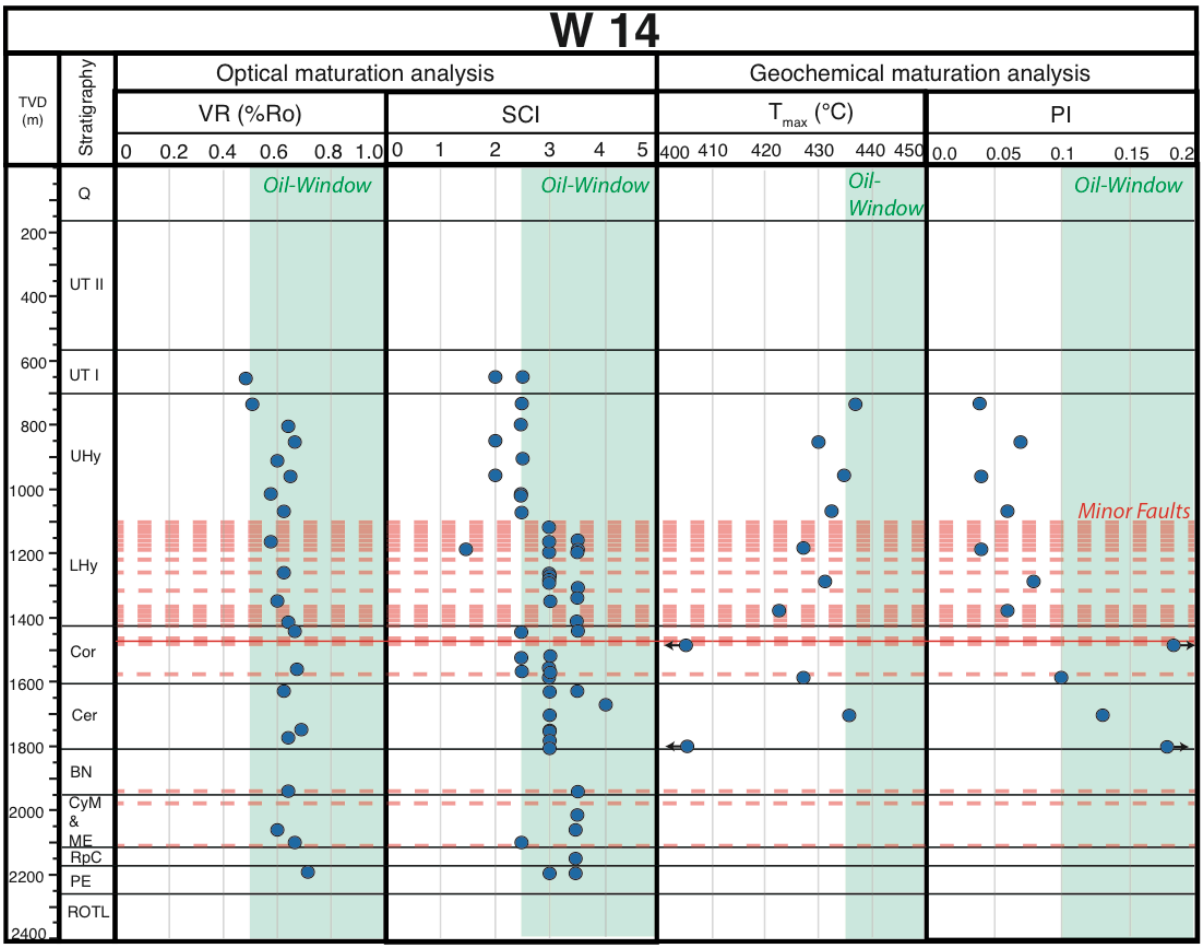

Figure 49: Maturation analysis in well W14, showing the results from VR, SCI and Rock-Eval (T_{max}, PI). Red dotted lines represent minor faults as indicated by well reports.

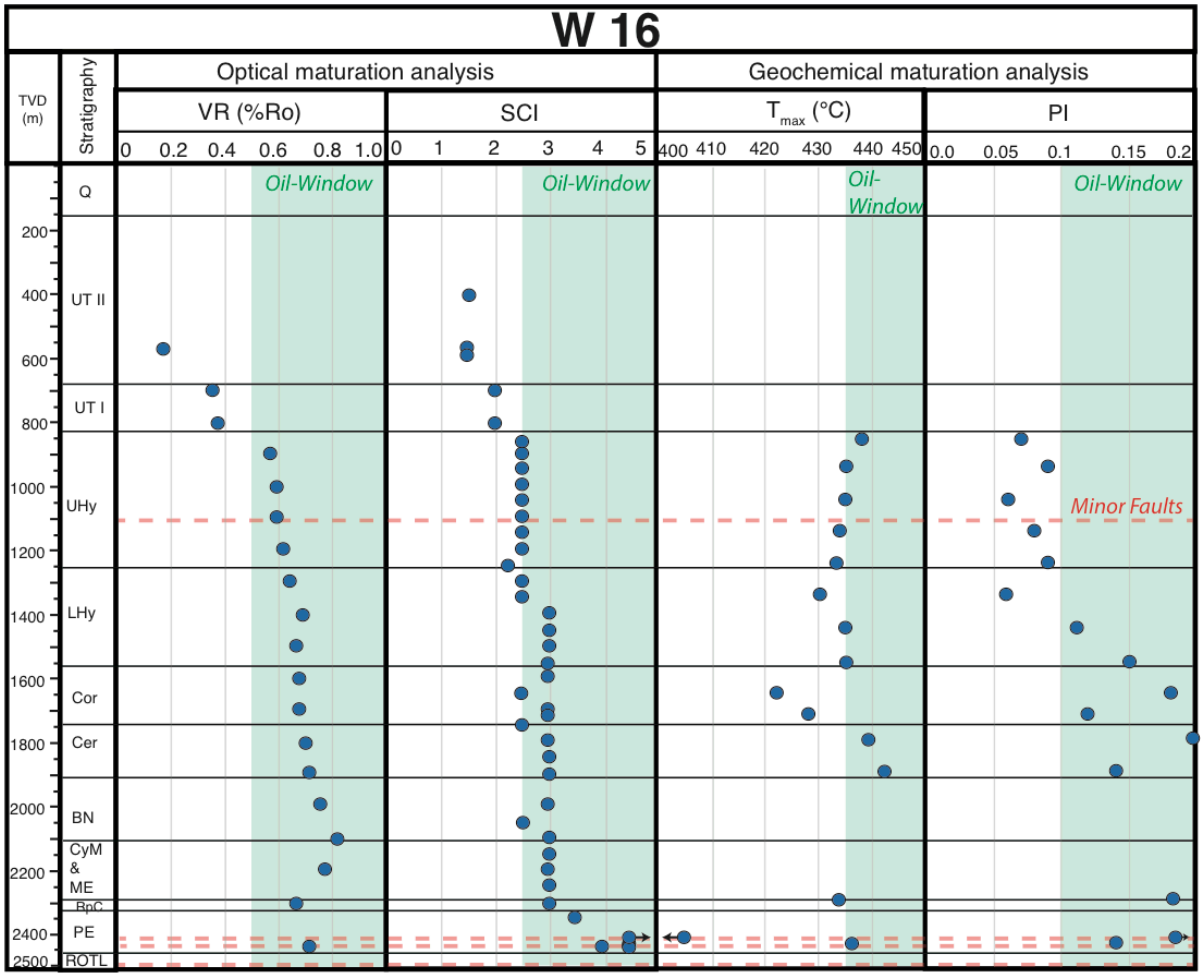

Figure 50: Maturation analysis in well W 16, showing the results from VR, SCI and Rock-Eval (T_{max}, PI). Red dotted lines represent minor faults as indicated by well reports.

Based on the profound and extensive VR data set, VR maps were created for the most prominent source rock intervals of the Pechelbronn Group, Rupel Clay Group, Lower- and Upper Hydrobia Formations (Fig. 51). For the Pechelbronn Group and Rupel Clay Group, few values were interpolated (red coloured values) and labelled accordingly: for the Rupel Clay Group, VR values have been extrapolated in case of available VR data from the overlying Meletta Group and/or underlying Pechelbronn Group to the known depth of the Rupel Clay Group. For the Pechelbronn Group, maturities from the overlying Rupel Clay Group were extrapolated with depth. These interpolated data must be considered with caution.

VR data of the early syn-rift Pechelbronn Group and Rupel Clay Group ranges from 0.51–0.88 %Ro and 0.40–0.80 %Ro. Within the Lower and Upper Hydrobia Formation dated to the Late Miocene, VR values range from 0.55–0.66 %Ro and 0.48–0.70 %Ro. For interpretation purposes, depth maps of the individual units are displayed as well. The fault systems shown were interpreted from 3D seismics.

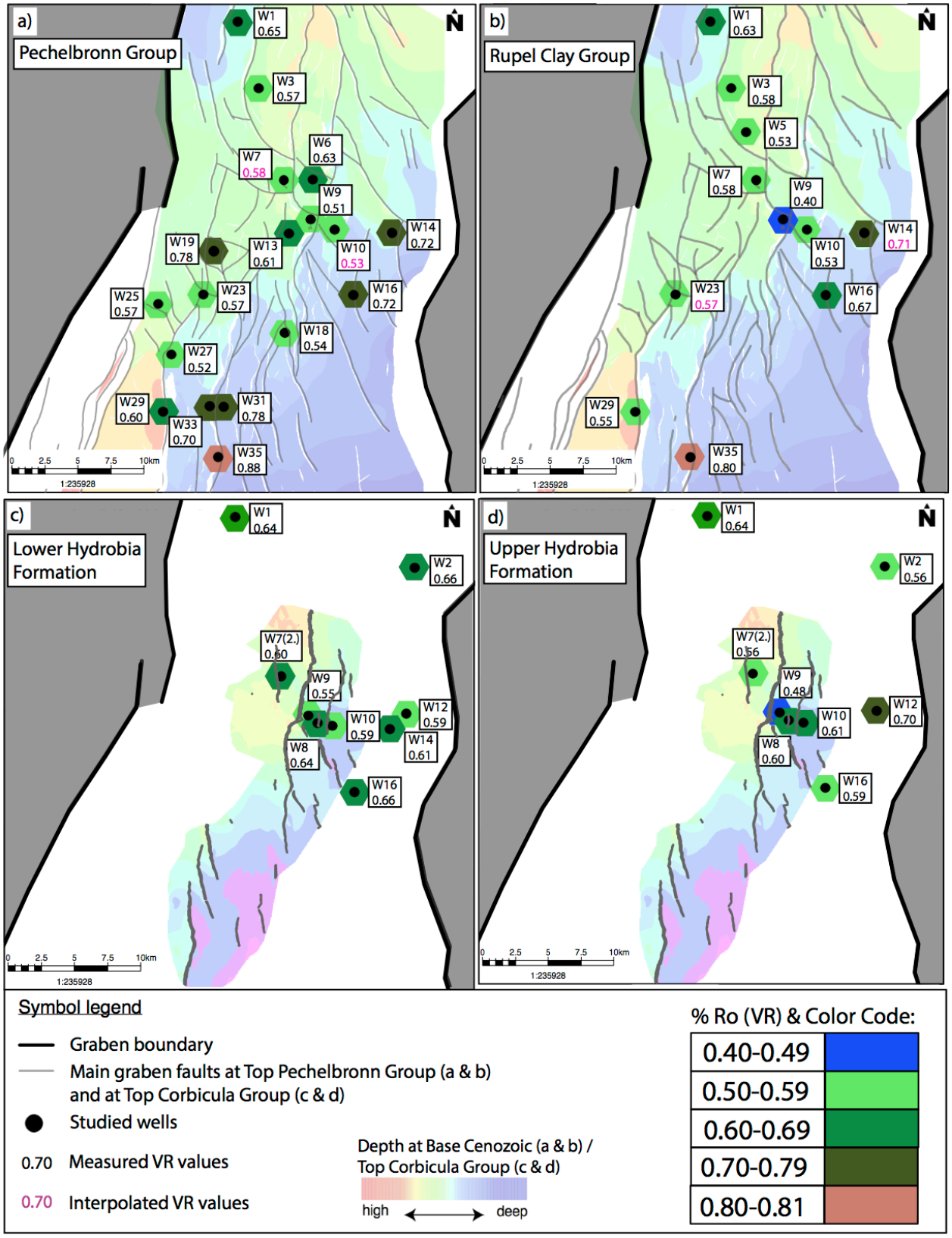

Figure 51: Vitrinite Reflectance maps of a) the Pechelbronn Group; b) the Rupel Clay Group; c) the Lower Hydrobia Formation; d) the Upper Hydrobia Formation. Maps include interpreted fault patterns at the interval of interest and rough depth maps. Note that all wells are in close vicinity (around 1–2 km distance) to major fault zones, which can be observed in seismic.

8.2. Interpretation

Data sets based on the integrated (optical and geochemical) maturation analysis show good consistency between the different data sets (Figs. 42–50). Overall, the VR, SCI and T_{max} values conformingly indicate immature conditions in the Upper Tertiary II, and immature to mid oil-window settings in the Upper Tertiary I to Pechelbronn Group. PI suggests that some hydrocarbon generation occurred in the Eocene to early Miocene formations.

Well W1

According to the results from VR and SCI analysis a downward slightly increasing maturation trend is observed in well W1, from the immature Upper Tertiary II interval at the top of the section to the basal oil-window maturation stage near the base (Fig. 42). Minor differences are detected between these two data sets down to the Corbicula Group. Elevated SCI values, such as in a sample from 1250 m depth, are probably related to higher coalified, recycled sporomorphs and the missing in-situ population. As vitrinite reflectance seems to be a more accurate reference parameter, a basal-oil window level of organic maturation is suggested for almost the entire Cenozoic succession. T_{max} data suggest, that the stage of potential oil generation was barely reached. In the Cerithium Group and below this unit, some samples show extremely low T_{max}. Unclear S2 peaks in the affected samples are the reason for this anomaly (T_{max}= Temperature at maximum S2 peak) (Fig. 52). Unusually low T_{max} values may represent pollution by drilling fluids or natural impregnation by migrating hydrocarbons (Bordenave et al. 1993); in consequence, these samples were applied to a special treatment to remove (eventually remaining) drilling mud. Afterwards, Rock-Eval pyrolysis has been repeated on the affected samples but the new measurements also provided results with an unclear S2 peak. One possible reason may be the occurrence of pyrobitumen in the affected samples.

Based on the PI data set, HC generation occurred in the (Lower) Hydrobia Formation and underlying lithostratigraphic units. As PI is derived from S1 and S2, and the S2 is questionable in samples with low T_{max} (<360°C), it is better to not over-interpret the PI data. Rupel Clay Group samples, on the other hand, show clear S2 peaks. This indicates that oil generation has taken place, as also suggested by VR data. Oil generation may have occurred in the Corbicula Group, based on the PI, VR and SCI data. Maturation stage in well W1 is thus elevated as compared to the other wells discussed here. This may been caused by the exceptional situation of the well in a small pull-apart basin on the western border of the URG, which has undergone a slightly different subsidence history than other wells in the area.

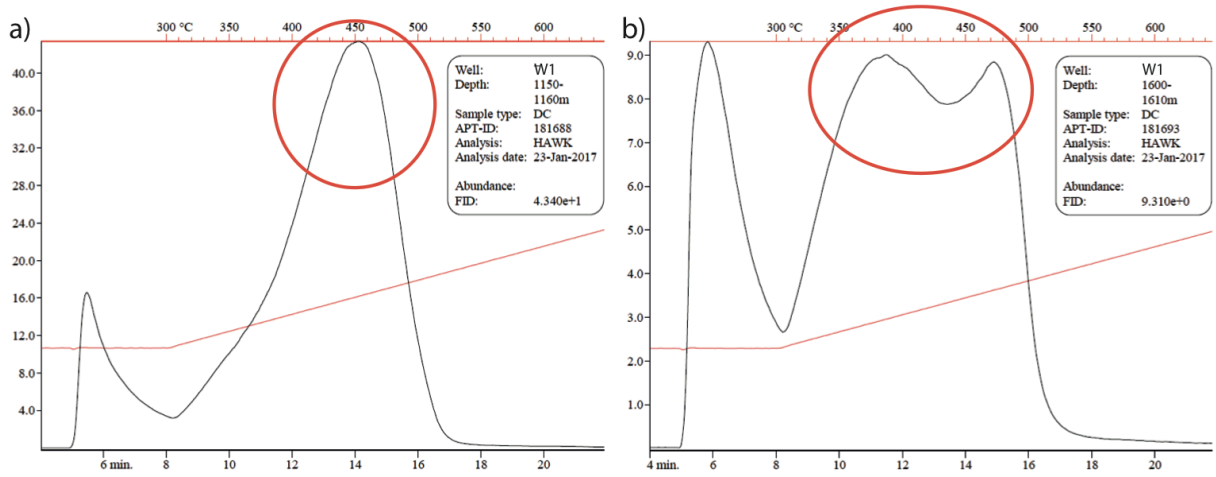

Figure 52: Rock-Eval pyrograms from well W1 indicating (a) a clean and reliable S2 peak; (b) an unclean S2 peak that is possibly the result of pyrobitumen, affecting the sample. As a result, T_{max} and PI are unreliable and must be interpreted with caution.

Well W2

Based on the VR, SCI and PI data obtained from well W2, maturation increases with depth (Fig. 43). The Upper Hydrobia Formation and overlying units are still immature, while samples from the underlying Lower Hydrobia Formation reached the mid oil-window. In contrast, immature conditions are suggested for this interval by SCI and T_{max} data. The latter T_{max} values from the Lower Hydrobia Formation are likely decreased slightly due to the high sulphur content (3.04–3.98 %) as previously described by Isaksen et al. (2000). Therefore, a basal oil-window level of organic maturation is inferred, as also suggested by the general maturation trend. This suggests minor HC generation.

Well W7

Maturation data from well W7 indicates immature to basal oil-window conditions throughout the Cenozoic succession (Fig. 44). A vertically almost uniform maturation trend is observed, based on VR, SCI, and T_{max} data, beginning in the Upper Hydrobia Formation. Only the overlying Upper Tertiary I and II samples are strongly immature based on VR data. Elevated SCI values for these samples are probably the result of recycled and higher mature sporomorphs, as also interpreted for one sample from the Cerithium Group. PI data suggest that hydrocarbon generation occurred within the Cyrena Marls Group and the Meletta Group. Yet this is very questionable, because silt lithologies with high carbonate content dominate lithologies. The potential source rocks of the Rupel Clay Group and Pechelbronn Group suggest no HC generation within these units.

Well W8:

Based on VR and SCI data, immature conditions are inferred for sediments of the Upper Tertiary I and II Groups of well W8, and a basal oil-window maturation stage in the underlying sediments (Fig. 45). Geochemical maturation analysis reveals similar but slightly less mature conditions. Decreased T_{max} values in the Lower Hydrobia Formation to Corbicula Group are likely caused by

elevated sulphur contents, as shown from another area by (Isaksen et al. 2000). Based on maturation analysis the generation of HCs is unlikely for these units, as also indicated by PI. Elevated PI values (indicating basal oil-window) in the Lower Hydrobia Formation and Corbicula Group may indicate oil generation within these units. In the Cerithium Group, where elevated PI were also measured, HC generation is unlikely due to unfavorable lithologies as confirmed by well logs and literature (Schwarz 1997).

Well W9

Based on VR and SCI data, an almost vertically uniform trend is inferred for the Cenozoic succession covering the immature to basal oil-window fields (Fig. 46). T_{max} data indicate that no major changes occur in maturation level. Slightly lower T_{max} values in the Lower Hydrobia Formation may again be related to the geochemical composition of the samples. The PI data suggest that oil generation took place in the late Eocene to early Oligocene sediments. This interpretation does, however, not fit optical maturation parameters. Elevated PI values correspond to elevated S1 peaks in the Rock-Eval pyrolysis. However, well W9 was drilled into a footwall structure, which produced HC until the 1960ies. The existence of small amounts of migrated, free hydrocarbons (S1) in the sediments is therefore likely, even though the well was classified as dry. No oil based drilling mud was used. To sum up, no hydrocarbon generation has occurred in well W9 based on integrated maturation analysis.

Well W10

Based on VR and SCI data the Upper Tertiary I and II Groups show slightly increasing values of organic maturation within the immature field (Fig. 47). Below, from the Hydrobia Group to the top of the Pechelbronn Group, an almost vertically uniform maturation trend is recognized. Low maturities within the Pechelbronn Group are most probably related to degraded dark vitrinite, which causes therefore low reflection values. The Lower Pechelbronn Formation was deposited under terrestrial-fluvial conditions; in consequence, degradation of organic material occurred during sediment transport from the graben shoulders to the depositional area in the basin. T_{max} corresponds well with the maturation values obtained by optical analysis. Except for the Lower Hydrobia Formation to Corbicula Group in which T_{max} values are slightly lower than those obtained by optical analysis. This difference is explained by high sulphur contents of this interval (2.55–3.73 wt.%) (Isaksen et al. 2000). Extremely low T_{max} values in the Pechelbronn Group are related with unclear S2 peaks (Fig. 52). PI values indicate that no HC generation took place. Elevated PI values in the Pechelbronn Group (and Meletta Group) are unreliable because these values are related to samples with an unclear S2 peak.

Wells W12 & W14

An almost vertically uniform, downwards only slightly increasing maturation trend is identified in these wells. Immature conditions are inferred for the Upper Tertiary I (Figs. 48 & 49). Based on optical (VR and SCI) analysis, maturation reaches the mid oil-window in the Pechelbronn Group in well W14 (2196.6 m) and in the Cerithium Group in well W12 (1634.3 m).

Elevated SCI values, as observed in the Cerithium Group in well W14, are caused by recycled sporomorphs. Based on geochemical analysis, a trend from an uppermost immature stage to a basal oil-window stage is observed in both wells.

Apparently low T_{max} and high PI values in well W14 are due to unreliable pyrograms. When maturation data from optical and geochemical analysis are combined it appears that oil generation has not been reached in the Hydrobia Group and the Corbicula Group. Yet, based on VR and SCI data, a maturation stage sufficient for oil generation (0.60–0.66 %Ro) is indicated for the underlying source rocks of the Rupel Clay Group (and Middle Pechelbronn Formation) in well W14. This example nicely shows that only the combination of different methods and the discussion of the data result in a conceivable interpretation.

Well W16

Well W16 well shows a downward increasing maturation trend ranging from immature conditions in the Upper Tertiary II/I to a mid-oil-window stage in the Pechelbronn Group (Fig. 50). This is indicated by VR and SCI data. Geochemical T_{max} data suggest, however, that no depth-related change occurred in organic maturation. Slightly lower T_{max} values in the Corbicula Group are again referred to elevated sulphur contents (2.92–3.14 %) as discussed earlier. Rock-Eval results from one sample of the Pechelbronn Group (2435.6 m) are apparently unreliable, most probably due to the presence of pyrobitumen (Fig. 52). Based on PI data, the source rocks of the Rupel Clay Group as well as the Corbicula - and Hydrobia Groups indicate maturation levels sufficiently high for oil generation, which fits well with the results from optical analysis.

The maturity level based on VR data for selected potential source rock intervals is shown in Fig. 52. For the Pechelbronn Group and Rupel Clay Group, the VR map shows a somewhat subsidence-controlled maturation trend from North (low-shallow), where VR values range around 0.53–0.65 towards the South, where VR values reach up to 0.88 %Ro for the Pechelbronn Group and 0.8 %Ro for the Rupel Clay Group (high-deep). Within the Hydrobia Group, similar VR maturation data in the range of 0.48–0.66 %Ro are measured for the Lower and Upper Hydrobia Formation. For these units, no clear trend can be observed within the study area. When comparing the different stratigraphic units, it becomes apparent that even though several 100s of meters of sediments were deposited in between the Rupel Clay Group and the Hydrobia Group, maturities expressed by VR do not correspond to a solely burial-controlled subsidence trend, with would we characterized by increasing maturities with depth.

9. Palaeothermal History and Basin Analysis

In order to grasp the principles of the palaeothermal history in the northern URG, the basin modeling software PetroMod® 1D was used to simulate the burial history and palaeothermal heat flow of few selected wells. The aim of this one-dimensional modeling is to get a better understanding of the subsidence and accumulation history of the Cenozoic graben fill and of the heat flow evolution during the complex and multiphase rifting evolution. Changing heat flows throughout Cenozoic were previously discussed e.g. by Bruss (2000), Lampe (2001), Lampe & Person (2000) and Lampe & Person (2002). In addition, regional heat flow variations and anomalies were observed (e.g. Teichmüller & Teichmüller 1979, Hoffers 1981, Clauser 1988, Schellschmidt & Clauser 1996, Baillieux et al. 2013).

The specific wells subjected to these one-dimensional simulations are illustrated in Fig. 53. These wells were chosen because of their different settings within the graben and because a full and continuous suite of samples was available: well W1 is located within a small pull-apart basin to the northwest of the study area; well W10 is located in the graben center on a hanging wall; well W16 represents a structural dome along the eastern graben boundary (Plein 1992).

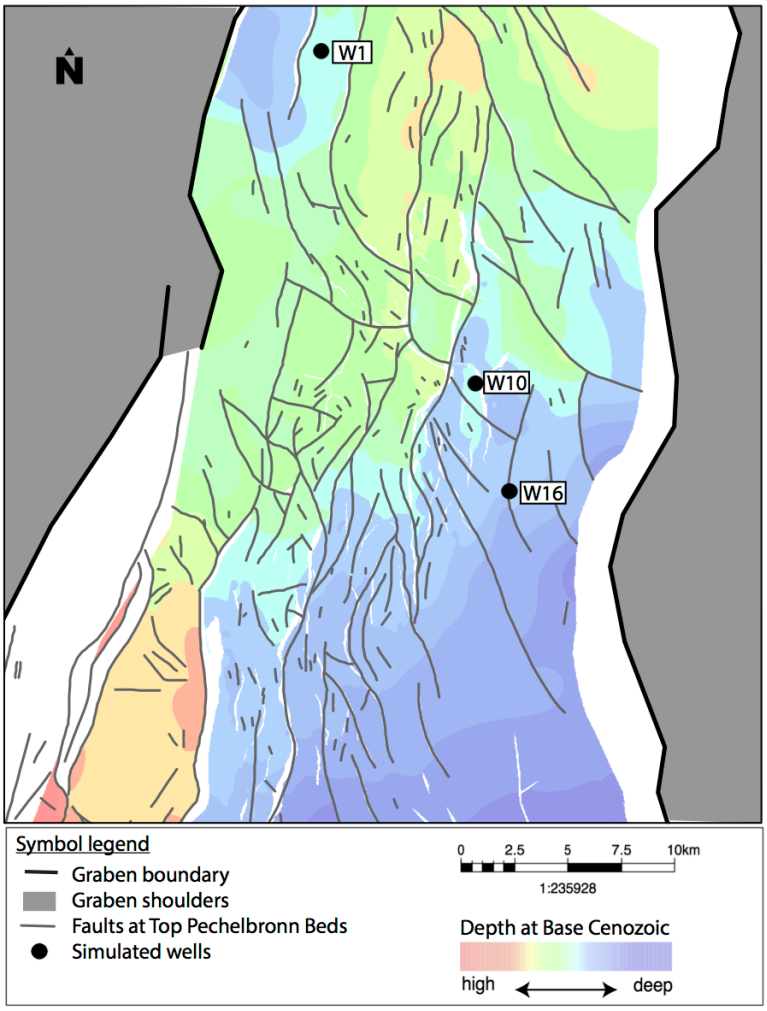

Figure 53: Location of wells, which are here used for one-dimensional numerical modeling

9.1. Input Parameters and Boundary Conditions

In order to obtain the most realistic simulation of palaeothermal evolution and subsidence and accumulation history, strong emphasis must be paid on input parameters and boundary conditions of the model. A close relationship and interpretation are given between the individual parameters. For example, heat flow exerts the main control on the temperature conditions within the sedimentary succession, which is modified by lithology, thermal conductivity (considering lithology and its pore filling) as well as sedimentation and subsidence (affecting together also compaction). The following input parameters, which describe the Cenozoic succession, are used:

- Lithology and thickness of lithostratigraphic intervals. These data are obtained from well log interpretation and the description of rock samples from cuttings and cores. The lithological description is detailed and includes alternations on cm-scale. Thus, the lithotypes need to be simplified and/or combined for simulation purposes to mixed lithologies with mean rock-properties.
- Petrophysical rock properties are used, that are assigned to the sedimentary units based on lithological classification
- Lithostratigraphic framework (modified after Schad 1964)
- Unconformities

Following the definition of the lithostratigraphic succession that is being modeled, boundary conditions need to be quantified:

- Palaeo-water-depth (m) and SWI temperature (°C)
  Palaeo-water depths (m) and temperature estimates at the sediment/water interface (SWI) are adapted from Bruss (2000) and Lampe (2001)
- Heat flow:
  Heat flow is estimated from the geotectonic framework during the different rifting phases. It has important impact on the thermal evolution and thus on the maturity level in the basin. Continental rifts such as the URG often are regions of elevated heat flow Illies 1972, Pauwels et al. 1993, Agemar et al. 2013, Freymark et al. 2017). Yet the URG is a passive rift and elevated heat flow rates are unrelated to the presence of plumes (active rift), but rather to tectonic stress and to a thinning of the lithosphere, the latter associated with the uplift of the Moho discontinuity (Illies & Fuchs 1974, Schumacher 2002, Grimmer et al. 2016, Freymark et al. 2017). In conclusion, the URG provides good potential for deep geothermal exploration, as for example in Soultz-sous-Forêts (Vosges, France), where the present day geothermal gradient exceeds 130°C/km, or in Landau (central URG, SW-Germany), where a vertical temperature gradient of 110°C/km is reached (Rybach 2007, Baillieux et al. 2013, Person & Garven 1992, Schellschmidt & Clauser 1996, Vidal et al. 2015, Freymark et al. 2017).
  Also low geothermal gradients are reported from the URG on a local scale in the areas of Stockstadt, Schwarzbach or the Heidelberg-Mannheim Basin with 45 °C/km (Doebl &

Teichmüller 1979, Agemar et al. 2013, 2014). The variation of heat flow during rift development and its controlling factors will be discussed in more detail in the Simulations Chapter (9.3.).

Following the definition of input parameters and boundary conditions, 1D simulations were carried out. During this forward modeling, simulations begin with the oldest defined sediment unit, continuing to the youngest recent unit.

9.2. Calibration

After entering input data and boundary conditions into the model (conceptual model) and running the simulations, an independent data set on the thermal evolution is necessary for calibration purposes. An optimization of the simulated one-dimensional model is achieved based on the measured VR data as calibration tool. VR is applied for calibration, because it is a reliable temperature sensitive maturation parameter. Similar to other maturation parameters such as the Sporomorph Coloration Index it is irreversible over time (Bostick 1979, Schenk et al. 1990, Suárez-Ruiz 2012).
Following the input of VR data, the simulation is modified respectively within a realistic framework in terms of graben evolution. The calibration is achieved by varying and adjusting input parameters and boundary conditions such as heat flow, thickness of eroded events, SWI temperatures, palaeo-water-depths and rock properties. Yet, for the one-dimensional simulation, the heat flow seems to be the main triggering parameter with the greatest impact on the thermal evolution (Table 1, Fig. 54).

9.3. 1D Simulation

The best fitting input parameters and the results of the one-dimensional simulations for the wells W1, W10 and W16 are shown in Fig. 54 and Fig. 55. In order to fit the calibration data, heat flow as the most influential input parameter on the distribution of heat (Gallagher et al. 1997) was adjusted in geologically reasonable ranges for each well.

A geodynamic conductive heat flow, which is closely linked to the geotectonic history of the URG, is proposed for one-dimensional simulations, in agreement with published data e.g. by Lampe (2001), Bruss (2000), Teichmüller & Teichmüller (1979) and Agemar et al. (2013): the first pulse of elevated heat flow (~120 °C) is correlated to crustal thinning with accompanying volcanism prior to rift development during Upper Cretaceous until Lower Eocene (e.g. Bruss 2000). During the following subsidence and cooling of the crust starting in the Middle Eocene to the Early Oligocene, low heat flow rates are assumed (down to ~70 mW/m^2). Yet, heat flow rates are assumed to be still higher than the continental average heat flow of 60mW/m^2 (Allen & Allen 1990). The second main phase of rifting began in the Early Miocene. Increased tectonic activity and sinistral shear movements are correlated to elevated heat flow rates of ~80 mW/m^2 to 90

mW/m². From the Late Pliocene until recent, lower heat flow rates of 72 mW/m² are assumed. In addition to the conductive heat flow, convective heat flow influences especially the youngest thermal evolution within the URG, as described e.g. by Clauser (1988) and Lampe (2001). This convective heat transport is evidenced in geothermal anomalies within the URG (Clauser 1988), yet it cannot be taken into account by one-dimensional numerical simulations.

In well W1, the best fitting simulated palaeothermal trend fits the VR data of the Upper Tertiary II and of the older Meletta Group, Rupel Clay Group and the Pechelbronn Group. The Early Oligocene to Pliocene Formations in between are consistently underestimated. These VR values cannot be reconstructed using only basal, conductive heat flow as is provided in one-dimensional modeling: By elevating the basal heat flow, much higher maturities (VR values) would be reconstructed for the early syn-rift sediments, yet the overlying formations would still be by far underestimated. The "best fitting" maturation trend for well W1 is characterized not by a steady and constant heat flow, but rather by a varying heat flow in geologically reasonable ranges under consideration of the geotectonic background as described above (Table 1, Fig. 54). The maximum heat flow rates were reached during the Late Miocene (5.3–7 Ma) and during Late Eocene to Early Oligocene (28.7–33.1 Ma).

A similar palaeothermal trend is reconstructed for well W10. The modeled trend fits best the calibration data for the Upper Tertiary II, Bunte Niederröderner Group, Cyrena Marls Group and Rupel Clay Group. The Upper Tertiary I Group to Cerithium Group interval is underestimated (Fig. 55). The reconstructed geodynamic heat flow again indicates maximum rates during Late Miocene (5.3–7 Ma) and during Late Eocene to Early Oligocene (28.7–33.1 Ma) (Table 1, Fig. 54).

For well W 16, the optimized palaeothermal trend matches calibration data of the Upper Tertiary II, Rupel Clay Group and the Pechelbronn Group (Fig. 55). The intermittent Upper Tertiary I to Meletta Group indicate elevated maturities that cannot be reconstructed using only basal, conductive heat flow. Heat flow rates are varying over the rifting period similar to the other wells. Much higher heat flow rates were reconstructed for the Late Miocene for well W16 (Table 1, Fig. 54). These results indicate that the heat flow within the URG was not only varying through time, but also within the rift basin. Thereby the eastern graben margin seems to be affected by much higher heat flow rates during Upper Miocene (7.0–5.3 Ma) than the western graben margin (W 1) and the graben center (W10). This may be related to higher subsidence at the eastern graben boundary and half-graben development tilting towards the east in the northern URG (Fig. 33)(e.g. Schnaebele 1948, Grimmer et al. 2016). This is contrary to the present situation, where the highest heat flow affects the western margin, for example in Landau or Soultz-sous-Forêts (Vosges, France)(Vidal et al. 2015, Agemar 2014).

Table 1: Paleo Water Depth, Sediment/Water Interface Temperature and Heat Flow for the simulated wells The maximum heat flow rates were reached during the Late Miocene (5.3-7 Ma) and during Late Eocene to Early Oligocene (28.7-33.1 Ma).

Age (Ma)	PWD (m)	SWIT (°C)
W1, W10 & W16		
0	0	13
1.6	3	14
5.3	0	14
10	0	16
16.2	0	18
18.3	5	19
20	5	19
22.2	10	19
23.9	30	19
24.5	30	19
26.4	45	19
28.7	65	19
29.9	65	21
31.32	100	21
33.1	150	21

Age (Ma)	HF (mW/m²)	HF (mW/m²)	HF (mW/m²)
	W1	W10	W16
0	72	72	72
1.6	72	72	72
5.3	80	80	95
7	80	80	90
10	74	74	74
16.2	72	72	72
18.3	73	73	73
20	73	73	73
22.2	73	73	73
23.9	72	72	72
24.5	72	72	72
26.4	75	75	75
28.7	85	85	85
29.9	91	91	91
31.32	96	96	96
33.1	105	105	105

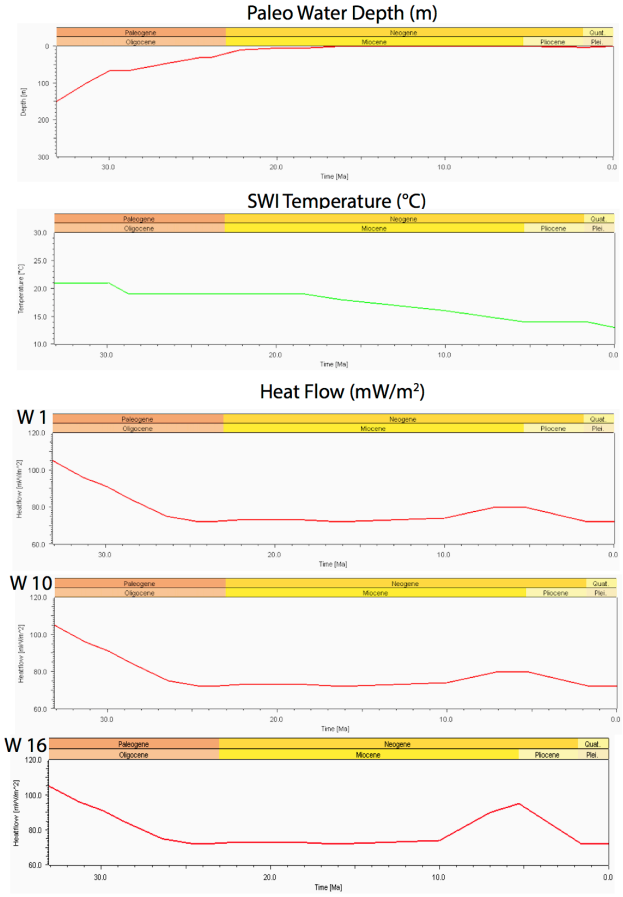

Figure 54: Input parameters and boundary parameters for the simulated wells W1, W10 and W16. Note the two phases of elevated heat flow during Oligocene and Late Miocene to Early Pliocene.

As illustrated in all three one-dimensional numerical simulations, the majority of calibration points below ~500 m down to ~2000 m depth, which mainly belong to the formations of the Upper Tertiary I to Cyrena Marls Group, is by far underestimated by the simulation. Thus, these intervals, comprising most of the sediment succession, are affected by a secondary thermal overprint that cannot be explained by using only a geodynamic basal (conductive) heat flow. As wells selected for the simulation have been drilled near major, deep-routed fault zones,

hydrothermal overprint is proposed to explain the elevated heat flow, as will be discussed in more detail in Chapter 10.3.. Although these effects cannot be modeled using one-dimensional numerical simulations, the misfit of the observed and modeled temperature evolution in much of the successions clearly shows the strong effects of this important additional factor. Increased heat flow along fault zones is a common phenomenon in the URG and elsewhere, for example in the Lower Saxony Basin (Wüstefeld et al. 2017). In the southern URG for example, elevated heat flow anomalies of 160 mW/m² and even reaching 300 mW/m² are described, associated with fault zones near the graben center (Illies et al. 1981, Person & Garven 1992), whereas lower heat flow rates of 60 mW/m² or even 30 mW/m² are reached along the graben shoulders (Clauser 1989). These anomalies are too high and too unevenly distributed to be accounted for solely by crustal doming (Lampe 2001).

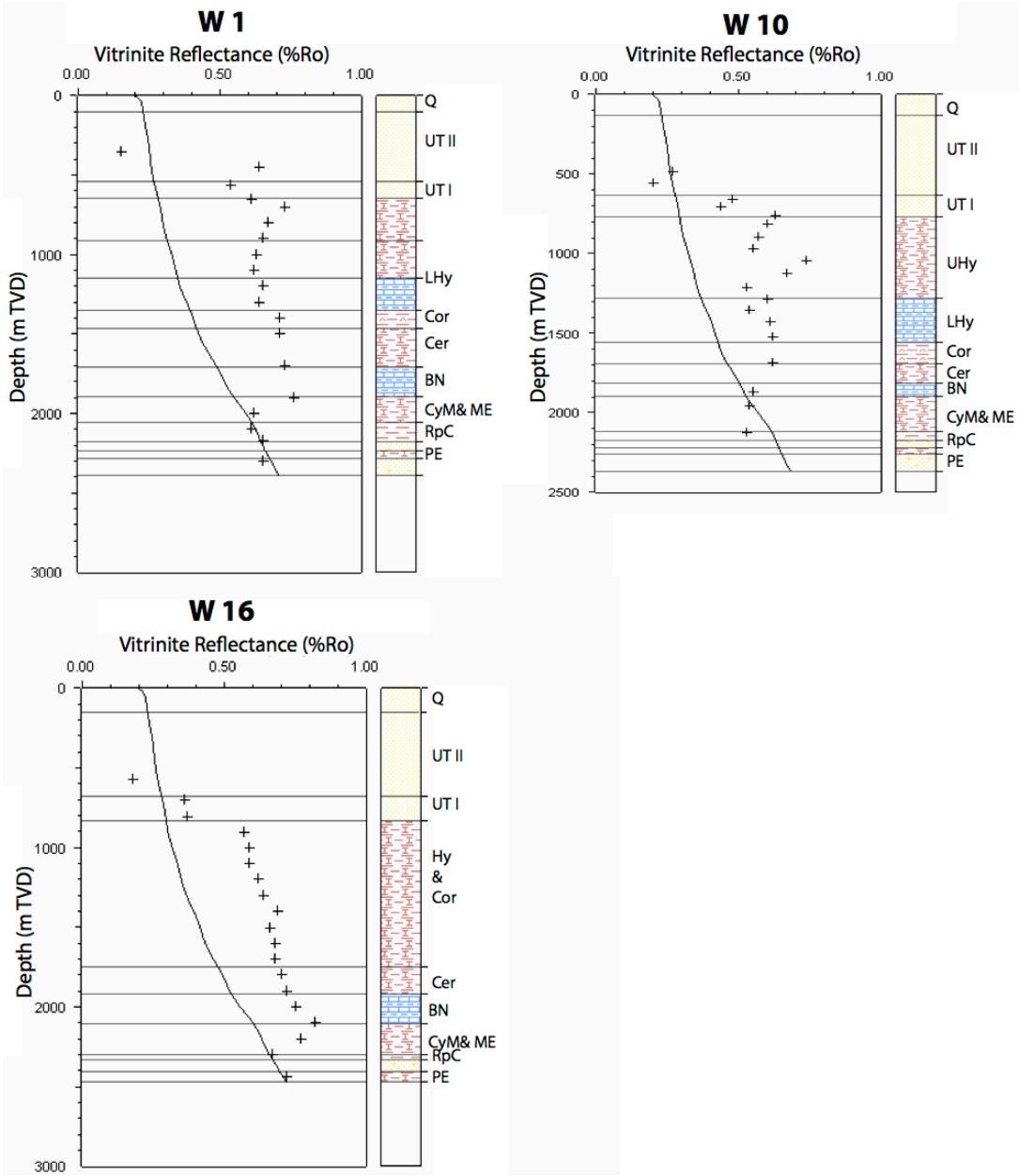

Figure 55: 1D simulations of VR maturation trends with depth for wells W1, W10 and W16. Crosses indicate VR calibration data.

Basin evolution is driven by subsidence and accommodation space. Using PetroMod® 1D, the subsidence history of the simulated wells is reconstructed. The variations of the subsidence rates through rift evolution are shown in Fig. 56 for the simulated wells W1, W10 and W16. Well W1, which was drilled into a small pull-apart basin within the northernmost URG, evidences high but fairly constant subsidence. The hiatus between the Upper Tertiary II and the Upper Tertiary I is thereby modeled by a phase of non-deposition and non-erosion. Well W10 is located on a hanging wall block in the graben center. This well does not reflect constant subsidence, but rather a multiphase subsidence history. Well 16, which represents the eastern graben margin, also indicates a multiphase subsidence history. The main subsidence phases in these wells do not correlate with the subsidence history of the graben center. Instead, a fairly long phase of non-deposition and non-erosion existed during the Late Oligocene to Early Miocene. The hiatus between the Upper Tertiary II and the Upper Tertiary I is thereby modeled with minor sediment deposition and erosion (50 m) for both wells W10 and W16.

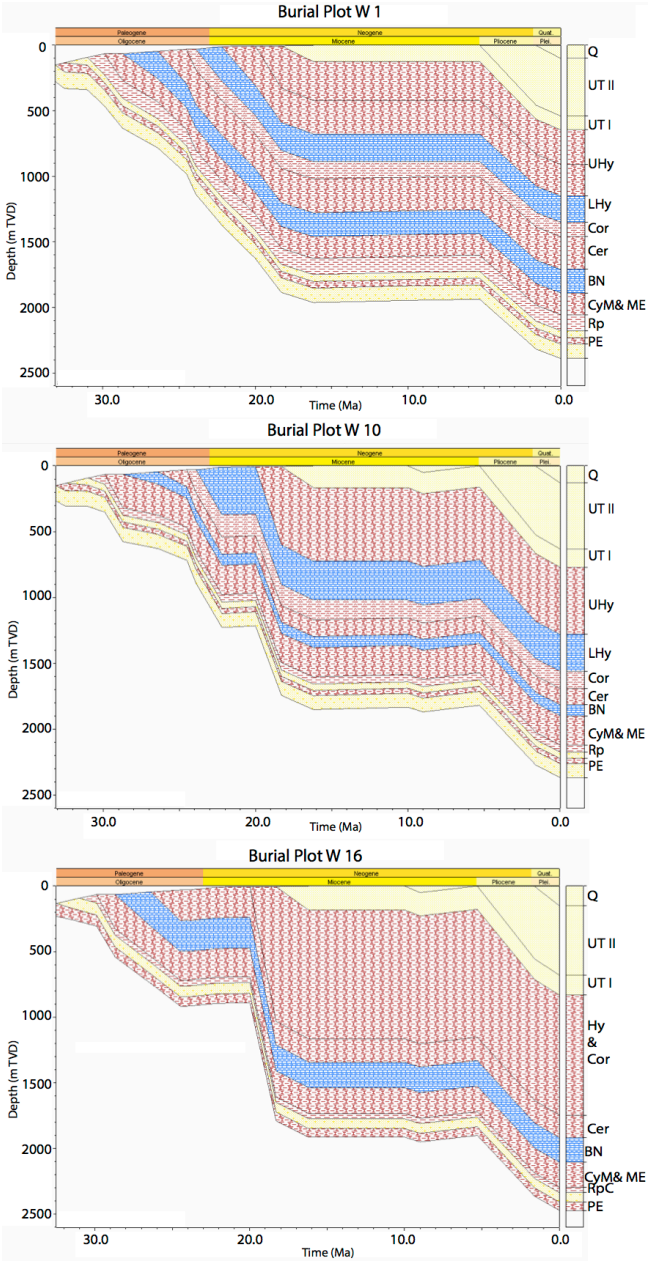

Figure 56: Burial plots for wells W1, W10 and W16

10. Discussion

10.1. Palaeoenvironment Conditions

10.1.1. Pechelbronn Group

A proximal-oxic setting of the **Lower Pechelbronn Formation** of the northern URG is here interpreted from palynofacies analysis. This interpretation is consistent with the fluvial-terrestrial setting assigned to this interval by Gaupp & Nickel (2001) and Derer (2003). Based on previous studies (Derer 2003, Perner 2014), indications of the first marine transgression (Hardenbol et al. 1998) are interpreted to have occurred in the uppermost Lower Pechelbronn Formation as found in wells W10 (and W31). Synsedimentary tectonic activity was particularly important during this time. As the Pechelbronn Formation was deposited during the first main phase of subsidence and rifting (Derer 2003), high amounts of terrestrial material were transported into the graben. This included terrestrial OM consisting in high amounts of terrestrial derived phytoclasts, AOM (degraded phytoclasts) and sporomorphs. The main input of sediment was derived from a less uplifted segment of the western border fault (Derer 2003). Additional but minor sediment input from the eastern graben shoulder is indicated in well W10 by the occurrence of quartz with magmatic-metamorphic origin, eroded from the Odenwald Massif (Perner 2014). Synsedimentary tectonic activity is manifested in high thickness variations of the Lower Pechelbronn Formation. Thicknesses are in the range of ten's of meters along the northern transfer zone (Derer 2003) and up to 330m in the Karlsruhe area (well Hagsfeld: Doebl 1967, Wirth 1969). Besides the basin-wide subsidence, where the depocenter during Pechelbronn times was located in the central URG (e.g. Grimm et al. 2011), also synsedimentary tectonic activity along reactivated pre-rift faults and newly formed major fault zones played a major role for sediment thickness distribution. The latter process led to the development of tilted fault blocks, sediment wedges and half graben structures in the northern URG. High thickness variations over a few 100s of meters lateral distance are found e.g. in wells W9 and W10 due to synsedimentary tectonic activity along the Stockstadt fault.

Palynofacies results for the **Middle Pechelbronn Formation** do not completely fit the widely established model of the first Cenozoic marine transgression in the URG. Even though high fractions of fine grained claystones and marlstones support the established model of a transgression prograding from the Palaeogene North Sea via the "Hessische Senke" (Grimm et al. 2000, Grimm & Grimm 2003, Grimm 2005), OM composition indicates a very distinct influence of rift-related, terrestrially derived OM and suggests rather proximal-oxic settings. The best indications for marine conditions are found in wells W10 and W16, which represent topographically deeper structures and thus more accommodation space and higher water depth compared with the rest of the studied wells. A propagation of the sea through the "Hessische Senke" along the eastern side of the northern URG appears likely. Berger et al. (2005) suggested that no marine connection existed at that time with the Alpine Sea, despite marine environments in the northern, central and southern URG. Comparable to the Lower Pechelbronn Formation, terrestrial OM input is derived mainly from the western-, and to a much smaller extent from the eastern graben shoulder. Even though the synsedimentary tectonic activity seems to have

decreased when compared with the preceding time (e.g. Grimm et al. 2011), high sediment thickness variations identified in the Middle Pechelbronn Formation. Variations in sediment thickness ranging from <5 m to > 50 m are described from the area of Eich-Königsgarten (Gaupp & Nickel 2001).

Palynofacies data of the **Upper Pechelbronn Formation** suggests a strong terrestrial influence with distinct lateral changes of the palaeoenvironment. In contrast to the Middle Pechelbronn Formation, the Upper Pechelbronn interval was deposited during a regressive phase (Hardenbold et al. 1998). Brackish-marine influence was present only intermittently due to short-term connection with the North Sea. Our data confirm that a strong terrestrial influence existed; it is therefore difficult to precisely distinguish between brackish-marine and terrestrial conditions. Based on the results presented by Gaupp & Nickel (2001), a delta/shoreface system prograded from the western graben shoulder into the graben. Distant from this delta/shoreface system, the amounts of terrestrial OM are reduced. The dominant sand intervals of the Lower and Upper Pechelbronn Group shows excellent reservoir properties and provide the most important reservoir rocks, productive in fields such as Eich, Stockstadt, Wattenheim, Hofheim and Schwarzbach (e.g. Straub 1956, 1962).

10.1.2. Rupel Clay Group

Palynofacies results in the northern URG reveal partly high variations in depositional setting and palaeoenvironmental conditions. These observations differ from the established model for the Rupel Clay Group in the central and southern URG and adjacent Mainz Basin (Grimm et al. 2011, Grimm 1991, Grimm et al. 2002), where the interval is assumed to consist of homogeneous offshore shales and marlstones deposited under more open marine conditions. OM composition in the study area is not homogeneous and neither the Foraminifera Marls Formation nor the Fish Shale Formation is dominated by a typically marine composition. The occurrence of sporomorphs within the entire Rupel Clay Group is in line with the results from Nickel (1996) and indicates the proximity of the system to the graben shoulders.

The Foraminifera Marls Formation has been described in literature as deposits of a fully marine, oxygenated milieu with good connections to the open sea and excellent life conditions (Martini 1990, Grimm et al. 2000, Grimm et al. 2011). At the base of the Foraminifera Marls Formation, Nickel (1996) describes the occurrence of marine dinoflagellates. The results presented in this study indicate, that despite the presence of dinoflagellate cysts, which suggest distal-oxic conditions, distal to restricted marine and anoxic conditions established during deposition of the Foraminifera Marls Formation within large areas of the northern URG, as can be inferred form the dominance of fluorescent AOM, acritarcs and prasinophytes (Fig. 35).

After a sea level stasis during the initial Fish Shale Formation, sea level rose again (Grimm et al. 1999, Nickel 1996) and normal marine conditions were re-established (Grimm 1991). Water depths of 200 to 300 m are postulated by Grimm et al. (2011). However, the results in this study indicate mostly restricted marine conditions in the study area. “Normal marine” oxic conditions established only in well W7 in the graben center based on palynofacies composition (Fig. 34).

Palynofacies data presented here from the northern URG suggest that not the Fish Shale Formation, but the Foraminifera Marls represent the main marine phase. During deposition of the Fish Shale Formation marine OM was mixed with high amounts of terrestrial phytoclasts and sporomorphs.

A sharp petrological boundary is reported from the eastern border of the central graben, between the Foraminifera Marls Formation and the overlying "bituminous" and finely laminated Fish Shale Formation (Micklich & Hildebrandt 2005). Well log GR data indicate, that this boundary is marked by a sand-dominated interval. Due to the wide sampling rates of the cuttings this boundary couldn't be observed in the rock samples. Core material was not available.

Although a deltaic/shoreface system is only reported for the (Upper) Pechelbronn deposits, palynofacies results from this study clearly indicate that terrestrial sediment and OM transport were still ongoing during deposition of the Rupel Clay Group. Terrestrial sediment input from areas outside the graben is indicated by the high continental OM content (phytoclasts, sporomorphs, lacustrine algae), which was most probably transported fluvially into the graben. Also Derer (2003) presumed that the first major phase of rifting/subsidence still continued at this time. The presence of bisaccate pollen (sporomorph group) in all studied wells (Fig. 13) is probably caused by largely aeolian transport from the graben shoulders into the basin (Tyson 1995, Traverse 2007). Under consideration of the assumption by Grimm (1994), that fresh water influx during the deposition of the Rupel Clay Group played a role only locally within the URG, it can be assumed, that the high amounts of continental OM were brought into the graben from only few "sediment entry points" from the graben shoulders (Derer 2003). The occurrence of phytoclasts, sporomorphs and lacustrine algae in all studied wells suggest that the OM was transported via fluvial transport into the graben, transported via water currents within the marine system and re-deposited even >10 km from the graben shoulders into the graben center.

10.1.3. Meletta Group, Cyrena Marls Group, Bunte Niederröderner Group and Cerithium Group

During the deposition of the Meletta Group a marine connection existed between the North Sea and the gradually more restricted Paratethys in the South. Despite on-going graben subsidence and further transgression in the northern URG, brackish conditions established due to high sediment influx (Grimm et al. 2005, Grimm et al. 2011). Most palynofacies samples in the study area illustrate proximal conditions with rather high terrestrial OM input, which confirms the high sediment input of terrestrial OM from the hinterland into the graben. Neither the eastern nor the western graben shoulder can be determined as dominant erosive source area.

The overlying Cyrena Marls Group was deposited in a brackish to brackish-marine environment (Rothausen & Sonne 1984, Reichenbacher 2000, Grimm et al. 2011). From the south, fluvial sediments were transported into the northern URG (Rothausen & Sonne 1984, Grimm et al. 2011), which can be confirmed by the presence of continental OM such as phytoclasts, sporomorphs and lacustrine algae in the graben (Fig. 17). A shallow marine connection is inferred of the northern URG with the North Sea via the Hessische Senke (Rothausen & Sonne 1984). Palynofacies data confirm a brackish-marine setting with mostly restricted marine-

anoxic conditions (dominance of fluorescing AOM) and only frequently distal-oxic conditions (dominance of dinoflagellates) (Fig. 36).

Deposition of the Bunte Niederröderner Group took place under limnic-fluviatile conditions with assumed high terrestrial sediment input (Schad 1964, Straub 1962, Grimm et al. 2011). In the northern URG this terrestrial sediment input is low, although certain amounts of fluorescing AOM that are normally interpreted as brackish-marine AOM in presence of phytoplankton, might actually represent degraded lacustrine algal material; they may therefore be assigned to the continental OM group. Nevertheless, palynofacies data reveal a distinct marine influence in some samples indicated by dinoflagellates. The OM composition therefore suggests an at least temporarily restricted marine setting under overall anoxic conditions.

The overlying Cerithium Group were deposited during the second Chattian transgression (Hardenbol et al. 1998), which enabled an intermittent connection to the North Sea Basin (Grimm & Grimm 2003, Grimm et al. 2011). OM composition suggests deposition in a rather distal setting, because of the influence of the transgression on palynofacies. The restricted marine conditions in the study area reconstructed from palynofacies, agree with the proposed brackish-marine setting of the Cerithium Group (Prell-Müssig 1965, Schwarz 1997).

10.1.4. Corbicula Group

The Corbicula Group was deposited during a regressive phase, under lagoonal conditions in a rather isolated basin (Kadolsky 1988, Grimm & Grimm 2003, Grimm et al. 2011). Terrestrial OM is particularly abundant in the lower part of the formation. Only wells W10 and W8 indicate higher amounts of terrestrial OM in the upper Corbicula Group. This increase of terrestrial and decrease of marine OM provides evidence for increased terrigenous sediment supply, caused by the second major phase of subsidence/rifting. The normal marine signatures in the lower part of the Corbicula Group in wells W10 and W8 can be explained by sediment bypassing the two wells situated on the hanging wall. All other wells indicate increased amounts of terrestrial OM. Only at the top of the Corbicula Group increased amounts of marine AOM as well as phytoplankton and decreasing amounts of phytoclasts indicate a new transgression. From the northern URG high variations in salinity (limnic to hypersaline) are reported (Wagner 1947, 1955). Salt layers in the area of Worms suggest brine influx from the central and southern URG (Wagner 1947, 1955, Schad 1964, Grimm et al. 2011). Abnormally high salinities, as they are evidenced by phytoplancton assemblages with high amounts of acritarcs, have been found in few samples from the well W8 and the eastern wells W12 and W14.

10.1.5. Hydrobia Group

Deposition of the Lower and Upper Hydrobia Formations took place in a limnic-brackish setting (Schad 1964, Grimm et al. 2011). The unit was intermittently connected with the North Sea as indicated by short-term brackish-marine ingressions and changes in salinity (Grimm et al. 2011). Palynofacies results suggest overall anoxic conditions for the deposits of the Hydrobia Group. The aquatic setting is restricted marine-anoxic, as it is typical for brackish-marine ingressions. Oxic conditions are (especially in the Lower Hydrobia Group) mostly restricted to wells located along the eastern graben shoulder. This may be related to higher subsidence rates

along the eastern graben (Doebl 1967), which led to higher accommodation space and thus to higher water depth and more oxic, "open marine" conditions. The changes in salinity as Grimm et al. (2011) describe them for the Hydrobia Group are confirmed only for the Upper Hydrobia Formation by the presence high amounts of acritarcs is few samples (e.g. from wells W1, W14, see Appendix 1). Few samples from the Lower Hydrobia Formation suggest deposition in a proximal setting, as indicated by high amounts of terrestrial OM (phytoclasts, non-fluorescent AOM and sporomorphs) (Fig. 24, 39). This is most probably related to the second major phase of rifting/subsidence in the northern URG. Higher subsidence within the graben led to higher accommodation space and thus to the deposition of eroded terrestrial sediments and OM from the graben shoulders.

Also in the Upper Hydrobia Formation, elevated amounts of terrestrial OM are present in few samples from the northern wells W1 and W2, as well as wells along the eastern graben border (W2, W12, W14)(Fig. 25, 41). This can be ascribed to sporadic input of terrestrial OM from the graben shoulders. Inner graben wells were apparently not affected by this terrestrial OM influx.

10.2. Hydrocarbon Potential

The combination of both kerogen analysis and maturation analysis provides the possibility to precisely estimate the HC potential in the northern URG. Considering the rapid lateral changes in palaeoenvironmental conditions, it must be kept in mind that the resulting source rock qualities may change rapidly over small-scale distances and even from one to another individual structural blocks, e.g. footwalls or hanging walls.

10.2.1. Pechelbronn Group

The Lower and Upper Pechelbronn Formations are known to represent favorable reservoir units (e.g. Böcker et al. 2016), e.g. in the oil fields of Eich, Stockstadt and Schwarzbach. Their source rock potential in the northern URG is low due to low clay contents, similar to the central URG (e.g. Welte 1979). A moderate source rock potential has been assigned to the Middle Pechelbronn Formation by Gaupp & Nickel (2001) and Derer (2003) in the northern URG. The subunit contains a moderate source rock potential in the central URG, with consistent TOC values of 1.0–1.5 %, type II/III kerogen and HI values of 140–220mg HC/g TOC (Espitalié 1979). In the present study of the northern URG, only few samples could clearly be attributed to the Middle Pechelbronn Formation. Their TOC values are low, ranging between 0.3–0.6 %; they show almost pure type III/IV kerogen and HI values of 30–113 mg HC/g TOC. These data indicate, that the Middle Pechelbronn Formation is much stronger influenced by the input of terrestrial, gas-prone type III kerogen than this is the case in the central URG.
The Pechelbronn Group in the northern URG thus indicate mainly gas-prone/ barren type III/IV kerogen and only small amounts of oil-prone type (I-/)II kerogen. HI values range from 30–112 mg HC/g TOC in the southern wells of the study area (W31, W19 and W16) and from 30-112 mg HC/g TOC in the northern wells (W1, W10, W9, W7). Similar to the northern URG, also from the

central URG a type III/IV kerogen composition and HI values of 50–110 mg HC/g TOC (Bruss 2000) are reported. Therefore kerogen distribution seems to be quite homogenous throughout the URG, with a slight increase in type II kerogen towards the northernmost URG, while type III kerogen still dominates. Also TOC values seem fairly consistent throughout the northern and central URG: samples from the northern URG do not exceed 2.6 % (except for one sample from well W19, which reaches 5.9 %), while TOC values of 0.2-3.0 % are reported from the central URG (Welte 1979).

As maturation of the Pechelbronn Group only reaches the basal to middle oil window in most parts of the study area (Fig. 51), only a minor expulsion of HC is suggested for the Middle Pechelbronn Formation. The highest maturities of up to 0.88 %Ro are reached in the southern wells W35 and W31 and W33, which are located at the vicinity of the northern edge of the Heidelberg-Mannheim Basin. Elevated maturities are also present in the northernmost well W1 (0.65 %Ro), which represents a small pull-apart basin within the URG, and along the eastern graben shoulder in wells W14 and W16 (both 0.72 %Ro). These elevated values correlate with areas with higher subsidence and thus higher depth of the Pechelbronn Group, as the base map (Base Cenozoic) shows. Lower maturities in the basal oil-window (0.51–0.63 %Ro) were measured in wells with lower subsidence. These results suggest a burial controlled maturation trend for the Pechelbronn Group. Hydrocarbons were most likely formed in the areas with high subsidence. Taking into account the results from kerogen analysis, the best oil potential is assigned to in the easternmost wells W12, W14 and W16. Even though maturities are slightly lower than in the southernmost wells W31 and W35, the amounts of oil-prone type I and type II kerogen are highest (Fig. 11).

10.2.2. Rupel Clay Group

The Rupel Clay Group, especially the Fish Shale Formation, is considered to represent the main source rock of the central and northern URG (Rückheim 1989, Bruss 2000, Böcker & Littke 2014). For the latter this is only partly correct. Kerogen analysis from the central URG suggests a purely oil-prone type II kerogen based on geochemical analyses (Langford & Blanc-Valleron 1990, Böcker & Littke 2014). The results presented in this study for the northern URG reveal a type III (and even type IV) kerogen dominance, implying a much higher gas-, rather than oil generation potential, due to the higher input of terrestrial OM. The highest amounts of oil-prone type I/II kerogen are reached in the Foraminifera Marls Formation in the northernmost well W1 and on the eastern side of the Stockstadt fault.

HI values of the Rupel Clay in the central URG range around 500–550 mg HC/g TOC. In the northern URG wider ranges of HI values of 95–309 mg HC/g TOC (Fish Shale Formation) and 44–413 mg HC/g TOC (Foraminifera Marls Formation) were measured, suggesting a more inhomogeneous kerogen composition. These contents are similar to the HI values published by Rückheim (1989) for the northern URG, reaching 47–540 mg HC/g TOC. Geochemical results confirm a complex kerogen composition for the Rupel Clay Group in the northern URG, which is observed in optical analysis.

In terms of OM quantity, the Fish Shale Formation from the central URG shows TOC values in the range of 3.0–5.0 % (Böcker et al. 2016, Böcker 2016) and 0.5–4.3 % (Welte 1979). In our samples from the northern URG, TOC values do not exceed 3.0 % and mostly range around 0.75–1.8 %. This reveals the generally lower and higher variable OM content in OM content of the Fish Shale Formation in this part of the graben. In contrast to the central URG, the Foraminifera Marls Formation reach increased TOC values of up to 3.32 %. This is evidence of the somewhat higher source rock potential of the Foraminifera Marls Formation in the northern URG compared to the Fish Shale Formation. Rückheim (1989) reports a mean TOC of 2.5 % for the Rupel Clay Group.
Maturation does not exceed the middle oil-window in the study area (0.40–0.80 %Ro) (Fig. 51). Similar to the Pechelbronn Group, the highest maturities are assigned to the wells with highest subsidence, suggesting burial controlled maturities for the Rupel Clay Group. The highest maturities of 0.63–0.80 %Ro assigned to wells W 35 (northern edge of the Heidelberg-Mannheim Basin), wells W12 and W14 (eastern graben margin) and well W1 (small pull apart basin in the northernmost URG). Taking into account the higher amounts of gas-prone kerogen, and lower TOC contents of the Rupel Clay compared to the central URG, the HC generation potential is expected to be lower than in the central URG. Yet, highest maturation is identified in wells, which also provide highest amounts of oil-prone kerogen (Fig. 14). Thus, (minor) oil generation likely existed along the eastern graben border and in the well W1 pull-apart basin, as also indicated by the Rock Eval parameter PI. In addition, high sulphur contents are measured in the Rupel Clay, which favor an early generation of hydrocarbons. Bruss (2000) links the high sulphur contents to type IIS kerogen, which generates hydrocarbons at lower temperatures. Even though these assumptions were made for the Corbicula group and Hydrobia Group, they are well applicable for the Rupel Clay group as well (pers. comm. Bruss, D.).

10.2.3. Meletta Group, Cyrena Marls Group, Bunte Niederröderner Group and Cerithium Group

Based on integrated kerogen analysis, which reveals high amounts of type III/ IV kerogen (Figs. 18, 20), and low TOC (0.5–0.7 wt.%), no significant amounts of HC can be expected from the Meletta Group and Cyrena Marls Group, despite maturation levels in the basal oil window. Compared with data from the central URG, the HC potential in the northern URG seems to be even poorer. Studies from the central URG indicate insufficient quantity and quality of organic material for these intervals (Bruss 2000), with TOC values of 0.4–3.0 %, type III kerogen composition and HI values of 50–180 mg HC/g TOC. These measurements refer to argillaceous intervals with coaly plant residues but do not reflect dominant lithological composition (e.g. Bruss 2000). Despite the low source rock potential of the Meletta Group and Cyrena Marls Group in the northern URG, reservoir properties of these units dominated by carbonate and clay are also minor.
For the overlying Bunte Niederröderner Group, a moderate oil generation potential is suggested for the fine-grained siliciclastic samples studied in this thesis, yet these lithologies are rare and HC generation potential of the unit is expected to be low. No source rock qualities are known from the URG.

In the study area, the Cerithium Group contains moderate amounts of oil-prone type I and type II kerogen, yet low TOC, which minimizes the source rock potential of the unit. Also this interval is dominated by silty/calcareous lithologies. In the central URG, the Cerithium Group has not been discussed to date in terms of their source rock potential. In this area, sandy intercalations occur mainly along the graben margins and may there act as potential reservoirs for HC, despite their sporadically occurrence and low thickness (Schad 1964). The potential of the Cerithium Group as a reservoir or source rocks unit is therefore negligible despite maturation in the basal oil window in the northern URG.

10.2.4. Corbicula Group

The results from this study are consistent with published data from the northern URG. For the areas of Eich, Stockstadt, Wolfskehlen, Pfungstadt, Frankenthal and Dudenhofen, the Corbicula Group and the overlying Hydrobia Group are characterized as favorable gas source rock units (Schad 1962). Also, small amounts of oil were detected in the area of Frankenthal and Worms (Schad 1962). Within the study area, HC potential of the Corbicula Group is characterized by moderate to high TOC (up to 2.4 wt.%), mixed kerogen type composition and HI values of up to 414 mg HC/g TOC. In the central URG, slightly higher TOC values of up to 3.0 % are reported. The organic material of the Corbicula Group consists of a mixture of primary type-IIS-kerogen (with elevated sulphur content) and secondary type III kerogen with variable HI (95–505 mg HC/g TOC) (Bruss 2000).
Maturation does not exceed the basal (to middle) oil window (Fig. 51). In consequence, minor amounts of oil may have formed in the study area. High sulphur contents of up to 3.8 wt.% may again favor the expulsion of hydrocarbons at lower temperatures (Bruss 2000).

10.2.5. Hydrobia Group

A good gas source rock potential has been described for the Hydrobia Group from the area of Eich, Stockstadt, Wolfskehlen, Pfungstadt, Frankenthal and Dudenhofen (Straub 1962). These results are only partly confirmed by the present study.
Based on our integrated kerogen analysis, the Upper Hydrobia Formation, but also the Hydrobia Group in general, are dominated by oil-prone type I and II kerogen. Gas-prone type III kerogen is highest in the Lower Hydrobia Formation along the eastern graben margin. In the rest of the northern URG oil-prone type I/II kerogen dominates, which is consistent with small oil occurrences in the areas of Frankenthal and Worms (Straub 1962). HI values of the Hydrobia Group from the central URG range from 95–505 mg HC/g TOC (Bruss 2000). Hi data from the northern URG correspond well, with similar HI values of 86–487 mg HC/g TOC for the Lower Hydrobia Formation and 227–592 mg HC/g TOC for the Upper Hydrobia Formation. This suggests a fairly homogenous kerogen composition throughout the URG. Also, TOC values of 0.6–3.0 % in the study area are similar to the central URG, where TOC reaches also up to 3.0 %.
Maturation of the Hydrobia Group is in the early to mid oil-window throughout the study area (Fig. 51): maturities of the Lower Hydrobia Formation range from 0.55 to 0.66 %Ro, the Upper

Hydrobia Formation reaches maturities of 0.48–0.7 %Ro. These maturities are high compared to the deeper buried sediments of the Pechelbronn Group and Rupel Clay Group, suggesting secondary overprint of burial controlled maturation of the Hydrobia Group. Highest maturation is detected along the Eastern graben shoulder and in the northernmost well W1. High sulphur contents (type IIS-kerogen) are present in the Lower Hydrobia Formation of the northern URG, which may have favored the generation of hydrocarbons (Bruss 2000).

10.3. Maturation Trends and Hydrothermal Anomalies

Fig. 57 illustrates the maturity trends based on VR for the studied wells. Additional VR data are included from the literature (Rückheim 1989, Lampe 2001). These additional maturation data fit well with the VR data from this thesis. It is important to note that maturation levels exceed burial depths and the "normal", burial-controlled subsidence trend in many samples. Only few samples may represent values of an in-situ, "basal heat flow controlled" maturation trend, as illustrated by numerical modeling (Chapter 9). The simulations clarify that conductive, basal heat flow alone cannot be responsible for the maturity level that is observed in the Cenozoic sediment succession studied here. These thermal anomalies, which affect almost the entire Cenozoic succession, start in 500 m depth or even above, in some wells within the Upper Hydrobia Formation (e.g. wells W16, W31, W12, W8), but in other wells also within the Upper Tertiary I or II (e.g. W1, W10, W29) (Figs. 57, 58).
In Fig. 58, the interpreted maturity trends with depth are displayed along with a subsidence controlled maturity trend as would be normally expected. The interpreted maturity trends for the studied wells are based on VR analysis, which are corroborated by other maturity data retrieved from SCI and Rock-Eval Pyrolysis, as can be inferred from Figs. 42–50. Because all maturation parameters indicate the same maturation level, VR data can be considered as reliable and do not represent e.g. reworked material brought into the basin from the hinterland and graben shoulders. With the specific refined method of VR measurements in this study, reworked material can clearly be avoided when taking the measurements. Even though wells W12, W14 and W16, which are located near the eastern graben border, indicate a slight increasing maturation with depth, VR is still much too high for burial-controlled maturation (Fig. 58). These trends are difficult to explain using conventional heat flow models. At least for wells W1 and W16, this is also shown by one-dimensional modeling (Fig. 55), which clearly indicated that the maturities within the Cenozoic sediments cannot be reached using solely conductive (basal) heat flow (see above).

Thermal anomalies are a well-known phenomena from the northern URG (Lampe & Person 2000), and the southern URG (Timar Geng et al. 2004), but also from sedimentary basins worldwide (e.g. Frings et al. 2004, Wisian & Blackwell 2004), even though the causes may be different.
One possibility to explain the elevated maturation stages observed in the results from the northern URG is volcanic activity. Yet, the volcanic activity known from the northern URG ends

in the early Eocene, prior to beginning of rifting in the URG (Keller et al. 2002). None of the investigated wells penetrated any volcanic rocks younger than early Eocene. Hence, the thermal event proven by VR and other maturation data must be unrelated to magmatic intrusions. Miocene volcanic activity is limited to the southern URG (Baranyi et al. 1976) (Fig. 5).
Another hypothesis to explain the thermal anomalies would be excess overburden and subsequent erosion during the 9 Ma hiatus between the Upper Tertiary I and Upper Tertiary II, which would have led to deeper burial and thus to higher maturities in the Miocene sediments. Yet, this would have led to higher maturities in the Late Eocene to Early Oligocene sediments (Pechelbronn Group and Rupel Clay Group), which does not fit the modeling. Maturation level in these latter sediments is not related to deeper burial. In consequence, the hypothesis of additional sedimentation and erosion during the Upper Tertiary II-Upper Tertiary I hiatus appears to be highly unlikely. Also, erosion of overburden is undocumented from the northern URG. Therefore, a mere hiatus without additional sedimentation or erosion seems plausible.

Thus, to explain these results, one or possibly more secondary thermal overprint(s) of an in-situ maturation must be assumed. Hydrothermally influenced maturation is a well-known phenomenon in sediment basins (e.g. Kennard et al. 1999). The level of overprint can reach a stage, where the hydrodynamic processes of hot groundwater aquifers in sedimentary basins can have a profound effect on thermal maturation (Person & Garven 1992, Hullen et al. 1994) and may enhance petroleum generation even at shallow depths, as shown e.g. from the Gulf of California (Kvenvolden and Simoneit 1990). For the URG, the migration of hot groundwater has been proposed to cause the variations of geothermal gradients e.g. by Doebl & Teichmüller (1979). Their assumptions are well established today (Clauser & Villinger 1990, Clauser & Neugebauer 1991, Person & Garven 1992, Le-Carlier et al. 1994, Ledesert et al. 1996, Schellschmidt & Clauser 1996).

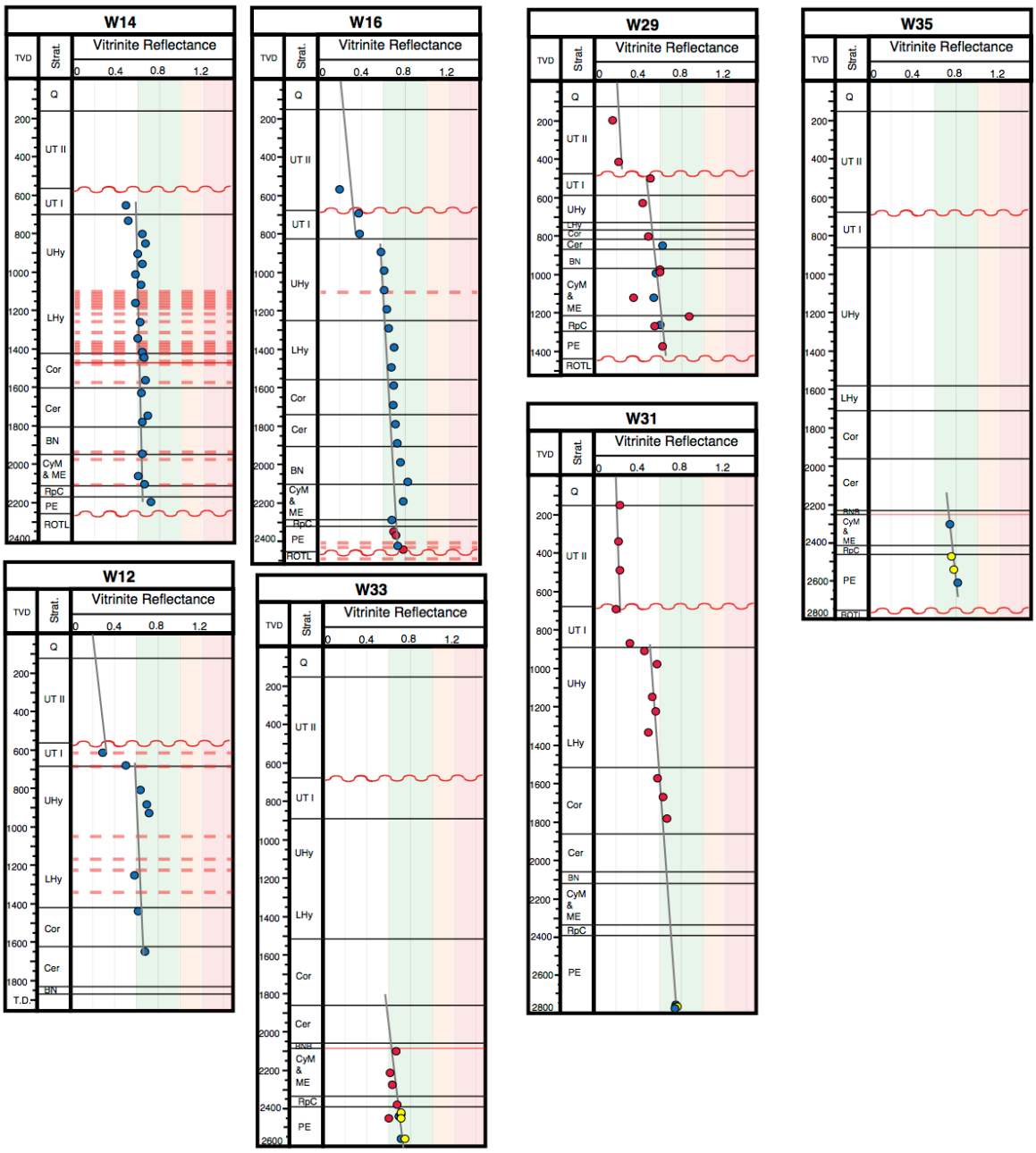
W14
W16
W29
W35
W12
W33
W31
TVD
Strat.
Vitrinite Reflectance
0
0.4
0.8
1.2
Q
UT II
UT I
UHy
LHy
Cor
Cer
BN
CyM & ME
RpC
PE
ROTL
T.D.

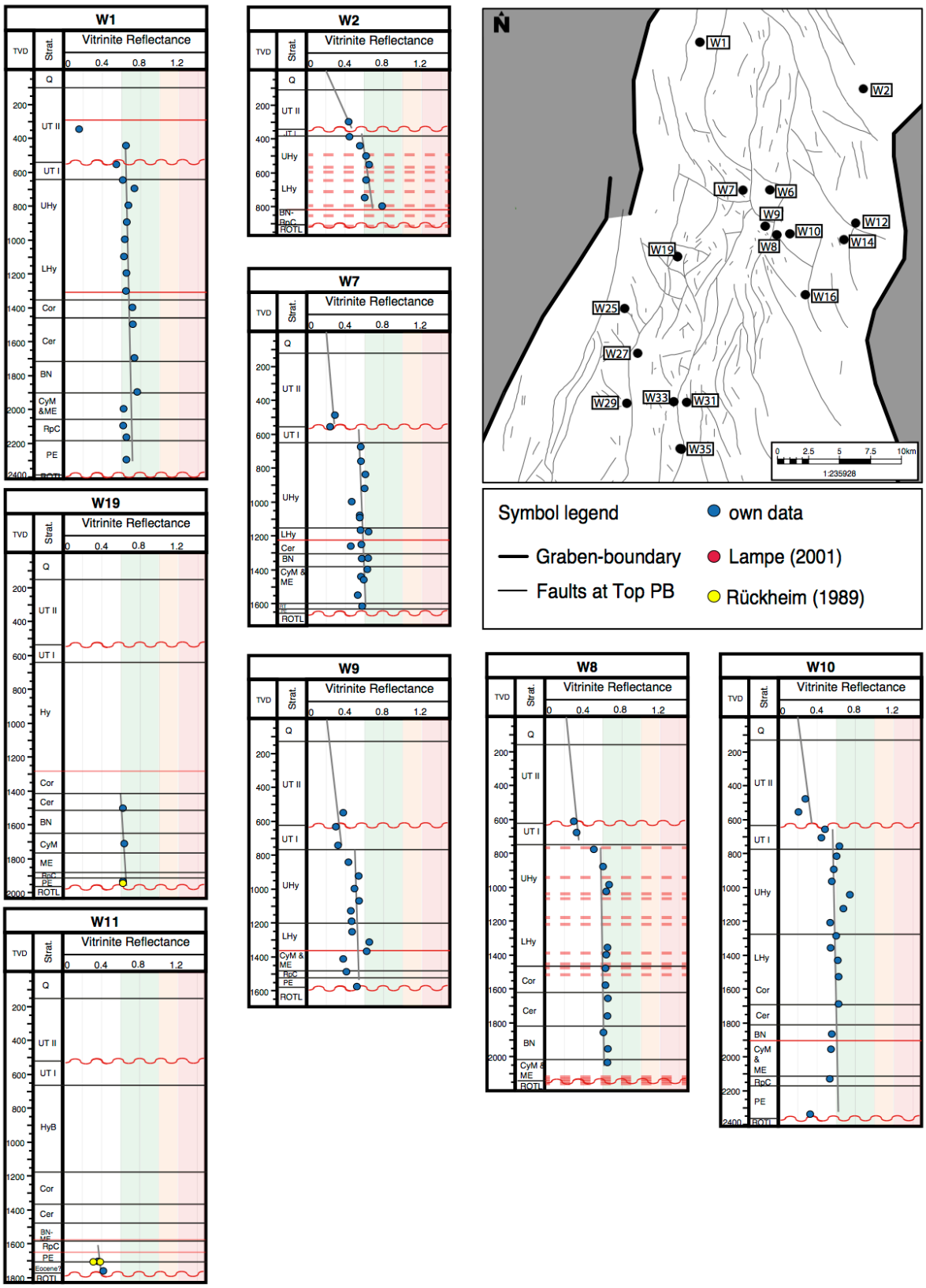

Figure 57: Vitrinite Reflectance (%Ro) variation with depth in the northern URG, including published data by Lampe (2001) and Rückheim (1989). Red lines represent major fault zones, red dotted lines indicate smaller faults (as indicated by well reports), hiatus are indicated by red wavy lines.

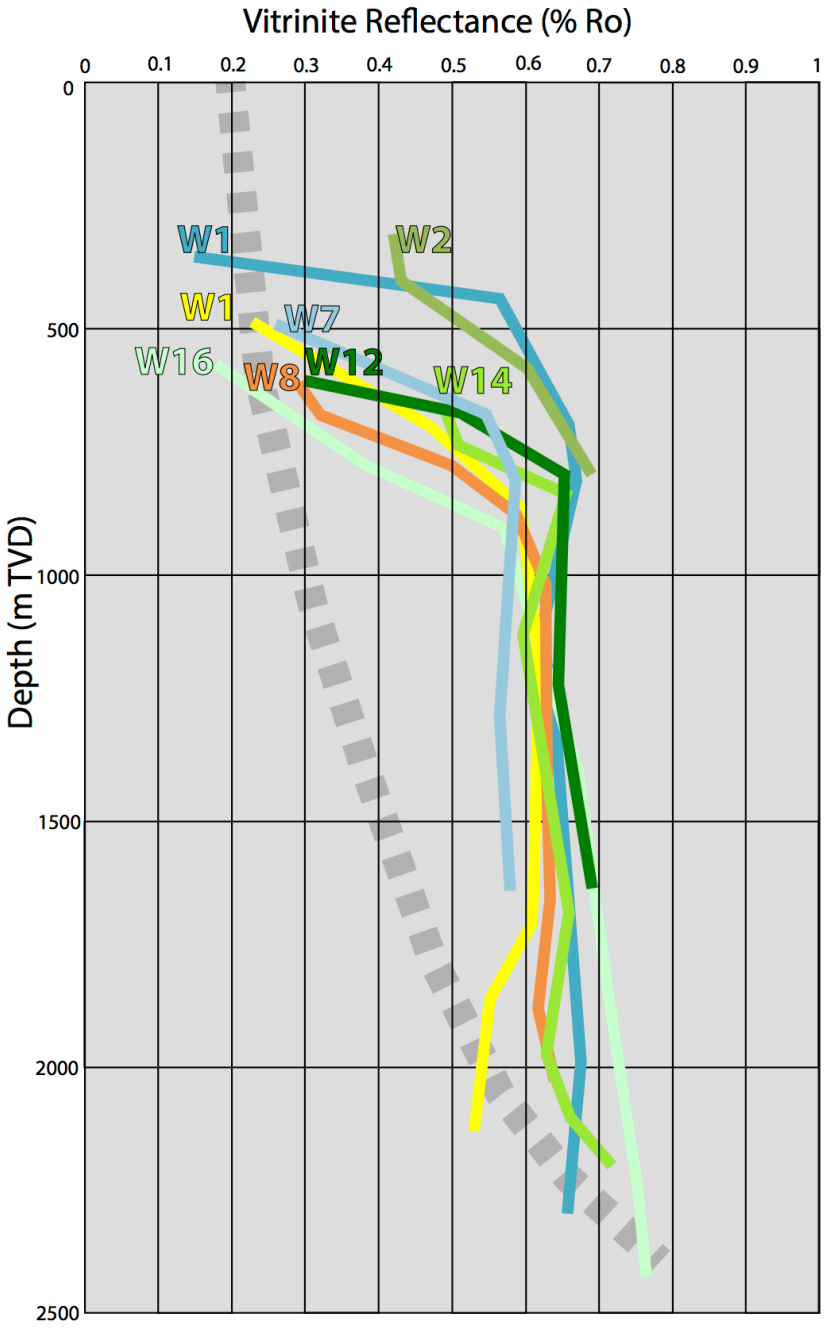

Figure 58: Ro variation with depth in selected wells, suggesting significant secondary thermal overprint in the studied wells. The grey dotted line represents a burial controlled maturation trend, as it would be expected in non-overprinted profiles (e.g. Böcker 2016). Note that even though some wells indicate overall increasing maturities with depth, samples from depths of 300/500 m to about 2000 m are too high for a subsidence controlled maturation trend.

In the northern URG, non-burial controlled maturation trends that are similar to the maturation trends presented in this thesis were previously proposed e.g. by Lampe (2001) and Lampe et al. (2001). These studies report maturity anomalies between 1000 to 1500 m depth within the Hydrobia Group and Corbicula Group in the area of wells W29, W31 and W33. These thermal anomalies are recognized in elevate maturation data such as VR data, ranging between 0.58 and 0.69 %Ro in the affected intervals. It is proposed that the elevated maturities caused by episodic lateral flow of hot groundwater along conductive fractures and bedding planes. Thereby an aquifer is presumed, which is sandwiched between two less permeable units. Vertical ascent of fluids from deep sourced groundwater aquifers in this model only plays a minor role. In a two-

dimensional numerical simulation, Lampe (2001) modeled the measured thermal anomalies and reconstructed possible fluid temperatures, as well as the duration of these hydrothermal events. Therefore, porosities of 19 to 20 % for sand intervals and 3 to 12 % for silt intervals were assumed. In more detail, a porosity of 24 % was assigned to the Bunte Niederröderner Group and porosities of 19-21 % were assigned to the Cyrena Marls Group, Meletta Group and Rupel Clay Group. These values are rather high and justified by the occurrence of coarse, rift-related alluvial fans in the area of the wells W29, W31 and W33 close to the graben boundary. Permeabilities between 10^{-16} to 10^{-13} m^2 are assumed for the Cenozoic sediments, in line with permeability data from the southern URG (Clauser & Villinger 1990).

Under consideration of well log data and rock samples, these high porosities and permeabilities may be questionable. Typical SP- and Resistivity log curves are published from the Stockstadt area in the graben center by Straub (1962) (Fig. 59). With few exceptions, these well logs can be considered as representative for the whole Cenozoic strata. Based on this compilation by Straub (1962), the Cenozoic sediments in the northern URG consist of mainly fine clastic lithologies such as claystones and marlstones. In addition, the Hydrobia Group, especially the Upper Hydrobia Formation, contains few layers of dolomite, which are well visible in the Resistivity Log (positive peaks). Silt and sand lithologies are mostly restricted to the Upper Tertiary I and II intervals, to the Bunte Niederröderner Group and to the Pechelbronn Group. The lithologies are verified by rocks samples from cutting and core material, which are used in this study. The dominance of fine clastic lithologies (claystone, marlstone) minimizes the possibility of lateral aquifers especially within the Hydrobia Group and Corbicula Group as described by Lampe (2001). Significantly lower porosities and permeabilities must be assumed based on log data for the northern URG, especially when focusing on the central graben area where the presence of coarse alluvial fans is unlikely. Even though the results presented in this thesis indicate similar thermal anomalies with similar maturation data (VR also ranging around 0.6 to 0.7 %Ro) within the Cenozoic sediments, the elevated maturities seem to be caused by another process than lateral fluid flow, as basin-wide lateral fluid flow is highly improbable considering the lithological properties of the strata.

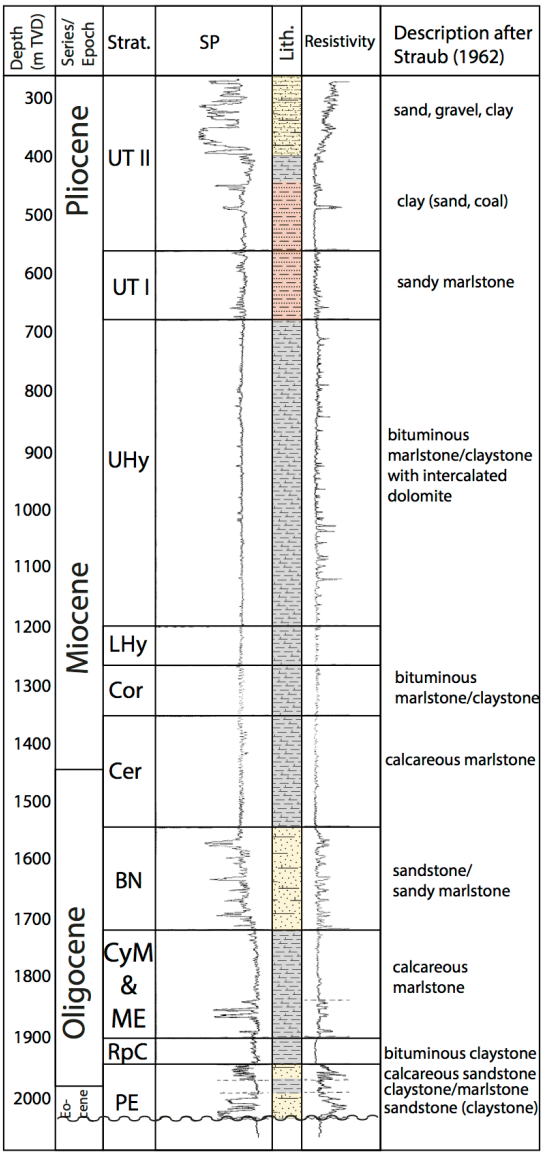

Figure 59: Standard well profile from the Stockstadt area with SP- and Resistivity well log data, modified from Straub (1962). The Cenozoic succession consists of mostly fine clastic claystones and marlstones. In addition, the Hydrobia Group, especially the Upper Hydrobia Formation, contains few layers of dolomite. Coarse clastic lithologies are mostly restricted to the Upper Tertiary I and II intervals, the Bunte Niederröderner Group and the Pechelbronn Group. Note that this profile does not include hiatus and faults.

On contrary to the hypothesis of lateral fluid flow, which leads to secondary thermal overprint (Lampe (2001), Lampe et al. (2001), the thermal anomalies that are observed in this study in wells within the northern URG may be rather effected by long-lasting hydrothermal fluid systems, which occur(ed) particularly along active fault zones. This hypothesis is supported by the position of the studied wells along major faults or fault zones (Figs. 3 & 6). Because of their often elevated permeabilities, fault zones may act as primary pathways for hot ascending (and also descending) fluids (Clauser & Villinger 1990, Person & Garven 1992, Wüstefeld et al. 2017). Most wells in this study cut such major fault systems, which are likely to favor the transport of hot hydrothermal fluids (Fig. 3 & 6), the latter causing the observed secondary thermal overprint of the sedimentary succession. Yet, in order to act as pathways for ascending fluids, the fault zones must be deep routed and connected to a deep sourced aquifer with high fluid temperatures. Under consideration of the lengths and the throw/vertical displacements of these

faults, conclusions on the height of the fault can be derived (e.g. Schlische et al. 1996, Torabi & Berg 2011, Wüstefeld et al. 2017). The studied wells are all located along such major deep-routed faults or fault zones, which is also visible from seismics, if available:

Well W1 is located on a minor horst structure within a small pull-apart basin within the URG, indicating a relatively independent subsidence history within the URG. Fault zones are cut in 300 m and 1300 m depth (Fig. 42). Yet, orientation and exact position of these faults cannot be reconstructed because seismic data and well reports were not obtained for this study.

Well W2 was drilled into an assumed anticlinal structural (Boigk & Krzywicki 1954), comprising Cenozoic sediments down to the Rupel Clay. A major fault zone is cut at 810 m depth within the Lower Hydrobia Formation. Due to this fault cut out, the Corbicula Group and Cerithium Group do not occur in the well. Additional indications of a smaller fracture network are reported from well reports (small fractures with calcite fillings)(Fig. 43).

Well W7 and the subsidiary wells W7(2.) and W7a are situated on a hanging wall structure west of the Stockstadt fault. The wells were drilled through the Cenozoic succession down to the Pechelbronn Group. A fault cut-out of about 400 m at 1225 m in the Lower Hydrobia Formation is estimated from seismics. The Corbicula Group and the upper section of the Cerithium Group were missing due to this fault (Fig. 44). Seismics clearly show, that the Stockstadt fault is a deep routed fault that reaches into the basement below the pre-rift Rotliegend sediments. This is illustrated in a seismic section few km south of the wells W7, W7(2.) and W7a in Fig. 33a. The total vertical offset of the Stockstadt fault ranges around >800 m at top PE.

Well W10 is situated on a hanging wall fault block, which is bordered to the west by the Stockstadt fault and to the east by the Allmend fault (Fig. 33a). The well cuts the Allmend fault, which is connected to the Stockstadt fault and was also active during the Miocene. The deep routed Allmend fault reaches into the basement with a vertical offset of ~180 m at top PE. Due to the fault cut-out of about 100 m at a depth of 900 m, a reduction of the Bunte Niederröderner Group results (Fig. 47).

Well W9 was drilled from the same well site as well W10, but reaches into a footwall structure west of the Stockstadt fault. The well cuts the Cenozoic succession down to the Pechelbronn Group. A fault cut-out of about 250 m at 1353 m reduces the thickness of the Lower Hydrobia Formation (Fig. 46). The Bunte Niederröderner Group and Corbicula Group are not drilled.

Situated on the same hanging wall fault block as well W10, well W8 was drilled through the Cenozoic succession down to the Cyrena Marls Group (Fig. 45). Besides the Stockstadt Fault, which is cut in 2145 m, indications of a smaller fracture network are described in the well reports (small fractures with calcite fillings).

The wells W12 and W14 are located near the eastern border of the URG. They are both drilled into a structural dome that is fragmented by large fault zones (Veit 1955). Based on seismic interpretation, one fault zone is present in well W14 in the Corbicula Group, but it did not cause a significant reduction of the formation thickness (Figs. 48 & 49). Abundant information exists on additional fracture zones, e.g. within the Hydrobia Group, but also in other formations.

Well W16 was drilled into a structural dome near the eastern graben shoulder (Plein 1992). It was drilled through the complete Cenozoic succession down to the Pechelbronn Group. No

major faults were reported nor observed in seismics, but smaller faults are documented in well reports.

Taking into account, that all wells cut through faults, of which most faults are deep basement faults as proven by seismics, the ascent of hydrothermal fluids from a deep sourced aquifer seems realistic. Yet it is necessary to discuss the origin of these hydrothermal fluids and also to get an idea of how the nearly vertically uniform maturation trends presented in Figs 42–50 could develop despite the fine clastic lithologies of the Cenozoic basin fill (e.g. Straub 1962), which apparently do not allow for large-scale convective fluid transport.
Published data suggest that the damage zones of such major fault zones are several tens to hundreds of meters wide, allowing for vertical fluid transport (e.g. Shipton et al. 2006; Torabi & Berg 2011, Wüstefeld et al. 2017). The authors Wüstefeld et al. (2017) explained a thermal anomaly in tight gas sandstones within the Lower Saxony Basin by circulating hydrothermal fluid flow along the fault damage zone of a major deep routed fault with up to 600 m displacement. The lateral extent of the thermal anomaly is evidenced by VR measurements and by the temperature-related diagenetic overprint and amounts up to 1 km. Yet, this overprint in 1 km distance is not related to convective fluid flow but rather to thermal heating, induced by hot) fluids (around 300°C), along the fault (damage) zone.
When transferring these results on the position of the wells in the northern URG (Fig. 6), all wells are in close vicinity and mostly even positioned < 1 km apart from major fault zones. It is probable, that the damage zones of these major deep routed fault zones show increased permeabilities, as described e.g. by Cherubini et al. (2013), allowing for advective heat transport.

In order to get an idea of the relationship between the distance between the well and adjacent major faults and the level of maturation, well W10, which is located within the 3 D seismic cube was studied in more detail. Fig. 60 shows the position of the well W10 and the orientation of the adjacent faults at different depth levels, at which also VR data exist. The well is located along the Allmend Fault (orange colored), which is connected to the Stockstadt Fault (e.g. Fig. 6). All displayed faults are major faults, which can be well detected in seismics. Yet, only the orange colored Allmend Fault reaches down into the pre-rift Rotliegend sediments and into the underlying basement. The visualization of different depth levels shows the complexity of a fault zone and the connected faults, with many “sub-faults” and branches.

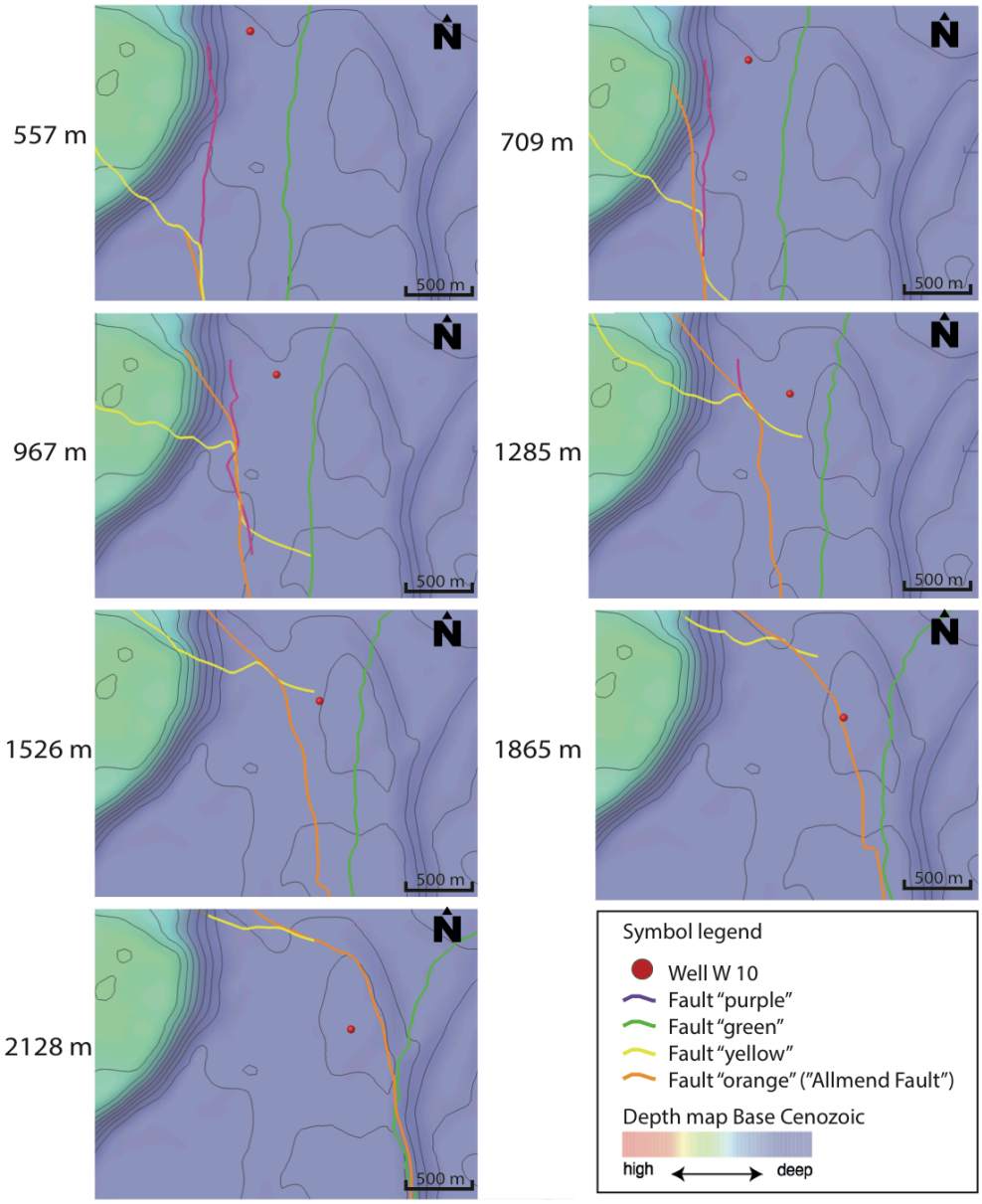

Figure 60: Visualization of the distance between the well path of well W10 and the adjacent faults at different depth levels, at which also VR measurements exist. The position of the well W10 changes due to the deviation of the well. All faults are visible on a seismic scale, yet the largest fault is the orange colored Allmend Fault.

Due to this complexity of fault systems, here illustrated for one exemplary well, no simple distance to fault- relationship can be derived. Fig. 61 illustrates the relation of the closest measured distance between the different colored faults and the well path of well W10 in Fig. 60 at the different depth levels. In addition, the measured VR data is plotted. It is important to keep in mind that the orange colored Allmend fault is the deepest routed fault, reaching into the Rotliegend and the underlying Basement. Ascending fluids, which migrate via the displayed fault system must have originated from this Allmend fault.

Fig. 61 shows that the nearest faults are located 10–1820 m apart from the well path. VR measurements do not correlate precisely with the distance of one of the four nearest faults. Thus it is probable that fluid transport occurred along several faults, if not the whole fault system. Yet it seems that fluid transport along some faults is more likely than for others. For example, low VR values are measured in the samples from 480 m and 560 m depth, whereas higher VR is

measured below 658 m. Elevated VR in the sample from 658 m correlates well with the decreasing distance to the “yellow” fault and the “orange” (Allmend) fault, suggesting fluid and heat transport especially along these faults. In this 480–658 m, the “green” and “purple” colored faults appear to not contribute to the hydrothermal system. Also it appears that the “purple” fault in general does not contribute significantly to the hydrothermal system. The extent of this fault down to about 1400 m does not cause changes in VR above or below.

Lower VR in the lowermost sample in well W10 correlates well with increasing distance of the faults “yellow”, “green” and “orange” (Allmend fault) from the well, suggesting fluid and heat transport along these faults.

Despite these correlations between VR data and the distance from the well path to faults, the distance to surrounding faults or fault segments cannot precisely reconstruct the “Zick-zack” curve that is indicated by VR data. Lithological properties must be kept in mind and the permeability and porosity of individual stratigraphic units plays a major role for lateral fluid transport away from the faults. Thereby higher porosities and permeabilities generally favor the possibility for laterally moving fluids, whereas low porosities and permeabilities lowers this possibility. Taking into account the previously discussed strongly fine clastic dominated composition of the Cenozoic basin fill in the northern URG, porosities and permeabilities are likely lower than predicted by Lampe (2001), at least for most parts of the graben area. Especially along the Stockstadt fault and the Allmend fault, where well W10 was drilled, much lower porosities and permeabilities must be assumed due to the absence of coarse clastic alluvial fans. The highest porosities are assumed for the (more siliciclastic) Bunte Niederröderner Group at 1800–1900 m and the Pechelbronn Group at 2150–2360 m depth (Fig. 47). Yet, when referring to these depth intervals in Fig. 61, no positive VR anomalies can be determined. Instead the highest VR values are measured within the Upper Hydrobia Formation at 1045–1125 m depth; an interval that consists of fine clastic claystones and marlstones with frequent intercalations of dolomite. Thus lateral fluid flow away from the faults is unlikely. Instead it seems that the hydrothermal events lasted long enough to significantly overprint the entire basin fill (almost) equally. As porosities and permeabilities are low, a purely conductive propagation of the high temperature overprint is assumed. Taking into account the studies from the Lower Saxony Basin by Wüstefeld et al. (2017), most VR measurements that indicate maturities higher than the expected subsidence-controlled maturation level are obtained from samples less than 600 m away from the surrounding faults. These distances lie within the 1 km radius that is proposed for a purely conductive thermal overprint (Wüstefeld et al. 2017, Turcotte & Schubert 2002).

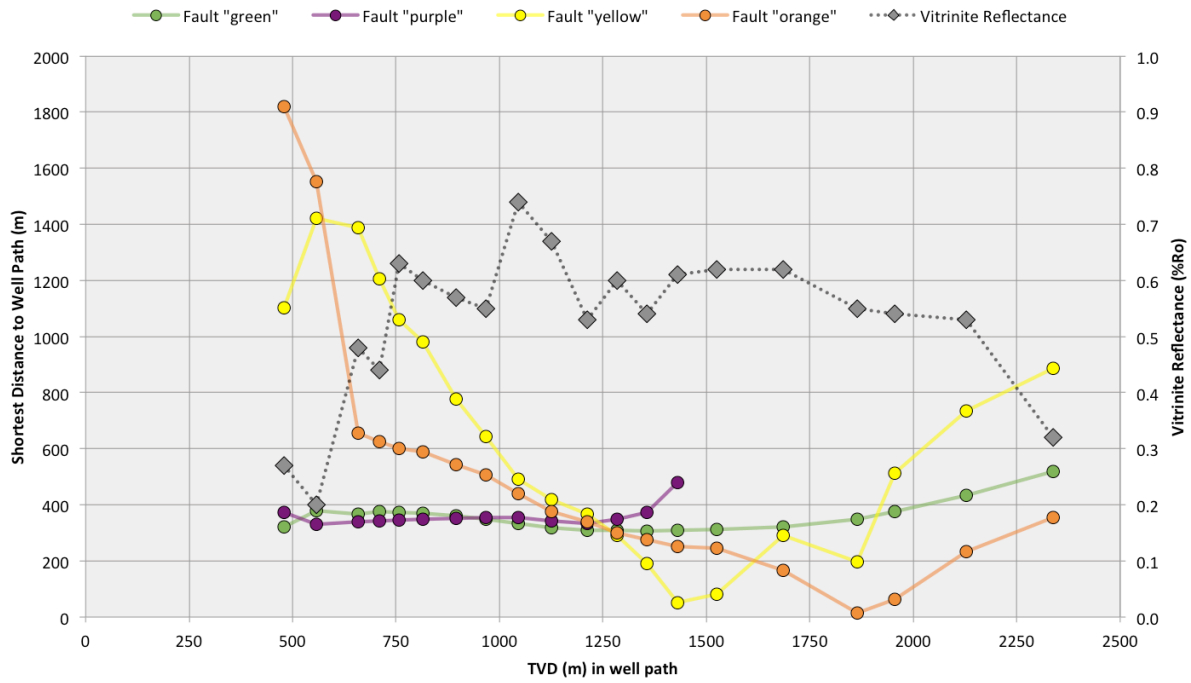

Figure 61: Distance of well W10 to the surrounding faults (see Fig. 60) and measured Vitrinite Reflectance versus depth (m TVD)

The presence of circulating hot groundwater and consequent regional redistribution of heat has been proposed for the URG e.g. by Doebl & Teichmüller (1979), Clauser (1989) and Clauser & Villinger (1990).

Yet, the origin of these fluids is not fully understood. The idea of a hot groundwater aquifer that is restricted to a 500 m thick and higher permeable stratigraphic interval, assigned to the Hydrobia Group (Lampe 2001) as discussed above mismatches the hypothesis of locally ascending hot deep sourced fluids via major fault zones reaching to the basement (e.g. AlNajem 2016, Schmidt et al. 2017). Results from this study suggest ascending hot hydrothermal fluids via fault zones, which act as pathways for fluid migration, as well as an origin of fluids in deep, pre-rift sediments.

Posteriorly, geochemical studies have evidenced deep-sourced fluids in shallow groundwater aquifers in the northern URG, supporting this hypothesis. In the northern URG, this was the case near well W1 in the northernmost study area, where fluids ascended along the Western Boundary Fault, which divides the Main Basin in the West from the URG (AlNajem 2016, Schmitt 1992, Schmidt et al. 2017). In the scope of the research and development project "TRACE" (*TiefenReservoir-Analyse und Charakterisierung von der Erdoberfläche/Deep sourced Reservoir Analysis and Characterization from the Surface*), the ascent of deep sourced fluids was proven based on a geochemical-isotopic concept. Here, $^{87}Sr/^{86}Sr$ ratios have been used as a tracer of fault-controlled fluid ascent into shallow aquifers. The Strontium isotope ratios are effective tracers to prove hydrogeological processes such as water-rock interaction and groundwater mixing, because they reflect the Strontium isotopic composition of the environment through which the water migrated. The authors Schmidt et al. (2017) suggest deformation process along the Western Boundary Fault, leading to permeability heterogeneities and thus enabling hydrothermal fluid circulation. Therefore fault zones may act as hydraulic conduits enabling the

ascent of deep saline groundwater and thus connecting shallow and deep geological environments. One result of the TRACE project was the detection of fluids in shallow aquifers that indicate long residence time in the crystalline basement at elevated temperatures. With increasing distance from the main fault, the proportion of these deep waters decrease and therefore lowing the $^{87}Sr/^{86}Sr$ ratios of the groundwater samples. The $^{87}Sr/^{86}Sr$ ratios of groundwater samples are in agreement with Sr isotopic data from granodiorite from the Odenwald Massif, which occurs also in the subsurface of the northern URG. Thus granodiorite is most likely the source rock for diagenetic Sr. Thereby Sr is derived from Rb rich minerals and enriched in groundwater. Ascending highly saline mineral waters contain high $^{87}Sr/^{86}Sr$ ratios derived from water-rock interaction with silicates from upper crustal crystalline basement (Schmidt et al. 2017). Within the scope of the TRACE project, AlNajem (2016) also identified NaCl dominated fluids in shallow groundwater along the Western Boundary Fault. These high NaCl contents are an additional indicator for a deep-sourced origin of fluids in the area and contrast to surface-near groundwater, which is less saline and Ca-HCO_3 dominated (e.g. Stober & Bucher 2000, AlNajem 2016). These geochemical differences are also based on the origin and development of the waters and influenced by e.g. water-rock interactions or dissolution of evaporates (He et al. 1999, Stober & Bucher 2000, Aubert et al. 2002, Göb et al. 2013).

Taking into account the work done by Stober & Jodocy 2011, both the Permian Rotliegend siliciclastic sediments as well as the crystalline basement presents porosities and permeabilities are high enough to allow for geothermal prospection. Yet, fracture density within the Rotliegend sediments may have been insufficient to account for high convection cells for ascending fluids. The authors Becker et al. (2012) correlated the Rotliegend in wells from the Saar-Nahe Basin. This work nicely shows, that the Rotliegend in the area consists of matrix-supported conglomerates with several volcanic intervals of partially >100 m thickness (Müller 1996, Marell 1989). Hydrogeological mapping in the Rotliegend in the area of Kaiserslautern west of the northern URG, also propose very few aquifers within the Rotliegend in the area (LGB/LfW 2004). These studies of Becker et al. (2012) and LGB/LfW (2004) suggest that large-scale aquifers could not develop within the Rotliegend. Even though the Rotliegend does seem to be not the main origin of hydrothermal fluids, high strontium and lithium concentrations in combination with high $^{87}Sr/^{86}Sr$ ratios from the Western Boundary Fault in the northern URG indicate some sort of influence of Permian Rotliegend sediments (AlNajem 2016). A greater potential is assigned to the fractured granodiorite (Walter 2007), which forms part of the crystalline basement and is underlying the Rotliegend (e.g. Pribnow & Schnellschmidt 2000). Fluids, which ascent via large fault zones might thus indicate the $^{87}Sr/^{86}Sr$ isotope ratios of the Rotliegend, which they migrate(d) through.

The thermal overprint of the affected sedimentary succession over hundreds of meters thickness (Figs. 42–50, 57) can only take place, if fluid temperatures are high and the hydrothermal pulse persists for some time. Higher temperatures may significantly reduce the time frame necessary to develop the observed thermally overprinted maturation trends identified here. As shown in Fig. 57, the thermal anomalies can be observed beginning in the Hydrobia Group to Upper

Tertiary II sediments. Thus more than one hydrothermal event must be assumed from Middle Miocene to Pliocene times in the studied wells.
For the area of Worms in the northern URG, Lampe et al. (2001) postulated a hydrothermal event of 10000-100000 a duration, which has been tentatively been correlated to Alpine tectonism at 5 Ma. During this 10000-100000 a period, hot fluids from depths of > 3.6 km ascended along large fault zones. Lampe et al. (2001) further suggested that after ascending to the Corbicula Group and Hydrobia Group, the fluids dispersed laterally to about 1.2 km out of the fault zones. Over the 100000 a period, the authors simulated fluid temperatures of 130–160°C using two-dimensional numerical simulations.

Possible information on fluid temperatures is also obtained from the Lower Triassic Buntsandstein in the central URG. Here, Soyk (2015) measured temperatures of fluid inclusions trapped in quartz cement. Thereby a hydrothermal origin of the cementing fluids was proven based on homogenization temperatures in the fluid conclusion. Homogenization temperatures of <250 °C were measured on the western flank, whereas up to or even above 350 °C were measured on the eastern graben shoulder in the Odenwald Massif. Homogenization temperatures indicate the minimum fluid temperatures at the time of cementation. Yet it must be kept in mind that these temperatures, even though they are pressure corrected, are assigned to certain burial depths. Hence the 250–350°C must be interpreted with caution, as these homogenization temperatures are strongly dependent on the pressure conditions, which are in turn dependent on the overlying succession and the existence of fluid pathways. Therefore temperatures may be lowered when the fluids ascend via deep routed fault zones. Nevertheless the study of Soyk shows that the fluid temperatures may differentiate throughout the URG.

Also from the area of Soultz-sous-Forêts in N-E France in the southern URG, fluid temperatures are known. The Soultz region has great potential for geothermal energy development (Genter & Traineau 1996, Guillou-Frottier et al. 2011, Gardien et al. 2016), even though the origin of the high basal heat flow remains unknown. It is probable that at least one part corresponds to the mantle uplift signature. Also radiogenic heat production of a granitic intrusion under the sedimentary cover may provide an excess heat from natural radioactivity (Guillou-Frottier et al. 2011, Gardien et al. 2016). The temperature of modern brines, which ascend in deep geothermal holes down to 5 km depth range from 130–160°C (Dubois et al. 1996). Temperatures of 230°C are described for the groundwater reservoir in the granitic basement (Aquilina et al. 1997). Complex circulation pathways within the crystalline basement are described for the Soultz region (Aquilina et al. 1997). The circulation of fluids is most probably related to the presence of faults and higher permeabilities within the damage zones, similar as it is the case for the northern URG (Fritz & Gérard 2010).

Overall, the URG holds great geothermal potential due to its increased geothermal gradient, as shown not only from the Soultz region, but also from Landau, Insheim and Bruchsal (e.g. Agemar et al. 2014, Vidal et al. 2015) located in the central URG. Large temperature variations are observed across the URG, as proven by Agemar et al. (2013, 2014), among others due to

additional descending fluid flow at the eastern graben boundary fault, which ascends again at the western boundary fault. (Clauser & Villinger 1990, Stober & Bucher 2015). In addition, Freymark et al. (2017) have shown that the temperature distribution is to a high degree influenced by the thick Cenozoic sediment interval, which causes a "thermal blanketing" effect, as well as by high radiogenic heat production in the underlying basement. The authors obtained indications for fluid flow, which affects the thermal field of the URG at a depth interval of 500 to 2500 m depth.

Long-term hydrothermalism and consequent overprint of maturities are of major importance for HC generation in the northern URG from the potential source rock units such as the Rupel Clay Group, the Corbicula Group or the Hydrobia Group, which consist of fine-clastic marine sediments. As shown in Fig. 51 and Figs. 42–50, similar levels of maturation are reached within these source rock intervals at least for some wells in the study area. Yet, it must be kept in mind, that the potential for HC generation, which is interpreted from integrated maturation analysis, is only given in the close vicinity of major faults and fault systems. At larger distances, levels of organic maturation are probably lower, but can only be verified by the analysis of wells located in unfaulted areas.

Previous maturation studies in the URG were mainly based on VR analysis. In contrast to the maturation trends in the northern URG presented in this, mostly logarithmically increased maturation trends were reported for the Cenozoic basin fill in the central URG. These trends are referred to as subsidence and heat flow controlled increase in maturation (Heling & Teichmüller 1974, Teichmüller 1979, Böcker & Littke 2014, Böcker 2016). Few elevated, but also burial-controlled maturation trends are identified near Scheibenhardt, Huttenheim, Rülzheim or Landau. These are linked to higher heat flows in these areas and are not influenced by secondary hydrothermal overprint (Böcker & Littke 2014, Teichmüller 1979). Yet, also few maturation trends similar to the ones documented here for the northern URG are described from the central URG. Robert (1985) measured similar, nearly vertically uniform maturation trends in the central URG. In the area of Landau (Knöringen) for example, VR values of 0.55 %Ro were measured at shallow 200 m depth, which also suggest significant hydrothermal overprint.

10.4. Limitations of PetroMod 1D

Models, whether one-dimensional or two-dimensional, only represent possible solutions to a measured data set. Entirely correct models do not exist, because simplifications e.g. on lithologic composition and rock properties must be made and not all governing factors will usually be known.

The one-dimensional simulations allow for a reconstruction of the geodynamic, conductive (basal) heat flow in the selected wells. Yet, most VR data do not fit the simulated models and cannot be fed into the simulations, because the hydrothermal overprint cannot be modeled in 1D. In order to simulate the interaction of conductive, basal heat flow and hydrothermally

induced convective heat flow, two-dimensional simulations need to be performed on carefully selected transects within the study area. These two-dimensional simulations would allow for an implementation of lateral fluid flow, as previously shown e.g. by Lampe (2001) for the southernmost northern URG. This complex task was not possible in the framework of this thesis.

The spatial position of faults and fault zones, which act as pathways for ascending fluids, can be implemented into a two-dimensional model, but the precise locations and of the faults and their distance to the well paths need to be known precisely. This is even a problem for a two-dimensional model. And would better be solved in 3D. In addition, it is important to insert permeability data of the faults, as faults act either as fluid pathways, or as seals, which hamper fluid flow. Problems for all these models are, that many of these factors are not or only roughly known.

As an output of multi-dimensional models, information on fluid inflow temperatures, fluid velocities within the sedimentary compartments, and on the duration and frequencies of hydrothermal events are obtained (e.g. Lampe 2001, Lampe & Person 2001).

Since only vertical heat flow was available for the present one-dimensional numerical simulations these simulations yield limitation with respect to the complex heat transfer mechanisms known to occur within sediment basins. Still, these simulations provide valuable information on possible temperature histories of the investigated wells considering for modeling only a conductive heat flow from below: from the differences between measured and modeled data, clear indications on the presence of long-lasting hydrothermal overprint can be drawn.

11. Conclusions

The URG in SW-Germany is a Cenozoic passive rift with complex tectonic setting and multiphase development. The basin fill contains fluvial-limnic terrestrial deposits, which provide potential reservoirs, and brackish-marine deposits, which provide potential source rock units. Several HC fields are known from the northern URG, yet the origin of these hydrocarbon accumulations and the overall hydrocarbon potential as well as palaeoenvironmental background is not fully understood. This thesis contributes to a better understanding of the northern URG sediment fill in terms of palaeoenvironmental conditions, source rock development and palaeothermal history.

The analysis of the palaeoenvironment development has evidenced major small-scale differences and fluctuations of oxygen levels and proximity to erosional sources throughout the graben. These are the result of various interconnected factors, including external system parameters (not directly describing the depositional system) and internal system parameters (directly describing the depositional system). The intensity of rift-tectonic activity and related uplift of the graben shoulders seems to be the main controlling factor for OM composition,

overwhelming other factors described below. Palynofacies investigations show very high fluctuations of the terrestrial OM components (phytoclasts, sporomorphs, terrestrial AOM). Specifically, the phases of active graben rifting in the Late Eocene to Early Oligocene (Pechelbronn Group and Rupel Clay Group) and in the Early Miocene (Corbicula Group and Lower Hydrobia Formation) result in high amounts of terrestrially derived OM, which is shed into the graben from the eastern, but mainly the western shoulders. Basin topography, subsidence rates and accommodation space of the various tilted fault blocks and horst/graben structures thereby trigger the details of the distribution of terrestrial OM input from the graben shoulders. As a consequence of this rift related dynamics, small-scale differences are evidenced by variations in the OM composition and oxygen levels.

Tectonic activity in the graben was low to negligible during the Late Oligocene to earliest Miocene (e.g. Bunte Niederröderner Group, Cerithium Group) and in the Late Miocene (Upper Hydrobia Formation), resulting in low amounts of terrestrial-originated OM. Thus, additional factors seem to control the composition of OM during these phases. OM composition of these intervals mainly consists in mainly marine phytoplancton and marine AOM. Therefore, OM composition seems to have been triggered mainly by changes in relative sea level (water depth), which is the second-most important factor.

Additional factors are likely contributing to OM composition in phases of low or negligible tectonic activity *and* constant sea level. Among these are oxygen ratios, marine currents, water stratification, the availability of light, and salinity. These factors cannot be precisely quantified or specifically assigned to the different constituents of the OM. Its composition and preservation state is therefore the result of complex interaction of processes, including large-scale rift related tectonic activity, topography, sea level changes as well as small-scale palaeoenvironmental conditions. In contrast to the published prevailing model of a sea level controlled marine depositional system (e.g. Grimm et al. 2011, Gaupp & Nickel 2001), the OM composition in the URG seems to be controlled to a much higher degree by rift-related tectonic processes and its impact on the topography of the graben shoulders, whereas sea level appears to have been less important.

The hydrocarbon potential of the Cenozoic succession is estimated based on an integrated kerogen analysis in the studied wells, determining the kerogen composition and TOC, and by determining maturities in the studied wells:

The Pechelbronn Group is subdivided into the Lower- Middle- and Upper Pechelbronn Formation; with the exception of the Middle Pechelbronn Formation these are known as good reservoir units e.g. from the oil fields Eich, Schwarzbach and Stockstadt. The analysis of these units verified low clay contents, suggesting a low source rock potential and better reservoir quality. Low source rock potential is assigned to the Middle Pechelbronn Formation. OM consists of mainly gas-prone and barren type III/IV kerogen and low amounts of oil-prone type I/II kerogen. Corresponding HI values of 30–113 mg HC/g TOC are reached. TOC is generally below 2.6 %. In comparison to the central URG, the Middle Pechelbronn Formation in the northern URG is much stronger influenced by input of terrestrial type III/IV kerogen input from the graben shoulders. If at all, gas generation potential is assigned to the Middle Pechelbronn Formation.

Maturities reach the basal to middle oil window (max. 0.88 %Ro), suggesting no expulsions of gaseous hydrocarbons. If at all, minor oil expulsion is assigned to the Middle Pechelbronn Formation in the southernmost and northernmost study area, where the maximum maturities are reached.

The analysis of the Rupel Clay Group (subdivided into Fish Shale Formation and Foraminifera Marls Formation) reveals a gas-prone, type III/IV kerogen dominance, implying a much higher gas-, rather than oil generation potential, due to the rifting-related higher input of terrestrial OM. In contrast to the central URG, where the best oil generation potential is assigned to the Fish Shale Formation, the highest amounts of oil-prone type I/II kerogen are reached in the Foraminifera Marls Formation in the northernmost part of the study area and along the eastern graben border. HI values are in the range of 95–309 mg HC/g TOC (Fish Shale Formation) and 44–413 mg HC/g TOC (Foraminifera Marls Formation). TOC does not exceed 3.0 % and mostly ranges around 0.75–1.8 %. Overall, kerogen quantity is lower than in the central URG and much higher gas generation potential is assigned to the northern URG. Maturation in the northern URG ranges up to 0.8 %Ro, which corresponds to the middle oil-window. In addition, high sulphur contents are measured in the Rupel Clay Group, which favor an early generation of hydrocarbons. Consequently, moderate oil generation is assigned to the eastern graben border and to the pull-apart basin in the northernmost northern URG.

Kerogen composition in the overlying Meletta Group and Cyrena Marls Group reveals high amounts of gas-prone and barren type III/ IV kerogen and low TOC contents of <0.7 wt.%. Despite maturities in the basal oil window within the study, argillaceous intervals are rare and carbonate contents are high, so that both the HC potential and reservoir qualities are low.

For the overlying Bunte Niederröderner Group, a moderate oil generation potential (dominance of type I/II kerogen) is suggested for the (very rare) fine clastic intervals. Thus, no considerable HC generation is attributed to the Bunte Niederröderner Group. Yet, the unit is known as reservoir unit from the URG.

In the study area the Cerithium Group indicates moderate amounts of oil-prone type I and II kerogen, but low TOC and high carbonate contents, which minimize the source rock potential.

From the central URG, no studies exist on the source rock potential of the Cerithium Group.

The Corbicula Group is characterized by moderate to high TOC (up to 2.4 wt.%), mixed kerogen composition and HI values of up to 414 mg HC/g TOC. Maturation does not exceed the basal (to mid) oil-window, yet high sulphur contents favor the generation of hydrocarbons at lower temperatures. Therefore, the unit provides good HC potential, especially along the eastern graben border and in the small pull-apart basin in the north of the study area.

The Hydrobia Group is subdivided into the Lower- and Upper Hydrobia Formation with differing HC potential in the study area. Moderate to very high amounts of oil-prone type I/II kerogen dominate the OM composition especially of the Upper Hydrobia Formation. Elevated amounts of type III/IV kerogen in the Lower Hydrobia Formation are related to rift-dynamics and high terrestrial OM influx from the graben shoulders. HI values range between 86–487 mg HC/g TOC for the Lower Hydrobia Formation and 227–592 mg HC/g TOC for the Upper Hydrobia Formation. TOC values of 0.6–3 wt.% were measured. These data are similar to the central URG, suggesting relatively homogenous source rock qualities. Maturities of the Lower and Upper

Hydrobia Formation are in an early to mid oil-window throughout the northern URG, and high sulphur contents facilitate the early oil generation. Thus, oil generation has likely occurred, especially along the eastern graben shoulder and in the small pull-apart basin in the north of the study area.

In the studied HC exploration wells maturities were influenced by both, conductive (basal) heat flow and by convective, hydrothermally induced heat flow. Relatively uniform, steep vertical maturation trends, which are untypical for a burial-controlled maturation, are observed in different, independent data sets. They are here interpreted to provide strong evidence for significant secondary thermal overprinting. This overprint must be related to long-lasting, very hot hydrothermal fluid systems, well known from the URG, which were mainly concentrated along reactivated fault zones. Therefore, maturation was tectonically controlled by the distribution of hydrothermal fluid systems, in addition to subsidence controlled burial maturation. In consequence, late syn-rift sediments such as the Hydrobia Group also provide a favorable oil- source rock potential based on kerogen analysis. Yet, these maturities only refer to the studied wells, which are all located along large fault zones. It appears likely that wells, which are located within structural blocks and do not cut through faults, indicate burial controlled maturation trends.

The reconstruction of palaeothermal history using PetroMod® 1D reveals geodynamic heat flow, with maximum heat flow rates (>75mW/m^2) during the Late Eocene to Early Oligocene, correlating to phases of high rift-related tectonic activity. Lower heat flow rates (~72 mW/m2) are identified during Early Miocene and Pliocene and thus correspond to phases of low rift-related tectonic activity. These assumptions are consistent with published heat flow data from the central (Bruss 2000) and northern URG (Lampe 2001), suggesting similar basin-wide geothermal anomalies during rift development. As these reconstructed palaeothermal simulations do not fit all calibration data (VR), secondary thermal overprint via ascending hot fluids is assumed.

Rift-related tectonic activity had a major impact on the palaeoenvironment and hydrocarbon generation potential within the URG rift basin, significantly exceeding the impact of sea level fluctuations. Also, hydrothermally controlled maturation within this complex rift setting is directly linked to rift tectonic activity. Hence, depositional settings, kerogen composition, thermal maturation and hydrocarbon potential are strongly linked to the geotectonic development of the rift system.

12. Outlook

The northern URG is a complex graben segment in terms of tectonic setting with a multiphase subsidence history. This thesis provides a better understanding of this graben segment in terms of palaeoenvironment development, kerogen composition, -quality and –distribution, as well as the palaeothermal evolution and the frequent influence of hydrothermal fluids on maturity. Despite the results of this research, several questions remain and several points need to be reconsidered or analyzed in more detail in the future in order to fully understand the complexity of the northern URG:

- The analyses performed in this study all refer to exploration wells, which were drilled in close vicinity of large faults or fault zones. With respect to the palaeoenvironmental setting and sediment transport routes, but also kerogen composition, palynofacies studies presented here would need to be applied to additional wells, which are located in the inner parts of structural blocks and do not cut faults; thereby generating information on lateral small-scale changes. As most exploration wells were drilled close to faults or cutting through faults, the possibility of gaining additional information on these small-scale changes within the inner parts of structural blocks is limited.

- Collecting more evidence concerning the hypothesis of hydrothermal overprint:
    - Additional information on smaller fractures and the fracture network and orientation may be gathered for example by the analysis of wells logs and additional seismic interpretation. This might enhance the process of building a realistic model of hydrothermal overprint in the northern URG
    - Two- or even three dimensional models on the palaeothermal history may provide important information on possible realistic fluid temperatures and the durations of the hydrothermal events
    - Regional geochemical analysis of hydrothermal fluids along major fault zones, such as the ones ascent in the area of Worms or Groß Gerau (“TRACE” project) may provide additional information for the discussion on the origin of hydrothermal fluids

- Information regarding the origin/source of existing hydrocarbon accumulations in the northern Upper Rhine Graben:
    - Oil analysis from the hydrocarbon fields will help to evaluate the attribution to individual source rock units, e.g. based on biomarker analysis.
    - With the knowledge regarding individual source rock units that fed the existing hydrocarbon fields, possible migration paths could be reconstructed under careful reconsideration of rock and fault properties.

References

Achauer, U. & Masson, F. (2002): Seismic tomography of continental rifts revisited: from relative to absolute heterogeneities. – Tectonophysics, 358: 17–37.

Agemar, T., Brunken, J., Jodocy, M., Schellschmidt, R., Schulz, R. & Stober, I. (2013): Untergrund-temperaturen in Baden-Württemberg. – Zeitschrift der Deutschen Gesellschaft für Geowissen-schaften, 164 (1): 49–62; Stuttgart.

Agemar, T., Weber, J., Schulz, R. (2014): Deep geothermal energy production in Germany. – Energies, 7 (7): 4397–4416.

Allen, P.A. & Allen J.R. (1990): Basin analysis: principles and applications. – Blackwell Scientific Publications, 451 pp.; Oxford.

Al Najam, S. (2016): Hydrogeochemische Charakterisierung von Grundwässern des Oberrheingrabens zur Identifizierung störungsbedingter Tiefenwasser-Einflüsse. – PhD Thesis Ruprecht-Karls University Heidelberg, 123 pp.

Aquilina, L., Pauwels, H., Genter, A., Fouillac, C. (1997): Water-rock interaction processes in the Triassic sandstone and the granitic basement of the Rhine Graben: geochemical investigation of a geothermal reservoir. – Geochimica et Cosmochimica Acta, 61 (20): 4281–4295.

Aubert, D., Stille, P., Probst, A., Gauthier- Lafaye, F., Pourcelot, L. & Del Nero, M. (2002): Characterization and migration of atmospheric REE in soils and surface waters. – Geochimica et Cosmochimica Acta, 66(19): 3339–3350.

Baillieux, P., Schill, E., Edel, J-B., Mauri, G. (2013): Localization of temperature anomalies in the Upper Rhine Graben: insights from geophysics and neotectonic activity. – International Geology Review, 55(14): 1744–1762.

Baranyi, I., Lippolt H., Todt W. (1976): Kalium-Argon-Altersbestimmung an tertiären Vulkaniten des Oberrheingraben-Gebietes. – Oberrheinische Geologische Abhandlungen, 25: 41–62.

Bartz, J. (1974): Die Mächtigkeit des Quartärs im Oberrheingraben. – Approaches to Taphrogenesis, Inter-Union Commission on Geodynamics, Scientific Reports, 8: 78–87; Stuttgart.

Batten, D.J. (1981): Palynofacies, organic maturation and source rock potential for petroleum. – Organic maturation Studies and Fossil Fuel Exploration. Academic Press, 201–223.

Batten, D.J. (1996): Chapter 26B. Palynofacies and petroleum potential. – Palynology: principles and applications, American Association of Stratigraphic Palynologists Foundation, 3: 1065–1084.

Becker, A., Schwarz, M., Schäfer, A. (2012): Lithostratigraphische Korrelation des Rotliegend im östlichen Saar-Nahe-Becken. – Jahresberichte und Mitteilungen des Oberrheinischen Geologischen Vereins, N.F. 94: 105–133; Stuttgart.

Berger, J.P. (1996): Cartes paléogéographiques-palinspastiques du basin molassique Suisse (Oligocène inférieur-Miocène moyen). – Neues Jahrbuch für Geologie und Paläontologie, Abhandlungen, 202(1): 1–44.

Berger, J.P., Reichenbacher, B., Becker, D., Grimm, M., Grimm, K., Picot, L., Storni, A., Pirkenseer, C., Derer, C., Schaefer, A. (2005): Paleogeography of the Upper Rhine Graben (URG) and the Swiss Molasse Basin (SMB) from Eocene to Pliocene. – International Journal of Earth Sciences, 94(4): 697–710.

Böcker, J. & Littke, R. (2014): Source rock characterization and thermal maturity of the Rupelian Fish Shale (Bodenheim Fm./Hochberg Subfm.) in the central Upper Rhine Graben. – Zeitschrift der Deutschen Gesellschaft für Geowissenschaften, 165: 247–274.

Böcker, J. (2016): Petroleum system and thermal history of the Upper Rhine Graben-Implications from organic geochemical analyses, oil-source rock correlations and numerical modelling. – PhD thesis RWTH Aachen, 154 pp.

Böcker, J. & Littke, R. (2016): Thermal maturity and petroleum kitchen areas of Liassic Black Shales (Lower Jurassic) in the central Upper Rhine Graben, Germany. – International Journal of Earth Sciences, 105: 611–636.

Böcker, J., Littke, R., Forster, A. (2016): An overview on source rocks and the petroleum system of the central Upper Rhine Graben. – International Journal of Earth Sciences, 106: 707–742.

Boigk, H. & Krzywicki, E. (1954): Die Erdölbohrtätigkeit des Jahres 1953 in Westdeutschland. – Erdöl und Kohle, 7: 137–148; Hamburg.

Boigk, H. & Schoeneich, H. (1970): Die Tiefenlage der Permbasis im nördlichen Oberrheingrabens. – Graben Problems, 45–55; Stuttgart (Schweizerbart)

Bordenave, M., Espitalié J., Leplat, P., Oudin, J.L. & Vandenbroucke, M. (1993): Screening techniques for source rock evaluation. – Applied Petroleum Geochemistry. - Editions Technip, 217–278; Paris.

Bostick, N.H. (1979): Microscopic measurements on the level of catagenesis of solid organic matter in sedimentary rocks to aid exploration for petroleum and to determine former burial temperatures – a review. – Society of Economic Palaeontologists and Mineralogists, Special Publications, 26: 17–43.

Brun, J.P., Gutscher, M.A., DEKORP-ECORS teams (1992): Deep crustal structure of the Rhine Graben from DEKORP-ECORS seismic reflection data: a summary. – Tectonophysics, 208 (1–3): 139–147.

Bruss, D. (2000): Zur Herkunft der Erdöle im mittleren Oberrheingraben und ihre Bedeutung für die Rekonstruktion der Migrationsgeschichte und der Speichergesteine. - Berichte des Forschungszentrums Jülich, 3831, 222 pp. – PhD thesis, Erlangen-Nürnberg University.

Cherubini, Y., Cacace, M., Scheck-Wenderoth, M., Moeck, I., and Lewerenz, B. (2013): Controls on the deep thermal field – implications from 3-D numerical simulations for the geothermal research site Groß Schönebeck. – Environmental Earth Sciences, 70, 3619–3642.

Clauser C. (1988): Untersuchungen zur Trennung der konduktiven und konvektiven Anteile im Wärmetransport in einem Sedimentbecken am Beispiel des Oberrheintalgrabens. – Fortschritt-Berichte VDI, 19(28), Düsseldorf, 134 pp. - PhD thesis, TU Berlin.

Clauser C. (1989): Conductive and convective heat flow components in the Rhinegraben and implications for the deep permeability distribution. – Hydrogeological regimes and their subsurface thermal effects. - American Geophysical Union, 59–64; Washington DC.

Clauser, C. & Villinger, H. (1990): Analysis of conductive and convective heat transfer in a sedimentary basin, demonstrated for the Rhinegraben. – Geophysical Journal International, 100(3): 393–414; London.

Clauser, C. & Neugebauer, H.J. (1991): Thermisch relevante Tiefenwasserzirkulation in der Oberkruste unter dem Oberrheingraben? Eingrenzungen mit Hilfe hydrothermischer Modellrechnungen. – Geologisches Jahrbuch, E48: 185–217; Hannover.

Collins, A. (1990): The 1-10 spore colour index (SCI) scale: a universally applicable colour maturation scale, based on graded, picked palynomorphs, Meded. – Rijks geolgische Dienst, 45: 39–47.

Derer, C.E. (2003): Tectono-sedimentary evolution of the northern Upper Rhine Graben (Germany), with special regard to the early syn-rift stage. – PhD thesis Bonn University; 99 pp.

Derer, C.E., Kosinowski, M., Luterbacher, H.P., Schäfer, A. & Süss, M.P. (2003): Sedimentary response to tectonics in extensional basins: the Pechelbronn Beds (late Eocene to early Oligocene) in the northern Upper Rhine Graben, Germany. – Tracing Tectonic Deformation Using the Sedimentary Record, Geological Society Special Publications, Geological Society London, 208: 55–69; London.

Derer, C.E., Schumacher, M.E. & Schäfer, A. (2005): The northern Upper Rhine Graben: basin geometry and early syn-rift tectono-sedimentary evolution. – International Journal of Earth Sciences (Geologische Rundschau), 94: 640–656; Berlin-Heidelberg.

Dèzes, P., Schmid, S.M., Ziegler, P.A. (2004): Evolution of the European Cenozoic Rift System: interaction of the Alpine and Pyrenean orogens with their foreland lithosphere. – Tectonophysics, 389: 1–33.

Dill, H.G., Sachsenhofer, R., Grecula, P., Sasvari, T., Palinkas, L.A., Borojevic-Sostaric, S., Strmic-Palinkas, S., Prochaska, W., Garuti, G., Zaccarini, F., Arbouille, D. & Schulz, H-M. (2008): Fossil fuels, ore and industrial minerals. – The Geology of Central Europe. Geological Society, London, 2: 1341–1449; London.

Doebl, F. (1958): Stratigraphische und paläogeographische Ergebnisse neuerer mikropaläontologischer Untersuchungen im Tertiär des Rheintal-Grabens. – Erdöl u. Kohle, 11, 373–376; Hamburg.

Doebl, F. (1961): Fazies und Mikropaläontologie des Miozäns im Rheintalgraben und seine Verbindung zu den benachbarten Tertiärgebieten. – Meyniana, 10: 89–93; Kiel.

Doebl, F. (1967): The Tertiary and Pleistocene sediments of the northern and central part of the upper Rhinegraben. – Abhandlungen GLA Baden-Württemberg, 6: 48–54.

Doebl, F. & Malz, H. (1962): Tertiär des Rheintalgrabens. – Arbeitskreis Deutscher Erdölgeologen: Leitfossilien der Mikropaläontologie, B, 10: 379–419; Berlin.

Doebl, F. & Olbrecht, W. (1974): An Isobath Map of the Tertiary Base in the Rhinegraben. – Approaches to Taphrogenesis: 71–72; Stuttgart.

Doebl, F. & Teichmüller, R. (1979): Zur Geologie und heutigen Geothermik im mittleren Oberrheintalgraben. – Fortschritte in der Geologie von Rheinland und Westfalen, 27:1–17; Krefeld.

Dubois, M., Ayt Ougougdal, M., Meere, P., Royer, J-J., Boiron, M.-V., Cathelineau, M. (1996): Temperature of paleo- to modern self-sealing within a continental rift basin: The fluid inclusion data (Soultz-sous-Forêts, Rhine Graben, France). –European Journal of Mineralogy, 8: 1065–1080; Stuttgart.

Durst, H. (1991): Aspects of exploration history and structural style in the Rhine graben area. – Generation, accumulation, and production of Europe's hydrocarbons. European Association of Petroleum Geoscientists, Special Publication, 1: 247–261.

Espitalié J., (1979): Charakterisierung der organischen Substanz und ihres Reifegrades in vier Bohrungen des mittleren Oberrhein-Grabens sowie Abschätzung der paläothermischen Gradienten. – Fortschritte in der Geologie von Rheinland und Westfalen, 27: 87–96.

Espitalié J., Deroo G., Marquis F. (1985): La pyrolyse Rock-Eval et ses applications. – Revue de l'Institut Français du Petrole, 40, 563–579.

Fekiacova, Z., Mertz, D., & Renne, P. (2007): Geodynamic setting of the tertiary Hocheifel volcanism (Germany), Part I: $^{40}Ar/^{39}Ar$ geochronology. – Mantle Plumes - A Multidisciplinary Approach, Springer, 185–206; Heidelberg.

Federal Geographic Data Committee (2006): FGDC Digital Cartographic Standard for Geologic Map Symbolization: Reston, Va. – Federal Geographic Data Committee Document Number FGDC-STD-013–2006, 290 p., 2 plates.

Fischer, M.J., Barnard, P.C., Cooper, B.S. (1981): Organic maturation and hydrocarbon generation in the Mesozoic sediments of the Sverdrup Basin, Arctic Canada. – Proceedings IV International Palynological Conference, Lucknow (1976-77), 2: 581–588.

Freymark, J., Sippel, J., Scheck-Wenderoth M., Bär K., Stiller, M., Fritsche J.-G., Kracht M. (2017): The deep thermal field of the Upper Rhine Graben. – Tectonophysics, 694: 114–129.

Frings, K., Lutz, R., de Wall, H., Warr, L.N. (2004): Coalification history of the Cinera-Matallana pull-apart basin (NW Spain). – International Journal of Earth Sciences, 93(1): 92–106.

Fritz, B. & Gérard, A. (2010): On the way to the exploitation of deep geothermal resources in naturally fractures environments. – Comptes Rendus Geosciences; 342: 493–501.

Gallagher K., Rmasdale M., Lonergan L., Morrow D. (1997): The role of thermal conductivity measurements in modeling thermal histories in sedimentary basins. – Marine and petroleum Geology, 14(2): 201–214, Amsterdam.

Gardien, V., Rabinowicz, M., Vigneresse, J.L., Dubois, M., Boulvais, P., Martini, R. (2016): Long-lived interaction between hydrothermal and magmatic fluids in the Soultz-sous-Forêts granitic system (Rhine Graben, France). – Lithos, 246–247: 110–127.

Gaupp, R. & Nickel, B. (2001): Die Pechelbronn-Schichten im Raum Eich-Stockstadt (Nördlicher Oberrheingraben; Blatt 6216 Gernsheim). – Geologisches Jahrbuch Hessen, 128: 19–27; Wiesbaden.

Gawenda, P. (2011): Germany – Overview about Renewed Petroleum Activities. – American Association of Petroleum Geologists-ER Newsletter - December 2011 - Exploration country focus.

Gawthorpe, R.L. & Hurst, J.M. (1993): Transfer zones in extensional basins: their structural style and influence on drainage development and stratigraphy. – Journal of the Geological Society, 150: 1137–1152.

Genter, A. & Traineau, H. (1996): Analysis of macroscopic fractures in granite in the HDR geothermal well EPS-1, Soultz-sous-Forêts, France. – Journal of Volcanology and Geothermal Research, 72: 121–141.

Geyer, O.F., Gwinner, M.P. (2011): Geologie von Baden-Württemberg. 5th edition, Schweizerbart, 627 pp; Stuttgart.

Glahn A. & Granet M. (1992): 3-D structure of the lithosphere beneath the southern Rhine graben area. – Tectonophysics, 208: 149–158.

Göb, S., Loges, A., Nolde, N., Bau, M., Jacob, D. E. & Markl, G. (2013): Major and trace element compositions (including REE) of mineral, thermal, mine and surface waters in SW Germany and implications for water–rock interaction. – Applied Geochemistry, 33: 127–152.

Grimm, K.I. (1991): Biostratigraphie, Paläogeographie und Paläoökologie des Fischschiefers (Mittlerer Rupelton/Mitteloligozän) im Mainzer Becken. – Mainzer geowissenschaftliche Mitteilungen, 20: 249–278; Mainz.

Grimm, K.I. (1994): Paläoökologie, Paläogeographie und Stratigraphie im Mainzer Becken, im Oberrheingraben, in der Hessischen Senke und in der Leipziger Bucht während des Mittleren Rupeltons (Fischschiefer/Rupelium/Unteroligozän). – Mitteilungen der Pollichia, 81: 7–193.

Grimm, K.I., Grimm, M.C. & Schindler, T. (1999): Der Meeressand (Rupelium, Oligozän) der Sandgrube „Faber“ bei Siefersheim in Rheinhessen (Mainzer Becken). – Mainzer geowissenschaftliche Mitteilungen, 28: 7–32; Mainz.

Grimm, K.I., Grimm, M.C. & Schindler, T. (2000): Lithostratigraphische Gliederung im Rupelium / Chattium des Mainzer Beckens, Deutschland. – Neues Jahrbuch für Geologie und Paläontologie, 218(3): 343–397; Stuttgart.

Grimm, K.I., Grimm, M.C., Schindler, T. & Köthe, A. (2002): Der „Rupelton“ (Rupelium, Oligozän) der Tongrube Bott- Eder bei Rauenberg (Oberrheingraben, Deutschland). – Courier Forschungsinstitut Senckenberg, 237, 229–253; Frankfurt a.M.

Grimm, K.I. & Grimm, M.C. (2003): Geologischer Führer durch das Mainzer Tertiärbecken. - Die fossilen Wirbellosen des Mainzer Tertiärbeckens. – Mainzer Naturwissenschaftliches Archiv, Beiheft, 26: 1–158; Mainz.

Grimm, K.I., Köthe, A. & Grimm, M.C. (2005): Sedimentologie und Biostratigraphie im Rupelium der Ziegeleigrube Jungk, Wöllstein (Mainzer Becken). – Senckenbergiana lethaea, 85 (2): 231–259; Frankfurt a.M.

Grimm, M.C. (2005): Beiträge zur Lithostratigraphie des Paläogens und Neogens im Oberrheingebiet (Oberrheingraben, Mainzer Becken, Hanauer Becken). – Geologisches Jahrbuch Hessen 132: 79–112; Wiesbaden.

Grimm, M.C., Wielandt-Schuster, U., Hottenrott, M., Grimm, K.I., Radtke, G. (2011): Oberrheingraben. – Deutsche Stratigraphische Kommission (ed) Stratigraphie von Deutschland IX; Tertiär, 1: Oberrheingraben und benachbarte Tertärgebiete. Schriftenreihe der Deutschen Gesellschaft für Geowissenschaften, 75: 57–132.

Grimmer, J.C., Ritter, J.R.R., Eisbacher, G.H., Fielitz, W. (2016): The late Variscan control on the location and asymmetry of the Upper Rhine Graben. – International Journal of Earth Sciences, 1–27.

Guillou-Frottier, L., Carré, C., Bourgine, B., (2011): Régimes thermiques actuels des bassins sédimentaires: traitement des données, cartographies et sources potentielles des anomalies. – Exemples du graben du Rhin et du bassin de Paris (Rapport final. BRGM/RP-60355-FR. 92).

Hardenbol, J., Thierry, J., Farley, M., Jacquin, T., De Gracuabsky, P.C. (1998): Mesozoic and Cenozoic chronostratigraphic framework of european basins. – Mesozoic and Cenozoic sequence stratigraphy of european basins, SEPM Special Publications, 60: 3–13; Tulsa, Oklahoma.

He, K., Stober, I. & Bucher, K. (1999): Chemical evolution of thermal waters from limestone aquifers of the Southern Upper Rhine Valley. – Applied Geochemistry, 14: 223–235.

Heling, D., Teichmüller, M. (1974): Die Grenze Montmorillonit / Mixed Layer-Minerale und ihre Beziehung zur Inkohlung in der Grauen Schichtenfolge des Oligozäns im Oberrheingraben. – Fortschritte in der Geologie von Rheinland und Westfalen (Krefeld), 24: 113–128.

Hillebrand, T, Leythaeuser, D. (1992): Reservoir geochemistry of the Stockstadt oilfield. – Advances in Organic Geochemistry 1991, Organic Geochemistry, 19: 119–131.

Hoffers, B. (1981): A model for hydrothermal convection in the Rhine graben and its tectonic implications. – Tectonophysics, 73 (1–3): 141–149.

Horn, P., Lippolt, H.J., Todt, W. (1972): Kalium-Argon-Bestimmungen an tertiären Vulkaniten des Oberrheingrabens- I. Gesamtgesteinsalter. – Eclogae geologicae Helvetiae, 65: 131–156.

Hullen, J.B., Goff, F., Bortz, L.C. & Bereskin, S.R. (1994): Geology and geothermal origin of Grand Canyon and Bacon Flat oil fields, Railroad Valley, Nevada. – The American Association of Petroleum Geologists Bulletin, 78: 596–623; Tulsa, OK.

Illies, J. H. (1970): Graben Tectonics as Related to Crust-Mantle Interaction. – Graben Problems, 4-27; Stuttgart.

Illies, J.H., (1972): The Rhine graben rift system-plate tectonics and transform faulting. – Surveys in Geophysics, 1 (1): 27–60; Dordrecht.

Illies, J.H. & Mueller, S. (1970): Graben problems. 316 pp. E. Schweizerbart'sche Verlagsbuchhandlung, Stuttgart.

Illies, J.H. & Fuchs, K. (1974): Approaches to Taphrogenesis. 469 pp. E. Schweizerbart'sche Verlagsbuchhandlung, Stuttgart.

Illies, J.H., Baumann, H., Hoffers, B., (1981): Stress Pattern and Strain Release in the Alpine Foreland (1981/01/10).

Isaksen, G.H., Wilkinson, D.R. & Hitchen, K. (2000): Geochemistry of organic-rich Cretaceous and Jurassic mudstones in the West Lewis and West Flannan basins, offshore north-west Scotland: implications for source rock presence in the north-east Rockall Trough. - Marine and Petroleum Geology, 17: 27–42.

Jäger, H. (2013): Optical kerogen analysis – a new workflow in unconventional shale play analysis, URTEC – Unconventional Resources Technology Conference, August 2013, Denver, Colorado, USA.

Kadolsky, D. (1988): Stratigraphie und Molluskenfaunen von „Landschneckenkalk" und „Cerithienschichten" im Mainzer Becken (Oberoligozän bis Untermiozän?). – Geologisches Jahrbuch (A), 110: 69–133; Hannover.

Keller, J., Kraml, M., Henjes-Kunst, F. (2002): ^{40} Ar/^{39} Ar single crystal laser dating of early volcanism in the Upper Rhine Graben and tectonic implications. – Schweizerische Mineralogische und Petrographische Mittelungen, 82: 121–130.

Kennard, J.M., Deighton, I., Edwards, D.S., Colwell, J.B., O'Brien, G.W. & Boreham, C.J. (1999): Thermal history modeling and transient heat pulses: new insights into hydrocarbon expulsion and "hot flushes" in the Vulcan Sub-basin, Timor Sea. - APPEA Journal: frontiers of opportunity/Australian Petroleum Production and Exploration Association Ltd., 39(1): 177–207; Canberra.

Kvenvolden, K.A. & Simoneit, B.R.T. (1990): Hydrothermally derived petroleum: examples from Guyamas basin, Gulf of California, and Escanaba Trough, northeast Pacific Ocean. - American Association of Petroleum Geologists Bulletin, 74: 223–237; Tulsa, OK.

Lampe, C. & Person, M. (2000): Episodic hydrothermal fluid flow in the Upper Rhinegraben (Germany). – Journal of Geochemical Exploration, 69/70: 37–40.

Lampe, C. (2001): The effects of hydrothermal fluid flow on the temperature history of the northern Upper Rhinegraben: Numerical simulation studies. – Kölner Forum für Geologie und Paläontologie, 8, 126 pp. - PhD thesis Köln University.

Lampe, C., Person, M., Nöth, S., Ricken, W. (2001): Episodic fluid flow within continental rift basins—some insights from field data and mathematical models. – Geofluids, 1:42–54.

Lampe, C. & Person, M. (2002): Advective cooling within sedimentary rift basins – application to the Upper Rhinegraben (Germany). – Marine and Petroleum Geology, 19: 361–375.

Langford, F.F., Blanc-Valleron, M.M. (1990): Interpreting rock-eval pyrolysis data using graphs of pyrolysable hydrocarbons vs. Total organic carbon. – American Association of Petroleum Geologists Bulletin, 74: 799–804.

Le-Carlier, C., Royer, J.J. & Flores, E.L. (1994): Convective heat transfer at the Soultz-sous-Forêts geothermal site; implications for oil potential. – First Break, 12(11): 553–560; Oxford.

Ledesert, B., Joffre, J., Ambles, A., Sardini, P., Genter, A. & Meunier, A. (1996): Organic matter in the Soultz HDR granitic thermal exchanger (France); natural tracer of fluid circulations between the basement and its sedimentary cover. – Journal of Volcanology and Geothermal Research, 70(3-4): 235–253; Amsterdam.

LGB, LfW (2004): Hydrogeologische Kartierung Kaiserslautern. – LGB-RLP, LfW-RLP, 96 pp.

Luis, J.F. (2007): Mirone: A multi-purpose tool for exploring grid data. – Computers & Geosciences, 22 (1): 31–41.

Lutz, M., Cleintuar, M. (1999): Geological results of a hydrocarbon exploration campaign in the southern Upper Rhine Graben (Alsace Centrale, France). – Bulletin für Angewandte Geologie, 4: 3–80.

Marell, D. (1989): Das Rotliegende zwischen Odenwald und Taunus. – Geologische Abhandlungen Hessen, 89: 128 pp.; Wiesbaden.

Martini, E. (1990): The Rhinegraben system, a connection between northern and southern seas in the European Tertiary. – Veröffentlichungen Übersee-Museum Bremen, A 10: 83–98, 208–211; Bremen.

Mauthe, G. Brink, H.J. & Burri, P. (1993): Kohlenwasserstoffvorkommen und -potential im deutschen Teil des Oberrheingrabens. – Bulletin der Vereinigung Schweiz, Petroleum-Geologen und -Ingenieure., 60 (137): 15–29; Zürich.

Meier, L. & Eisbacher, G.H. (1991): Crustal kinematics and deep-structure of the northern Rhine Graben, Germany. – Tectonics, 10: 621–630.

Micklich, N. & Hildebrandt, L. (2005): The Frauenweiler clay pit ("GrubeUnterfeld"). – Kaupia, 14: 113–118.

Müller, H. (1996): Das Permokarbon im nördlichen Oberrheingraben. Paläogeographische und strukturelle Entwicklung des permokarbonen Saar-Nahe-Beckens im nördlichen Oberrhein-graben. – Geologische Abhandlungen Hessen, 99, 85 pp.; Wiesbaden.

Mukhopadhyay, P.K. (1994): Vitrinite reflectance as a maturity parameter. – Vitrinite reflectance as a maturity parameter, American Chemical Society, 1–24.; Washington , DC .

Nickel, B. (1996): Palynofazies und Palynostratigraphie der Pechelbronn Schichten im nördlichen Oberrheintalgraben. – Palaeontographica, B/240: 1–151; Stuttgart.

Nielsen, S., Clausen, O. & Mcgregor, E. (2015): basin%Ro : A Vitrinite reflectance model derived from basin and laboratory data. – Basin Research, 29(S1): 515–536.

Pauwels, H. & Fouillac, C. & Fouillac, A.-M.. (1993): Chemistry and isotopes of deep geothermal saline fluids in the Upper Rhine Graben: Origin of compounds and water-rock interactions. – Geochimica et Cosmochimica Acta, 57(12): 2737–2749.

Perner, M. (2014): Sedimentpetrographie und Ablagerungsbedingungen der Pechelbronn-Gruppe (Ober-Eozän bis Unter-Oligozän) und der Bodenheim-Formation (Unter-Oligozän) im nördlichen Oberrheingraben, – M.Sc. thesis, 90 pp., Ruprecht-Karls-University Heidelberg.

Person, M. & Garven, G. (1992): Hydrogeologic constraints on petroleum generation within continental rift basins; theory and application to the Rhine Graben. – American Association of Petroleum Geologists Bulletin, 76(4): 468–488; Tulsa, OK.

Peters, K.E. (1986): Guidelines for evaluating petroleum source rocks using programmed pyrolysis. – American Association of Petroleum Geologists Bulletin, 70: 318–329.

Peters, K.E. & Cassa, M.R. (1994): Applied Source-Rock Geochemistry. – The Petroleum System. From Source to Trap, American Association of Petroleum Geologists, 93–120; Tulsa.

Pflug, R. (1982): Bau und Entwicklung des Oberrheingrabens. – Wissenschaftliche Buchgesellschaft Darmstadt, 145 pp.; Darmstadt.

Plein, E. (1992): Das Erdölfeld Eich-Königsgarten (Exkursion E am 23.4.1992). – Jahresberichte und Mitteilungen des Oberrheinischen Geologischen Vereines, N.F. 74: 41–54; Stuttgart.

Prell-Müssig, R. (1965): Das jüngere Tertiär (Oberes Rupel bis Aquitan) bei Bruchsal (Foraminiferen, Fazies, Stratigraphie). – Jahreshefte des Geologischen Landesamtes Baden-Württemberg, 7: 229–301; Freiburg.i.Br.

Pribnow, D. & Schnellschmidt, R. (2000): Thermal Tracking of Upper Crustal Fluid Flow in the Rhine graben. – Geophysical Research Letters, 27: 1957–1960.

Reichenbacher, B. (2000): Das brackisch-lakustrine Oligozän und Unter-Miozän im Mainzer Becken und Hanauer Becken: Fischfaunen, Paläoökologie. – Biostratigraphie, Paläogeographie. Courier Forschungsinstitut Senckenberg, 222, 1–143; Frankfurt am Main.

Reinhold, C., Schwarz, M., Bruss, D., Heesbeen, B., Perner, M., Suana, M. (2016): The Northern Upper Rhine Graben- Re-dawn of a mature petroleum province? – Swiss Bulletin, 21/2, 2016: 35–56.

Robert, P. (1985): Histoire géothermique et diagenèse organique. – Bulletin des Centres de Recherches Exploration-Production Elf-Aquitaine, Mém. 8; Pau.

Rothausen, K. & Sonne, V. (1984): Mainzer Becken. – Sammlung geologischer Führer, 79: 203 pp.; Berlin-Stuttgart.

Rückheim, J. (1989): Migrations- und Akkumulationsgeschichte der Erdöle des nördlichen Oberrheingrabens und deren Beziehung zur Diagenese der klastischen Speichergesteine. Berichte der Kernforschungsanlage Jülich. K. J. GmbH. – PhD thesis RWTH Aachen University, 282pp.

Rybach, L. (2007): The geothermal conditions in the Rhine Graben - a summary. – Bulletin für Angewandte Geologie, 12(1): 29–32.

Schad, A. (1962): Voraussetzungen für die Bildung von Erdöllagerstätten im Rheingraben. – Abhandlungen des Geologischen Landesamtes Baden-Württemberg, 5: 29–40; Freiburg i.Br.

Schad, A. (1962): Das Erdölfeld Landau. – Abhandlungen des Geologischen Landesamtes Baden-Württemberg, 5: 81–101; Freiburg i.Br.

Schad, A. (1964): Feingliederung des Miozäns und die Deutung der nacholigozänen Bewegungen im Mittleren Rheingraben. – Abhandlungen des Geologischen Landesamtes Baden-Württemberg, 5: 1–56; Freiburg i.Br.

Schellschmidt, R. & Clauser, C. (1996): The Thermal Regime of the Upper Rhine Graben and the Anomaly at Soultz. – Zeitschrift für Angewandte Geologie, 42(1): 40–44; Hannover.

Schenk, H.J., Witte, E.G., Littke, R., Schwochau, K., (1990): Structural modifications of vitrinite and alginite concentrates during pyrolytic maturation at different heating rates. A combined infrared, 13C NMR and microscopical study. – Organic Geochemistry, 16: 943–950.

Schlische, R.W., Young, S.S., Ackermann, R.V., Gupta, A. (1996): Geometry and scaling relatios of a population of very small rift: Related normal faults. – Geology, 24: 683–686.

Schmidt, G., Al Najem, S., Isenbeck- Schröter, M., Freundt, F., Kraml, M. & Aeschbach- Hertig, W. (2017): $^{87}Sr/^{86}Sr$ ratios in shallow and deep aquifers and thermal water from the Eastern Boundary Fault of the northern Upper Rhine Graben at the Heidelberg Basin, Germany. – Procedia Earth and Planetary Science, 17: 108–111.

Schmitt, M. (1992): Ursache und Ablauf der Versalzung der oberen Grundwasserleiter im nördlichen Oberrheingraben. – PhD thesis Technische Hochschule Darmstadt, 237 pp.

Schnaebele, R.J. (1948): Monographie Géologique du Champ Pétrolifere de Pechelbronn. – Mémoires du Service de la Carte Géologique d'Alsace et de Lorraine, 7: 1–254.

Schumacher, M.E. (2002): Upper Rhine Graben: Role of preexisting structures during rift evolution. – Tectonics, 21(1): 6–1–6–17.

Schwarz, J. (1997): Charophyten aus dem Tertiär des Oberrheingrabens (Mitteleozän-Untermiozän). – Palaeontographica (B), 243: 1–84; Stuttgart.

Schwarz, M. (2005): Evolution und Struktur des oberrheingrabens- quantitative Einblicke mit Hilfe dreidimensionaler thermomechanischer Modellrechnungen. – PhD thesis Albert-Ludwigs University Freiburg i.Br., 337 pp.

Shipton, Z., Soden, A.M., Kirkpatrick, J.D., Bright, A.M., Lunn, R.J. (2006): How thick is a fault? Fault displacement-thickness scaling revisted. – Earthquakes: Radiated Energy and the Physics of Faulting, Geophysical Monograph Series, 170: 193–198; Washington D.C.

Sissingh, W. (1998): Comparative Tertiary stratigraphy of the Rhine Graben, Bresse Graben and Molasse Basin: correlation of Alpine foreland events. – Tectononphysics, 300: 249–284; Amsterdam.

Sittler, C. (1965): Le Paléogène des fossés rhénan et rhodanien. Études sédimentologiques et paléoclimatiques. – Mém. Service de la Carte Géollogique Alsace Lorraine, 24: 1–392; Strasbourg.

Sittler, C. (1967): Le soubassement et le remplissage sédimentaire du fossé rhénan au niveau du bassin de Pechelbronn et du seuil d'Erstein. Coupes géologiques à traverse le fossé rhénan. - Abhandlungen des Geologischen Landesamtes Amt Baden-Württemberg, 6 (26): 69–80.

Sittler, C. (1988): Rhine graben sections. - The northwest European Tertiary basin. – Geologisches Jahrbuch, (A) 100: 135–136; Hannover.

Soyk, D. (2015): Diagenesis and reservoir quality of the Lower and Middle Buntsandstein (Lower Triassic), SW-Germany. – PhD Thesis Ruprecht-Karls University Heidelberg, 179 pp.

Stober, I. & Bucher, K. (2000): Herkunft der Salinität in Tiefenwässern des Grundgebirges - unter besonderer Berücksichtigung der Kristallinwässer des Schwarzwaldes. – Grundwasser, Zeitschrift der Fachsektion Hydrogeologie, 5(3): 125–140.

Stober, I. & Bucher, K. (2015): Hydraulic and hydrochemical properties of deep sedimentary reservoirs of the Upper Rhine Graben, Europe. – Geofluids, 15: 464–482.

Stober, I. & Jodocy, M. (2011): Geothermische Verhältnisse südlich des Kaiserstuhls - Das Hartheimer Becken im südlichen Oberrheingraben. – Grundwasser, Zeitschrift der Fachsektion Hydrogeologie, 16: 113–123.

Straub, E. (1956): Erdöl- und Erdgasfeld Stockstadt. – Symposium sobre Yacimentos de Petroleo y Gas, 20. Congress geológ. Internat., 5 (Europa): 141–147; Mexico-City.

Straub, E. (1962): Die Erdöl- und Erdgaslagerstätten in Hessen und Rheinhessen. – Abhandlungen des Geologischen Landesamtes Baden-Württemberg, 4, 123–136; Freiburg i.Br.

Suárez-Ruiz, I., Flores, D., Filho, J.G.M., Hackley, P.C. (2012): Review and update of the applications of organic petrology: Part 1, geological applications. – International Journal of Coal Geology, 99: 54–112.

Teichmüller, M. (1979): Die Diagenese der kohligen Substanzen in den Gesteinen des Tertiärs und Mesozoikums des mittleren Oberrhein-Grabens. – Fortschritte in der Geologie von Rheinland und Westfalen, 27: 19–49.

Teichmüller, M. & Teichmüller, R. (1979): Zur geothermischen Geschichte des Oberrhein-Grabens. Zusammenfassung und Auswertung eines Symposiums. – Fortschritte in der Geologie von Rheinland und Westfalen, 27: 109–120.

Timar Geng, Z., Fügenschuh, B., Schaltegger, U. & Wetzel, A. (2004): The impact oft he Jurassic hydrothermal activity on zircon fission track data from the southern Upper Rhine Graben area. – Schweizerische Mineralogische und Petrographische Mitteilungen, 84: 257–269.

Tissot, B.P. & Welte, D.H. (1984): Petroleum Formation and Occurrence, 699 pp.; Berlin.

Torabi, A. & Berg, S.S. (2011): Scaling of fault attributes: A review. – Marine and Petroleum Geology, 28: 1444–1460.

Traverse A. (2007): Paleopalynology. Second edition. Springer; xviii + 813 pp.; Dordrecht, NL.

Turcotte, D.L. & Schubert, G. (2002): Geodynamics. – Cambridge University Press, 456 pp.; New York.

Tyson R.V. (1989): Late Jurassic palynofacies trends, Piper and Kimmeridge Clay Formation, UK onshore and offshore. – Northwest European Micropalaeontology and palynology. British Micropalaeontological Society Series, 135–172.

Tyson, R.V. (1995): Sedimentary Organic Matter. – Organic Facies and Palynofacies. Chapman & Hall, London, 615 pp.

Veit, E. (1955): Die Tiefbohrungen bei Pfungstadt und der Bau des Rheintalgrabens im Raum um Darmstadt. – Zeitschrift der Deutschen Geologischen Gesellschaft, 105: 150–151; Hannover.

Vidal, J., Genter, A., Schmittbuhl, J., Whitechurch, H., Baujard, C. & Dalmais, E. (2015): Evolution of concepts for the geothermal projects in the Upper Rhine Graben. – European Geothermal Workshop 2015; Strasbourg.

Villemin, T. & Coletta, B. (1990): Subsidence in the Rhine Graben: a new compilation of borehole data. – Symposium on Rhine-Rhone Rift System; ICL-WG-3 Symp., Geological Institute University Basel, 31 pp.

Wagner, W. (1947): Miozänes Steinsalz im hessischen Rheintalgraben. – Wissenschaftliche Veröffentlichung TH Darmstadt, (1)3: 93–96; Darmstadt.

Wagner, W. (1955): Die tertiären Salzlagerstätten im Oberrheintal-Graben. – Zeitschrift der Deutschen Geologischen Gesellschaft (1953), 105 (4): 706–728; Stuttgart.

Walter, R. (2007): Geologie von Mitteleuropa. 7th edition. Schweizbart`sche Verlagsbuchhandlung (Nägele u. Obermiller) Stuttgart: 511pp.

Welte, D.H. (1979): Organisch-geochemische Untersuchungen zur Bildung von Erdöl Kohlenwasserstoffen an Gesteinen des mittleren Oberrhein-Grabens. – Fortschritte in der Geologie von Rheinland und Westfalen, 27: 51–73.

Welte, D.H. & Yükler, M.A. (1981): Petroleum origin and accumulation in basin evolution- a quantitive model. – American Association of Petroleum Geologists Bulletin, 65: 1387–1396.

Wisian, K.W. & Blackwell, D.D. (2004): Numerical modeling of Basin and Range geothermal systems. - Geothermics, 33: 713–741.

Wirth, E. (1954): Die nördliche Verbreitungsgrenze des Unteroligozäns im Rheintalgraben und ihre wirtschaftliche Bedeutung. – Notizblatt des hessischen Landesamtes für Bodenforschung, 82: 168–189; Wiesbaden.

Wirth, E. (1969): Die Probleme des Eozäns im deutschen Anteil der Oberrheinebene und ihrer Randzonen. Memoires B.R.G.M., 69:287–306; Paris.

Wüstefeld, P., Hilse, U., Luders, V., Wemmer, K., Koehrer, B. & Hilgers, C. (2017): Kilometer-scale Fault-related Thermal Anomalies in Tight Gas Sandstones. – Marine and Petroleum Geology, 86: 288–303.

Yalcin, M.N., Littke, R. & Sachsenhofer, R.F. (1997): Thermal history of sedimentary basins. – Petroleum and basin evolution, 71–167; Berlin.

Ziegler, P.A. (1992): European Cenozoic rift system. – Tectonophysics, 208: 91–111; Amsterdam.

Ziegler, P.A. (1994): Cenozoic rift system of western and central Europe: An overview. – Geologie en Mijnbouw, 73: 99–127.

Ziegler, P.A. & Dezes, P. (2007): Cenozoic uplift of Variscan Massifs in the Alpine foreland: timing and controlling mechanisms. – Global and Planetary Change, 58: 237–269.

List of Abbreviations

AOM	Amorphous Organic Material
BGL	Below Ground Level
CNS	C-N-S analysis
HC	Hydrocarbons
HI	Hydrogen Index [mg HC/g TOC]; HI = (100 x S2)/TOC
Ma	„millions of years“
OI	Oxygen Index [mg CO_2/g TOC]; OI = (100 x S3)/TOC
OM	Organic Material
ORG	Oberrheingraben
PI	Production Index; PI=S1/(S1+S2)
S1	Amount of free HCs present in the sample before the Rock-Eval pyrolysis [mg HC/g rock]
S2	Volume of HCs that formed during Rock Eval pyrolysis [mg HC / g rock]
S3	Amounts of CO_2 [mg CO_2 / g rock] produced during pyrolysis
SCI	Spore Coloration Index (1-10)
T_{max}	Temperature of maximum release of HC during pyrolysis (top of S2)
TOC	Total Organic Carbon (%)
TS	Total sulphur (%)
TVD	True Vertical Depth (m)
URG	Upper Rhine Graben
VR	Vitrinite reflectance
Wt.%	Weight-%

Stratigraphic formations:

BN	Bunte Niederröderner Group
Cer	Cerithien Group
Cor	Corbicula Group
CyM	Cyrena Marls Group
FM	Fish Shale Formation (Rupel Clay Group)
FS	Foraminifera Marls Formation (Rupel Clay Group)
Hy	Hydrobia Group
LPE	Lower Pechelbronn Formation
LHy	Lower Hydrobia Formation
ME	Meletta Group
MPE	Middle Pechelbronn Formation
PE	Pechelbronn Group
RpC	Rupel Clay Group
UHy	Upper Hydrobia Formation
UPE	Upper Pechelbronn Group
UT I	Upper Tertiary I
UT II	Upper Tertiary II

Appendix

Well	TVD (m)	Stratigraphy	# of particels	Preservation of Phytoclasts			Phyclasts%/ total OM	Preservation of Inertinite			Inertinite %/ total OM	Preservation of Vitrinite			Vitrinite %/ total OM	Preservation of Cutinite			Cutinite %/ total OM	Preservation of Sporomorphs			Sporomorphs %/ total OM	Preservation of Spores			Spores %/ total OM	Preservation of Pollen			Pollen %/ total OM	terr. AOM %/ total OM	marine AOM %/ total OM	total AOM %/ total OM
				good (%/Phytoclasts)	moderate (%/Phytoclasts)	poor (%/Phytoclasts)		good (%/Inertinite)	moderate (%/Inertinite)	poor (%/Inertinite)		good (%/Vitrinite)	moderate (%/Vitrinite)	poor (%/Vitrinite)		good (%/Cutinite)	moderate (%/Cutinite)	poor (%/Cutinite)		good (%/Sporomorphs)	moderate(%/Sporomorphs)	poor (%/Sporomorphs)		good (%/Spores)	moderate (%/Spores)	poor (%/Spores)		good (%/Spores)	moderate (%/Spores)	poor (%/Spores)				
W1	650.0	UHy	385	30	41	29	48.3	0	100	0	3.4	31	39	31	34.0	38	29	33	10.9	52	48	0	6.5	100	0	0	3.4	0	100	0	3.1	3.9	11.7	15.6
W1	660.0	UHy	320	0	45	55	26.6	0	100	0	1.9	0	47	53	18.1	0	24	76	6.6	44	38	17	19.7	77	12	12	8.1	22	57	22	11.6	3.1	50.0	53.1
W1	700.0	UHy	283	22	48	30	9.5	43	57	0	2.5	15	45	40	7.1	0	0	0	0.0	49	51	0	13.1	60	40	0	5.3	41	59	0	7.8	10.6	63.6	74.2
W1	750.0	UHy	324	12	41	47	15.1	0	100	0	0.9	13	37	50	14.2	0	0	0	0.0	55	35	10	18.5	100	0	0	7.7	23	60	17	10.8	4.6	61.7	66.4
W1	800.0	UHy	241	0	56	44	13.3	0	100	0	7.5	0	0	100	5.8	0	0	0	0.0	66	9	25	18.3	88	12	0	13.7	0	0	100	4.6	8.3	60.2	68.5
W1	850.0	UHy	352	13	45	43	24.7	33	67	0	6.8	5	37	59	17.9	0	0	0	0.0	14	46	40	24.1	40	37	23	8.5	0	51	49	15.6	7.1	34.1	41.2
W1	900.0	UHy	232	0	69	31	6.9	0	100	0	0.9	0	75	25	5.2	0	0	100	0.9	58	35	8	22.4	55	27	18	9.5	60	40	0	12.9	5.6	62.5	68.1
W1	950.0	UHy	264	23	60	17	93.6	70	30	0	12.5	15	66	19	63.3	19	60	21	17.8	57	43	0	2.7	100	0	0	1.5	0	100	0	1.1	3.8	0.0	3.8
W1	1000.0	UHy	330	0	54	46	18.5	0	100	0	1.2	0	47	53	16.1	0	100	0	1.2	59	38	3	36.7	78	22	0	16.7	42	52	6	20.0	7.6	36.4	43.9
W1	1050.0	UHy	318	0	51	49	21.4	0	100	0	2.2	0	40	60	15.1	0	69	31	4.1	28	40	32	18.9	75	0	25	3.8	17	50	33	15.1	7.9	45.6	53.5
W1	1100.0	UHy	288	23	53	25	18.4	46	54	0	9.0	0	52	48	9.4	0	0	0	0.0	25	57	18	15.3	64	36	0	3.8	12	64	24	11.5	12.2	47.9	60.1
W1	1150.0	UHy	265	15	54	31	19.6	31	69	0	9.8	0	33	67	9.1	0	100	0	0.8	39	44	17	15.5	55	45	0	8.3	21	42	37	7.2	6.4	54.7	61.1
W1	1200.0	UHy	281	0	54	46	17.1	0	100	0	1.1	0	51	49	16.0	0	0	0	0.0	41	38	21	21.7	100	0	0	5.7	20	51	29	16.0	10.3	45.6	55.9
W1	1250.0	UHy	381	15	48	37	19.2	70	30	0	2.6	8	46	46	13.6	0	73	27	2.9	30	42	28	31.5	80	20	0	3.9	23	45	32	27.6	5.2	28.9	34.1
W1	1300.0	UHy	380	12	44	45	26.6	0	100	0	1.1	12	41	46	25.5	0	0	0	0.0	42	31	27	21.3	67	33	0	1.6	40	31	29	19.7	0.0	34.2	34.2
W1	1370.0	Cor	341	16	53	32	16.7	0	100	0	2.1	18	46	36	14.7	0	0	0	0.0	50	36	14	37.2	76	24	0	5.0	45	38	16	32.3	2.9	38.1	41.1
W1	1400.0	Cor	347	5	60	36	12.1	0	100	0	0.6	5	58	38	11.5	0	0	0	0.0	45	40	15	30.3	67	24	9	9.5	35	47	18	20.7	5.8	51.9	57.6
W1	1430.0	Cor	322	0	47	53	31.4	0	100	0	3.1	0	35	65	24.5	0	75	25	3.7	29	53	19	33.5	37	43	20	15.8	21	61	18	17.7	20.2	14.0	34.2
W1	1500.0	Cer	308	18	45	37	12.3	0	100	0	2.6	23	30	47	9.7	0	0	0	0.0	6	59	35	21.4	57	43	0	2.3	0	61	39	19.2	6.5	51.9	58.4
W1	1600.0	Cer	359	7	52	41	26.5	0	100	0	3.3	9	45	46	20.6	0	44	56	2.5	39	37	24	30.4	100	0	0	3.6	31	42	27	26.7	4.2	32.0	36.2
W1	1700.0	Cer	289	2	31	67	57.4	18	82	0	5.9	0	27	73	48.8	0	0	100	2.8	0	0	100	1.0	0	0	0	0.0	0	0	100	1.0	39.8	1.7	41.5
W1	1800.0	BN	214	0	0	100	2.3	0	0	0	0.0	0	0	100	2.3	0	0	0	0.0	0	0	0	0.0	0	0	0	0.0	0	0	0	0.0	35.0	58.4	93.5
W1	1900.0	CyM	247	9	48	43	35.2	0	100	0	4.5	11	41	49	30.8	0	0	0	0.0	0	60	40	8.1	0	100	0	4.9	0	0	100	3.2	2.0	54.7	56.7
W1	2000.0	ME	260	18	61	21	44.2	48	52	0	9.6	12	61	27	28.5	0	75	25	6.2	0	50	50	3.8	0	100	0	1.2	0	29	71	2.7	0.0	51.9	51.9
W1	2070.0	FS (RpC)	304	11	45	44	36.5	0	100	0	5.3	14	41	45	27.3	0	0	100	3.9	23	36	41	12.8	0	0	0	0.0	23	36	41	12.8	39.5	11.2	50.7
W1	2074.0	FS (RpC)	318	16	43	41	26.1	26	74	0	7.2	13	34	54	17.6	0	0	100	1.3	0	60	40	6.3	0	100	0	0.9	0	53	47	5.3	15.7	51.9	67.6
W1	2080.0	FS (RpC)	278	0	29	71	30.9	0	100	0	4.3	0	19	81	24.1	0	0	100	2.5	26	59	15	16.5	46	54	0	9.4	0	65	35	7.2	39.6	10.8	50.4
W1	2100.0	FM (RpC)	302	0	62	38	19.2	0	0	0	0.0	0	56	44	16.6	0	100	0	2.6	19	23	58	10.3	67	33	0	3.0	0	18	82	7.3	24.8	45.7	70.5
W1	2120.0	FM (RpC)	313	11	41	47	31.0	13	88	0	7.7	13	30	58	20.4	0	0	100	2.9	20	40	40	14.4	75	25	0	3.8	0	45	55	10.5	39.9	11.2	51.1
W1	2140.0	FM (RpC)	253	0	50	50	17.4	0	100	0	2.8	0	27	73	11.9	0	100	0	2.8	0	56	44	3.6	0	100	0	1.2	0	33	67	2.4	7.9	65.2	73.1
W1	2160.0	FM (RpC)	229	4	36	59	30.1	0	100	0	1.7	5	31	64	25.3	0	43	57	3.1	0	80	20	6.6	0	100	0	1.7	0	73	27	4.8	24.0	39.3	63.3
W1	2210.0	PE	228	0	57	43	28.5	0	100	0	7.9	0	40	60	20.6	0	0	0	0.0	0	0	0	0.0	0	0	0	0.0	0	0	0	0.0	15.4	54.8	70.2
W1	2300.0	PE	321	16	33	51	28.0	50	50	0	8.7	0	30	70	16.8	0	0	100	2.5	0	0	100	0.9	0	0	0	0.0	0	0	100	0.9	21.2	49.8	71.0
W1	2400.0	PE	270	0	71	29	25.9	0	100	0	11.1	0	50	50	14.8	0	0	0	0.0	0	0	0	0.0	0	0	0	0.0	0	0	0	0.0	37.0	37.0	74.1

Well	TVD (m)	Stratigraphy	Preservation of Phytoplancton			Phytoplancton %/ total OM	Preservation of Prasinophytes			Prasinophytes %/ total OM	Preservation of Acritarchs			Acritarchs %/ total OM	Preservation of Dinoflagellate cysts			Dinoflagellate cysts %/ total OM	Preservation of Leiospheres			Leiospheres %/ total OM	Preservation of Lacustrine Algae			Lacustrine Algae %/ total OM	Foraminifera %/ total OM	Fungi %/ total OM	Ter. Comp. % / total OM	Marine Comp. % / total OM	ter. palynomorphs/ total OM	marine palynomorphs/ total OM
			good (%/Phytoplancton)	moderate (%/Phytoplancton)	poor (%/Phytoplancton)		good (%/Pras.)	moderate (%/Pras.)	poor (%/Pras.)		good (%/Acritarchs)	moderate (%/Acritarchs)	poor (%/Acritarchs)		good (%/Dino.)	moderate (%/Dino.)	poor (%/Dino.)		good (%/Leiospheres)	moderate (%/Leiospheres)	poor (%/Leiospheres)		good (%/Lac. Algae)	moderate (%/Lac. Algae)	poor (%/Lac. Algae)						
W1	650.0	UHy	0	0	0	0.0	0	0	0	0.0	0	0	0	0.0	0	0	0	0.0	0	0	0	0.0	49	38	13	29.6	0.0	0.0	58.7	11.7	6.5	0.0
W1	660.0	UHy	0	100	0	0.6	0	0	0	0.0	0	0	0	0.0	0	100	0	0.6	0	0	0	0.0	0	0	0	0.0	0.0	0.0	49.4	50.6	19.7	0.6
W1	700.0	UHy	100	0	0	0.7	100	0	0	0.7	0	0	0	0.0	0	0	0	0.0	0	0	0	0.0	0	100	0	2.5	0.0	0.0	33.2	64.3	13.1	0.7
W1	750.0	UHy	0	0	0	0.0	0	0	0	0.0	0	0	0	0.0	0	0	0	0.0	0	0	0	0.0	0	0	0	0.0	0.0	0.0	38.3	61.7	18.5	0.0
W1	800.0	UHy	0	0	0	0.0	0	0	0	0.0	0	0	0	0.0	0	0	0	0.0	0	0	0	0.0	0	0	0	0.0	0.0	0.0	39.8	60.2	18.3	0.0
W1	850.0	UHy	0	24	76	4.8	0	67	33	1.7	0	0	100	3.1	0	0	0	0.0	0	0	0	0.0	0	100	0	5.1	0.0	0.0	56.0	38.9	24.1	4.8
W1	900.0	UHy	100	0	0	0.9	0	0	0	0.0	0	0	0	0.0	100	0	0	0.9	0	0	0	0.0	100	0	0	1.7	0.0	0.0	34.9	63.4	22.4	0.9
W1	950.0	UHy	0	0	0	0.0	0	0	0	0.0	0	0	0	0.0	0	0	0	0.0	0	0	0	0.0	0	0	0	0.0	0.0	0.0	100.0	0.0	2.7	0.0
W1	1000.0	UHy	0	0	100	0.9	0	0	0	0.0	0	0	100	0.9	0	0	0	0.0	0	0	0	0.0	0	0	0	0.0	0.0	0.0	62.7	37.3	36.7	0.9
W1	1050.0	UHy	45	55	0	6.3	0	0	0	0.0	0	0	0	0.9	53	47	0	5.3	0	0	0	0.0	0	0	0	0.0	0.0	0.0	48.1	51.9	18.9	6.3
W1	1100.0	UHy	0	0	100	3.8	0	0	0	0.0	0	0	100	0.7	0	0	100	3.1	0	0	0	0.0	43	57	0	2.4	0.0	0.0	45.8	51.7	15.3	3.8
W1	1150.0	UHy	0	0	100	0.8	0	0	0	0.0	0	0	0	0.0	0	0	100	0.8	0	0	0	0.0	0	100	0	3.0	0.0	0.0	41.5	55.5	15.5	0.8
W1	1200.0	UHy	60	20	20	5.3	0	0	0	0.0	0	0	0	0.0	50	25	25	4.3	100	0	0	1.1	0	0	0	0.0	0.0	0.0	49.1	50.9	21.7	5.3
W1	1250.0	UHy	12	52	37	13.6	100	0	0	0.5	0	56	44	4.2	12	53	35	8.9	0	0	0	0.0	100	0	0	1.6	0.0	0.0	55.9	42.5	31.5	13.6
W1	1300.0	UHy	32	32	35	17.9	0	0	0	0.0	0	31	69	6.8	52	33	14	11.1	0	0	0	0.0	0	0	0	0.0	0.0	0.0	47.9	52.1	21.3	17.9
W1	1370.0	Cor	0	24	76	5.0	0	0	0	0.0	0	0	0	0.0	0	24	76	5.0	0	0	0	0.0	0	0	0	0.0	0.0	0.0	56.9	43.1	37.2	5.0
W1	1400.0	Cor	0	0	0	0.0	0	0	0	0.0	0	0	0	0.0	0	0	0	0.0	0	0	0	0.0	0	0	0	0.0	0.0	0.0	48.1	51.9	30.3	0.0
W1	1430.0	Cor	0	0	100	0.9	0	0	0	0.0	0	0	100	2.3	0	0	100	2.9	0	0	0	0.0	0	100	0	2.6	0.0	0.0	85.1	14.9	33.5	0.9
W1	1500.0	Cer	0	0	100	5.2	0	0	0	0.0	0	0	100	0.0	55	32	14	6.1	0	0	0	0.0	0	100	0	0.8	0.0	0.0	40.3	57.1	21.4	5.2
W1	1600.0	Cer	55	32	14	6.1	0	0	0	0.0	0	0	0	0.0	0	0	0	0.0	0	0	0	0.0	0	0	0	0.0	0.0	0.0	61.0	38.2	30.4	6.1
W1	1700.0	Cer	0	0	0	0.0	0	0	0	0.0	0	0	0	0.0	0	0	0	0.0	0	0	0	0.0	0	0	0	0.0	0.0	0.0	98.3	1.7	1.0	0.0
W1	1800.0	BN	0	0	100	4.2	0	0	0	0.0	0	0	100	0.0	0	0	100	4.2	0	0	0	0.0	0	0	0	0.0	0.0	0.0	37.4	62.6	0.0	4.2
W1	1900.0	CyM	0	0	0	0.0	0	0	0	0.0	0	0	0	0.0	0	0	0	0.0	0	0	0	0.0	0	0	0	0.0	0.0	0.0	45.3	54.7	8.1	0.0
W1	2000.0	ME	0	0	0	0.0	0	0	0	0.0	0	0	0	0.0	0	0	0	0.0	0	0	0	0.0	0	0	0	0.0	0.0	0.0	48.1	51.9	3.8	0.0
W1	2070.0	FS (RpC)	0	0	0	0.0	0	0	0	0.0	0	0	0	0.0	0	0	0	0.0	0	0	0	0.0	0	0	0	0.0	0.0	0.0	88.8	11.2	12.8	0.0
W1	2074.0	FS (RpC)	0	0	0	0.0	0	0	0	0.0	0	0	0	0.0	0	0	0	0.0	0	0	0	0.0	0	0	0	0.0	0.0	0.0	48.1	51.9	6.3	0.0
W1	2080.0	FS (RpC)	0	0	100	2.2	0	0	0	0.0	0	0	100	1.1	0	0	100	1.1	0	0	0	0.0	0	0	0	0.0	0.0	0.0	87.1	12.9	16.5	2.2
W1	2100.0	FM (RpC)	0	0	0	0.0	0	0	0	0.0	0	0	0	0.0	0	0	0	0.0	0	0	0	0.0	0	0	0	0.0	0.0	0.0	54.3	45.7	10.3	0.0
W1	2120.0	FM (RpC)	0	27	73	3.5	0	0	0	0.0	0	0	0	0.0	0	27	73	3.5	0	0	0	0.0	0	0	0	0.0	0.0	0.0	85.3	14.7	14.4	3.5
W1	2140.0	FM (RpC)	0	0	100	5.9	0	0	0	0.0	0	0	100	1.2	0	0	100	4.7	0	0	0	0.0	0	0	0	0.0	0.0	0.0	28.9	71.1	3.6	5.9
W1	2160.0	FM (RpC)	0	0	0	0.0	0	0	0	0.0	0	0	0	0.0	0	0	0	0.0	0	0	0	0.0	0	0	0	0.0	0.0	0.0	60.7	39.3	6.6	0.0
W1	2210.0	PE	0	0	100	1.3	0	0	0	0.0	0	0	100	1.3	0	0	0	0.0	0	0	0	0.0	0	0	0	0.0	0.0	0.0	43.9	56.1	0.0	1.3
W1	2300.0	PE	0	0	0	0.0	0	0	0	0.0	0	0	0	0.0	0	0	0	0.0	0	0	0	0.0	0	0	0	0.0	0.0	0.0	50.2	49.8	0.9	0.0
W1	2400.0	PE	0	0	0	0.0	0	0	0	0.0	0	0	0	0.0	0	0	0	0.0	0	0	0	0.0	0	0	0	0.0	0.0	0.0	63.0	37.0	0.0	0.0

Well	TVD (m)	Stratigraphy	# of particels	Preservation of Phytoclasts			Phyclasts%/ total OM	Preservation of Inertinite			Inertinite %/ total OM	Preservation of Vitrinite			Vitrinite %/ total OM	Preservation of Cutinite			Cutinite %/ total OM	Preservation of Sporomorphs			Sporomorphs %/ total OM	Preservation of Spores			Spores %/ total OM	Preservation of Pollen			Pollen %/ total OM	terr. AOM %/ total OM	marine AOM %/ total OM	total AOM %/ total OM
				good (%/Phytoclasts)	moderate (%/Phytoclasts)	poor (%/Phytoclasts)		good (%/Intertinite)	moderate (%/Interlinite)	poor (%/Interlinite)		good (%/Vitrinite)	moderate (%/Vitrinite)	poor (%/Vitrinite)		good (%/Cutinite)	moderate (%/Cutinite)	poor (%/Cutinite)		good (%/Sporomorphs)	moderate(%/Sporomorphs)	poor (%/Sporomorphs)		good (%/Spores)	moderate (%/Spores)	poor (%/Spores)		good (%/Spores)	moderate (%/Spores)	poor (%/Spores)				
W2	391.4	UHy	183.0	22.5	65.0	12.5	43.7	27.3	72.7	0.0	6.0	31.9	57.4	10.6	25.7	0.0	77.3	22.7	12.0	67.6	32.4	0.0	38.8	83.3	16.7	0.0	13.1	59.6	40.4	0.0	25.7	0.0	0.0	0.0
W2	398.8	UHy	237.0	38.3	38.3	23.5	34.2	100.0	0.0	0.0	3.4	34.8	36.4	28.8	27.8	0.0	100.0	0.0	3.0	46.2	46.2	7.7	16.5	100.0	0.0	0.0	3.8	30.0	60.0	10.0	12.7	3.8	44.3	48.1
W2	449.0	UHy	258.0	33.3	52.2	14.5	26.7	50.0	50.0	0.0	6.2	27.1	52.1	20.8	18.6	40.0	60.0	0.0	1.9	33.9	57.6	8.5	22.9	35.7	64.3	0.0	5.4	33.3	55.6	11.1	17.4	4.7	44.6	49.2
W2	503.3	UHy	321.0	18.6	39.0	42.4	18.4	100.0	0.0	0.0	0.9	19.5	31.7	48.8	12.8	0.0	66.7	33.3	4.7	0.0	0.0	0.0	0.0	0.0	0.0	0.0	0.0	0.0	0.0	0.0	0.0	6.2	40.5	46.7
W2	510.4	UHy	358.0	56.3	39.3	4.5	31.3	69.0	31.0	0.0	8.1	39.7	51.7	8.6	16.2	80.0	20.0	0.0	7.0	56.4	43.6	0.0	26.3	42.1	57.9	0.0	5.3	60.0	40.0	0.0	20.9	5.6	29.3	34.9
W2	556.0	UHy	299.0	49.5	42.1	8.4	31.8	56.3	43.8	0.0	5.4	22.2	55.6	22.2	12.0	69.8	30.2	0.0	14.4	49.2	50.8	0.0	20.4	72.7	27.3	0.0	3.7	44.0	56.0	0.0	16.7	3.3	41.8	45.2
W2	561.9	UHy	278.0	30.6	33.3	36.1	64.7	57.1	42.9	0.0	12.6	26.9	26.9	46.2	46.8	0.0	66.7	33.3	5.4	44.2	44.2	11.6	15.5	69.2	30.8	0.0	4.7	33.3	50.0	16.7	10.8	7.9	9.4	17.3
W2	650.8	UHy	302.0	34.0	43.6	22.3	31.1	58.8	41.2	0.0	5.6	37.9	41.4	20.7	19.2	0.0	52.6	47.4	6.3	60.2	39.8	0.0	29.1	61.5	38.5	0.0	4.3	60.0	40.0	0.0	24.8	4.0	29.5	33.4
W2	670.5	UHy	300.0	37.3	53.0	9.6	27.7	69.2	30.8	0.0	8.7	27.7	59.6	12.8	15.7	0.0	80.0	20.0	3.3	74.7	25.3	0.0	31.7	100.0	0.0	0.0	9.3	64.2	35.8	0.0	22.3	1.7	35.0	36.7
W2	671.0	UHy	301.0	38.5	36.5	25.0	34.6	62.5	37.5	0.0	15.9	17.9	35.7	46.4	18.6	0.0	0.0	0.0	0.0	51.6	48.4	0.0	21.3	75.0	25.0	0.0	8.0	37.5	62.5	0.0	13.3	6.6	36.5	43.2
W2	673.0	UHy	256.0	25.8	30.3	43.9	25.8	81.3	18.8	0.0	6.3	9.5	31.0	59.5	16.4	0.0	50.0	50.0	3.1	17.5	30.0	52.5	15.6	100.0	0.0	0.0	2.7	0.0	36.4	63.6	12.9	5.9	39.1	44.9
W2	709.3	UHy	333.0	49.0	38.8	12.2	29.4	70.4	29.6	0.0	8.1	40.8	42.3	16.9	21.3	0.0	0.0	0.0	0.0	54.2	43.2	2.5	35.4	72.1	27.9	0.0	12.9	44.0	52.0	4.0	22.5	3.0	28.5	31.5
W2	747.7	UHy	312.0	38.8	42.1	19.1	58.7	60.3	39.7	0.0	20.2	29.2	39.6	31.3	30.8	20.8	58.3	20.8	7.7	32.9	67.1	0.0	22.4	56.5	43.5	0.0	7.4	21.3	78.7	0.0	15.1	8.0	8.0	16.0
W2	755.9	UHy	367.0	30.6	52.8	16.7	19.6	80.0	20.0	0.0	4.1	19.2	57.7	23.1	14.2	0.0	100.0	0.0	1.4	83.5	16.5	0.0	34.6	93.2	6.8	0.0	12.0	78.3	21.7	0.0	22.6	0.0	16.3	16.3
W2	801.0	UHy	300.0	46.2	36.6	17.2	62.0	66.7	33.3	0.0	19.0	41.4	37.9	20.7	38.7	0.0	38.5	61.5	4.3	28.4	64.2	7.5	22.3	68.8	31.3	0.0	5.3	15.7	74.5	9.8	17.0	7.7	3.3	11.0
W2	805.2	UHy	393.0	10.6	52.9	36.5	26.5	38.1	61.9	0.0	5.3	5.2	51.7	43.1	14.8	0.0	48.0	52.0	6.4	52.1	36.7	11.2	43.0	71.4	28.6	0.0	19.6	35.9	43.5	20.7	23.4	8.9	18.6	27.5

Well	TVD (m)	Stratigraphy	Preservation of Phytoplancton		Phytoplancton %/ total OM	Preservation of Prasinophytes			Prasinophytes %/ total OM	Preservation of Acritarchs			Acritarchs %/ total OM	Preservation of Dinoflagellate cysts			Dinoflagellate cysts %/ total OM	Preservation of Leiospheres			Leiospheres %/ total OM	Preservation of Lacustrine Algae			Lacustrine Algae %/ total OM	Foramnifera %/ total OM	Fungi %/ total OM	Terr Comp. % / total OM	Marine Comp. % / total OM	terr. palynomorphs/ total OM	marine palynomorphs/ total OM
			good (%/Phytoplancton)	moderate (%/Phytoplancton)	poor (%/Phytoplancton)	good (%/Pras.)	moderate (%/Pras.)	poor (%/Pras.)		good (%/Acritarchs)	moderate (%/Acritarchs)	poor (%/Acritarchs)		good (%/Dino.)	moderate (%/Dino.)	poor (%/Dino.)		good (%/Leiospheres)	moderate (%/Leiospheres)	poor (%/Leiospheres)		good (%/Lac. Algae)	moderate (%/Lac. Algae)	poor (%/Lac. Algae)							
W2	391.4	UHy	100.0	0.0	17.5	0.0	0.0	0.0	0.0	0.0	0.0	0.0	0.0	100.0	0.0	0.0	15.8	100.0	0.0	0.0	1.6	0.0	0.0	0.0	0.0	0.0	0.0	0.0	82.5	17.5	38.8	17.5
W2	398.8	UHy	0.0	100.0	0.0	0.0	0.0	0.0	0.0	0.0	0.0	0.0	0.0	0.0	100.0	0.0	1.3	0.0	0.0	0.0	0.0	0.0	0.0	0.0	0.0	0.0	0.0	0.0	54.4	45.6	16.5	1.3
W2	449.0	UHy	0.0	0.0	100.0	1.2	0.0	0.0	0.0	0.0	0.0	0.0	0.0	0.0	0.0	100.0	1.2	0.0	0.0	0.0	0.9	0.0	0.0	0.0	0.0	0.0	0.0	0.0	54.3	45.7	22.9	1.2
W2	503.3	UHy	64.3	29.5	6.3	34.9	0.0	0.0	0.0	0.0	0.0	100.0	2.2	67.6	32.4	0.0	31.8	100.0	0.0	0.0	0.9	0.0	0.0	0.0	0.0	0.0	0.0	0.0	24.6	75.4	0.0	34.9
W2	510.4	UHy	16.0	8.0	76.0	7.0	0.0	0.0	0.0	0.0	0.0	100.0	4.2	40.0	20.0	40.0	2.8	0.0	0.0	0.0	0.0	0.0	100.0	0.0	0.0	0.0	0.0	0.0	63.1	36.3	26.3	7.0
W2	556.0	UHy	100.0	0.0	0.0	2.7	0.0	0.0	0.0	0.0	0.0	0.0	0.0	100.0	0.0	0.0	2.7	0.0	0.0	0.0	0.0	0.0	0.0	0.0	0.0	0.0	0.0	0.0	55.5	44.5	20.4	2.7
W2	561.9	UHy	100.0	0.0	0.0	2.5	0.0	0.0	0.0	0.0	0.0	0.0	0.0	100.0	0.0	0.0	2.5	0.0	0.0	0.0	0.0	0.0	0.0	0.0	0.0	0.0	0.0	0.0	88.1	11.9	15.5	2.5
W2	650.8	UHy	84.2	0.0	15.8	6.3	0.0	0.0	0.0	0.0	0.0	100.0	1.0	100.0	0.0	0.0	5.3	0.0	0.0	0.0	0.0	0.0	0.0	0.0	0.0	0.0	0.0	0.0	64.2	35.8	29.1	6.3
W2	670.5	UHy	0.0	0.0	0.0	0.0	0.0	0.0	0.0	0.0	0.0	0.0	0.0	0.0	0.0	0.0	0.0	0.0	0.0	0.0	0.0	0.0	100.0	0.0	0.0	0.0	0.0	0.0	61.0	35.0	31.7	0.0
W2	671.0	UHy	0.0	0.0	100.0	1.0	0.0	0.0	0.0	0.0	0.0	100.0	1.0	0.0	0.0	0.0	0.0	0.0	0.0	0.0	0.0	0.0	0.0	0.0	0.0	0.0	0.0	0.0	62.5	37.5	21.3	1.0
W2	673.0	UHy	22.9	20.0	57.1	13.7	0.0	0.0	0.0	0.0	0.0	0.0	0.0	25.0	12.5	62.5	12.5	0.0	0.0	100.0	0.0	0.0	1.2	0.0	0.0	0.0	0.0	0.0	47.3	52.7	15.6	13.7
W2	709.3	UHy	100.0	0.0	0.0	3.6	100.0	0.0	0.0	0.0	0.0	0.0	0.0	0.0	0.0	0.0	0.0	100.0	0.0	0.0	0.9	0.0	0.0	0.0	0.0	0.0	0.0	0.0	67.9	32.1	35.4	3.6
W2	747.7	UHy	22.2	77.8	0.0	2.9	22.2	77.8	0.0	0.0	0.0	0.0	0.0	0.0	0.0	0.0	0.0	0.0	0.0	0.0	0.0	0.0	0.0	0.0	0.0	0.0	0.0	0.0	89.1	10.9	22.4	2.9
W2	755.9	UHy	95.4	4.6	0.0	29.4	0.0	0.0	0.0	0.0	0.0	0.0	0.0	100.0	0.0	0.0	21.8	82.1	17.9	0.0	7.6	0.0	0.0	0.0	0.0	0.0	0.0	0.0	54.2	45.8	34.6	29.4
W2	801.0	UHy	100.0	0.0	0.0	4.7	0.0	0.0	0.0	0.0	0.0	0.0	0.0	100.0	0.0	0.0	4.7	0.0	0.0	0.0	0.0	0.0	0.0	0.0	0.0	0.0	0.0	0.0	92.0	8.0	22.3	4.7
W2	805.2	UHy	0.0	0.0	100.0	3.1	0.0	0.0	0.0	0.0	0.0	0.0	2.3	0.0	0.0	0.0	0.0	0.0	0.0	100.0	0.8	0.0	0.0	0.0	0.0	0.0	0.0	0.0	78.4	21.6	43.0	3.1

Well	TVD (m)	Stratigraphy	# of particels	Preservation of Phytoclasts			Phyclasts%/ total OM	Preservation of Inertinite			Inertinite %/ total OM	Preservation of Vitrinite			Vitrinite %/ total OM	Preservation of Cutinite			Cutinite %/ total OM	Preservation of Sporomorphs			Sporomorphs %/ total OM	Preservation of Spores			Spores %/ total OM	Preservation of Pollen			Pollen %/ total OM	terr. AOM %/ total OM	marine AOM %/ total OM	total AOM %/ total OM
				good (%/Phytoclasts)	moderate (%/Phytoclasts)	poor (%/Phytoclasts)		good (%/Inertinite)	moderate (%/Inertinite)	poor (%/Inertinite)		good (%/Vitrinite)	moderate (%/Vitrinite)	poor (%/Vitrinite)		good (%/Cutinite)	moderate (%/Cutinite)	poor (%/Cutinite)		good (%/Sporomorphs)	moderate(%/Sporomorphs)	poor (%/Sporomorphs)		good (%/Spores)	moderate (%/Spores)	poor (%/Spores)		good (%/Spores)	moderate (%/Spores)	poor (%/Spores)				
W3	1727.7	FM (RpC)	102	25	34	41	66.7	33	67	0	8.8	24	29	47	57.8	0	0	0	0.0	9	38	53	33.3	100	0	0	2.9	0	42	58	30.4	0.0	0.0	0.0
W3	1728.3	FM (RpC)	230	12	44	44	22.6	67	33	0	2.6	4	46	50	20.0	0	0	0	0.0	0	48	52	26.5	0	50	50	13.0	0	45	55	13.5	17.0	24.8	41.7
W3	1728.7	FM (RpC)	306	0	36	64	23.9	0	73	27	3.6	0	31	69	14.7	0	24	76	5.6	3	35	62	30.1	6	25	69	17.0	0	48	53	13.1	26.5	0.0	26.5
W3	1729.3	FM (RpC)	244	9	32	60	33.6	27	73	0	4.5	7	23	70	24.6	0	36	64	4.5	4	33	63	20.9	7	27	67	12.3	0	43	57	8.6	28.3	0.0	28.3
W3	1729.7	FM (RpC)	386	45	55	0	29.0	35	65	0	9.6	62	38	0	15.5	0	100	0	3.9	24	55	22	41.7	31	69	0	6.7	22	52	26	35.0	2.6	9.1	11.7
W3	1735.5	FM (RpC)	402	0	69	31	60.4	0	100	0	3.2	0	59	41	27.4	0	75	25	29.9	51	49	0	10.2	100	0	0	5.2	0	100	0	5.0	24.9	1.2	26.1
W3	1737.5	PE	240	6	42	51	49.7	50	20	30	3.4	5	51	45	28.6	0	33	67	17.6	23	35	42	10.7	19	43	38	7.2	30	20	50	3.4	15.5	0.0	15.5
W3	1743.8	PE	274	8	42	50	64.6	26	66	9	12.8	4	36	60	42.7	0	40	60	9.1	0	0	100	3.6	0	0	100	1.1	0	0	100	2.6	30.3	0.0	30.3
W3	1744.2	PE	308	7	41	52	63.6	100	0	0	1.3	3	63	33	20.5	6	32	62	41.9	9	33	58	18.5	10	40	50	15.6	0	0	100	2.9	17.9	0.0	17.9

Well	TVD (m)	Stratigraphy	Phytoplancton %/ total OM	Preservation of Phytoplancton			Prasinophytes %/ total OM	Preservation of Prasinophytes			Acritarchs %/ total OM	Preservation of Acritarchs			Dinoflagellate cysts %/ total OM	Preservation of Dinoflagellate cysts			Leiospheres %/ total OM	Preservation of Leiospheres			Lacustrine Algae %/ total OM	Preservation of Lacustrine Algae			Foraminifera %/ total OM	Fungi %/ total OM	Terr Comp. % / total OM	Marine Comp. % / total OM	terr. palynomorphs/ total OM	marine palynomorphs/ total OM
				good (%/Phytoplancton)	moderate (%/Phytoplancton)	poor (%/Phytoplancton)		good (%/Pras.)	moderate (%/Pras.)	poor (%/Pras.)		good (%/Acritarchs)	moderate (%/Acritarchs)	poor (%/Acritarchs)		good (%/Dino.)	moderate (%/Dino.)	poor (%/Dino.)		good (%/Leiospheres)	moderate (%/Leiospheres)	poor (%/Leiospheres)		good (%/Lac. Algae)	moderate (%/Lac. Algae)	poor (%/Lac. Algae)							
W3	1727.7	FM (RpC)	0	0	0	0.0	0.0	0	0	0	0.0	0	0	0	0.0	0	0	0	0.0	0	0	0	0.0	0	0	0	0.0	0.0	100.0	0.0	33.3	0.0
W3	1728.3	FM (RpC)	0	52	48	9.1	0.0	0	0	0	5.7	54	46	0	3.5	0	50	50	0.0	0	0	0	0.0	0	0	0	0.0	0.0	66.1	33.9	26.5	9.1
W3	1728.7	FM (RpC)	12	28	60	19.6	1.0	19	6	75	5.2	10	32	59	13.4	0	0	0	0.0	0	0	0	0.0	0	0	0	0.0	0.0	80.4	19.6	30.1	19.6
W3	1729.3	FM (RpC)	21	26	52	17.2	0.0	0	0	100	1.6	24	29	47	15.6	0	0	0	0.0	0	0	0	0.0	0	0	0	0.0	0.0	82.8	17.2	20.9	17.2
W3	1729.7	FM (RpC)	4	44	51	17.6	0.0	43	57	0	13.7	20	47	33	3.9	0	0	0	0.0	0	0	0	0.0	0	0	0	0.0	0.0	73.3	26.7	41.7	17.6
W3	1735.5	FM (RpC)	0	100	0	3.2	0.0	0	0	100	0.0	0	0	0	0.0	0	100	0	3.2	0	0	0	0.0	0	0	0	0.0	0.0	95.5	4.5	10.2	3.2
W3	1737.5	PE	0	0	100	6.9	1.0	0	0	100	2.8	0	0	100	2.1	0	0	100	1.0	0	0	0	0.0	0	0	0	0.0	17.2	75.9	24.1	10.7	24.1
W3	1743.8	PE	0	0	100	1.5	0.0	0	0	0	0.0	0	0	100	1.5	0	0	0	0.0	0	0	0	0.0	0	0	0	0.0	0.0	98.5	1.5	3.6	1.5
W3	1744.2	PE	0	0	0	0.0	0.0	0	0	0	0.0	0	0	0	0.0	0	0	0	0.0	0	0	0	0.0	0	0	0	0.0	0.0	100.0	0.0	18.5	0.0

Well	TVD (m)	Stratigraphy	# of particels	Preservation of Phytoclasts			Phyclasts%/ total OM	Preservation of Inertinite			Inertinite %/ total OM	Preservation of Vitrinite			Vitrinite %/ total OM	Preservation of Cutinite			Cutinite %/ total OM	Preservation of Sporomorphs			Sporomorphs %/ total OM	Preservation of Spores			Spores %/ total OM	Preservation of Pollen			Pollen %/ total OM	terr. AOM %/ total OM	marine AOM %/ total OM	total AOM %/ total OM
				good (%/Phytoclasts)	moderate (%/Phytoclasts)	poor (%/Phytoclasts)		good (%/Inertinite)	moderate (%/Inertinite)	poor (%/Inertinite)		good (%/Vitrinite)	moderate (%/Vitrinite)	poor (%/Vitrinite)		good (%/Cutinite)	moderate (%/Cutinite)	poor (%/Cutinite)		good (%/Sporomorphs)	moderate(%/Sporomorphs)	poor (%/Sporomorphs)		good (%/Spores)	moderate (%/Spores)	poor (%/Spores)		good (%/Spores)	moderate (%/Spores)	poor (%/Spores)				
W4	1400.0-1404.2	BN	219	52	48	0	91.3	66	34	0	62.1	27	73	0	23.3	0	100	0	5.9	0	0	100	3.7	0	0	100	3.7	0	0	0	0.0	5.0	0.0	5.0
W4	1454.5-1455.3	CyM	231	21	50	30	56.7	57	43	0	18.2	3	53	44	38.5	0	0	0	0.0	12	62	26	21.6	100	0	0	1.7	4	67	28	19.9	1.7	3.9	5.6
W4	1553.5	ME	299	16	51	33	47.2	45	55	0	16.4	0	46	54	26.8	0	67	33	4.0	22	45	32	25.8	0	40	60	3.3	25	46	28	22.4	13.4	8.4	21.7
W4	1554.4	ME	292	22	42	36	63.4	64	36	0	12.3	16	47	37	38.7	0	33	67	12.3	0	49	51	14.7	0	50	50	2.1	0	49	51	12.7	11.0	0.0	11.0
W4	1555.5	ME	289	26	48	26	66.1	100	0	0	9.7	19	54	27	40.1	0	60	40	16.3	32	57	11	21.8	47	53	0	5.2	27	58	15	16.6	4.5	0.0	4.5
W4	1556.5	ME	275	20	46	34	33.1	55	45	0	12.0	0	39	61	16.7	0	75	25	4.4	10	35	54	28.7	0	0	100	4.0	12	41	47	24.7	17.5	3.6	21.1
W4	1557.5	ME	334	23	46	31	52.4	60	40	0	15.0	12	47	41	25.4	0	50	50	12.0	0	60	40	27.2	0	84	16	5.7	0	54	46	21.6	6.0	0.0	6.0

Well	TVD (m)	Stratigraphy	Preservation of Phytoplancton			Phytoplancton %/ total OM	Preservation of Prasinophytes			Prasinophytes %/ total OM	Preservation of Acritarchs			Acritarchs %/ total OM	Preservation of Dinoflagellate cysts			Dinoflagellate cysts %/ total OM	Preservation of Leiospheres			Leiospheres %/ total OM	Preservation of Lacustrine Algae			Lacustrine Algae %/ total OM	Foraminifera %/ total OM	Fungi %/ total OM	Terr Comp. % / total OM	Marine Comp. % / total OM	terr. palynomorphs/ total OM	marine palynomorphs/ total OM
			good (%/Phytoplancton)	moderate (%/Phytoplancton)	poor (%/Phytoplancton)		good (%/Pras.)	moderate (%/Pras.)	poor (%/Pras.)		good (%/Acritarchs)	moderate (%/Acritarchs)	poor (%/Acritarchs)		good (%/Dino.)	moderate (%/Dino.)	poor (%/Dino.)		good (%/Leiospheres)	moderate (%/Leiospheres)	poor (%/Leiospheres)		good (%/Lac. Algae)	moderate (%/Lac. Algae)	poor (%/Lac. Algae)							
W4	1400.0-1404.2	BN	0	0	0	0.0	0	0	0	0.0	0	0	0	0.0	0	0	0	0.0	0	0	0	0.0	0	0	0	0.0	0.0	0.0	100.0	0.0	3.7	0.0
W4	1454.5-1455.3	CyM	49	35	16	16.0	0	0	0	0.0	0	0	100	2.6	58	42	0	13.4	0	0	0	0.0	0	0	0	0.0	0.0	0.0	80.1	19.9	21.6	16.0
W4	1553.5	ME	50	0	50	5.4	0	0	0	0.0	50	0	50	5.4	0	0	0	0.0	0	0	0	0.0	0	0	0	0.0	0.0	0.0	86.3	13.7	25.8	5.4
W4	1554.4	ME	0	22	78	11.0	0	0	0	0.0	0	0	100	2.7	0	29	71	8.2	0	0	0	0.0	0	0	0	0.0	0.0	0.0	89.0	11.0	14.7	11.0
W4	1555.5	ME	55	32	14	7.6	0	0	0	0.0	0	0	0	0.0	55	32	14	7.6	0	0	0	0.0	0	0	0	0.0	0.0	0.0	92.4	7.6	21.8	7.6
W4	1556.5	ME	60	23	17	17.1	0	0	0	0.0	0	20	80	3.6	76	24	0	13.5	0	0	0	0.0	0	0	0	0.0	0.0	0.0	79.3	20.7	28.7	17.1
W4	1557.5	ME	19	33	48	14.4	0	0	0	0.0	0	18	82	5.1	29	42	29	9.3	0	0	0	0.0	0	0	0	0.0	0.0	0.0	85.6	14.4	27.2	14.4

Well	TVD (m)	Stratigraphy	# of particels	Preservation of Phytoclasts			Preservation of Inertinite			Preservation of Vitrinite			Preservation of Cutinite			Preservation of Sporomorphs			Preservation of Spores			Preservation of Pollen			Pollen %/ total OM	terr. AOM %/ total OM	marine AOM %/ total OM	total AOM %/ total OM
				good (%/Phytoclasts)	moderate (%/Phytoclasts)	poor (%/Phytoclasts)	good (%/Inertinite)	moderate (%/Inertinite)	poor (%/Inertinite)	good (%/Vitrinite)	moderate (%/Vitrinite)	poor (%/Vitrinite)	good (%/Cutinite)	moderate (%/Cutinite)	poor (%/Cutinite)	good (%/Sporomorphs)	moderate(%/Sporomorphs)	poor (%/Sporomorphs)	good (%/Spores)	moderate (%/Spores)	moderate (%/Spores)	good (%/Spores)	moderate (%/Spores)	poor (%/Spores)				
W5	1569.5	FM (RpC)	248	38	56	6	55	45	0	34	57	9	0	100	0	4	70	26	12	80	8	0	65	35	20.6	28.2	0.0	28.2
W5	1570.0	FM (RpC)	250	46	30	24	100	0	0	0	51	49	0	100	0	27	50	23	26	57	17	28	45	28	11.6	30.0	0.0	30.0
W5	1571.5	FM (RpC)	233	40	60	0	64	36	0	37	63	0	0	100	0	49	47	4	78	22	0	21	71	8	16.3	34.3	10.7	45.1
W5	1572.0	FM (RpC)	236	38	63	0	64	36	0	0	100	0	0	0	0	38	54	8	53	47	0	24.6	16	65	18.2	36.0	0.0	36.0
W5	1573.7	FM (RpC)	257	31	26	43	75	25	0	0	26	74	0	0	0	46	54	0	59	41	0	12.5	14	86	5.4	33.1	0.0	33.1
W5	1577.0	FM (RpC)	277	51	39	11	90	10	0	10	66	24	0	81	19	0	63	37	0	100	0	3.2	0	44	16.2	7.2	0.0	7.2
W5	1579.0	FM (RpC)	384	21	31	48	52	39	9	9	14	77	0	100	0	5	48	47	14	86	0	9.1	0	72	17.4	13.0	1.3	14.3
W5	1581.0	FM (RpC)	15	0	0	0	0	0	0	0	0	0	0	0	0	53	33	13	0	0	0	0.0	53	13	100.0	0.0	0.0	0.0

Well	TVD (m)	Stratigraphy	Phytoplancton %/ total OM			Prasinophytes %/ total OM			Acritarchs %/ total OM			Dinoflagellate cysts %/ total OM			Leiospheres %/ total OM			Lacustrine Algae %/ total OM			Foraminifera %/ total OM	Fungi %/ total OM	Terr Comp. % / total OM	Marine Comp. % / total OM	terr. palynomorphs/ total OM	marine palynomorphs/ total OM
			good (%/Phytoplancton)	moderate (%/Phytoplancton)	poor (%/Phytoplancton)	good (%/Pras.)	moderate (%/Pras.)	poor (%/Pras.)	good (%/Acritarchs)	moderate (%/Acritarchs)	poor (%/Acritarchs)	good (%/Dino.)	moderate (%/Dino.)	poor (%/Dino.)	good (%/Leiospheres)	moderate (%/Leiospheres)	poor (%/Leiospheres)	good (%/Lac. Algae)	moderate (%/Lac. Algae)	poor (%/Lac. Algae)						
W5	1569.5	FM (RpC)	30	13	57	9.3	0	0	0	0	0.0	30	13	57	9.3	0	0	0.0	0	0	0.0	0.0	90.7	9.3	30.6	9.3
W5	1570.0	FM (RpC)	30	40	30	21.2	67	33	0	47	53	6.8	0	42	58	4.8	0	0.0	0	0	0.0	0.0	78.8	21.2	20.8	21.2
W5	1571.5	FM (RpC)	0	21	79	6.0	0	0	0	0	100	3.0	0	43	57	3.0	0	0.0	0	0	0.0	0.0	83.3	16.7	31.8	6.0
W5	1572.0	FM (RpC)	19	81	0	11.0	0	100	0	0	0	0.0	28	72	0	7.6	0	0.0	0	0	0.0	0.0	89.0	11.0	42.8	11.0
W5	1573.7	FM (RpC)	0	41	59	11.3	0	100	0	0	100	6.6	0	0	0.0	0	0	0.0	0	0	0.0	0.0	88.7	11.3	17.9	11.3
W5	1577.0	FM (RpC)	35	39	26	39.0	0	0	0	50	50	13.7	54	33	13	25.3	0	0.0	0	0	0.0	0.0	61.0	39.0	19.5	39.0
W5	1579.0	FM (RpC)	11	42	47	39.6	0	57	43	1.8	39	61	18.5	23	43	34	19.3	0	0	0	0.0	0.0	0.0	59.1	40.9	26.6	39.6
W5	1581.0	FM (RpC)	0	0	0	0.0	0	0	0.0	0	0	0.0	0	0	0.0	0	0	0.0	0	0	0.0	0.0	0.0	100.0	0.0	100.0	0.0

Well	TVD (m)	Stratigraphy	# of particels	Preservation of Phytoclasts			Phyclasts%/ total OM	Preservation of Inertinite			Inertinite %/ total OM	Preservation of Vitrinite			Vitrinite %/ total OM	Preservation of Cutinite			Cutinite %/ total OM	Preservation of Sporomorphs			Sporomorphs %/ total OM	Preservation of Spores			Spores %/ total OM	Preservation of Pollen			Pollen %/ total OM	terr. AOM %/ total OM	marine AOM %/ total OM	total AOM %/ total OM
				good (%/Phytoclasts)	moderate (%/Phytoclasts)	poor (%/Phytoclasts)		good (%/Inertinite)	moderate (%/Inertinite)	poor (%/Inertinite)		good (%/Vitrinite)	moderate (%/Vitrinite)	poor (%/Vitrinite)		good (%/Cutinite)	moderate (%/Cutinite)	poor (%/Cutinite)		good (%/Sporomorphs)	moderate(%/Sporomorphs)	poor (%/Sporomorphs)		good (%/Spores)	moderate (%/Spores)	poor (%/Spores)		good (%/Spores)	moderate (%/Spores)	poor (%/Spores)				
W7	560.0	UT I	303	36	39	25	98.3	62	29	10	6.9	34	40	26	91.4	0	0	0	0.0	20	80	0	1.7	20	80	0	1.7	0	0	0	0.0	0.0	0.0	0.0
W7	690.0	UHy	250	38	13	49	15.6	50	25	25	4.8	28	8	64	10.0	100	0	0	0.8	84	16	0	12.8	88	13	0	9.6	75	25	0	3.2	0.0	64.8	64.8
W7	760.0	UHy	222	27	30	42	14.9	18	45	36	5.0	32	23	45	9.9	0	0	0	0.0	100	0	0	7.7	100	0	0	4.5	100	0	0	3.2	0.0	74.3	74.3
W7	838.0	UHy	290	24	30	46	26.2	29	14	57	7.2	22	36	42	19.0	0	0	0	0.0	73	27	0	25.5	79	21	0	14.8	65	35	0	10.7	0.0	39.7	39.7
W7	920.0	UHy	337	27	33	40	31.2	14	39	46	8.3	24	34	41	20.8	100	0	0	2.1	82	18	0	14.8	88	13	0	4.7	79	21	0	10.1	0.0	43.0	43.0
W7	997.0	UHy	392	30	35	36	34.4	55	23	23	7.9	13	43	44	23.7	100	0	0	2.8	80	20	0	10.2	76	24	0	4.3	83	17	0	5.9	0.0	45.2	45.2
W7	1097.0	UHy	354	26	23	51	19.5	25	42	33	3.4	26	19	54	16.1	0	0	0	0.0	76	24	0	18.6	77	23	0	8.5	75	25	0	10.2	0.0	40.4	40.4
W7	1173.0	LHy	242	12	33	55	13.6	0	25	75	3.3	9	39	52	9.5	100	0	0	0.8	79	21	0	19.4	72	28	0	10.3	86	14	0	9.1	0.0	47.5	47.5
W7	1257.0	Cer	303	31	34	35	25.4	22	39	39	5.9	30	34	36	18.5	100	0	0	1.0	20	51	29	18.2	37	63	0	6.3	11	44	44	11.9	1.7	31.4	33.0
W7	1330.0	BN	361	50	29	21	21.6	52	35	13	6.4	49	27	24	15.2	0	0	0	0.0	87	13	0	17.5	100	0	0	4.7	83	17	0	12.7	0.0	49.3	49.3
W7	1435.0	BN	333	46	32	22	29.1	45	40	14	12.6	43	27	29	15.3	100	0	0	1.2	69	25	6	20.1	66	34	0	8.7	71	18	11	11.4	0.0	46.5	46.5
W7(2.)	1080.0	UHy	274	27	25	47	20.1	25	25	50	5.8	28	26	46	14.2	0	0	0	0.0	82	18	0	22.6	78	22	0	6.6	84	16	0	16.1	0.0	46.0	46.0
W7(2.)	1165.0	LHy	244	26	19	55	17.2	18	36	45	4.5	21	14	64	11.5	100	0	0	1.2	84	16	0	23.8	89	11	0	7.4	83	18	0	16.4	4.1	49.2	53.3
W7(2.)	1250.0	Cer	229	24	29	48	9.2	25	50	25	3.5	23	15	62	5.7	0	0	0	0.0	84	16	0	18.8	67	33	0	5.2	90	10	0	13.5	0.0	34.9	34.9
W7(2.)	1334.0	BN & CyM & ME	297	25	26	49	19.2	0	55	45	3.7	17	19	64	12.1	80	20	0	3.4	74	26	0	19.5	68	32	0	7.4	78	22	0	12.1	0.0	47.5	47.5
W7(2.)	1396.0	BN & CyM & ME	246	6	34	60	28.5	8	38	54	15.0	3	30	67	13.4	0	0	0	0.0	91	9	0	14.2	100	0	0	4.1	88	12	0	10.2	2.4	40.7	43.1
W7(2.)	1460.0	BN & CyM & ME	289	41	29	29	20.1	0	56	44	3.1	44	27	29	15.6	100	0	0	1.4	70	30	0	15.2	83	17	0	8.0	57	43	0	7.3	0.0	38.1	38.1
W7(2.)	1550.0	BN & CyM & ME	337	30	20	50	45.7	26	10	65	9.2	26	24	50	34.1	100	0	0	2.4	54	35	11	11.0	75	25	0	4.7	38	43	19	6.2	0.0	34.4	34.4
W7(2.)	1647.0	RpC	347	25	32	43	78.7	25	28	48	11.5	19	35	46	62.2	100	0	0	4.9	30	70	0	6.6	56	44	0	2.6	14	86	0	4.0	0.0	8.6	8.6

Well	TVD (m)	Stratigraphy	Preservation of Phytoplancton		Phytoplancton %/ total OM	Preservation of Prasinophytes			Prasinophytes %/ total OM	Preservation of Acritarchs			Acritarchs %/ total OM	Preservation of Dinoflagellate cysts			Dinoflagellate cysts %/ total OM	Preservation of Leiospheres			Leiospheres %/ total OM	Preservation of Lacustrine Algae			Lacustrine Algae %/ total OM	Foraminifera %/ total OM	Fungi %/ total OM	Terr Comp. % / total OM	Marine Comp. % / total OM	terr. palynomorphs/ total OM	marine palynomorphs/ total OM
			good (%/Phytoplancton)	moderate (%/Phytoplancton)	poor (%/Phytoplancton)	good (%/Pras.)	moderate (%/Pras.)	poor (%/Pras.)		good (%/Acritarchs)	moderate (%/Acritarchs)	poor (%/Acritarchs)		good (%/Dino.)	moderate (%/Dino.)	poor (%/Dino.)		good (%/Leiospheres)	moderate (%/Leiospheres)	poor (%/Leiospheres)		good (%/Lac. Algae)	moderate (%/Lac. Algae)	poor (%/Lac. Algae)						
W7	560.0	UT I	0	0	0	0	0	0	0.0	0	0	0	0.0	0	0	0	0.0	0	0	0	0.0	0	0	0	0.0	0.0	0.0	100.0	0.0	1.7	0.0
W7	690.0	UHy	81	19	0	6.4	100	0	0	0	0	0	0.0	57	43	0	2.8	100	0	0	3.2	100	0	0	0.4	0.0	0.0	28.4	71.2	12.8	6.4
W7	760.0	UHy	86	14	0	3.2	100	0	0	0	0	0	0.0	0	100	0	0.5	100	0	0	1.8	0	0	0	0.0	0.0	0.0	22.5	77.5	7.7	3.2
W7	838.0	UHy	60	40	0	8.6	100	0	0	0	0	0	0.0	43	57	0	4.8	80	20	0	3.4	0	0	0	0.0	0.0	0.0	51.7	48.3	25.5	8.6
W7	920.0	UHy	65	35	0	11.0	100	0	0	0	0	0	0.0	50	50	0	7.7	100	0	0	2.4	0	0	0	0.0	0.0	0.0	46.0	54.0	14.8	11.0
W7	997.0	UHy	13	65	23	10.2	0	100	0	0	0	0	0.0	6	68	26	8.7	100	0	0	0.8	0	0	0	0.0	0.0	0.0	44.6	55.4	10.2	10.2
W7	1097.0	UHy	58	37	5	20.6	0	0	0	0	0	0	0.0	55	39	6	19.5	100	0	0	1.1	100	0	0	0.8	0.0	0.0	38.1	61.0	18.6	20.6
W7	1173.0	LHy	56	36	9	18.6	78	22	0	0	0	0	0.0	36	48	16	10.3	82	18	0	4.5	100	0	0	0.8	0.0	0.0	33.1	66.1	19.4	18.6
W7	1257.0	Cer	34	57	9	11.6	0	100	0	2.3	0	0	0.0	41	48	11	8.9	100	0	0	0.3	61	39	0	11.9	0.0	0.0	45.2	42.9	18.2	11.6
W7	1330.0	BN	92	8	0	6.6	0	0	0	0.0	0	0	0.0	90	10	0	5.8	100	0	0	0.8	67	33	0	5.0	0.0	0.0	39.1	56.0	17.5	6.6
W7	1435.0	BN	69	31	0	3.9	0	0	0	0.0	0	0	0.0	69	31	0	3.9	0	0	0	0.0	100	0	0	0.3	0.0	0.0	49.2	50.5	20.1	3.9
W7(2.)	1080.0	UHy	60	40	0	7.3	0	0	0	0.0	0	0	0.0	53	47	0	6.2	100	0	0	1.1	55	18	27	4.0	0.0	0.0	42.7	53.3	22.6	7.3
W7(2.)	1165.0	LHy	100	0	0	4.5	100	0	0	0.8	0	0	0.0	100	0	0	3.7	0	0	0	0.0	0	0	100	1.2	0.0	0.0	45.1	53.7	23.8	4.5
W7(2.)	1250.0	Cer	88	12	0	7.4	100	0	0	1.3	0	0	0.0	86	14	0	6.1	0	0	0	0.0	100	0	0	29.7	0.0	0.0	27.9	42.4	18.8	7.4
W7(2.)	1334.0	BN & CyM & ME	63	38	0	5.4	33	67	0	2.0	0	0	0.0	80	20	0	3.4	0	0	0	0.0	88	12	0	8.4	0.0	0.0	38.7	52.9	19.5	5.4
W7(2.)	1396.0	BN & CyM & ME	80	20	0	12.2	100	0	0	1.2	0	0	0.0	75	25	0	9.8	100	0	0	1.2	100	0	0	2.0	0.0	0.0	45.1	52.8	14.2	12.2
W7(2.)	1460.0	BN & CyM & ME	50	28	22	20.1	50	50	0	0.7	0	0	0.0	49	27	24	19.0	100	0	0	0.3	84	16	0	6.6	0.0	0.0	35.3	58.1	15.2	20.1
W7(2.)	1550.0	BN & CyM & ME	63	37	0	8.0	100	0	0	0.6	0	0	0.0	57	43	0	6.8	100	0	0	0.6	100	0	0	0.9	0.0	0.0	56.7	42.4	11.0	8.0
W7(2.)	1647.0	RpC	67	33	0	1.7	0	0	0	0.0	0	0	0.0	67	33	0	1.7	0	0	0	0.0	100	0	0	4.3	0.0	0.0	85.3	10.4	6.6	1.7

Well	TVD (m)	Stratigraphy	# of particels	Preservation of Phytoclasts			Phyclasts%/ total OM	Preservation of Inertinite			Inertinite %/ total OM	Preservation of Vitrinite			Vitrinite %/ total OM	Preservation of Cutinite			Cutinite %/ total OM	Preservation of Spromorphs			Spromorphs %/ total OM	Preservation of Spores			Spores %/ total OM	Preservation of Pollen			Pollen %/ total OM	terr. AOM %/ total OM	marine AOM %/ total OM	total AOM %/ total OM
				good (%/Phytoclasts)	moderate (%/Phytoclasts)	poor (%/Phytoclasts)		good (%/Interlinite)	moderate (%/Interlinite)	poor (%/Interlinite)		good (%/Vitrinite)	moderate (%/Vitrinite)	poor (%/Vitrinite)		good (%/Cutinite)	moderate (%/Cutinite)	poor (%/Cutinite)		good (%/Spromorphs)	moderate(%/Spromorphs)	poor (%/Spromorphs)		good (%/Spores)	moderate (%/Spores)	poor (%/Spores)		good (%/Spores)	moderate (%/Spores)	poor (%/Spores)				
W7	560.0	UT I	303	36	39	25	98.3	62	29	10	6.9	34	40	26	91.4	0	0	0	0.0	20	80	0	1.7	20	80	0	1.7	0	0	0	0.0	0.0	0.0	0.0
W7	690.0	UHy	250	38	13	49	15.6	50	25	25	4.8	28	8	64	10.0	100	0	0	0.8	84	16	0	12.8	88	13	0	9.6	75	25	0	3.2	0.0	64.8	64.8
W7	760.0	UHy	222	27	30	42	14.9	18	45	36	5.0	32	23	45	9.9	0	0	0	0.0	100	0	0	7.7	100	0	0	4.5	100	0	0	3.2	0.0	74.3	74.3
W7	838.0	UHy	290	24	30	46	26.2	29	14	57	7.2	22	36	42	19.0	0	0	0	0.0	73	27	0	25.5	79	21	0	14.8	65	35	0	10.7	0.0	39.7	39.7
W7	920.0	UHy	337	27	33	40	31.2	14	39	46	8.3	24	34	41	20.8	100	0	0	2.1	82	18	0	14.8	88	13	0	4.7	79	21	0	10.1	0.0	43.0	43.0
W7	997.0	UHy	392	30	35	36	34.4	55	23	23	7.9	13	43	44	23.7	100	0	0	2.8	80	20	0	10.2	76	24	0	4.3	83	17	0	5.9	0.0	45.2	45.2
W7	1097.0	UHy	354	26	23	51	19.5	25	42	33	3.4	26	19	54	16.1	0	0	0	0.0	76	24	0	18.6	77	23	0	8.5	75	25	0	10.2	0.0	40.4	40.4
W7	1173.0	LHy	242	12	33	55	13.6	0	25	75	3.3	9	39	52	9.5	100	0	0	0.8	79	21	0	19.4	72	28	0	10.3	86	14	0	9.1	0.0	47.5	47.5
W7	1257.0	Cer	303	31	34	35	25.4	22	39	39	5.9	30	34	36	18.5	100	0	0	1.0	20	51	29	18.2	37	63	0	6.3	11	44	44	11.9	1.7	31.4	33.0
W7	1330.0	BN	361	50	29	21	21.6	52	35	13	6.4	49	27	24	15.2	0	0	0	0.0	87	13	0	17.5	100	0	0	4.7	83	17	0	12.7	0.0	49.3	49.3
W7	1435.0	BN	333	46	32	22	29.1	45	40	14	12.6	43	27	29	15.3	100	0	0	1.2	69	25	6	20.1	66	34	0	8.7	71	18	11	11.4	0.0	46.5	46.5
W7a	1070.0	UHy	319	23	25	52	24.1	26	11	63	6.0	22	29	48	18.2	0	0	0	0.0	81	15	4	15.0	77	23	0	4.1	83	11	6	11.0	0.0	43.9	43.9
W7a	1110.0	UHy	281	26	26	48	20.6	38	31	31	5.7	21	24	55	14.9	0	0	0	0.0	80	20	0	19.9	77	23	0	10.7	85	15	0	9.3	0.0	40.6	40.6
W7a	1125.0	UHy	293	51	18	31	22.2	60	15	25	6.8	33	25	42	12.3	100	0	0	3.1	86	14	0	29.0	85	15	0	6.8	86	14	0	22.2	0.0	41.0	41.0
W7a	1135.0	UHy	332	50	13	37	11.4	38	38	25	2.4	48	7	44	8.1	100	0	0	0.9	91	9	0	19.6	92	8	0	7.5	90	10	0	12.0	0.0	24.7	24.7
W7a	1155.0	LHy	277	28	22	49	24.2	33	27	40	5.4	12	22	66	14.8	82	18	0	4.0	69	31	0	19.5	40	60	0	5.4	79	21	0	14.1	0.0	38.3	38.3
W7a	1163.0	LHy	277	12	24	65	30.7	0	0	100	2.5	13	24	63	27.4	0	100	0	0.7	76	24	0	23.8	50	50	0	5.1	83	17	0	18.8	3.6	32.9	36.5
W7a	1167.0	LHy	303	50	6	44	20.5	45	10	45	7.9	47	5	47	12.5	100	0	0	1.3	55	39	6	16.8	56	44	0	5.9	55	36	9	10.9	0.0	47.9	47.9
W7a	1172.0	LHy	335	37	24	39	22.4	62	38	0	6.3	18	18	64	13.4	78	22	0	2.7	73	27	0	25.4	50	50	0	3.6	77	23	0	21.8	0.0	36.4	36.4
W7a	1191.0	LHy	363	38	18	44	30.6	57	13	30	6.3	33	19	48	24.2	0	0	0	0.0	70	22	8	20.4	38	38	23	3.6	77	18	5	16.8	0.0	35.0	35.0
W7a	1200.0	LHy	341	28	31	41	22.9	15	65	20	5.9	22	22	56	14.7	100	0	0	2.3	75	25	0	18.5	63	38	0	7.0	82	18	0	11.4	0.0	34.9	34.9
W7a	1210.0	LHy	261	58	27	15	19.9	66	26	9	13.4	23	38	38	5.0	100	0	0	1.5	61	39	0	12.6	46	54	0	5.0	70	30	0	7.7	0.0	27.2	27.2
W7a	1220.0	LHy	313	6	29	66	11.2	10	15	75	6.4	0	47	53	4.8	0	0	0	0.0	91	9	0	27.2	100	0	0	16.9	75	25	0	10.2	1.6	37.1	38.7
W7a	1288.0	Cer	329	13	15	73	24.3	18	9	74	10.3	9	20	72	14.0	0	0	0	0.0	85	15	0	21.9	100	0	0	2.7	83	17	0	19.1	8.2	36.2	44.4
W7a	1418.0	CyM & ME	540	20	42	38	90.6	38	19	42	14.4	21	44	35	40.4	11	49	40	35.7	29	71	0	3.1	25	75	0	1.5	33	67	0	1.7	4.6	0.0	4.6
W7a	1537.0	CyM & ME	335	55	21	24	76.7	36	17	47	22.4	62	23	15	50.1	71	29	0	4.2	50	50	0	5.4	56	44	0	2.7	44	56	0	2.7	13.7	0.0	13.7
W7a	1557.0	CyM & ME	284	70	10	20	84.5	46	7	46	19.0	77	11	12	63.4	100	0	0	2.1	70	30	0	3.5	70	30	0	3.5	0	0	0	0.0	4.2	0.0	4.2
W7a	1596.0	CyM & ME	389	46	29	24	84.6	40	22	38	40.9	50	37	13	39.3	71	29	0	4.4	83	17	0	4.6	100	0	0	0.8	80	20	0	3.9	6.9	0.0	6.9
W7a	1601.0	FS (RpC)	348	36	33	32	79.3	44	15	41	15.5	29	40	31	59.8	100	0	0	4.0	50	43	7	8.6	43	43	14	4.0	56	44	0	4.6	4.3	0.0	4.3
W7a	1608.0	FS (RpC)	386	32	33	35	80.6	63	22	15	7.0	26	35	39	68.9	78	22	0	4.7	46	43	11	7.3	0	100	0	0.8	52	36	12	6.5	7.8	0.0	7.8
W7a	1611.0	FS (RpC)	356	18	47	34	72.2	43	57	0	3.9	13	48	38	64.9	83	17	0	3.4	21	21	58	5.3	33	33	33	3.4	0	0	100	2.0	12.6	0.0	12.6
W7a	1618.0	FM (RpC)	288	14	30	56	81.9	23	31	46	9.0	12	29	59	70.8	67	33	0	2.1	33	67	0	2.1	33	67	0	2.1	0	0	0	0.0	15.3	0.0	15.3
W7a	1622.0	FM (RpC)	357	21	39	40	72.8	45	31	24	8.1	16	41	43	61.3	58	25	17	3.4	37	42	21	5.3	50	29	21	3.9	0	80	20	1.4	14.3	0.0	14.3
W7a	1628.0	FM (RpC)	266	9	38	53	70.7	100	0	0	3.0	3	40	57	66.2	50	50	0	1.5	20	30	50	3.8	33	17	50	2.3	0	50	50	1.5	22.6	0.0	22.6
W7a	1631.0	PE	274	15	32	53	79.2	24	56	20	9.1	14	29	57	70.1	0	0	0	0.0	40	60	0	7.3	47	53	0	6.2	0	100	0	1.1	7.3	1.1	8.4
W7a	1633.0	PE	224	15	35	51	75.0	40	60	0	4.5	9	34	56	67.4	100	0	0	3.1	100	0	0	1.8	100	0	0	1.8	0	0	0	0.0	12.5	2.2	14.7
W7a	1637.0	PE	259	10	34	56	81.5	21	58	21	14.7	8	29	64	66.8	0	0	0	0.0	56	38	6	6.2	33	50	17	2.3	70	30	0	3.9	3.1	6.2	9.3
W7a	1641.0	PE	264	12	28	60	80.3	21	32	46	10.6	10	27	63	69.7	0	0	0	0.0	0	100	0	1.5	0	0	0	0.0	0	100	0	1.5	4.9	4.9	9.8
W7a	1647.0	PE	235	17	34	50	90.2	31	44	26	16.6	13	32	55	73.6	0	0	0	0.0	50	30	20	4.3	63	38	0	3.4	0	0	100	0.9	2.1	3.0	5.1
W7a	1646.0	PE	331	19	47	34	66.2	20	44	37	12.4	14	51	36	50.8	100	0	0	3.0	60	40	0	7.6	58	42	0	5.7	67	33	0	1.8	1.5	13.6	15.1
W7a	1648.0	PE	281	17	42	41	79.7	35	28	37	16.4	12	46	42	63.3	0	0	0	0.0	88	13	0	8.5	100	0	0	4.6	73	27	0	3.9	5.3	2.8	8.2
W7a	1651.0	PE	238	20	29	50	61.8	35	20	45	16.8	13	34	54	43.7	100	0	0	1.3	63	37	0	11.3	60	40	0	6.3	67	33	0	5.0	3.4	18.9	22.3
W7a	1658.0	PE	310	14	36	51	69.0	15	44	41	19.0	8	34	58	47.4	100	0	0	2.6	67	33	0	9.7	80	20	0	4.8	53	47	0	4.8	12.9	5.8	18.7

Well	TVD (m)	Stratigraphy	Preservation of Phytoplancton			Phytoplancton %/ total OM	Preservation of Prasinophytes			Prasinophytes %/ total OM	Preservation of Acritarchs			Acritarchs %/ total OM	Preservation of Dinoflagellate cysts			Dinoflagellate cysts %/ total OM	Preservation of Leiospheres			Leiospheres %/ total OM	Preservation of Lacustrine Algae			Lacustrine Algae %/ total OM	Foraminifera %/ total OM	Fungi %/ total OM	Terr Comp. % / total OM	Marine Comp. % / total OM	terr. palynomorphs/ total OM	marine palynomorphs/ total OM
			good (%/Phytoplancton)	moderate (%/Phytoplancton)	poor (%/Phytoplancton)		good (%/Pras.)	moderate (%/Pras.)	poor (%/Pras.)		good (%/Acritarchs)	moderate (%/Acritarchs)	poor (%/Acritarchs)		good (%/Dino.)	moderate (%/Dino.)	poor (%/Dino.)		good (%/Leiospheres)	moderate (%/Leiospheres)	poor (%/Leiospheres)		good (%/Lac. Algae)	moderate (%/Lac. Algae)	poor (%/Lac. Algae)						
W7	560.0	UT I	0	0	0	0.0	0	0	0	0.0	0	0	0	0.0	0	0	0	0.0	0	0	0	0.0	0	0	0	0.0	0.0	0.0	100.0	0.0	1.7	0.0
W7	690.0	UHy	81	19	0	6.4	100	0	0	0.4	0	0	0	0.0	57	43	0	2.8	100	0	0	3.2	100	0	0	0.4	0.0	0.0	28.4	71.2	12.8	6.4
W7	760.0	UHy	86	14	0	3.2	100	0	0	0.9	0	0	0	0.0	0	100	0	0.5	100	0	0	1.8	0	0	0	0.0	0.0	0.0	22.5	77.5	7.7	3.2
W7	838.0	UHy	60	40	0	8.6	100	0	0	0.3	0	0	0	0.0	43	57	0	4.8	80	20	0	3.4	0	0	0	0.0	0.0	0.0	51.7	48.3	25.5	8.6
W7	920.0	UHy	65	35	0	11.0	100	0	0	0.9	0	0	0	0.0	50	50	0	7.7	100	0	0	2.4	0	0	0	0.0	0.0	0.0	46.0	54.0	14.8	11.0
W7	997.0	UHy	13	65	23	10.2	0	100	0	0.8	0	0	0	0.0	6	68	26	8.7	100	0	0	0.8	0	0	0	0.0	0.0	0.0	44.6	55.4	10.2	10.2
W7	1097.0	UHy	58	37	5	20.6	0	0	0	0.0	0	0	0	0.0	55	39	6	19.5	100	0	0	1.1	100	0	0	0.8	0.0	0.0	38.1	61.0	18.6	20.6
W7	1173.0	LHy	56	36	9	18.6	78	22	0	3.7	0	0	0	0.0	36	48	16	10.3	82	18	0	4.5	100	0	0	0.8	0.0	0.0	33.1	66.1	19.4	18.6
W7	1257.0	Cer	34	57	9	11.6	0	100	0	2.3	0	0	0	0.0	41	48	11	8.9	100	0	0	0.3	61	39	0	11.9	0.0	0.0	45.2	42.9	18.2	11.6
W7	1330.0	BN	92	8	0	6.6	0	0	0	0.0	0	0	0	0.0	90	10	0	5.8	100	0	0	0.8	67	33	0	5.0	0.0	0.0	39.1	56.0	17.5	6.6
W7	1435.0	BN	69	31	0	3.9	0	0	0	0.0	0	0	0	0.0	69	31	0	3.9	0	0	0	0.0	100	0	0	0.3	0.0	0.0	49.2	50.5	20.1	3.9
W7a	1070.0	UHy	70	17	13	16.9	100	0	0	1.3	0	0	0	0.0	68	18	14	15.7	0	0	0	0.0	0	0	0	0.0	0.0	0.0	39.2	60.8	15.0	16.9
W7a	1110.0	UHy	62	30	8	18.9	80	20	0	5.3	0	0	0	0.0	55	35	10	11.0	57	29	14	2.5	0	0	0	0.0	0.0	0.0	40.6	59.4	19.9	18.9
W7a	1125.0	UHy	78	9	13	7.8	100	0	0	1.4	0	0	0	0.0	58	17	25	4.1	100	0	0	2.4	0	0	0	0.0	0.0	0.0	51.2	48.8	29.0	7.8
W7a	1135.0	UHy	68	22	10	44.3	0	0	0	0.0	0	0	0	0.0	66	23	11	42.2	100	0	0	2.1	0	0	0	0.0	0.0	0.0	31.0	69.0	19.6	44.3
W7a	1155.0	LHy	72	24	4	18.1	0	100	0	0.7	0	0	0	0.0	73	22	5	13.4	82	18	0	4.0	0	0	0	0.0	0.0	0.0	43.7	56.3	19.5	18.1
W7a	1163.0	LHy	72	20	8	9.0	80	20	0	1.8	0	0	0	0.0	70	20	10	7.2	0	0	0	0.0	0	0	0	0.0	0.0	0.0	58.1	41.9	23.8	9.0
W7a	1167.0	LHy	59	25	16	14.5	0	43	57	2.3	0	0	0	0.0	64	25	11	9.2	89	11	0	3.0	0	100	0	0.3	0.0	0.0	37.3	62.4	16.8	14.5
W7a	1172.0	LHy	74	26	0	15.8	100	0	0	1.2	0	0	0	0.0	65	35	0	11.9	100	0	0	2.7	0	0	0	0.0	0.0	0.0	47.8	52.2	25.4	15.8
W7a	1191.0	LHy	73	27	0	13.5	100	0	0	2.5	0	0	0	0.0	68	33	0	11.0	0	0	0	0.0	100	0	0	0.6	0.0	0.0	51.0	48.5	20.4	13.5
W7a	1200.0	LHy	54	30	16	23.8	0	0	0	0.0	0	0	0	0.0	53	30	16	23.2	100	0	0	0.6	0	0	0	0.0	0.0	0.0	41.3	58.7	18.5	23.8
W7a	1210.0	LHy	43	23	34	40.2	0	0	0	0.0	0	0	0	0.0	41	24	36	38.7	100	0	0	1.5	0	0	0	0.0	0.0	0.0	32.6	67.4	12.6	40.2
W7a	1220.0	LHy	78	21	2	20.1	100	0	0	0.6	0	0	0	0.0	76	22	2	18.5	100	0	0	1.0	100	0	0	2.9	0.0	0.0	39.9	57.2	27.2	20.1
W7a	1288.0	Cer	70	3	27	9.1	67	33	0	0.9	0	0	0	0.0	70	0	30	8.2	0	0	0	0.0	0	100	0	0.3	0.0	0.0	54.4	45.3	21.9	9.1
W7a	1418.0	CyM & ME	0	0	100	1.7	0	0	0	0.0	0	0	0	0.0	0	0	100	1.7	0	0	0	0.0	0	0	0	0.0	0.0	0.0	98.3	1.7	3.1	1.7
W7a	1537.0	CyM & ME	0	21	79	4.2	0	0	0	0.0	0	0	0	0.0	0	21	79	4.2	0	0	0	0.0	0	0	0	0.0	0.0	0.0	95.8	4.2	5.4	4.2
W7a	1557.0	CyM & ME	41	41	18	7.7	100	0	0	0.4	0	0	0	0.0	38	43	19	7.4	0	0	0	0.0	0	0	0	0.0	0.0	0.0	92.3	7.7	3.5	7.7
W7a	1596.0	CyM & ME	46	38	15	3.3	0	100	0	0.5	0	0	0	0.0	44	33	22	2.3	100	0	0	0.5	0	100	0	0.5	0.0	0.0	96.1	3.3	4.6	3.3
W7a	1601.0	FS (RpC)	59	41	0	7.8	100	0	0	0.9	0	0	0	0.0	54	46	0	6.9	0	0	0	0.0	0	0	0	0.0	0.0	0.0	92.2	7.8	8.6	7.8
W7a	1608.0	FS (RpC)	35	41	24	4.4	0	0	0	0.0	0	0	0	0.0	22	33	44	2.3	50	50	0	2.1	0	0	0	0.0	0.0	0.0	95.6	4.4	7.3	4.4
W7a	1611.0	FS (RpC)	26	37	37	9.8	67	33	0	0.8	0	0	0	0.0	22	38	41	9.0	0	0	0	0.0	0	0	0	0.0	0.0	0.0	90.2	9.8	5.3	9.8
W7a	1618.0	FM (RpC)	0	0	100	0.7	0	0	0	0.0	0	0	0	0.0	0	0	100	0.7	0	0	0	0.0	0	0	0	0.0	0.0	0.0	99.3	0.7	2.1	0.7
W7a	1622.0	FM (RpC)	33	44	22	7.6	0	0	0	0.0	0	0	0	0.0	33	44	22	7.6	0	0	0	0.0	0	0	0	0.0	0.0	0.0	92.4	7.6	5.3	7.6
W7a	1628.0	FM (RpC)	17	17	67	2.3	50	50	0	0.8	0	0	0	0.0	0	0	100	1.5	0	0	0	0.0	0	0	100	0.8	0.0	0.0	97.0	2.3	3.8	2.3
W7a	1631.0	PE	25	38	38	2.9	0	0	0	0.0	0	0	0	0.0	0	50	50	2.2	100	0	0	0.7	100	0	0	2.2	0.0	0.0	93.8	4.0	7.3	2.9
W7a	1633.0	PE	21	16	63	8.5	0	0	0	0.0	0	0	0	0.0	21	16	63	8.5	0	0	0	0.0	0	0	0	0.0	0.0	0.0	89.3	10.7	1.8	8.5
W7a	1637.0	PE	0	63	38	3.1	0	100	0	0.8	0	0	0	0.0	0	50	50	2.3	0	0	0	0.0	0	0	0	0.0	0.0	0.0	90.7	9.3	6.2	3.1
W7a	1641.0	PE	14	23	64	8.3	60	0	40	1.9	0	0	0	0.0	0	38	62	4.9	0	0	100	1.5	0	0	0	0.0	0.0	0.0	86.7	13.3	1.5	8.3
W7a	1647.0	PE	0	100	0	0.4	0	0	0	0.0	0	0	0	0.0	0	100	0	0.4	0	0	0	0.0	0	0	0	0.0	0.0	0.0	96.6	3.4	4.3	0.4
W7a	1646.0	PE	59	41	0	11.2	0	0	0	0.0	0	0	0	0.0	59	41	0	11.2	0	0	0	0.0	0	0	0	0.0	0.0	0.0	75.2	24.8	7.6	11.2
W7a	1648.0	PE	60	20	20	3.6	0	0	0	0.0	0	0	0	0.0	60	20	20	3.6	0	0	0	0.0	0	0	0	0.0	0.0	0.0	93.6	6.4	8.5	3.6
W7a	1651.0	PE	45	55	0	4.6	0	100	0	0.8	0	0	0	0.0	56	44	0	3.8	0	0	0	0.0	0	0	0	0.0	0.0	0.0	76.5	23.5	11.3	4.6
W7a	1658.0	PE	13	75	13	2.6	0	100	0	0.6	0	0	0	0.0	0	80	20	1.6	100	0	0	0.3	0	0	0	0.0	0.0	0.0	91.6	8.4	9.7	2.6

Well	TVD (m)	Stratigraphy	# of particels	Preservation of Phytoclasts			Phyclasts%/ total OM	Preservation of Inertinite			Inertinite %/ total OM	Preservation of Vitrinite			Vitrinite %/ total OM	Preservation of Cutinite			Cutinite %/ total OM	Preservation of Sporomorphs			Sporomorphs %/ total OM	Preservation of Spores			Spores %/ total OM	Preservation of Pollen			Pollen %/ total OM	terr. AOM %/ total OM	marine AOM %/ total OM	total AOM %/ total OM
				good (%/Phytoclasts)	moderate (%/Phytoclasts)	poor (%/Phytoclasts)		good (%/Inertinite)	moderate (%/Inertinite)	poor (%/Inertinite)		good (%/Vitrinite)	moderate (%/Vitrinite)	poor (%/Vitrinite)		good (%/Cutinite)	moderate (%/Cutinite)	poor (%/Cutinite)		good (%/Sporomorphs)	moderate(%/Sporomorphs)	poor (%/Sporomorphs)		good (%/Spores)	moderate (%/Spores)	poor (%/Spores)		good (%/Spores)	moderate (%/Spores)	poor (%/Spores)				
W8	675.0	UT I	444	8	27	64	35.4	46	54	0	6.3	0	24	76	23.6	0	13	88	5.4	39	48	13	7.0	80	20	0	3.4	0	75	25	3.6	40.5	2.3	42.8
W8	765.0	UHy	251	3	57	40	28.7	0	100	0	2.8	4	54	43	22.3	0	44	56	3.6	55	45	0	12.4	100	0	0	1.6	48	52	0	10.8	4.0	53.8	57.8
W8	775.0	UHy	326	0	44	56	18.1	0	100	0	2.8	0	34	66	15.3	0	0	0	0.0	26	48	26	15.3	64	36	0	4.3	11	53	36	11.0	3.1	53.7	56.7
W8	825.0	UHy	305	16	45	39	24.3	31	69	0	4.3	0	41	59	16.1	67	33	0	3.9	48	38	14	18.4	40	60	0	1.6	49	35	16	16.7	4.9	50.8	55.7
W8	875.0	UHy	295	16	44	40	15.3	47	53	0	5.1	0	33	67	7.1	0	56	44	3.1	36	30	34	23.7	60	40	0	1.7	34	29	37	22.0	8.5	52.5	61.0
W8	915.0	UHy	296	7	52	41	18.9	33	67	0	4.1	0	48	52	14.9	0	0	0	0.0	20	37	43	11.8	100	0	0	1.4	10	42	48	10.5	6.8	62.5	69.3
W8	985.0	UHy	275	0	43	57	16.7	0	100	0	2.5	0	37	63	12.7	0	0	100	1.5	27	27	45	16.0	100	0	0	1.5	20	30	50	14.5	7.3	60.0	67.3
W8	1020.0	UHy	377	0	40	60	18.0	0	100	0	2.1	0	21	79	11.1	0	56	44	4.8	30	34	36	24.4	57	43	0	1.9	28	33	39	22.5	6.6	41.1	47.7
W8	1353.4	UHy	379	23	46	32	24.3	30	70	0	7.1	24	36	40	14.5	0	30	70	2.6	0	57	43	43.3	0	100	0	0.8	0	57	43	42.5	0.0	4.5	4.5
W8	1395.0	UHy	390	20	43	37	12.6	50	50	0	4.1	6	39	55	8.5	0	0	0	0.0	27	55	18	18.7	100	0	0	0.5	25	56	18	18.2	9.0	46.2	55.1
W8	1405.0	UHy	295	0	75	25	8.1	0	100	0	3.1	0	60	40	5.1	0	0	0	0.0	12	44	44	28.5	0	100	0	0.7	12	43	45	27.8	5.1	45.8	50.8
W8	1430.0	UHy	267	0	39	61	21.3	0	100	0	1.1	0	41	59	17.2	0	0	100	3.0	32	36	32	16.5	0	0	0	0.0	32	36	32	16.5	0.0	56.2	56.2
W8	1450.0	UHy	360	26	48	26	15.0	40	60	0	5.6	18	41	41	9.4	0	0	0	0.0	43	38	20	32.5	33	67	0	3.3	44	34	22	29.2	0.0	38.9	38.9
W8	1475.0	Cor	268	14	55	31	21.6	0	100	0	1.5	15	52	33	20.1	0	0	0	0.0	26	40	34	13.1	0	0	0	0.0	26	40	34	13.1	20.5	37.3	57.8
W8	1505.0	Cor	380	30	58	13	18.6	24	76	0	4.5	38	62	0	11.8	0	0	100	2.4	0	19	81	29.6	0	27	73	2.9	0	19	81	26.7	36.6	5.2	41.9
W8	1525.0	Cor	322	0	33	67	10.2	0	100	0	2.5	0	18	82	5.2	0	0	100	2.5	15	35	50	36.9	50	50	0	2.5	13	34	54	34.5	43.1	1.5	44.6
W8	1555.0	Cor	329	13	52	35	18.1	31	69	0	7.8	0	41	59	9.6	0	0	100	0.6	17	44	38	35.2	47	53	0	5.1	12	43	45	30.1	1.5	31.6	33.1
W8	1575.0	Cor	363	10	39	51	19.3	31	69	0	3.6	6	38	56	13.2	0	0	100	2.5	12	48	40	30.3	0	100	0	0.8	12	47	41	29.5	4.1	41.3	45.5
W8	1600.0	Cor	332	20	41	39	22.3	27	73	0	3.3	20	38	43	18.1	0	0	100	0.9	22	48	30	21.7	57	43	0	2.1	18	48	33	19.6	6.8	46.3	53.1
W8	1603.6	Cor	288	16	47	37	17.6	47	53	0	5.9	0	54	46	9.7	0	0	100	2.1	6	61	33	18.6	30	70	0	3.4	0	59	41	15.2	4.1	58.6	62.8
W8	1624.0	Cer	352	21	36	43	21.6	30	57	13	6.5	18	27	55	14.5	0	0	100	0.6	32	45	23	20.7	0	0	0	0.0	32	45	23	20.7	9.4	43.2	52.6
W8	1650.0	Cer	371	5	44	51	21.7	36	64	0	2.9	0	42	58	14.7	0	40	60	4.0	29	50	21	18.8	17	83	0	3.2	31	43	26	15.5	10.7	40.2	50.9
W8	1674.0	Cer	349	34	50	16	19.4	57	43	0	6.0	24	53	24	9.7	23	54	23	3.7	28	47	25	34.0	0	100	0	2.3	30	43	27	31.7	5.7	35.7	41.4
W8	1700.0	Cer	293	24	45	30	11.3	0	0	0	0.0	27	40	33	10.2	0	100	0	1.0	18	50	32	24.6	0	100	0	1.0	19	48	33	23.5	6.1	49.5	55.6
W8	1714.0	Cer	304	27	46	27	18.4	100	0	0	1.3	24	42	33	14.8	0	100	0	2.3	35	25	40	20.7	0	0	0	0.0	35	25	40	20.7	10.9	41.1	52.0
W8	1756.0	Cer	294	4	32	65	26.9	19	81	0	5.4	0	24	76	16.7	0	0	100	4.8	14	45	41	9.9	100	0	0	1.4	0	52	48	8.5	57.8	1.7	59.5
W8	1764.7	Cer	392	12	45	43	12.5	0	100	0	3.3	21	32	46	7.1	0	0	100	2.0	11	49	40	16.6	0	0	100	0.8	11	52	37	15.8	10.2	0.0	10.2
W8	1795.0	Cer	333	10	35	55	23.1	0	0	0	0.0	16	35	49	15.3	0	35	65	7.8	45	38	17	20.7	100	0	0	0.9	42	39	18	19.8	43.5	3.0	46.5
W8	1820.0	BN	278	9	48	44	28.8	37	63	0	6.8	0	55	45	14.4	0	19	81	7.6	25	39	35	28.4	67	33	0	3.2	20	40	40	25.2	6.8	30.6	37.4
W8	1850.0	BN	280	9	35	57	16.4	0	100	0	1.4	11	32	58	13.5	0	0	100	1.4	0	47	53	26.0	0	60	40	7.1	0	42	58	18.9	14.2	28.5	42.7
W8	1875.0	BN	268	23	47	30	23.7	33	67	0	3.3	26	52	22	17.0	0	0	100	3.3	27	29	44	21.9	43	57	0	2.6	25	25	50	19.3	2.2	33.3	35.6
W8	1905.0	BN	269	14	37	49	27.1	33	67	0	3.3	15	36	49	17.5	0	24	76	6.3	6	45	48	11.5	0	0	100	3.0	9	61	30	8.6	5.6	40.9	46.5
W8	1930.0	BN	329	14	35	51	17.3	24	76	0	5.2	12	21	67	10.0	0	0	100	2.1	6	30	64	21.3	0	25	75	3.6	7	31	62	17.6	7.0	33.4	40.4
W8	1950.0	BN	285	5	55	41	15.4	14	86	0	4.9	0	35	65	8.1	0	57	43	2.5	21	49	29	26.3	30	40	30	3.5	20	51	29	22.8	10.5	40.4	50.9
W8	1975.0	BN	289	13	50	37	23.5	43	57	0	7.3	0	43	57	10.4	0	53	47	5.9	30	41	30	18.7	50	0	50	2.1	27	46	27	16.6	6.9	41.5	48.4
W8	1980.0	BN	246	20	43	37	19.9	50	50	0	3.3	20	43	37	12.2	0	36	64	4.5	18	48	34	25.2	33	67	0	3.7	15	45	40	21.5	4.1	44.7	48.8
W8	2000.0	BN	265	14	39	47	22.3	0	100	0	2.6	28	41	31	10.9	0	17	83	8.7	10	32	59	15.5	50	50	0	3.0	0	27	73	12.5	3.8	47.2	50.9
W8	2025.0	CyM & ME	262	5	57	39	16.8	20	80	0	3.8	0	47	53	6.5	0	53	47	6.5	26	45	29	16.0	57	0	43	2.7	20	54	26	13.4	7.6	49.6	57.3
W8	2050.0	CyM & ME	311	10	36	54	25.1	31	69	0	4.2	8	37	56	16.7	0	0	100	4.2	22	48	30	20.6	46	54	0	4.2	16	47	37	16.4	3.2	45.0	48.2

Well	TVD (m)	Stratigraphy	Preservation of Phytoplancton			Phytoplancton %/ total OM	Preservation of Prasinophytes			Prasinophytes %/ total OM	Preservation of Acritarchs			Acritarchs %/ total OM	Preservation of Dinoflagellate cysts			Dinoflagellate cysts %/ total OM	Preservation of Leiospheres			Leiospheres %/ total OM	Preservation of Lacustrine Algae			Lacustrine Algae %/ total OM	Foraminifera %/ total OM	Fungi %/ total OM	Terr Comp. % / total OM	Marine Comp. % / total OM	terr. palynomorphs/ total OM	marine palynomorphs/ total OM
			good (%/Phytoplancton)	moderate (%/Phytoplancton)	poor (%/Phytoplancton)		good (%/Pras.)	moderate (%/Pras.)	poor (%/Pras.)		good (%/Acritarchs)	moderate (%/Acritarchs)	poor (%/Acritarchs)		good (%/Dino.)	moderate (%/Dino.)	poor (%/Dino.)		good (%/Leiospheres)	moderate (%/Leiospheres)	poor (%/Leiospheres)		good (%/Lac. Algae)	moderate (%/Lac. Algae)	poor (%/Lac. Algae)						
W8	675.0	UT I	67	0	33	2.7	0	0	0	0.0	0	0	100	0.9	0	0	0	0.0	100	0	0	1.8	24	59	17	12.2	0.0	0.0	82.9	5.0	7.0	2.7
W8	765.0	UHy	0	0	0	0.0	0	0	0	0.0	0	0	0	0.0	0	0	0	0.0	0	0	0	0.0	0	100	0	1.2	0.0	0.0	45.0	53.8	12.4	0.0
W8	775.0	UHy	0	0	100	9.8	0	0	0	0.0	0	0	100	1.2	0	0	100	8.6	0	0	0	0.0	0	0	0	0.0	0.0	0.0	36.5	63.5	15.3	9.8
W8	825.0	UHy	0	100	0	1.6	0	0	0	0.0	0	0	0	0.0	0	100	0	1.6	0	0	0	0.0	0	0	0	0.0	0.0	0.0	47.5	52.5	18.4	1.6
W8	875.0	UHy	0	0	0	0.0	0	0	0	0.0	0	0	0	0.0	0	0	0	0.0	0	0	0	0.0	0	0	0	0.0	0.0	0.0	47.5	52.5	23.7	0.0
W8	915.0	UHy	0	0	0	0.0	0	0	0	0.0	0	0	0	0.0	0	0	0	0.0	0	0	0	0.0	0	0	0	0.0	0.0	0.0	37.5	62.5	11.8	0.0
W8	985.0	UHy	0	0	0	0.0	0	0	0	0.0	0	0	0	0.0	0	0	0	0.0	0	0	0	0.0	0	0	0	0.0	0.0	0.0	40.0	60.0	16.0	0.0
W8	1020.0	UHy	0	0	0	0.0	0	0	0	0.0	0	0	0	0.0	0	0	0	0.0	11	51	38	9.8	0	0	0	0.0	0.0	0.0	49.1	41.1	24.4	0.0
W8	1353.4	UHy	60	40	0	25.3	0	0	0	0.0	0	0	0	0.0	60	40	0	25.3	70	30	0	2.6	0	0	0	0.0	0.0	0.0	67.5	29.8	43.3	25.3
W8	1395.0	UHy	53	47	0	12.1	0	0	0	0.0	0	0	0	0.0	53	47	0	12.1	0	33	67	1.5	0	0	0	0.0	0.0	0.0	40.3	58.2	18.7	12.1
W8	1405.0	UHy	38	43	19	12.5	0	0	0	0.0	0	33	67	2.0	45	45	10	10.5	0	0	0	0.0	0	0	0	0.0	0.0	0.0	41.7	58.3	28.5	12.5
W8	1430.0	UHy	0	25	75	6.0	0	0	0	0.0	0	0	0	0.0	0	25	75	6.0	0	0	0	0.0	0	0	0	0.0	0.0	0.0	37.8	62.2	16.5	6.0
W8	1450.0	UHy	20	20	59	13.6	0	0	0	0.0	0	0	100	3.9	29	29	43	9.7	0	0	0	0.0	0	0	0	0.0	0.0	0.0	47.5	52.5	32.5	13.6
W8	1475.0	Cor	40	40	20	7.5	0	0	0	0.0	0	0	0	0.0	40	40	20	7.5	0	0	0	0.0	0	0	0	0.0	0.0	0.0	55.2	44.8	13.1	7.5
W8	1505.0	Cor	8	36	56	9.4	0	0	0	0.0	0	0	100	2.1	11	46	43	7.3	0	0	0	0.0	0	0	0	0.0	0.5	0.5	84.8	15.2	29.6	9.9
W8	1525.0	Cor	8	38	54	7.4	100	0	0	0.6	0	0	0	0.0	0	41	59	6.8	0	0	0	0.0	0	0	0	0.0	0.0	0.9	90.2	9.8	36.9	8.3
W8	1555.0	Cor	5	55	40	12.7	0	0	0	0.0	0	0	100	1.2	5	61	34	11.4	0	0	0	0.0	0	0	0	0.0	0.9	0.4	54.8	45.2	35.2	13.6
W8	1575.0	Cor	50	25	25	4.4	0	0	0	0.0	0	0	0	0.0	50	25	25	4.4	0	0	0	0.0	0	0	100	0.6	0.0	0.7	53.7	45.7	30.3	4.4
W8	1600.0	Cor	0	100	0	1.5	0	0	0	0.0	0	0	0	0.0	0	100	0	0.9	0	100	0	0.6	0	0	0	0.0	0.0	1.5	50.7	49.3	21.7	3.0
W8	1603.6	Cor	0	0	100	0.3	0	0	0	0.0	0	0	100	0.3	0	0	0	0.0	0	0	0	0.0	0	0	0	0.0	0.0	0.7	40.3	59.7	18.6	1.0
W8	1624.0	Cer	0	28	72	5.1	0	0	0	0.0	0	100	0	0.9	0	13	87	4.3	0	0	0	0.0	0	0	0	0.0	0.0	0.0	51.7	48.3	20.7	5.1
W8	1650.0	Cer	13	63	23	8.0	50	50	0	2.1	0	50	50	1.6	0	75	25	4.3	0	0	0	0.0	0	0	0	0.0	0.0	0.5	51.2	48.8	18.8	8.6
W8	1674.0	Cer	0	41	59	4.9	0	0	0	0.0	0	0	100	1.1	0	33	67	2.6	0	100	0	1.1	0	0	0	0.0	0.0	0.3	59.1	40.9	34.0	5.1
W8	1700.0	Cer	0	50	50	1.4	0	0	0	0.0	0	0	100	0.7	0	100	0	0.7	0	0	0	0.0	38	62	0	7.2	0.0	0.0	42.0	50.9	24.6	1.4
W8	1714.0	Cer	14	38	48	6.9	0	0	0	0.0	0	0	100	0.7	16	42	42	6.3	0	0	0	0.0	0	50	50	2.0	0.0	0.0	50.0	48.0	20.7	6.9
W8	1756.0	Cer	0	36	64	3.7	0	0	0	0.0	0	0	100	1.4	0	57	43	2.4	0	0	0	0.0	0	0	0	0.0	0.0	0.0	94.6	5.4	9.9	3.7
W8	1764.7	Cer	1	46	53	59.9	0	0	0	0.0	1	42	57	56.4	0	100	0	3.6	0	0	0	0.0	0	100	0	0.8	0.0	0.0	39.3	59.9	16.6	59.9
W8	1795.0	Cer	19	50	31	4.8	0	0	0	0.0	0	67	33	1.8	30	40	30	3.0	0	0	0	0.0	75	25	0	4.8	0.0	0.0	87.4	7.8	20.7	4.8
W8	1820.0	BN	50	0	50	1.4	0	0	100	0.7	0	0	0	0.0	100	0	0	0.7	0	0	0	0.0	27	73	0	4.0	0.0	0.0	64.0	32.0	28.4	1.4
W8	1850.0	BN	0	30	70	10.7	0	0	0	0.0	0	0	100	4.3	0	56	44	5.7	0	0	100	0.7	64	36	0	3.9	0.0	0.4	56.6	39.5	26.0	11.0
W8	1875.0	BN	8	35	57	18.1	0	0	0	0.0	0	40	60	5.6	12	32	56	12.6	0	0	0	0.0	0	0	0	0.0	0.0	0.7	47.8	52.2	21.9	18.9
W8	1905.0	BN	0	67	33	2.2	0	0	0	0.0	0	0	0	0.0	0	67	33	2.2	0	0	0	0.0	47	53	0	12.6	0.0	0.0	44.2	43.1	11.5	2.2
W8	1930.0	BN	0	41	59	10.3	0	0	0	0.0	0	30	70	3.0	0	38	62	6.4	0	100	0	0.9	49	51	0	10.6	0.0	0.0	45.6	43.8	21.3	10.3
W8	1950.0	BN	0	35	65	6.0	0	0	0	0.0	0	0	100	2.8	0	57	43	2.5	0	100	0	0.7	100	0	0	1.4	0.0	0.0	52.3	46.3	26.3	6.0
W8	1975.0	BN	0	0	100	4.2	0	0	0	0.0	0	0	100	2.4	0	0	100	1.7	0	0	0	0.0	87	13	0	5.2	0.0	0.0	49.1	45.7	18.7	4.2
W8	1980.0	BN	0	100	0	1.6	0	0	0	0.0	0	0	0	0.0	0	100	0	1.6	0	0	0	0.0	73	27	0	4.5	0.0	0.0	49.2	46.3	25.2	1.6
W8	2000.0	BN	0	10	90	7.9	0	0	0	0.0	0	0	100	2.6	0	0	100	4.5	0	100	0	0.8	67	33	0	3.4	0.0	0.0	41.5	55.1	15.5	7.9
W8	2025.0	CyM & ME	46	23	31	9.9	0	0	0	0.0	0	0	0	0.0	46	23	31	9.9	0	0	0	0.0	100	0	0	0.0	0.0	0.0	40.5	59.5	16.0	9.9
W8	2050.0	CyM & ME	25	33	42	3.9	0	0	0	0.0	0	0	100	0.6	30	40	30	3.2	0	0	0	0.0	100	0	0	2.3	0.0	0.0	48.9	48.9	20.6	3.9

Well	TVD (m)	Stratigraphy	# of particels	Preservation of Phytoclasts			Phyclasts%/ total OM	Preservation of Inertinite			Inertinite % total OM	Preservation of Vitrinite			Vitrinite % total OM	Preservation of Cutinite			Cutinite % total OM	Preservation of Sporomorphs			Sporomorphs %/ total OM	Preservation of Spores			Spores %/ total OM	Preservation of Pollen			Pollen %/ total OM	terr. AOM %/ total OM	marine AOM %/ total OM	total AOM %/ total OM
				good (%/Phytoclasts)	moderate (%/Phytoclasts)	poor (%/Phytoclasts)		good (%/Inertinite)	moderate (%/Inertinite)	poor (%/Inertinite)		good (%/Vitrinite)	moderate (%/Vitrinite)	poor (%/Vitrinite)		good (%/Cutinite)	moderate (%/Cutinite)	poor (%/Cutinite)		good (%/Sporomorphs)	moderate(%/Sporo morphs)	poor (%/Sporomorphs)		good (%/Spores)	moderate (%/Spores)	moderate (%/Spores)		good (%/Spores)	moderate (%/Spores)	poor (%/Spores)				
W9	839.0	UHy	321	28	34	38	40.5	11	44	44	5.6	28	34	38	33.3	100	0	0	1.6	89	11	0	11.2	100	0	0	5.0	80	20	0	6.2	1.6	45.2	46.7
W9	920.0	UHy	303	23	33	44	31.4	20	35	45	6.6	24	32	44	24.8	0	0	0	0.0	87	13	0	14.9	87	13	0	7.6	86	14	0	7.3	3.3	47.9	51.2
W9	993.0	UHy	318	57	11	31	17.0	56	44	0	2.8	47	6	47	11.3	100	0	0	2.8	92	8	0	11.6	89	11	0	8.8	100	0	0	2.8	0.0	59.7	59.7
W9	1063.0	UHy	316	0	100	0	1.9	0	0	0	0.0	0	100	0	1.9	0	0	0	0.0	76	14	10	29.4	86	0	14	11.4	70	23	7	18.0	0.0	61.7	61.7
W9	1124.0	UHy	288	31	23	46	4.5	50	0	50	1.4	25	38	38	2.8	0	0	100	0.3	52	15	33	16.0	61	0	39	6.3	46	25	29	9.7	0.0	46.9	46.9
W9	1155.0	UHy	372	44	31	25	22.6	50	36	14	3.8	36	32	32	15.9	82	18	0	3.0	63	29	8	25.0	57	28	15	12.6	70	30	0	12.4	0.0	48.4	48.4
W9	1171.0	UHy	383	22	32	46	32.6	0	38	62	5.5	27	28	45	26.1	0	100	0	1.0	49	22	28	17.5	18	24	58	8.6	79	21	0	8.9	0.0	43.6	43.6
W9	1183.0	UHy	276	34	9	57	15.9	0	0	100	4.0	25	17	58	8.7	100	0	0	3.3	80	20	0	16.3	72	28	0	9.1	90	10	0	7.2	0.0	54.7	54.7
W9	1192.0	UHy	269	31	18	51	14.5	30	40	30	3.7	31	10	59	10.8	0	0	0	0.0	67	21	12	24.9	45	35	20	14.9	100	0	0	10.0	0.0	56.1	56.1
W9	1201.0	LHy	269	33	29	38	7.8	0	0	100	1.1	39	33	28	6.7	0	0	0	0.0	64	22	14	21.9	50	50	0	9.7	76	0	24	12.3	0.0	59.1	59.1
W9	1214.0	LHy	250	30	40	30	8.0	0	0	0	0.0	30	40	30	8.0	0	0	0	0.0	65	16	19	14.8	47	32	21	7.6	83	0	17	7.2	0.0	61.2	61.2
W9	1220.0	LHy	287	38	22	40	15.7	67	33	0	2.1	33	21	46	13.6	0	0	0	0.0	71	23	6	27.2	47	26	26	6.6	78	22	0	20.6	0.0	40.4	40.4
W9	1230.0	LHy	307	40	17	43	23.5	33	38	29	7.8	39	7	55	14.3	100	0	0	1.3	65	30	5	18.6	25	56	19	5.2	80	20	0	13.4	0.0	43.3	43.3
W9	1248.0	LHy	300	33	0	67	13.0	14	0	86	4.7	33	0	67	7.0	100	0	0	1.3	75	13	12	23.0	76	0	24	5.7	75	17	8	17.3	0.0	41.3	41.3
W9	1266.0	LHy	325	19	28	53	22.2	0	50	50	2.5	23	21	56	18.8	0	100	0	0.9	64	34	2	18.8	59	41	0	8.9	69	28	3	9.8	0.0	41.8	41.8
W9	1284.0	LHy	332	28	21	50	37.0	37	23	40	10.5	26	21	52	25.3	0	0	100	1.2	65	30	4	26.8	53	47	0	5.7	69	26	6	21.1	0.9	22.0	22.9
W9	1308.0	LHy	291	25	23	52	35.1	58	25	17	8.2	16	20	64	25.4	0	50	50	1.4	65	32	3	23.7	71	29	0	4.8	64	33	4	18.9	0.0	35.1	35.1
W9	1320.0	LHy	255	26	13	61	20.8	20	27	53	5.8	26	9	65	13.1	40	0	60	1.9	72	28	0	9.6	50	50	0	2.3	79	21	0	7.3	0.0	46.5	46.5
W9	1341.0	LHy	284	15	23	62	35.2	41	18	41	6.0	10	24	66	29.2	0	0	0	0.0	77	23	0	18.7	67	33	0	4.2	80	20	0	14.4	0.0	35.6	35.6
W9	1353.0	LHy	297	33	14	53	42.8	47	27	27	10.1	27	7	66	30.0	50	50	0	2.7	90	3	7	20.2	33	22	44	3.0	100	0	0	17.2	0.0	31.3	31.3
W9	1362.0	LHy	334	31	21	48	41.0	47	27	27	9.0	26	20	54	32.0	0	0	0	0.0	100	0	0	24.3	100	0	0	5.1	100	0	0	19.2	0.0	26.9	26.9
W9	1377.0	CyM & ME	374	37	17	46	48.4	52	17	30	12.3	29	18	53	34.5	100	0	0	1.6	95	0	5	16.8	100	0	0	5.6	93	0	7	11.2	0.0	32.1	32.1
W9	1400.0	CyM & ME	350	22	19	59	31.8	29	14	57	6.0	21	20	59	25.9	0	0	0	0.0	69	21	10	20.2	65	35	0	7.4	71	13	16	12.8	0.0	43.2	43.2
W9	1482.0	FS (RpC)	343	31	23	47	55.1	33	23	43	8.7	22	24	54	40.5	85	15	0	5.8	69	31	0	14.3	70	30	0	2.9	69	31	0	11.4	0.0	20.7	20.7
W9	1488.0	FS (RpC)	291	17	44	39	83.2	31	33	36	12.4	11	48	41	67.7	100	0	0	3.1	50	50	0	4.8	40	60	0	1.7	56	44	0	3.1	0.0	9.6	9.6
W9	1496.0	FS (RpC)	304	21	25	54	67.4	80	20	0	4.9	17	25	58	62.5	0	0	0	0.0	40	37	23	11.5	0	100	0	2.3	50	21	29	9.2	1.6	14.1	15.8
W9	1504.0	FM (RpC)	337	19	39	42	69.4	45	28	28	8.6	12	41	47	56.4	53	47	0	4.5	67	33	0	6.2	0	100	0	0.9	78	22	0	5.3	11.6	7.1	18.7
W9	1525.0	FM (RpC)	285	7	42	51	50.5	25	42	33	4.2	3	43	54	45.3	100	0	0	1.1	38	57	5	7.4	31	62	8	4.6	50	50	0	2.8	0.0	37.2	37.2
W9	1527.0	FM (RpC)	292	9	31	60	52.5	33	33	33	3.1	8	31	62	49.5	0	0	0	0.0	73	27	0	13.9	27	73	0	3.7	90	10	0	10.2	0.0	32.5	32.5
W9	1532.0	UPE	276	9	42	49	62.7	50	50	0	1.4	5	43	52	59.1	100	0	0	2.2	56	44	0	5.8	50	50	0	2.2	60	40	0	3.6	15.9	13.0	29.0
W9	1544.0	UPE	306	25	38	37	69.4	90	10	0	6.5	18	41	41	62.9	0	0	0	0.0	63	29	9	11.3	59	24	18	5.5	67	33	0	5.8	3.2	12.3	15.5
W9	1553.0	MPE	338	25	21	54	55.9	28	56	17	5.3	19	19	62	47.4	100	0	0	3.2	26	53	21	10.0	13	58	29	7.1	60	40	0	2.9	17.4	13.5	30.9
W9	1563.0	LPE	223	11	29	61	79.8	35	65	0	9.0	6	24	70	69.5	67	33	0	1.3	25	75	0	3.6	33	67	0	2.7	0	100	0	0.9	16.6	0.0	16.6
W9	1570.0	LPE	298	17	38	45	82.6	23	23	54	18.8	15	43	42	63.8	0	0	0	0.0	38	25	38	2.7	38	25	38	2.7	0	0	0	0.0	9.4	1.7	11.1

Well	TVD (m)	Stratigraphy	Preservation of Phytoplancton			Phytoplancton %/ total OM	Preservation of Prasinophytes			Prasinophytes %/ total OM	Preservation of Acritarchs			Acritarchs %/ total OM	Preservation of Dinoflagellate cysts			Dinoflagellate cysts %/ total OM	Preservation of Leiospheres			Leiospheres %/ total OM	Preservation of Lacustrine Algae			Lacustrine Algae %/ total OM	Foraminifera %/ total OM	Fungi %/ total OM	Ter Comp. % / total OM	Marine Comp. % / total OM	ter. palynomorphs/ total OM	marine palynomorphs/ total OM
			good (%/Phytoplancton)	moderate (%/Phytoplancton)	poor (%/Phytoplancton)		good (%/Pras.)	moderate (%/Pras.)	poor (%/Pras.)		good (%/Acritarchs)	moderate (%/Acritarchs)	poor (%/Acritarchs)		good (%/Dino.)	moderate (%/Dino.)	poor (%/Dino.)		good (%/Leiospheres)	moderate (%/Leiospheres)	poor (%/Leiospheres)		good (%/Lac. Algae)	moderate (%/Lac. Algae)	poor (%/Lac. Algae)						
W9	839.0	UHy	40	20	40	1.6	100	0	0	0.6	0	0	0	0.0	0	33	67	0.9	0	0	0	0.0	0	0	0	0.0	0.0	0.0	53.3	46.7	11.2	1.6
W9	920.0	UHy	75	25	0	2.6	100	0	0	1.0	0	0	0	0.0	0	0	0	0.0	0	0	0	0.0	0	0	0	0.0	0.0	0.0	49.5	50.5	14.9	2.6
W9	993.0	UHy	43	32	24	11.6	82	18	0	3.5	0	0	0	0.0	0	47	53	5.3	0	0	0	0.0	0	0	0	0.0	0.0	0.0	28.6	71.4	11.6	11.6
W9	1063.0	UHy	68	9	23	7.0	73	0	27	3.5	0	0	0	0.0	0	50	50	1.3	100	0	0	2.2	0	0	0	0.0	0.0	0.0	31.3	68.7	29.4	7.0
W9	1124.0	UHy	35	37	28	32.6	0	47	53	5.2	0	0	0	0.0	0	35	23	27.4	0	0	0	0.0	0	0	0	0.0	0.0	0.0	20.5	79.5	16.0	32.6
W9	1155.0	UHy	23	38	38	3.5	100	0	0	0.8	0	0	0	0.0	0	38	63	2.2	0	100	0	0.5	100	0	0	0.5	0.0	0.0	47.6	51.9	25.0	3.5
W9	1171.0	UHy	46	17	38	6.3	0	0	0	0.0	0	0	0	0.0	46	17	38	6.3	0	0	0	0.0	0	0	0	0.0	0.0	0.0	50.1	49.9	17.5	6.3
W9	1183.0	UHy	39	19	42	13.0	0	0	0	0.0	0	0	0	0.0	39	19	42	13.0	0	0	0	0.0	0	0	0	0.0	0.0	0.0	32.2	67.8	16.3	13.0
W9	1192.0	UHy	75	25	0	4.5	0	0	0	0.0	0	0	0	0.0	75	25	0	4.5	0	0	0	0.0	0	0	0	0.0	0.0	0.0	39.4	60.6	24.9	4.5
W9	1201.0	LHy	70	20	10	11.2	100	0	0	1.1	0	0	0	0.0	64	24	12	9.3	100	0	0	0.7	0	0	0	0.0	0.0	0.0	29.7	70.3	21.9	11.2
W9	1214.0	LHy	31	49	21	15.6	67	33	0	3.6	0	0	0	0.0	22	48	30	10.8	0	100	0	1.2	100	0	0	0.4	0.0	0.0	22.8	76.8	14.8	15.6
W9	1220.0	LHy	78	22	0	14.3	56	44	0	3.1	0	0	0	0.0	82	18	0	9.8	100	0	0	1.4	100	0	0	2.4	0.0	0.0	42.9	54.7	27.2	14.3
W9	1230.0	LHy	61	29	10	13.4	0	0	100	0.3	0	0	0	0.0	67	24	9	10.7	43	57	0	2.3	100	0	0	1.3	0.0	0.0	42.0	56.7	18.6	13.4
W9	1248.0	LHy	36	38	27	21.3	25	75	0	2.7	0	0	0	0.0	33	33	33	17.0	80	20	0	1.7	100	0	0	1.3	0.0	0.0	36.0	62.7	23.0	21.3
W9	1266.0	LHy	37	43	20	14.2	100	0	0	1.2	0	0	0	0.0	34	42	24	11.7	0	100	0	1.2	80	20	0	3.1	0.0	0.0	40.9	59.0	18.8	14.2
W9	1284.0	LHy	50	32	18	13.3	0	100	0	0.6	0	0	0	0.0	52	29	19	12.7	0	0	0	0.0	0	0	0	0.0	0.0	0.0	64.8	35.2	26.8	13.3
W9	1308.0	LHy	27	64	9	3.8	0	0	0	0.0	0	0	0	0.0	27	64	9	3.8	0	0	0	0.0	57	43	0	2.4	0.0	0.0	58.8	38.8	23.7	3.8
W9	1320.0	LHy	29	27	44	21.2	70	30	0	3.8	0	0	0	0.0	20	27	53	17.3	0	0	0	0.0	0	0	0	0.0	0.0	1.9	30.4	69.6	9.6	23.1
W9	1341.0	LHy	40	47	13	10.6	60	40	0	1.8	0	0	0	0.0	36	48	16	8.8	0	0	0	0.0	0	0	0	0.0	0.0	0.0	53.9	46.1	18.7	10.6
W9	1353.0	LHy	65	35	0	5.7	100	0	0	1.3	0	0	0	0.0	54	46	0	4.4	0	0	0	0.0	0	0	0	0.0	0.0	0.0	63.0	37.0	20.2	5.7
W9	1362.0	LHy	100	0	0	7.8	100	0	0	0.9	0	0	0	0.0	100	0	0	4.8	100	0	0	2.1	0	0	0	0.0	0.0	0.0	65.3	34.7	24.3	7.8
W9	1377.0	CyM & ME	100	0	0	2.7	100	0	0	0.5	0	0	0	0.0	100	0	0	0.5	100	0	0	1.6	0	0	0	0.0	0.0	0.0	65.2	34.8	16.8	2.7
W9	1400.0	CyM & ME	40	47	13	4.3	100	0	0	0.6	0	0	0	0.0	31	54	15	3.7	0	0	0	0.0	0	0	0	0.0	0.0	0.6	52.0	48.0	20.2	4.8
W9	1482.0	FS (RpC)	43	46	11	8.2	0	0	0	0.0	0	0	0	0.0	33	54	13	7.0	100	0	0	1.2	67	33	0	1.7	0.0	0.0	69.4	28.9	14.3	8.2
W9	1488.0	FS (RpC)	100	0	0	2.4	0	0	0	0.0	0	0	0	0.0	100	0	0	2.4	0	0	0	0.0	0	0	0	0.0	0.0	0.0	88.0	12.0	4.8	2.4
W9	1496.0	FS (RpC)	75	25	0	5.3	100	0	0	0.3	0	0	0	0.0	71	29	0	4.6	100	0	0	0.3	0	0	0	0.0	0.0	0.0	80.6	19.4	11.5	5.3
W9	1504.0	FM (RpC)	36	64	0	3.3	0	0	0	0.0	0	0	0	0.0	36	64	0	3.3	0	0	0	0.0	100	0	0	2.4	0.0	0.0	87.2	10.4	6.2	3.3
W9	1525.0	FM (RpC)	57	29	14	4.9	0	0	0	0.0	0	0	0	0.0	57	29	14	4.9	0	0	0	0.0	0	0	0	0.0	0.0	0.0	57.9	42.1	7.4	4.9
W9	1527.0	FM (RpC)	0	0	0	0.0	0	0	0	0.0	0	0	0	0.0	0	0	0	0.0	0	0	0	0.0	0	0	0	0.0	0.0	1.0	66.4	33.6	13.9	1.0
W9	1532.0	UPE	57	43	0	2.5	0	0	0	0.0	0	0	0	0.0	57	43	0	2.5	0	0	0	0.0	0	0	0	0.0	0.0	0.0	84.4	15.6	5.8	2.5
W9	1544.0	UPE	13	38	50	2.6	0	0	0	0.0	0	0	0	0.0	13	38	50	2.6	0	0	0	0.0	0	0	0	0.0	0.0	1.3	83.9	16.1	11.3	3.9
W9	1553.0	MPE	33	44	22	2.6	100	0	0	0.9	0	0	0	0.0	0	67	33	1.8	0	0	0	0.0	0	0	0	0.0	0.0	0.6	83.2	16.8	10.0	3.2
W9	1563.0	LPE	0	0	0	0.0	0	0	0	0.0	0	0	0	0.0	0	0	0	0.0	0	0	0	0.0	0	0	0	0.0	0.0	0.0	100.0	0.0	3.6	0.0
W9	1570.0	LPE	0	27	73	3.7	0	0	0	0.0	0	0	0	0.0	0	27	73	3.7	0	0	0	0.0	0	0	0	0.0	0.0	0.0	94.6	5.4	2.7	3.7

Well	TVD (m)	Stratigraphy	# of particels	Preservation of Phytoclasts			Phyclasts%/ total OM	Preservation of Inertinite			Inertinite %/ total OM	Preservation of Vitrinite			Vitrinite %/ total OM	Preservation of Cutinite			Cutinite %/ total OM	Preservation of Sporomorphs			Sporomorphs %/ total OM	Preservation of Spores			Spores %/ total OM	Preservation of Pollen			Pollen %/ total OM	terr. AOM %/ total OM	marine AOM %/ total OM	total AOM %/ total OM
				good (%/Phytoclasts)	moderate (%/Phytoclasts)	poor (%/Phytoclasts)		good (%/Intertinite)	moderate (%/Intertinite)	poor (%/Intertinite)		good (%/Vitrinite)	moderate (%/Vitrinite)	poor (%/Vitrinite)		good (%/Cutinite)	moderate (%/Cutinite)	poor (%/Cutinite)		good (%/Sporomorphs)	moderate(%/Sporomorphs)	poor (%/Sporomorphs)		good (%/Spores)	moderate (%/Spores)	moderate (%/Spores)		good (%/Spores)	moderate (%/Spores)	poor (%/Spores)				
W10	759.0	UT I	136	41	41	19	99.3	-999	-999	0	0.0	40	40	20	91.9	50	50	0	7.4	100	0	0	0.7	0	0	0	0.0	100	0	0	0.7	0.0	0.0	0.0
W10	782.0	UHy	321	54	27	19	30.5	67	33	0	2.8	45	30	25	23.7	100	0	0	4.0	71	29	0	6.5	100	0	0	2.5	54	46	0	4.0	0.0	42.1	42.1
W10	816.0	UHy	291	26	38	36	39.9	20	20	60	3.4	26	40	34	36.4	0	0	0	0.0	87	13	0	10.7	100	0	0	6.2	69	31	0	4.5	0.0	44.7	44.7
W10	896.0	UHy	370	27	25	48	17.0	17	42	42	3.2	16	26	58	11.6	100	0	0	2.2	76	24	0	12.2	72	28	0	7.8	81	19	0	4.3	0.0	68.9	68.9
W10	967.0	UHy	295	41	36	23	13.2	20	40	40	5.1	54	33	13	8.1	0	0	0	0.0	20	80	0	1.7	50	50	0	0.7	0	100	0	1.0	0.0	84.7	84.7
W10	1046.0	UHy	292	35	31	34	21.2	28	24	48	9.9	42	36	21	11.3	0	0	0	0.0	55	42	3	13.0	74	22	4	9.2	9	91	0	3.8	0.0	62.3	62.3
W10	1125.0	UHy	266	28	30	42	31.2	38	25	38	3.0	23	32	45	26.7	100	0	0	1.5	69	31	0	9.8	86	14	0	5.3	50	50	0	4.5	0.0	56.4	56.4
W10	1211.0	UHy	337	30	23	47	19.0	44	38	19	4.7	26	15	59	13.6	0	100	0	0.6	47	45	8	14.5	50	37	13	8.9	42	58	0	5.6	0.0	62.3	62.3
W10	1258.0	UHy	261	25	31	44	12.3	67	33	0	2.3	12	32	56	9.6	100	0	0	0.4	64	36	0	14.9	69	31	0	6.1	61	39	0	8.8	0.0	59.4	59.4
W10	1282.0	LHy	269	49	31	20	18.2	42	46	13	8.9	56	16	28	9.3	0	0	0	0.0	64	36	0	12.3	82	18	0	6.3	44	56	0	5.9	0.0	67.7	67.7
W10	1324.0	LHy	266	16	37	47	21.4	18	36	45	4.1	13	38	49	16.9	100	0	0	0.4	48	52	0	10.9	40	60	0	1.9	50	50	0	9.0	0.0	62.4	62.4
W10	1356.0	LHy	286	26	40	34	24.5	33	33	33	3.1	22	42	36	20.6	100	0	0	0.7	38	32	30	16.4	64	36	0	3.8	31	31	39	12.6	0.0	45.5	45.5
W10	1372.0	LHy	266	0	32	68	23.3	0	100	0	1.1	0	29	71	22.2	0	0	0	0.0	55	39	5	14.3	56	44	0	6.8	55	35	10	7.5	0.0	45.1	45.1
W10	1428.0	LHy	227	16	21	63	57.7	5	10	86	9.3	12	23	65	44.1	80	20	0	4.4	0	63	37	8.4	0	56	44	4.0	0	70	30	4.4	11.5	19.4	30.8
W10	1461.0	LHy	287	22	34	44	29.6	32	14	54	9.8	15	43	42	18.5	50	50	0	1.4	17	54	29	8.4	31	46	23	4.5	0	64	36	3.8	4.5	44.3	48.8
W10	1494.0	LHy	371	15	9	76	42.3	16	12	72	20.5	9	6	84	20.8	100	0	0	1.1	43	57	0	10.0	70	30	0	2.7	33	67	0	7.3	8.1	29.1	37.2
W10	1527.0	LHy	301	12	25	64	51.2	12	17	71	32.9	11	38	51	18.3	0	0	0	0.0	18	58	24	12.6	23	62	15	4.3	16	56	28	8.3	23.3	13.0	36.2
W10	1555.0	LHy	323	10	37	53	47.4	5	41	54	12.1	13	33	55	34.1	0	100	0	1.2	42	38	20	18.6	39	33	28	5.6	43	40	17	13.0	17.3	13.9	31.3
W10	1564.0	LHy	278	15	46	39	43.2	31	54	15	4.7	8	48	45	36.3	100	0	0	2.2	56	32	12	14.7	56	31	13	5.8	56	32	12	9.0	19.8	21.6	41.4
W10	1576.0	Cor	215	12	43	45	32.1	0	60	40	9.3	16	37	47	22.8	0	0	0	0.0	74	26	0	19.5	78	22	0	8.4	71	29	0	11.2	12.1	28.8	40.9
W10	1600.0	Cor	306	22	34	44	59.8	40	35	25	6.5	16	34	50	48.7	57	43	0	4.6	49	51	0	12.7	11	89	0	2.9	60	40	0	9.8	22.9	3.3	26.1
W10	1617.0	Cor	255	16	28	57	47.8	7	22	71	16.1	16	32	52	30.2	100	0	0	1.6	42	58	0	18.8	44	56	0	6.3	41	59	0	12.5	11.4	18.4	29.8
W10	1634.0	Cor	328	9	36	55	14.3	9	43	48	7.0	8	29	63	7.3	0	0	0	0.0	56	30	15	18.6	66	28	6	9.8	45	31	24	8.8	14.3	41.5	55.8
W10	1649.0	Cor	312	30	45	25	6.4	0	75	25	2.6	0	0	0	0.0	50	25	25	3.8	71	16	13	20.2	56	28	17	5.8	78	11	11	14.4	14.7	51.6	66.3
W10	1665.0	Cor	276	24	41	35	12.3	0	67	33	2.2	31	38	31	9.4	0	0	100	0.7	80	18	3	14.5	77	23	0	10.9	90	0	10	3.6	5.8	54.7	60.5
W10	1681.0	Cor	295	35	24	41	5.8	0	100	0	1.4	55	0	45	3.7	0	0	100	0.7	79	21	0	22.4	77	23	0	10.5	80	20	0	11.9	2.7	54.9	57.6
W10	1730.0	Cer	268	25	42	33	4.5	0	43	57	2.6	60	40	0	1.9	0	0	0	0.0	57	33	10	25.0	29	58	13	11.6	81	11	8	13.4	3.4	54.9	58.2
W10	1747.0	BN	274	21	44	35	12.4	0	50	50	2.9	27	42	31	9.5	0	0	0	0.0	68	21	11	19.3	52	33	15	9.9	85	8	8	9.5	0.7	39.4	40.1
W10	1780.0	BN	314	10	52	39	29.6	0	30	70	7.3	14	64	22	20.4	0	0	100	1.9	49	28	23	13.7	41	27	32	7.0	57	29	14	6.7	2.9	45.2	48.1
W10	1965.0	CyM & ME	317	17	38	45	9.1	17	25	58	3.8	18	47	35	5.4	0	0	0	0.0	72	28	0	9.1	64	36	0	4.4	80	20	0	4.7	2.8	69.1	71.9
W10	1954.0	CyM & ME	282	43	41	15	36.9	31	69	0	4.6	49	39	12	27.3	21	29	50	5.0	84	16	0	6.7	75	25	0	4.3	100	0	0	2.5	2.1	44.0	46.1
W10	2045.0	CyM & ME	297	49	31	20	28.3	53	29	18	5.7	53	35	12	20.2	0	0	100	2.4	100	0	0	10.8	100	0	0	5.4	100	0	0	5.4	2.7	50.5	53.2
W10	2110.0	CyM & ME	263	13	63	24	46.0	26	35	39	8.7	10	69	20	37.3	0	0	0	0.0	71	18	11	10.6	100	0	0	1.5	67	21	13	9.1	3.8	36.9	40.7
W10	2119.0	CyM & ME	283	29	55	16	36.4	35	53	12	6.0	28	56	15	30.0	0	0	100	0.4	67	33	0	7.4	100	0	0	2.1	53	47	0	5.3	0.0	55.1	55.1
W10	2132.0	FS (RpC)	312	19	36	45	34.3	33	22	44	2.9	19	41	40	28.8	0	0	100	2.6	22	43	35	7.4	28	39	33	5.8	0	60	40	1.6	44.2	10.6	54.8
W10	2141.0	FS (RpC)	263	9	33	58	24.3	0	40	60	1.9	10	32	58	22.4	0	0	0	0.0	65	15	21	12.9	79	5	16	7.2	47	27	27	5.7	28.9	33.1	62.0
W10	2155.0	FM (RpC)	283	17	5	79	14.8	0	0	0	0.0	17	5	79	14.8	0	0	0	0.0	31	69	0	9.2	31	69	0	9.2	0	0	0	0.0	21.2	52.7	73.9
W10	2165.0	FM (RpC)	362	24	24	53	10.5	25	0	75	1.1	26	29	45	8.6	0	0	100	0.8	100	0	0	2.2	100	0	0	2.2	0	0	0	0.0	53.3	32.0	85.4
W10	2172.0	FM (RpC)	271	13	26	60	25.1	67	0	33	1.1	11	29	60	22.9	0	0	100	1.1	45	18	36	8.1	27	0	73	4.1	64	36	0	4.1	10.7	50.9	61.6
W10	2251.0	MPE	283	26	37	37	44.9	26	40	34	12.4	27	38	35	31.1	0	0	100	1.4	0	60	40	1.8	0	100	0	1.1	0	0	100	0.7	20.5	14.5	35.0
W10	2257.0	MPE	223	60	27	13	85.7	56	27	18	20.2	59	28	13	55.2	78	22	0	10.3	33	42	25	5.4	44	56	0	4.0	0	0	100	1.3	0.9	1.3	2.2
W10	2260.0	LPE	337	27	25	47	33.8	0	0	100	0.6	28	26	46	33.2	0	0	0	0.0	60	27	13	4.5	40	40	20	3.0	100	0	0	1.5	18.1	1.5	19.6
W10	2307.0	LPE	294	77	17	6	73.1	74	15	11	9.2	75	18	7	50.0	85	15	0	13.9	64	36	0	8.5	44	56	0	3.1	75	25	0	5.4	0.0	14.6	14.6
W10	2311.0	LPE	509	16	42	42	43.0	8	27	65	5.1	17	44	39	37.9	0	0	0	0.0	74	26	0	8.4	84	16	0	3.7	67	33	0	4.7	5.9	33.4	39.3
W10	2337.0	LPE	326	9	66	25	93.6	0	0	0	0.0	9	66	25	93.6	0	0	0	0.0	0	0	0	0.0	0	0	0	0.0	0	0	0	0.0	6.4	0.0	6.4
W10	2342.0	LPE	261	20	74	6	96.9	0	100	0	1.1	20	74	6	95.8	0	0	0	0.0	0	0	0	0.0	0	0	0	0.0	0	0	0	0.0	3.1	0.0	3.1
W10	2346.0	LPE	234	1	83	16	95.3	60	40	0	2.1	0	83	17	93.2	0	0	0	0.0	0	0	0	0.0	0	0	0	0.0	0	0	0	0.0	4.7	0.0	4.7
W10	2349.0	LPE	310	18	52	30	85.2	26	30	43	7.4	14	56	30	75.2	100	0	0	2.6	100	0	0	0.3	100	0	0	0.3	0	0	0	0.0	12.9	1.6	14.5
W10	2354.0	LPE	322	58	27	15	95.7	0	33	67	1.9	57	28	15	90.1	100	0	0	3.7	0	100	0	1.2	0	0	0	0.0	0	100	0	1.2	3.1	0.0	3.1
W10	2356.0	LPE	371	46	34	20	100.0	50	41	9	12.4	46	33	21	87.6	0	0	0	0.0	0	0	0	0.0	0	0	0	0.0	0	0	0	0.0	0.0	0.0	0.0
W10	2361.0	LPE	306	57	25	18	91.2	58	17	25	3.9	53	28	19	77.1	87	13	0	10.1	0	100	0	2.6	0	100	0	2.3	0	100	0	0.3	0.0	4.6	4.6

Well	TVD (m)	Stratigraphy	Preservation of Phytoplancton			Phytoplancton %/ total OM	Preservation of Prasinophytes			Prasinophytes %/ total OM	Preservation of Acritarchs			Acritarchs %/ total OM	Preservation of Dinoflagellate cysts			Dinoflagellate cysts %/ total OM	Preservation of Leiospheres			Leiospheres %/ total OM	Preservation of Lacustrine Algae			Lacustrine Algae %/ total OM	Foraminifera %/ total OM	Fungi %/ total OM	Terr Comp. % / total OM	Marine Comp. % / total OM	terr. palynomorphs/ total OM	marine palynomorphs/ total OM
			good (%/Phytoplancton)	moderate (%/Phytoplancton)	poor (%/Phytoplancton)		good (%/Pras.)	moderate (%/Pras.)	poor (%/Pras.)		good (%/Acritarchs)	moderate (%/Acritarchs)	poor (%/Acritarchs)		good (%/Dino.)	moderate (%/Dino.)	poor (%/Dino.)		good (%/Leiospheres)	moderate (%/Leiospheres)	poor (%/Leiospheres)		good (%/Lac. Algae)	moderate (%/Lac. Algae)	poor (%/Lac. Algae)						
W10	759.0	UT 1	0	0	0	0.0	0	0	0	0.0	0	0	0	0.0	0	0	0	0.0	0	0	0	0.0	0	0	0	0.0	0.0	0.0	100.0	0.0	0.7	0.0
W10	782.0	UHy	74	26	0	9.7	100	0	0	1.2	0	0	0	0.0	70	30	0	8.4	0	0	0	0.0	47	53	0	11.2	0.0	0.0	37.1	51.7	6.5	9.7
W10	816.0	UHy	67	33	0	4.1	100	0	0	0.3	0	0	0	0.0	56	44	0	3.1	100	0	0	0.7	0	100	0	0.7	0.0	0.0	50.5	48.8	10.7	4.1
W10	896.0	UHy	0	43	57	1.9	0	0	0	0.0	0	0	0	0.0	0	0	100	1.1	0	100	0	0.8	0	0	0	0.0	0.0	0.0	29.2	70.8	12.2	1.9
W10	967.0	UHy	0	100	0	0.3	0	0	0	0.0	0	0	0	0.0	0	0	100	0.0	0	100	0	0.3	0	0	0	0.0	0.0	0.0	14.9	85.1	1.7	0.3
W10	1046.0	UHy	30	20	50	3.4	0	0	0	0.0	0	0	0	0.0	0	0	100	1.7	60	40	0	1.7	0	0	0	0.4	0.0	0.0	34.2	65.8	13.0	3.4
W10	1125.0	UHy	100	0	0	2.3	0	0	0	0.0	0	0	0	0.0	0	0	0	0.0	100	0	0	2.3	100	0	0	0.4	0.0	0.0	41.0	58.6	9.8	2.3
W10	1211.0	UHy	36	29	36	4.2	100	0	0	0.9	0	0	0	0.0	18	36	45	3.3	0	0	0	0.0	0	0	0	0.0	0.0	0.0	33.5	66.5	14.5	4.2
W10	1258.0	UHy	14	28	59	11.1	100	0	0	0.4	0	0	0	0.0	11	29	61	10.7	0	100	0	0.0	100	0	0	2.3	0.0	0.0	27.2	70.5	14.9	11.1
W10	1282.0	LHy	40	60	0	1.9	100	0	0	0.7	0	0	0	0.0	0	100	0	0.7	0	100	0	0.4	0	0	0	0.0	0.0	0.0	30.5	69.5	12.3	1.9
W10	1324.0	LHy	0	36	64	5.3	0	100	0	0.4	0	0	0	0.0	0	31	69	4.9	0	0	0	0.0	0	0	0	0.0	0.0	0.0	32.3	67.7	10.9	5.3
W10	1356.0	LHy	33	44	23	13.6	75	25	0	1.4	0	0	0	0.0	24	48	27	11.5	100	0	0	0.7	0	0	0	0.0	0.0	0.0	40.9	59.1	16.4	13.6
W10	1372.0	LHy	24	48	28	17.3	100	0	0	0.8	0	0	0	0.0	20	50	30	16.5	0	0	0	0.0	0	0	0	0.0	0.0	0.0	37.6	62.4	14.3	17.3
W10	1428.0	LHy	14	43	43	3.1	0	0	0	0.0	0	0	0	0.0	50	50	50	2.6	100	0	0	0.4	0	0	0	0.0	0.0	0.0	77.5	22.5	8.4	3.1
W10	1461.0	LHy	39	42	18	13.2	60	40	0	1.7	0	0	0	0.0	36	42	21	11.5	0	0	0	0.0	0	0	0	0.0	0.0	0.0	42.5	57.5	8.4	13.2
W10	1494.0	LHy	26	28	46	10.5	50	50	0	1.1	0	0	0	0.0	23	26	51	9.4	0	0	0	0.0	0	0	0	0.0	0.0	0.0	60.4	39.6	10.0	10.5
W10	1527.0	LHy	0	0	0	0.0	0	0	0	0.0	0	0	0	0.0	0	0	0	0.0	0	0	0	0.0	0	0	0	0.0	0.0	0.0	87.0	13.0	12.6	0.0
W10	1555.0	LHy	33	33	33	2.8	0	100	0	0.3	0	0	0	0.0	38	25	38	2.5	0	0	0	0.0	0	0	0	0.0	0.0	0.0	83.3	16.7	18.6	2.8
W10	1564.0	LHy	0	100	0	0.7	0	0	0	0.0	0	0	0	0.0	0	100	0	0.7	0	0	0	0.0	0	0	0	0.0	0.0	0.0	77.7	22.3	14.7	0.7
W10	1576.0	Cor	13	50	38	7.4	100	0	0	0.9	0	0	0	0.0	0	57	43	6.5	0	0	0	0.0	0	0	0	0.0	0.0	0.0	63.7	36.3	19.5	7.4
W10	1600.0	Cor	75	0	25	1.3	100	0	0	1.0	0	0	0	0.0	0	0	100	0.3	0	0	0	0.0	0	0	0	0.0	0.0	0.0	95.4	4.6	12.7	1.3
W10	1617.0	Cor	0	67	33	3.5	0	0	0	0.0	0	0	0	0.0	0	40	60	2.0	0	100	0	1.6	0	0	0	0.0	0.0	0.0	78.0	22.0	18.8	3.5
W10	1634.0	Cor	57	38	5	11.3	0	0	0	0.0	0	0	0	0.0	57	38	5	11.3	0	0	0	0.0	0	0	0	0.0	0.0	0.0	47.3	52.7	18.6	11.3
W10	1649.0	Cor	27	59	14	7.1	0	0	100	0.3	0	0	0	0.0	29	62	10	6.7	0	0	0	0.0	0	0	0	0.0	0.0	0.0	41.3	58.7	20.2	7.1
W10	1665.0	Cor	54	26	20	12.7	100	0	0	1.8	0	0	0	0.0	45	31	24	10.5	100	0	0	0.4	0	0	0	0.0	0.0	0.0	32.6	67.4	14.5	12.7
W10	1681.0	Cor	52	33	14	14.2	100	0	0	0.3	0	0	0	0.0	50	35	15	13.6	100	0	0	0.3	0	0	0	0.0	0.0	0.0	30.8	69.2	22.4	14.2
W10	1730.0	Cer	33	30	36	12.3	80	20	0	1.9	0	0	0	0.0	25	32	43	10.4	0	0	0	0.0	0	0	0	0.0	0.0	0.0	32.8	67.2	25.0	12.3
W10	1747.0	BN	70	25	5	28.1	100	0	0	0.4	0	0	0	0.0	70	25	5	27.7	0	0	0	0.0	0	0	0	0.0	0.0	0.0	32.5	67.5	19.3	28.1
W10	1780.0	BN	33	44	22	8.6	0	0	0	0.0	0	0	0	0.0	33	44	22	8.6	0	0	0	0.0	0	0	0	0.0	0.0	0.0	46.2	53.8	13.7	8.6
W10	1965.0	CyM & ME	33	37	30	9.5	67	33	0	0.9	0	0	0	0.0	30	37	33	8.5	0	0	0	0.0	0	100	0	0.3	0.0	0.0	21.1	78.5	9.1	9.5
W10	1954.0	CyM & ME	55	24	21	10.3	0	0	0	0.0	0	0	0	0.0	55	24	21	10.3	0	0	0	0.0	0	0	0	0.0	0.0	0.0	45.7	54.3	6.7	10.3
W10	2045.0	CyM & ME	26	30	43	7.7	0	0	0	0.0	0	0	0	0.0	26	30	43	7.7	0	0	0	0.0	0	0	0	0.0	0.0	0.0	41.8	58.2	10.8	7.7
W10	2110.0	CyM & ME	57	43	0	2.7	100	0	0	1.1	0	0	0	0.0	0	100	0	1.1	100	0	0	0.4	0	0	0	0.0	0.0	0.0	60.5	39.5	10.6	2.7
W10	2119.0	FS (RpC)	0	33	67	1.1	0	100	0	0.4	0	0	0	0.0	0	0	100	0.7	0	0	0	0.0	0	0	0	0.0	0.0	0.0	43.8	56.2	7.4	1.1
W10	2132.0	FS (RpC)	18	18	64	3.5	0	0	0	0.0	0	0	0	0.0	18	18	64	3.5	0	0	0	0.0	0	0	0	0.0	0.0	0.0	85.9	14.1	7.4	3.5
W10	2141.0	FS (RpC)	100	0	0	0.8	0	0	0	0.0	0	0	0	0.0	100	0	0	0.8	0	0	0	0.0	0	0	0	0.0	0.0	0.0	66.2	33.8	12.9	0.8
W10	2155.0	FM (RpC)	33	33	33	2.1	0	0	0	0.0	0	0	0	0.0	33	33	33	2.1	0	0	0	0.0	0	0	0	0.0	0.0	0.0	45.2	54.8	9.2	2.1
W10	2165.0	FM (RpC)	29	43	29	1.9	100	0	0	0.6	0	0	0	0.0	0	60	40	1.4	0	0	0	0.0	0	0	0	0.0	0.0	0.0	66.0	34.0	2.2	1.9
W10	2172.0	FM (RpC)	50	21	29	5.2	0	0	0	0.0	0	0	0	0.0	50	21	29	5.2	0	0	0	0.0	0	0	0	0.0	0.0	0.0	43.9	56.1	8.1	5.2
W10	2251.0	MPE	17	38	44	18.4	0	40	60	1.8	0	0	0	0.0	19	38	43	16.6	0	0	0	0.0	0	0	0	0.0	0.0	0.0	67.1	32.9	1.8	18.4
W10	2257.0	MPE	31	54	15	5.8	0	0	0	0.0	0	0	0	0.0	31	54	15	5.8	0	0	0	0.0	0	0	0	0.9	0.0	0.0	91.9	7.2	5.4	5.8
W10	2260.0	LPE	36	27	36	40.7	0	0	100	0.6	0	0	0	0.0	39	24	37	38.3	0	100	0	1.8	40	0	60	1.5	0.0	0.0	56.4	42.1	4.5	40.7
W10	2307.0	LPE	73	27	0	3.7	0	0	0	0.0	0	0	0	0.0	73	27	0	3.7	0	0	0	0.0	59	0	0	6.3	0.0	0.0	81.6	18.4	8.5	3.7
W10	2311.0	LPE	73	27	0	2.9	100	0	0	1.2	0	0	0	0.0	56	44	0	1.8	0	0	0	0.0	59	41	0	6.3	0.0	0.0	57.4	36.3	8.4	2.9
W10	2337.0	LPE	0	0	0	0.0	0	0	0	0.0	0	0	0	0.0	0	0	0	0.0	0	0	0	0.0	0	0	0	0.0	0.0	0.0	100.0	0.0	0.0	0.0
W10	2342.0	LPE	0	0	0	0.0	0	0	0	0.0	0	0	0	0.0	0	0	0	0.0	0	0	0	0.0	0	0	0	0.0	0.0	0.0	100.0	0.0	0.0	0.0
W10	2346.0	LPE	0	0	0	0.0	0	0	0	0.0	0	0	0	0.0	0	0	0	0.0	0	0	0	0.0	0	0	0	0.0	0.0	0.0	100.0	0.0	0.0	0.0
W10	2349.0	LPE	0	0	0	0.0	0	0	0	0.0	0	0	0	0.0	0	0	0	0.0	0	0	0	0.0	0	0	0	0.0	0.0	0.0	98.4	1.6	0.3	0.0
W10	2354.0	LPE	0	0	0	0.0	0	0	0	0.0	0	0	0	0.0	0	0	0	0.0	0	0	0	0.0	0	0	0	0.0	0.0	0.0	100.0	0.0	1.2	0.0
W10	2356.0	LPE	0	0	0	0.0	0	0	0	0.0	0	0	0	0.0	0	0	0	0.0	0	0	0	0.0	0	0	0	0.0	0.0	0.0	100.0	0.0	0.0	0.0
W10	2361.0	LPE	40	0	60	1.6	100	0	0	0.7	0	0	0	0.0	0	0	100	1.0	0	0	0	0.0	0	0	0	0.0	0.0	0.0	93.8	6.2	2.6	1.6

Well	TVD (m)	Stratigraphy	# of particels	Preservation of Phytoclasts			Phyclasts%/ total OM	Preservation of Inertinite			Inertinite %/ total OM	Preservation of Vitrinite			Vitrinite %/ total OM	Preservation of Cutinite			Cutinite %/ total OM	Preservation of Sporomorphs			Sporomorphs %/ total OM	Preservation of Spores			Spores %/ total OM	Preservation of Pollen			Pollen %/ total OM	terr. AOM %/ total OM	marine AOM %/ total OM	total AOM %/ total OM
				good (%/Phytoclasts)	moderate (%/Phytoclasts)	poor (%/Phytoclasts)		good (%/Inertinite)	moderate (%/Inertinite)	poor (%/Inertinite)		good (%/Vitrinite)	moderate (%/Vitrinite)	poor (%/Vitrinite)		good (%/Cutinite)	moderate (%/Cutinite)	poor (%/Cutinite)		good (%/Sporomorphs)	moderate(%/Sporomorphs)	poor (%/Sporomorphs)		good (%/Spores)	moderate (%/Spores)	poor (%/Spores)		good (%/Spores)	moderate (%/Spores)	poor (%/Spores)				
W12	676.2	UT l	345	42	37	21	31.6	40	60	0	5.8	43	31	26	25.8	0	0	0	0.0	50	48	2	35.7	62	38	0	7.5	46	3	28.1	2.9	29.9	32.8
W12	797.5	UHy	261	20	33	47	21.1	67	33	0	2.3	18	32	50	14.6	0	36	64	4.2	55	27	18	8.4	100	0	0	3.8	17	33	4.6	1.5	69.0	70.5
W12	875.2	UHy	322	15	27	58	16.1	67	33	0	1.9	10	31	59	12.1	0	0	100	2.2	64	32	4	30.1	74	26	0	15.5	53	38	9	14.6	4.0	49.7	53.7
W12	914.4	UHy	221	36	53	11	16.3	72	28	0	8.1	0	71	29	6.3	0	100	0	1.8	42	53	4	33.0	60	40	0	18.1	21	70	9	14.9	0.0	47.5	47.5
W12	1040.0	UHy	309	15	42	43	30.1	0	100	0	2.3	18	41	42	25.6	0	0	100	2.3	55	41	5	21.4	80	20	0	4.9	47	47	6	16.5	0.0	48.5	48.5
W12	1042.0	UHy	280	50	45	5	22.1	54	46	0	8.6	58	42	0	11.1	0	57	43	2.5	67	27	6	62.9	82	18	0	7.9	65	29	6	55.0	2.5	12.5	15.0
W12	1042.5	UHy	356	23	39	38	34.3	59	41	0	9.0	12	35	54	21.9	0	67	33	3.4	41	44	15	42.7	64	36	0	12.6	31	48	21	30.1	0.0	21.1	21.1
W12	1236.2	LHy	342	16	31	52	37.3	73	27	0	4.4	11	32	58	26.8	0	33	67	6.1	42	37	21	20.7	46	27	27	7.6	40	42	18	13.1	1.5	40.2	41.7
W12	1426.2	Cor	254	16	49	34	31.1	52	48	0	9.8	0	47	53	20.1	0	100	0	1.2	48	47	4	35.0	45	55	0	13.0	50	43	7	22.0	0.0	26.8	26.8
W12	1428.0	Cor	313	34	32	34	62.9	100	0	0	2.6	35	37	28	54.3	0	0	100	6.1	26	49	25	24.6	100	0	0	2.6	17	55	28	22.0	0.0	2.2	2.2
W12	1429.0	Cor	354	12	46	41	51.1	53	47	0	4.8	8	48	44	45.2	0	0	100	1.1	20	35	45	33.1	27	20	53	4.2	19	37	44	28.8	6.2	5.6	11.9
W12	1634.3	Cer	206	0	43	57	11.2	0	59	41	8.3	0	0	100	2.9	0	0	0	0.0	60	40	0	37.4	47	53	0	16.5	70	30	0	20.9	36.4	9.7	46.1
W12	1841.2	BN	242	24	45	30	84.7	52	48	0	39.7	0	43	57	45.0	0	0	0	0.0	0	0	100	2.9	0	0	0	0.0	0	0	100	2.9	8.3	4.1	12.4

Well	TVD (m)	Stratigraphy	Preservation of Phytoplancton		Phytoplancton %/ total OM	Preservation of Prasinophytes			Prasinophytes %/ total OM	Preservation of Acritarchs			Acritarchs %/ total OM	Preservation of Dinoflagellate cysts			Dinoflagellate cysts %/ total OM	Preservation of Leiospheres			Leiospheres %/ total OM	Preservation of Lacustrine Algae			Lacustrine Algae %/ total OM	Foraminifera %/ total OM	Fungi %/ total OM	Terr Comp. % / total OM	Marine Comp. % / total OM	terr. palynomorphs/ total OM	marine palynomorphs/ total OM
			good (%/Phytoplancton)	moderate (%/Phytoplancton)	poor (%/Phytoplancton)	good (%/Pras.)	moderate (%/Pras.)	poor (%/Pras.)		good (%/Acritarchs)	moderate (%/Acritarchs)	poor (%/Acritarchs)		good (%/Dino.)	moderate (%/Dino.)	poor (%/Dino.)		good (%/Leiospheres)	moderate (%/Leiospheres)	poor (%/Leiospheres)		good (%/Lac. Algae)	moderate (%/Lac. Algae)	poor (%/Lac. Algae)							
W12	676.2	UT l	0	0	0.0	0	0	0	0.0	0	0	0	0.0	0	0	0	0.0	0	0	0	0.0	0	0	0	0.0	0.0	0.0	70.1	29.9	35.7	0.0
W12	797.5	UHy	0	0	0.0	0	0	0	0.0	0	0	0	0.0	0	0	0	0.0	0	0	0	0.0	0	0	0	0.0	0.0	0.0	31.0	69.0	8.4	0.0
W12	875.2	UHy	0	0	0.0	0	0	0	0.0	0	0	0	0.0	0	0	0	0.0	0	0	0	0.0	0	0	0	0.0	0.0	0.0	50.3	49.7	30.1	0.0
W12	914.4	UHy	57	43	0	3.2	0	0	0.0	0	0	0	0.0	57	43	0	3.2	0	0	0	0.0	0	0	0	0.0	0.0	0.0	49.3	50.7	33.0	3.2
W12	1040.0	UHy	0	0	0	0.0	0	0	0.0	0	0	0	0.0	0	0	0	0.0	0	0	0	0.0	0	0	0	0.0	0.0	0.0	51.5	48.5	21.4	0.0
W12	1042.0	UHy	0	0	0	0.0	0	0	0.0	0	0	0	0.0	0	0	0	0.0	0	0	0	0.0	0	0	0	0.0	0.0	0.0	87.5	12.5	62.9	0.0
W12	1042.5	UHy	0	100	0	0	0	0	0.0	0	0	0	0.0	0	100	0	1.1	0	0	0	0.0	0	0	0	0.8	0.0	0.0	77.0	22.2	42.7	1.1
W12	1236.2	LHy	0	0	0	0	0	0	0.0	0	0	0	0.0	0	0	0	0.0	0	0	0	0.0	100	0	0	0.0	0.0	0.3	59.5	40.5	20.7	0.3
W12	1426.2	Cor	39	22	39	7.1	0	0	0.0	50	29	21	5.5	0	0	100	1.6	0	0	0	0.0	0	0	0	0.0	0.0	0.0	66.1	33.9	35.0	7.1
W12	1428.0	Cor	6	50	44	10.2	0	0	0.0	7	43	50	8.9	0	100	0	1.3	0	0	0	0.0	0	0	0	0.0	0.0	0.0	87.5	12.5	24.6	10.2
W12	1429.0	Cor	0	60	40	2.8	0	0	0.0	0	0	100	1.1	0	100	0	1.7	0	0	0	0.0	0	0	100	1.1	0.0	0.0	90.4	8.5	33.1	2.8
W12	1634.3	Cer	18	18	64	5.3	0	0	0.0	0	0	0	0.0	18	18	64	5.3	0	0	0	0.0	0	0	0	0.0	0.0	0.0	85.0	15.0	37.4	5.3
W12	1841.2	BN	0	0	0	0.0	0	0	0.0	0	0	0	0.0	0	0	0	0.0	0	0	0	0.0	0	0	0	0.0	0.0	0.0	95.9	4.1	2.9	0.0

Well	TVD (m)	Stratigraphy	# of particels	Preservation of Phytoclasts			Phyclasts%/ total OM	Preservation of Inertinite			Inertinite %/ total OM	Preservation of Vitrinite			Vitrinite %/ total OM	Preservation of Cutinite			Cutinite %/ total OM	Preservation of Sporomorphs			Sporomorphs %/ total OM	Preservation of Spores			Spores %/ total OM	Preservation of Pollen			Pollen %/ total OM	terr. AOM %/ total OM	marine AOM %/ total OM	total AOM %/ total OM
				good (%/Phytoclasts)	moderate (%/Phytoclasts)	poor (%/Phytoclasts)		good (%/Intertinite)	moderate (%/Interlinite)	poor (%/Interlinite)		good (%/Vitrinite)	moderate (%/Vitrinite)	poor (%/Vitrinite)		good (%/Cutinite)	moderate (%/Cutinite)	poor (%/Cutinite)		good (%/Sporomorphs)	moderate(%/Sporomorphs)	poor (%/Sporomorphs)		good (%/Spores)	moderate (%/Spores)	poor (%/Spores)		good (%/Spores)	moderate (%/Spores)	poor (%/Spores)				
W13	1801.0	PE	250	52	27	21	96.0	70	30	0	46.0	36	24	40	50.0	0	0	0	0.0	0	0	100	1.2	0	0	100	1.2	0	0	0	0.0	0.0	0.0
W13	1831.0	PE	210	3	15	82	71.4	0	0	0	0.0	3	15	82	71.4	0	0	0	0.0	31	38	31	20.0	59	18	23	10.5	0	60	40	9.5	0.0	0.0	0.0
W13	1851.0	PE	214	20	14	66	87.9	69	31	0	6.1	16	13	71	81.8	0	0	0	0.0	0	50	50	9.3	0	73	27	5.1	0	22	78	4.2	0.0	0.0	0.0
W13	1861.0	PE	245	32	35	33	33.5	58	42	0	15.5	9	30	61	18.0	0	0	0	0.0	5	28	67	15.9	6	26	68	13.9	0	40	60	2.0	38.8	6.1	44.9
W13	1862.5	PE	302	1	36	63	91.4	0	0	100	3.0	1	20	78	69.9	0	0	100	18.5	23	77	0	8.6	27	73	0	5.0	18	82	0	3.6	0.0	0.0	0.0

Well	TVD (m)	Stratigraphy	Preservation of Phytoplancton		Phytoplancton %/ total OM	Preservation of Prasinophytes			Prasinophytes %/ total OM	Preservation of Acritarchs			Acritarchs %/ total OM	Preservation of Dinoflagellate cysts			Dinoflagellate cysts %/ total OM	Preservation of Leiospheres			Leiospheres %/ total OM	Preservation of Lacustrine Algae			Lacustrine Algae %/ total OM	Foraminifera %/ total OM	Fungi %/ total OM	Terr Comp. % / total OM	Marine Comp. % / total OM	terr. palynomorphs/ total OM	marine palynomorphs/ total OM
			good (%/Phytoplancton)	moderate (%/Phytoplancton)	poor (%/Phytoplancton)	good (%/Pras.)	moderate (%/Pras.)	poor (%/Pras.)		good (%/Acritarchs)	moderate (%/Acritarchs)	poor (%/Acritarchs)		good (%/Dino.)	moderate (%/Dino.)	poor (%/Dino.)		good (%/Leiospheres)	moderate (%/Leiospheres)	poor (%/Leiospheres)		good (%/Lac. Algae)	moderate (%/Lac. Algae)	poor (%/Lac. Algae)							
W13	1801.0	PE	0	0	100	2.8	0	0	0	0	0	0	0.0	0	0	100	2.8	0	0	0	0.0	0	0	0	0.0	0.0	0.0	97.2	2.8	1.2	2.8
W13	1831.0	PE	72	22	6	8.6	0	0	0	0	0	0	0.0	72	22	6	8.6	0	0	0	0.0	0	0	0	0.0	0.0	0.0	91.4	8.6	20.0	8.6
W13	1851.0	PE	0	0	100	2.8	0	0	0	0	0	0	0.0	0	0	100	2.8	0	0	0	0.0	0	0	0	0.0	0.0	0.0	97.2	2.8	9.3	2.8
W13	1861.0	PE	0	0	100	5.7	0	0	0	0	0	0	3.3	0	0	100	2.4	0	0	0	0.0	0	0	0	0.0	0.0	0.0	88.2	11.8	15.9	5.7
W13	1862.5	PE	0	0	0	0.0	0	0	0	0	0	0	0.0	0	0	0	0.0	0	0	0	0.0	0	0	0	0.0	0.0	0.0	100.0	0.0	8.6	0.0

Well	TVD (m)	Stratigraphy	# of particels	Preservation of Phytoclasts			Phyclasts%/ total OM	Preservation of Inertinite			Inertinite %/ total OM	Preservation of Vitrinite			Vitrinite %/ total OM	Preservation of Cutinite			Cutinite %/ total OM	Preservation of Sporomorphs			Sporomorphs %/ total OM	Preservation of Spores			Spores %/ total OM	Preservation of Pollen			Pollen %/ total OM	terr. AOM %/ total OM	marine AOM %/ total OM	total AOM %/ total OM
				good (%/Phytoclasts)	moderate (%/Phytoclasts)	poor (%/Phytoclasts)		good (%/Inertinite)	moderate (%/Inertinite)	poor (%/Inertinite)		good (%/Vitrinite)	moderate (%/Vitrinite)	poor (%/Vitrinite)		good (%/Cutinite)	moderate (%/Cutinite)	poor (%/Cutinite)		good (%/Sporomorphs)	moderate(%/Sporomorphs)	poor (%/Sporomorphs)		good (%/Spores)	moderate (%/Spores)	poor (%/Spores)		good (%/Spores)	moderate (%/Spores)	poor (%/Spores)				
W14	657.5	UT I	342	28	44	28	62.8	52	48	0	22.4	17	39	44	29.9	8	50	42	10.5	16	34	50	11.0	46	0	54	3.8	0	52	48	7.3	7.6	0.0	7.6
W14	738.4	UHy	257	63	37	0	13.6	100	0	0	3.1	52	48	0	10.5	0	0	0	0.0	86	14	0	35.8	90	10	0	16.0	82	18	0	19.8	0.0	50.6	50.6
W14	805.0	UHy	203	38	50	13	15.8	60	40	0	7.4	18	59	24	8.4	0	0	0	0.0	72	28	0	49.8	75	25	0	26.1	69	31	0	23.6	0.0	34.5	34.5
W14	855	UHy	292	0	85	15	6.8	0	100	0	4.5	0	100	0	1.4	0	0	100	1.0	42	37	21	21.2	72	28	0	12.3	0	50	50	8.9	0.0	71.9	71.9
W14	910	UHy	223	63	21	16	8.5	100	0	0	4.0	30	40	30	4.5	0	0	0	0.0	83	17	0	18.8	90	10	0	13.0	69	31	0	5.8	0.0	55.6	55.6
W14	962.9	UHy	286	20	53	27	22.3	29	71	0	10.8	19	38	43	7.3	0	33	67	4.2	68	32	0	18.5	88	12	0	9.1	48	52	0	9.4	3.5	45.3	48.8
W14	1016	UHy	202	10	38	52	28.7	40	60	0	2.5	9	42	49	22.3	0	0	100	4.0	60	34	6	71.3	69	31	0	43.1	47	39	14	28.2	0.0	0.0	0.0
W14	1022.7	UHy	301	34	47	19	42.2	86	14	0	4.7	23	46	30	18.6	32	56	12	18.9	55	41	4	34.9	71	29	0	12.6	46	48	6	22.3	4.3	15.0	19.3
W14	1070	UHy	307	13	48	39	18.1	33	67	0	2.9	10	45	45	12.9	0	43	57	2.3	31	37	31	17.5	89	11	0	6.1	0	51	49	11.3	1.6	55.0	56.6
W14	1124	UHy	325	46	43	11	11.4	82	18	0	5.2	15	65	20	6.2	0	0	0	0.0	32	59	9	27.1	39	61	0	10.2	27	58	15	16.9	0.0	61.5	61.5
W14	1163	UHy	257	48	37	15	10.5	80	20	0	1.9	41	41	18	8.6	0	0	0	0.0	79	21	0	20.6	86	14	0	11.3	71	29	0	9.3	0.0	66.1	66.1
W14	1164	UHy	323	8	37	55	11.8	60	40	0	1.5	0	36	64	10.2	0	0	0	0.0	74	23	3	35.0	83	17	0	18.6	64	30	6	16.4	5.6	40.2	45.8
W14	1165	UHy	197	19	43	38	10.7	25	75	0	4.1	15	23	62	6.6	0	0	0	0.0	20	29	51	40.1	42	32	26	19.3	0	27	73	20.8	30.5	12.7	43.1
W14	1167.8	UHy	241	0	46	54	11.6	0	0	0	0.0	0	40	60	10.4	0	100	0	1.2	45	40	15	56.4	51	44	5	17.0	42	39	19	39.4	6.2	24.9	31.1
W14	1188.9	UHy	335	29	52	19	43.0	85	15	0	3.9	34	43	22	22.7	9	73	18	16.4	44	40	16	20.9	74	26	0	6.9	30	47	23	14.0	3.6	31.3	34.9
W14	1189	UHy	309	18	31	51	15.9	29	71	0	5.5	16	12	72	8.1	0	0	100	2.3	22	48	30	23.6	50	50	0	4.5	15	47	37	19.1	3.2	55.0	58.3
W14	1189.9	UHy	301	12	57	31	16.3	18	82	0	3.7	11	53	36	12.0	0	0	100	0.7	74	18	9	11.3	93	7	0	9.0	0	57	43	2.3	3.3	63.1	66.4
W14	1193	UHy	410	4	45	51	20.0	0	0	0	0.0	6	43	51	12.9	0	48	52	7.1	44	37	18	28.0	91	9	0	5.6	33	45	23	22.4	2.4	24.4	26.8
W14	1199.3	UHy	328	27	33	40	15.8	54	46	0	3.9	23	30	47	9.1	0	22	78	2.7	59	37	4	22.7	73	27	0	4.5	55	40	5	18.2	0.0	51.5	51.5
W14	1265	LHy	356	16	44	40	29.5	18	82	0	6.2	18	38	45	20.8	0	0	100	2.5	44	34	23	17.4	83	17	0	5.1	27	41	32	12.4	4.2	47.8	52.0
W14	1271.6	LHy	346	28	43	30	27.2	75	25	0	4.6	23	54	23	17.6	0	18	82	4.9	41	35	24	44.2	77	23	0	11.3	28	39	32	32.9	17.3	4.3	21.7
W14	1289.6	LHy	381	29	33	37	26.8	62	38	0	5.5	21	32	47	21.3	0	0	0	0.0	29	36	36	7.3	33	67	0	2.4	26	21	53	5.0	1.8	4.7	6.6
W14	1300	LHy	384	16	44	40	32.3	70	30	0	2.6	15	43	43	23.2	0	52	48	6.5	21	56	23	20.1	46	54	0	6.8	8	57	35	13.3	1.3	2.3	3.6
W14	1312.9	LHy	326	29	41	30	52.5	69	31	0	4.0	37	42	21	33.7	0	42	58	14.7	24	43	33	27.0	47	53	0	11.7	6	36	58	15.3	1.5	12.3	13.8
W14	1347.8	LHy	391	11	49	40	57.5	44	56	0	4.1	12	51	37	36.6	0	42	58	16.9	26	40	33	25.3	67	13	21	6.1	13	49	37	19.2	0.0	8.2	8.2
W14	1351	LHy	349	14	51	35	63.9	67	33	0	3.4	16	52	32	42.7	0	52	48	17.8	41	40	19	34.4	66	28	7	17.5	15	53	32	16.9	0.0	1.1	1.1
W14	1384.5	LHy	377	2	54	45	33.2	33	67	0	1.6	0	51	49	20.7	0	56	44	10.9	31	32	37	35.0	61	39	0	9.5	20	29	51	25.5	5.3	22.0	27.3
W14	1418.8	LHy	329	23	37	40	39.5	64	36	0	3.3	26	40	33	26.4	0	28	72	9.7	35	48	18	25.5	66	34	0	9.7	15	56	29	15.8	15.2	18.2	33.4
W14	1446.5	Cor	326	13	45	43	28.7	0	0	0	0.0	17	46	38	22.0	0	41	59	6.7	48	43	9	22.9	58	32	10	9.5	41	50	9	13.5	33.6	9.2	42.8
W14	1448	Cor	368	20	26	54	27.7	69	31	0	3.5	15	32	52	19.3	0	0	100	4.9	53	39	8	39.1	81	19	0	14.4	37	51	12	24.7	1.4	21.7	23.1
W14	1449	Cor	332	42	40	18	31.0	65	35	0	15.7	22	56	22	12.3	0	0	100	3.0	41	49	9	45.8	68	32	0	7.5	36	53	11	38.3	6.0	12.0	18.1
W14	1483.8	Cor	241	0	0	100	18.7	0	0	100	18.7	0	0	0	0.0	0	0	0	0.0	0	0	0	0.0	0	0	0	0.0	0	0	0	0.0	76.8	2.9	79.7
W14	1523.1	Cor	420	14	51	34	33.3	14	86	0	3.3	17	45	38	24.8	0	59	41	5.2	68	30	2	61.9	72	28	0	11.9	67	31	2	50.0	1.0	1.7	2.6
W14	1526	Cor	371	0	51	49	52.7	0	100	0	2.2	0	51	49	38.2	0	39	61	12.4	45	48	7	29.6	85	15	0	7.0	32	58	10	22.6	7.8	4.0	11.8
W14	1566.4	Cor	247	19	60	21	17.4	100	0	0	2.4	8	56	36	10.1	0	100	0	4.9	82	18	0	59.9	79	21	0	13.4	83	17	0	46.6	0.0	11.7	11.7
W14	1567	Cor	277	37	24	39	27.4	68	32	0	9.0	22	20	59	18.4	0	0	0	0.0	5	57	38	33.2	10	69	22	18.4	0	41	59	14.8	21.7	12.6	34.3
W14	1569	Cor	287	23	44	33	39.7	58	42	0	10.8	10	45	46	28.9	0	0	0	0.0	0	44	56	24.4	0	49	51	13.6	0	39	61	10.8	31.4	3.5	34.8
W14	1571	Cor	347	0	58	42	9.5	0	0	0	0.0	0	58	42	9.5	0	0	0	0.0	56	32	12	50.1	60	40	0	21.6	53	26	21	28.5	8.6	10.1	18.7
W14	1591.3	Cor	347	10	52	38	32.6	24	76	0	4.9	10	46	43	19.9	0	52	48	7.8	0	48	52	51.6	0	50	50	30.0	0	45	55	21.6	14.4	0.0	14.4
W14	1631.8	Cer	263	6	50	44	48.3	64	36	0	4.2	0	48	52	29.3	0	59	41	14.8	19	57	24	27.4	33	52	15	10.3	11	60	29	17.1	3.8	15.6	19.4
W14	1637.6	Cer	323	9	41	50	22.9	0	100	0	5.6	18	21	61	11.8	0	22	78	5.6	18	23	59	22.6	39	17	43	7.1	8	26	66	15.5	1.5	40.2	41.8
W14	1672	Cer	314	50	37	13	29.3	65	35	0	6.4	49	34	18	21.7	0	100	0	1.3	22	40	38	39.8	0	50	50	4.5	24	39	37	35.4	0.0	27.1	27.1
W14	1704.5	Cer	251	16	32	52	24.7	60	40	0	2.0	13	34	53	21.1	0	0	100	1.6	61	34	5	56.6	80	20	0	15.9	54	39	7	40.6	8.0	3.2	11.2
W14	1749	Cer	320	16	57	27	31.3	19	81	0	13.4	26	45	29	9.7	0	31	69	8.1	17	35	48	32.8	0	0	0	0.0	17	35	48	32.8	26.6	9.4	35.9
W14	1754.9	Cer	278	80	20	0	5.4	57	43	0	2.5	100	0	0	2.9	0	0	0	0.0	20	36	44	39.9	17	30	52	8.3	20	38	42	31.7	5.4	34.2	39.6
W14	1780.0	Cer	265	18	50	32	18.9	0	100	0	1.1	25	36	39	13.6	0	82	18	4.2	39	44	17	39.6	33	67	0	4.5	40	41	19	35.1	0.0	11.3	11.3
W14	1808.6	Cer	225	40	60	0	11.1	67	33	0	6.7	0	100	0	4.4	0	0	0	0.0	0	0	100	8.9	0	0	0	0.0	0	0	100	8.9	13.3	66.7	80.0
W14	1851	BN	225	14	71	14	15.6	50	50	0	4.4	0	80	20	11.1	0	0	0	0.0	0	0	0	0.0	0	0	0	0.0	0	0	0	0.0	80.0	4.4	84.4
W14	1922.2	BN	270	50	42	8	88.9	60	40	0	74.1	0	50	50	14.8	0	0	0	0.0	0	0	0	0.0	0	0	0	0.0	0	0	0	0.0	3.7	7.4	11.1
W14	1945.8	BN	328	23	42	34	84.1	80	20	0	3.0	31	43	26	54.6	0	44	56	26.5	12	39	49	14.9	25	38	38	4.9	6	39	55	10.1	0.0	0.0	0.0
W14	2019	CyM & ME	335	36	36	29	83.6	77	23	0	38.8	0	50	50	29.9	0	40	60	14.9	50	37	13	11.3	0	100	0	0.9	54	31	14	10.4	0.0	3.9	3.9
W14	2064.3	CyM & ME	372	8	59	33	56.7	27	53	20	8.1	9	48	43	26.9	0	75	25	21.8	38	44	18	24.2	44	40	15	14.0	29	50	21	10.2	12.1	0.0	12.1
W14	2104.2	CyM & ME	309	48	36	16	86.4	55	45	0	21.7	51	31	19	58.3	0	60	40	6.5	63	25	13	12.9	89	11	0	6.1	38	38	24	6.8	0.0	0.0	0.0
W14	2152.9	RpC	277	18	42	40	55.2	73	27	0	4.0	17	30	53	41.5	0	100	0	9.7	0	77	23	23.1	0	100	0	6.9	0	67	33	16.2	3.2	2.5	5.8
W14	2154	RpC	208	25	49	25	30.3	52	38	10	10.1	14	66	20	16.8	0	0	100	3.4	0	38	63	15.4	0	53	47	8.2	0	20	80	7.2	50.5	0.0	50.5
W14	2196.6	PE	198	50	24	26	23.2	100	0	0	7.1	45	55	0	10.1	0	0	100	6.1	59	28	13	16.2	68	32	0	14.1	0	0	100	2.0	60.6	0.0	60.6
W14	2197	PE	302	25	44	31	21.2	100	0	0	2.6	14	50	36	18.5	0	0	0	0.0	31	24	45	31.5	24	17	59	19.5	42	36	22	11.9	43.0	0.0	43.0

Well	TVD (m)	Stratigraphy		Preservation of Phytoplancton			Phytoplancton %/ total OM	Preservation of Prasinophytes			Prasinophytes %/ total OM	Preservation of Acritarchs			Acritarchs %/ total OM	Preservation of Dinoflagellate cysts			Dinoflagellate cysts %/ total OM	Preservation of Leiospheres			Leiospheres %/ total OM	Preservation of Lacustrine Algae			Lacustrine Algae %/ total OM	Foraminifera %/ total OM	Fungi %/ total OM	Terr Comp. % / total OM	Marine Comp. % / total OM	terr. palynomorphs/ total OM	marine palynomorphs/ total OM
				good (%/Phytoplancton)	moderate (%/Phytoplancton)	poor (%/Phytoplancton)		good (%/Pras.)	moderate (%/Pras.)	poor (%/Pras.)		good (%/Acritarchs)	moderate (%/Acritarchs)	poor (%/Acritarchs)		good (%/Dino.)	moderate (%/Dino.)	poor (%/Dino.)		good (%/Leiospheres)	moderate (%/Leiospheres)	poor (%/Leiospheres)		good (%/Lac. Algae)	moderate (%/Lac. Algae)	poor (%/Lac. Algae)							
W14	657.5	UT I		0	0	100	0.6	0	0	0	0.0	0	0	0	0.0	0	0	0	0.0	0	0	100	0.6	33	67	0	17.4	0.0	0.6	81.4	1.2	11.0	1.2
W14	738.4	UHy		0	0	0	0.0	0	0	0	0.0	0	0	0	0.0	0	0	0	0.0	0	0	0	0.0	0	0	0	0.0	0.0	0.0	49.4	50.6	35.8	0.0
W14	805.0	UHy		0	0	0	0.0	0	0	0	0.0	0	0	0	0.0	0	0	0	0.0	0	0	0	0.0	0	0	0	0.0	0.0	0.0	65.5	34.5	49.8	0.0
W14	855	UHy		0	0	0	0.0	0	0	0	0.0	0	0	0	0.0	0	0	0	0.0	0	0	0	0.0	0	0	0	0.0	0.0	0.0	28.1	71.9	21.2	0.0
W14	910	UHy		50	39	11	17.0	0	0	0	0.0	0	0	0	0.0	53	36	11	16.1	0	100	0	0.9	0	0	100	0.7	0.0	0.3	27.4	72.6	18.8	17.0
W14	962.9	UHy		30	26	44	9.4	0	0	0	0.0	0	0	0	0.0	30	26	44	9.4	0	0	0	0.0	0	0	0	0.0	0.0	0.3	44.3	55.1	18.5	9.8
W14	1016	UHy		0	0	0	0.0	0	0	0	0.0	0	0	0	0.0	0	0	0	0.0	0	0	0	0.0	0	0	0	0.0	0.0	0.0	100.0	0.0	71.3	0.0
W14	1022.7	UHy		100	0	0	2.3	0	0	0	0.0	0	0	0	0.0	0	0	0	0.0	100	0	0	2.3	100	0	0	1.3	0.0	0.0	81.4	17.3	34.9	2.3
W14	1070	UHy		0	55	45	7.1	0	0	0	0.0	0	0	100	0.6	0	60	40	6.5	0	0	0	0.0	0	0	0	0.0	0.0	0.6	37.2	62.8	17.5	7.8
W14	1124	UHy		0	0	0	0.0	0	0	0	0.0	0	0	0	0.0	0	43	57	2.7	0	0	0	0.0	0	0	0	0.0	0.0	0.0	38.5	61.5	27.1	0.0
W14	1163	UHy		0	43	57	2.7	0	0	0	0.0	0	0	0	0.0	0	43	57	2.7	0	0	0	0.0	0	100	0	0.0	0.0	0.0	31.1	68.9	20.6	2.7
W14	1164	UHy		0	79	21	7.4	0	0	0	0.0	0	0	0	0.0	0	79	21	7.4	0	0	0	0.0	0	0	0	0.0	0.0	0.0	52.3	47.7	35.0	7.4
W14	1165	UHy		0	0	100	3.0	0	0	0	0.0	0	0	0	0.0	0	0	100	3.0	0	0	0	0.0	100	0	0	3.0	0.0	0.0	81.2	15.7	40.1	3.0
W14	1167.8	UHy		0	0	100	0.8	0	0	0	0.0	0	0	0	0.0	0	0	100	0.8	0	0	0	0.0	0	0	0	0.0	0.0	0.0	74.3	25.7	56.4	0.8
W14	1188.9	UHy		0	0	100	1.2	0	0	0	0.0	0	0	100	1.2	0	0	0	0.0	0	0	0	0.0	0	0	0	0.0	0.0	0.0	67.5	32.5	20.9	1.2
W14	1189	UHy		0	57	43	2.3	0	0	0	0.0	0	0	0	0.0	0	57	43	2.3	0	0	0	0.0	0	0	0	0.0	0.0	0.0	42.7	57.3	23.6	2.3
W14	1189.9	UHy		0	25	75	5.3	0	0	0	0.0	0	0	100	1.0	0	0	100	3.0	0	100	0	1.3	0	100	0	0.7	0.0	0.0	30.9	68.4	11.3	5.3
W14	1193	UHy		31	43	26	25.1	0	100	0	0.7	0	0	100	1.0	43	43	24	23.4	0	0	0	0.0	0	0	0	0.0	0.0	0.0	50.5	49.5	28.0	25.1
W14	1199.3	UHy		61	16	23	9.4	0	100	0	0.6	0	0	100	0.9	0	0	100	1.2	86	14	0	6.7	0	0	0	0.0	0.0	0.6	38.5	61.5	22.7	10.0
W14	1265	LHy		0	0	100	1.1	0	0	0	0.0	0	0	0	0.0	0	0	100	1.1	0	0	0	0.0	0	0	0	0.0	0.0	0.0	51.1	48.9	17.4	1.1
W14	1271.6	LHy		33	21	46	6.9	0	0	0	0.0	0	0	100	1.2	44	17	39	5.2	0	100	0	0.6	0	0	0	0.0	0.0	0.0	88.7	11.3	44.2	6.9
W14	1289.6	LHy		20	45	35	59.3	0	0	0	0.0	0	0	100	6.0	22	50	28	53.3	0	0	0	0.0	0	0	0	0.0	0.0	0.0	36.0	64.0	7.3	59.3
W14	1300	LHy		15	49	36	43.2	0	0	0	0.0	0	36	64	2.9	14	51	35	39.6	100	0	0	0.8	0	100	0	0.8	0.0	0.0	53.6	45.6	20.1	43.2
W14	1312.9	LHy		47	16	37	5.8	0	0	0	0.0	0	0	100	0.9	0	0	100	1.2	75	25	0	3.7	0	100	0	0.9	0.0	0.0	81.0	18.1	27.0	5.8
W14	1347.8	LHy		40	29	31	9.0	40	60	0	1.3	0	0	100	0.8	44	26	30	6.9	0	0	0	0.0	0	0	0	0.0	0.0	0.0	82.9	17.1	25.3	9.0
W14	1351	LHy		0	100	0	0.6	0	0	0	0.0	0	0	0	0.0	0	0	0	0.0	0	100	0	0.6	0	0	0	0.0	0.0	0.0	98.3	1.7	34.4	0.6
W14	1384.5	LHy		41	24	35	4.5	0	0	0	0.0	0	0	100	0.8	50	29	21	3.7	0	0	0	0.0	0	0	0	0.0	0.0	0.0	73.5	26.5	35.0	4.5
W14	1418.8	LHy		0	60	40	1.5	0	0	0	0.0	0	0	100	0.6	0	0	100	0.6	0	100	0	0.9	0	0	0	0.0	0.0	0.0	80.2	19.8	25.5	1.5
W14	1446.5	Cor		24	0	76	5.2	0	0	0	0.0	0	0	100	2.8	50	0	50	2.4	0	0	0	0.0	0	0	0	0.0	0.0	0.3	85.3	14.7	22.9	5.5
W14	1448	Cor		62	11	27	10.1	0	0	0	0.0	0	0	100	2.2	79	14	7	7.9	0	0	0	0.0	0	0	0	0.0	0.0	0.0	68.2	31.8	39.1	10.1
W14	1449	Cor		80	20	0	4.5	0	0	0	0.0	0	0	0	0.0	20	0	0	4.5	0	0	0	0.0	100	0	0	0.6	0.0	0.0	82.8	16.6	45.8	4.5
W14	1483.8	Cor		0	0	100	1.7	0	0	0	0.0	0	0	100	0.4	0	0	100	1.2	0	0	0	0.0	0	0	0	0.0	0.0	0.0	95.4	4.6	0.0	1.7
W14	1523.1	Cor		0	0	100	1.7	0	0	0	0.0	0	0	100	1.0	0	0	100	0.7	0	0	0	0.0	100	0	0	0.5	0.0	0.0	96.2	3.3	61.9	1.7
W14	1526	Cor		50	33	17	4.8	0	0	0	0.0	0	0	100	0.8	54	46	0	3.5	100	0	0	0.5	100	0	0	0.8	0.0	0.3	90.1	9.1	29.6	5.1
W14	1566.4	Cor		19	15	67	10.9	0	0	0	0.0	0	0	0	0.0	19	15	67	10.9	0	0	0	0.0	0	0	0	0.0	0.0	0.0	77.3	22.7	59.9	10.9
W14	1567	Cor		0	50	50	5.1	0	0	0	0.0	0	0	0	0.0	0	50	50	5.1	0	0	0	0.0	0	0	0	0.0	0.0	0.0	82.3	17.7	33.2	5.1
W14	1569	Cor		0	0	100	1.0	0	0	0	0.0	0	0	0	0.0	0	0	100	1.0	0	0	0	0.0	0	0	0	0.0	0.0	0.0	95.5	4.5	24.4	1.0
W14	1571	Cor		0	44	56	21.6	0	0	0	0.0	0	50	50	6.9	0	32	68	11.0	0	69	31	3.7	0	0	0	0.0	0.0	0.0	68.3	31.7	50.1	21.6
W14	1591.3	Cor		0	0	100	1.4	0	0	0	0.0	0	0	0	0.0	0	0	100	0.6	0	0	100	0.9	0	0	0	0.0	0.0	0.0	98.6	1.4	51.6	1.4
W14	1631.8	Cer		0	31	69	4.9	0	0	0	0.0	0	0	100	1.1	0	57	43	2.7	0	0	100	1.1	0	0	0	0.0	0.0	0.0	79.5	20.5	27.4	4.9
W14	1637.6	Cer		17	39	44	12.7	0	0	0	0.0	0	0	100	1.2	19	43	38	11.5	0	0	0	0.0	0	0	0	0.0	0.0	0.0	47.1	52.9	22.6	12.7
W14	1672	Cer		0	0	0	0.0	0	0	0	0.0	0	0	0	0.0	0	0	0	0.0	0	0	0	0.0	0	0	0	3.8	0.0	0.0	69.1	27.1	39.8	0.0
W14	1704.5	Cer		0	25	75	4.8	0	0	0	0.0	0	0	100	3.6	0	0	0	0.0	0	100	0	1.2	100	0	0	2.8	0.0	0.0	89.2	8.0	56.6	4.8
W14	1749	Cer		0	0	0	0.0	0	0	0	0.0	0	0	0	0.0	0	0	0	0.0	0	0	0	0.0	0	0	0	0.0	0.0	0.0	90.6	9.4	32.8	0.0
W14	1754.9	Cer		0	33	67	2.2	0	0	0	0.0	0	0	100	1.4	0	0	0	0.0	0	100	0	0.7	0	22	78	12.9	0.0	0.0	50.7	36.3	39.9	2.2
W14	1780.0	Cer		0	13	88	30.2	0	0	0	0.0	0	15	85	24.5	0	0	100	5.7	0	0	0	0.0	0	0	0	0.0	0.0	0.0	58.5	41.5	39.6	30.2
W14	1808.6	Cer		0	0	0	0.0	0	0	0	0.0	0	0	0	0.0	0	0	0	0.0	0	0	0	0.0	0	0	0	0.0	0.0	0.0	33.3	66.7	8.9	0.0
W14	1851	BN		0	0	0	0.0	0	0	0	0.0	0	0	0	0.0	0	0	0	0.0	0	0	0	0.0	0	100	0	0.0	0.0	0.0	95.6	4.4	0.0	0.0
W14	1922.2	BN		0	0	0	0.0	0	0	0	0.0	0	0	0	0.0	0	0	0	0.0	0	0	0	0.0	0	0	0	0.0	0.0	0.0	92.6	7.4	0.0	0.0
W14	1945.8	BN		0	0	100	0.9	0	0	0	0.0	0	0	100	0.9	0	0	0	0.0	0	0	0	0.0	0	0	0	0.0	0.0	0.0	99.1	0.9	14.9	0.9
W14	2019	CyM & ME		0	0	100	1.2	0	0	0	0.0	0	0	100	1.2	0	0	0	0.0	0	0	0	0.0	0	0	0	0.0	0.0	0.0	94.9	5.1	11.3	1.2
W14	2064.3	CyM & ME		27	42	31	7.0	0	0	0	0.0	64	36	0	3.0	0	0	47	4.0	0	0	0	0.0	0	0	0	0.0	0.0	0.0	93.0	7.0	24.2	7.0
W14	2104.2	CyM & ME		0	0	100	0.6	0	0	0	0.0	0	0	100	0.6	0	0	0	0.0	0	0	0	0.0	0	0	0	0.0	0.0	0.0	99.4	0.6	12.9	0.6
W14	2152.9	RpC		16	32	52	15.9	0	0	0	0.0	43	57	0	2.5	20	31	49	12.6	0	0	100	0.7	0	0	0	0.0	0.0	0.0	81.6	18.4	23.1	15.9
W14	2154	RpC		0	0	100	3.8	0	0	0	0.0	0	0	0	0.0	0	0	100	3.8	0	0	0	0.0	0	0	0	0.0	0.0	0.0	96.2	3.8	15.4	3.8
W14	2196.6	PE		0	0	0	0.0	0	0	0	0.0	0	0	0	0.0	0	0	0	0.0	0	0	0	0.0	0	0	0	0.0	0.0	0.0	100.0	0.0	16.2	0.0
W14	2197	PE		31	0	69	4.3	100	0	0	1.3	0	0	100	2.3	0	0	100	0.7	0	0	0	0.0	0	0	0	0.0	0.0	0.0	95.7	4.3	31.5	4.3

Well	TVD (m)	Stratigraphy	# of particels	Preservation of Phytoclasts			Phyclasts%/ total OM	Preservation of Inertinite			Inertinite %/ total OM	Preservation of Vitrinite			Vitrinite %/ total OM	Preservation of Cutinite			Cutinite %/ total OM	Preservation of Sporomorphs			Sporomorphs %/ total OM	Preservation of Spores			Spores %/ total OM	Preservation of Pollen			Pollen %/ total OM	terr. AOM %/ total OM	marine AOM %/ total OM	total AOM %/ total OM
				good (%/Phytoclasts)	moderate (%/Phytoclasts)	poor (%/Phytoclasts)		good (%/Intertinite)	moderate (%/Interlinite)	poor (%/Interlinite)		good (%/Vitrinite)	moderate (%/Vitrinite)	poor (%/Vitrinite)		good (%/Cutinite)	moderate (%/Cutinite)	poor (%/Cutinite)		good (%/Sporomorphs)	moderate(%/Sporomorphs)	poor (%/Sporomorphs)		good (%/Spores)	moderate (%/Spores)	poor (%/Spores)		good (%/Spores)	moderate (%/Spores)	poor (%/Spores)				
W15	1997.1	MPE	238	47	53	0	46.6	58	42	0	26.9	41	59	0	15.5	0	100	0	4.2	22	58	20	38.2	43	50	8	16.8	6	65	29	21.4	5.0	0.0	5.0
W15	1998.4	MPE	220	50	50	0	100.0	65	35	0	77.3	0	100	0	22.7	0	0	0	0.0	0	0	0	0.0	0	0	0	0.0	0	0	0	0.0	0.0	0.0	0.0
W15	2044.6	LPE	246	21	57	22	69.5	65	35	0	22.4	0	61	39	39.8	0	100	0	7.3	0	0	0	0.0	0	0	0	0.0	0	0	0	0.0	18.3	12.2	30.5
W15	2044.9	LPE	230	45	55	0	87.0	60	40	0	65.2	0	100	0	8.7	0	100	0	13.0	0	0	0	0.0	0	0	0	0.0	0	0	0	0.0	13.0	0.0	13.0
W15	2046.2	LPE	225	22	42	36	80.0	71	29	0	24.4	0	40	60	33.3	0	60	40	22.2	0	0	0	0.0	0	0	0	0.0	0	0	0	0.0	8.9	11.1	20.0

Well	TVD (m)	Stratigraphy	Phytoplancton %/ total OM	Preservation of Phytoplancton			Prasinophytes %/ total OM	Preservation of Prasinophytes			Acritarchs %/ total OM	Preservation of Acritarchs			Dinoflagellate cysts %/ total OM	Preservation of Dinoflagellate cysts			Leiospheres %/ total OM	Preservation of Leiospheres			Lacustrine Algae %/ total OM	Preservation of Lacustrine Algae			Foraminifera %/ total OM	Fungi %/ total OM	Terr Comp. % / total OM	Marine Comp. % / total OM	terr. palynomorphs/ total OM	marine palynomorphs/ total OM
				good (%/Phytoplancton)	moderate (%/Phytoplancton)	poor (%/Phytoplancton)		good (%/Pras.)	moderate (%/Pras.)	poor (%/Pras.)		good (%/Acritarchs)	moderate (%/Acritarchs)	poor (%/Acritarchs)		good (%/Dino.)	moderate (%/Dino.)	poor (%/Dino.)		good (%/Leiospheres)	moderate (%/Leiospheres)	poor (%/Leiospheres)		good (%/Lac. Algae)	moderate (%/Lac. Algae)	poor (%/Lac. Algae)						
W15	1997.1	MPE	10.1	0	33	67	0	0	0	0	2.9	0	100	0	7.1	0	53	47	0.0	0	0	0	0.0	0	0	0	0.0	0.0	89.9	10.1	38.2	10.1
W15	1998.4	MPE	0.0	0	0	0	0.0	0	0	0	0.0	0	0	0	0.0	0	0	0	0.0	0	0	0	0.0	0	0	0	0.0	0.0	100.0	0.0	0.0	0.0
W15	2044.6	LPE	0.0	0	0	0	0.0	0	0	0	0.0	0	0	0	0.0	0	0	0	0.0	0	0	0	0.0	0	0	0	0.0	0.0	87.8	12.2	0.0	0.0
W15	2044.9	LPE	0.0	0	0	0	0.0	0	0	0	0.0	0	0	0	0.0	0	0	0	0.0	0	0	0	0.0	0	0	0	0.0	0.0	100.0	0.0	0.0	0.0
W15	2046.2	LPE	0.0	0	0	0	0.0	0	0	0	0.0	0	0	0	0.0	0	0	0	0.0	0	0	0	0.0	0	0	0	0.0	0.0	88.9	11.1	0.0	0.0

Well	TVD (m)	Stratigraphy	# of particels	Preservation of Phytoclasts			Phyclasts%/ total OM	Preservation of Inertinite			Inertinite %/ total OM	Preservation of Vitrinite			Vitrinite %/ total OM	Preservation of Cutinite			Cutinite %/ total OM	Preservation of Sporomorphs			Sporomorphs %/ total OM	Preservation of Spores			Spores %/ total OM	Preservation of Pollen			Pollen %/ total OM	terr. AOM %/ total OM	marine AOM %/ total OM	total AOM %/ total OM
				good (%/Phytoclasts)	moderate (%/Phytoclasts)	poor (%/Phytoclasts)		good (%/Inertinite)	moderate (%/Inertinite)	poor (%/Inertinite)		good (%/Vitrinite)	moderate (%/Vitrinite)	poor (%/Vitrinite)		good (%/Cutinite)	moderate (%/Cutinite)	poor (%/Cutinite)		good (%/Sporomorphs)	moderate(%/Sporo morphs)	poor (%/Sporomorphs)		good (%/Spores)	moderate (%/Spores)	poor (%/Spores)		good (%/Spores)	moderate (%/Spores)	poor (%/Spores)				
W16	808.0	UTI	249.0	28.5	41.5	30.1	49.4	70.0	30.0	0.0	4.0	26.7	38.1	35.2	42.2	0.0	0.0	100.0	3.2	53.6	41.1	5.4	22.5	60.0	33.3	6.7	18.1	27.3	72.7	0.0	4.4	0.0	28.1	28.1
W16	865.0	UHy	278.0	11.9	38.1	50.0	30.2	35.0	65.0	0.0	7.2	6.7	42.2	51.1	16.2	0.0	0.0	100.0	6.8	31.9	19.1	48.9	16.9	100.0	0.0	0.0	5.4	0.0	28.1	71.9	11.5	2.9	49.3	52.2
W16	900.9	UHy	291.0	35.8	38.8	25.4	23.0	100.0	0.0	0.0	1.0	23.5	52.9	23.5	11.7	43.3	26.7	30.0	10.3	63.3	31.7	5.0	20.6	92.1	7.9	0.0	13.1	13.6	72.7	13.6	7.6	11.0	43.0	54.0
W16	950.0	UHy	279.0	0.0	18.8	81.3	22.9	0.0	100.0	0.0	1.1	0.0	19.1	80.9	16.8	0.0	0.0	100.0	5.0	28.3	56.5	15.2	16.5	61.9	38.1	0.0	7.5	0.0	72.0	28.0	9.0	6.5	50.2	56.6
W16	1000.0	UHy	245.0	26.8	63.4	9.8	16.7	57.1	42.9	0.0	2.9	20.6	67.6	11.8	13.9	0.0	0.0	0.0	0.0	40.0	60.0	0.0	18.4	81.8	18.2	0.0	9.0	0.0	100.0	0.0	9.4	5.7	59.2	64.9
W16	1050.0	UHy	253.0	6.5	54.3	39.1	18.2	0.0	100.0	0.0	1.6	12.0	32.0	56.0	9.9	0.0	76.5	23.5	6.7	31.5	51.9	16.7	21.3	100.0	0.0	0.0	4.3	14.0	65.1	20.9	17.0	3.2	57.3	60.5
W16	1100.0	UHy	264.0	0.0	25.8	74.2	11.7	0.0	0.0	0.0	0.0	0.0	25.8	74.2	11.7	0.0	0.0	100.0	0.0	37.0	48.1	14.8	20.5	76.2	23.8	0.0	8.0	12.1	63.6	24.2	12.5	7.2	60.6	67.8
W16	1150.0	UHy	254.0	0.0	56.7	43.3	11.8	0.0	100.0	0.0	3.5	0.0	61.5	38.5	5.1	0.0	0.0	100.0	3.1	14.5	57.8	27.7	32.7	52.2	47.8	0.0	9.1	0.0	61.7	38.3	23.6	7.5	45.3	52.8
W16	1200.0	UHy	342.0	10.3	30.8	59.0	22.8	0.0	0.0	0.0	0.0	10.3	30.8	59.0	22.8	0.0	0.0	0.0	0.0	46.7	41.1	12.2	26.3	71.0	29.0	0.0	9.1	33.9	47.5	18.6	17.3	1.5	36.5	38.0
W16	1250.0	LHy	365.0	6.3	27.1	66.7	13.2	0.0	0.0	0.0	0.0	6.3	27.1	66.7	13.2	0.0	0.0	0.0	0.0	12.8	47.9	39.4	25.8	50.0	50.0	0.0	6.6	0.0	47.1	52.9	19.2	12.3	35.3	47.7
W16	1300.0	LHy	300.0	9.1	54.5	36.4	11.0	60.0	40.0	0.0	1.7	0.0	57.1	42.9	9.3	0.0	0.0	0.0	0.0	29.3	37.9	32.8	19.3	100.0	0.0	0.0	2.7	18.0	44.0	38.0	16.7	7.7	45.0	52.7
W16	1350.0	LHy	244.0	0.0	57.1	42.9	17.2	0.0	100.0	0.0	2.9	0.0	65.4	34.6	10.7	0.0	0.0	100.0	3.7	9.4	62.5	28.1	13.1	33.3	66.7	0.0	3.7	0.0	60.9	39.1	9.4	11.1	51.2	62.3
W16	1400.0	LHy	340.0	0.0	44.0	56.0	14.7	0.0	100.0	0.0	2.4	0.0	33.3	66.7	12.4	0.0	0.0	100.0	0.0	19.6	62.3	18.1	40.6	26.9	73.1	0.0	15.3	15.1	55.8	29.1	25.3	7.4	32.4	39.7
W16	1450.0	LHy	290.0	20.6	41.2	38.2	23.4	63.6	36.4	0.0	3.8	15.2	52.2	32.6	15.9	0.0	0.0	100.0	3.8	26.3	55.3	18.4	26.2	44.0	56.0	0.0	8.6	17.6	54.9	27.5	17.6	8.6	39.7	48.3
W16	1502.0	LHy	348.0	13.0	45.5	41.6	22.1	60.0	40.0	0.0	1.4	10.1	47.8	42.0	19.8	0.0	0.0	100.0	0.9	34.1	61.5	4.4	26.1	54.5	45.5	0.0	9.5	22.4	70.7	6.9	16.7	4.9	33.9	38.8
W16	1560.0	LHy	266.0	10.7	60.7	28.6	10.5	100.0	0.0	0.0	1.1	0.0	66.7	33.3	4.5	0.0	69.2	30.8	4.9	26.3	43.4	30.3	28.6	76.9	23.1	0.0	9.8	0.0	54.0	46.0	18.8	5.3	37.6	42.9
W16	1597.5	Cor	374.0	0.0	47.4	52.6	15.2	0.0	0.0	0.0	0.0	0.0	47.4	52.6	15.2	0.0	0.0	0.0	0.0	18.5	54.8	26.6	33.2	43.4	56.6	0.0	14.2	0.0	53.5	46.5	19.0	3.2	35.6	38.8
W16	1652.5	Cor	319.0	33.3	28.0	38.7	23.5	76.5	23.5	0.0	5.3	30.8	43.6	25.6	12.2	0.0	0.0	100.0	6.0	33.3	50.0	16.7	24.5	52.0	48.0	0.0	7.8	24.5	50.9	24.5	16.6	7.5	26.6	34.2
W16	1700.0	Cor	330.0	28.9	38.6	32.5	25.2	52.6	47.4	0.0	5.8	21.9	35.9	42.2	19.4	0.0	0.0	0.0	0.0	17.2	56.3	26.4	26.4	21.2	48.5	30.3	10.0	14.8	61.1	24.1	16.4	35.8	8.5	44.2
W16	1720.0	Cor	274.0	17.6	54.4	27.9	24.8	47.1	52.9	0.0	6.2	7.8	54.9	37.3	18.6	0.0	0.0	0.0	0.0	37.1	48.6	14.3	12.8	100.0	0.0	0.0	1.5	29.0	54.8	16.1	11.3	21.5	29.6	51.1
W16	1750.0	Cer	300.0	19.3	44.5	36.1	39.4	29.2	70.8	0.0	7.9	20.5	37.2	42.3	25.8	0.0	41.2	58.8	5.6	17.1	47.4	35.5	25.2	61.1	38.9	0.0	6.0	3.4	50.0	46.6	19.2	23.2	5.0	28.1
W16	1800.0	Cer	301.0	4.4	38.2	57.4	22.6	0.0	100.0	0.0	1.0	5.6	35.2	59.3	17.9	0.0	36.4	63.6	3.7	8.8	51.3	40.0	26.6	50.0	50.0	0.0	2.7	4.2	51.4	44.4	23.9	39.9	8.3	48.2
W16	1850.0	Cer	321.0	6.7	46.7	46.7	14.0	20.0	80.0	0.0	4.7	0.0	40.9	59.1	6.9	0.0	0.0	100.0	2.5	40.7	39.8	19.4	33.6	39.3	35.7	25.0	8.7	41.3	41.3	17.5	24.9	12.5	26.5	38.9
W16	1900.0	Cer	320.0	3.4	40.9	55.7	27.5	0.0	100.0	0.0	5.6	4.8	29.0	66.1	19.4	0.0	0.0	100.0	2.5	11.3	60.6	28.2	22.2	0.0	54.5	45.5	3.4	13.3	61.7	25.0	18.8	16.9	23.4	40.3
W16	2000.0	BN	297.0	4.5	42.4	53.0	22.2	0.0	100.0	0.0	1.3	8.8	26.5	64.7	11.4	0.0	53.6	46.4	9.4	23.1	76.9	0.0	17.5	32.0	68.0	0.0	8.4	14.8	85.2	0.0	9.1	42.1	6.7	48.8
W16	2055.0	BN	263.0	27.5	47.1	25.5	19.4	0.0	100.0	0.0	3.0	66.7	33.3	0.0	8.0	0.0	40.9	59.1	8.4	16.4	47.8	35.8	25.5	50.0	50.0	0.0	2.3	13.1	47.5	39.3	23.2	7.6	39.9	47.5
W16	2100.0	BN	370.0	0.0	58.8	41.2	18.4	0.0	100.0	0.0	3.5	0.0	39.1	60.9	12.4	0.0	100.0	0.0	2.4	9.5	58.1	32.4	28.4	12.5	87.5	0.0	4.3	9.0	52.8	38.2	24.1	3.2	22.7	25.9
W16	2150.0	CyM & ME	363.0	3.4	47.4	49.1	32.0	18.2	81.8	0.0	6.1	0.0	46.8	53.2	17.1	0.0	25.0	75.0	8.8	29.5	51.9	18.6	35.5	50.0	50.0	0.0	8.8	22.7	52.6	24.7	26.7	5.0	20.4	25.3
W16	2200.0	CyM & ME	426.0	3.4	36.1	60.5	27.9	30.8	69.2	0.0	3.1	0.0	31.4	68.6	16.4	0.0	33.3	66.7	8.5	24.5	62.7	12.7	25.8	50.0	50.0	0.0	12.7	0.0	75.0	25.0	13.1	5.4	19.5	24.9
W16	2250.0	CyM & ME	358.0	7.9	43.3	48.8	35.5	40.9	59.1	0.0	6.1	1.2	48.8	50.0	24.0	0.0	0.0	100.0	5.3	13.4	62.9	23.7	27.1	39.4	60.6	0.0	9.2	0.0	64.1	35.9	17.9	3.4	20.4	23.7
W16	2300.0	RpC	413.0	0.0	43.8	56.3	27.1	0.0	100.0	0.0	3.1	0.0	27.9	72.1	16.5	0.0	54.8	45.2	7.5	34.1	51.6	14.3	30.5	36.6	63.4	0.0	9.9	32.9	45.9	21.2	20.6	6.8	27.1	33.9
W16	2350.0	UPE	271.0	13.2	50.5	36.3	33.6	63.2	36.8	0.0	7.0	0.0	54.8	45.2	22.9	0.0	50.0	50.0	3.7	18.6	58.1	23.3	15.9	61.5	38.5	0.0	4.8	0.0	66.7	33.3	11.1	8.9	39.9	48.7
W16	2398.20	UPE	260.0	52.2	39.1	8.7	88.5	63.2	36.8	0.0	73.1	0.0	50.0	50.0	15.4	0.0	0.0	0.0	0.0	0.0	0.0	0.0	0.0	0.0	0.0	0.0	0.0	0.0	0.0	0.0	0.0	7.7	3.8	11.5
W16	2398.44	MPE	276.0	23.3	41.9	34.9	31.2	52.6	47.4	0.0	13.8	0.0	40.0	60.0	16.3	0.0	0.0	100.0	1.1	0.0	0.0	0.0	0.0	0.0	0.0	0.0	0.0	0.0	0.0	0.0	0.0	61.6	7.2	68.8
W16	2414.28	MPE	240.0	27.8	50.0	22.2	75.0	55.6	44.4	0.0	37.5	0.0	55.6	44.4	37.5	0.0	0.0	0.0	0.0	0.0	0.0	0.0	0.0	0.0	0.0	0.0	0.0	0.0	0.0	0.0	0.0	22.9	2.1	25.0
W16	2420.37	MPE	260.0	50.0	37.5	12.5	61.5	57.1	42.9	0.0	53.8	0.0	0.0	100.0	7.7	0.0	0.0	0.0	0.0	0.0	0.0	0.0	0.0	0.0	0.0	0.0	0.0	0.0	0.0	0.0	0.0	34.6	3.8	38.5
W16	2425.3	MPE	452.0	18.8	47.1	34.1	46.0	34.2	65.8	0.0	8.4	22.0	45.8	32.2	26.1	0.0	36.5	63.5	11.5	0.0	46.2	53.8	26.3	0.0	34.5	65.5	6.4	0.0	50.0	50.0	19.9	5.5	22.1	27.7
W16	2425.74	MPE	310.0	44.9	32.7	22.4	79.0	63.0	37.0	0.0	43.5	23.8	23.8	52.4	33.9	0.0	100.0	0.0	1.6	0.0	0.0	0.0	43.3	56.7	0.0	0.0	0.0	0.0	0.0	0.0	0.0	19.4	1.6	21.0
W16	2431	MPE	394.0	26.5	49.7	23.8	45.9	50.5	49.5	0.0	24.1	0.0	100.0	0.0	1.0	0.0	47.6	52.4	20.8	0.0	43.3	56.7	15.2	0.0	0.0	0.0	0.0	0.0	43.3	56.7	15.2	15.2	2.5	17.8
W16	2435.6	MPE	355.0	12.7	42.8	44.5	66.5	56.3	43.8	0.0	9.0	10.2	44.9	44.9	33.2	0.0	39.5	60.5	24.2	12.8	76.9	10.3	11.0	0.0	100.0	0.0	3.4	18.5	66.7	14.8	7.6	10.7	2.8	13.5
W16	2438	MPE	287.0	2.7	59.3	37.9	63.4	0.0	100.0	0.0	5.6	4.1	57.9	38.0	42.2	0.0	48.9	51.1	15.7	0.0	50.0	50.0	9.1	0.0	0.0	100.0	3.1	0.0	76.5	23.5	5.9	12.9	3.5	16.4
W16	2440.68	MPE	323.0	0.0	56.7	43.3	55.1	0.0	100.0	0.0	2.2	0.0	60.5	39.5	36.8	0.0	42.3	57.7	16.1	10.0	62.5	27.5	12.4	14.8	77.8	7.4	8.4	0.0	30.8	69.2	4.0	7.1	1.5	8.7
W16	2444.9	MPE	333.0	1.3	58.6	40.1	68.2	0.0	100.0	0.0	1.5	2.7	61.9	35.4	33.9	0.0	53.2	46.8	32.7	10.3	79.3	10.3	8.7	42.9	57.1	0.0	2.1	0.0	86.4	13.6	6.6	10.5	3.0	13.5
W16	2443.83	MPE	303.0	23.3	43.2	33.4	94.7	37.5	62.5	0.0	15.8	25.9	39.2	34.9	62.4	0.0	40.0	60.0	16.5	0.0	42.9	57.1	2.3	0.0	42.9	57.1	2.3	0.0	0.0	0.0	0.0	0.0	0.0	0.0

Well	TVD (m)	Stratigraphy	Preservation of Phytoplancton			Phytoplancton %/ total OM	Preservation of Prasinophytes			Prasinophytes %/ total OM	Preservation of Acritarchs			Acritarchs %/ total OM	Preservation of Dinoflagellate cysts			Dinoflagellate cysts %/ total OM	Preservation of Leiospheres			Leiospheres %/ total OM	Preservation of Lacustrine Algae			Lacustrine Algae %/ total OM	Foraminifera %/ total OM	Fungi %/ total OM	Terr Comp. % / total OM	Marine Comp. % / total OM	terr. palynomorphs/ total OM	marine palynomorphs/ total OM
			good (%/Phyto.)	moderate (%/Phyto.)	poor (%/Phytoplancton)		good (%/Pras.)	moderate (%/Pras.)	poor (%/Pras.)		good (%/Acritarchs)	moderate (%/Acritarchs)	poor (%/Acritarchs)		good (%/Dino.)	moderate (%/Dino.)	poor (%/Dino.)		good (%/Leiospheres)	moderate (%/Leiospheres)	poor (%/Leiospheres)		good (%/Lac. Algae)	moderate (%/Lac. Algae)	poor (%/Lac. Algae)						
W16	808.0	UT I	0.0	0.0	0.0	0.0	0.0	0.0	0.0	0.0	0.0	0.0	0.0	0.0	0.0	0.0	0.0	0.0	0.0	0.0	0.0	0.0	0.0	0.0	0.0	0.0	0.0	0.0	71.9	28.1	22.5	0.0
W16	865.0	UHy	0.0	0.0	100.0	0.7	0.0	0.0	0.0	0.0	0.0	0.0	0.0	0.0	0.0	0.0	100.0	0.7	0.0	0.0	0.0	0.0	0.0	0.0	0.0	0.0	0.0	0.0	50.0	50.0	16.9	0.7
W16	900.9	UHy	0.0	14.3	85.7	2.4	0.0	0.0	0.0	0.0	0.0	14.3	85.7	2.4	0.0	0.0	0.0	0.0	0.0	0.0	0.0	0.0	0.0	0.0	0.0	0.0	0.0	0.0	54.6	45.4	20.6	2.4
W16	950.0	UHy	27.3	0.0	72.7	3.9	0.0	0.0	0.0	0.0	0.0	0.0	100.0	2.9	100.0	0.0	0.0	1.1	0.0	0.0	0.0	0.0	0.0	0.0	0.0	0.0	0.0	0.0	45.9	54.1	16.5	3.9
W16	1000.0	UHy	0.0	0.0	0.0	0.0	0.0	0.0	0.0	0.0	0.0	0.0	0.0	0.0	0.0	0.0	0.0	0.0	0.0	0.0	0.0	0.0	0.0	0.0	0.0	0.0	0.0	0.0	40.8	59.2	18.4	0.0
W16	1050.0	UHy	0.0	0.0	0.0	0.0	0.0	0.0	0.0	0.0	0.0	0.0	0.0	0.0	0.0	0.0	0.0	0.0	0.0	0.0	0.0	0.0	0.0	0.0	0.0	0.0	0.0	0.0	42.7	57.3	21.3	0.0
W16	1100.0	UHy	0.0	0.0	0.0	0.0	0.0	0.0	0.0	0.0	0.0	0.0	0.0	0.0	0.0	0.0	0.0	0.0	0.0	0.0	0.0	0.0	0.0	100.0	0.0	0.0	0.0	0.0	39.4	60.6	20.5	0.0
W16	1150.0	UHy	0.0	60.0	40.0	2.0	0.0	0.0	0.0	0.0	0.0	0.0	0.0	0.0	0.0	60.0	40.0	2.0	0.0	0.0	0.0	0.0	0.0	0.0	0.0	0.8	0.0	0.0	52.0	47.2	32.7	2.0
W16	1200.0	UHy	54.5	25.0	20.5	12.9	0.0	0.0	0.0	0.0	0.0	0.0	0.0	0.0	54.5	25.0	20.5	12.9	0.0	0.0	0.0	0.0	0.0	0.0	0.0	0.0	0.0	0.0	50.6	49.4	26.3	12.9
W16	1250.0	LHy	26.5	36.7	36.7	13.4	0.0	0.0	0.0	0.0	0.0	0.0	100.0	0.5	27.7	38.3	34.0	12.9	0.0	0.0	0.0	0.0	0.0	0.0	0.0	0.0	0.0	0.0	51.2	48.8	25.8	13.4
W16	1300.0	LHy	23.7	23.7	52.6	12.7	0.0	0.0	0.0	0.0	0.0	0.0	100.0	1.0	25.7	25.7	48.6	11.7	0.0	0.0	0.0	0.0	100.0	0.0	0.0	4.3	0.0	0.0	38.0	57.7	19.3	12.7
W16	1350.0	LHy	22.2	55.6	22.2	7.4	0.0	0.0	0.0	0.0	0.0	0.0	0.0	0.0	0.0	66.7	33.3	4.9	66.7	33.3	0.0	2.5	0.0	0.0	0.0	0.0	0.0	0.0	41.4	58.6	13.1	7.4
W16	1400.0	LHy	0.0	58.8	41.2	5.0	0.0	0.0	0.0	0.0	0.0	0.0	100.0	0.9	0.0	63.6	36.4	3.2	0.0	100.0	0.0	0.9	0.0	0.0	0.0	0.0	0.0	0.0	62.6	37.4	40.6	5.0
W16	1450.0	LHy	33.3	66.7	0.0	2.1	0.0	0.0	0.0	0.0	0.0	0.0	0.0	0.0	33.3	66.7	0.0	2.1	0.0	0.0	0.0	0.0	0.0	0.0	0.0	0.0	0.0	0.0	58.3	41.7	26.2	2.1
W16	1502.0	LHy	6.7	53.3	40.0	12.9	0.0	0.0	0.0	0.0	0.0	0.0	0.0	0.0	6.7	53.3	40.0	12.9	0.0	0.0	0.0	0.0	0.0	0.0	0.0	0.0	0.0	0.0	53.2	46.8	26.1	12.9
W16	1560.0	LHy	0.0	60.4	39.6	18.0	0.0	0.0	0.0	0.0	0.0	0.0	0.0	0.0	0.0	60.4	39.6	18.0	0.0	0.0	0.0	0.0	0.0	0.0	0.0	0.0	0.0	0.0	44.4	55.6	28.6	18.0
W16	1597.5	Cor	0.0	31.3	68.8	12.8	0.0	0.0	0.0	0.0	0.0	17.6	82.4	4.5	0.0	38.7	61.3	8.3	0.0	0.0	0.0	0.0	0.0	0.0	0.0	0.0	0.0	0.0	51.6	48.4	33.2	12.8
W16	1652.5	Cor	29.8	47.4	22.8	17.9	0.0	0.0	0.0	0.0	0.0	100.0	0.0	2.5	34.7	38.8	26.5	15.4	0.0	0.0	0.0	0.0	0.0	0.0	0.0	0.0	0.0	0.0	55.5	44.5	24.5	17.9
W16	1700.0	Cor	71.4	28.6	0.0	4.2	100.0	0.0	0.0	0.0	0.0	0.0	0.0	0.0	50.0	50.0	0.0	2.4	100.0	0.0	0.0	0.9	0.0	0.0	0.0	0.0	0.0	0.0	87.3	12.7	26.4	4.2
W16	1720.0	Cor	27.6	27.6	44.8	10.6	0.0	0.0	0.0	0.0	0.0	0.0	0.0	0.0	27.6	27.6	44.8	10.6	0.0	0.0	0.0	0.0	100.0	0.0	0.0	0.7	0.0	0.0	59.1	40.1	12.8	10.6
W16	1750.0	Cer	40.0	30.0	30.0	6.6	0.0	0.0	0.0	0.0	0.0	100.0	100.0	1.0	47.1	35.3	17.6	5.6	0.0	0.0	0.0	0.0	0.0	0.0	0.0	0.0	0.0	0.7	87.7	12.3	25.2	7.3
W16	1800.0	Cer	0.0	0.0	100.0	1.3	0.0	0.0	0.0	0.0	0.0	100.0	100.0	1.3	0.0	0.0	0.0	0.0	0.0	0.0	0.0	0.0	100.0	0.0	0.0	1.3	0.0	0.0	89.0	9.6	26.6	1.3
W16	1850.0	Cer	0.0	63.2	36.8	5.9	0.0	0.0	0.0	0.0	0.0	0.0	0.0	0.0	0.0	63.2	36.8	5.9	0.0	0.0	0.0	0.0	0.0	100.0	0.0	7.5	0.0	0.0	60.1	32.4	33.6	5.9
W16	1900.0	Cer	8.7	56.5	34.8	7.2	0.0	0.0	0.0	0.0	0.0	0.0	100.0	2.5	13.3	86.7	0.0	4.7	0.0	0.0	0.0	0.0	0.0	100.0	0.0	2.8	0.0	0.0	66.6	30.6	22.2	7.2
W16	2000.0	BN	14.3	25.0	60.7	9.4	0.0	0.0	0.0	0.0	0.0	0.0	0.0	0.0	16.7	29.2	54.2	8.1	0.0	0.0	100.0	1.3	100.0	0.0	0.0	2.0	0.0	0.0	81.8	16.2	17.5	9.4
W16	2055.0	BN	0.0	40.0	60.0	7.6	0.0	0.0	0.0	0.0	0.0	0.0	0.0	0.0	0.0	40.0	60.0	7.6	0.0	0.0	0.0	0.0	0.0	0.0	0.0	0.0	0.0	0.0	52.5	47.5	25.5	7.6
W16	2100.0	BN	0.0	25.5	74.5	13.8	0.0	0.0	0.0	0.0	0.0	0.0	0.0	0.0	0.0	25.5	74.5	13.8	0.0	0.0	0.0	0.0	60.0	40.0	0.0	13.5	0.0	0.0	50.0	36.5	28.4	13.8
W16	2150.0	CyM & ME	15.4	69.2	15.4	7.2	0.0	0.0	0.0	0.0	0.0	0.0	100.0	4.5	15.4	69.2	15.4	7.2	0.0	0.0	0.0	0.0	17.4	82.6	0.0	5.4	0.0	0.0	72.5	27.5	35.5	7.2
W16	2200.0	CyM & ME	4.4	35.3	60.3	16.0	0.0	0.0	0.0	0.0	0.0	0.0	100.0	4.5	6.1	49.0	44.9	11.5	0.0	0.0	0.0	0.0	0.0	0.0	0.0	0.0	0.0	0.0	59.2	35.4	25.8	16.0
W16	2250.0	CyM & ME	34.7	38.8	26.5	13.7	0.0	0.0	0.0	0.0	0.0	0.0	0.0	0.0	34.7	38.8	26.5	13.7	0.0	0.0	0.0	0.0	0.0	0.0	0.0	0.0	0.0	0.0	65.9	34.1	27.1	13.7
W16	2300.0	RpC	52.9	0.0	47.1	4.1	0.0	0.0	0.0	0.0	0.0	0.0	100.0	1.9	100.0	0.0	0.0	2.2	0.0	0.0	0.0	0.0	0.0	100.0	0.0	4.4	0.0	0.0	64.4	31.2	30.5	4.1
W16	2350.0	UPE	0.0	0.0	0.0	0.0	0.0	0.0	0.0	0.0	0.0	0.0	0.0	0.0	0.0	0.0	0.0	0.0	0.0	0.0	0.0	0.0	0.0	100.0	0.0	1.8	0.0	0.0	58.3	39.9	15.9	0.0
W16	2398.20	UPE	0.0	0.0	0.0	0.0	0.0	0.0	0.0	0.0	0.0	0.0	0.0	0.0	0.0	0.0	0.0	0.0	0.0	0.0	0.0	0.0	0.0	0.0	0.0	0.0	0.0	0.0	96.2	3.8	0.0	0.0
W16	2398.44	MPE	0.0	0.0	0.0	0.0	0.0	0.0	0.0	0.0	0.0	0.0	0.0	0.0	0.0	0.0	0.0	0.0	0.0	0.0	0.0	0.0	0.0	0.0	0.0	0.0	0.0	0.0	92.8	7.2	0.0	0.0
W16	2414.28	MPE	0.0	0.0	0.0	0.0	0.0	0.0	0.0	0.0	0.0	0.0	0.0	0.0	0.0	0.0	0.0	0.0	0.0	0.0	0.0	0.0	0.0	0.0	0.0	0.0	0.0	0.0	97.9	2.1	0.0	0.0
W16	2420.37	MPE	0.0	0.0	0.0	0.0	0.0	0.0	0.0	0.0	0.0	0.0	0.0	0.0	0.0	0.0	0.0	0.0	0.0	0.0	0.0	0.0	0.0	0.0	0.0	0.0	0.0	0.0	96.2	3.8	0.0	0.0
W16	2425.3	MPE	0.0	0.0	0.0	0.0	0.0	0.0	0.0	0.0	0.0	0.0	0.0	0.0	0.0	0.0	0.0	0.0	0.0	0.0	0.0	0.0	0.0	0.0	0.0	0.0	0.0	0.0	77.9	22.1	26.3	0.0
W16	2425.74	MPE	0.0	0.0	0.0	0.0	0.0	0.0	0.0	0.0	0.0	0.0	0.0	0.0	0.0	0.0	0.0	0.0	0.0	0.0	0.0	0.0	0.0	0.0	0.0	0.0	0.0	0.0	98.4	1.6	0.0	0.0
W16	2431	MPE	0.0	9.6	90.4	21.1	0.0	0.0	0.0	0.0	0.0	11.6	88.4	17.5	0.0	0.0	100.0	3.6	0.0	0.0	0.0	0.0	0.0	0.0	0.0	0.0	0.0	0.0	76.4	23.6	15.2	21.1
W16	2435.6	MPE	12.5	15.6	71.9	9.0	0.0	0.0	0.0	0.0	0.0	100.0	100.0	6.5	44.4	55.6	0.0	2.5	0.0	0.0	0.0	0.0	0.0	0.0	0.0	0.0	0.0	0.0	88.2	11.8	11.0	9.0
W16	2438	MPE	0.0	65.6	34.4	11.1	0.0	0.0	0.0	0.0	0.0	0.0	100.0	3.8	0.0	100.0	0.0	4.9	0.0	100.0	0.0	2.4	0.0	0.0	0.0	0.0	0.0	0.0	85.4	14.6	9.1	11.1
W16	2440.68	MPE	0.0	41.6	58.4	23.8	0.0	0.0	0.0	0.0	0.0	26.0	74.0	15.5	0.0	70.4	29.6	8.4	0.0	0.0	0.0	0.0	0.0	0.0	0.0	0.0	0.0	0.0	74.6	25.4	12.4	23.8
W16	2444.9	MPE	0.0	18.8	81.3	9.6	0.0	0.0	0.0	0.0	0.0	10.0	90.0	6.0	0.0	33.3	66.7	3.6	0.0	0.0	0.0	0.0	0.0	0.0	0.0	0.0	0.0	0.0	87.4	12.6	8.7	9.6
W16	2443.83	MPE	0.0	0.0	100.0	3.0	0.0	0.0	0.0	0.0	0.0	100.0	100.0	3.0	0.0	0.0	0.0	0.0	0.0	0.0	0.0	0.0	0.0	0.0	0.0	0.0	0.0	0.0	97.0	3.0	2.3	3.0

Well	TVD (m)	Stratigraphy	# of particels	Preservation of Phytoclasts			Phyclasts%/ total OM	Preservation of Inertinite			Inertinite %/ total OM	Preservation of Vitrinite			Vitrinite %/ total OM	Preservation of Cutinite			Cutinite %/ total OM	Preservation of Sporomorphs			Sporomorphs %/ total OM	Preservation of Spores			Spores %/ total OM	Preservation of Pollen			Pollen %/ total OM	terr. AOM %/ total OM	marine AOM %/ total OM	total AOM %/ total OM
				good (%/Phytoclasts)	moderate (%/Phytoclasts)	poor (%/Phytoclasts)		good (%/Interitnite)	moderate (%/Interitnite)	poor (%/Interitnite)		good (%/Vitrinite)	moderate (%/Vitrinite)	poor (%/Vitrinite)		good (%/Cutinite)	moderate (%/Cutinite)	poor (%/Cutinite)		good (%/Sporomorphs)	moderate(%/Sporomorphs)	poor (%/Sporomorphs)		good (%/Spores)	moderate (%/Spores)	poor (%/Spores)		good (%/Spores)	moderate (%/Spores)	poor (%/Spores)				
W18	2399.7	PE	290	33	18	49	47.9	60	22	18	15.5	26	14	61	25.5	0	25	75	6.9	18	51	32	29.3	18	52	29	22.4	15	45	40	6.9	21.7	0.0	21.7
W18	2400.5	PE	404	21	37	41	64.1	66	34	0	9.4	24	38	38	30.9	0	38	63	23.8	51	39	10	20.3	56	37	7	18.6	0	57	43	1.7	14.9	0.0	14.9
W18	2403.4	PE	225	38	62	0	93.3	53	47	0	66.7	0	100	0	26.7	0	0	0	0.0	0	0	0	0.0	0	0	0	0.0	0	0	0	0.0	4.4	2.2	6.7

Well	TVD (m)	Stratigraphy	Preservation of Phytoplancton		Phytoplancton %/ total OM	Preservation of Prasinophytes		Prasinophytes %/ total OM	Preservation of Acritarchs		Acritarchs %/ total OM	Preservation of Dinoflagellate cysts			Dinoflagellate cysts %/ total OM	Preservation of Leiospheres			Leiospheres %/ total OM	Preservation of Lacustrine Algae			Lacustrine Algae %/ total OM	Foraminifera %/ total OM	Fungi %/ total OM	Terr Comp. % / total OM	Marine Comp. % / total OM	terr. palynomorphs/ total OM	marine palynomorphs/ total OM
			good (%/Phytoplancton)	moderate (%/Phytoplancton)	poor (%/Phytoplancton)	good (%/Pras.)	moderate (%/Pras.)	poor (%/Pras.)	good (%/Acritarchs)	moderate (%/Acritarchs)	poor (%/Acritarchs)	good (%/Dino.)	moderate (%/Dino.)	poor (%/Dino.)		good (%/Leiospheres)	moderate (%/Leiospheres)	poor (%/Leiospheres)		good (%/Lac. Algae)	moderate (%/Lac. Algae)	poor (%/Lac. Algae)							
W18	2399.7	PE	0	0	100	1.0	0	0	0	0	100	1.0	0	0	0.0	0	0	0	0.0	0	0	0	0.0	0.0	0.0	99.0	1.0	29.3	1.0
W18	2400.5	PE	0	0	100	0.7	0	0	0	0	0	0	0	100	0.7	0	0	0	0.0	0	0	0	0.0	0.0	0.0	99.3	0.7	20.3	0.7
W18	2403.4	PE	0	0	0	0.0	0	0	0	0	0	0	0	0	0.0	0	0	0	0.0	0	0	0	0.0	0.0	0.0	97.8	2.2	0.0	0.0

Well	TVD (m)	Stratigraphy	# of particels	Preservation of Phytoclasts			Phyclasts%/ total OM	Preservation of Inertinite			Inertinite % / total OM	Preservation of Vitrinite			Vitrinite % / total OM	Preservation of Cutinite			Cutinite % / total OM	Preservation of Sporomorphs			Sporomorphs % / total OM	Preservation of Spores			Spores % / total OM	Preservation of Pollen			Pollen % / total OM	terr. AOM % / total OM	marine AOM % / total OM	total AOM % / total OM
				good (%/Phytoclasts)	moderate (%/Phytoclasts)	poor (%/Phytoclasts)		good (%/Inertinite)	moderate (%/Inertinite)	poor (%/Inertinite)		good (%/Vitrinite)	moderate (%/Vitrinite)	poor (%/Vitrinite)		good (%/Cutinite)	moderate (%/Cutinite)	poor (%/Cutinite)		good (%/Sporomorphs)	moderate(%/Sporomorphs)	poor (%/Sporomorphs)		good (%/Spores)	moderate (%/Spores)	good (%/Spores)		good (%/Spores)	moderate (%/Spores)	poor (%/Spores)				
W19	1455.0	Cer	238	46	39	15	19.3	73	27	0	4.6	37	43	20	14.7	0	0	0	0.0	2	44	54	45.0	0	41	59	24.8	4	48	48	20.2	1.7	25.2	26.9
W19	1457.0	Cer	317	40	52	8	33.1	47	53	0	5.4	27	55	18	13.9	50	50	0	13.9	34	61	5	32.5	44	56	0	19.6	20	68	12	12.9	4.4	15.1	19.6
W19	1640.0	CyM	300	22	40	38	77.7	59	35	5	12.3	36	48	16	26.7	0	37	63	38.7	15	63	22	13.7	26	74	0	7.7	0	50	50	6.0	7.3	0.0	7.3
W19	1850.0	RpC	274	13	21	65	40.9	60	40	0	9.1	0	100	0	3.3	0	6	94	28.5	26	45	28	36.1	53	47	0	17.9	0	44	56	18.2	9.1	5.5	14.6
W19	1851.0	RpC	226	1	36	63	75.7	7	69	24	12.8	0	38	62	9.3	0	27	73	53.5	33	50	17	13.3	56	44	0	8.0	0	58	42	5.3	6.6	0.0	6.6
W19	1852.0	RpC	215	9	12	80	52.6	100	0	0	4.7	0	33	67	7.0	0	9	91	40.9	15	45	40	31.2	37	48	15	12.6	0	43	58	18.6	11.6	4.7	16.3
W19	1853.0	PE	251	7	39	53	76.1	0	100	0	4.8	17	38	45	32.7	0	33	67	38.7	0	23	77	12.0	0	58	42	4.8	0	0	100	7.2	9.2	0.0	9.2
W19	1854.0	PE	294	8	65	27	73.1	55	45	0	11.2	0	72	28	37.1	0	62	38	24.8	18	48	34	20.8	55	35	10	6.8	0	54	46	13.9	0.0	0.0	0.0
W19	1856.0	PE	215	43	55	2	97.7	45	55	0	93.0	0	50	50	4.7	0	0	0	0.0	0	0	0	0.0	0	0	0	0.0	0	0	0	0.0	2.3	0.0	2.3
W19	1878.0	PE	250	32	52	16	100.0	35	52	13	92.0	0	50	50	8.0	0	0	0	0.0	0	0	0	0.0	0	0	0	0.0	0	0	0	0.0	0.0	0.0	0.0

Well	TVD (m)	Stratigraphy	Preservation of Phytoplancton			Phytoplancton % / total OM	Preservation of Prasinophytes			Prasinophytes % / total OM	Preservation of Acritarchs			Acritarchs % / total OM	Preservation of Dinoflagellate cysts			Dinoflagellate cysts % / total OM	Preservation of Leiospheres			Leiospheres % / total OM	Preservation of Lacustrine Algae			Lacustrine Algae % / total OM	Foraminifera % / total OM	Fungi % / total OM	Terr Comp. % / total OM	Marine Comp. % / total OM	terr. palynomorphs/ total OM	marine palynomorphs/ total OM
			good (%/Phytoplancton)	moderate (%/Phytoplancton)	poor (%/Phytoplancton)		good (%/Pras.)	moderate (%/Pras.)	poor (%/Pras.)		good (%/Acritarchs)	moderate (%/Acritarchs)	poor (%/Acritarchs)		good (%/Dino.)	moderate (%/Dino.)	poor (%/Dino.)		good (%/Leiospheres)	moderate (%/Leiospheres)	poor (%/Leiospheres)		good (%/Lac. Algae)	moderate (%/Lac. Algae)	poor (%/Lac. Algae)							
W19	1455.0	Cer	0	0	100	8.8	0	0	0	0.0	0	0	100	3.8	0	0	100	5.0	0	0	0	0.0	0	0	0	0.0	0.0	66.0	34.0	45.0	8.8	
W19	1457.0	Cer	0	49	51	14.8	0	0	0	0.0	0	0	100	0.0	0	49	51	14.8	0	0	0	0.0	0	0	0	0.0	0.0	70.0	30.0	32.5	14.8	
W19	1640.0	CyM	0	0	100	1.3	0	0	0	0.0	0	0	100	1.3	0	0	0	0.0	0	0	0	0.0	0	0	0	0.0	0.0	98.7	1.3	13.7	1.3	
W19	1850.0	RpC	0	52	48	8.4	0	0	0	0.0	0	60	40	7.3	0	0	100	1.1	0	0	0	0.0	0	0	0	0.0	0.0	86.1	13.9	36.1	8.4	
W19	1851.0	RpC	0	20	80	4.4	0	0	0	0.0	0	0	100	0.0	0	20	80	4.4	0	0	0	0.0	0	0	0	0.0	0.0	95.6	4.4	13.3	4.4	
W19	1852.0	RpC	0	0	0	0.0	0	0	0	0.0	0	0	100	0.0	0	0	0	0.0	0	0	0	0.0	0	0	0	0.0	0.0	95.3	4.7	31.2	0.0	
W19	1853.0	PE	0	0	100	2.8	0	0	0	0.0	0	0	100	1.2	0	0	100	1.6	0	0	0	0.0	0	0	0	0.0	0.0	97.2	2.8	12.0	2.8	
W19	1854.0	PE	0	0	100	6.1	0	0	0	0.0	0	0	100	6.1	0	0	0	0.0	0	0	0	0.0	0	0	0	0.0	0.0	93.9	6.1	20.7	6.1	
W19	1856.0	PE	0	0	0	0.0	0	0	0	0.0	0	0	0	0.0	0	0	0	0.0	0	0	0	0.0	0	0	0	0.0	0.0	100.0	0.0	0.0	0.0	
W19	1878.0	PE	0	0	0	0.0	0	0	0	0.0	0	0	0	0.0	0	0	0	0.0	0	0	0	0.0	0	0	0	0.0	0.0	100.0	0.0	0.0	0.0	

Well	TVD (m)	Stratigraphy	# of particels	Preservation of Phytoclasts			Phyclasts%/ total OM	Preservation of Inertinite			Inertinite %/ total OM	Preservation of Vitrinite			Vitrinite %/ total OM	Preservation of Cutinite			Cutinite %/ total OM	Preservation of Sporomorphs			Sporomorphs %/ total OM	Preservation of Spores			Spores %/ total OM	Preservation of Pollen			Pollen %/ total OM	terr. AOM %/ total OM	marine AOM %/ total OM	total AOM %/ total OM
				good (%/Phytoclasts)	moderate (%/Phytoclasts)	poor (%/Phytoclasts)		good (%/Inertinite)	moderate (%/Inertinite)	poor (%/Inertinite)		good (%/Vitrinite)	moderate (%/Vitrinite)	poor (%/Vitrinite)		good (%/Cutinite)	moderate (%/Cutinite)	poor (%/Cutinite)		good (%/Sporomorphs)	moderate(%/Sporomorphs)	poor (%/Sporomorphs)		good (%/Spores)	moderate (%/Spores)	poor (%/Spores)		good (%/Spores)	moderate (%/Spores)	poor (%/Spores)				
W21	1455.3	CyM & ME	272	31	38	32	76.8	80	20	0	25.7	7	50	44	44.5	0	28	72	6.6	0	32	68	21.0	0	29	71	11.4	0	35	65	9.6	0.0	0.0	0.0
W21	1461.1	CyM & ME	262	35	36	30	85.9	88	8	4	19.5	19	44	37	66.4	0	0	0	0.0	43	43	13	11.5	47	32	21	7.3	36	64	0	4.2	0.0	0.0	0.0
W21	1575.6	CyM & ME	269	28	39	33	69.5	86	14	0	5.2	24	40	36	64.3	0	0	0	0.0	22	28	50	18.6	10	38	52	7.8	31	21	48	10.8	0.0	5.2	5.2
W21	1581.6	CyM & ME	266	23	37	39	82.8	74	26	0	11.6	15	39	46	71.3	0	0	0	0.0	23	43	34	16.4	31	34	34	11.9	0	67	33	4.5	0.0	0.0	0.0
W21	1587.5	CyM & ME	278	31	41	29	83.5	82	18	0	20.5	15	43	42	57.6	0	100	0	5.4	6	45	48	11.2	12	35	53	6.1	0	57	43	5.0	0.0	0.0	0.0
W21	1590.2	CyM & ME	318	32	38	30	82.4	72	26	2	15.7	23	41	36	66.7	0	0	0	0.0	0	36	64	14.8	0	8	92	4.1	0	47	53	10.7	0.0	2.8	2.8
W21	1753.2	UPE	274	14	47	38	88.3	52	44	5	23.4	1	48	51	65.0	0	0	0	0.0	0	0	100	11.3	0	0	100	8.4	0	0	100	2.9	0.0	0.0	0.0
W21	1772.9	MPE	312	23	44	33	65.7	66	34	0	16.0	13	38	48	33.3	0	65	35	16.3	7	51	41	13.1	15	65	20	6.4	0	38	62	6.7	12.8	7.1	19.9

Well	TVD (m)	Stratigraphy	Preservation of Phytoplancton			Phytoplancton %/ total OM	Preservation of Prasinophytes			Prasinophytes %/ total OM	Preservation of Acritarchs			Acritarchs %/ total OM	Preservation of Dinoflagellate cysts			Dinoflagellate cysts %/ total OM	Preservation of Leiospheres			Leiospheres %/ total OM	Preservation of Lacustrine Algae			Lacustrine Algae %/ total OM	Foraminifera %/ total OM	Fungi %/ total OM	Terr Comp. % / total OM	Marine Comp. % / total OM	terr. palynomorphs/ total OM	marine palynomorphs/ total OM
			good (%/Phytoplancton)	moderate (%/Phytoplancton)	poor (%/Phytoplancton)		good (%/Pras.)	moderate (%/Pras.)	poor (%/Pras.)		good (%/Acritarchs)	moderate (%/Acritarchs)	poor (%/Acritarchs)		good (%/Dino.)	moderate (%/Dino.)	poor (%/Dino.)		good (%/Leiospheres)	moderate (%/Leiospheres)	poor (%/Leiospheres)		good (%/Lac. Algae)	moderate (%/Lac. Algae)	poor (%/Lac. Algae)							
W21	1455.3	CyM & ME	0	0	100	2.2	0	0	100	1.5	0	0	100	0.7	0	0	0	0.0	0	0	0	0.0	0	0	0	0.0	0.0	97.8	2.2	21.0	2.2
W21	1461.1	CyM & ME	0	57	43	2.7	0	0	100	1.5	0	0	100	1.1	0	0	0	0.0	0	0	0	0.0	0	0	0	0.0	0.0	97.3	2.7	11.5	2.7
W21	1575.6	CyM & ME	0	22	78	6.7	0	0	100	0.4	0	18	82	6.3	0	0	0	0.0	0	0	0	0.0	0	0	0	0.0	0.0	88.1	11.9	18.6	6.7
W21	1581.6	CyM & ME	0	0	0	0.0	0	0	0	0.0	0	0	0	0.0	0	0	0	0.0	0	0	0	0.0	0	0	0	0.0	0.7	99.3	0.7	16.4	0.7
W21	1587.5	CyM & ME	0	0	100	5.4	0	0	100	1.1	0	0	100	4.3	0	0	0	0.0	0	0	0	0.0	0	0	0	0.0	0.0	94.6	5.4	11.2	5.4
W21	1590.2	CyM & ME	0	0	0	0.0	0	0	0	0.0	0	0	0	0.0	0	0	0	0.0	0	0	0	0.0	0	0	0	0.0	0.0	97.2	2.8	14.8	0.0
W21	1753.2	UPE	0	0	100	0.4	0	0	100	0.4	0	0	100	0.0	0	0	0	0.0	0	0	0	0.0	0	0	0	0.0	0.0	99.6	0.4	11.3	0.4
W21	1772.9	MPE	0	0	100	1.3	0	0	100	1.3	0	0	100	0.0	0	0	0	0.0	0	0	0	0.0	0	0	0	0.0	0.0	91.7	8.3	13.1	1.3

Well	TVD (m)	Stratigraphy	# of particels	Preservation of Phytoclasts			Phyclasts%/ total OM	Preservation of Inertinite			Inertinite %/ total OM	Preservation of Vitrinite			Vitrinite %/ total OM	Preservation of Cutinite			Cutinite %/ total OM	Preservation of Sporomorphs			Sporomorphs %/ total OM	Preservation of Spores			Spores %/ total OM	Preservation of Pollen			Pollen %/ total OM	ter. AOM %/ total OM	marine AOM %/ total OM	total AOM %/ total OM
				good (%/Phytoclasts)	moderate (%/Phytoclasts)	poor (%/Phytoclasts)		good (%/Interitnite)	moderate (%/Inertitnite)	poor (%/Inertitnite)		good (%/Vitrinite)	moderate (%/Vitrinite)	poor (%/Vitrinite)		good (%/Cutinite)	moderate (%/Cutinite)	poor (%/Cutinite)		good (%/Sporomorphs)	moderate(%/Sporomorphs)	poor (%/Sporomorphs)		good (%/Spores)	moderate (%/Spores)	poor (%/Spores)		good (%/Spores)	moderate (%/Spores)	poor (%/Spores)				
W23	1136.5	Cor	352	20	37	42	23.6	45	55	0	5.7	13	32	56	17.9	0	0	0	0.0	0	11	89	27.3	0	26	74	7.7	0	6	94	19.6	22.7	6.3	29.0
W23	1245.0	Cor	270	39	39	22	34.1	61	39	0	8.5	32	39	29	25.6	0	0	0	0.0	0	1	99	25.6	0	13	88	3.0	0	0	100	22.6	33.3	1.9	35.2
W23	1350	Cer	330	9	36	55	23.0	70	30	0	3.0	0	36	64	20.0	0	0	0	0.0	0	21	79	39.7	0	43	57	13.3	0	9	91	26.4	19.7	0.0	19.7
W23	1642.3	BN	282	36	46	18	77.2	67	33	0	15.8	24	52	24	31.9	32	48	20	29.5	0	50	50	8.4	0	55	45	3.9	0	46	54	4.6	3.5	0.0	3.5
W23	1773.6	CyM & ME	258	25	47	28	73.6	53	47	0	13.2	34	45	21	34.5	0	49	51	26.0	0	19	81	6.2	0	43	57	2.7	0	0	100	3.5	8.1	0.0	8.1
W23	1812.6	CyM & ME	268	16	49	35	74.3	51	49	0	14.6	13	54	33	34.3	0	41	59	25.4	6	48	45	12.3	15	62	23	4.9	0	40	60	7.5	4.1	5.6	9.7
W23	1955	PE	221	16	43	41	48.0	68	32	0	11.3	0	69	31	11.8	0	36	64	24.9	0	17	83	5.4	0	22	78	4.1	0	0	100	1.4	43.0	2.3	45.2
W23	1965.0	PE	340	35	50	15	100.0	57	43	0	61.8	0	62	38	38.2	0	0	0	0.0	0	0	0	0.0	0	0	0	0.0	0	0	0	0.0	0.0	0.0	0.0
W23	1969.5	PE	282	24	33	42	39.4	86	14	0	9.9	5	41	54	21.6	0	36	64	7.8	23	50	26	44.3	29	55	16	35.1	0	35	65	9.2	8.9	1.1	9.9
W23	1986.1	PE	200	50	50	0	100.0	50	50	0	100.0	0	0	0	0.0	0	0	0	0.0	0	0	0	0.0	0	0	0	0.0	0	0	0	0.0	0.0	0.0	0.0
W23	1996.7	PE	306	33	46	21	78.4	53	47	0	49.0	0	44	56	29.4	0	0	0	0.0	0	0	100	2.0	0	0	0	2.0	0	0	0	0.0	19.6	0.0	19.6

Well	TVD (m)	Stratigraphy	Preservation of Phytoplancton		Phytoplancton %/ total OM	Preservation of Prasinophytes			Prasinophytes %/ total OM	Preservation of Acritarchs			Acritarchs %/ total OM	Preservation of Dinoflagellate cysts			Dinoflagellate cysts %/ total OM	Preservation of Leiospheres			Preservation of Lacustrine Algae			Lacustrine Algae %/ total OM	Foraminifera %/ total OM	Fungi %/ total OM	Terr Comp. % / total OM	Marine Comp. % / total OM	terr. palynomorphs/ total OM	marine palynomorphs/ total OM
			good (%/Phytoplancton)	moderate (%/Phytoplancton)	poor (%/Phytoplancton)	good (%/Pras.)	moderate (%/Pras.)	poor (%/Pras.)		good (%/Acritarchs)	moderate (%/Acritarchs)	poor (%/Acritarchs)		good (%/Dino.)	moderate (%/Dino.)	poor (%/Dino.)		good (%/Leiospheres)	moderate (%/Leiospheres)	poor (%/Leiospheres)	good (%/Lac. Algae)	moderate (%/Lac. Algae)	poor (%/Lac. Algae)							
W23	1136.5	Cor	0	41	59	20.2	0	0	0	0.0	54	46	3.7	0	38	62	16.5	0	0	0	0	0	0	0.0	0.0	0.0	73.6	26.4	27.3	20.2
W23	1245.0	Cor	0	0	100	5.2	0	0	0	0.0	0	0	0.0	0	0	100	5.2	0	0	0	0	0	0	0.0	0.0	0.0	93.0	7.0	25.6	5.2
W23	1350	Cer	0	17	83	17.6	0	0	0	0.0	0	0	0.0	0	17	83	17.6	0	0	0	0	0	0	0.0	0.0	0.0	82.4	17.6	39.7	17.6
W23	1642.3	BN	0	39	61	9.8	0	0	0	0.0	0	0	0.0	0	44	56	8.8	0	0	100	1.1	0	0	0.0	0.0	1.1	89.1	10.9	8.4	10.9
W23	1773.6	CyM & ME	0	39	61	12.0	0	0	0	0.0	0	36	64	4.3	0	40	60	7.8	0	0	0	0	0	0.0	0.0	0.0	88.0	12.0	6.2	12.0
W23	1812.6	CyM & ME	0	0	100	3.7	0	0	0	0.0	0	0	100	1.1	0	100	2.6	0	0	0	0	0	0	0.0	0.0	0.0	90.7	9.3	12.3	3.7
W23	1955	PE	0	0	100	1.4	0	0	0	0.0	0	0	100	1.4	0	0	0.0	0	0	0	0	0	0	0.0	0.0	0.0	96.4	3.6	5.4	1.4
W23	1965.0	PE	0	0	0	0.0	0	0	0	0.0	0	0	0	0.0	0	0	0.0	0	0	0	0	0	0	0.0	0.0	0.0	100.0	0.0	0.0	0.0
W23	1969.5	PE	0	0	100	6.4	0	0	0	0.0	0	0	100	3.2	0	0	3.2	0	0	0	0	0	0	0.0	0.0	0.0	92.6	7.4	44.3	6.4
W23	1986.1	PE	0	0	0	0.0	0	0	0	0.0	0	0	0	0.0	0	0	0.0	0	0	0	0	0	0	0.0	0.0	0.0	100.0	0.0	0.0	0.0
W23	1996.7	PE	0	0	0	0.0	0	0	0	0.0	0	0	0	0.0	0	0	0.0	0	0	0	0	0	0	0.0	0.0	0.0	100.0	0.0	2.0	0.0

Well	TVD (m)	Stratigraphy	# of particels	Preservation of Phytoclasts			Phyclasts%/ total OM	Preservation of Inertinite			Inertinite %/ total OM	Preservation of Vitrinite			Vitrinite %/ total OM	Preservation of Cutinite			Cutinite %/ total OM	Preservation of Sporomorphs			Sporomorphs %/ total OM	Preservation of Spores			Spores %/ total OM	Preservation of Pollen			Pollen %/ total OM	terr. AOM %/ total OM	marine AOM %/ total OM	total AOM %/ total OM
				good (%/Phytoclasts)	moderate (%/Phytoclasts)	poor (%/Phytoclasts)		good (%/Interlinite)	moderate (%/Interlinite)	poor (%/Interlinite)		good (%/Vitrinite)	moderate (%/Vitrinite)	poor (%/Vitrinite)		good (%/Cutinite)	moderate (%/Cutinite)	poor (%/Cutinite)		good (%/Sporomorphs)	moderate(%/Sporomorphs)	poor (%/Sporomorphs)		good (%/Spores)	moderate (%/Spores)	poor (%/Spores)		good (%/Spores)	moderate (%/Spores)	poor (%/Spores)				
W25	1705.0	PE	228	9	23	68	59.2	18	64	18	4.8	7	17	76	51.8	33	67	0	2.6	44	25	31	15.8	50	0	50	7.0	40	45	15	8.8	15.8	1.8	17.5
W25	1796.0	PE	371	1	58	41	68.7	50	50	0	1.1	1	30	70	40.7	0	100	0	27.0	21	42	36	8.9	31	38	31	4.3	12	47	41	4.6	1.3	17.5	18.9

Well	TVD (m)	Stratigraphy	Preservation of Phytoplancton			Phytoplancton %/ total OM	Preservation of Prasinophytes			Prasinophytes %/ total OM	Preservation of Acritarchs			Acritarchs %/ total OM	Preservation of Dinoflagellate cysts			Dinoflagellate cysts %/ total OM	Preservation of Leiospheres			Leiospheres %/ total OM	Preservation of Lacustrine Algae			Lacustrine Algae %/ total OM	Foraminifera %/ total OM	Fungi %/ total OM	Terr Comp. % / total OM	Marine Comp. % / total OM	terr. palynomorphs/ total OM	marine palynomorphs/ total OM
			good (%/Phytoplancton)	moderate (%/Phytoplancton)	poor (%/Phytoplancton)		good (%/Pras.)	moderate (%/Pras.)	poor (%/Pras.)		good (%/Acritarchs)	moderate (%/Acritarchs)	poor (%/Acritarchs)		good (%/Dino.)	moderate (%/Dino.)	poor (%/Dino.)		good (%/Leiospheres)	moderate (%/Leiospheres)	poor (%/Leiospheres)		good (%/Lac. Algae)	moderate (%/Lac. Algae)	poor (%/Lac. Algae)							
W25	1705.0	PE	29	65	6	7.5	0	0	0	0.0	0	89	11	3.9	63	38	0	3.5	0	0	0	0.0	0	0	0	0.0	0.0	0.0	90.8	9.2	15.8	7.5
W25	1796.0	PE	31	62	8	3.5	0	0	0	0.0	14	86	0	1.9	50	33	17	1.6	0	0	0	0.0	0	0	0	0.0	0.0	0.0	79.0	21.0	8.9	3.5

Well	TVD (m)	Stratigraphy	# of particels	Preservation of Phytoclasts			Phyclasts%/ total OM	Preservation of Inertinite			Inertinite %/ total OM	Preservation of Vitrinite			Vitrinite %/ total OM	Preservation of Cutinite			Cutinite %/ total OM	Preservation of Sporomorphs			Sporomorphs %/ total OM	Preservation of Spores			Spores %/ total OM	Preservation of Pollen			Pollen %/ total OM	terr. AOM %/ total OM	marine AOM %/ total OM	total AOM %/ total OM
				good (%/Phytoclasts)	moderate (%/Phytoclasts)	poor (%/Phytoclasts)		good (%/Interlinite)	moderate (%/Interlinite)	poor (%/Interlinite)		good (%/Vitrinite)	moderate (%/Vitrinite)	poor (%/Vitrinite)		good (%/Cutinite)	moderate (%/Cutinite)	poor (%/Cutinite)		good (%/Sporomorphs)	moderate(%/Sporomorphs)	poor (%/Sporomorphs)		good (%/Spores)	moderate (%/Spores)	poor (%/Spores)		good (%/Spores)	moderate (%/Spores)	poor (%/Spores)				
W29	853.1	BN	254	24	31	46	52.8	12	32	56	42.9	76	24	0	9.8	0	0	0	0.0	0	0	0	0.0	0	0	0	0.0	0	0	0	0.0	47.2	0.0	47.2
W29	908.4	BN	228	63	34	3	100.0	71	27	2	68.0	45	49	5	32.0	0	0	0	0.0	0	0	0	0.0	0	0	0	0.0	0	0	0	0.0	0.0	0.0	0.0
W29	1001.2	CyM & ME	207	45	40	16	89.9	74	23	3	16.9	38	44	19	72.9	0	0	0	0.0	0	73	27	7.2	0	0	100	1.4	0	67	33	5.8	0.0	0.0	0.0
W29	1121.1	CyM & ME	195	47	45	8	76.9	50	50	0	6.2	47	44	9	70.8	0	0	0	0.0	22	78	0	4.6	0	0	0	0.0	22	78	0	4.6	4.1	9.2	13.3
W29	1133.2	CyM & ME	314	49	30	21	58.3	74	17	9	7.3	39	32	29	39.5	69	31	0	11.5	42	33	25	23.2	64	0	36	3.5	39	39	23	19.7	3.5	3.8	7.3
W29	1267	PE	224	42	39	19	96.9	71	18	12	7.6	36	44	20	79.9	71	14	14	9.4	14	43	43	3.1	33	0	67	1.3	0	75	25	1.8	0.0	0.0	0.0
W29	1268.5	PE	230	10	52	37	46.5	21	79	0	16.5	0	38	63	27.8	60	40	0	2.2	0	0	0	0.0	0	0	0	0.0	0	0	0	0.0	3.5	50.0	53.5

Well	TVD (m)	Stratigraphy	Preservation of Phytoplancton			Phytoplancton %/ total OM	Preservation of Prasinophytes			Prasinophytes %/ total OM	Preservation of Acritarchs			Acritarchs %/ total OM	Preservation of Dinoflagellate cysts			Dinoflagellate cysts %/ total OM	Preservation of Leiospheres			Leiospheres %/ total OM	Preservation of Lacustrine Algae			Lacustrine Algae %/ total OM	Foraminifera %/ total OM	Fungi %/ total OM	Terr Comp. % / total OM	Marine Comp. % / total OM	terr. palynomorphs/ total OM	marine palynomorphs/ total OM
			good (%/Phytoplancton)	moderate (%/Phytoplancton)	poor (%/Phytoplancton)		good (%/Pras.)	moderate (%/Pras.)	poor (%/Pras.)		good (%/Acritarchs)	moderate (%/Acritarchs)	poor (%/Acritarchs)		good (%/Dino.)	moderate (%/Dino.)	poor (%/Dino.)		good (%/Leiospheres)	moderate (%/Leiospheres)	poor (%/Leiospheres)		good (%/Lac. Algae)	moderate (%/Lac. Algae)	poor (%/Lac. Algae)							
W29	853.1	BN	0	0	0	0.0	0	0	0	0.0	0	0	0	0.0	0	0	0	0.0	0	0	0	0.0	0	0	0	0.0	0.0	0.0	100.0	0.0	0.0	0.0
W29	908.4	BN	0	0	0	0.0	0	0	0	0.0	0	0	0	0.0	0	0	0	0.0	0	0	0	0.0	0	0	0	0.0	0.0	0.0	100.0	0.0	0.0	0.0
W29	1001.2	CyM & ME	0	33	67	2.9	0	0	0	0.0	0	100	0	1.0	0	0	100	1.9	0	0	0	0.0	0	0	0	0.0	0.0	0.0	97.1	2.9	7.2	2.9
W29	1121.1	CyM & ME	70	0	30	5.1	0	0	0	0.0	0	0	0	0.0	70	0	30	5.1	0	0	0	0.0	0	0	0	0.0	0.0	0.0	85.6	14.4	4.6	5.1
W29	1133.2	CyM & ME	59	31	9	10.2	100	0	0	0.3	56	25	19	5.1	60	40	0	4.8	0	0	0	0.0	100	0	0	1.0	0.0	0.0	85.0	14.0	23.2	10.2
W29	1267	PE	0	0	0	0.0	0	0	0	0.0	0	0	0	0.0	0	0	0	0.0	0	0	0	0.0	0	0	0	0.0	0.0	0.0	100.0	0.0	3.1	0.0
W29	1268.5	PE	0	0	0	0.0	0	0	0	0.0	0	0	0	0.0	0	0	0	0.0	0	0	0	0.0	0	0	0	0.0	0.0	0.0	50.0	50.0	0.0	0.0

Well	TVD (m)	Stratigraphy	# of particels	Preservation of Phytoclasts			Phytoclasts%/ total OM	Preservation of Inertinite			Inertinite %/ total OM	Preservation of Vitrinite			Vitrinite %/ total OM	Preservation of Cutinite			Cutinite %/ total OM	Preservation of Sporomorphs			Sporomorphs %/ total OM	Preservation of Spores			Spores %/ total OM	Preservation of Pollen			Pollen %/ total OM	terr. AOM %/ total OM	marine AOM %/ total OM	total AOM %/ total OM
				good (%/Phytoclasts)	moderate (%/Phytoclasts)	poor (%/Phytoclasts)		good (%/Inertinite)	moderate (%/Inertinite)	poor (%/Inertinite)		good (%/Vitrinite)	moderate (%/Vitrinite)	poor (%/Vitrinite)		good (%/Cutinite)	moderate (%/Cutinite)	poor (%/Cutinite)		good (%/Sporomorphs)	moderate(%/Sporomorphs)	poor (%/Sporomorphs)		good (%/Spores)	moderate (%/Spores)	poor (%/Spores)		good (%/Spores)	moderate (%/Spores)	poor (%/Spores)				
W31	2646.8	UPE	290	8	46	45	82.4	37	63	0	6.6	10	46	44	45.2	0	44	56	30.7	0	55	45	3.8	0	75	25	2.8	0	0	100	1.0	13.8	0.0	13.8
W31	2646.9	UPE	205	0	20	80	85.9	0	100	0	2.9	0	18	82	82.9	0	0	0	0.0	0	50	50	2.0	0	50	50	2.0	0	0	0	0.0	10.7	0.0	10.7
W31	2687.9	MPE	277	21	58	21	25.6	50	50	0	9.4	4	62	33	16.2	0	0	0	0.0	0	5	95	44.4	0	0	100	12.3	0	7	93	32.1	19.1	0.0	19.1
W31	2752.5	MPE	240	63	29	8	100.0	68	23	9	91.7	0	100	0	8.3	0	0	0	0.0	0	0	0	0.0	0	0	0	0.0	0	0	0	0.0	0.0	0.0	0.0
W31	2767.0	LPE	224	5	41	54	57.1	0	100	0	4.0	15	33	52	20.5	0	38	62	32.6	0	17	83	8.0	0	17	83	8.0	0	0	0	0.0	34.8	0.0	34.8
W31	2767.8	LPE	265	1	35	63	63.0	0	0	0	0.0	6	53	41	12.1	0	31	69	50.9	10	25	65	19.2	17	17	66	10.9	0	36	64	8.3	17.7	0.0	17.7
W31	2768.0	LPE	296	2	51	47	64.5	0	0	0	0.0	0	53	47	17.2	3	51	46	47.3	0	48	52	10.5	0	65	35	7.8	0	0	100	2.7	22.6	0.0	22.6
W31	2768.4	LPE	314	16	43	40	78.7	100	0	0	3.8	24	40	36	36.9	0	51	49	37.9	0	33	67	1.9	0	33	67	1.9	0	0	0	0.0	11.1	4.5	15.6

Well	TVD (m)	Stratigraphy	Preservation of Phytoplancton			Phytoplancton %/ total OM	Preservation of Prasinophytes			Prasinophytes %/ total OM	Preservation of Acritarchs			Acritarchs %/ total OM	Preservation of Dinoflagellate cysts			Dinoflagellate cysts %/ total OM	Preservation of Leiospheres			Leiospheres %/ total OM	Preservation of Lacustrine Algae			Lacustrine Algae %/ total OM	Foraminifera %/ total OM	Fungi %/ total OM	Terr Comp. % / total OM	Marine Comp. % / total OM	terr. palynomorphs/ total OM	marine palynomorphs/ total OM
			good (%/Phytoplancton)	moderate (%/Phytoplancton)	poor (%/Phytoplancton)		good (%/Pras.)	moderate (%/Pras.)	poor (%/Pras.)		good (%/Acritarchs)	moderate (%/Acritarchs)	poor (%/Acritarchs)		good (%/Dino.)	moderate (%/Dino.)	poor (%/Dino.)		good (%/Leiospheres)	moderate (%/Leiospheres)	poor (%/Leiospheres)		good (%/Lac. Algae)	moderate (%/Lac. Algae)	poor (%/Lac. Algae)							
W31	2646.8	UPE	0	0	0	0.0	0	0	0	0.0	0	0	0	0.0	0	0	0	0.0	0	0	0	0.0	0	0	0	0.0	0.0	0.0	100.0	0.0	3.8	0.0
W31	2646.9	UPE	0	0	100	1.5	0	0	0	0.0	0	0	0	0.0	0	0	100	1.5	0	0	0	0.0	0	0	0	0.0	0.0	0.0	98.5	1.5	2.0	1.5
W31	2687.9	MPE	0	0	100	10.8	0	0	0	0.0	0	0	100	7.2	0	0	100	3.2	0	0	100	0.4	0	0	0	0.0	0.0	0.0	89.2	10.8	44.4	10.8
W31	2752.5	MPE	0	0	0	0.0	0	0	0	0.0	0	0	0	0.0	0	0	0	0.0	0	0	0	0.0	0	0	0	0.0	0.0	0.0	100.0	0.0	0.0	0.0
W31	2767.0	LPE	0	0	0	0.0	0	0	0	0.0	0	0	0	0.0	0	0	0	0.0	0	0	0	0.0	0	0	0	0.0	0.0	0.0	100.0	0.0	8.0	0.0
W31	2767.8	LPE	0	0	0	0.0	0	0	0	0.0	0	0	0	0.0	0	0	0	0.0	0	0	0	0.0	0	0	0	0.0	0.0	0.0	100.0	0.0	19.2	0.0
W31	2768.0	LPE	0	43	57	2.4	0	100	0	1.0	0	0	0	0.0	0	0	100	1.4	0	0	0	0.0	0	0	0	0.0	0.0	0.0	97.6	2.4	10.5	2.4
W31	2768.4	LPE	0	0	100	3.8	0	0	0	0.0	0	0	100	3.8	0	0	0	0.0	0	0	0	0.0	0	0	0	0.0	0.0	0.0	91.7	8.3	1.9	3.8

Well	TVD (m)	Stratigraphy	# of particels	Preservation of Phytoclasts			Phyclasts%/ total OM	Preservation of Inertinite			Inertinite %/ total OM	Preservation of Vitrinite			Vitrinite %/ total OM	Preservation of Cutinite			Cutinite %/ total OM	Preservation of Sporomorphs			Sporomorphs %/ total OM	Preservation of Spores			Spores %/ total OM	Preservation of Pollen			Pollen %/ total OM	terr. AOM %/ total OM	marine AOM %/ total OM	total AOM %/ total OM
				good (%/Phytoclasts)	moderate (%/Phytoclasts)	poor (%/Phytoclasts)		good (%/Inertinite)	moderate (%/Inertinite)	poor (%/Inertinite)		good (%/Vitrinite)	moderate (%/Vitrinite)	poor (%/Vitrinite)		good (%/Cutinite)	moderate (%/Cutinite)	poor (%/Cutinite)		good (%/Sporomorphs)	moderate(%/Sporomorphs)	poor (%/Sporomorphs)		good (%/Spores)	moderate (%/Spores)	poor (%/Spores)		good (%/Spores)	moderate (%/Spores)	poor (%/Spores)				
W35	2314.0	CyM	265	20	37	43	54.0	100	0	0	2.3	21	39	40	41.5	0	37	63	10.2	0	67	33	9.1	0	54	46	4.9	0	82	18	4.2	18.5	0.0	18.5
W35	2515.0	UPE	292	18	35	48	64.0	71	29	0	5.8	15	40	44	46.6	0	15	85	11.6	0	30	70	11.3	0	37	63	6.5	0	21	79	4.8	15.4	0.0	15.4
W35	2516.2	UPE	261	21	42	37	74.7	60	40	0	3.8	19	42	39	70.9	0	0	0	0.0	0	0	0	0.0	0	0	0	0.0	0	0	0	0.0	25.3	0.0	25.3
W35	2623.3	LPE	297	17	37	46	85.2	47	53	0	5.1	19	31	50	46.8	9	43	47	33.3	0	0	0	0.0	0	0	0	0.0	0	0	0	0.0	14.8	0.0	14.8
W35	2625.0	LPE	216	10	26	63	66.7	43	57	0	3.2	11	31	59	51.4	0	0	100	12.0	0	0	100	1.9	0	0	100	1.9	0	0	0	0.0	31.5	0.0	31.5

Well	TVD (m)	Stratigraphy	Phytoplancton %/ total OM	Preservation of Phytoplancton			Prasinophytes %/ total OM	Preservation of Prasinophytes			Acritarchs %/ total OM	Preservation of Acritarchs			Dinoflagellate cysts %/ total OM	Preservation of Dinoflagellate cysts			Leiospheres %/ total OM	Preservation of Leiospheres			Lacustrine Algae %/ total OM	Preservation of Lacustrine Algae			Foraminifera %/ total OM	Fungi %/ total OM	Terr Comp. % / total OM	Marine Comp. % / total OM	terr. palynomorphs/ total OM	marine palynomorphs/ total OM
				good (%/Phytoplancton)	moderate (%/Phytoplancton)	poor (%/Phytoplancton)		good (%/Pras.)	moderate (%/Pras.)	poor (%/Pras.)		good (%/Acritarchs)	moderate (%/Acritarchs)	poor (%/Acritarchs)		good (%/Dino.)	moderate (%/Dino.)	poor (%/Dino.)		good (%/Leiospheres)	moderate (%/Leiospheres)	poor (%/Leiospheres)		good (%/Lac. Algae)	moderate (%/Lac. Algae)	poor (%/Lac. Algae)						
W35	2314.0	CyM	14	35	51	18.5	0	0	0	0.0	0	40	60	3.8	18	33	49	14.7	0	0	0	0.0	0	0	0	0.0	0.0	81.5	18.5	9.1	18.5
W35	2515.0	UPE	22	22	56	9.2	0	0	0	0.0	0	0	100	1.0	0	30	40	6.8	0	0	100	1.4	0	0	0	0.0	0.0	90.8	9.2	11.3	9.2
W35	2516.2	UPE	0	0	0	0.0	0	0	0	0.0	0	0	0	0.0	0	0	0	0.0	0	0	0	0.0	0	0	0	0.0	0.0	100.0	0.0	0.0	0.0
W35	2623.3	LPE	0	0	0	0.0	0	0	0	0.0	0	0	0	0.0	0	0	0	0.0	0	0	0	0.0	0	0	0	0.0	0.0	100.0	0.0	0.0	0.0
W35	2625.0	LPE	0	0	0	0.0	0	0	0	0.0	0	0	0	0.0	0	0	0	0.0	0	0	0	0.0	0	0	0	0.0	0.0	100.0	0.0	1.9	0.0

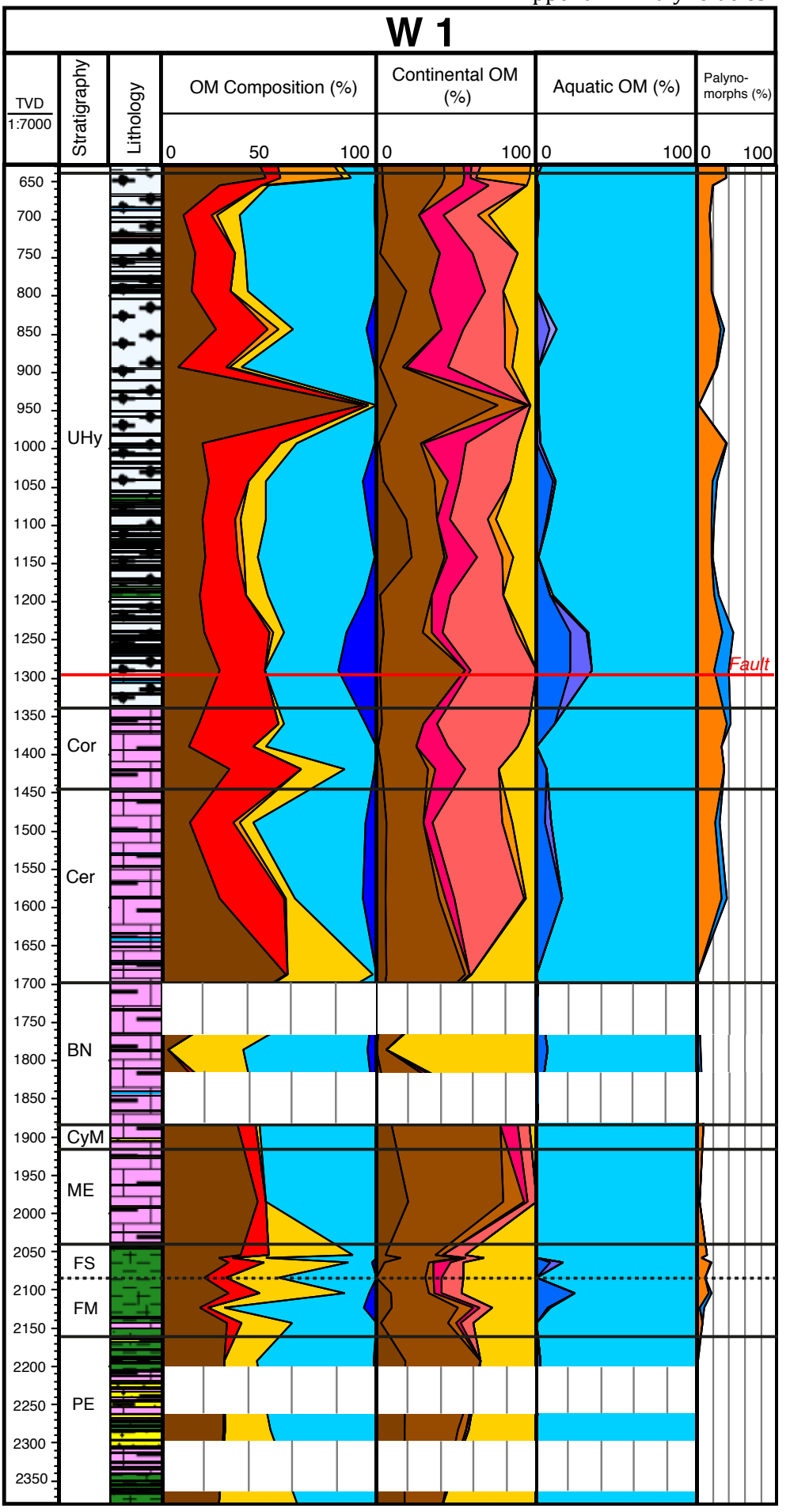
W 1
TVD
1:7000
Stratigraphy
Lithology
OM Composition (%)
0
50
100
Continental OM (%)
0
100
Aquatic OM (%)
0
100
Palyno-morphs (%)
0
100
650
700
750
800
850
900
950
1000
1050
1100
1150
1200
1250
1300
1350
1400
1450
1500
1550
1600
1650
1700
1750
1800
1850
1900
1950
2000
2050
2100
2150
2200
2250
2300
2350
UHy
Cor
Cer
BN
CyM
ME
FS
FM
PE
Fault

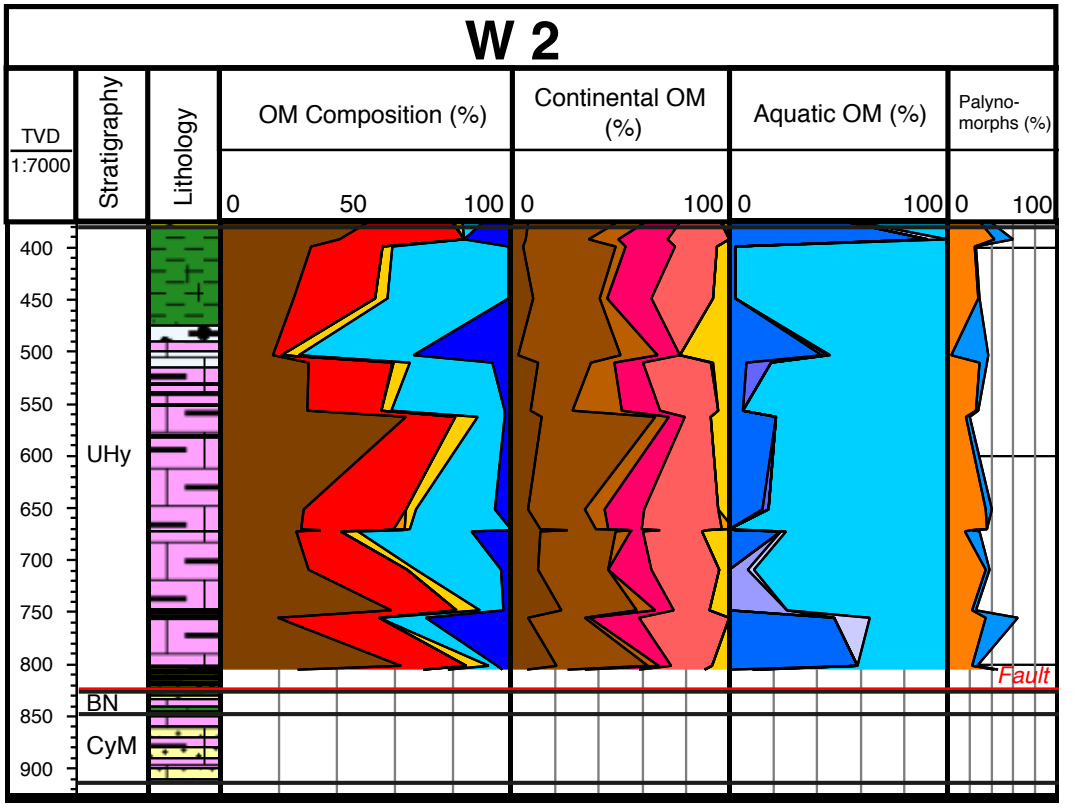

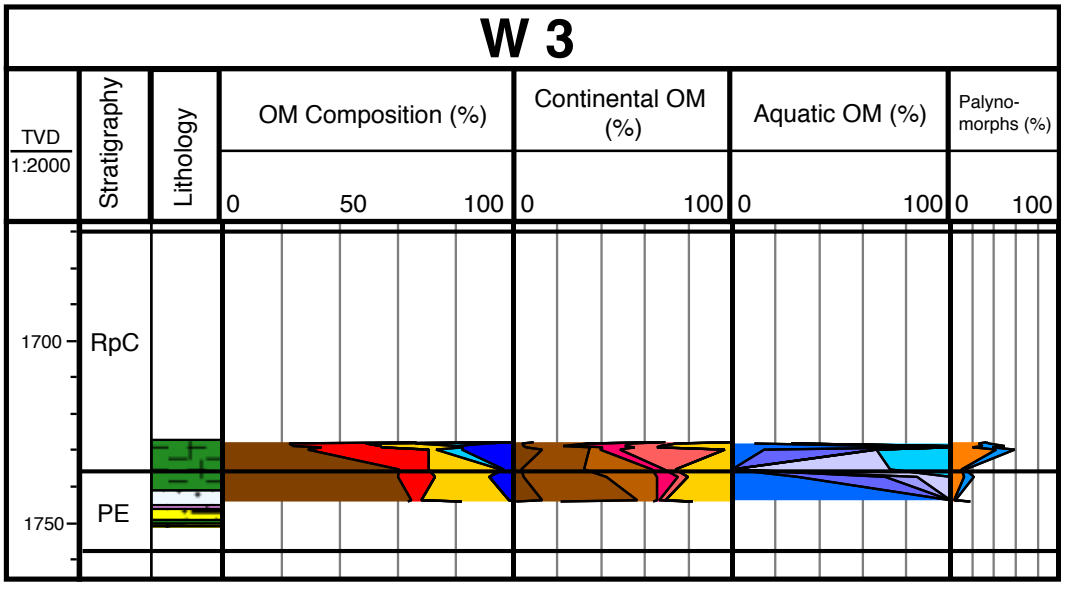

TVD	Strati-graphy	Lithology	OM composition (100%)	Continental components	Aquatic components	Palynomorphs (aquatic, continental)
m (BGL)			% / total OM	% / continental OM	% / aquatic OM	% / total OM
			Phytoclasts	Inertinite	Dinoflaggelate cysts	Continental palynomorphs
			Sporomorphs	Vitrinite	Acritarcs	Aquatic palynomorphs
			Lacustrine algae	Cutinite	Prasinophytes	
			Terrestrial AOM	Spores	Leiospheres	
			Brackish-marine AOM	Pollen	Brackish-marine AOM	
			Phytoplankton	Lacustrine algae		
				Terrestrial AOM		

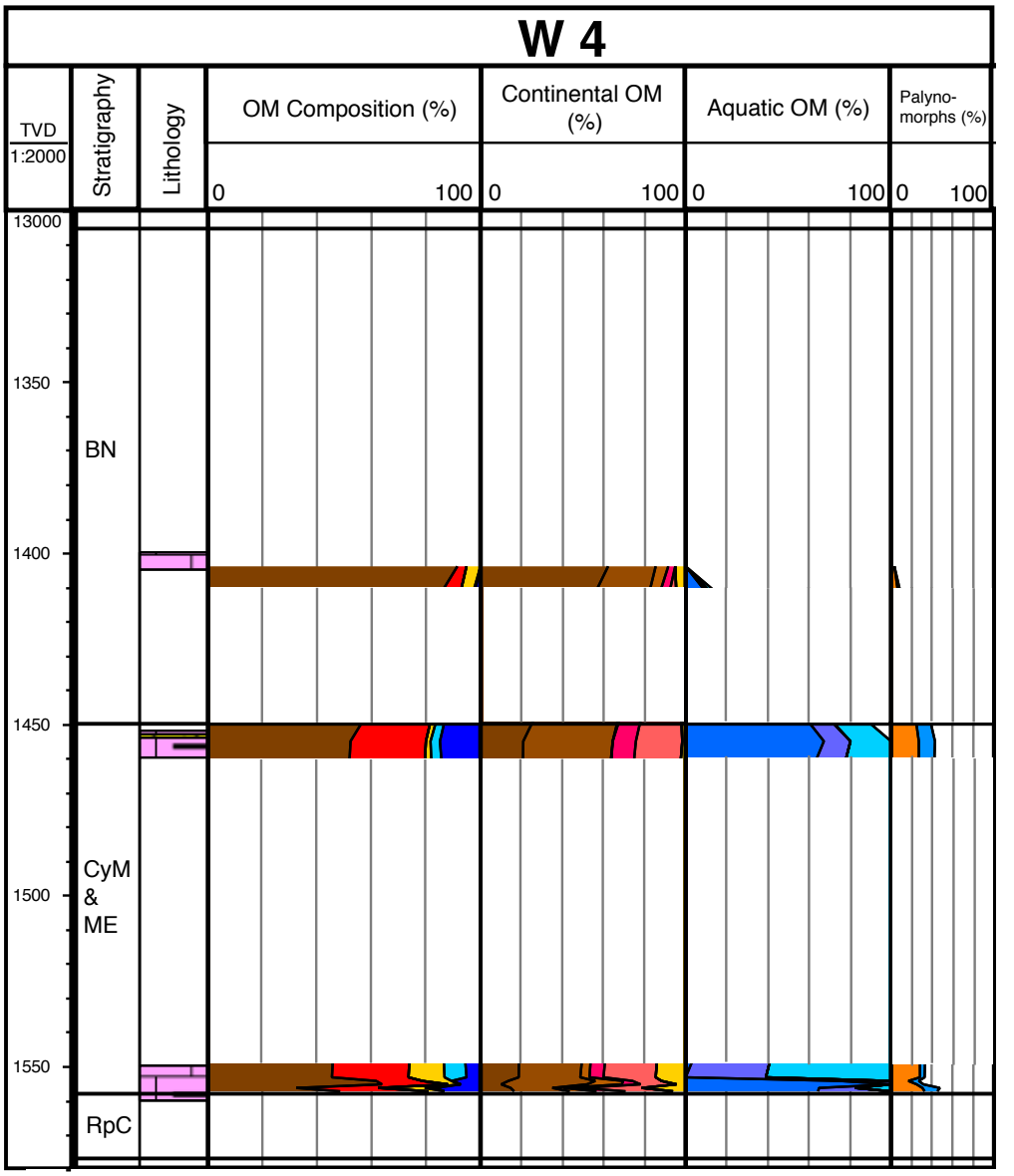
W 4
TVD
1:2000
Stratigraphy
Lithology
OM Composition (%)
Continental OM (%)
Aquatic OM (%)
Palyno-morphs (%)
0
100
13000
1350
1400
1450
1500
1550
BN
CyM & ME
RpC

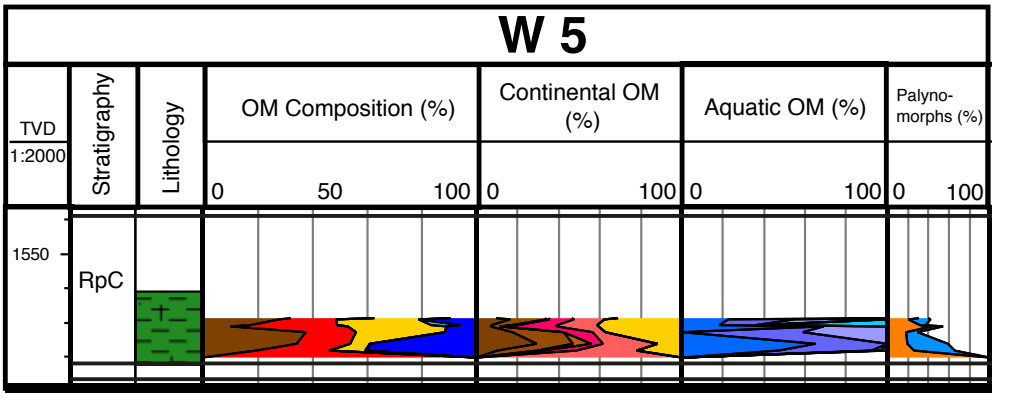
W 5
TVD
1:2000
Stratigraphy
Lithology
OM Composition (%)
Continental OM (%)
Aquatic OM (%)
Palyno-morphs (%)
0
50
100
1550
RpC

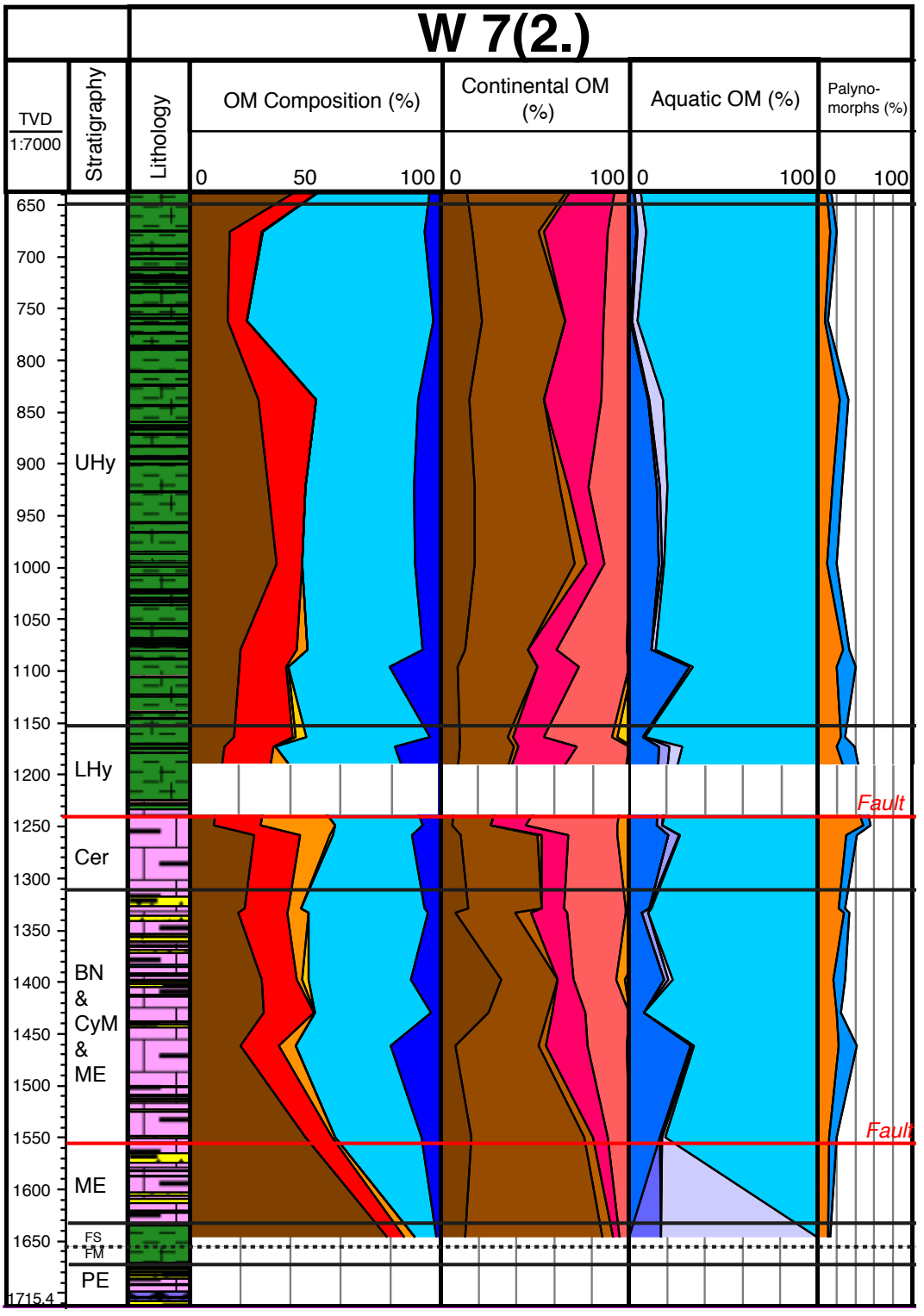

TVD	Strati-graphy	Lithology	OM composition (100%)	Continental components	Aquatic components	Palynomorphs (aquatic, continental)
m (BGL)			% / total OM	% / continental OM	% / aquatic OM	% / total OM
			Phytoclasts	Inertinite	Dinoflaggelate cysts	Continental palynomorphs
			Sporomorphs	Vitrinite	Acritarcs	Aquatic palynomorphs
			Lacustrine algae	Cutinite	Prasinophytes	
			Terrestrial AOM	Spores	Leiospheres	
			Brackish-marine AOM	Pollen	Brackish-marine AOM	
			Phytoplankton	Lacustrine algae		
				Terrestrial AOM		

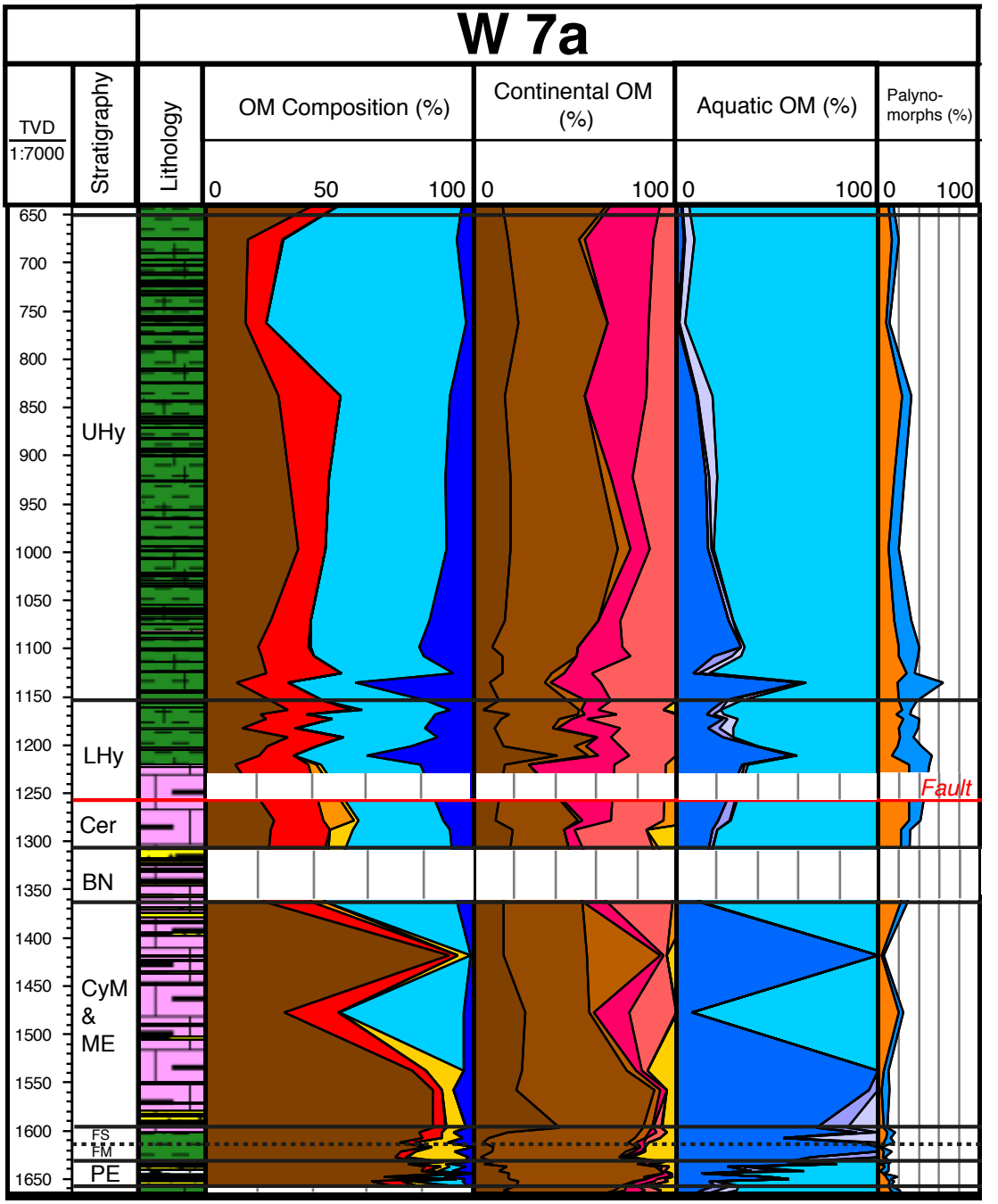
W 7a
TVD
1:7000
Stratigraphy
Lithology
OM Composition (%)
Continental OM (%)
Aquatic OM (%)
Palyno-morphs (%)
0
50
100
650
700
750
800
850
900
950
1000
1050
1100
1150
1200
1250
1300
1350
1400
1450
1500
1550
1600
1650
UHy
LHy
Cer
BN
CyM & ME
FS
FM
PE
Fault

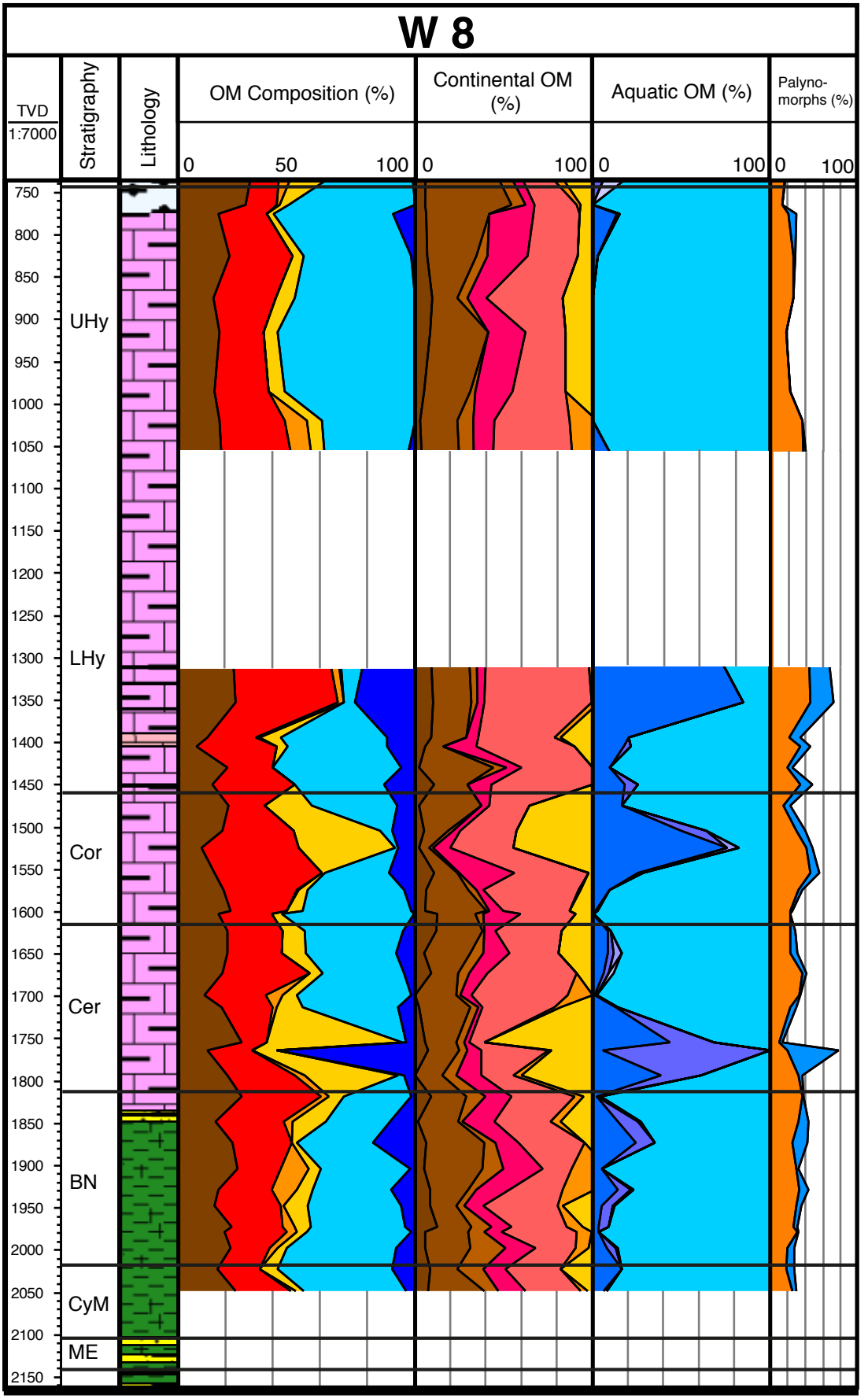
W 8
TVD
1:7000
Stratigraphy
Lithology
OM Composition (%)
0
50
100
Continental OM (%)
0
100
Aquatic OM (%)
0
100
Palyno-morphs (%)
0
100
750
800
850
900
950
1000
1050
1100
1150
1200
1250
1300
1350
1400
1450
1500
1550
1600
1650
1700
1750
1800
1850
1900
1950
2000
2050
2100
2150
UHy
LHy
Cor
Cer
BN
CyM
ME

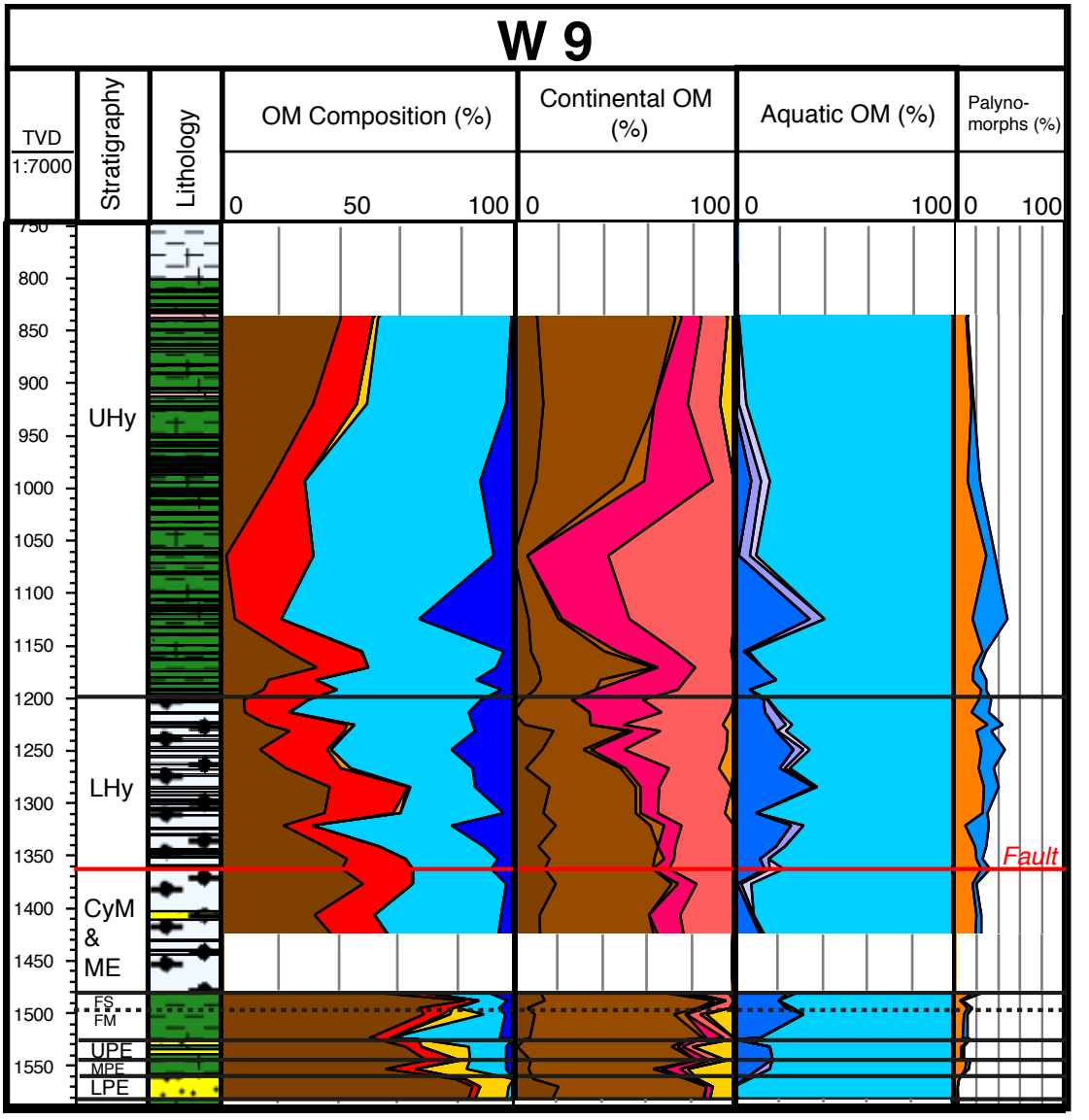

TVD	Strati-graphy	Lithology	OM composition (100%)	Continental components	Aquatic components	Palynomorphs (aquatic, continental)
m (BGL)			% / total OM	% / continental OM	% / aquatic OM	% / total OM
			Phytoclasts	Inertinite	Dinoflaggelate cysts	Continental palynomorphs
			Sporomorphs	Vitrinite	Acritarcs	Aquatic palynomorphs
			Lacustrine algae	Cutinite	Prasinophytes	
			Terrestrial AOM	Spores	Leiospheres	
			Brackish-marine AOM	Pollen	Brackish-marine AOM	
			Phytoplankton	Lacustrine algae		
				Terrestrial AOM		

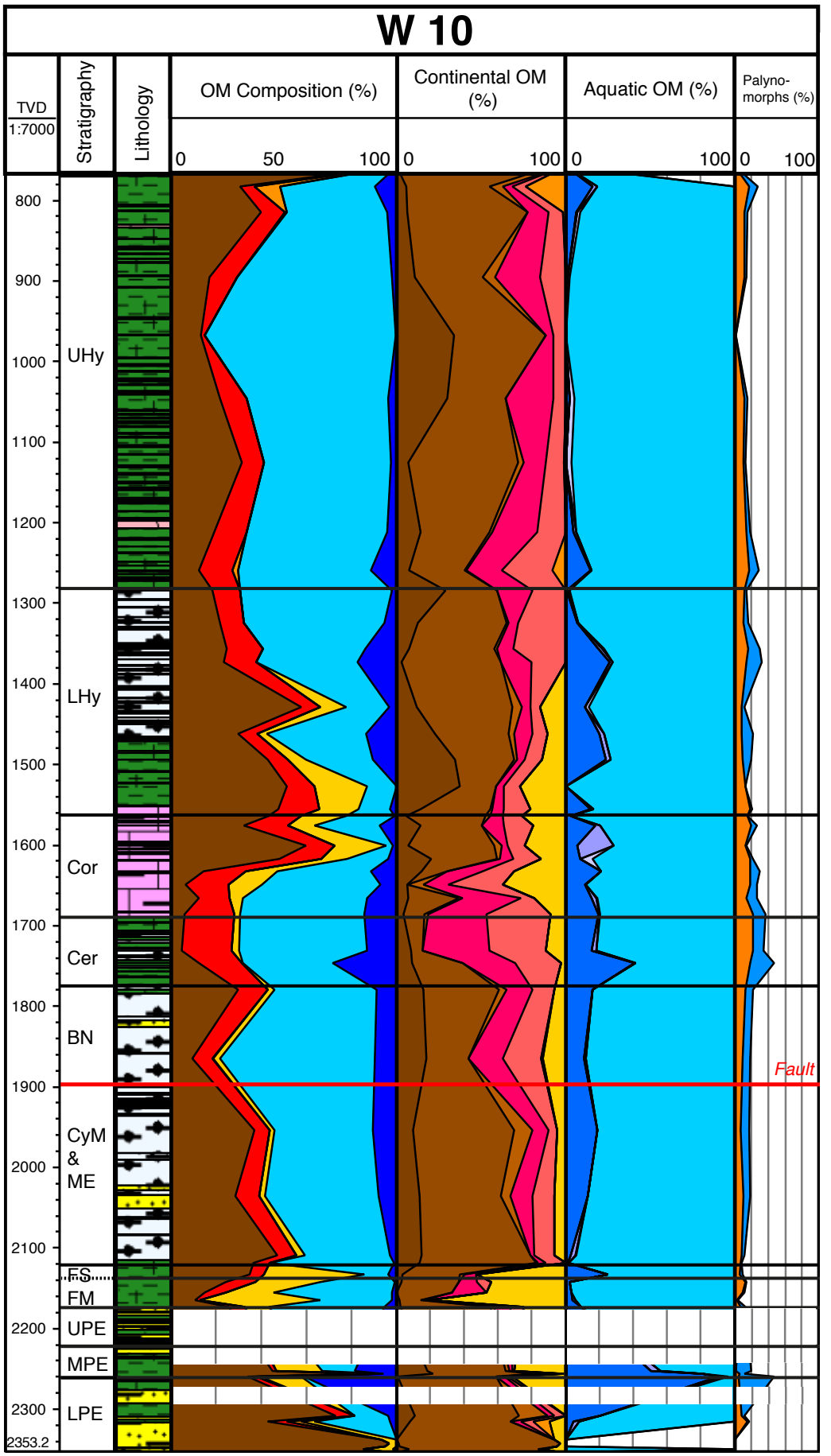
W 10
TVD
1:7000
Stratigraphy
Lithology
OM Composition (%)
0
50
100
Continental OM (%)
0
100
Aquatic OM (%)
0
100
Palyno-morphs (%)
0
100
800
900
1000
1100
1200
1300
1400
1500
1600
1700
1800
1900
2000
2100
2200
2300
2353.2
UHy
LHy
Cor
Cer
BN
CyM & ME
FS
FM
UPE
MPE
LPE
Fault

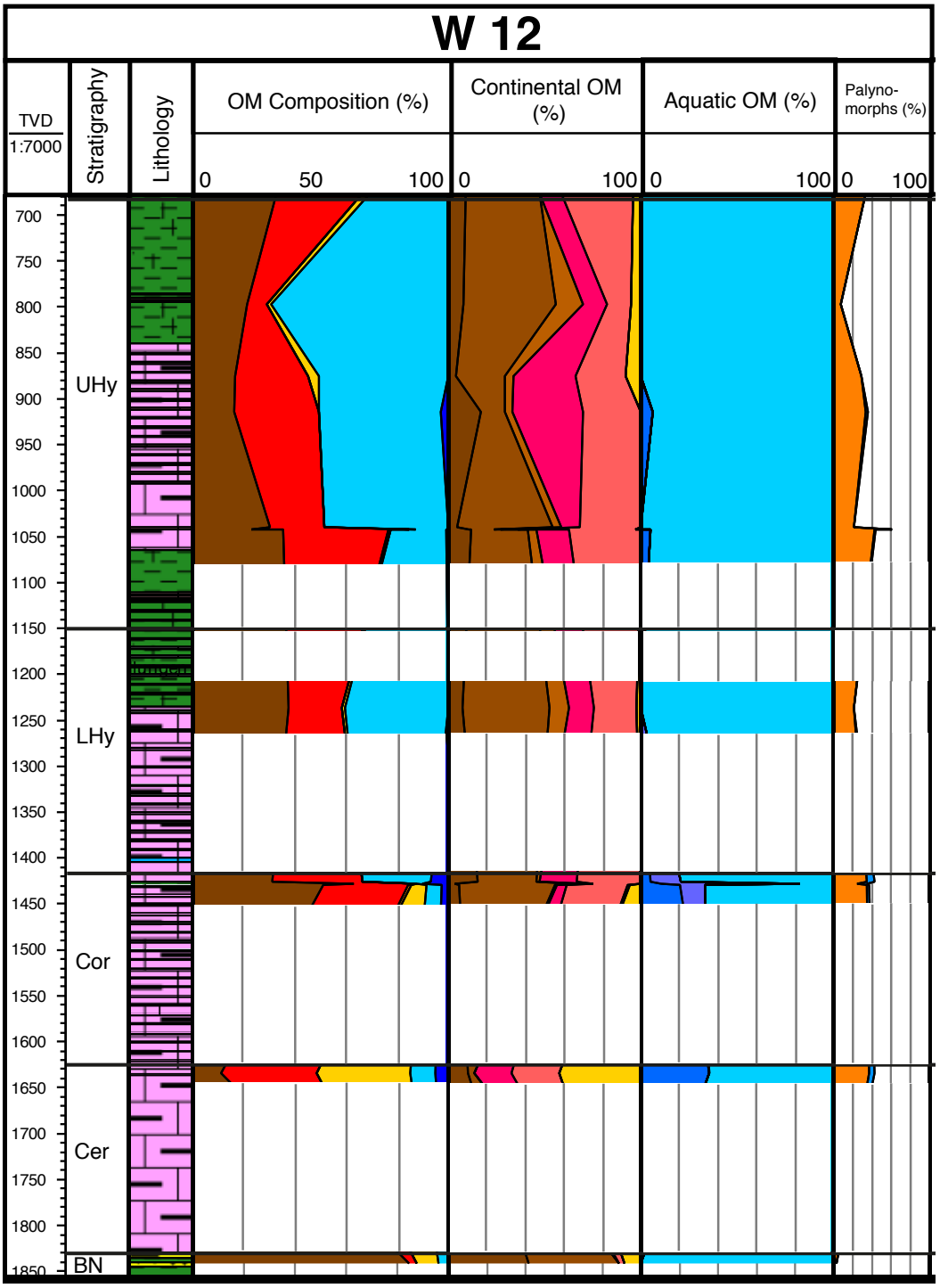

TVD	Strati-graphy	Lithology	OM composition (100%)	Continental components	Aquatic components	Palynomorphs (aquatic, continental)
m (BGL)			% / total OM	% / continental OM	% / aquatic OM	% / total OM
			Phytoclasts	Inertinite	Dinoflaggelate cysts	Continental palynomorphs
			Sporomorphs	Vitrinite	Acritarcs	Aquatic palynomorphs
			Lacustrine algae	Cutinite	Prasinophytes	
			Terrestrial AOM	Spores	Leiospheres	
			Brackish-marine AOM	Pollen	Brackish-marine AOM	
			Phytoplankton	Lacustrine algae		
				Terrestrial AOM		

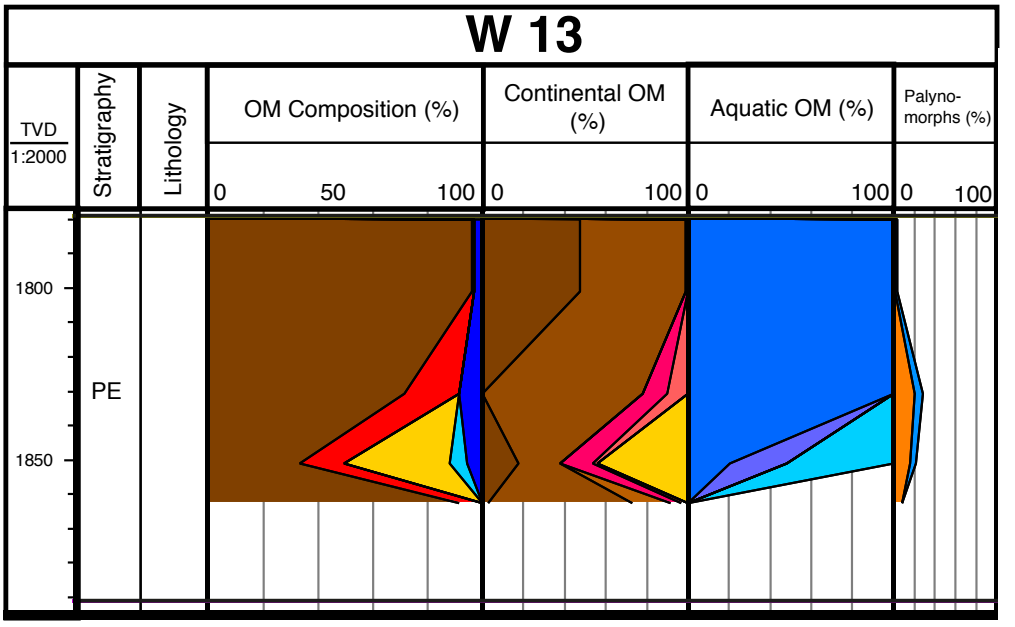
W 13
TVD
1:2000
Stratigraphy
Lithology
OM Composition (%)
Continental OM (%)
Aquatic OM (%)
Palyno-morphs (%)
0
50
100
1800
1850
PE

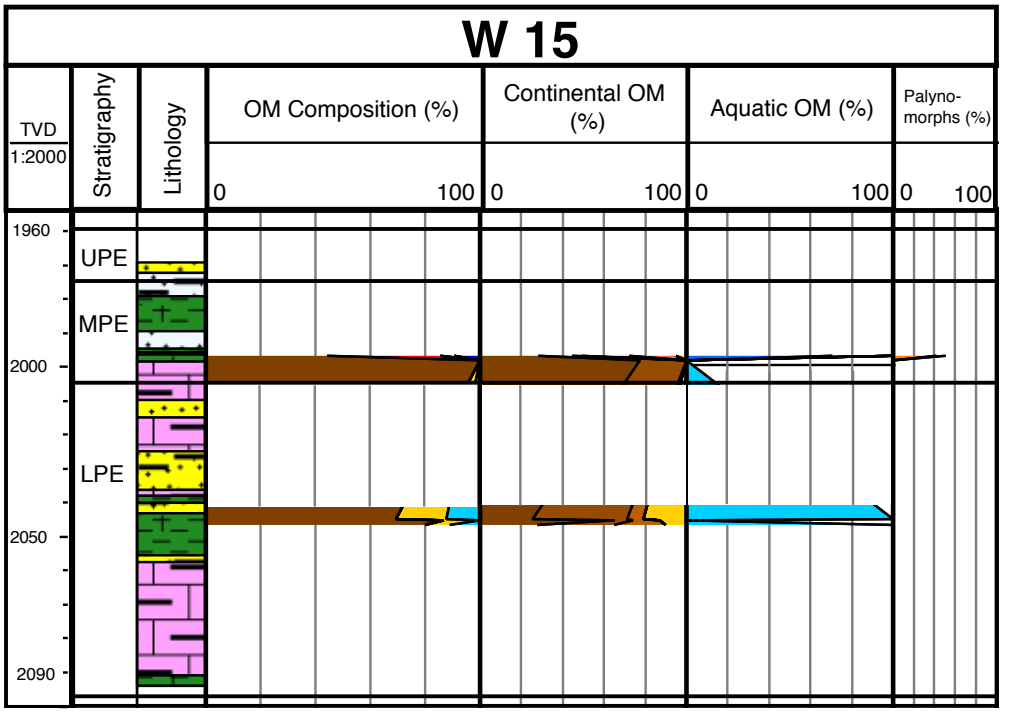
W 15
TVD
1:2000
Stratigraphy
Lithology
OM Composition (%)
Continental OM (%)
Aquatic OM (%)
Palyno-morphs (%)
0
100
1960
2000
2050
2090
UPE
MPE
LPE

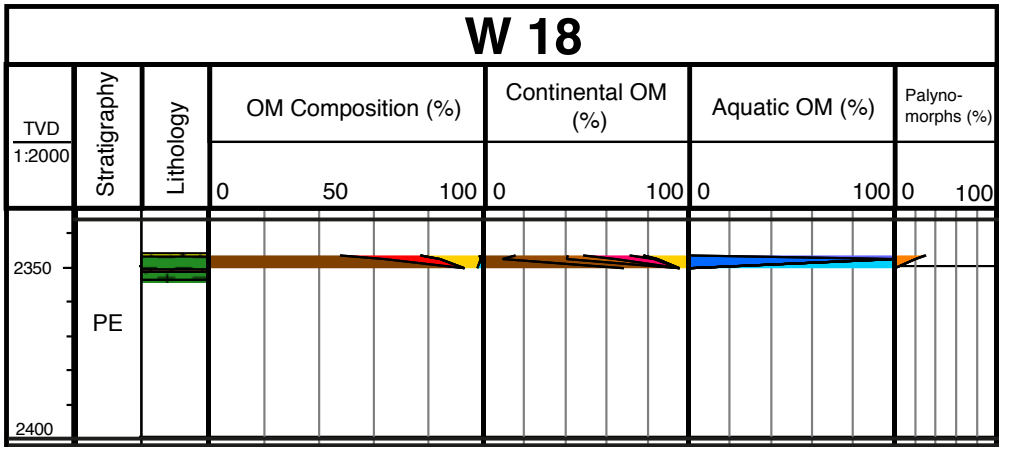
W 18
TVD
1:2000
Stratigraphy
Lithology
OM Composition (%)
Continental OM (%)
Aquatic OM (%)
Palyno-morphs (%)
0
50
100
2350
2400
PE

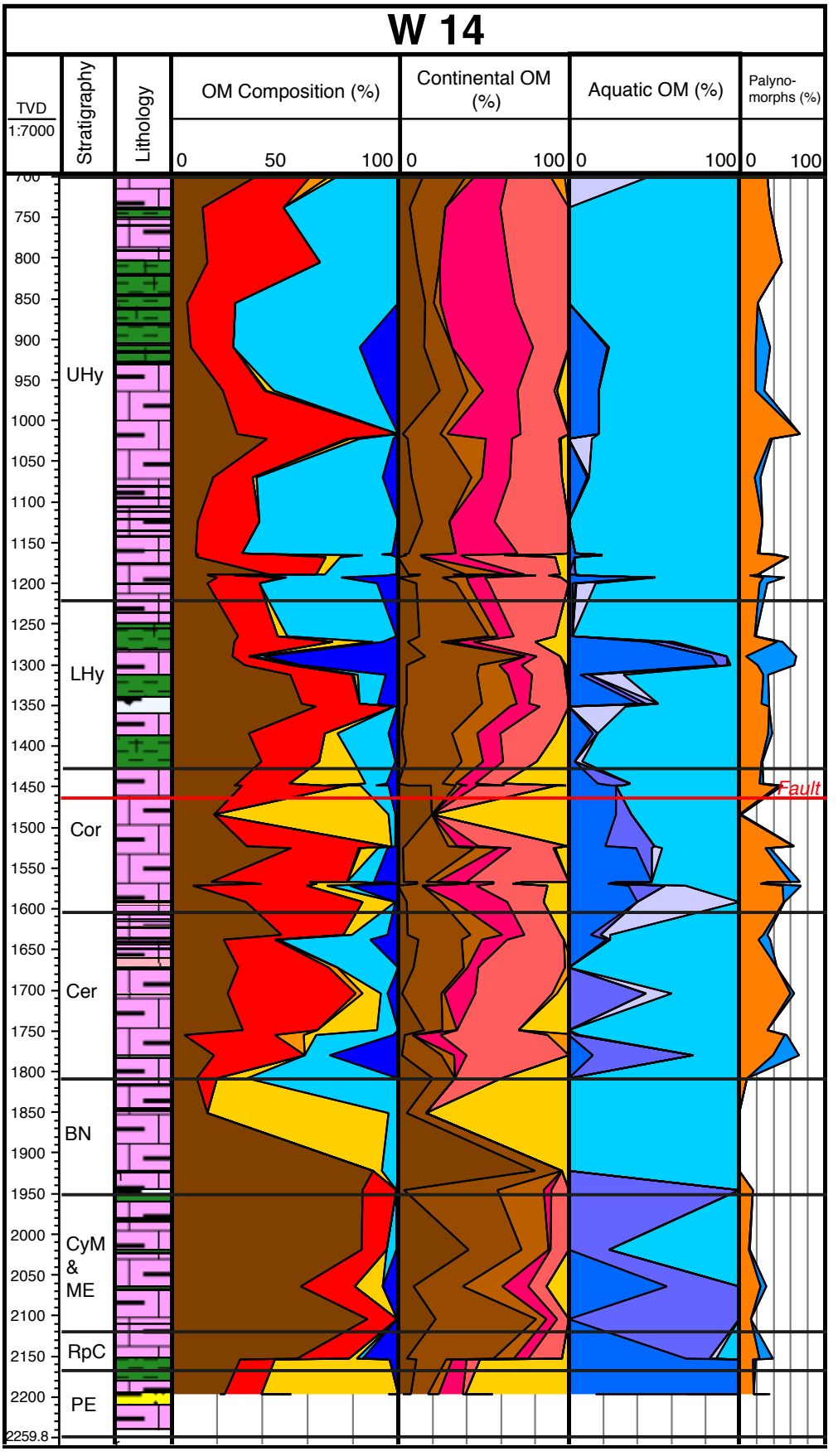
W 14
TVD
1:7000
Stratigraphy
Lithology
OM Composition (%)
0
50
100
Continental OM (%)
0
100
Aquatic OM (%)
0
100
Palyno-morphs (%)
0
100
750
800
850
900
950
1000
1050
1100
1150
1200
1250
1300
1350
1400
1450
1500
1550
1600
1650
1700
1750
1800
1850
1900
1950
2000
2050
2100
2150
2200
2259.8
UHy
LHy
Cor
Cer
BN
CyM & ME
RpC
PE
Fault

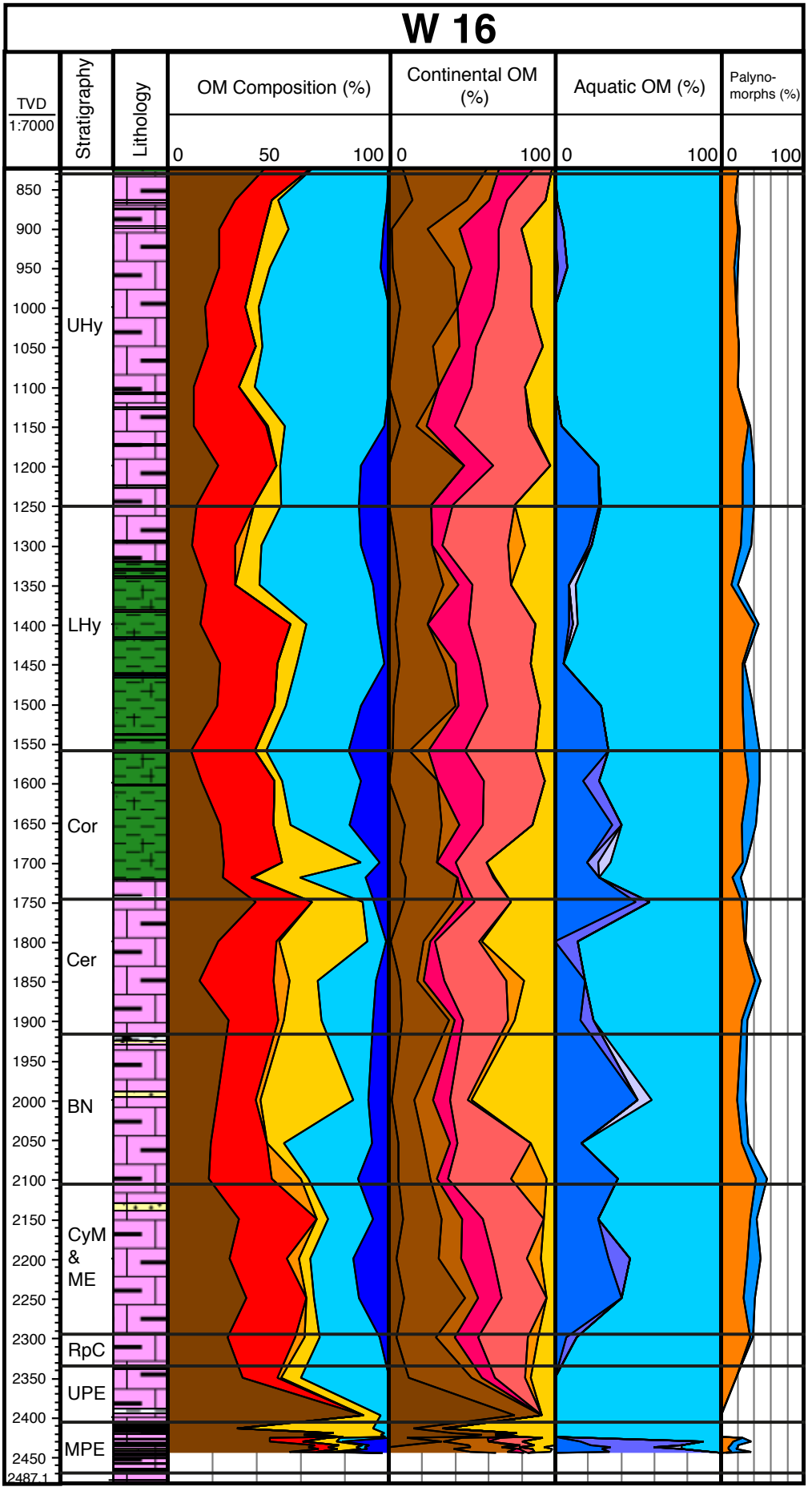
W 16
TVD
1:7000
Stratigraphy
Lithology
OM Composition (%)
0
50
100
Continental OM (%)
0
100
Aquatic OM (%)
0
100
Palyno-morphs (%)
0
100
850
900
950
1000
1050
1100
1150
1200
1250
1300
1350
1400
1450
1500
1550
1600
1650
1700
1750
1800
1850
1900
1950
2000
2050
2100
2150
2200
2250
2300
2350
2400
2450
2487.1
UHy
LHy
Cor
Cer
BN
CyM & ME
RpC
UPE
MPE

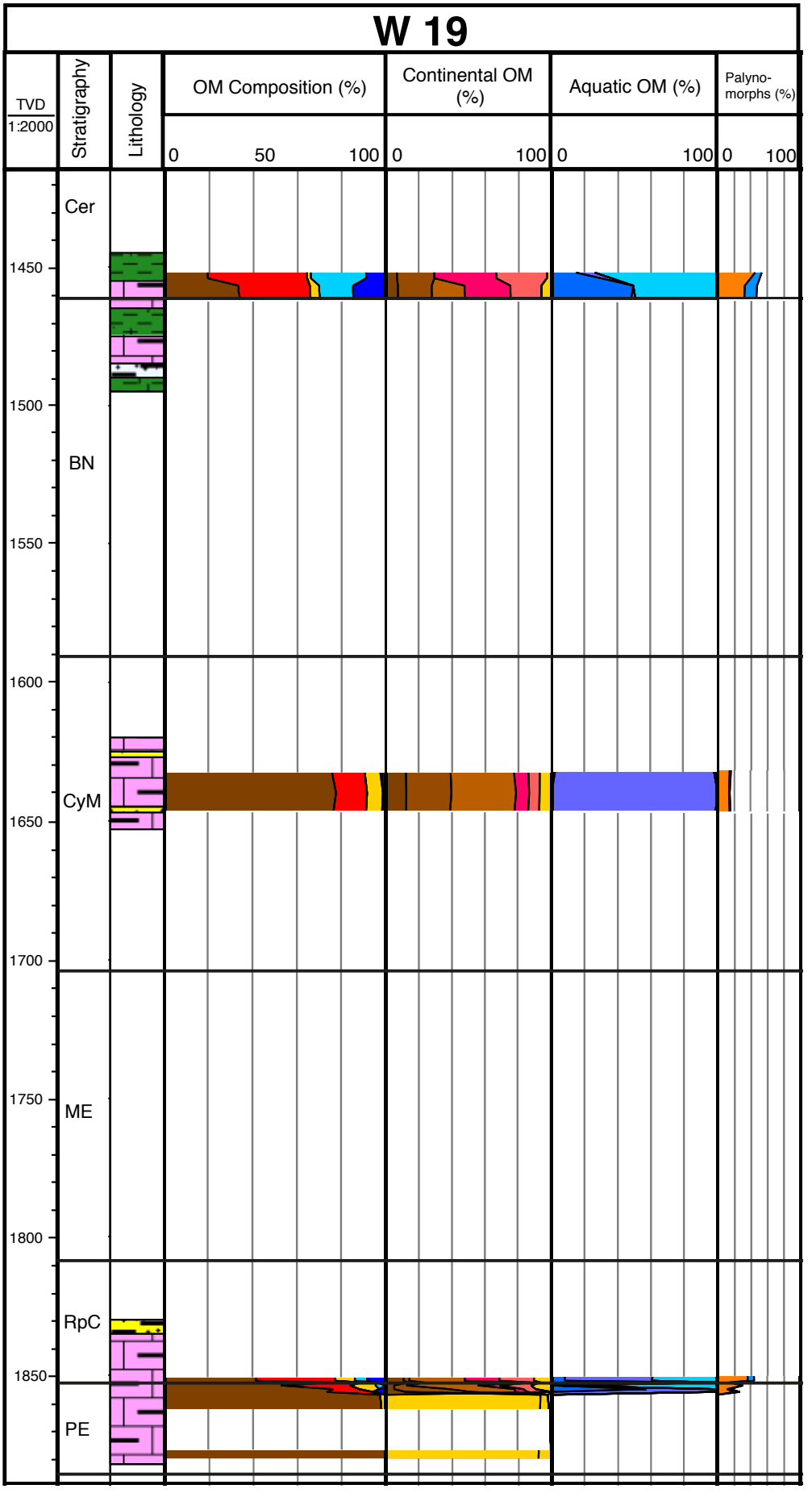
W 19
TVD
1:2000
Stratigraphy
Lithology
OM Composition (%)
0
50
100
Continental OM (%)
0
100
Aquatic OM (%)
0
100
Palyno-morphs (%)
0
100
Cer
BN
CyM
ME
RpC
PE
1450
1500
1550
1600
1650
1700
1750
1800
1850

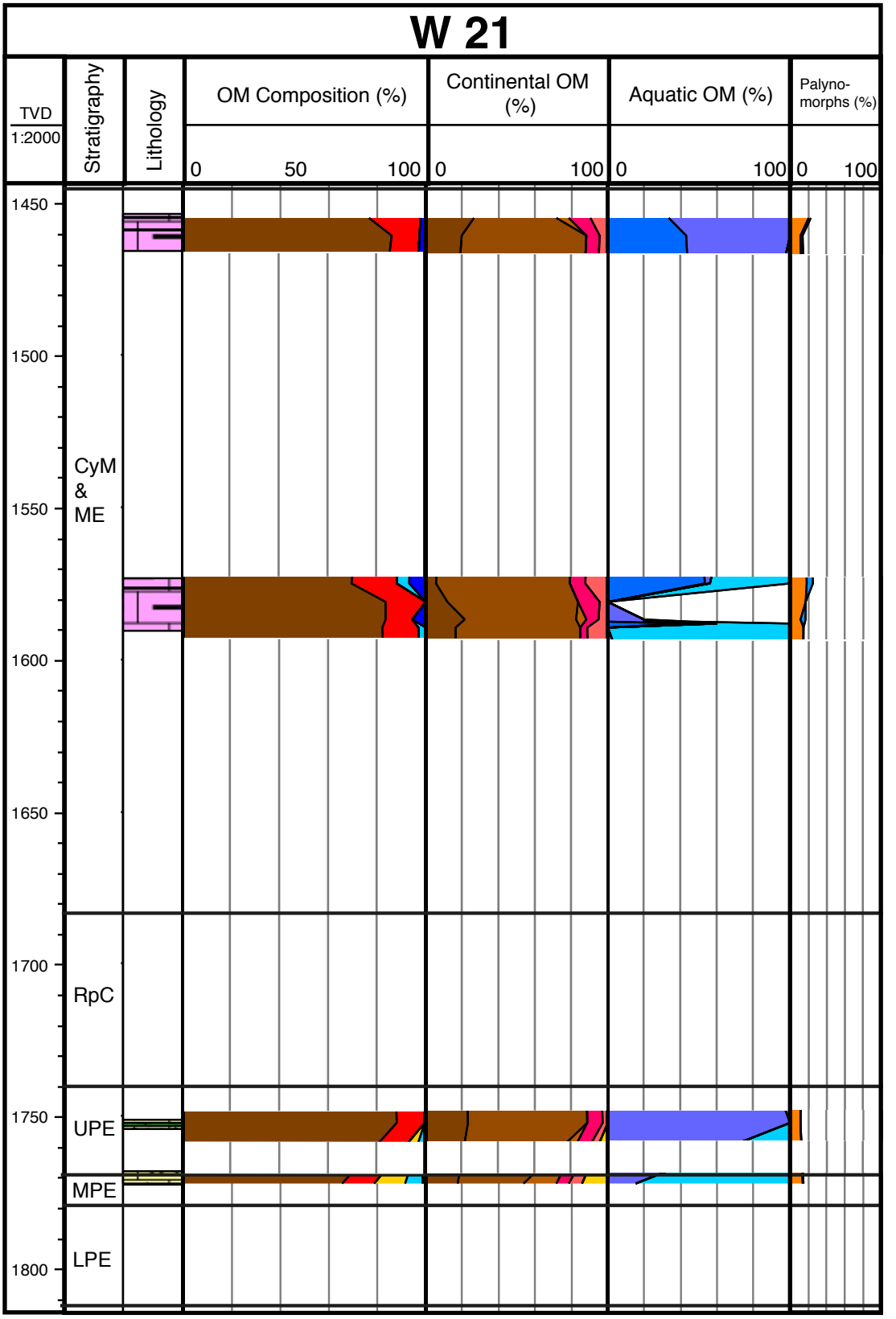
W 21
TVD
1:2000
Stratigraphy
Lithology
OM Composition (%)
Continental OM (%)
Aquatic OM (%)
Palyno-morphs (%)
0
50
100
1450
1500
1550
1600
1650
1700
1750
1800
CyM & ME
RpC
UPE
MPE
LPE

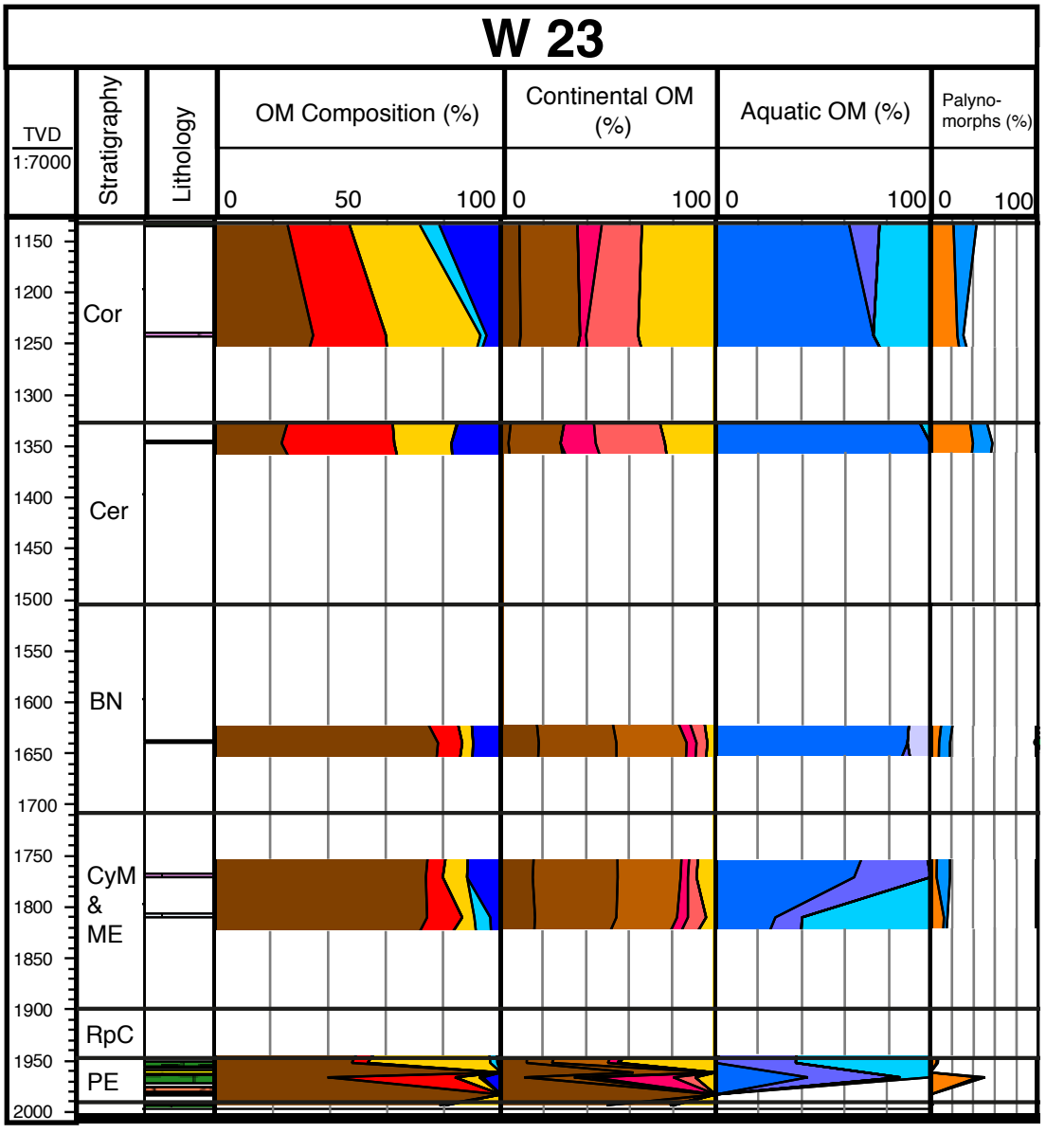

TVD	Strati-graphy	Lithology	OM composition (100%)	Continental components	Aquatic components	Palynomorphs (aquatic, continental)
m (BGL)			% / total OM	% / continental OM	% / aquatic OM	% / total OM
			Phytoclasts	Inertinite	Dinoflaggelate cysts	Continental palynomorphs
			Sporomorphs	Vitrinite	Acritarcs	Aquatic palynomorphs
			Lacustrine algae	Cutinite	Prasinophytes	
			Terrestrial AOM	Spores	Leiospheres	
			Brackish-marine AOM	Pollen	Brackish-marine AOM	
			Phytoplankton	Lacustrine algae		
				Terrestrial AOM		

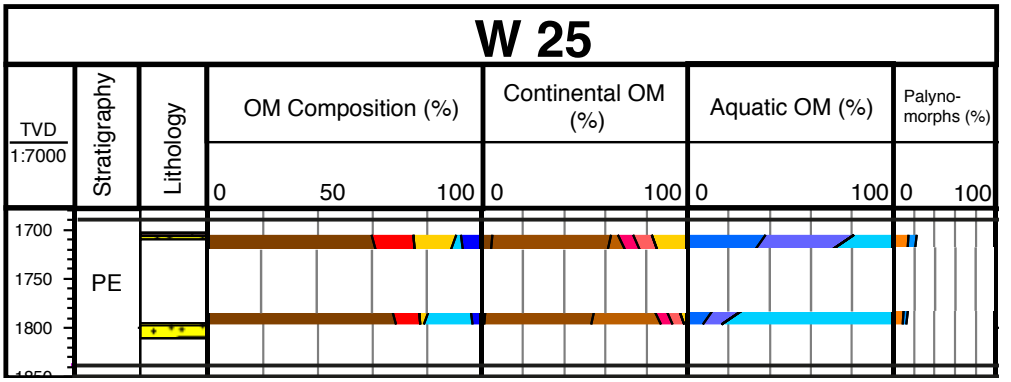

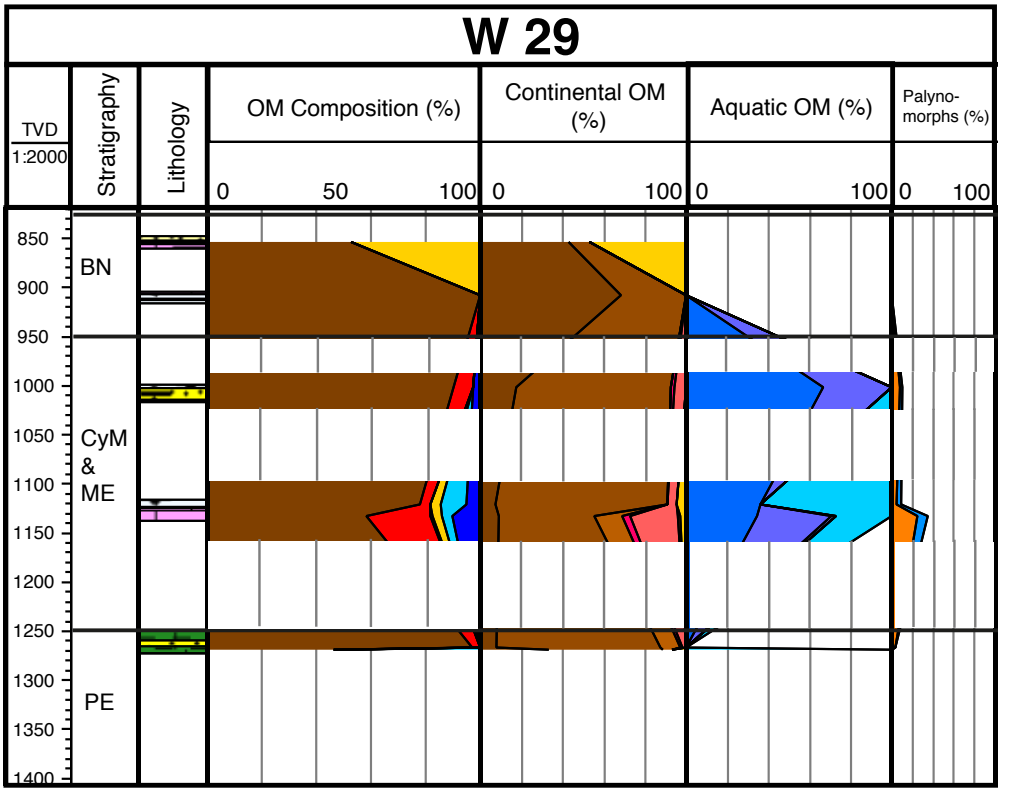

TVD	Strati-graphy	Lithology	OM composition (100%)	Continental components	Aquatic components	Palynomorphs (aquatic, continental)
m (BGL)			% / total OM	% / continental OM	% / aquatic OM	% / total OM
			Phytoclasts	Inertinite	Dinoflaggelate cysts	Continental palynomorphs
			Sporomorphs	Vitrinite	Acritarcs	Aquatic palynomorphs
			Lacustrine algae	Cutinite	Prasinophytes	
			Terrestrial AOM	Spores	Leiospheres	
			Brackish-marine AOM	Pollen	Brackish-marine AOM	
			Phytoplankton	Lacustrine algae		
				Terrestrial AOM		

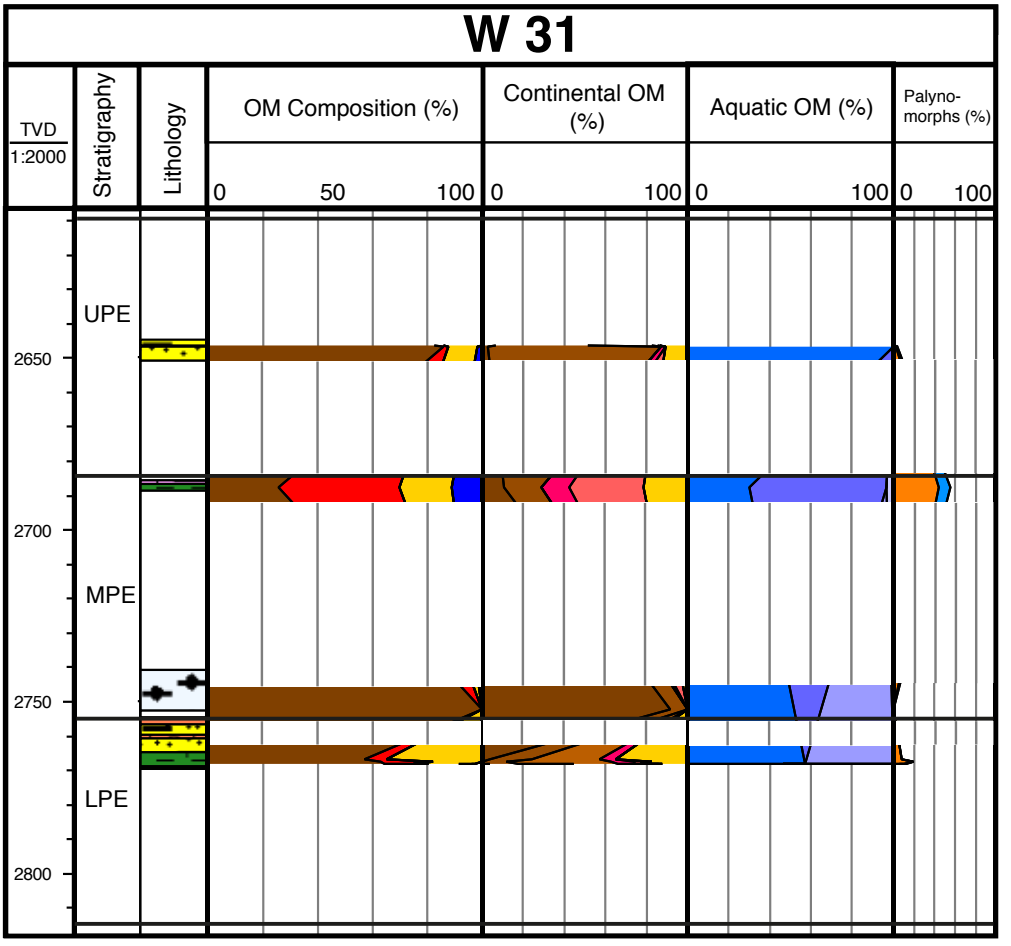
W 31
TVD
1:2000
Stratigraphy
Lithology
OM Composition (%)
0
50
100
Continental OM (%)
0
100
Aquatic OM (%)
0
100
Palyno-morphs (%)
0
100
UPE
MPE
LPE
2650
2700
2750
2800

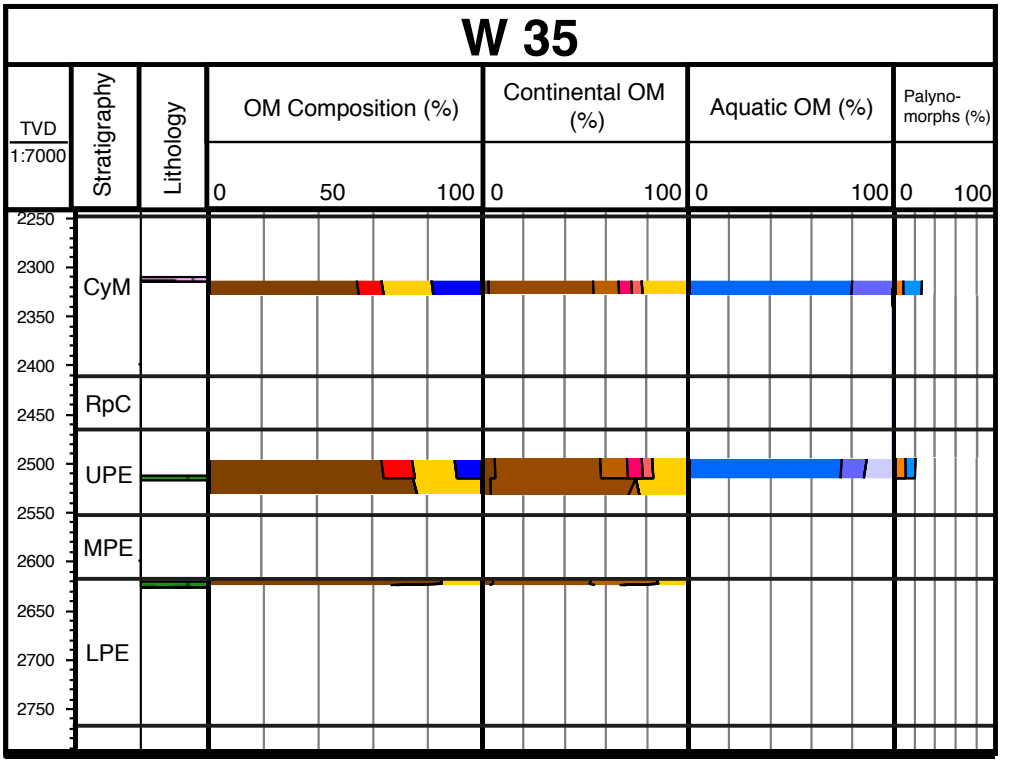
W 35
TVD
1:7000
Stratigraphy
Lithology
OM Composition (%)
0
50
100
Continental OM (%)
0
100
Aquatic OM (%)
0
100
Palyno-morphs (%)
0
100
2250
2300
2350
2400
2450
2500
2550
2600
2650
2700
2750
CyM
RpC
UPE
MPE
LPE

Well	TVD (m)	Stratigraphy	# of particels	Kerogen type			
				I	II	III	IV
W1	650.0	UHy	385	41.3	6.5	48.8	3.4
W1	660.0	UHy	320	50.0	20.3	27.8	1.9
W1	700.0	UHy	283	66.8	13.1	17.7	2.5
W1	750.0	UHy	324	61.7	18.5	18.8	0.9
W1	800.0	UHy	241	60.2	18.3	14.1	7.5
W1	850.0	UHy	352	44.0	24.1	25.0	6.8
W1	900.0	UHy	232	64.2	23.3	11.6	0.9
W1	950.0	UHy	264	0.0	2.7	84.8	12.5
W1	1000.0	UHy	330	37.3	36.7	24.8	1.2
W1	1050.0	UHy	318	46.5	24.2	27.0	2.2
W1	1100.0	UHy	288	51.0	18.4	21.5	9.0
W1	1150.0	UHy	265	57.7	16.2	16.2	9.8
W1	1200.0	UHy	281	46.6	26.0	26.3	1.1
W1	1250.0	UHy	381	35.7	39.5	22.1	2.7
W1	1300.0	UHy	380	41.1	32.4	25.5	1.1
W1	1370.0	Cor	341	38.1	42.2	17.6	2.1
W1	1400.0	Cor	347	51.9	30.3	17.3	0.6
W1	1430.0	Cor	322	14.0	34.5	48.4	3.1
W1	1500.0	Cer	308	57.4	23.6	16.4	2.6
W1	1600.0	Cer	359	32.9	36.5	27.3	3.3
W1	1700.0	Cer	289	1.7	1.0	91.3	5.9
W1	1800.0	BN	214	58.4	4.2	37.4	0.0
W1	1900.0	CyM	247	54.7	8.1	32.8	4.5
W1	2000.0	ME	260	51.9	3.8	34.6	9.6
W1	2070.0	FS (RpC)	304	11.2	12.8	70.7	5.3
W1	2074.0	FS (RpC)	318	51.9	6.3	34.6	7.2
W1	2080.0	FS (RpC)	278	11.9	17.6	66.2	4.3
W1	2100.0	FM (RpC)	302	45.7	10.3	44.0	0.0
W1	2120.0	FM (RpC)	313	11.2	17.9	63.3	7.7
W1	2140.0	FM (RpC)	253	66.4	8.3	22.5	2.8
W1	2160.0	FM (RpC)	229	39.3	6.6	52.4	1.7
W1	2210.0	PE	228	54.8	1.3	36.0	7.9
W1	2300.0	PE	321	49.8	0.9	40.5	8.7
W1	2400.0	PE	270	37.0	0.0	51.9	11.1
W2	391.4	UHy	183.0	1.5	57.7	35.2	5.6
W2	398.8	UHy	237.0	39.9	25.9	31.2	3.0
W2	449.0	UHy	258.0	41.7	29.0	23.6	5.8
W2	503.3	UHy	321.0	42.4	33.6	23.0	0.9
W2	510.4	UHy	358.0	33.0	31.4	27.8	7.8
W2	556.0	UHy	299.0	39.1	28.1	27.8	5.0
W2	561.9	UHy	278.0	9.2	19.4	59.0	12.4
W2	650.8	UHy	302.0	28.0	39.8	27.1	5.2
W2	670.5	UHy	300.0	39.0	31.7	20.7	8.7
W2	671.0	UHy	301.0	37.5	21.3	25.2	15.9
W2	673.0	UHy	256.0	40.2	28.1	25.4	6.3
W2	709.3	UHy	333.0	32.7	34.3	24.8	8.3
W2	747.7	UHy	312.0	10.9	22.4	46.5	20.2
W2	755.9	UHy	367.0	24.0	56.4	15.5	4.1
W2	801.0	UHy	300.0	3.3	27.0	50.7	19.0
W2	805.2	UHy	393.0	21.6	43.0	30.0	5.3

Well	TVD (m)	Stratigraphy	# of particels	Kerogen type			
				I	II	III	IV
W3	1727.7	FM (RpC)	102	0.0	33.3	57.8	8.8
W3	1728.3	FM (RpC)	230	30.4	30.0	37.0	2.6
W3	1728.7	FM (RpC)	306	6.2	43.5	46.7	3.6
W3	1729.3	FM (RpC)	244	1.6	36.5	57.4	4.5
W3	1729.7	FM (RpC)	386	22.8	45.6	22.0	9.6
W3	1735.5	FM (RpC)	402	4.5	10.2	82.1	3.2
W3	1737.5	PE	240	5.8	15.4	74.6	4.2
W3	1743.8	PE	274	0.0	5.1	82.1	12.8
W3	1744.2	PE	308	0.0	18.5	80.2	1.3
W4	1400.0-1404.2	BN	219	0.0	3.7	34.2	62.1
W4	1454.5-1455.3	CyM	231	6.0	40.0	37.2	16.8
W4	1553.5	ME	299	13.3	27.9	42.9	15.9
W4	1554.4	ME	292	2.7	24.7	60.5	12.0
W4	1555.5	ME	289	0.0	31.8	58.9	9.4
W4	1556.5	ME	275	7.1	43.6	37.6	11.7
W4	1557.5	ME	334	4.7	40.9	40.4	13.9
W5	1569.5	FM (RpC)	248	0.0	39.9	51.2	8.9
W5	1570.0	FM (RpC)	250	16.4	25.6	45.2	12.8
W5	1571.5	FM (RpC)	233	13.7	34.8	45.5	6.0
W5	1572.0	FM (RpC)	236	3.4	50.4	40.3	5.9
W5	1573.7	FM (RpC)	257	11.3	17.9	55.3	15.6
W5	1577.0	FM (RpC)	277	13.7	44.8	23.5	18.1
W5	1579.0	FM (RpC)	384	21.6	45.8	26.6	6.0
W5	1581.0	FM (RpC)	15	0.0	100.0	0.0	0.0
W7	560.0	UT I	303	0.7	1.6	90.8	6.9
W7	690.0	UHy	250	68.8	15.6	10.8	4.8
W7	760.0	UHy	222	77.0	8.1	9.9	5.0
W7	838.0	UHy	290	45.0	27.9	19.6	7.5
W7	920.0	UHy	337	46.3	22.6	22.8	8.3
W7	997.0	UHy	392	46.7	18.9	26.5	7.9
W7	1097.0	UHy	354	42.4	38.1	16.1	3.4
W7	1173.0	UHy	242	56.6	29.8	10.3	3.3
W7	1257.0	Cer	303	45.9	27.1	21.1	5.9
W7	1330.0	BN	361	55.1	23.3	15.2	6.4
W7	1435.0	BN	333	46.8	24.0	16.5	12.6
W7(2.)	1080.0	UHy	274	51.1	28.8	14.2	5.8
W7(2.)	1165.0	LHy	244	51.2	27.5	16.8	4.5
W7(2.)	1250.0	Cer	229	65.9	24.9	5.7	3.5
W7(2.)	1334.0	BN-ME	297	57.9	22.9	15.5	3.7
W7(2.)	1396.0	BN-ME	246	45.1	24.0	15.9	15.0
W7(2.)	1460.0	BN-ME	289	45.7	34.3	17.0	3.1
W7(2.)	1550.0	BN-ME	337	36.5	17.8	36.5	9.2
W7(2.)	1647.0	RpC	347	13.0	8.4	67.1	11.5

Well	TVD (m)	Stratigraphy	# of particels	Kerogen type			
				I	II	III	IV
W7a	1070.0	UHy	319	45.1	30.7	18.2	6.0
W7a	1110.0	UHy	281	48.4	31.0	14.9	5.7
W7a	1125.0	UHy	293	45.2	32.4	15.5	6.9
W7a	1135.0	UHy	332	27.0	61.5	9.1	2.4
W7a	1155.0	LHy	277	43.0	32.9	18.8	5.4
W7a	1163.0	LHy	277	34.7	31.0	31.8	2.5
W7a	1167.0	LHy	303	53.5	26.1	13.9	6.6
W7a	1172.0	LHy	335	40.8	36.6	16.3	6.3
W7a	1191.0	LHy	363	38.2	31.0	24.4	6.4
W7a	1200.0	LHy	341	35.5	41.6	17.0	5.9
W7a	1210.0	LHy	261	28.7	51.3	6.5	13.4
W7a	1220.0	LHy	313	41.5	45.7	6.4	6.4
W7a	1288.0	Cer	329	37.4	30.1	22.2	10.3
W7a	1418.0	CyM & ME	540	0.0	4.8	80.7	14.4
W7a	1537.0	CyM & ME	335	0.0	9.6	68.1	22.4
W7a	1557.0	CyM & ME	284	0.4	10.9	69.7	19.0
W7a	1596.0	CyM & ME	389	1.5	6.9	50.6	40.9
W7a	1601.0	FS (RpC)	348	0.9	15.5	68.1	15.5
W7a	1608.0	FS (RpC)	386	2.1	9.6	81.3	7.0
W7a	1611.0	FS (RpC)	356	0.8	14.3	80.9	3.9
W7a	1618.0	FM (RpC)	288	0.0	2.8	88.2	9.0
W7a	1622.0	FM (RpC)	357	0.0	12.9	79.0	8.1
W7a	1628.0	FM (RpC)	266	1.5	5.3	90.2	3.0
W7a	1631.0	PE	274	4.0	9.5	77.4	9.1
W7a	1633.0	PE	224	2.2	10.3	83.0	4.5
W7a	1637.0	PE	259	6.9	8.5	69.9	14.7
W7a	1641.0	PE	264	8.3	6.4	74.6	10.6
W7a	1647.0	PE	235	3.0	4.7	75.7	16.6
W7a	1646.0	PE	331	13.6	18.7	55.3	12.4
W7a	1648.0	PE	281	2.8	12.1	68.7	16.4
W7a	1651.0	PE	238	19.7	15.1	48.3	16.8
W7a	1658.0	PE	310	6.8	11.3	62.9	19.0
W8	675.0	UT I	444	16.6	10.0	67.3	6.1
W8	765.0	UHy	251	54.5	13.0	29.6	2.8
W8	775.0	UHy	326	51.6	28.5	17.3	2.6
W8	825.0	UHy	305	45.6	28.2	22.4	3.8
W8	875.0	UHy	295	50.7	26.5	18.0	4.9
W8	915.0	UHy	296	57.8	18.4	20.0	3.8
W8	985.0	UHy	275	55.2	22.7	19.7	2.3
W8	1020.0	UHy	377	48.7	27.7	21.6	2.0
W8	1353.4	UHy	379	7.1	68.6	17.2	7.1
W8	1395.0	UHy	390	46.6	32.3	17.0	4.0
W8	1405.0	UHy	295	44.1	43.8	9.4	2.8
W8	1430.0	UHy	267	54.3	25.0	19.6	1.1
W8	1450.0	UHy	360	41.3	44.2	9.1	5.4
W8	1475.0	Cor	268	36.4	22.5	39.6	1.5
W8	1505.0	Cor	380	7.3	37.4	50.8	4.5
W8	1525.0	Cor	322	2.0	47.7	48.0	2.3
W8	1555.0	Cor	329	28.1	55.2	10.1	6.7
W8	1575.0	Cor	363	41.3	35.6	19.6	3.5
W8	1600.0	Cor	332	46.6	24.5	25.7	3.2
W8	1603.6	Cor	288	56.4	22.8	15.2	5.6
W8	1624.0	Cer	352	42.6	27.5	23.6	6.3
W8	1650.0	Cer	371	42.1	26.9	28.2	2.8
W8	1674.0	Cer	349	36.5	39.3	18.4	5.8
W8	1700.0	Cer	293	56.4	26.5	17.1	0.0

Well	TVD (m)	Stratigraphy	# of particels	Kerogen type			
				I	II	III	IV
W8	1714.0	Cer	304	43.3	27.7	27.7	1.3
W8	1756.0	Cer	294	3.0	13.1	78.5	5.4
W8	1764.7	Cer	392	55.7	22.1	18.9	3.2
W8	1795.0	Cer	333	8.7	31.0	60.3	0.0
W8	1820.0	BN	278	32.9	33.9	26.8	6.4
W8	1850.0	BN	280	36.1	34.4	28.2	1.4
W8	1875.0	BN	268	37.6	37.3	21.9	3.2
W8	1905.0	BN	269	49.3	20.5	27.1	3.1
W8	1930.0	BN	329	47.3	28.7	18.9	5.1
W8	1950.0	BN	285	44.2	30.5	20.5	4.8
W8	1975.0	BN	289	47.3	23.3	22.3	7.0
W8	1980.0	BN	246	48.6	27.7	20.5	3.2
W8	2000.0	BN	265	53.2	21.2	23.0	2.6
W8	2025.0	CyM & ME	262	48.3	27.9	20.1	3.7
W8	2050.0	CyM & ME	311	46.1	26.6	23.2	4.0
W9	839.0	UHy	321	46.1	11.6	36.7	5.6
W9	920.0	UHy	303	50.5	14.9	28.1	6.6
W9	993.0	UHy	318	66.0	17.0	14.2	2.8
W9	1063.0	UHy	316	67.4	30.7	1.9	0.0
W9	1124.0	UHy	288	52.1	43.4	3.1	1.4
W9	1155.0	UHy	372	50.3	27.2	18.8	3.8
W9	1171.0	UHy	383	43.6	23.8	27.2	5.5
W9	1183.0	UHy	276	54.7	29.3	12.0	4.0
W9	1192.0	UHy	269	56.1	29.4	10.8	3.7
W9	1201.0	LHy	269	61.0	31.2	6.7	1.1
W9	1214.0	LHy	250	66.4	25.6	8.0	0.0
W9	1220.0	LHy	287	47.4	36.9	13.6	2.1
W9	1230.0	LHy	307	47.2	29.3	15.6	7.8
W9	1248.0	LHy	300	47.0	40.0	8.3	4.7
W9	1266.0	LHy	325	47.4	30.5	19.7	2.5
W9	1284.0	LHy	332	22.6	39.5	27.4	10.5
W9	1308.0	LHy	291	37.5	27.5	26.8	8.2
W9	1320.0	LHy	255	51.4	27.5	15.3	5.9
W9	1341.0	LHy	284	37.3	27.5	29.2	6.0
W9	1353.0	LHy	297	32.7	24.6	32.7	10.1
W9	1362.0	LHy	334	29.9	29.0	32.0	9.0
W9	1377.0	CyM & ME	374	34.2	17.4	36.1	12.3
W9	1400.0	CyM & ME	350	44.0	24.0	26.0	6.0
W9	1482.0	FS (RpC)	343	23.6	21.3	46.4	8.7
W9	1488.0	FS (RpC)	291	9.6	7.2	70.8	12.4
W9	1496.0	FS (RpC)	304	14.8	16.1	64.1	4.9
W9	1504.0	FM (RpC)	337	9.5	9.5	72.4	8.6
W9	1525.0	FM (RpC)	285	37.2	12.3	46.3	4.2
W9	1527.0	FM (RpC)	292	32.9	14.0	50.0	3.1
W9	1532.0	UPE	276	13.0	8.3	77.2	1.4
W9	1544.0	UPE	306	12.4	14.1	67.0	6.5
W9	1553.0	MPE	338	14.5	11.8	68.3	5.3
W9	1563.0	LPE	223	0.0	3.6	87.4	9.0
W9	1570.0	LPE	298	1.7	2.8	76.0	19.5

Well	TVD (m)	Stratigraphy	# of particels	Kerogen type			
				I	II	III	IV
W10	759.0	UT I	136	0.0	0.7	99.3	0.0
W10	782.0	UHy	321	54.5	15.0	27.7	2.8
W10	816.0	UHy	291	46.4	13.7	36.4	3.4
W10	896.0	UHy	370	69.7	13.2	13.8	3.2
W10	967.0	UHy	295	85.1	1.7	8.1	5.1
W10	1046.0	UHy	292	64.9	13.5	11.5	10.1
W10	1125.0	UHy	266	59.0	9.8	28.2	3.0
W10	1211.0	UHy	337	63.2	17.8	14.2	4.7
W10	1258.0	UHy	261	62.1	25.7	10.0	2.3
W10	1282.0	LHy	269	68.8	13.0	9.3	8.9
W10	1324.0	LHy	266	62.8	15.8	17.3	4.1
W10	1356.0	LHy	286	47.6	28.0	21.3	3.1
W10	1372.0	LHy	266	45.9	30.8	22.2	1.1
W10	1428.0	LHy	227	19.8	11.0	59.9	9.3
W10	1461.0	LHy	287	46.0	19.9	24.4	9.8
W10	1494.0	LHy	371	30.5	18.5	30.2	20.7
W10	1527.0	LHy	301	13.0	12.6	41.5	32.9
W10	1555.0	LHy	323	14.2	21.1	52.6	12.1
W10	1564.0	LHy	278	21.6	15.5	58.3	4.7
W10	1576.0	Cor	215	29.8	26.0	34.9	9.3
W10	1600.0	Cor	306	4.2	13.1	76.1	6.5
W10	1617.0	Cor	255	20.0	20.8	43.1	16.1
W10	1634.0	Cor	328	41.5	29.9	21.6	7.0
W10	1649.0	Cor	312	52.8	25.7	18.9	2.6
W10	1665.0	Cor	276	57.5	24.2	16.1	2.2
W10	1681.0	Cor	295	55.8	35.7	7.1	1.4
W10	1730.0	Cer	268	58.9	32.9	5.4	2.7
W10	1747.0	BN	274	40.1	46.7	10.3	2.9
W10	1780.0	BN	314	45.5	21.8	25.3	7.4
W10	1965.0	CyM & ME	317	70.3	17.7	8.2	3.8
W10	1954.0	CyM & ME	282	44.0	17.0	34.4	4.6
W10	2045.0	CyM & ME	297	50.5	18.5	25.3	5.7
W10	2110.0	CyM & ME	263	39.3	9.7	42.0	8.9
W10	2119.0	CyM & ME	283	55.7	7.8	30.5	6.0
W10	2132.0	FS (RpC)	312	10.7	10.0	76.4	2.9
W10	2141.0	FS (RpC)	263	33.1	13.7	51.3	1.9
W10	2155.0	FM (RpC)	283	52.7	11.3	36.0	0.0
W10	2165.0	FM (RpC)	362	32.6	3.6	62.7	1.1
W10	2172.0	FM (RpC)	271	51.3	12.6	34.9	1.1
W10	2251.0	MPE	283	16.3	18.4	53.0	12.4
W10	2257.0	MPE	223	2.2	11.2	66.4	20.2
W10	2260.0	LPE	337	5.4	42.4	51.6	0.6
W10	2307.0	LPE	294	14.6	12.2	63.9	9.2
W10	2311.0	LPE	509	40.9	10.2	43.8	5.1
W10	2337.0	LPE	326	0.0	0.0	100.0	0.0
W10	2342.0	LPE	261	0.0	0.0	98.9	1.1
W10	2346.0	LPE	234	0.0	0.0	97.9	2.1
W10	2349.0	LPE	310	1.6	0.3	90.6	7.4
W10	2354.0	LPE	322	0.0	1.2	96.9	1.9
W10	2356.0	LPE	371	0.0	0.0	87.6	12.4
W10	2361.0	LPE	306	5.2	3.6	87.3	3.9

Well	TVD (m)	Stratigraphy	# of particels	Kerogen type			
				I	II	III	IV
W12	676.2	UT I	345	30.8	33.5	29.6	6.0
W12	797.5	UHy	261	69.5	7.7	20.5	2.3
W12	875.2	UHy	322	50.8	28.6	18.7	1.9
W12	914.4	UHy	221	47.5	36.2	8.1	8.1
W12	1040.0	UHy	309	48.5	21.4	27.8	2.3
W12	1042.0	UHy	280	13.1	61.2	16.8	9.0
W12	1042.5	UHy	356	22.4	42.5	25.9	9.2
W12	1236.2	LHy	342	40.4	20.8	34.5	4.4
W12	1426.2	Cor	254	32.3	36.6	21.3	9.8
W12	1428.0	Cor	313	11.2	25.9	60.4	2.6
W12	1429.0	Cor	354	7.9	34.7	52.5	4.8
W12	1634.3	Cer	206	9.7	42.7	39.3	8.3
W12	1841.2	BN	242	4.1	2.9	53.3	39.7
W13	1801.0	PE	250	0.0	4.0	50.0	46.0
W13	1831.0	PE	210	0.0	28.6	71.4	0.0
W13	1851.0	PE	214	9.4	18.4	56.7	15.5
W13	1862.5	PE	302	0.0	8.6	88.4	3.0
W14	657.5	UT I	342	18.1	11.1	48.2	22.5
W14	738.4	UHy	257	50.6	35.8	10.5	3.1
W14	805.0	UHy	203	34.5	49.8	8.4	7.4
W14	855	UHy	292	71.9	21.2	2.4	4.5
W14	910	UHy	223	56.5	35.0	4.5	4.0
W14	962.9	UHy	286	46.2	28.0	15.0	10.8
W14	1016	UHy	202	0.0	71.3	26.2	2.5
W14	1022.7	UHy	301	18.6	34.9	41.9	4.7
W14	1070	UHy	307	56.0	24.1	16.9	2.9
W14	1124	UHy	325	61.5	27.1	6.2	5.2
W14	1163	UHy	257	66.1	23.3	8.6	1.9
W14	1164	UHy	323	40.2	42.4	15.8	1.5
W14	1165	UHy	197	15.7	43.1	37.1	4.1
W14	1167.8	UHy	241	24.9	57.3	17.8	0.0
W14	1188.9	UHy	335	32.5	20.9	42.7	3.9
W14	1189	UHy	309	55.0	25.9	13.6	5.5
W14	1189.9	UHy	301	66.1	14.3	15.9	3.7
W14	1193	UHy	410	26.1	51.5	22.4	0.0
W14	1199.3	UHy	328	60.1	24.1	11.9	4.0
W14	1265	LHy	356	47.8	18.5	27.5	6.2
W14	1271.6	LHy	346	6.1	48.8	40.4	4.7
W14	1289.6	LHy	381	10.8	60.6	23.1	5.5
W14	1300	LHy	384	6.8	59.6	31.0	2.6
W14	1312.9	LHy	326	17.8	28.2	50.0	4.0
W14	1347.8	LHy	391	10.2	32.2	53.5	4.1
W14	1351	LHy	349	1.7	34.4	60.5	3.4
W14	1384.5	LHy	377	23.2	37.6	37.6	1.6
W14	1418.8	LHy	329	19.1	26.1	51.4	3.3
W14	1446.5	Cor	326	12.0	25.5	62.6	0.0
W14	1448	Cor	368	23.9	47.0	25.5	3.5
W14	1449	Cor	332	12.7	50.3	21.4	15.7
W14	1483.8	Cor	241	3.3	1.2	76.8	18.7
W14	1523.1	Cor	420	3.1	62.6	31.0	3.3
W14	1526	Cor	371	6.2	33.2	58.5	2.2
W14	1566.4	Cor	247	11.7	70.9	15.0	2.4
W14	1567	Cor	277	12.6	38.3	40.1	9.0
W14	1569	Cor	287	3.5	25.4	60.3	10.8
W14	1571	Cor	347	20.7	61.1	18.2	0.0

Well	TVD (m)	Stratigraphy	# of particels	Kerogen type			
				I	II	III	IV
W14	1591.3	Cor	347	0.9	52.2	42.1	4.9
W14	1631.8	Cer	263	17.9	30.0	47.9	4.2
W14	1637.6	Cer	323	41.5	34.1	18.9	5.6
W14	1672	Cer	314	30.9	39.8	22.9	6.4
W14	1704.5	Cer	251	10.8	56.6	30.7	2.0
W14	1749	Cer	320	9.4	32.8	44.4	13.4
W14	1754.9	Cer	278	49.3	39.9	8.3	2.5
W14	1780.0	Cer	265	35.8	45.3	17.7	1.1
W14	1808.6	Cer	225	66.7	8.9	17.8	6.7
W14	1851	BN	225	4.4	0.0	91.1	4.4
W14	1922.2	BN	270	7.4	0.0	18.5	74.1
W14	1945.8	BN	328	0.9	14.9	81.1	3.0
W14	2019	CyM & ME	335	5.1	11.3	44.8	38.8
W14	2064.3	CyM & ME	372	3.0	28.2	60.8	8.1
W14	2104.2	CyM & ME	309	0.6	12.9	64.7	21.7
W14	2152.9	RpC	277	5.8	35.7	54.5	4.0
W14	2154	RpC	208	0.0	19.2	70.7	10.1
W14	2196.6	PE	198	0.0	16.2	76.8	7.1
W14	2197	PE	302	3.6	32.1	61.6	2.6
W15	1997.1	MPE	238	2.8	48.2	23.5	25.5
W15	1998.4	MPE	220	0.0	0.0	22.7	77.3
W15	2044.6	LPE	246	12.2	0.0	65.4	22.4
W15	2044.9	LPE	230	0.0	0.0	34.8	65.2
W15	2046.2	LPE	225	11.1	0.0	64.4	24.4
W16	808.0	UT I	249.0	28.1	22.5	45.4	4.0
W16	865.0	UHy	278.0	49.3	17.6	25.9	7.2
W16	900.9	UHy	291.0	45.4	20.6	33.0	1.0
W16	950.0	UHy	279.0	53.0	17.6	28.3	1.1
W16	1000.0	UHy	245.0	59.2	18.4	19.6	2.9
W16	1050.0	UHy	253.0	57.3	21.3	19.8	1.6
W16	1100.0	UHy	264.0	60.6	20.5	18.9	0.0
W16	1150.0	UHy	254.0	46.1	34.6	15.7	3.5
W16	1200.0	UHy	342.0	36.5	39.2	24.3	0.0
W16	1250.0	LHy	365.0	35.9	38.6	25.5	0.0
W16	1300.0	LHy	300.0	50.3	31.0	17.0	1.7
W16	1350.0	LHy	244.0	53.7	18.0	25.4	2.9
W16	1400.0	LHy	340.0	34.1	43.8	19.7	2.4
W16	1450.0	LHy	290.0	39.7	28.3	28.3	3.8
W16	1502.0	LHy	348.0	33.9	39.1	25.6	1.4
W16	1560.0	LHy	266.0	37.6	46.6	14.7	1.1
W16	1597.5	Cor	374.0	40.1	41.4	18.4	0.0
W16	1652.5	Cor	319.0	29.2	39.8	25.7	5.3
W16	1700.0	Cor	330.0	10.3	28.8	55.2	5.8
W16	1720.0	Cor	274.0	30.3	23.4	40.1	6.2
W16	1750.0	Cer	300.0	6.0	31.0	55.0	8.0
W16	1800.0	Cer	301.0	11.0	26.6	61.5	1.0
W16	1850.0	Cer	321.0	34.0	39.6	21.8	4.7
W16	1900.0	Cer	320.0	28.8	26.9	38.8	5.6
W16	2000.0	BN	297.0	10.1	25.6	63.0	1.3
W16	2055.0	BN	263.0	39.9	33.1	24.0	3.0
W16	2100.0	BN	370.0	36.2	42.2	18.1	3.5
W16	2150.0	CyM & ME	363.0	20.4	42.7	30.9	6.1
W16	2200.0	CyM & ME	426.0	29.3	37.3	30.3	3.1
W16	2250.0	CyM & ME	358.0	20.4	40.8	32.7	6.1
W16	2300.0	RpC	413.0	33.4	32.7	30.8	3.1

Well	TVD (m)	Stratigraphy	# of particels	Kerogen type			
				I	II	III	IV
W16	2350.0	UPE	271.0	41.7	15.9	35.4	7.0
W16	2398.20	UPE	260.0	3.8	0.0	23.1	73.1
W16	2398.44	MPE	276.0	7.2	0.0	79.0	13.8
W16	2414.28	MPE	240.0	2.1	0.0	60.4	37.5
W16	2420.37	MPE	260.0	3.8	0.0	42.3	53.8
W16	2425.3	MPE	452.0	1.6	0.0	54.8	43.5
W16	2425.74	MPE	310.0	22.1	26.3	43.1	8.4
W16	2431	MPE	394.0	20.1	18.8	37.1	24.1
W16	2435.6	MPE	355.0	9.3	13.5	68.2	9.0
W16	2438	MPE	287.0	9.8	13.9	70.7	5.6
W16	2440.68	MPE	323.0	17.0	20.7	60.1	2.2
W16	2444.9	MPE	333.0	9.0	12.3	77.2	1.5
W16	2443.83	MPE	303.0	3.0	2.3	78.9	15.8
W18	2399.7	PE	290	1.0	29.3	54.1	15.5
W18	2400.5	PE	404	0.0	21.0	69.6	9.4
W18	2403.4	PE	225	2.2	0.0	31.1	66.7
W19	1455.0	Cer	238	29.0	50.0	16.4	4.6
W19	1457.0	Cer	317	15.1	47.3	32.2	5.4
W19	1640.0	CyM	300	1.3	13.7	72.7	12.3
W19	1850.0	RpC	274	12.8	37.2	40.9	9.1
W19	1851.0	RpC	226	0.0	17.7	69.5	12.8
W19	1852.0	RpC	215	4.7	31.2	59.5	4.7
W19	1853.0	PE	251	1.2	13.5	80.5	4.8
W19	1854.0	PE	294	6.1	20.7	61.9	11.2
W19	1856.0	PE	215	0.0	0.0	7.0	93.0
W19	1878.0	PE	250	0.0	0.0	8.0	92.0
W21	1455.3	CyM & ME	272	1.5	21.7	51.1	25.7
W21	1461.1	CyM & ME	262	1.5	12.6	66.4	19.5
W21	1575.6	CyM & ME	269	5.6	24.9	64.3	5.2
W21	1581.6	CyM & ME	266	0.0	16.5	71.8	11.7
W21	1587.5	CyM & ME	278	1.1	15.5	62.9	20.5
W21	1590.2	CyM & ME	318	2.8	14.8	66.7	15.7
W21	1753.2	UPE	274	0.4	11.3	65.0	23.4
W21	1772.9	MPE	312	8.3	13.1	62.5	16.0
W23	1136.5	Cor	352	10.7	39.4	43.7	6.1
W23	1245.0	Cor	270	1.9	30.7	58.9	8.5
W23	1350	Cer	330	0.0	57.3	39.7	3.0
W23	1642.3	BN	282	1.1	17.4	65.6	16.0
W23	1773.6	CyM & ME	258	4.3	14.0	68.6	13.2
W23	1812.6	CyM & ME	268	6.7	14.9	63.8	14.6
W23	1955	PE	221	3.6	5.4	79.6	11.3
W23	1965.0	PE	340	0.0	0.0	38.2	61.8
W23	1969.5	PE	282	4.3	47.5	38.3	9.9
W23	1986.1	PE	200	0.0	0.0	0.0	100.0
W23	1996.7	PE	306	0.0	2.0	49.0	49.0
W25	1705.0	PE	228	5.8	18.6	70.8	4.9
W25	1796.0	PE	371	19.4	10.5	69.0	1.1

Well	TVD (m)	Stratigraphy	# of particels	Kerogen type			
				I	II	III	IV
W29	853.1	BN	254	0.0	0.0	57.1	42.9
W29	908.4	BN	228	0.0	0.0	32.0	68.0
W29	1001.2	CyM & ME	207	1.0	9.2	72.9	16.9
W29	1121.1	CyM & ME	195	9.3	8.8	75.6	6.2
W29	1133.2	CyM & ME	314	10.2	28.0	54.5	7.3
W29	1267	PE	224	0.0	3.1	89.3	7.6
W29	1268.5	PE	230	50.0	0.0	33.5	16.5
W31	2646.8	UPE	290	0.0	3.8	89.7	6.6
W31	2646.9	UPE	205	0.0	3.4	93.7	2.9
W31	2687.9	MPE	277	7.6	47.7	35.4	9.4
W31	2752.5	MPE	240	0.0	0.0	8.3	91.7
W31	2767.0	LPE	224	0.0	8.0	87.9	4.0
W31	2767.8	LPE	265	0.0	19.2	80.8	0.0
W31	2768.0	LPE	296	1.0	11.8	87.2	0.0
W31	2768.4	LPE	314	8.3	1.9	86.0	3.8
W35	2314.0	CyM	265	3.8	23.8	70.2	2.3
W35	2515.0	UPE	292	2.4	18.2	73.6	5.8
W35	2516.2	UPE	261	0.0	0.0	96.2	3.8
W35	2623.3	LPE	297	0.0	0.0	94.9	5.1
W35	2625.0	LPE	216	0.0	1.9	94.9	3.2

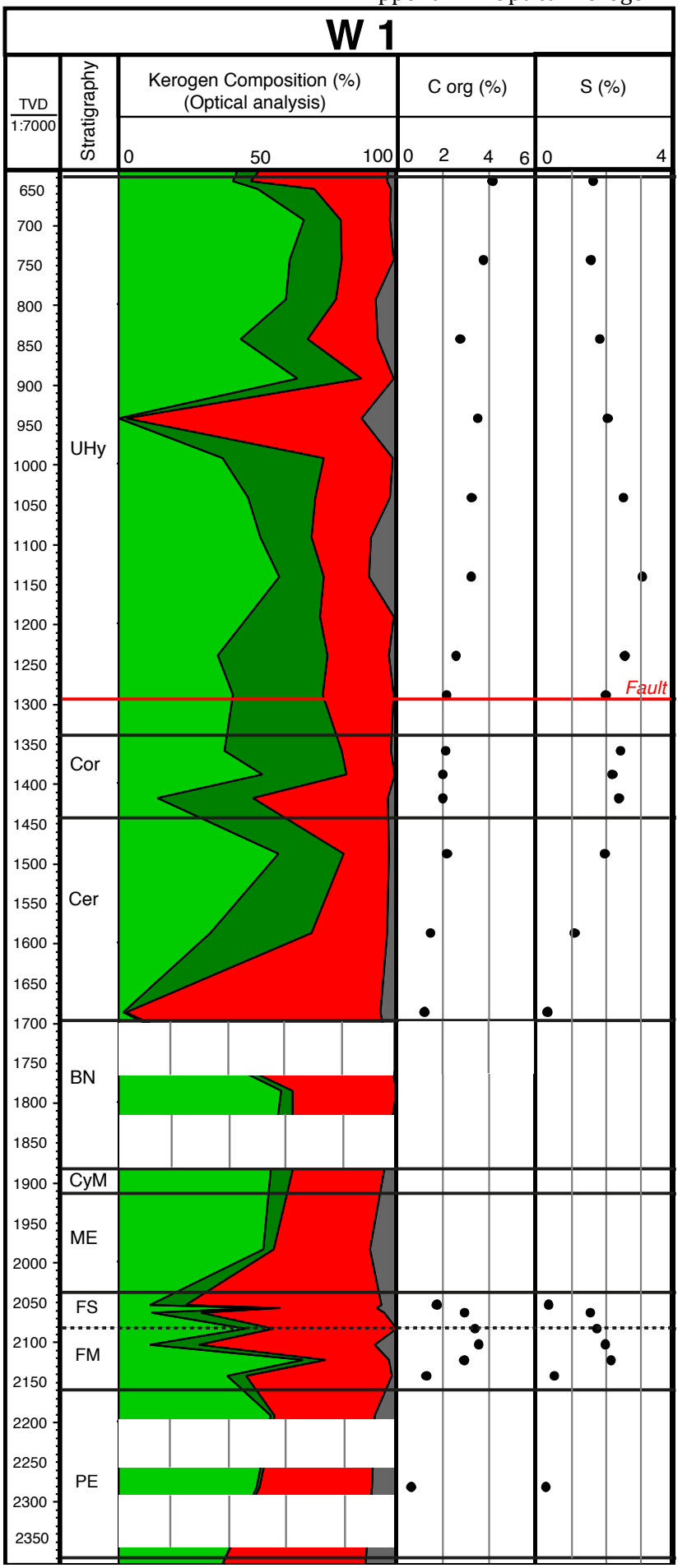
W 1
TVD
1:7000
Stratigraphy
Kerogen Composition (%)
(Optical analysis)
0
50
100
C org (%)
0
2
4
6
S (%)
0
4
650
700
750
800
850
900
950
1000
1050
1100
1150
1200
1250
1300
1350
1400
1450
1500
1550
1600
1650
1700
1750
1800
1850
1900
1950
2000
2050
2100
2150
2200
2250
2300
2350
UHy
Cor
Cer
BN
CyM
ME
FS
FM
PE
Fault

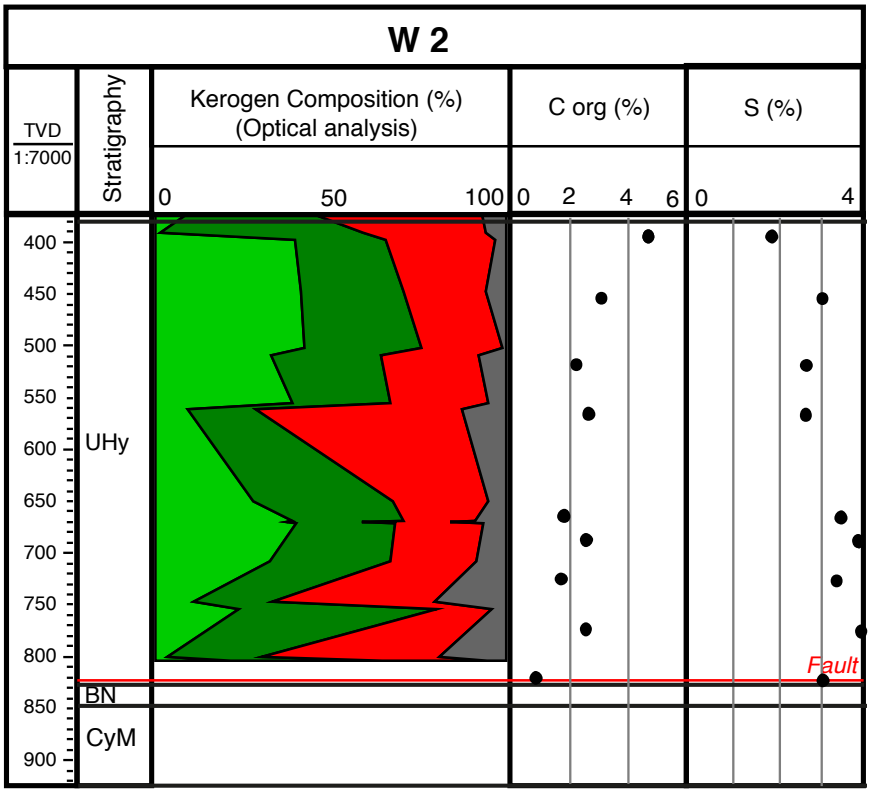

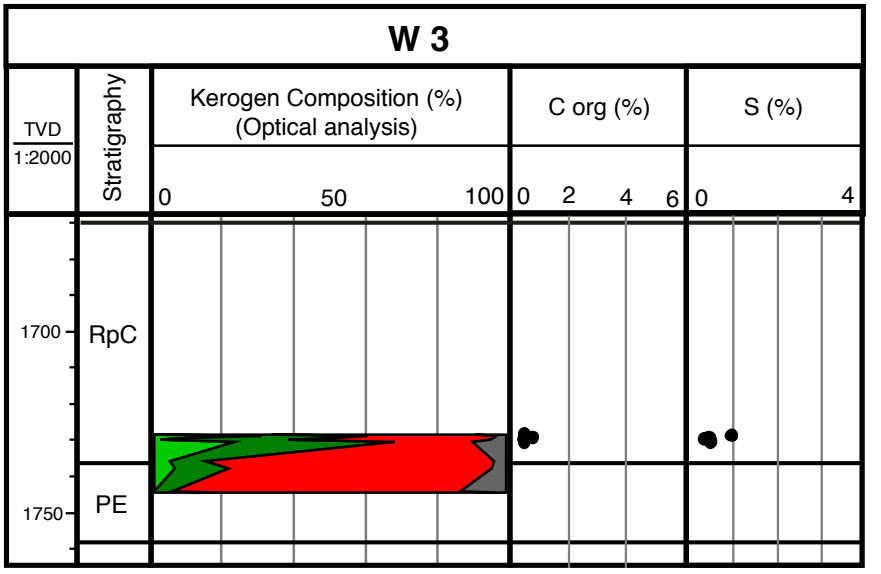

TVD	Strati-graphy	Kerogen composition (Optical analysis)	C org	S
m (BGL)		% / total OM	0 (%) 6	0 (%) 4
		Kerogen type I		
		Kerogen type II		
		Kerogen type III		
		Kerogen type IV		

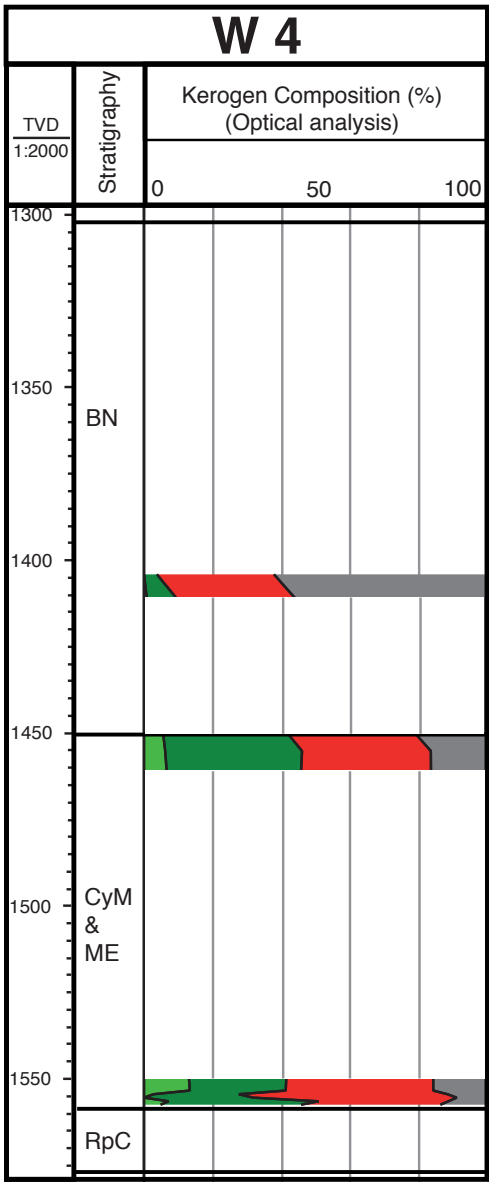
W 4
TVD
1:2000
Stratigraphy
Kerogen Composition (%)
(Optical analysis)
0
50
100
1300
1350
1400
1450
1500
1550
BN
CyM
&
ME
RpC

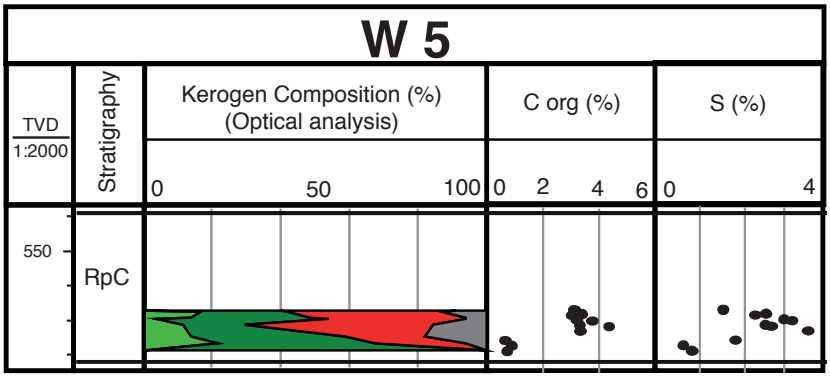
W 5
TVD
1:2000
Stratigraphy
Kerogen Composition (%)
(Optical analysis)
0
50
100
C org (%)
0
2
4
6
S (%)
0
4
550
RpC

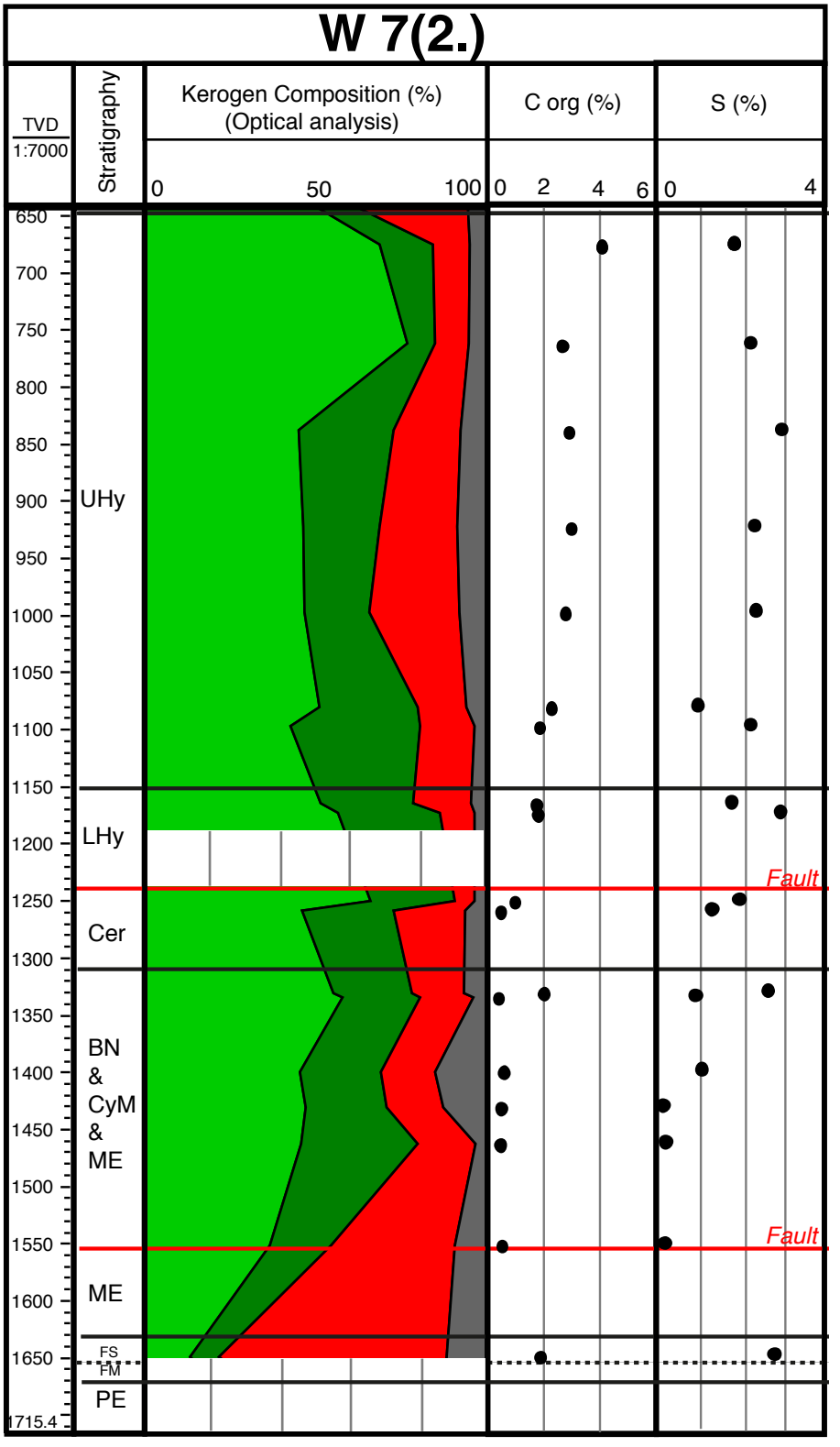
W 7(2.)
TVD
1:7000
Stratigraphy
Kerogen Composition (%)
(Optical analysis)
0
50
100
C org (%)
0
2
4
6
S (%)
0
4
650
700
750
800
850
900
950
1000
1050
1100
1150
1200
1250
1300
1350
1400
1450
1500
1550
1600
1650
1715.4
UHy
LHy
Cer
BN
&
CyM
&
ME
ME
FS
FM
PE
Fault
Fault

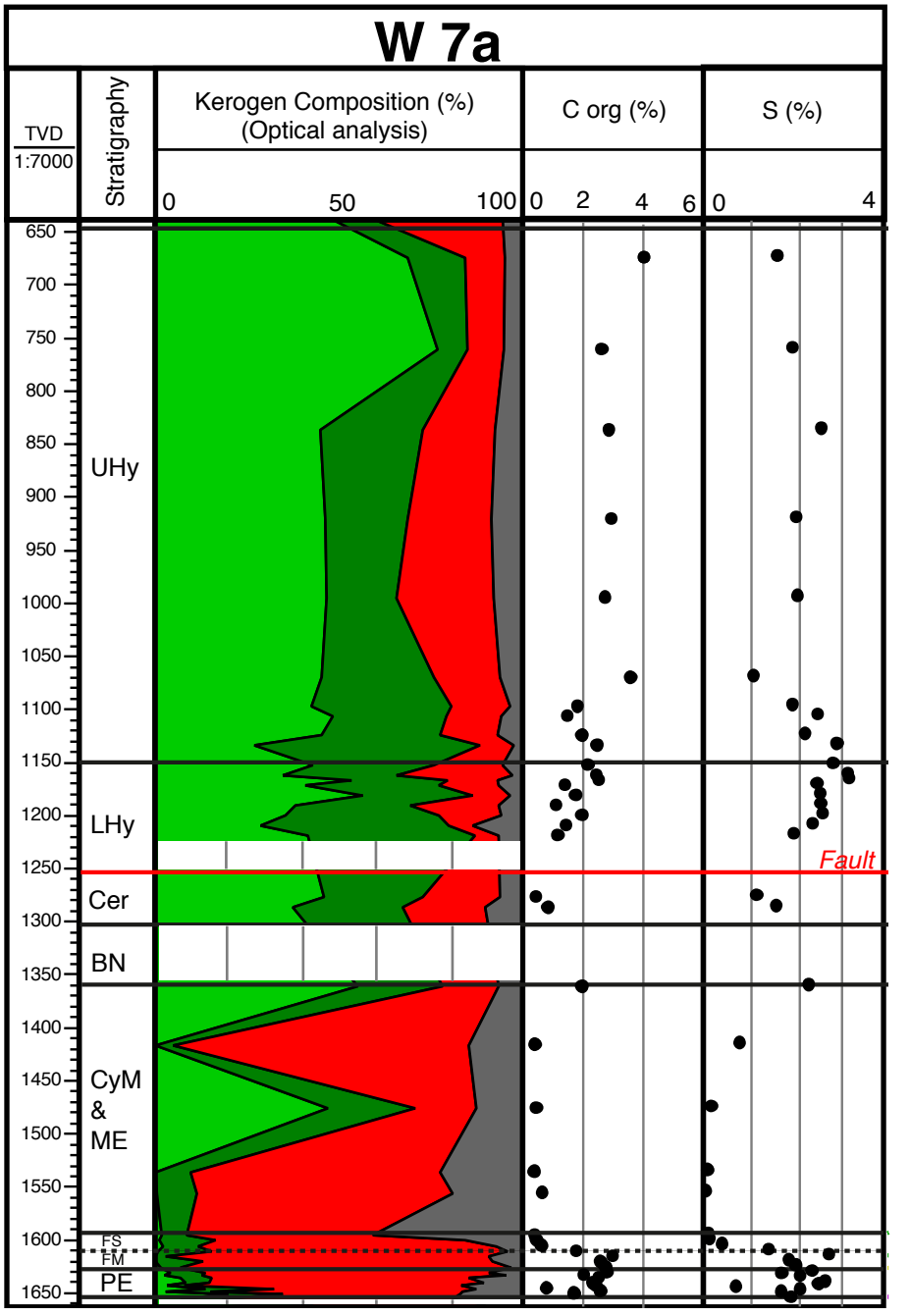

TVD	Strati-graphy	Kerogen composition (Optical analysis)	C org	S
m (BGL)		% / total OM	0 (%) 6	0 (%) 4
		Kerogen type I		
		Kerogen type II		
		Kerogen type III		
		Kerogen type IV		

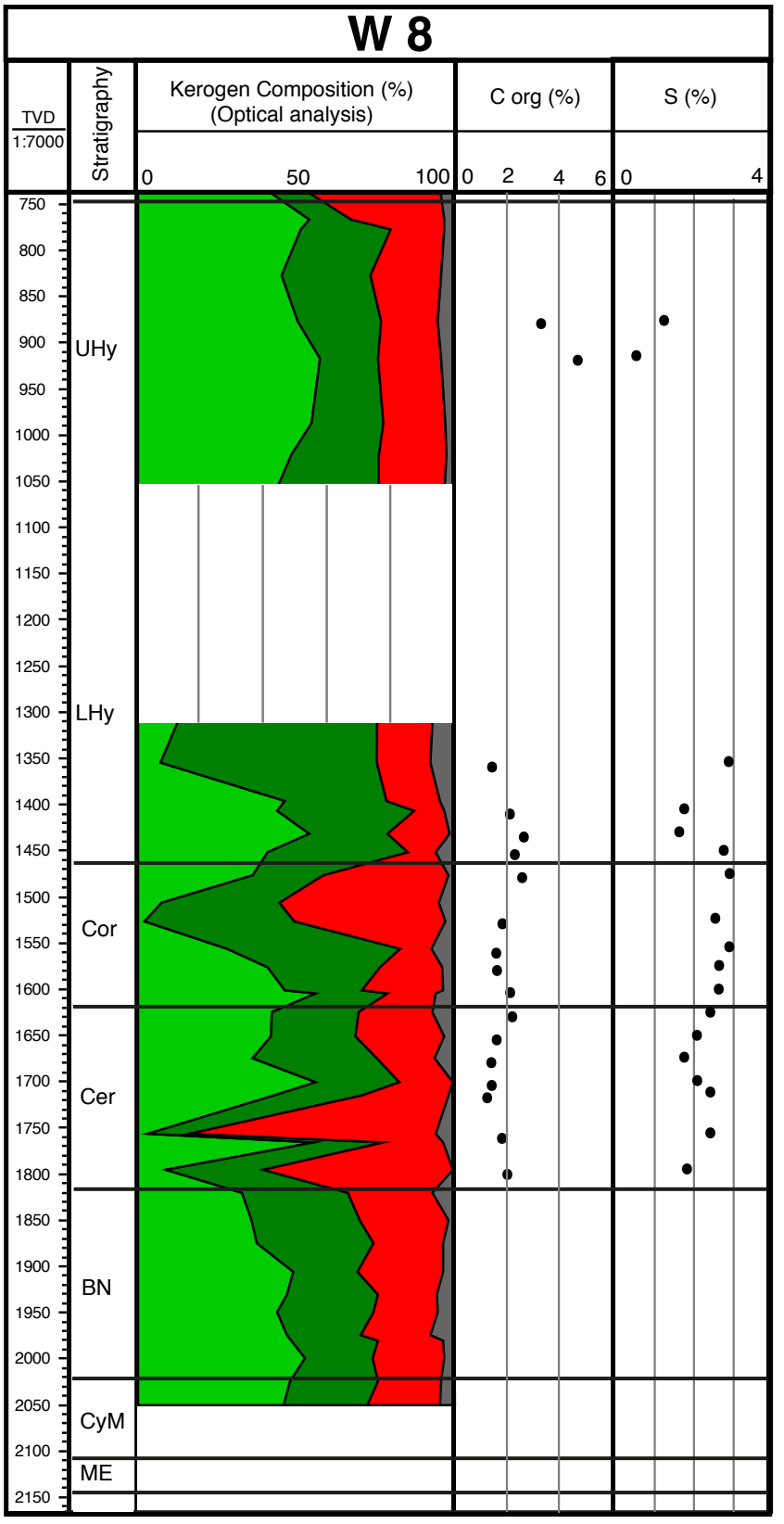
W 8
TVD
1:7000
Stratigraphy
Kerogen Composition (%)
(Optical analysis)
0
50
100
C org (%)
0
2
4
6
S (%)
0
4
750
800
850
900
950
1000
1050
1100
1150
1200
1250
1300
1350
1400
1450
1500
1550
1600
1650
1700
1750
1800
1850
1900
1950
2000
2050
2100
2150
UHy
LHy
Cor
Cer
BN
CyM
ME

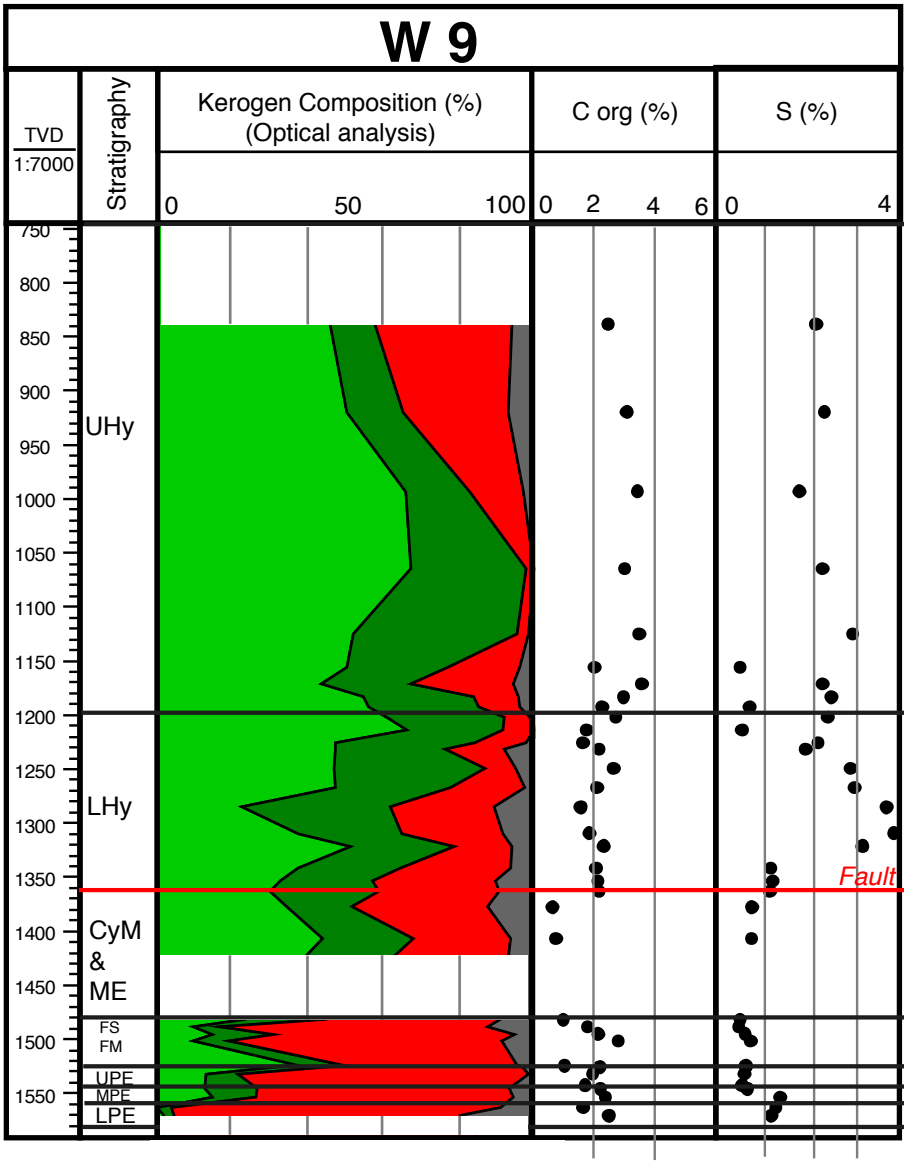

TVD	Strati-graphy	Kerogen composition (Optical analysis)	C org	S
m (BGL)		% / total OM	0 (%) 6	0 (%) 4
		Kerogen type I		
		Kerogen type II		
		Kerogen type III		
		Kerogen type IV		

Appendix 2: Optical Kerogen Analysis

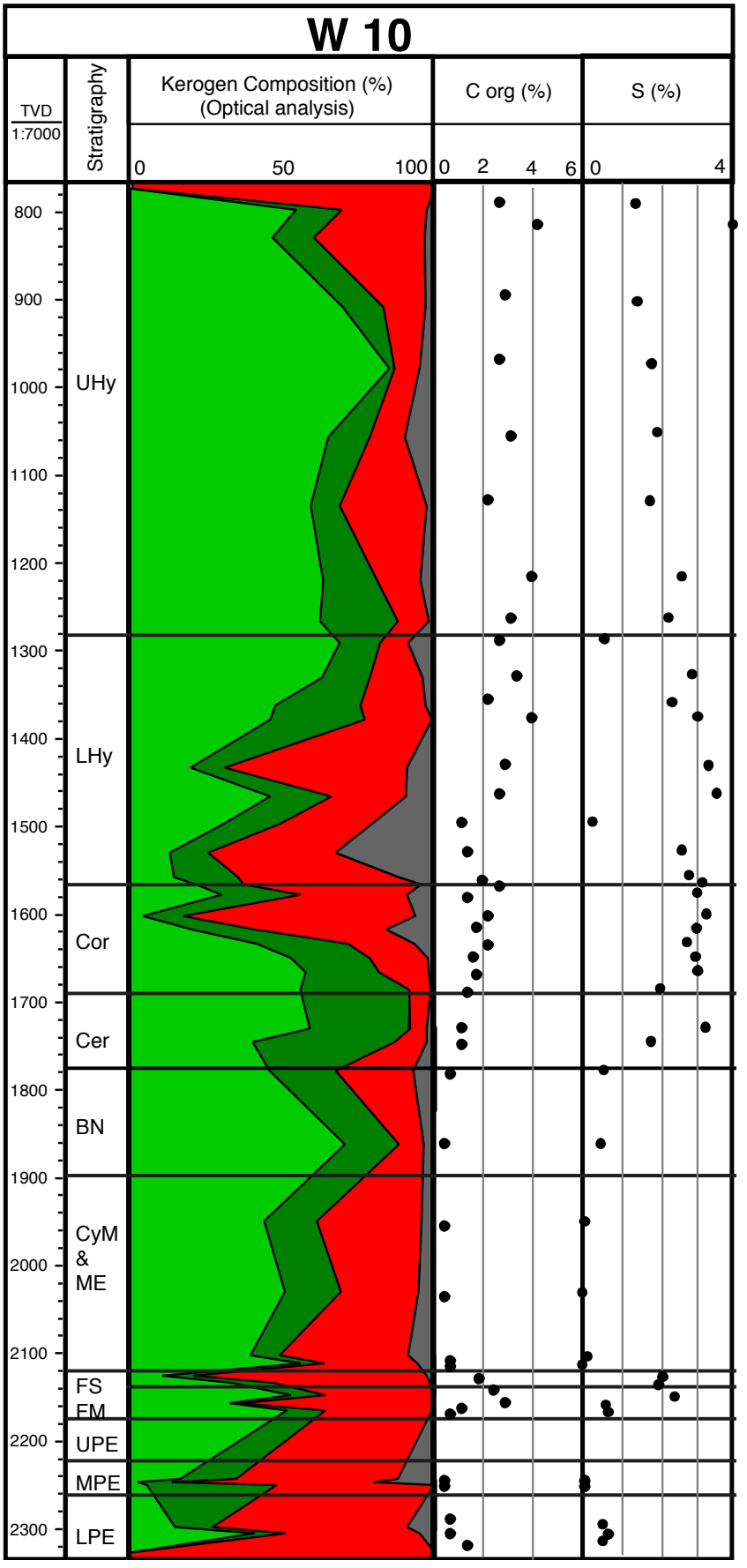

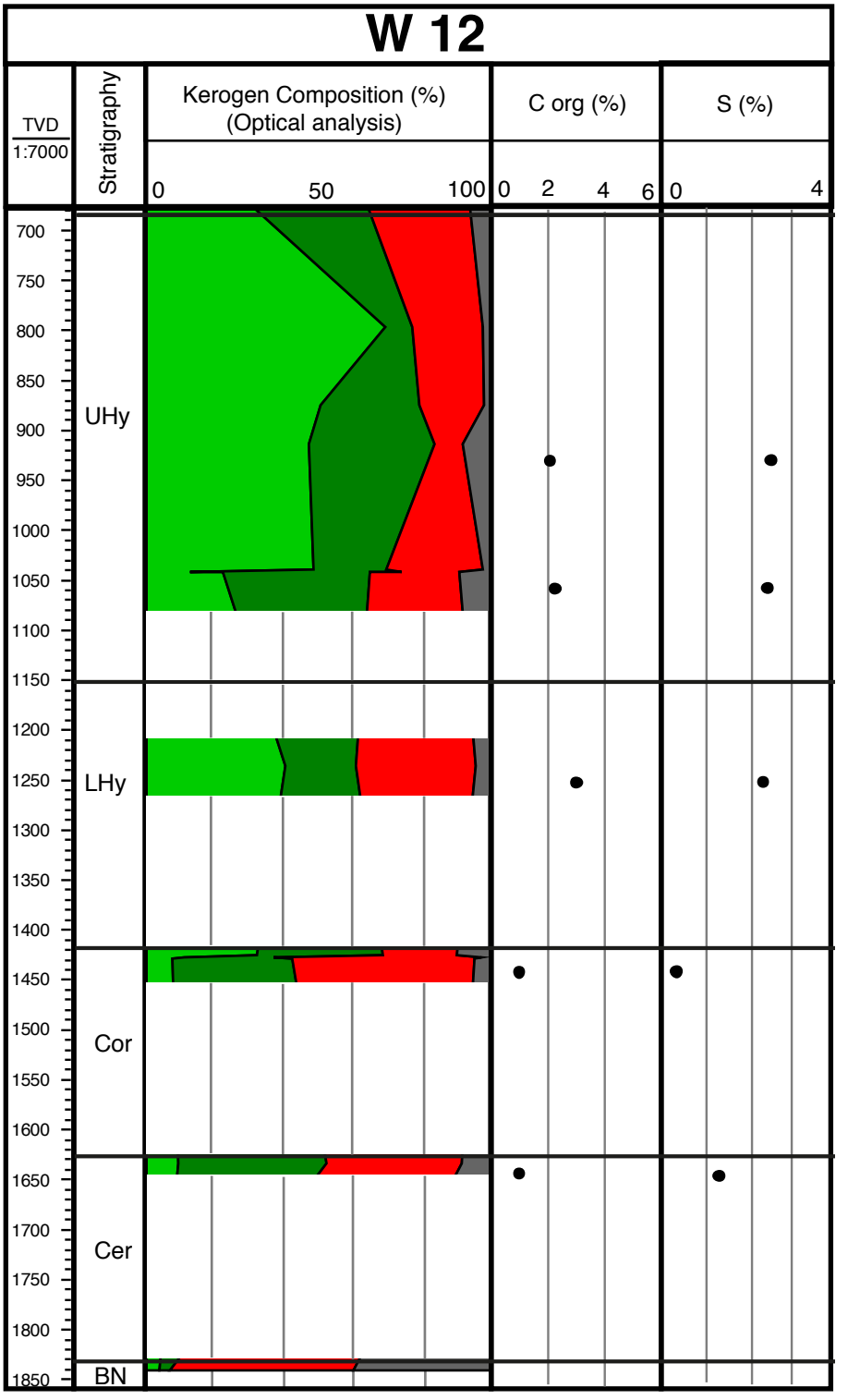

TVD	Strati-graphy	Kerogen composition (Optical analysis)	C org	S
m (BGL)		% / total OM	0 (%) 6	0 (%) 4
		Kerogen type I		
		Kerogen type II		
		Kerogen type III		
		Kerogen type IV		

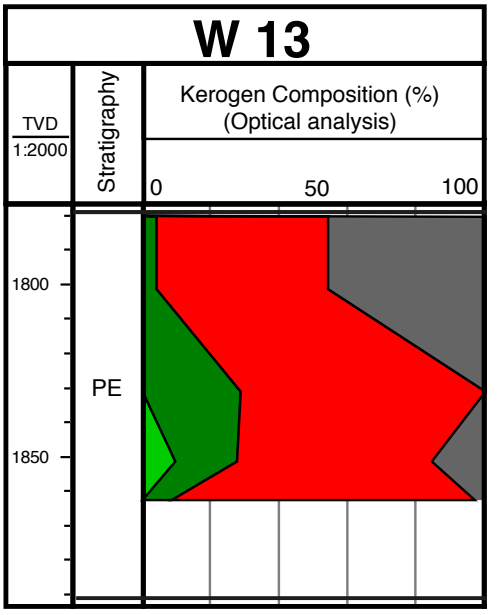
W 13
TVD
1:2000
Stratigraphy
Kerogen Composition (%)
(Optical analysis)
0
50
100
1800
PE
1850

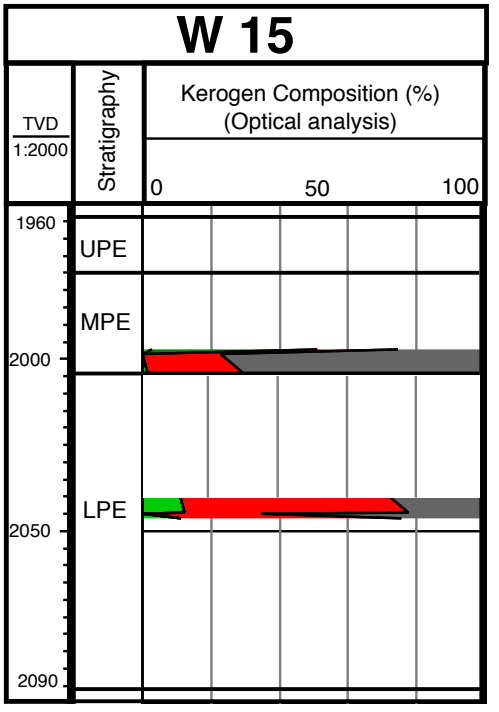
W 15
TVD
1:2000
Stratigraphy
Kerogen Composition (%)
(Optical analysis)
0
50
100
1960
UPE
MPE
2000
LPE
2050
2090

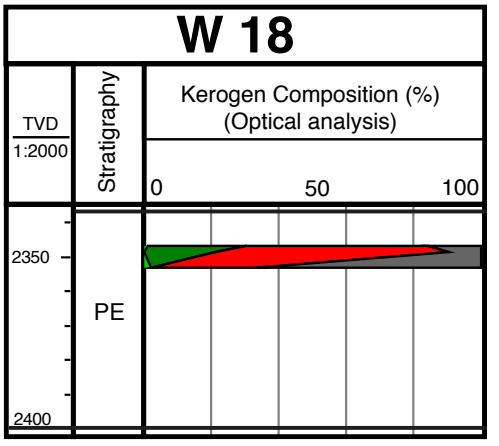
W 18
TVD
1:2000
Stratigraphy
Kerogen Composition (%)
(Optical analysis)
0
50
100
2350
PE
2400

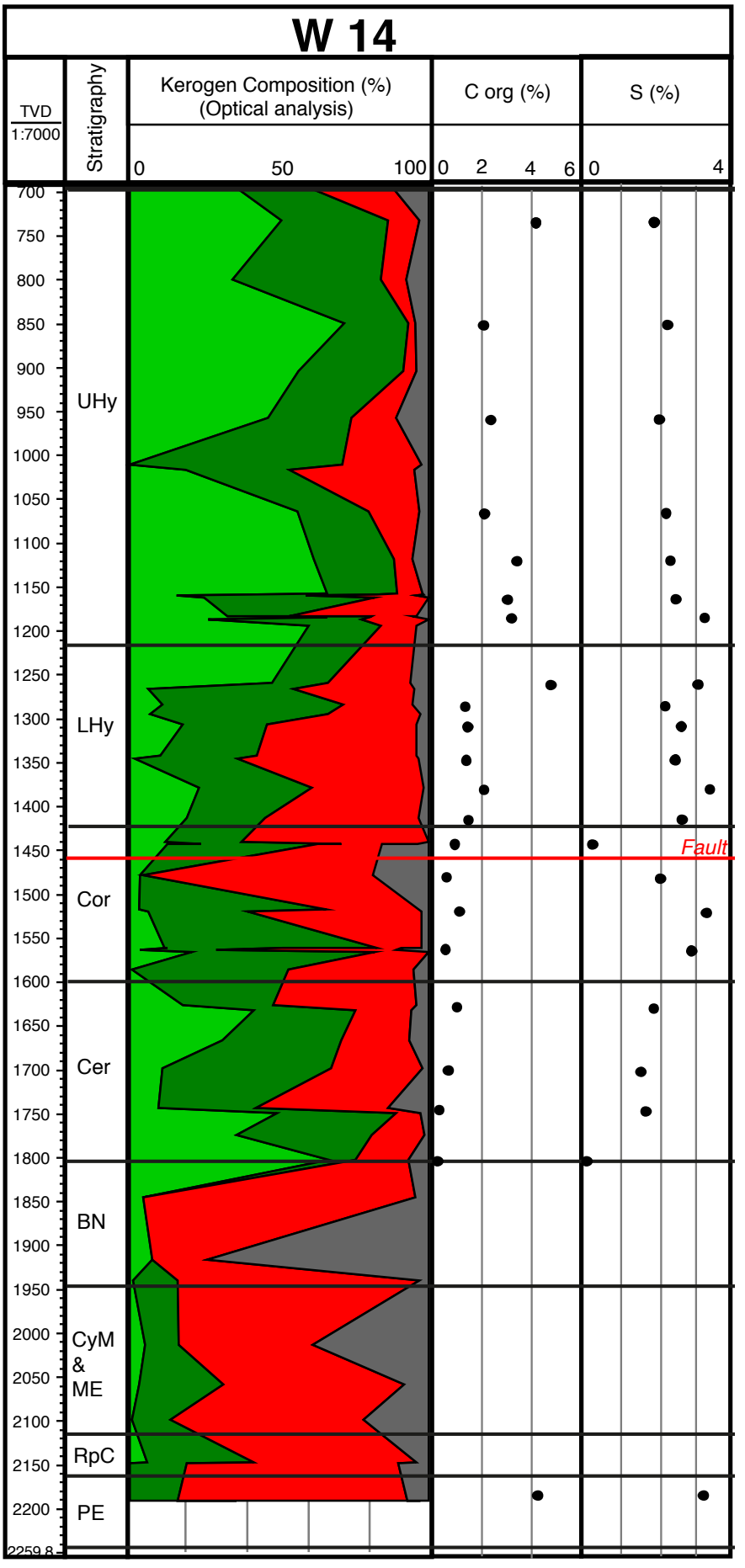
W 14
TVD
1:7000
Stratigraphy
Kerogen Composition (%)
(Optical analysis)
0
50
100
C org (%)
0
2
4
6
S (%)
0
4
700
750
800
850
900
950
1000
1050
1100
1150
1200
1250
1300
1350
1400
1450
1500
1550
1600
1650
1700
1750
1800
1850
1900
1950
2000
2050
2100
2150
2200
2259.8
UHy
LHy
Fault
Cor
Cer
BN
CyM
&
ME
RpC
PE

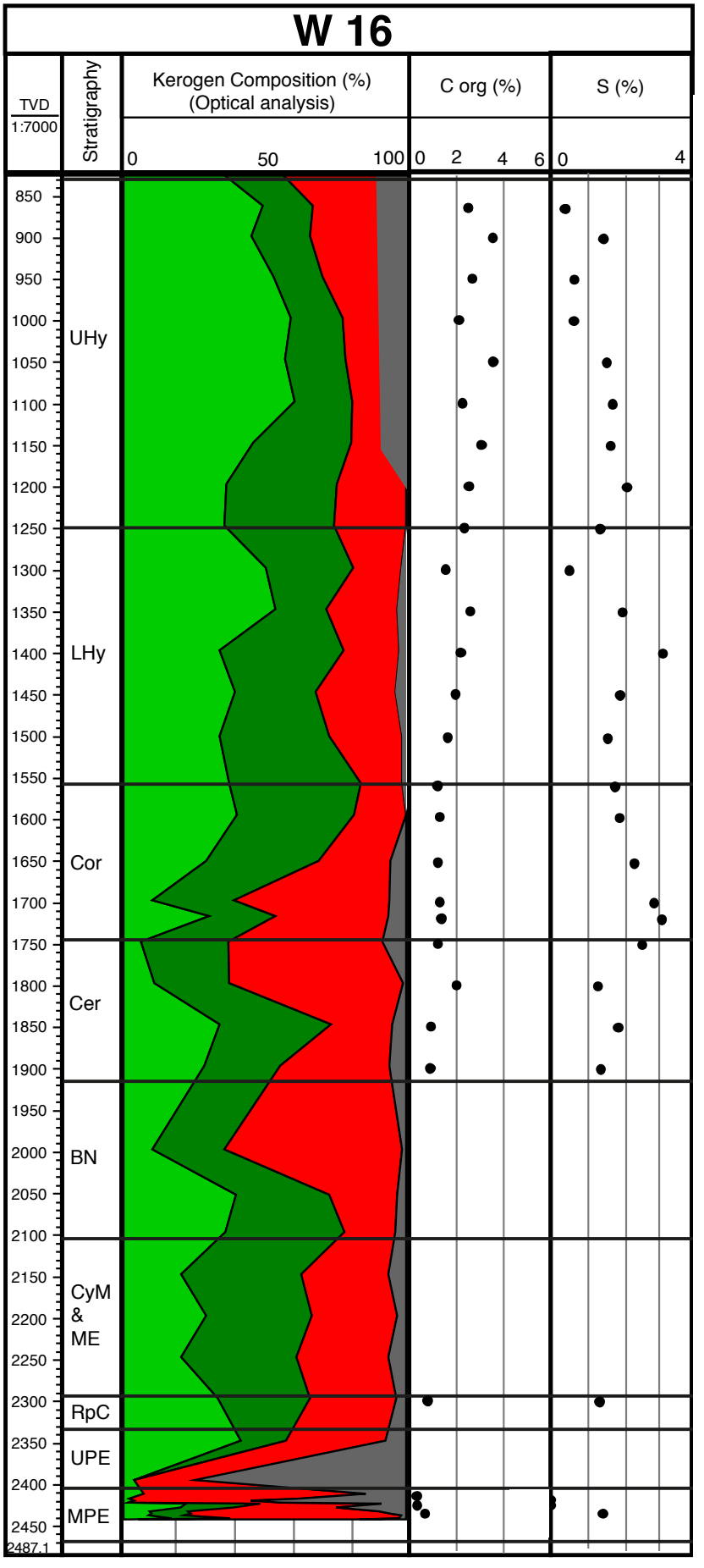
W 16
TVD
1:7000
Stratigraphy
Kerogen Composition (%)
(Optical analysis)
0
50
100
C org (%)
0
2
4
6
S (%)
0
4
850
900
950
1000
1050
1100
1150
1200
1250
1300
1350
1400
1450
1500
1550
1600
1650
1700
1750
1800
1850
1900
1950
2000
2050
2100
2150
2200
2250
2300
2350
2400
2450
2487.1
UHy
LHy
Cor
Cer
BN
CyM
&
ME
RpC
UPE
MPE

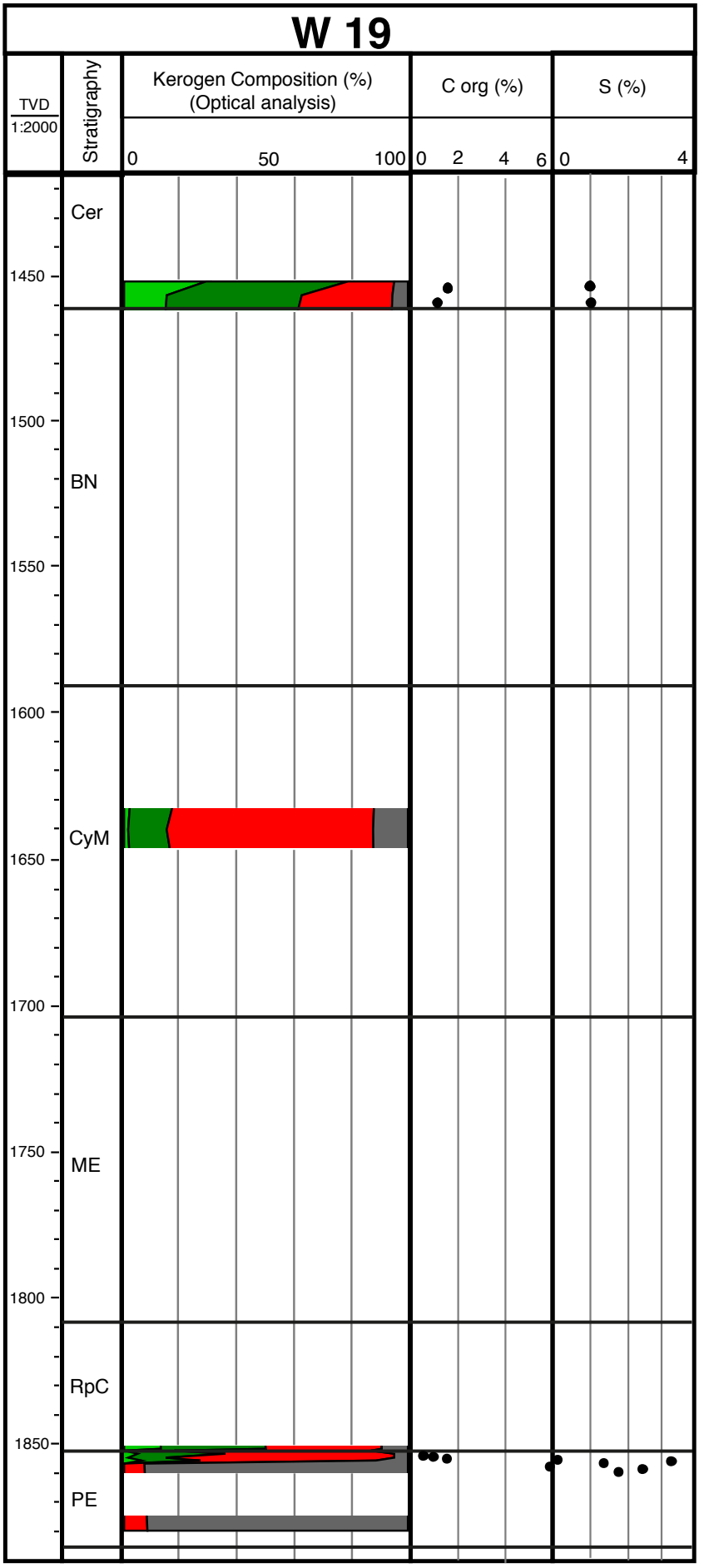
W 19
TVD
1:2000
Stratigraphy
Kerogen Composition (%)
(Optical analysis)
0
50
100
C org (%)
0
2
4
6
S (%)
0
4
Cer
BN
CyM
ME
RpC
PE
1450
1500
1550
1600
1650
1700
1750
1800
1850

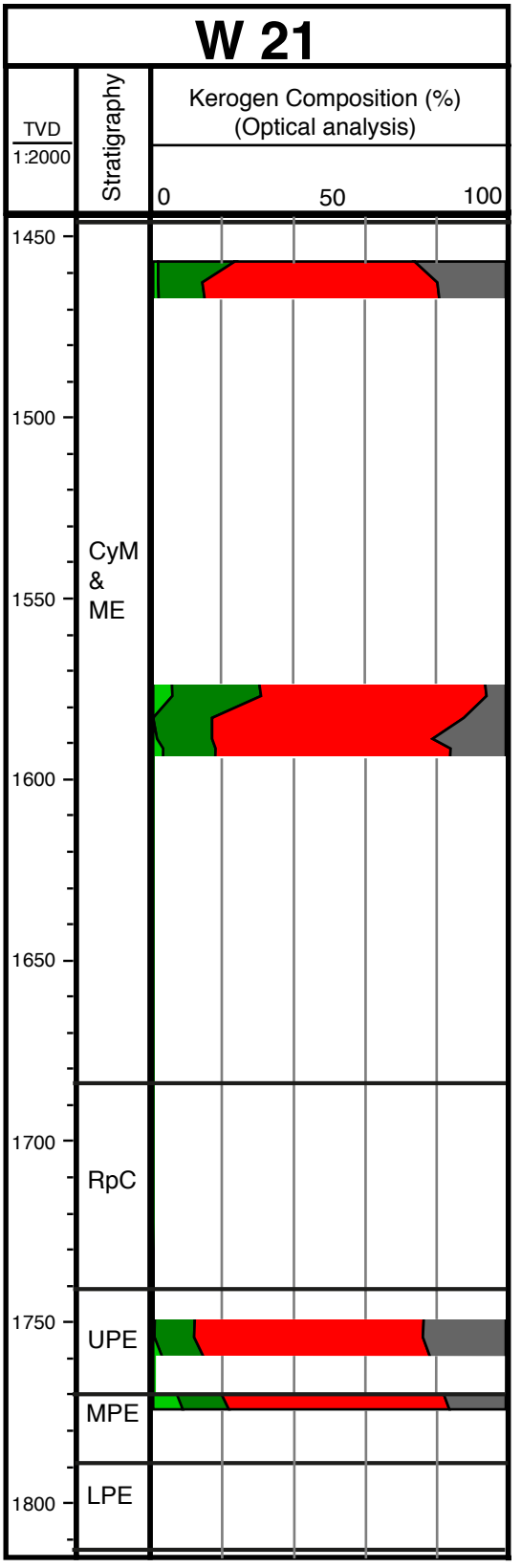
W 21
TVD
1:2000
Stratigraphy
Kerogen Composition (%)
(Optical analysis)
0
50
100
1450
1500
1550
1600
1650
1700
1750
1800
CyM
&
ME
RpC
UPE
MPE
LPE

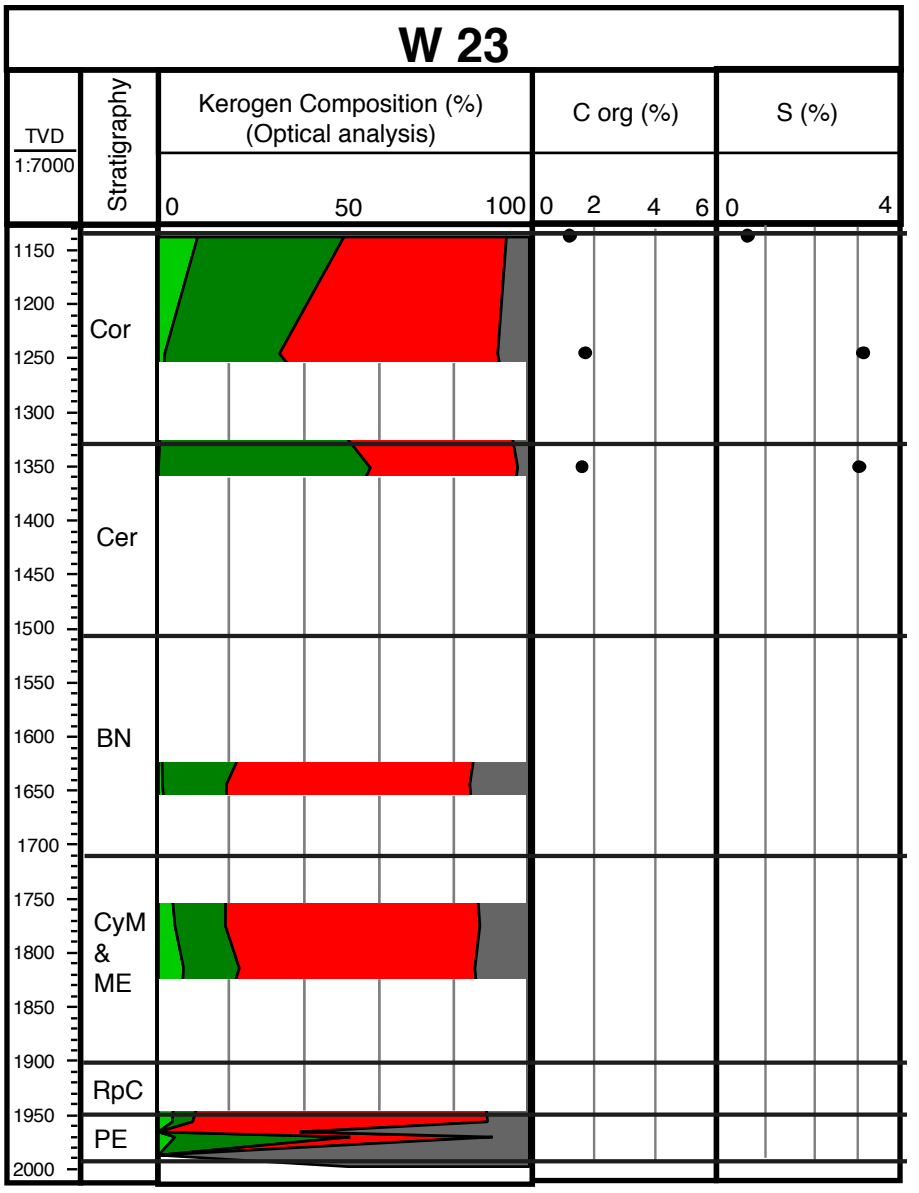

TVD	Strati-graphy	Kerogen composition (Optical analysis)	C org	S
m (BGL)		% / total OM	0 (%) 6	0 (%) 4
		Kerogen type I		
		Kerogen type II		
		Kerogen type III		
		Kerogen type IV		

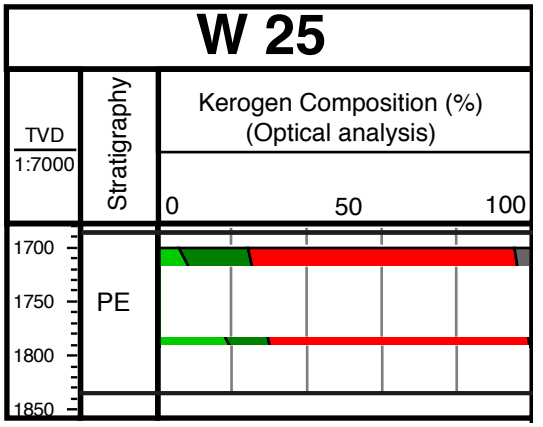

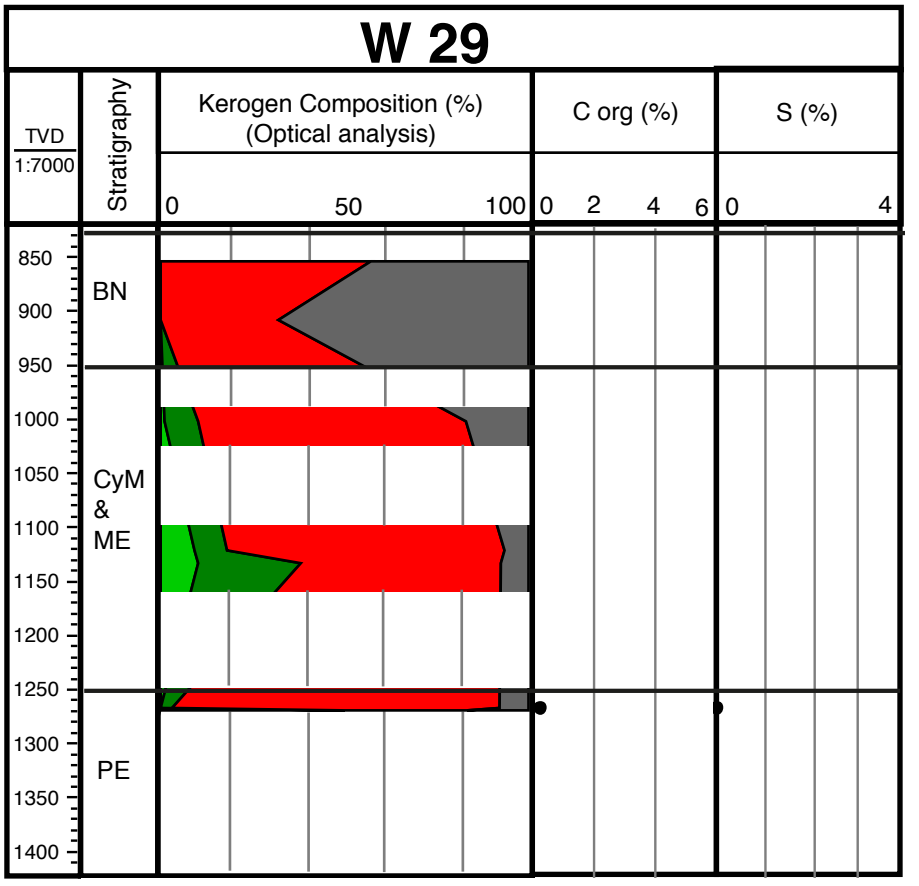

TVD	Strati-graphy	Kerogen composition (Optical analysis)	C org	S
m (BGL)		% / total OM	0 (%) 6	0 (%) 4
		Kerogen type I		
		Kerogen type II		
		Kerogen type III		
		Kerogen type IV		

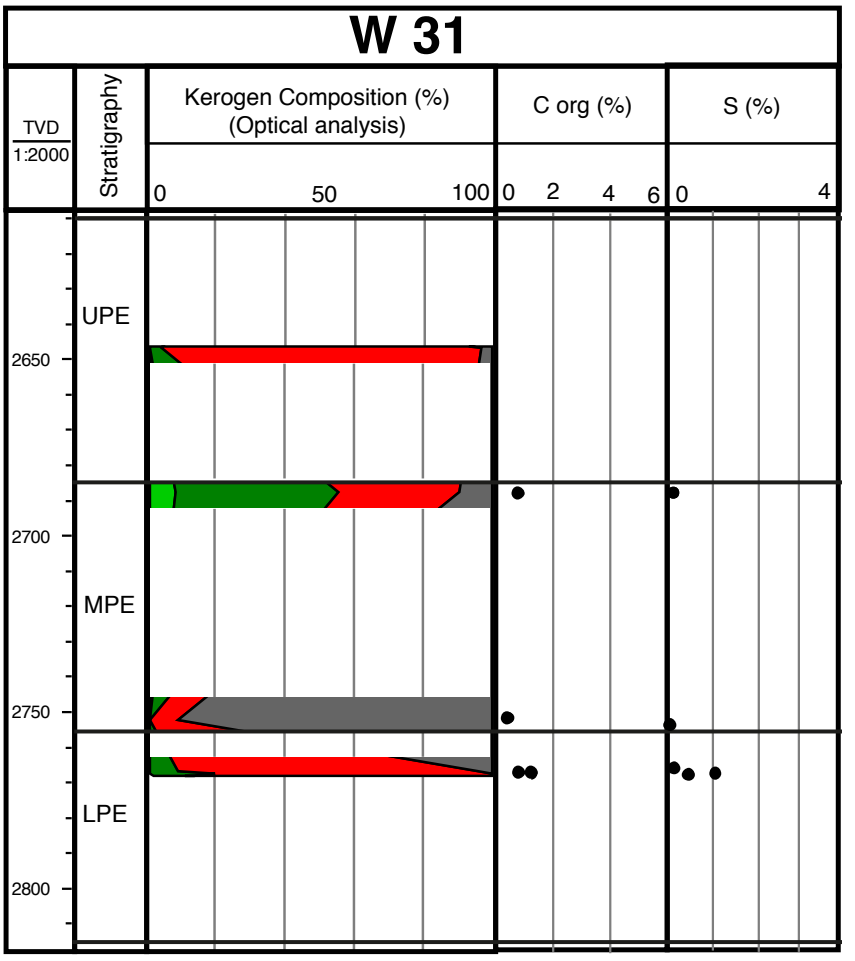
W 31
TVD
1:2000
Stratigraphy
Kerogen Composition (%)
(Optical analysis)
0
50
100
C org (%)
0
2
4
6
S (%)
0
4
UPE
MPE
LPE
2650
2700
2750
2800

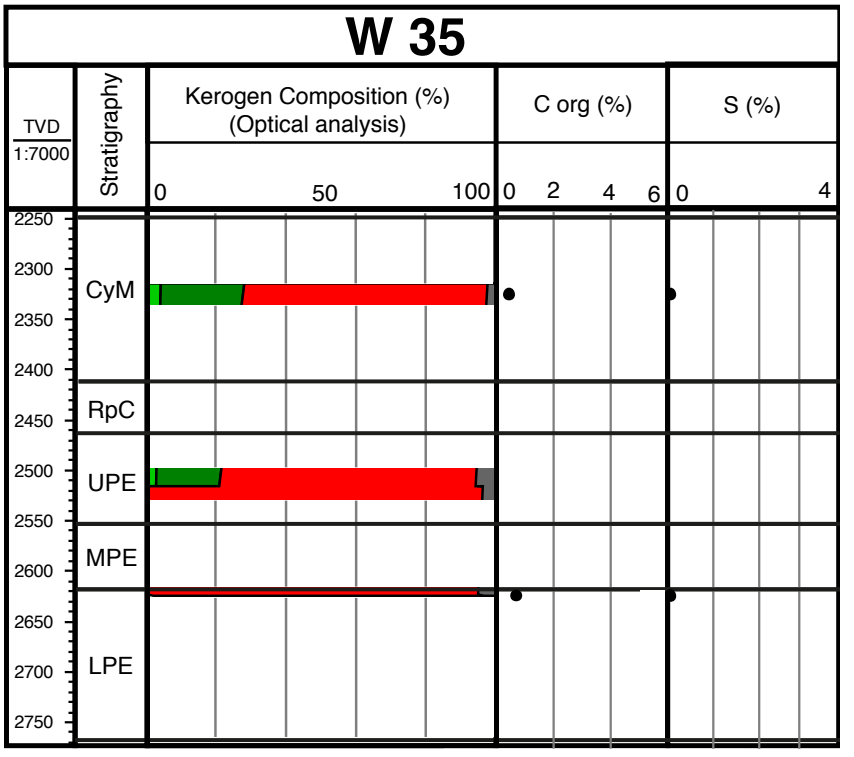
W 35
TVD
1:7000
Stratigraphy
Kerogen Composition (%)
(Optical analysis)
0
50
100
C org (%)
0
2
4
6
S (%)
0
4
CyM
RpC
UPE
MPE
LPE
2250
2300
2350
2400
2450
2500
2550
2600
2650
2700
2750

Well	Depth (TVD)	Formation	S1 (mg/g)	S2 (mg/g)	S3 (mg/g)	Tmax (°C)	PP (mg/g)	PI (wt ratio)	HI (mg HC/g TOC)	OI (mg CO_2/g TOC)
W1	650.0	UHy	1.91	21.35	1.85	441	23.26	0.08	514	45
W1	750.0	UHy	1.73	18.11	1.21	435	19.84	0.09	480	32
W1	850.0	UHy	1.34	10.78	1.00	430	12.12	0.11	390	36
W1	950.0	UHy	1.45	15.42	1.05	430	16.87	0.09	439	30
W1	1050.0	LHy	1.15	12.69	0.87	425	13.84	0.08	390	27
W1	1150.0	LHy	1.78	13.76	0.82	417	15.54	0.11	425	25
W1	1250.0	LHy	0.98	8.57	0.76	426	9.55	0.1	333	30
W1	1370.0	Cor	1.50	7.02	0.75	415	8.52	0.18	332	35
W1	1430.0	Cor	1.30	6.35	0.94	415	7.65	0.17	316	47
W1	1500.0	Cer	1.31	7.90	0.75	429	9.21	0.14	362	34
W1	1600.0	Cer	1.33	4.56	0.76	351	5.89	0.23	310	52
W1	1600.0	Cer	0.91	3.87	0.41	438	4.78	0.19	263	28
W1	1700.0	Cer	0.94	2.95	0.58	341	3.89	0.24	243	48
W1	2070.0	FS (RpC)	2.20	4.66	0.63	336	6.86	0.32	267	36
W1	2070.0	FS (RpC)	1.34	3.92	0.31	338	5.26	0.25	224	18
W1	2080.0	FS (RpC)	1.45	9.12	0.63	435	10.57	0.14	309	21
W1	2100.0	FS (RpC)	2.32	11.48	0.49	434	13.8	0.17	338	14
W1	2120.0	FM (RpC)	2.52	14.68	0.51	436	17.2	0.15	413	14
W1	2140.0	FM (RpC)	2.27	10.15	0.54	435	12.42	0.18	347	18
W1	2160.0	FM (RpC)	1.01	3.24	0.51	338	4.25	0.24	250	39
W1	2160.0	FM (RpC)	0.80	3.39	0.56	337	4.19	0.19	262	43
W1	2300.0	PE	0.74	1.83	0.42	328	2.57	0.29	286	66
W1	2300.0	PE	0.53	1.74	0.33	331	2.27	0.23	272	52
W2	391.4	UHy	0.69	25.67	1.07	446	26.36	0.03	554	23
W2	510.4	UHy	0.46	5.91	0.82	429	6.37	0.07	269	37
W2	709.3	LHy	0.33	2.51	0.53	414	2.84	0.12	150	32
W2	801.0	LHy	0.15	0.71	0.44	420	0.86	0.17	86	54
W3	1727.3	FM (RpC)	0.05	0.16	0.53	424	0.21	0.24	35	115
W3	1728.3	FM (RpC)	0.07	0.24	0.57	436	0.31	0.23	33	78
W3	1729.3	FM (RpC)	0.07	0.27	0.43	432	0.34	0.21	61	97
W5	1566.0	FM (RpC)	0.67	8.94	0.3	436	9.61	0.07	294	10
W5	1567.5	FM (RpC)	0.75	12.52	0.45	435	13.27	0.06	377	14
W5	1569.5	FM (RpC)	0.72	10.44	0.39	432	11.16	0.06	334	12
W5	1571.5	FM (RpC)	0.86	10.91	0.43	432	11.77	0.07	338	13
W5	1573.7	FM (RpC)	0.78	11.06	0.39	431	11.84	0.07	340	12
W5	1577.0	FM (RpC)	0.09	0.28	0.47	426	0.37	0.24	44	74
W5	1579.0	FM (RpC)	0.15	0.49	0.3	428	0.64	0.23	56	35
W5	1581.0	FM (RpC)	0.13	0.58	0.51	433	0.71	0.18	82	72
W7a	690.0	UHy	0.32	19.28	0.9	435	19.6	0.02	481	22
W7a	980.0	UHy	0.15	13.51	0.69	434	13.66	0.01	460	24
W7a	1160.0	UHy	0.38	17.39	2.96	424	17.77	0.02	486	83
W7a	1200.0	UHy	0.12	4.36	2.05	430	4.48	0.03	286	134
W7a	1220.0	UHy	0.17	7.03	0.95	430	7.2	0.02	354	48
W7a	1260.0	LHy	0.58	10.2	1.14	427	10.78	0.05	415	46
W7a	1265.0	LHy	0.5	11.12	0.87	425	11.62	0.04	438	34
W7a	1310.0	LHy	0.34	4.9	2.61	429	5.24	0.06	332	177
W7a	1390.0	Cer	0.06	1.62	3.15	431	1.68	0.04	181	352
W7a	1520.0	CyM & ME	0.04	0.36	1.68	437	0.4	0.1	76	356

Well	Depth (TVD)	Formation	S1 (mg/g)	S2 (mg/g)	S3 (mg/g)	Tmax (°C)	PP (mg/g)	PI (wt ratio)	HI (mg HC/g TOC)	OI (mg CO_2/g TOC)
W7a	1660.0	CyM & ME	0.04	0.38	2.37	433	0.42	0.1	55	345
W7a	1700.0	CyM & ME	0.07	0.32	3	433	0.39	0.18	69	652
W7a	1715.0	FS (RpC)	0.17	4.23	1.02	437	4.4	0.04	234	56
W7a	1720.0	FS (RpC)	0.24	8.69	0.67	432	8.93	0.03	292	22
W7a	1730.0	FM (RpC)	0.5	10.29	0.67	434	10.79	0.05	372	24
W7a	1737.5	UPE	0.23	5.95	0.71	435	6.18	0.04	291	35
W7a	1752.5	PE	0.22	6.89	0.68	435	7.11	0.03	266	26
W7a	1760.0	LPE	0.12	2.97	0.64	436	3.09	0.04	136	29
W8	875.0	UHy	0.52	13.79	0.88	437	14.31	0.04	439	28
W8	1353.4	LHy	0.29	2.48	0.73	414	2.77	0.1	186	55
W8	1450.0	LHy	0.48	5.4	0.63	420	5.88	0.08	253	29
W8	1525.0	CoB	0.58	4.29	0.49	420	4.87	0.12	251	29
W8	1600.0	CoB	0.63	5.74	0.54	423	6.37	0.1	280	26
W8	1700.0	CeB	0.36	2.66	0.45	434	3.02	0.12	198	34
W8	1795.0	CeB	0.34	3.54	0.53	433	3.88	0.09	186	28
W9	850.0	UHy	0.21	7.51	1.4	437	7.72	0.03	316	59
W9	945.0	UHy	0.26	13.47	1.22	434	13.73	0.02	454	41
W9	1145.0	UHy	0.24	14.52	0.88	433	14.76	0.02	500	30
W9	1240.0	UHy	0.26	13.86	0.87	432	14.12	0.02	411	26
W9	1290.0	UHy	0.18	7.77	0.61	428	7.95	0.02	401	31
W9	1315.0	UHy	0.33	13.39	1.16	429	13.72	0.02	388	34
W9	1365.0	LHy	0.38	11.67	0.83	429	12.05	0.03	445	32
W9	1385.0	LHy	0.13	4.64	0.46	429	4.77	0.03	275	27
W9	1445.0	LHy	0.35	12.42	0.77	428	12.77	0.03	487	30
W9	1475.0	LHy	0.29	7.81	0.85	426	8.1	0.04	387	42
W9	1565.0	LHy	0.29	9.27	0.92	426	9.56	0.03	415	41
W9	1635.0	LHy	0.54	8.29	0.87	425	8.83	0.06	397	42
W9	1660.0	CyM	0.09	0.59	0.83	427	0.68	0.13	98	138
W9	1705.0	CyM/ME	0.08	1.06	0.72	429	1.14	0.07	150	102
W9	1815.0	FS (RpC)	1.52	18.54	0.22	430	20.06	0.08	1959	23
W9	1825.0	FS (RpC)	0.11	1.63	1.01	430	1.74	0.06	95	59
W9	1845.0	FM (RpC)	0.19	8.19	0.69	431	8.38	0.02	304	26
W9	1880.0	FM (RpC)	0.37	2.31	0.81	432	2.68	0.14	233	82
W9	1892.0	UPE	0.37	4.68	0.66	432	5.05	0.07	248	35
W9	1944.0	LPE	0.92	4.35	0.75	430	5.27	0.17	276	48
W9	1956.0	LPE	2.49	8.07	0.97	428	10.56	0.24	337	40
W10	820.0	UHy	0.26	12.1	1.3	445	12.36	0.02	469	50
W10	860.0	UHy	0.43	19.97	1.4	435	20.4	0.02	501	35
W10	1050.0	UHy	0.22	10.06	0.97	433	10.28	0.02	411	40
W10	1250.0	UHy	0.13	5.34	1.38	434	5.47	0.02	250	65
W10	1360.0	UHy	0.29	19.36	0.89	432	19.65	0.01	516	24
W10	1500.0	LHy	0.35	14.98	0.83	422	15.33	0.02	477	26
W10	1540.0	LHy	0.19	7.6	0.81	433	7.79	0.02	353	38
W10	1630.0	LHy	0.3	8.15	1.02	422	8.45	0.04	306	38
W10	1670.0	LHy	0.45	11.19	0.81	432	11.64	0.04	449	32
W10	1710.0	LHy	0.09	1.78	0.66	424	1.87	0.05	172	64
W10	1795.0	Cor	0.53	9.72	0.76	427	10.25	0.05	414	32
W10	1810.0	Cor	0.24	2.94	0.79	424	3.18	0.08	235	63
W10	1920.0	Cor	0.22	5.14	0.81	428	5.36	0.04	311	49
W10	2000.0	Cer	0.12	2.89	0.84	437	3.01	0.04	278	81
W10	2020.0	Cer	0.09	2.43	0.81	438	2.52	0.04	253	84
W10	2350.0	CyM & ME	0.05	0.31	0.63	433	0.36	0.14	67	136
W10	2465.0	FM (RpC)	0.29	6.07	0.67	437	6.36	0.05	257	28
W10	2490.0	FM (RpC)	0.12	1.63	0.6	441	1.75	0.07	166	61
W10	2499.0	FM (RpC)	0.07	1.03	0.38	434	1.1	0.06	157	58

Well	Depth (TVD)	Formation	S1 (mg/g)	S2 (mg/g)	S3 (mg/g)	Tmax (°C)	PP (mg/g)	PI (wt ratio)	HI (mg HC/g TOC)	OI (mg CO_2/g TOC)
W10	2584.0	MPE	0.17	0.38	0.57	332	0.55	0.31	113	169
W10	2680.0	LPE	0.84	3.83	0.34	436	4.67	0.18	203	18
W10	2684.0	LPE	0.22	0.45	0.28	336	0.67	0.33	69	43
W10	2692.0	LPE	0.69	1.96	0.33	326	2.65	0.26	172	29
W12	914.4	UHy	0.3	6.1	0.92	433	6.4	0.05	295	44
W12	1042.0	UHy	0.37	7	0.82	437	7.37	0.05	313	37
W12	1236.2	LHy	0.44	8.88	0.84	428	9.32	0.05	298	28
W12	1426.2	Cor	0.25	1.47	0.8	432	1.72	0.15	146	79
W12	1634.3	Cer	0.16	1.42	0.81	436	1.58	0.1	148	85
W14	738.4	UHy	0.86	18.34	0.87	437	19.2	0.04	432	20
W14	855.9	UHy	0.55	7.42	0.98	430	7.97	0.07	338	45
W14	962.9	UHy	0.44	9.67	1.03	435	10.11	0.04	389	41
W14	1070.1	UHy	0.43	6.21	0.81	433	6.64	0.06	278	36
W14	1188.9	LHy	0.56	12.59	0.83	427	13.15	0.04	382	25
W14	1289.6	LHy	0.2	2.21	0.77	432	2.41	0.08	150	52
W14	1384.5	LHy	0.28	4.15	0.49	423	4.43	0.06	187	22
W14	1483.8	Cor	0.13	0.06	1.14	369	0.19	0.68	8	153
W14	1591.3	Cor	0.13	1.22	0.64	427	1.35	0.1	125	65
W14	1704.5	Cer	0.12	0.78	0.59	436	0.9	0.13	96	73
W14	1808.6	Cer	0.03	0.05	0.53	330	0.08	0.38	22	234
W16	865.0	UHy	0.65	8.71	0.65	438	9.36	0.07	359	27
W16	950.0	UHy	0.58	5.9	0.58	435	6.48	0.09	227	22
W16	1050.0	UHy	0.99	14.61	0.94	435	15.6	0.06	421	27
W16	1150.0	UHy	0.67	8.22	0.56	434	8.89	0.08	276	19
W16	1250.0	LHy	0.42	4.29	0.66	433	4.71	0.09	189	29
W16	1350.0	LHy	0.55	8.64	0.51	430	9.19	0.06	344	20
W16	1450.0	LHy	0.53	4.34	0.59	435	4.87	0.11	229	31
W16	1560.0	LHy	0.37	2.07	0.5	435	2.44	0.15	179	43
W16	1652.5	Cor	0.3	1.39	0.52	422	1.69	0.18	119	44
W16	1720.0	Cor	0.4	2.97	0.34	428	3.37	0.12	224	26
W16	1800.0	Cer	0.38	1.54	0.39	439	1.92	0.2	163	41
W16	1900.0	Cer	0.25	1.49	0.32	442	1.74	0.14	174	37
W16	2300.0	FS (RpC)	0.22	1.01	0.33	434	1.23	0.18	134	44
W16	2414.3	MPE	0.08	0.09	0.49	307	0.17	0.47	30	163
W16	2435.6	LPE?	0.06	0.37	0.22	436	0.43	0.14	58	34
W17	674.3	UHy	0.83	23.97	0.69	442	24.8	0.03	592	17
W17	676.8	UHy	0.51	12.11	0.67	441	12.62	0.04	450	25
W17	750.8	UHy	0.5	9.7	0.56	436	10.2	0.05	427	25
W19	1509.6	Cer	0.13	1.27	0.39	438	1.4	0.09	121	37
W19	1927.0	FM (RpC)	0.09	0.3	0.13	442	0.39	0.23	64	28
W19	1927.6	UPE	0.25	0.99	0.14	433	1.24	0.2	112	16
W19	1928.2	UPE	0.37	4.49	0.34	430	4.86	0.08	77	6
W23	1136.5	Cor	0.27	1.63	0.69	418	1.9	0.14	141	60
W23	1245.0	Cor	0.6	4.06	0.65	423	4.66	0.13	245	39
W23	1350.0	Cor	0.39	4.2	0.59	429	4.59	0.08	269	38
W31	2768.0	LPE	0.16	0.23	0.14	438	0.39	0.41	43	26

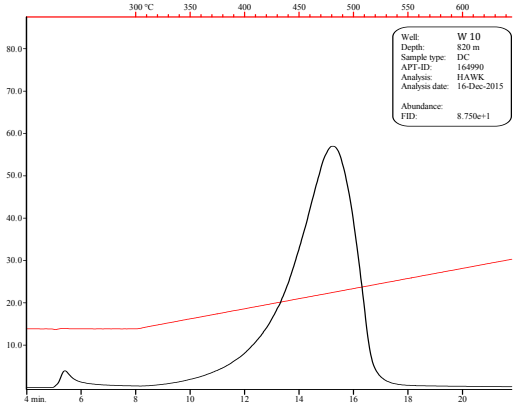
300 °C 350 400 450 500 550 600
Well: W 10
Depth: 820 m
Sample type: DC
APT-ID: 164990
Analysis: HAWK
Analysis date: 16-Dec-2015
Abundance:
FID: 8.750e+1
80.0 70.0 60.0 50.0 40.0 30.0 20.0 10.0
4 min. 6 8 10 12 14 16 18 20

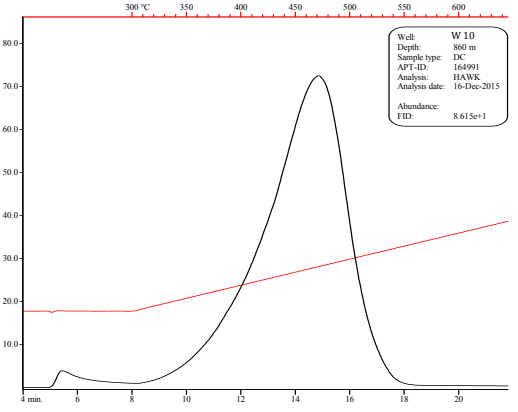
300 °C 350 400 450 500 550 600
Well: W 10
Depth: 860 m
Sample type: DC
APT-ID: 164991
Analysis: HAWK
Analysis date: 16-Dec-2015
Abundance:
FID: 8.615e+1
80.0 70.0 60.0 50.0 40.0 30.0 20.0 10.0
4 min. 6 8 10 12 14 16 18 20

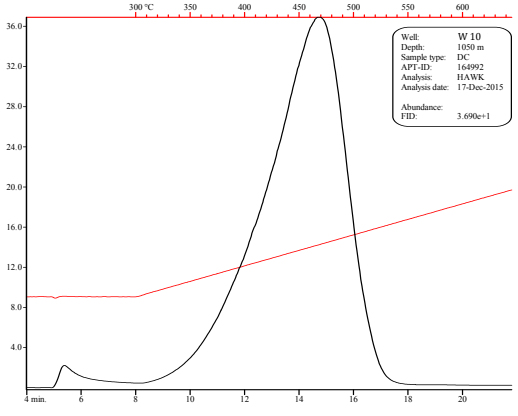
300 °C 350 400 450 500 550 600
Well: W 10
Depth: 1050 m
Sample type: DC
APT-ID: 164992
Analysis: HAWK
Analysis date: 17-Dec-2015
Abundance:
FID: 3.690e+1
36.0 32.0 28.0 24.0 20.0 16.0 12.0 8.0 4.0
4 min. 6 8 10 12 14 16 18 20

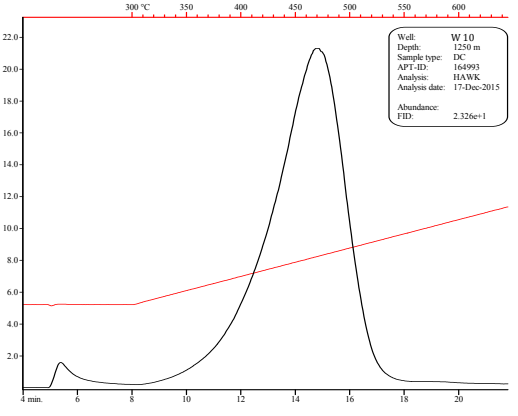
300 °C 350 400 450 500 550 600
Well: W 10
Depth: 1250 m
Sample type: DC
APT-ID: 164993
Analysis: HAWK
Analysis date: 17-Dec-2015
Abundance:
FID: 2.326e+1
22.0 20.0 18.0 16.0 14.0 12.0 10.0 8.0 6.0 4.0 2.0
4 min. 6 8 10 12 14 16 18 20

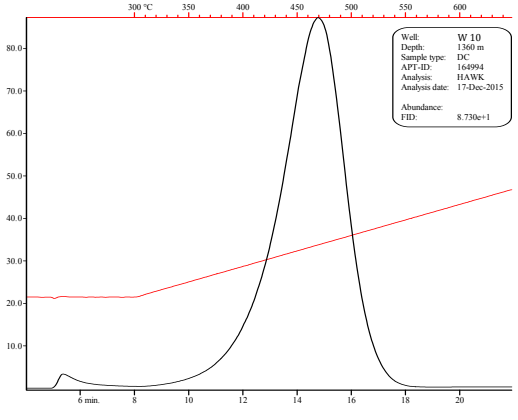
300 °C 350 400 450 500 550 600
Well: W 10
Depth: 1360 m
Sample type: DC
APT-ID: 164994
Analysis: HAWK
Analysis date: 17-Dec-2015
Abundance:
FID: 8.730e+1
80.0 70.0 60.0 50.0 40.0 30.0 20.0 10.0
6 min. 8 10 12 14 16 18 20

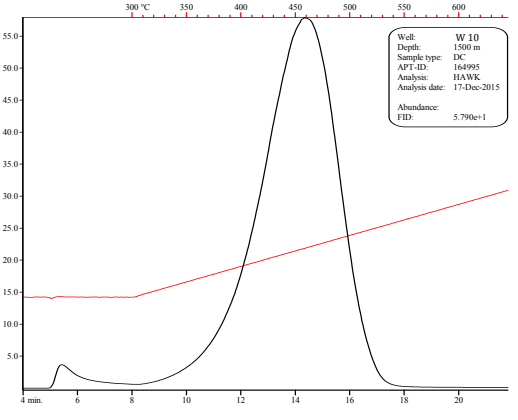
300 °C 350 400 450 500 550 600
Well: W 10
Depth: 1500 m
Sample type: DC
APT-ID: 164995
Analysis: HAWK
Analysis date: 17-Dec-2015
Abundance:
FID: 5.790e+1
55.0 50.0 45.0 40.0 35.0 30.0 25.0 20.0 15.0 10.0 5.0
4 min. 6 8 10 12 14 16 18 20

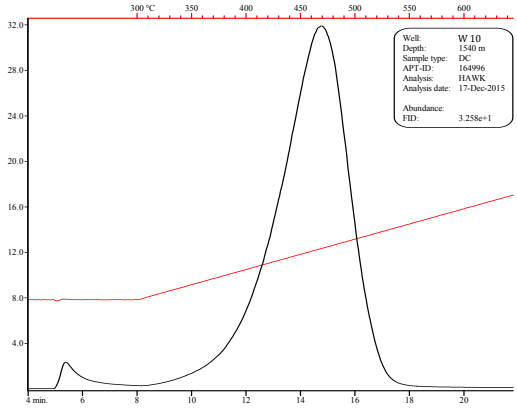
Well: W 10
Depth: 1540 m
Sample type: DC
APT-ID: 164996
Analysis: HAWK
Analysis date: 17-Dec-2015
Abundance:
FID: 3.258e+1

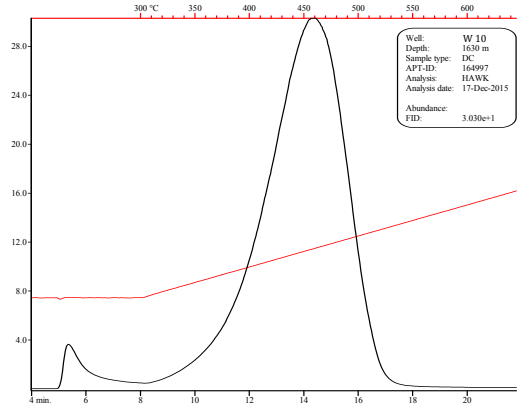
Well: W 10
Depth: 1630 m
Sample type: DC
APT-ID: 164997
Analysis: HAWK
Analysis date: 17-Dec-2015
Abundance:
FID: 3.030e+1

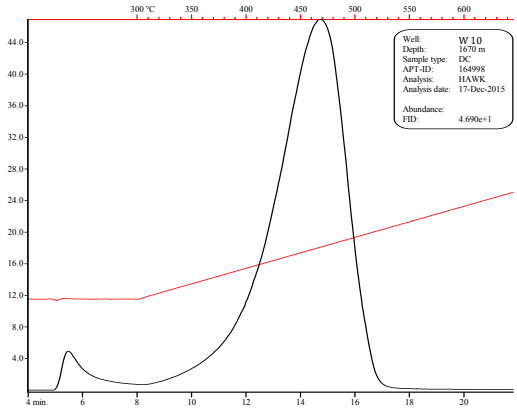
Well: W 10
Depth: 1670 m
Sample type: DC
APT-ID: 164998
Analysis: HAWK
Analysis date: 17-Dec-2015
Abundance:
FID: 4.690e+1

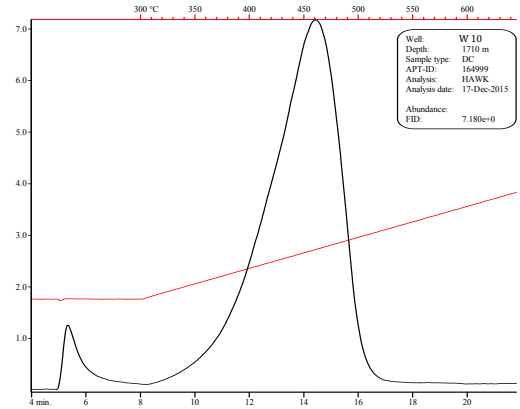
Well: W 10
Depth: 1710 m
Sample type: DC
APT-ID: 164999
Analysis: HAWK
Analysis date: 17-Dec-2015
Abundance:
FID: 7.180e+0

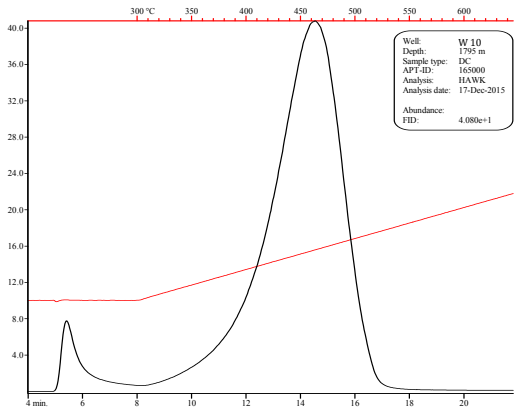
Well: W 10
Depth: 1795 m
Sample type: DC
APT-ID: 165000
Analysis: HAWK
Analysis date: 17-Dec-2015
Abundance:
FID: 4.080e+1

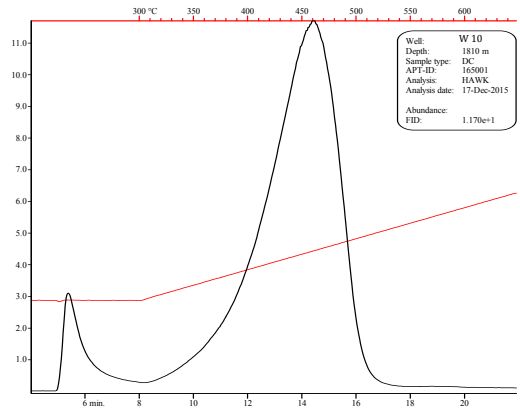
Well: W 10
Depth: 1810 m
Sample type: DC
APT-ID: 165001
Analysis: HAWK
Analysis date: 17-Dec-2015
Abundance:
FID: 1.170e+1

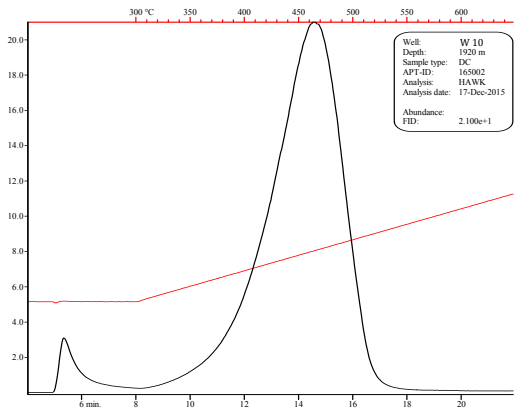
Well: W 10
Depth: 1920 m
Sample type: DC
APT-ID: 165002
Analysis: HAWK
Analysis date: 17-Dec-2015
Abundance:
FID: 2.100e+1

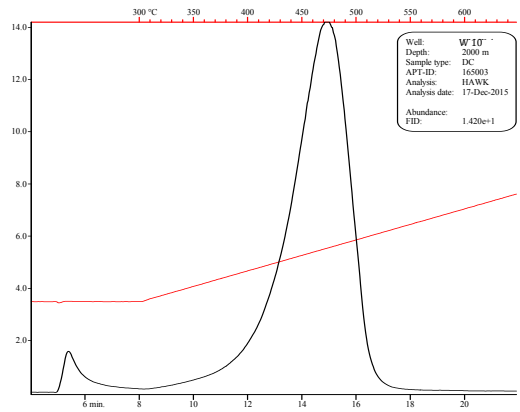
Well: W 10
Depth: 2000 m
Sample type: DC
APT-ID: 165003
Analysis: HAWK
Analysis date: 17-Dec-2015
Abundance:
FID: 1.420e+1

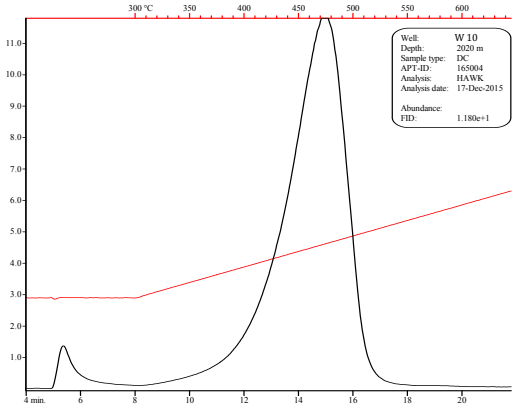
300 °C 350 400 450 500 550 600
Well: W 10
Depth: 2020 m
Sample type: DC
APT-ID: 165004
Analysis: HAWK
Analysis date: 17-Dec-2015
Abundance:
FID: 1.180e+1
4 min. 6 8 10 12 14 16 18 20

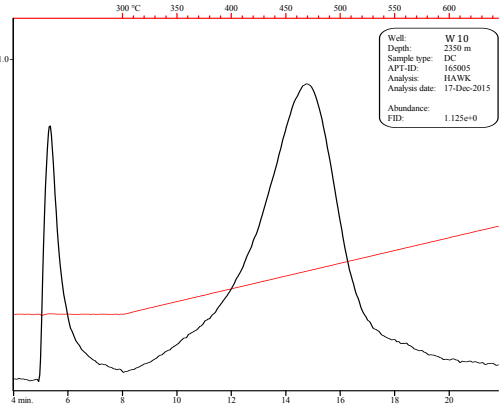
300 °C 350 400 450 500 550 600
Well: W 10
Depth: 2350 m
Sample type: DC
APT-ID: 165005
Analysis: HAWK
Analysis date: 17-Dec-2015
Abundance:
FID: 1.125e+0
4 min. 6 8 10 12 14 16 18 20

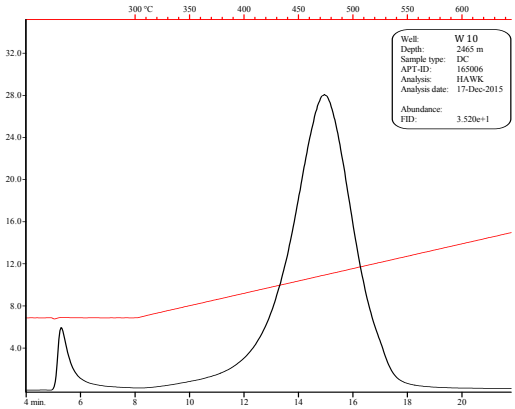
300 °C 350 400 450 500 550 600
Well: W 10
Depth: 2465 m
Sample type: DC
APT-ID: 165006
Analysis: HAWK
Analysis date: 17-Dec-2015
Abundance:
FID: 3.520e+1
4 min. 6 8 10 12 14 16 18 20

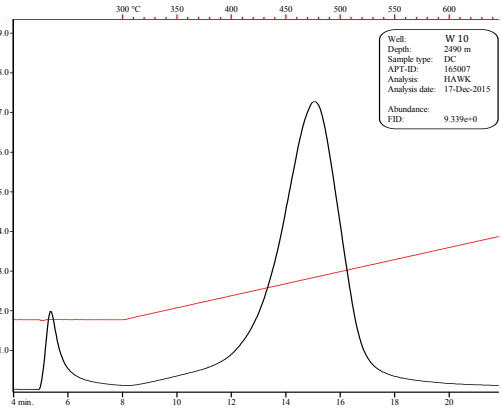
300 °C 350 400 450 500 550 600
Well: W 10
Depth: 2490 m
Sample type: DC
APT-ID: 165007
Analysis: HAWK
Analysis date: 17-Dec-2015
Abundance:
FID: 9.339e+0
4 min. 6 8 10 12 14 16 18 20

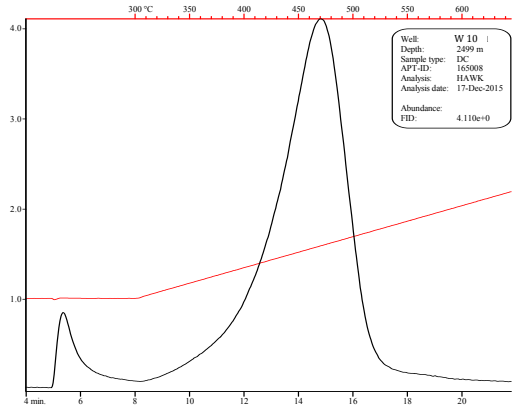
300 °C 350 400 450 500 550 600
Well: W 10
Depth: 2499 m
Sample type: DC
APT-ID: 165008
Analysis: HAWK
Analysis date: 17-Dec-2015
Abundance:
FID: 4.110e+0
4 min. 6 8 10 12 14 16 18 20

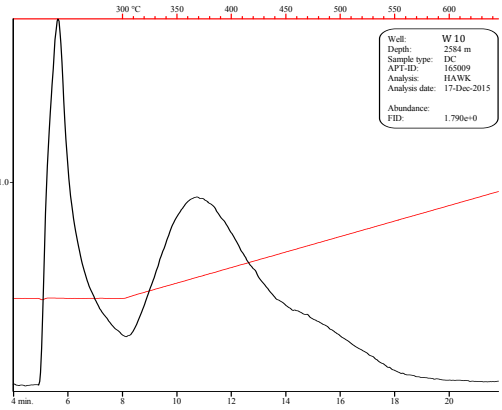
300 °C 350 400 450 500 550 600
Well: W 10
Depth: 2584 m
Sample type: DC
APT-ID: 165009
Analysis: HAWK
Analysis date: 17-Dec-2015
Abundance:
FID: 1.790e+0
4 min. 6 8 10 12 14 16 18 20

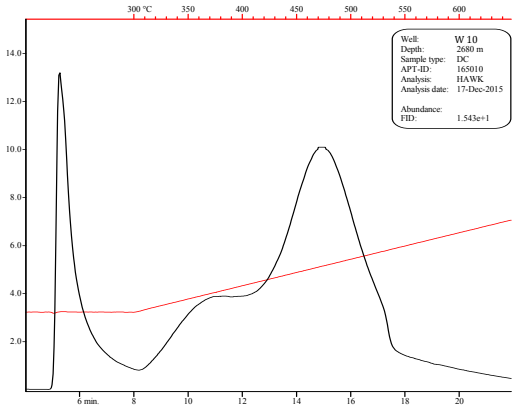
300 °C 350 400 450 500 550 600
Well: W 10
Depth: 2680 m
Sample type: DC
APT-ID: 165010
Analysis: HAWK
Analysis date: 17-Dec-2015
Abundance:
FID: 1.543e+1
6 min. 8 10 12 14 16 18 20

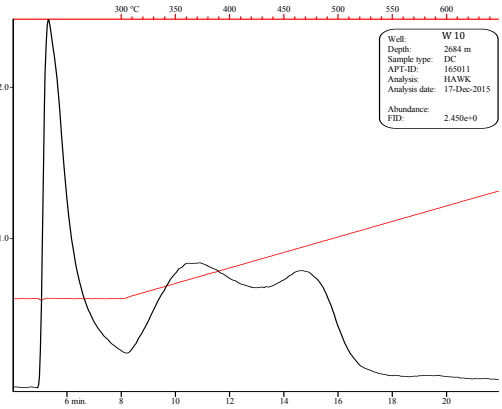
300 °C 350 400 450 500 550 600
Well: W 10
Depth: 2684 m
Sample type: DC
APT-ID: 165011
Analysis: HAWK
Analysis date: 17-Dec-2015
Abundance:
FID: 2.450e+0
6 min. 8 10 12 14 16 18 20

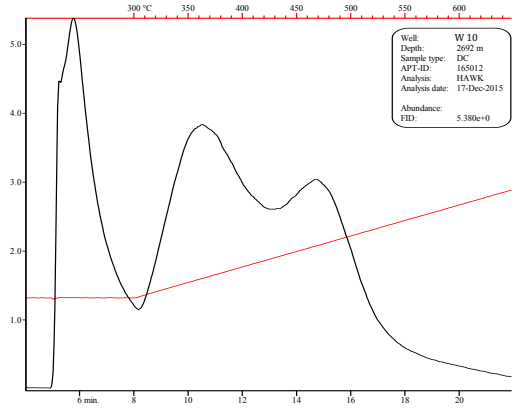
Well: W 10
Depth: 2692 m
Sample type: DC
APT-ID: 165012
Analysis: HAWK
Analysis date: 17-Dec-2015
Abundance:
FID: 5.380e+0

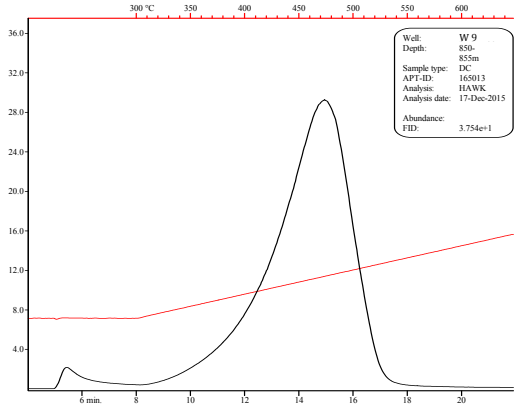
Well: W 9
Depth: 850-855m
Sample type: DC
APT-ID: 165013
Analysis: HAWK
Analysis date: 17-Dec-2015
Abundance:
FID: 3.754e+1

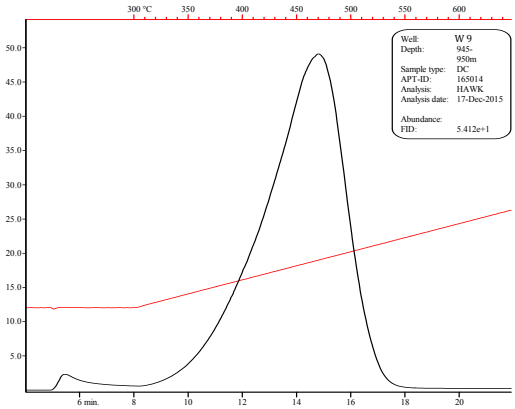
Well: W 9
Depth: 945-950m
Sample type: DC
APT-ID: 165014
Analysis: HAWK
Analysis date: 17-Dec-2015
Abundance:
FID: 5.412e+1

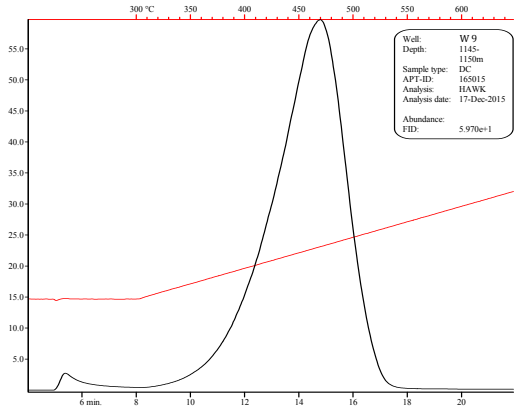
Well: W 9
Depth: 1145-1150m
Sample type: DC
APT-ID: 165015
Analysis: HAWK
Analysis date: 17-Dec-2015
Abundance:
FID: 5.970e+1

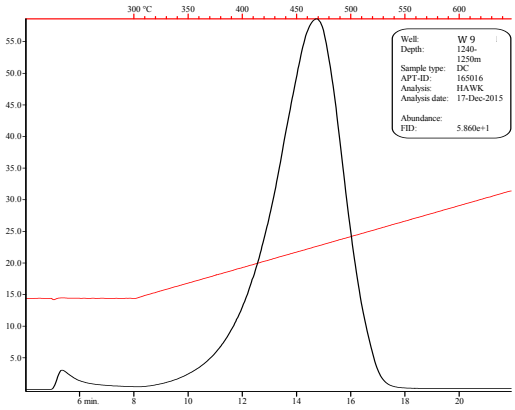
Well: W 9
Depth: 1240-1250m
Sample type: DC
APT-ID: 165016
Analysis: HAWK
Analysis date: 17-Dec-2015
Abundance:
FID: 5.860e+1

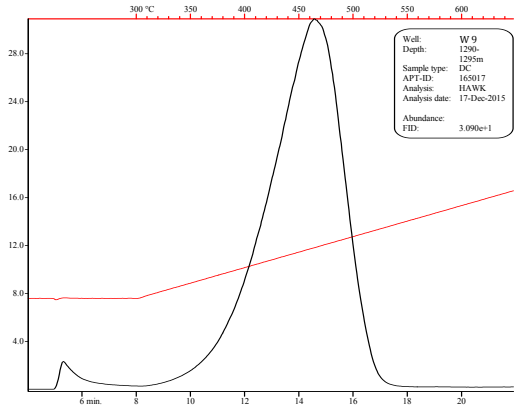
Well: W 9
Depth: 1290-1295m
Sample type: DC
APT-ID: 165017
Analysis: HAWK
Analysis date: 17-Dec-2015
Abundance:
FID: 3.090e+1

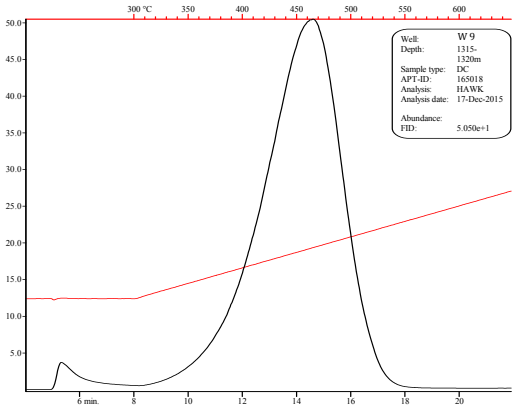
Well: W 9
Depth: 1315-1320m
Sample type: DC
APT-ID: 165018
Analysis: HAWK
Analysis date: 17-Dec-2015
Abundance:
FID: 5.050e+1

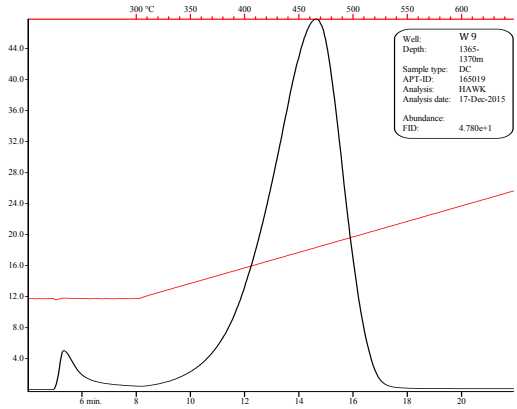
Well: W 9
Depth: 1365-1370m
Sample type: DC
APT-ID: 165019
Analysis: HAWK
Analysis date: 17-Dec-2015
Abundance:
FID: 4.780e+1

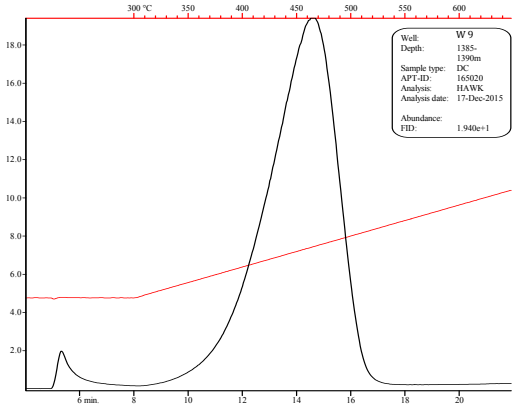
300 °C 350 400 450 500 550 600
Well: W 9
Depth: 1385-1390m
Sample type: DC
APT-ID: 165020
Analysis: HAWK
Analysis date: 17-Dec-2015
Abundance:
FID: 1.940e+1
6 min. 8 10 12 14 16 18 20

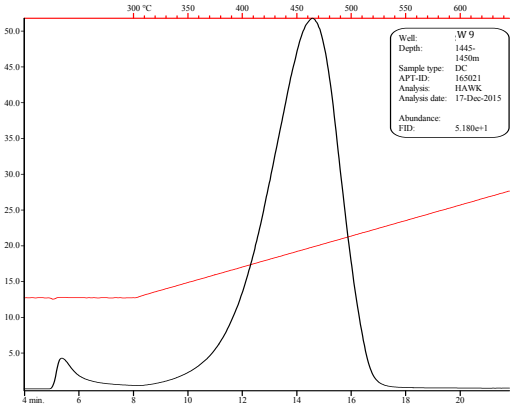
300 °C 350 400 450 500 550 600
Well: W 9
Depth: 1445-1450m
Sample type: DC
APT-ID: 165021
Analysis: HAWK
Analysis date: 17-Dec-2015
Abundance:
FID: 5.180e+1
4 min. 6 8 10 12 14 16 18 20

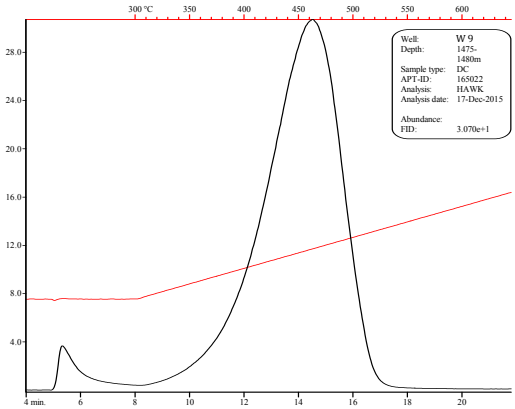
300 °C 350 400 450 500 550 600
Well: W 9
Depth: 1475-1480m
Sample type: DC
APT-ID: 165022
Analysis: HAWK
Analysis date: 17-Dec-2015
Abundance:
FID: 3.070e+1
4 min. 6 8 10 12 14 16 18 20

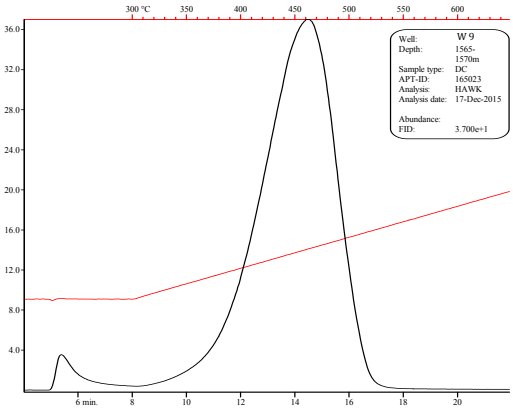
300 °C 350 400 450 500 550 600
Well: W 9
Depth: 1565-1570m
Sample type: DC
APT-ID: 165023
Analysis: HAWK
Analysis date: 17-Dec-2015
Abundance:
FID: 3.700e+1
6 min. 8 10 12 14 16 18 20

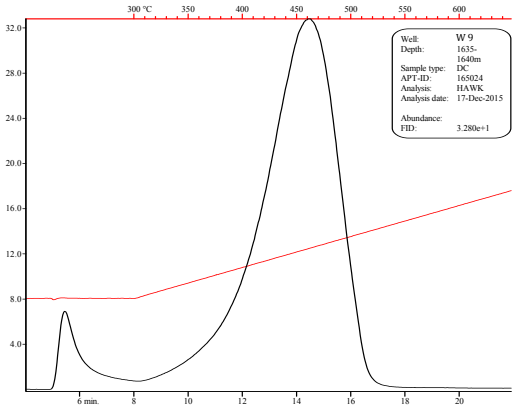
300 °C 350 400 450 500 550 600
Well: W 9
Depth: 1635-1640m
Sample type: DC
APT-ID: 165024
Analysis: HAWK
Analysis date: 17-Dec-2015
Abundance:
FID: 3.280e+1
6 min. 8 10 12 14 16 18 20

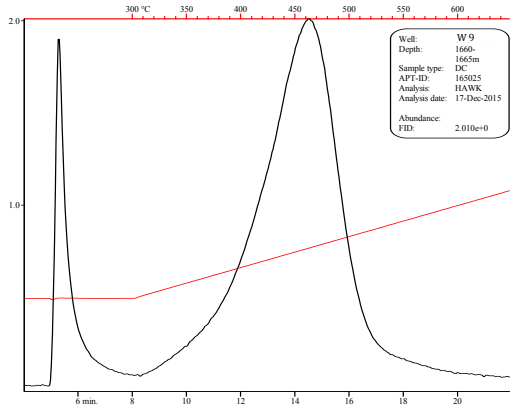
300 °C 350 400 450 500 550 600
Well: W 9
Depth: 1660-1665m
Sample type: DC
APT-ID: 165025
Analysis: HAWK
Analysis date: 17-Dec-2015
Abundance:
FID: 2.010e+0
6 min. 8 10 12 14 16 18 20

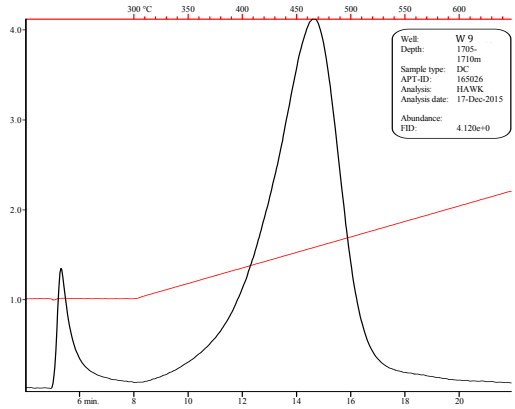
300 °C 350 400 450 500 550 600
Well: W 9
Depth: 1705-1710m
Sample type: DC
APT-ID: 165026
Analysis: HAWK
Analysis date: 17-Dec-2015
Abundance:
FID: 4.120e+0
6 min. 8 10 12 14 16 18 20

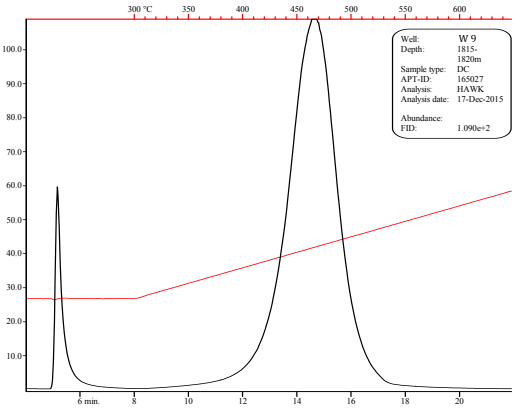
300 °C 350 400 450 500 550 600
Well: W 9
Depth: 1815-1820m
Sample type: DC
APT-ID: 165027
Analysis: HAWK
Analysis date: 17-Dec-2015
Abundance:
FID: 1.090e+2
6 min. 8 10 12 14 16 18 20

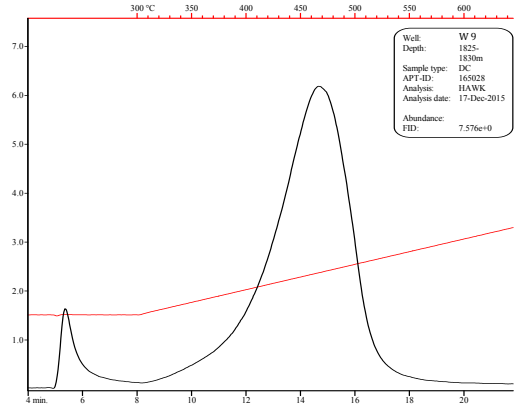
300 °C 350 400 450 500 550 600
Well: W 9
Depth: 1825-1830m
Sample type: DC
APT-ID: 165028
Analysis: HAWK
Analysis date: 17-Dec-2015
Abundance:
FID: 7.576e+0
4 min. 6 8 10 12 14 16 18 20

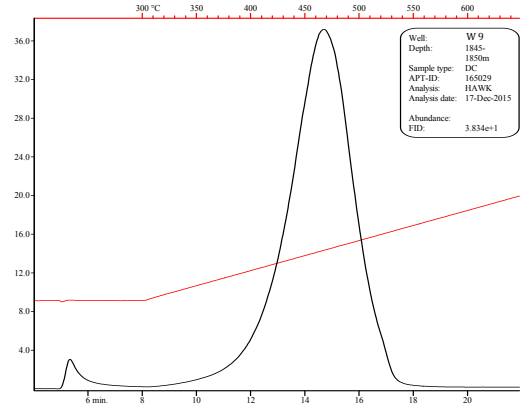
300 °C 350 400 450 500 550 600
Well: W 9
Depth: 1845-1850m
Sample type: DC
APT-ID: 165029
Analysis: HAWK
Analysis date: 17-Dec-2015
Abundance:
FID: 3.834e+1
6 min. 8 10 12 14 16 18 20

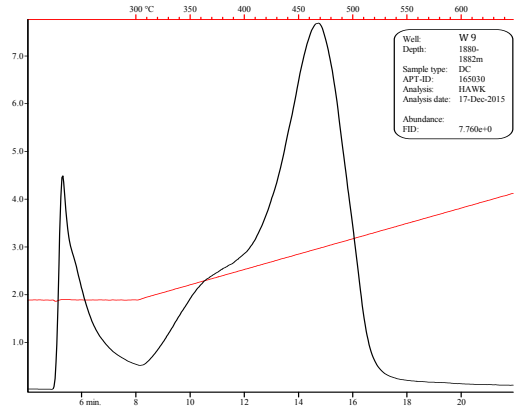
300 °C 350 400 450 500 550 600
Well: W 9
Depth: 1880-1882m
Sample type: DC
APT-ID: 165030
Analysis: HAWK
Analysis date: 17-Dec-2015
Abundance:
FID: 7.760e+0
6 min. 8 10 12 14 16 18 20

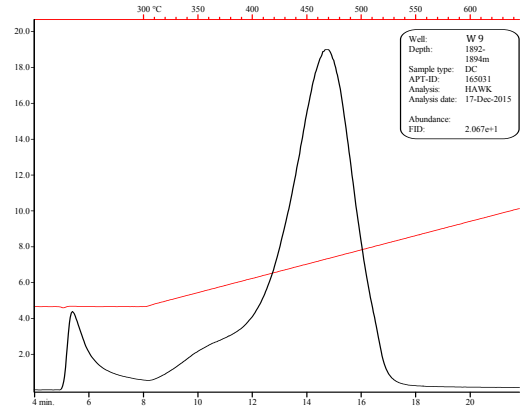
300 °C 350 400 450 500 550 600
Well: W 9
Depth: 1892-1894m
Sample type: DC
APT-ID: 165031
Analysis: HAWK
Analysis date: 17-Dec-2015
Abundance:
FID: 2.067e+1
4 min. 6 8 10 12 14 16 18 20

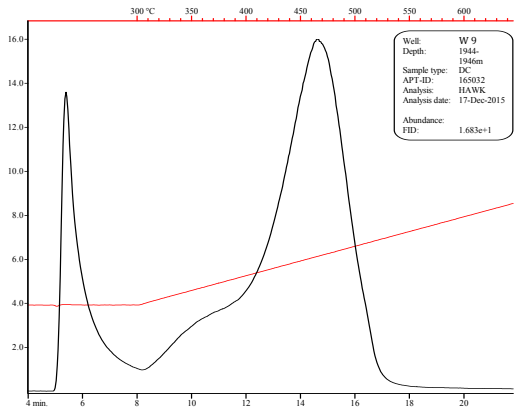
300 °C 350 400 450 500 550 600
Well: W 9
Depth: 1944-1946m
Sample type: DC
APT-ID: 165032
Analysis: HAWK
Analysis date: 17-Dec-2015
Abundance:
FID: 1.683e+1
4 min. 6 8 10 12 14 16 18 20

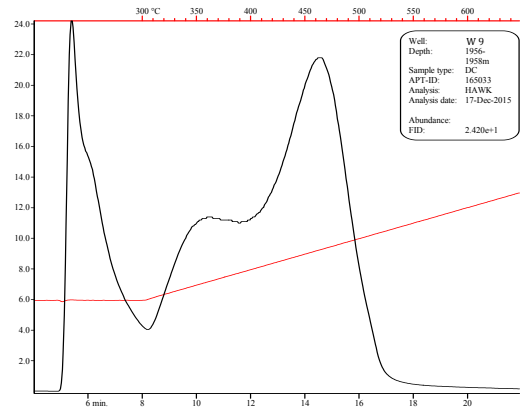
300 °C 350 400 450 500 550 600
Well: W 9
Depth: 1956-1958m
Sample type: DC
APT-ID: 165033
Analysis: HAWK
Analysis date: 17-Dec-2015
Abundance:
FID: 2.420e+1
6 min. 8 10 12 14 16 18 20

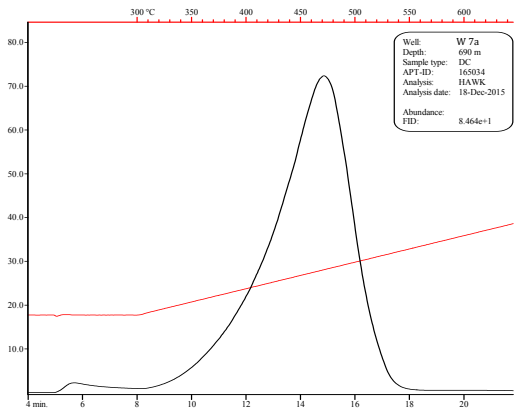
300 °C 350 400 450 500 550 600
Well: W 7a
Depth: 690 m
Sample type: DC
APT-ID: 165034
Analysis: HAWK
Analysis date: 18-Dec-2015
Abundance:
FID: 8.464e+1
4 min. 6 8 10 12 14 16 18 20

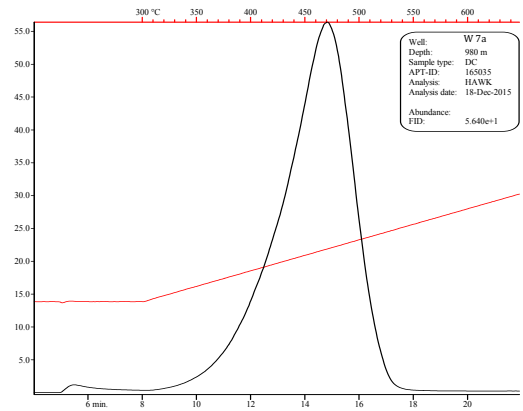
300 °C 350 400 450 500 550 600
Well: W 7a
Depth: 980 m
Sample type: DC
APT-ID: 165035
Analysis: HAWK
Analysis date: 18-Dec-2015
Abundance:
FID: 5.640e+1
6 min. 8 10 12 14 16 18 20

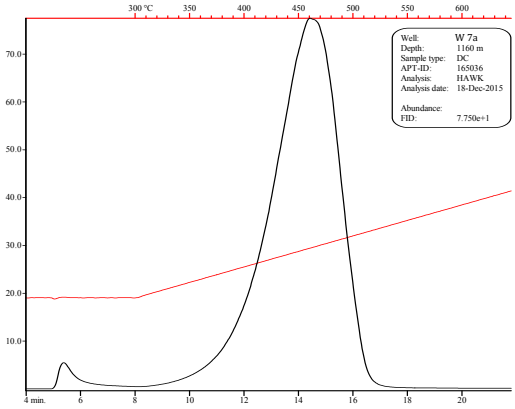
300 °C 350 400 450 500 550 600
Well: W 7a
Depth: 1160 m
Sample type: DC
APT-ID: 165036
Analysis: HAWK
Analysis date: 18-Dec-2015
Abundance:
FID: 7.750e+1
4 min. 6 8 10 12 14 16 18 20

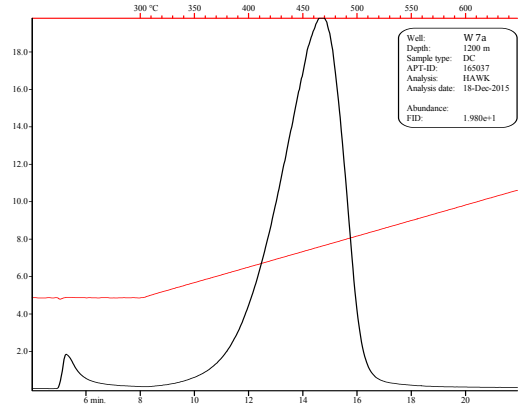
300 °C 350 400 450 500 550 600
Well: W 7a
Depth: 1200 m
Sample type: DC
APT-ID: 165037
Analysis: HAWK
Analysis date: 18-Dec-2015
Abundance:
FID: 1.980e+1
6 min. 8 10 12 14 16 18 20

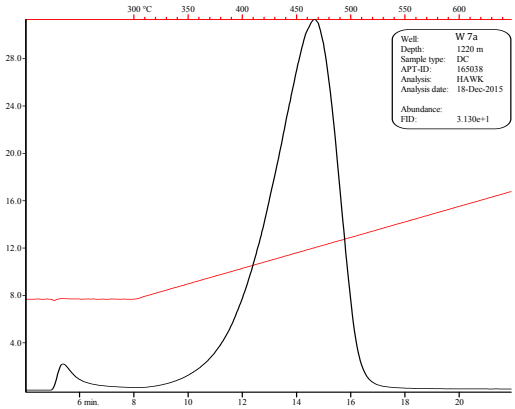
300 °C 350 400 450 500 550 600
Well: W 7a
Depth: 1220 m
Sample type: DC
APT-ID: 165038
Analysis: HAWK
Analysis date: 18-Dec-2015
Abundance:
FID: 3.130e+1
6 min. 8 10 12 14 16 18 20

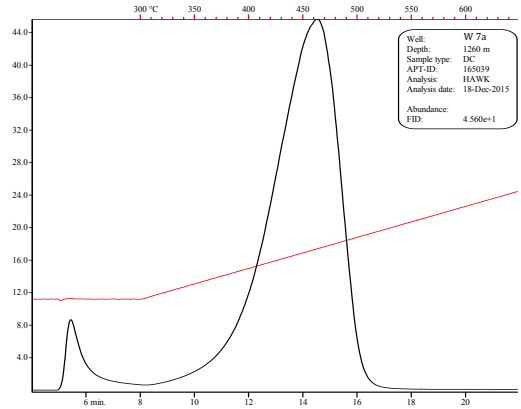
300 °C 350 400 450 500 550 600
Well: W 7a
Depth: 1260 m
Sample type: DC
APT-ID: 165039
Analysis: HAWK
Analysis date: 18-Dec-2015
Abundance:
FID: 4.560e+1
6 min. 8 10 12 14 16 18 20

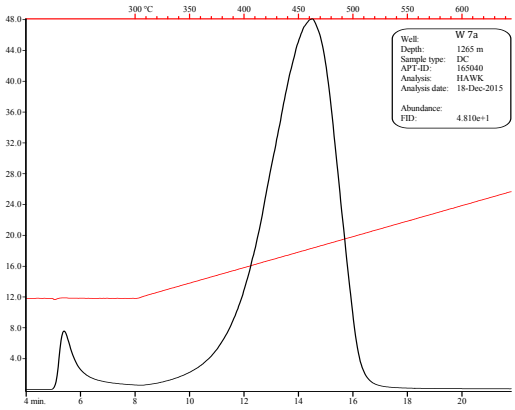
300 °C 350 400 450 500 550 600
Well: W 7a
Depth: 1265 m
Sample type: DC
APT-ID: 165040
Analysis: HAWK
Analysis date: 18-Dec-2015
Abundance:
FID: 4.810e+1
4 min. 6 8 10 12 14 16 18 20

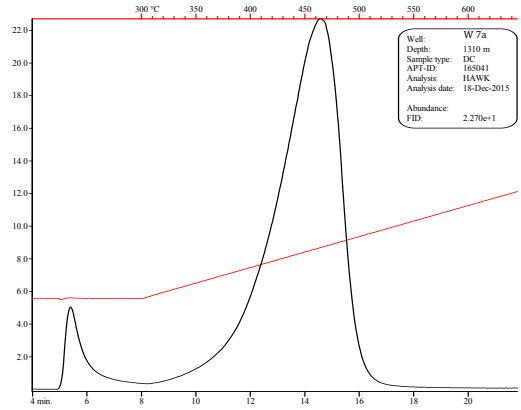
300 °C 350 400 450 500 550 600
Well: W 7a
Depth: 1310 m
Sample type: DC
APT-ID: 165041
Analysis: HAWK
Analysis date: 18-Dec-2015
Abundance:
FID: 2.270e+1
4 min. 6 8 10 12 14 16 18 20

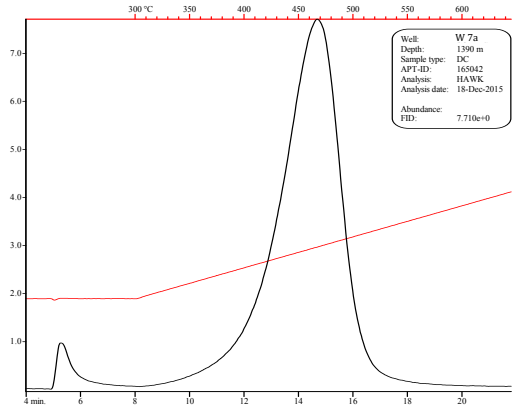
300 °C 350 400 450 500 550 600
Well: W 7a
Depth: 1390 m
Sample type: DC
APT-ID: 165042
Analysis: HAWK
Analysis date: 18-Dec-2015
Abundance:
FID: 7.710e+0
4 min. 6 8 10 12 14 16 18 20

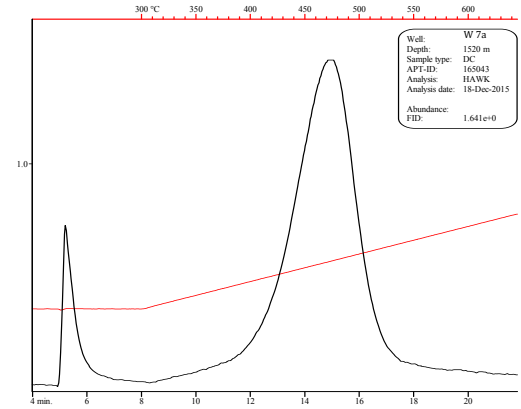
300 °C 350 400 450 500 550 600
Well: W 7a
Depth: 1520 m
Sample type: DC
APT-ID: 165043
Analysis: HAWK
Analysis date: 18-Dec-2015
Abundance:
FID: 1.641e+0
4 min. 6 8 10 12 14 16 18 20

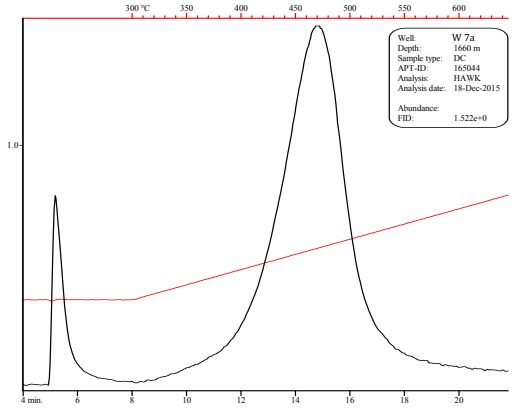
300 °C 350 400 450 500 550 600
Well: W 7a
Depth: 1660 m
Sample type: DC
APT-ID: 165044
Analysis: HAWK
Analysis date: 18-Dec-2015
Abundance:
FID: 1.522e+0
1.0
4 min. 6 8 10 12 14 16 18 20

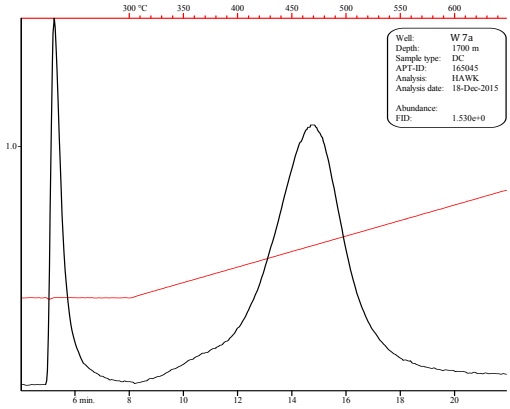
300 °C 350 400 450 500 550 600
Well: W 7a
Depth: 1700 m
Sample type: DC
APT-ID: 165045
Analysis: HAWK
Analysis date: 18-Dec-2015
Abundance:
FID: 1.530e+0
1.0
6 min. 8 10 12 14 16 18 20

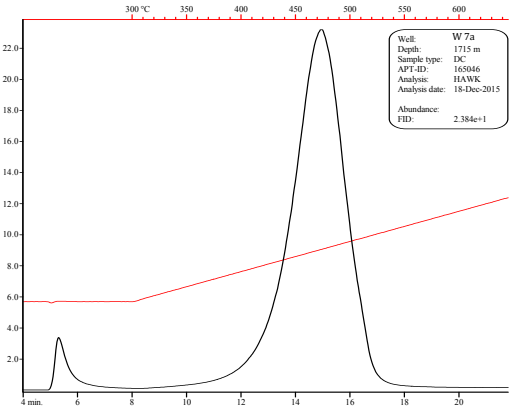
300 °C 350 400 450 500 550 600
Well: W 7a
Depth: 1715 m
Sample type: DC
APT-ID: 165046
Analysis: HAWK
Analysis date: 18-Dec-2015
Abundance:
FID: 2.384e+1
22.0 20.0 18.0 16.0 14.0 12.0 10.0 8.0 6.0 4.0 2.0
4 min. 6 8 10 12 14 16 18 20

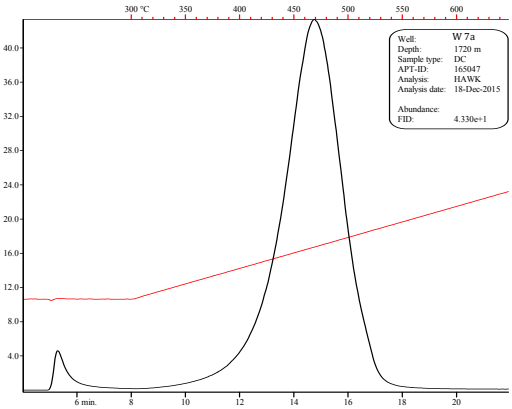
300 °C 350 400 450 500 550 600
Well: W 7a
Depth: 1720 m
Sample type: DC
APT-ID: 165047
Analysis: HAWK
Analysis date: 18-Dec-2015
Abundance:
FID: 4.330e+1
40.0 36.0 32.0 28.0 24.0 20.0 16.0 12.0 8.0 4.0
6 min. 8 10 12 14 16 18 20

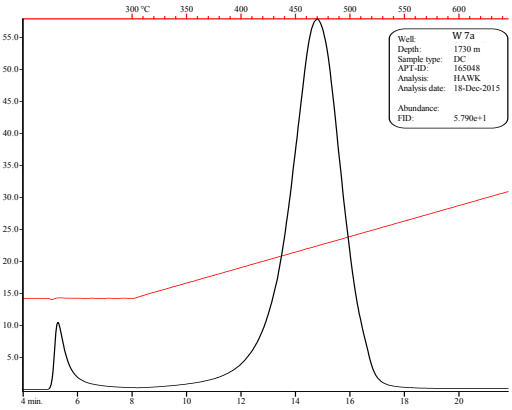
300 °C 350 400 450 500 550 600
Well: W 7a
Depth: 1730 m
Sample type: DC
APT-ID: 165048
Analysis: HAWK
Analysis date: 18-Dec-2015
Abundance:
FID: 5.790e+1
55.0 50.0 45.0 40.0 35.0 30.0 25.0 20.0 15.0 10.0 5.0
4 min. 6 8 10 12 14 16 18 20

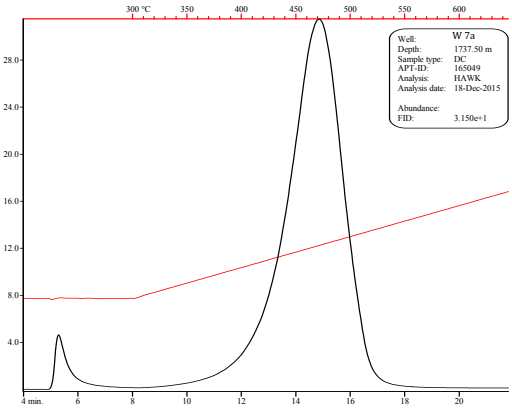
300 °C 350 400 450 500 550 600
Well: W 7a
Depth: 1737.50 m
Sample type: DC
APT-ID: 165049
Analysis: HAWK
Analysis date: 18-Dec-2015
Abundance:
FID: 3.150e+1
28.0 24.0 20.0 16.0 12.0 8.0 4.0
4 min. 6 8 10 12 14 16 18 20

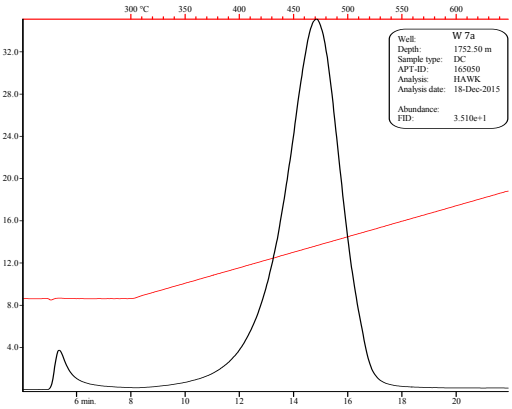
300 °C 350 400 450 500 550 600
Well: W 7a
Depth: 1752.50 m
Sample type: DC
APT-ID: 165050
Analysis: HAWK
Analysis date: 18-Dec-2015
Abundance:
FID: 3.510e+1
32.0 28.0 24.0 20.0 16.0 12.0 8.0 4.0
6 min. 8 10 12 14 16 18 20

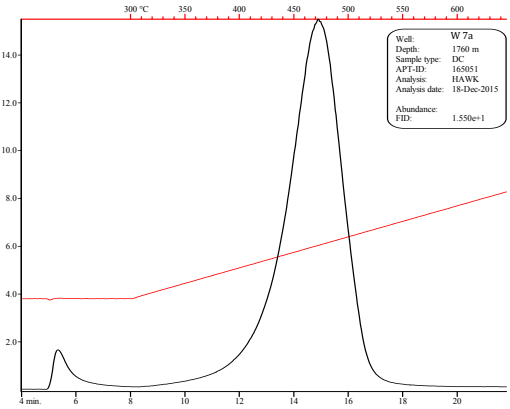
300 °C 350 400 450 500 550 600
Well: W 7a
Depth: 1760 m
Sample type: DC
APT-ID: 165051
Analysis: HAWK
Analysis date: 18-Dec-2015
Abundance:
FID: 1.550e+1
14.0 12.0 10.0 8.0 6.0 4.0 2.0
4 min. 6 8 10 12 14 16 18 20

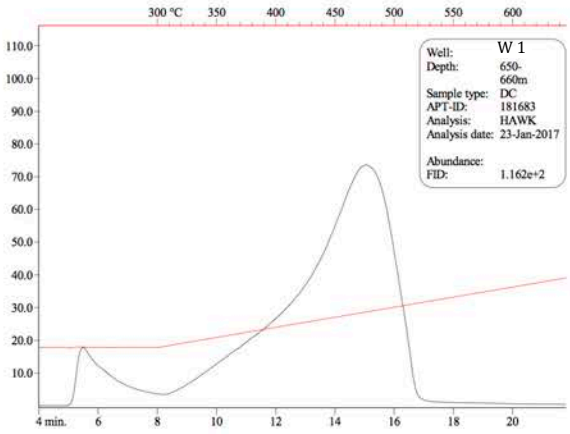
300 °C 350 400 450 500 550 600
110.0 100.0 90.0 80.0 70.0 60.0 50.0 40.0 30.0 20.0 10.0
4 min. 6 8 10 12 14 16 18 20
Well: W 1
Depth: 650-660m
Sample type: DC
APT-ID: 181683
Analysis: HAWK
Analysis date: 23-Jan-2017
Abundance:
FID: 1.162e+2

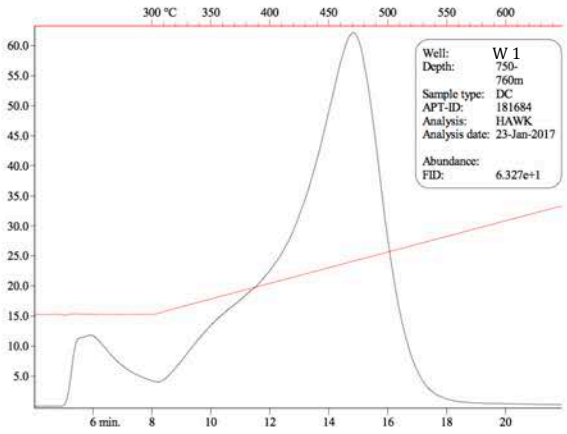
300 °C 350 400 450 500 550 600
60.0 55.0 50.0 45.0 40.0 35.0 30.0 25.0 20.0 15.0 10.0 5.0
6 min. 8 10 12 14 16 18 20
Well: W 1
Depth: 750-760m
Sample type: DC
APT-ID: 181684
Analysis: HAWK
Analysis date: 23-Jan-2017
Abundance:
FID: 6.327e+1

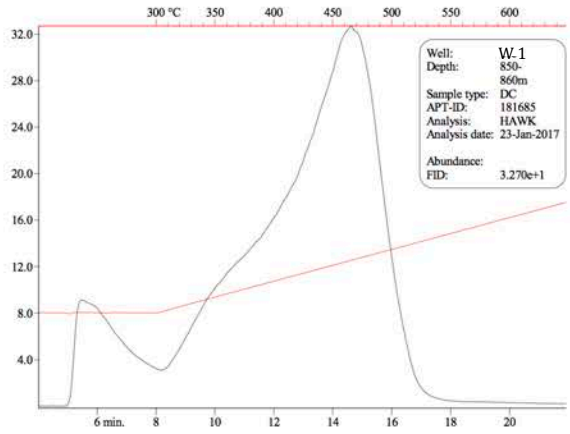
300 °C 350 400 450 500 550 600
32.0 28.0 24.0 20.0 16.0 12.0 8.0 4.0
6 min. 8 10 12 14 16 18 20
Well: W 1
Depth: 850-860m
Sample type: DC
APT-ID: 181685
Analysis: HAWK
Analysis date: 23-Jan-2017
Abundance:
FID: 3.270e+1

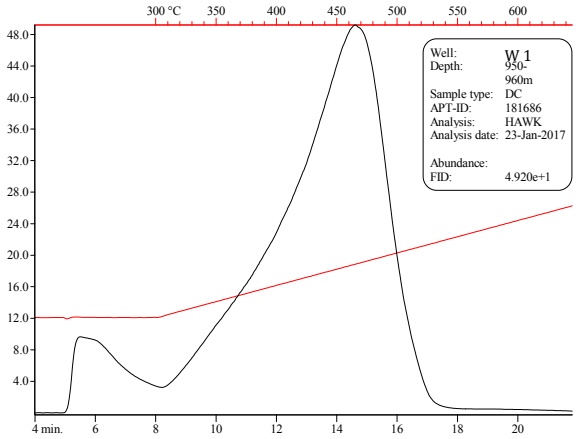
Well: W 1
Depth: 950-960m
Sample type: DC
APT-ID: 181686
Analysis: HAWK
Analysis date: 23-Jan-2017
Abundance:
FID: 4.920e+1

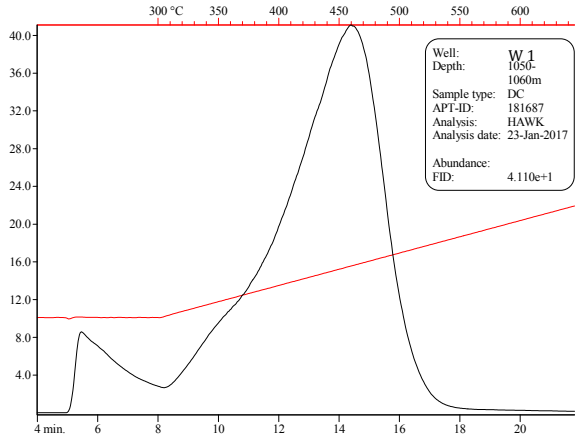
Well: W 1
Depth: 1050-1060m
Sample type: DC
APT-ID: 181687
Analysis: HAWK
Analysis date: 23-Jan-2017
Abundance:
FID: 4.110e+1

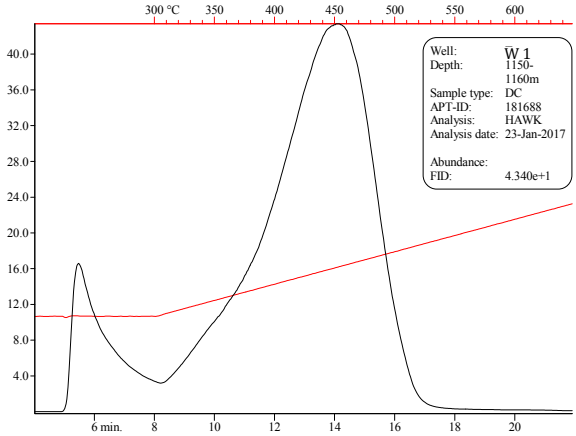
Well: W 1
Depth: 1150-1160m
Sample type: DC
APT-ID: 181688
Analysis: HAWK
Analysis date: 23-Jan-2017
Abundance:
FID: 4.340e+1

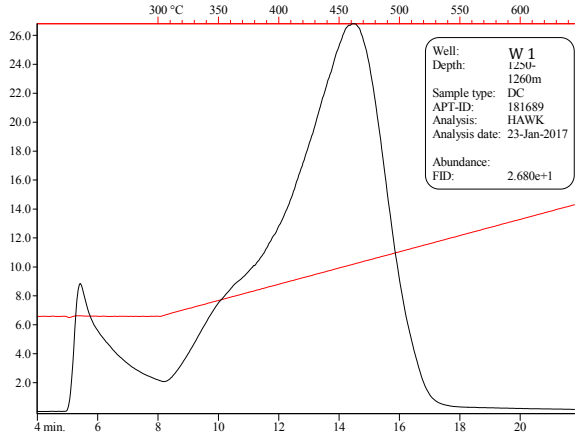
Well: W 1
Depth: 1250-1260m
Sample type: DC
APT-ID: 181689
Analysis: HAWK
Analysis date: 23-Jan-2017
Abundance:
FID: 2.680e+1

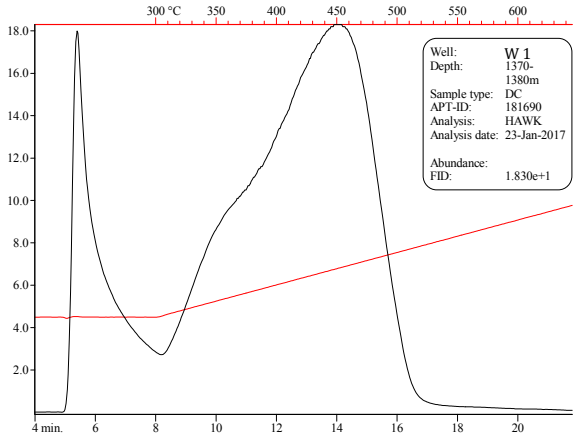
Well: W 1
Depth: 1370-1380m
Sample type: DC
APT-ID: 181690
Analysis: HAWK
Analysis date: 23-Jan-2017
Abundance:
FID: 1.830e+1

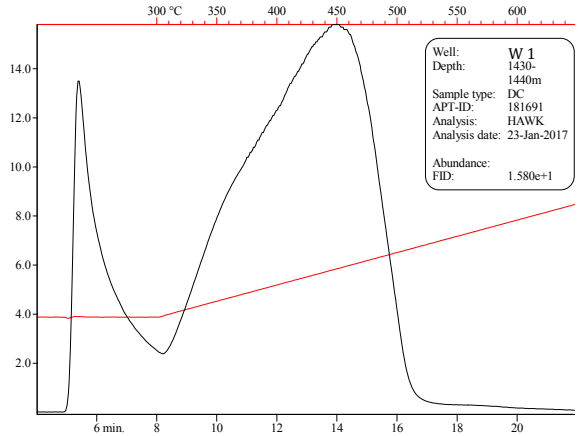
Well: W 1
Depth: 1430-1440m
Sample type: DC
APT-ID: 181691
Analysis: HAWK
Analysis date: 23-Jan-2017
Abundance:
FID: 1.580e+1

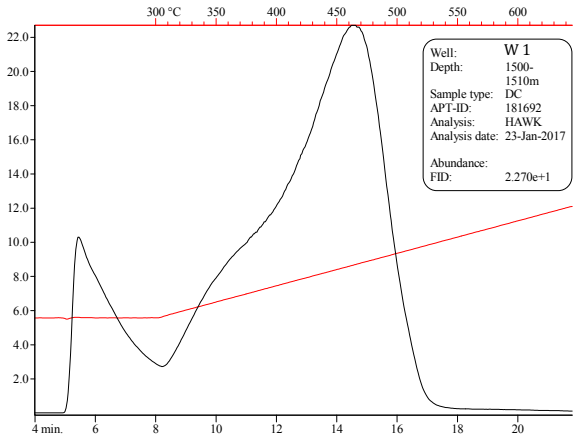
Well: W 1
Depth: 1500-1510m
Sample type: DC
APT-ID: 181692
Analysis: HAWK
Analysis date: 23-Jan-2017
Abundance:
FID: 2.270e+1

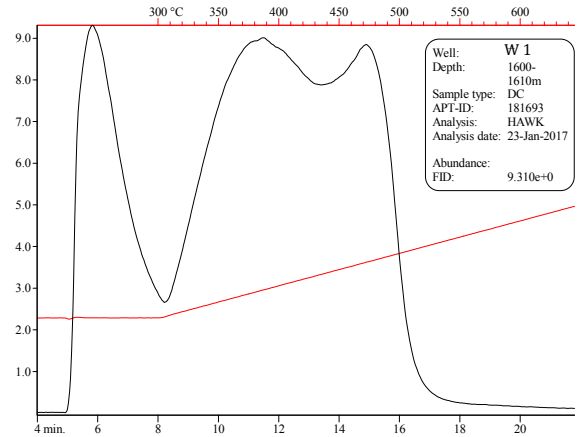
Well: W 1
Depth: 1600-1610m
Sample type: DC
APT-ID: 181693
Analysis: HAWK
Analysis date: 23-Jan-2017
Abundance:
FID: 9.310e+0

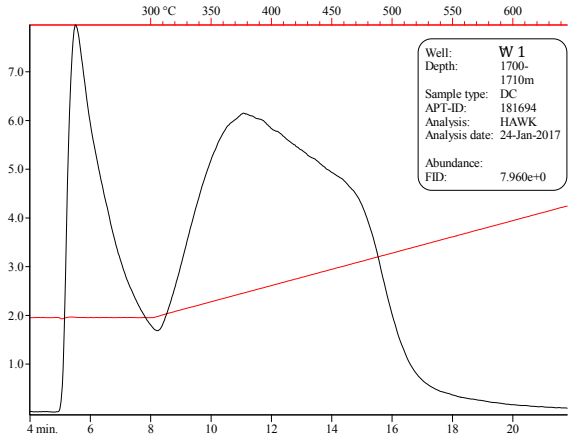
300 °C 350 400 450 500 550 600
Well: W 1
Depth: 1700-1710m
Sample type: DC
APT-ID: 181694
Analysis: HAWK
Analysis date: 24-Jan-2017
Abundance:
FID: 7.960e+0
4 min. 6 8 10 12 14 16 18 20

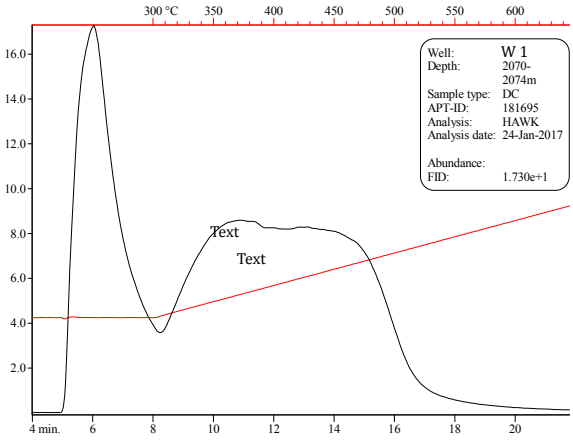
300 °C 350 400 450 500 550 600
Well: W 1
Depth: 2070-2074m
Sample type: DC
APT-ID: 181695
Analysis: HAWK
Analysis date: 24-Jan-2017
Abundance:
FID: 1.730e+1
Text
Text
4 min. 6 8 10 12 14 16 18 20

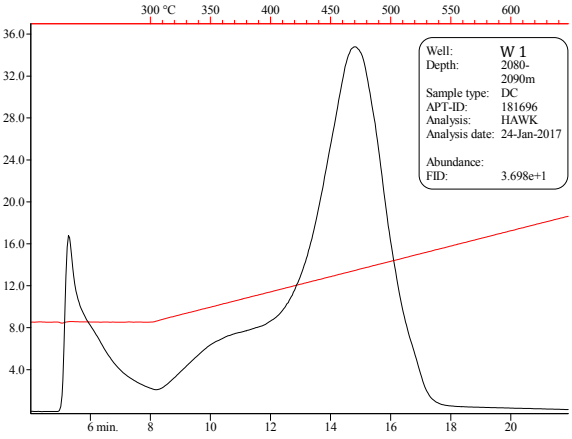
300 °C 350 400 450 500 550 600
Well: W 1
Depth: 2080-2090m
Sample type: DC
APT-ID: 181696
Analysis: HAWK
Analysis date: 24-Jan-2017
Abundance:
FID: 3.698e+1
6 min. 8 10 12 14 16 18 20

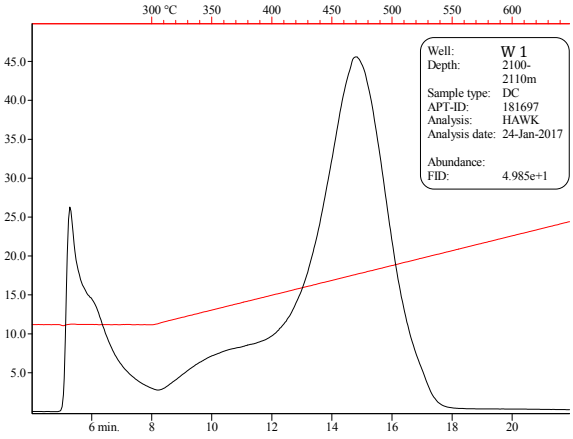
300 °C 350 400 450 500 550 600
Well: W 1
Depth: 2100-2110m
Sample type: DC
APT-ID: 181697
Analysis: HAWK
Analysis date: 24-Jan-2017
Abundance:
FID: 4.985e+1
6 min. 8 10 12 14 16 18 20

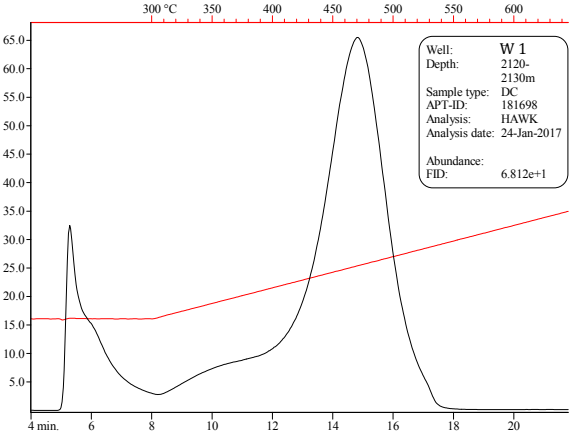
300 °C 350 400 450 500 550 600
Well: W 1
Depth: 2120-2130m
Sample type: DC
APT-ID: 181698
Analysis: HAWK
Analysis date: 24-Jan-2017
Abundance:
FID: 6.812e+1
4 min. 6 8 10 12 14 16 18 20

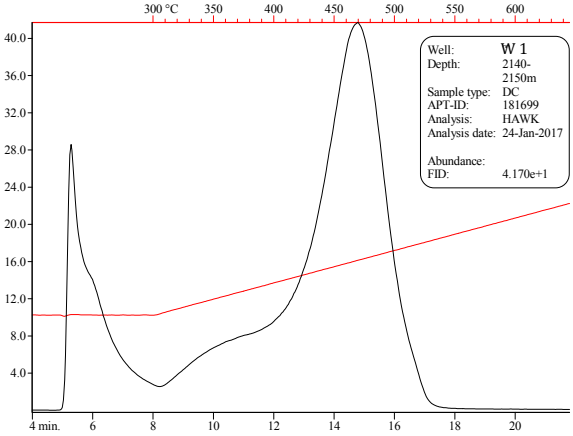
300 °C 350 400 450 500 550 600
Well: W 1
Depth: 2140-2150m
Sample type: DC
APT-ID: 181699
Analysis: HAWK
Analysis date: 24-Jan-2017
Abundance:
FID: 4.170e+1
4 min. 6 8 10 12 14 16 18 20

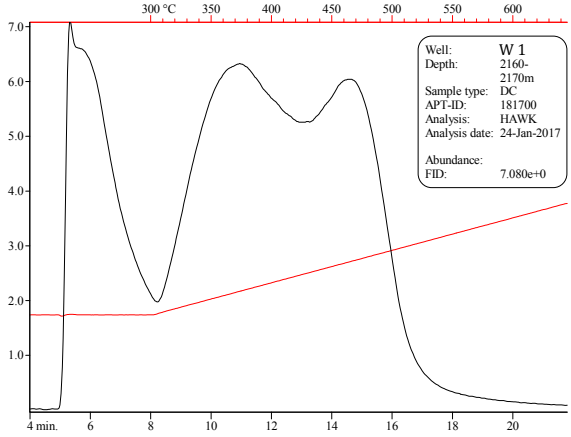
300 °C 350 400 450 500 550 600
Well: W 1
Depth: 2160-2170m
Sample type: DC
APT-ID: 181700
Analysis: HAWK
Analysis date: 24-Jan-2017
Abundance:
FID: 7.080e+0
4 min. 6 8 10 12 14 16 18 20

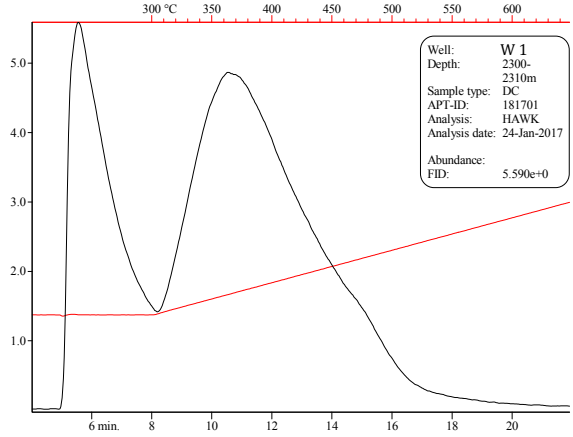
300 °C 350 400 450 500 550 600
Well: W 1
Depth: 2300-2310m
Sample type: DC
APT-ID: 181701
Analysis: HAWK
Analysis date: 24-Jan-2017
Abundance:
FID: 5.590e+0
6 min. 8 10 12 14 16 18 20

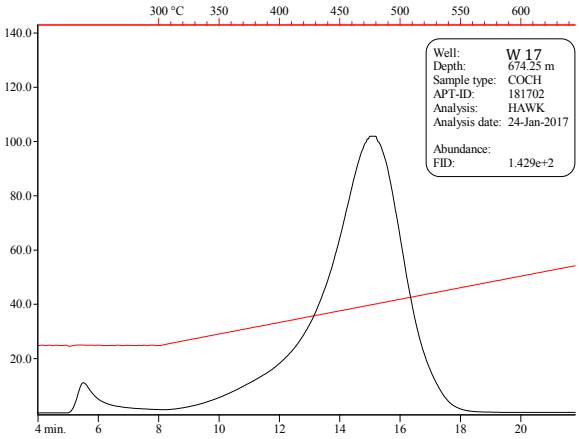
Well: W 17
Depth: 674.25 m
Sample type: COCH
APT-ID: 181702
Analysis: HAWK
Analysis date: 24-Jan-2017
Abundance:
FID: 1.429e+2

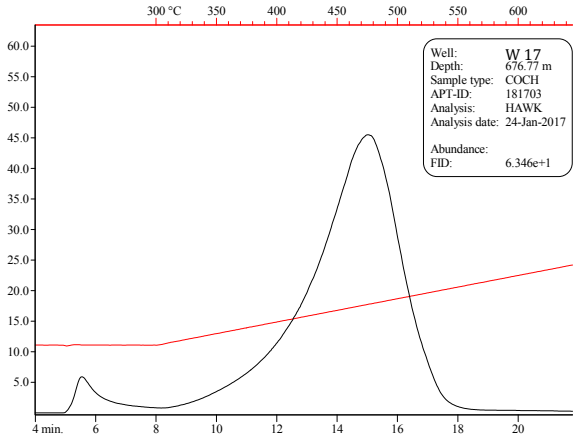
Well: W 17
Depth: 676.77 m
Sample type: COCH
APT-ID: 181703
Analysis: HAWK
Analysis date: 24-Jan-2017
Abundance:
FID: 6.346e+1

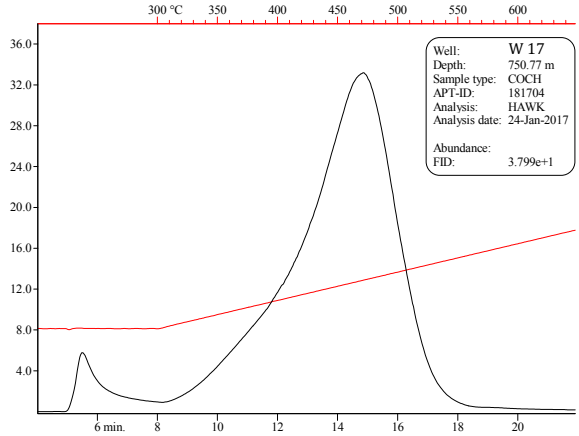
Well: W 17
Depth: 750.77 m
Sample type: COCH
APT-ID: 181704
Analysis: HAWK
Analysis date: 24-Jan-2017
Abundance:
FID: 3.799e+1

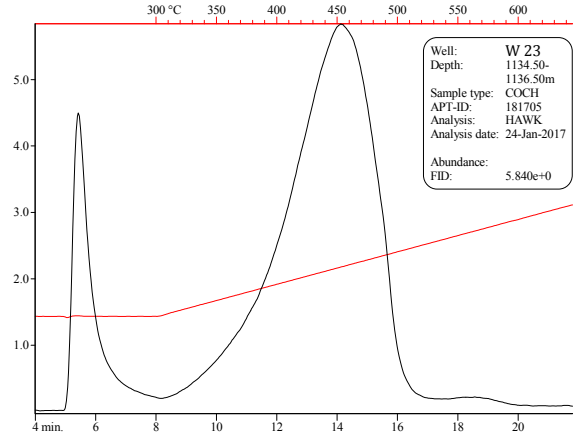
Well: W 23
Depth: 1134.50-1136.50m
Sample type: COCH
APT-ID: 181705
Analysis: HAWK
Analysis date: 24-Jan-2017
Abundance:
FID: 5.840e+0

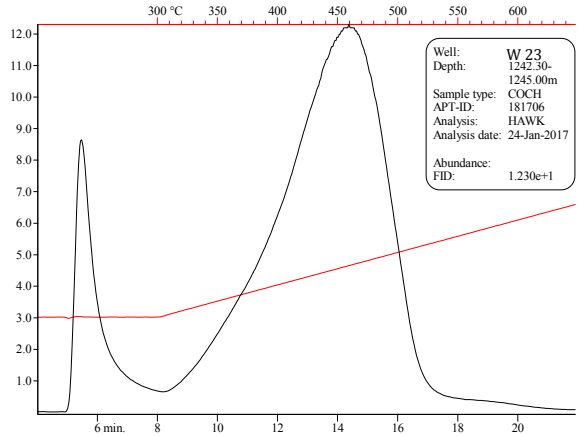
Well: W 23
Depth: 1242.30-1245.00m
Sample type: COCH
APT-ID: 181706
Analysis: HAWK
Analysis date: 24-Jan-2017
Abundance:
FID: 1.230e+1

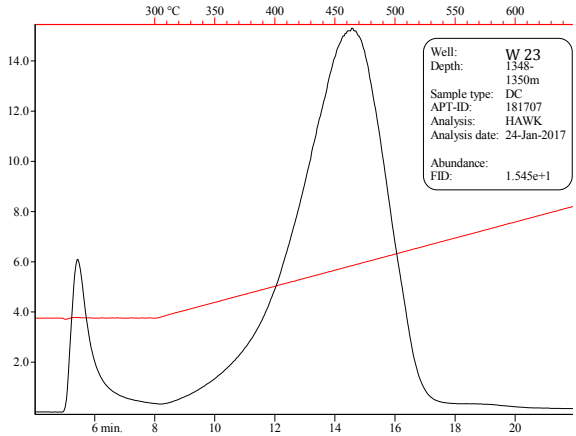
Well: W 23
Depth: 1348-1350m
Sample type: DC
APT-ID: 181707
Analysis: HAWK
Analysis date: 24-Jan-2017
Abundance:
FID: 1.545e+1

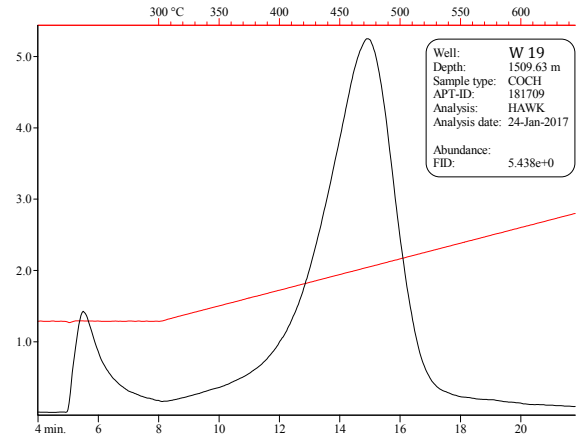
Well: W 19
Depth: 1509.63 m
Sample type: COCH
APT-ID: 181709
Analysis: HAWK
Analysis date: 24-Jan-2017
Abundance:
FID: 5.438e+0

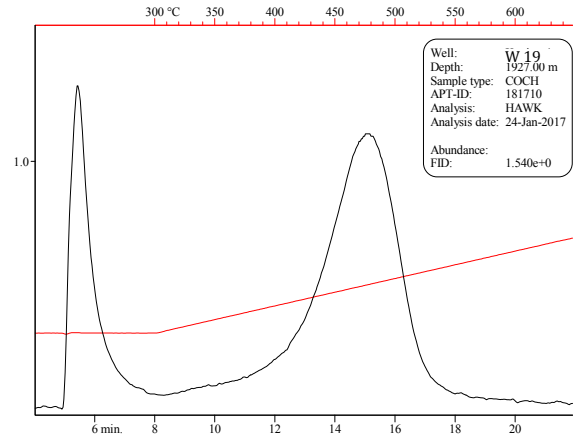
Well: W 19
Depth: 1927.00 m
Sample type: COCH
APT-ID: 181710
Analysis: HAWK
Analysis date: 24-Jan-2017
Abundance:
FID: 1.540e+0

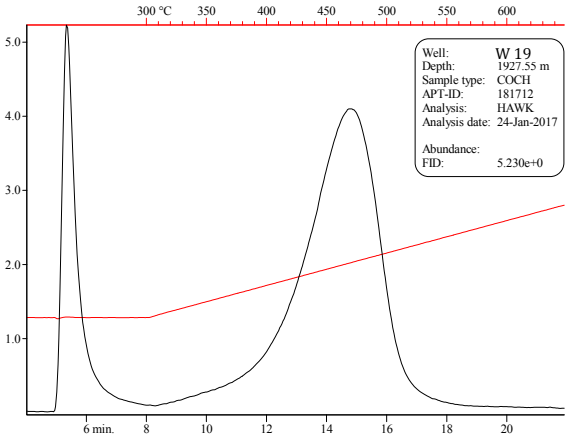
300 °C 350 400 450 500 550 600
Well: W 19
Depth: 1927.55 m
Sample type: COCH
APT-ID: 181712
Analysis: HAWK
Analysis date: 24-Jan-2017
Abundance:
FID: 5.230e+0
6 min. 8 10 12 14 16 18 20

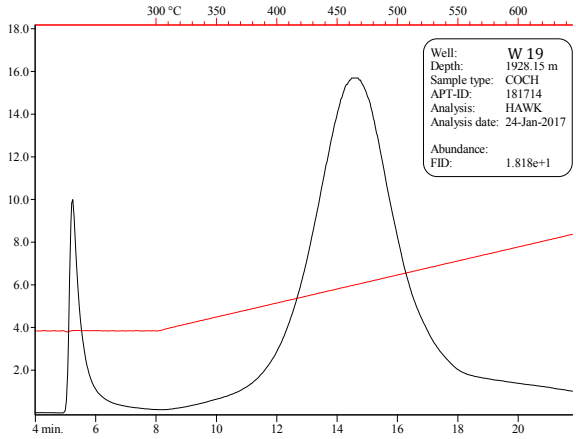
300 °C 350 400 450 500 550 600
Well: W 19
Depth: 1928.15 m
Sample type: COCH
APT-ID: 181714
Analysis: HAWK
Analysis date: 24-Jan-2017
Abundance:
FID: 1.818e+1
4 min. 6 8 10 12 14 16 18 20

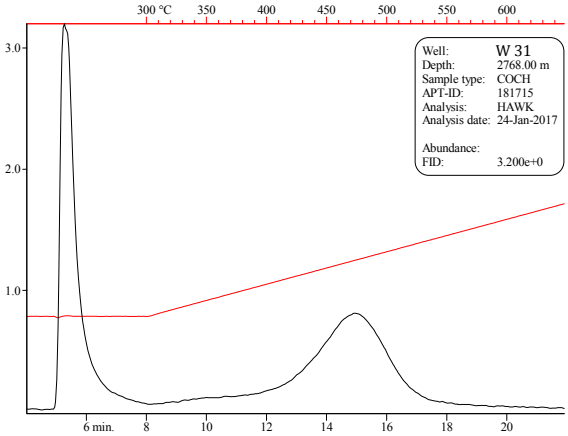
300 °C 350 400 450 500 550 600
Well: W 31
Depth: 2768.00 m
Sample type: COCH
APT-ID: 181715
Analysis: HAWK
Analysis date: 24-Jan-2017
Abundance:
FID: 3.200e+0
6 min. 8 10 12 14 16 18 20

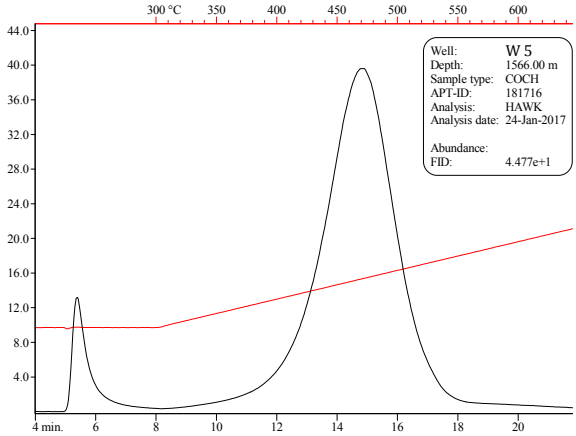
300 °C 350 400 450 500 550 600
Well: W 5
Depth: 1566.00 m
Sample type: COCH
APT-ID: 181716
Analysis: HAWK
Analysis date: 24-Jan-2017
Abundance:
FID: 4.477e+1
4 min. 6 8 10 12 14 16 18 20

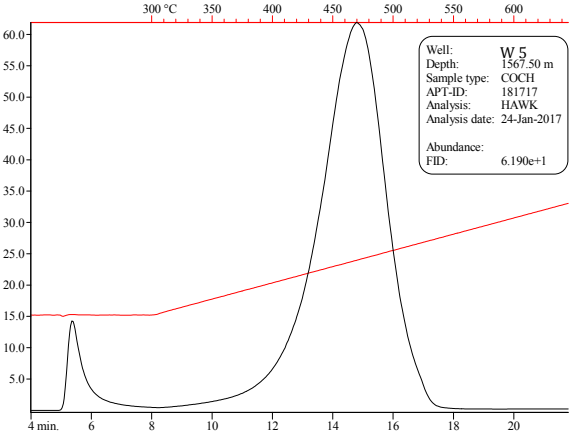
300 °C 350 400 450 500 550 600
Well: W 5
Depth: 1567.50 m
Sample type: COCH
APT-ID: 181717
Analysis: HAWK
Analysis date: 24-Jan-2017
Abundance:
FID: 6.190e+1
4 min. 6 8 10 12 14 16 18 20

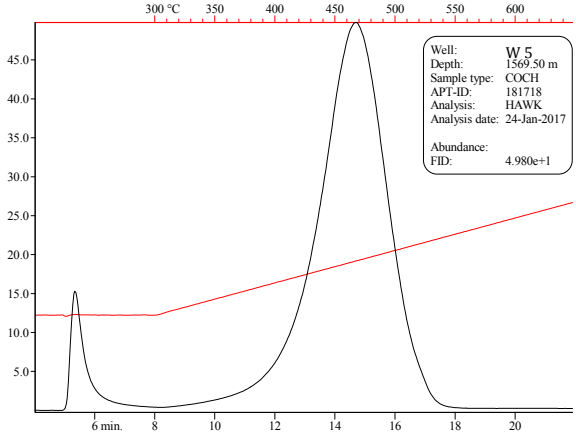
300 °C 350 400 450 500 550 600
Well: W 5
Depth: 1569.50 m
Sample type: COCH
APT-ID: 181718
Analysis: HAWK
Analysis date: 24-Jan-2017
Abundance:
FID: 4.980e+1
6 min. 8 10 12 14 16 18 20

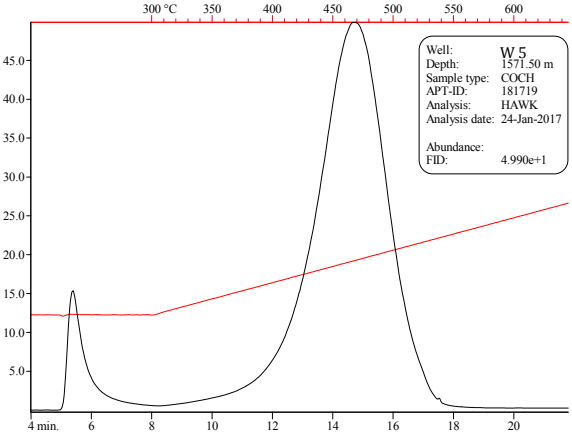
300 °C 350 400 450 500 550 600
Well: W 5
Depth: 1571.50 m
Sample type: COCH
APT-ID: 181719
Analysis: HAWK
Analysis date: 24-Jan-2017
Abundance:
FID: 4.990e+1
4 min. 6 8 10 12 14 16 18 20

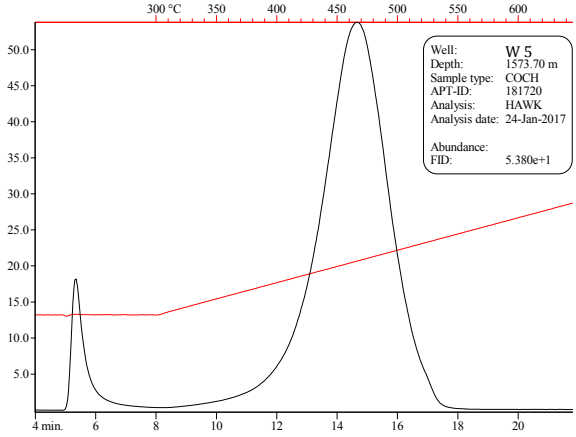
300 °C 350 400 450 500 550 600
Well: W 5
Depth: 1573.70 m
Sample type: COCH
APT-ID: 181720
Analysis: HAWK
Analysis date: 24-Jan-2017
Abundance:
FID: 5.380e+1
4 min. 6 8 10 12 14 16 18 20

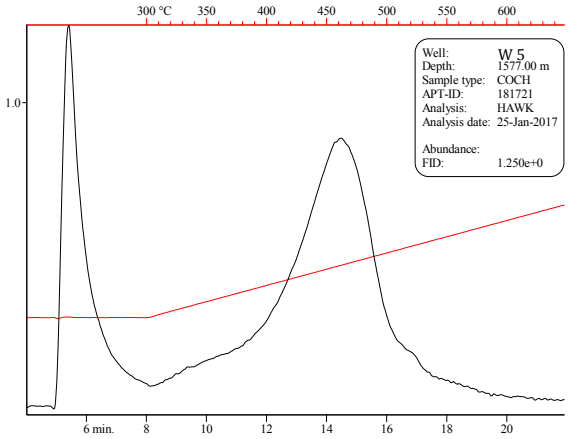
300 °C 350 400 450 500 550 600
1.0
6 min. 8 10 12 14 16 18 20
Well: W 5
Depth: 1577.00 m
Sample type: COCH
APT-ID: 181721
Analysis: HAWK
Analysis date: 25-Jan-2017
Abundance:
FID: 1.250e+0

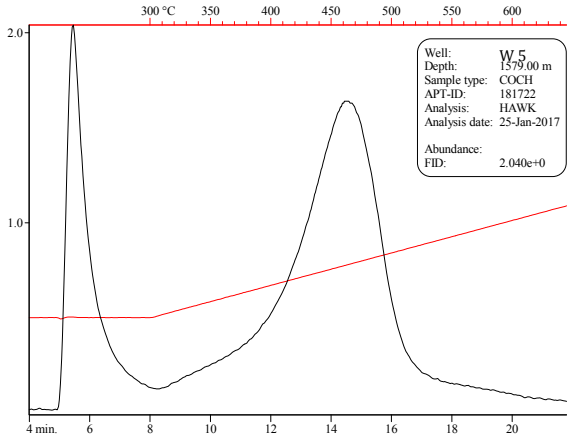
300 °C 350 400 450 500 550 600
2.0
1.0
4 min. 6 8 10 12 14 16 18 20
Well: W 5
Depth: 1579.00 m
Sample type: COCH
APT-ID: 181722
Analysis: HAWK
Analysis date: 25-Jan-2017
Abundance:
FID: 2.040e+0

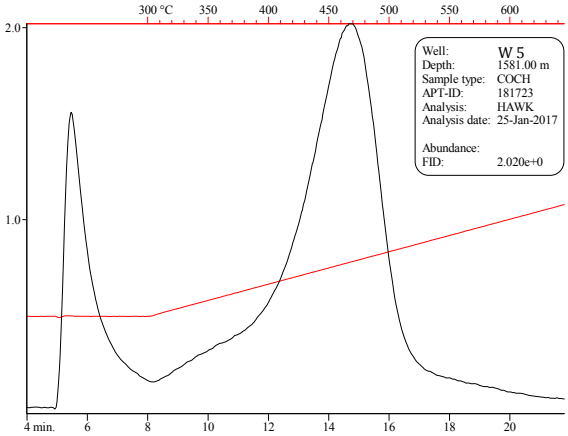
300 °C 350 400 450 500 550 600
2.0
1.0
4 min. 6 8 10 12 14 16 18 20
Well: W 5
Depth: 1581.00 m
Sample type: COCH
APT-ID: 181723
Analysis: HAWK
Analysis date: 25-Jan-2017
Abundance:
FID: 2.020e+0

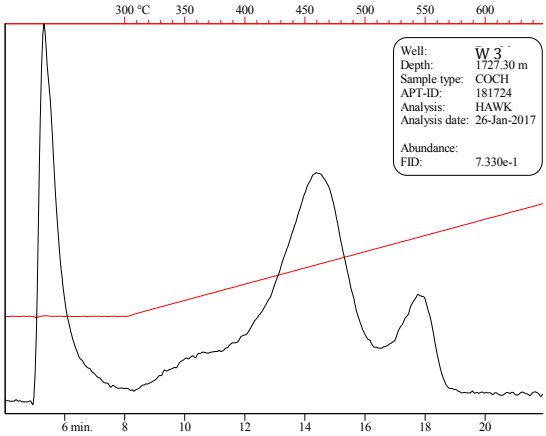
300 °C 350 400 450 500 550 600
6 min. 8 10 12 14 16 18 20
Well: W 3
Depth: 1727.30 m
Sample type: COCH
APT-ID: 181724
Analysis: HAWK
Analysis date: 26-Jan-2017
Abundance:
FID: 7.330e-1

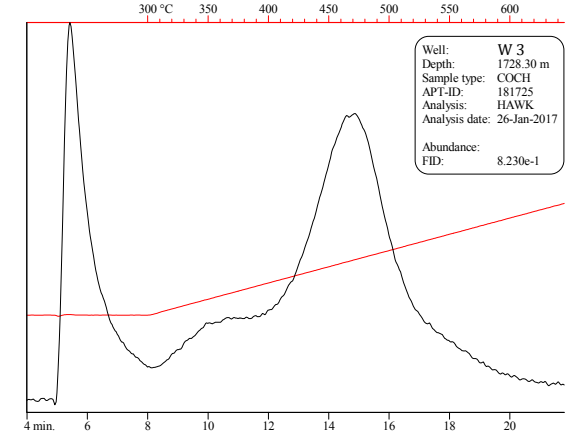
300 °C 350 400 450 500 550 600
4 min. 6 8 10 12 14 16 18 20
Well: W 3
Depth: 1728.30 m
Sample type: COCH
APT-ID: 181725
Analysis: HAWK
Analysis date: 26-Jan-2017
Abundance:
FID: 8.230e-1

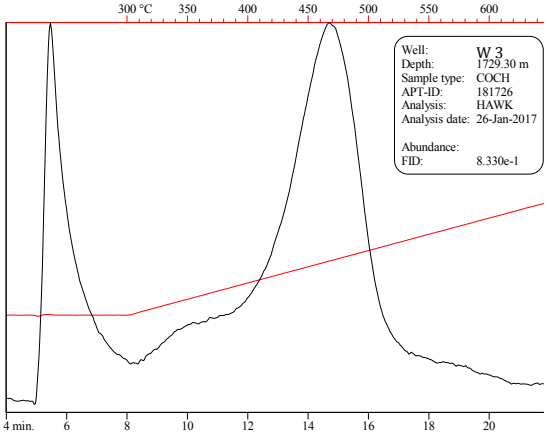
300 °C 350 400 450 500 550 600
4 min. 6 8 10 12 14 16 18 20
Well: W 3
Depth: 1729.30 m
Sample type: COCH
APT-ID: 181726
Analysis: HAWK
Analysis date: 26-Jan-2017
Abundance:
FID: 8.330e-1

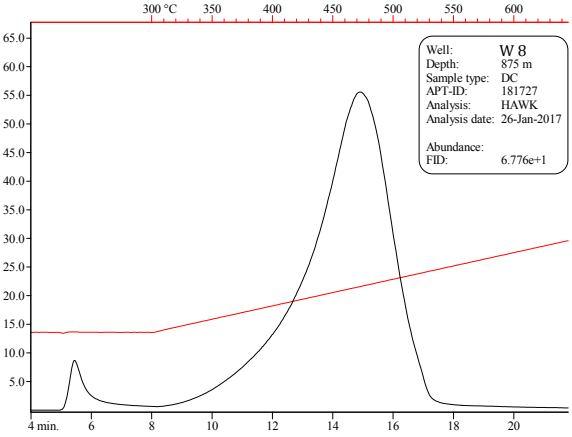
300 °C 350 400 450 500 550 600
65.0
60.0
55.0
50.0
45.0
40.0
35.0
30.0
25.0
20.0
15.0
10.0
5.0
4 min. 6 8 10 12 14 16 18 20
Well: W 8
Depth: 875 m
Sample type: DC
APT-ID: 181727
Analysis: HAWK
Analysis date: 26-Jan-2017
Abundance:
FID: 6.776e+1

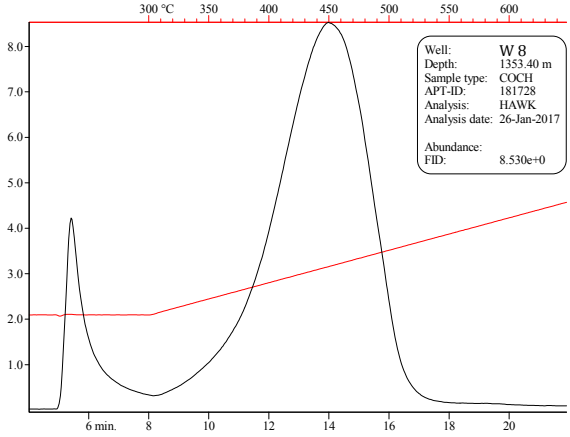
300 °C 350 400 450 500 550 600
8.0
7.0
6.0
5.0
4.0
3.0
2.0
1.0
6 min. 8 10 12 14 16 18 20
Well: W 8
Depth: 1353.40 m
Sample type: COCH
APT-ID: 181728
Analysis: HAWK
Analysis date: 26-Jan-2017
Abundance:
FID: 8.530e+0

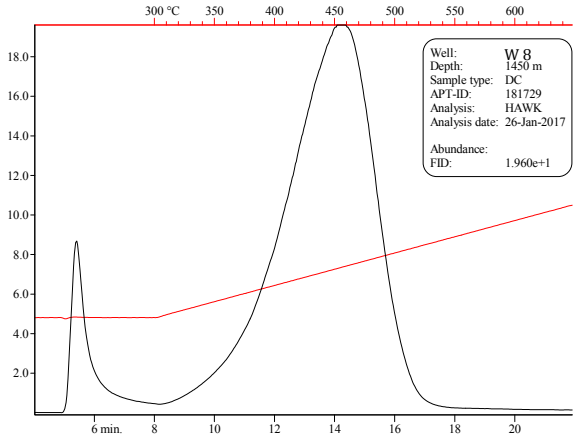
300 °C 350 400 450 500 550 600
Well: W 8
Depth: 1450 m
Sample type: DC
APT-ID: 181729
Analysis: HAWK
Analysis date: 26-Jan-2017
Abundance:
FID: 1.960e+1
6 min. 8 10 12 14 16 18 20

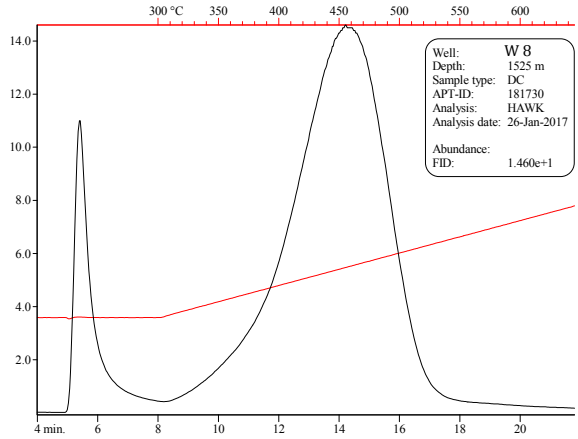
300 °C 350 400 450 500 550 600
Well: W 8
Depth: 1525 m
Sample type: DC
APT-ID: 181730
Analysis: HAWK
Analysis date: 26-Jan-2017
Abundance:
FID: 1.460e+1
4 min. 6 8 10 12 14 16 18 20

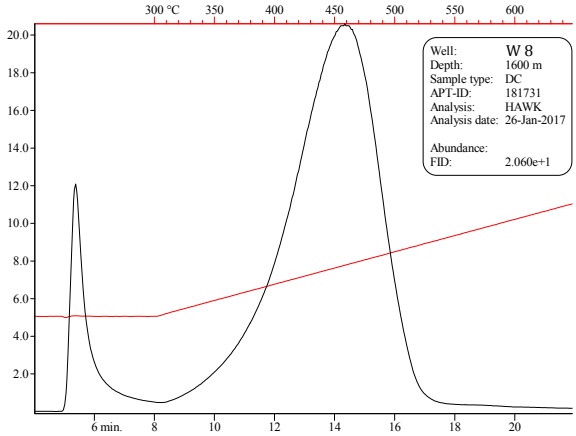
300 °C 350 400 450 500 550 600
Well: W 8
Depth: 1600 m
Sample type: DC
APT-ID: 181731
Analysis: HAWK
Analysis date: 26-Jan-2017
Abundance:
FID: 2.060e+1
6 min. 8 10 12 14 16 18 20

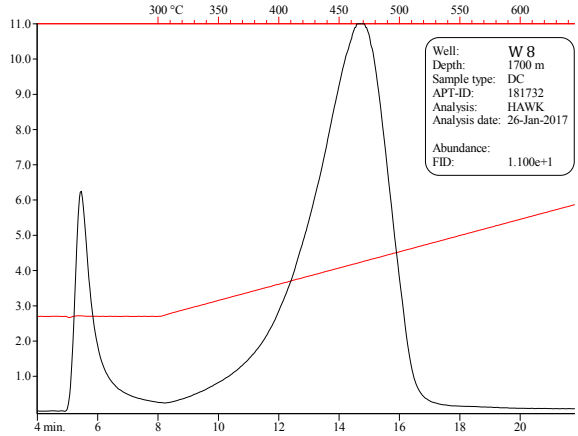
300 °C 350 400 450 500 550 600
Well: W 8
Depth: 1700 m
Sample type: DC
APT-ID: 181732
Analysis: HAWK
Analysis date: 26-Jan-2017
Abundance:
FID: 1.100e+1
4 min. 6 8 10 12 14 16 18 20

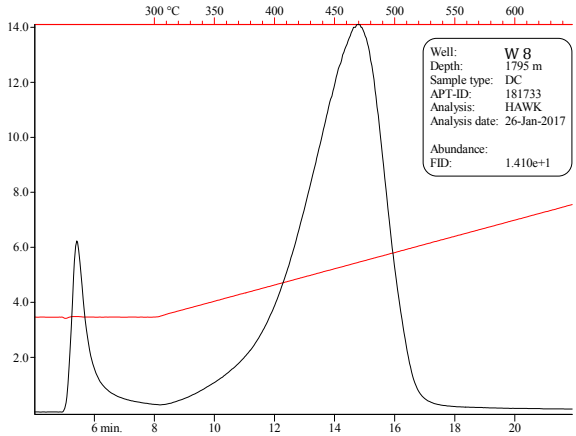
300 °C 350 400 450 500 550 600
Well: W 8
Depth: 1795 m
Sample type: DC
APT-ID: 181733
Analysis: HAWK
Analysis date: 26-Jan-2017
Abundance:
FID: 1.410e+1
6 min. 8 10 12 14 16 18 20

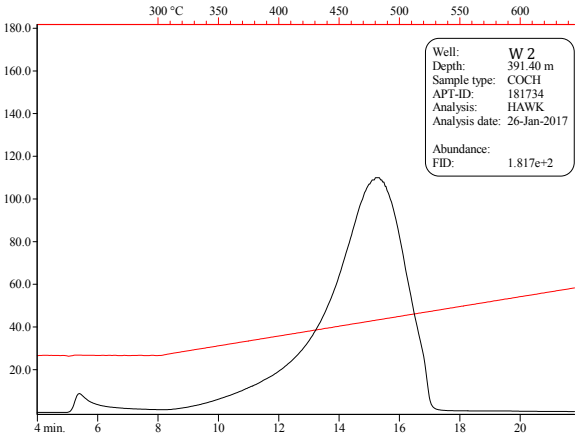
300 °C 350 400 450 500 550 600
Well: W 2
Depth: 391.40 m
Sample type: COCH
APT-ID: 181734
Analysis: HAWK
Analysis date: 26-Jan-2017
Abundance:
FID: 1.817e+2
4 min. 6 8 10 12 14 16 18 20

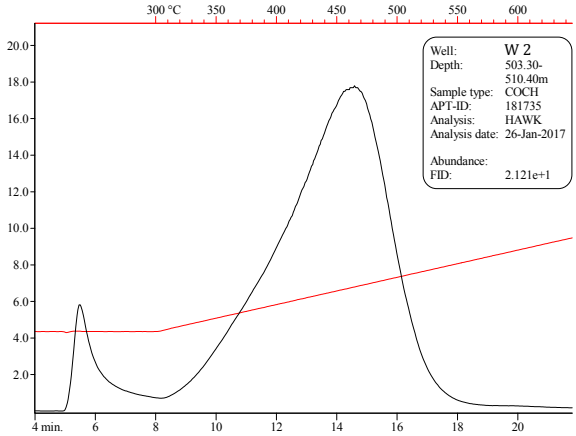
300 °C 350 400 450 500 550 600
Well: W 2
Depth: 503.30-510.40m
Sample type: COCH
APT-ID: 181735
Analysis: HAWK
Analysis date: 26-Jan-2017
Abundance:
FID: 2.121e+1
4 min. 6 8 10 12 14 16 18 20

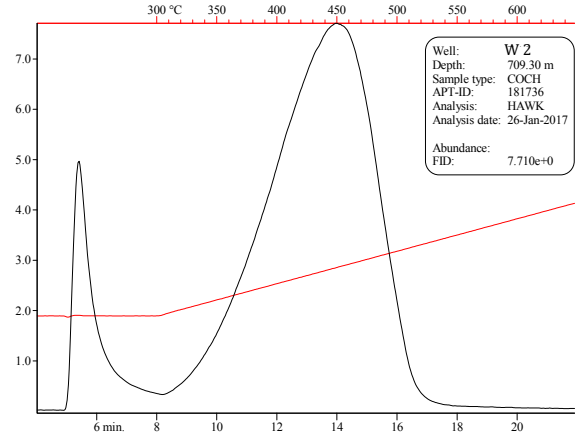
300 °C 350 400 450 500 550 600
Well: W 2
Depth: 709.30 m
Sample type: COCH
APT-ID: 181736
Analysis: HAWK
Analysis date: 26-Jan-2017
Abundance:
FID: 7.710e+0
6 min. 8 10 12 14 16 18 20

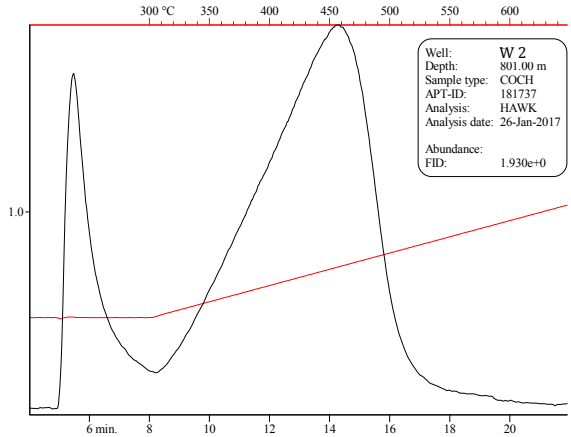
300 °C 350 400 450 500 550 600
Well: W 2
Depth: 801.00 m
Sample type: COCH
APT-ID: 181737
Analysis: HAWK
Analysis date: 26-Jan-2017
Abundance:
FID: 1.930e+0
1.0
6 min. 8 10 12 14 16 18 20

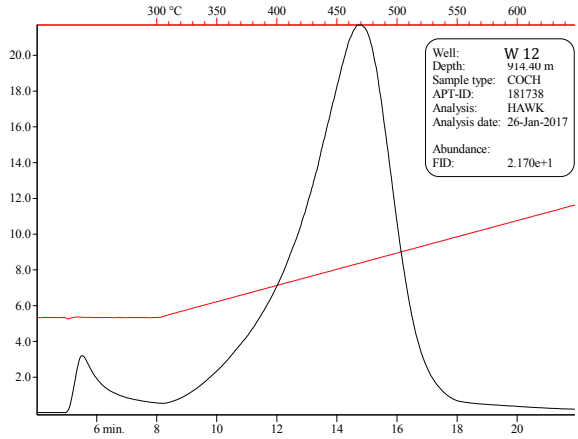
300 °C 350 400 450 500 550 600
Well: W 12
Depth: 914.40 m
Sample type: COCH
APT-ID: 181738
Analysis: HAWK
Analysis date: 26-Jan-2017
Abundance:
FID: 2.170e+1
20.0 18.0 16.0 14.0 12.0 10.0 8.0 6.0 4.0 2.0
6 min. 8 10 12 14 16 18 20

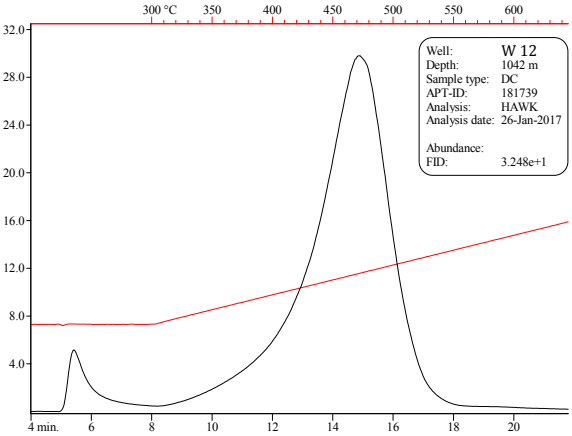
300 °C 350 400 450 500 550 600
Well: W 12
Depth: 1042 m
Sample type: DC
APT-ID: 181739
Analysis: HAWK
Analysis date: 26-Jan-2017
Abundance:
FID: 3.248e+1
32.0 28.0 24.0 20.0 16.0 12.0 8.0 4.0
4 min. 6 8 10 12 14 16 18 20

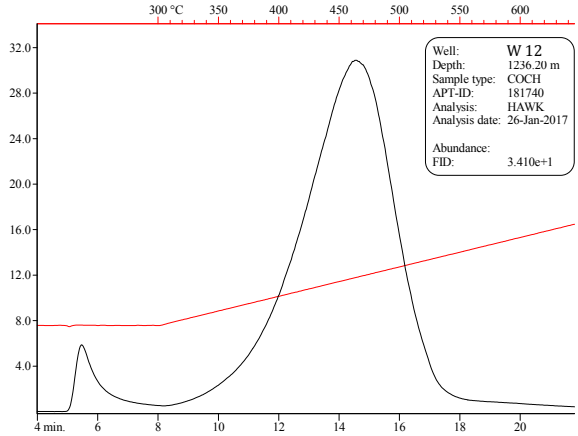
300 °C 350 400 450 500 550 600
Well: W 12
Depth: 1236.20 m
Sample type: COCH
APT-ID: 181740
Analysis: HAWK
Analysis date: 26-Jan-2017
Abundance:
FID: 3.410e+1
32.0 28.0 24.0 20.0 16.0 12.0 8.0 4.0
4 min. 6 8 10 12 14 16 18 20

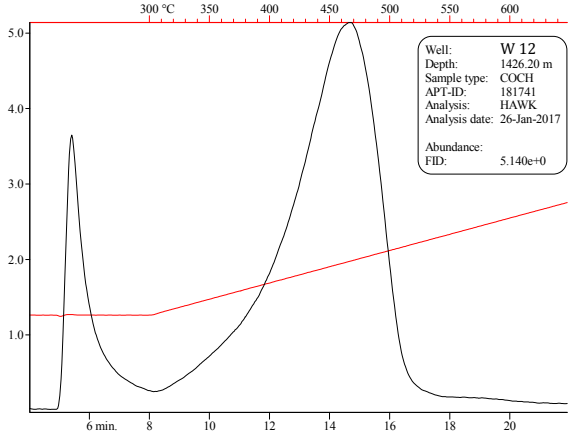
300 °C 350 400 450 500 550 600
Well: W 12
Depth: 1426.20 m
Sample type: COCH
APT-ID: 181741
Analysis: HAWK
Analysis date: 26-Jan-2017
Abundance:
FID: 5.140e+0
5.0 4.0 3.0 2.0 1.0
6 min. 8 10 12 14 16 18 20

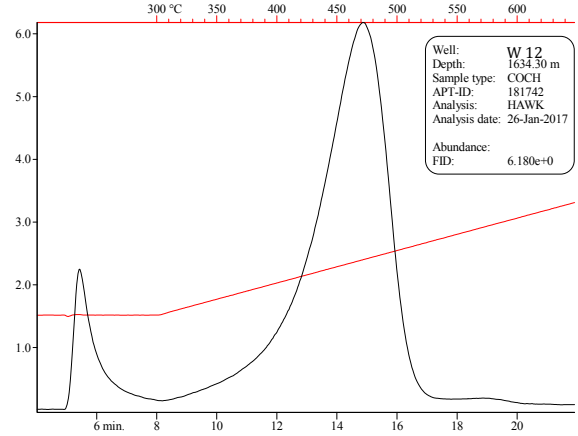
300 °C 350 400 450 500 550 600
Well: W 12
Depth: 1634.30 m
Sample type: COCH
APT-ID: 181742
Analysis: HAWK
Analysis date: 26-Jan-2017
Abundance:
FID: 6.180e+0
6.0 5.0 4.0 3.0 2.0 1.0
6 min. 8 10 12 14 16 18 20

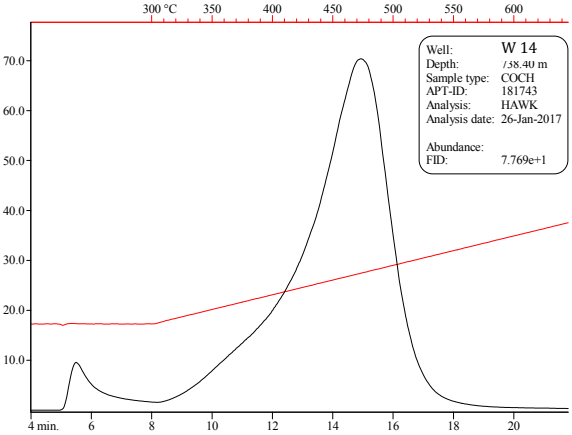
300 °C 350 400 450 500 550 600
Well: W 14
Depth: 738.40 m
Sample type: COCH
APT-ID: 181743
Analysis: HAWK
Analysis date: 26-Jan-2017
Abundance:
FID: 7.769e+1
70.0 60.0 50.0 40.0 30.0 20.0 10.0
4 min. 6 8 10 12 14 16 18 20

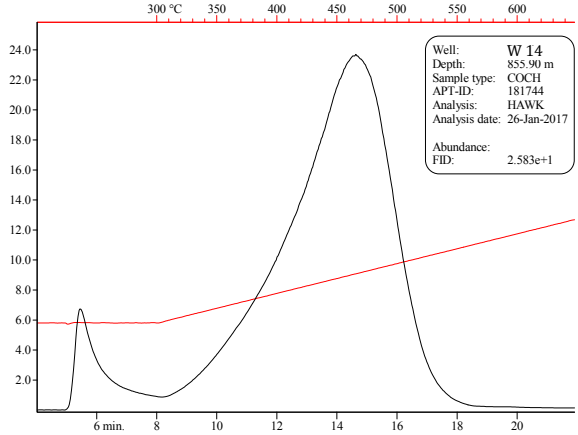
300 °C 350 400 450 500 550 600
Well: W 14
Depth: 855.90 m
Sample type: COCH
APT-ID: 181744
Analysis: HAWK
Analysis date: 26-Jan-2017
Abundance:
FID: 2.583e+1
24.0 22.0 20.0 18.0 16.0 14.0 12.0 10.0 8.0 6.0 4.0 2.0
6 min. 8 10 12 14 16 18 20

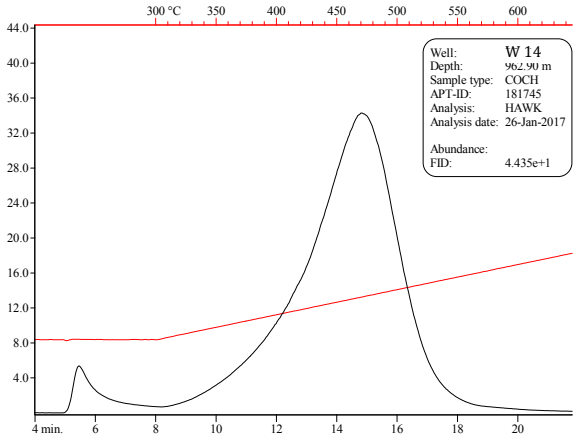
300 °C 350 400 450 500 550 600
Well: W 14
Depth: 962.90 m
Sample type: COCH
APT-ID: 181745
Analysis: HAWK
Analysis date: 26-Jan-2017
Abundance:
FID: 4.435e+1
4 min. 6 8 10 12 14 16 18 20

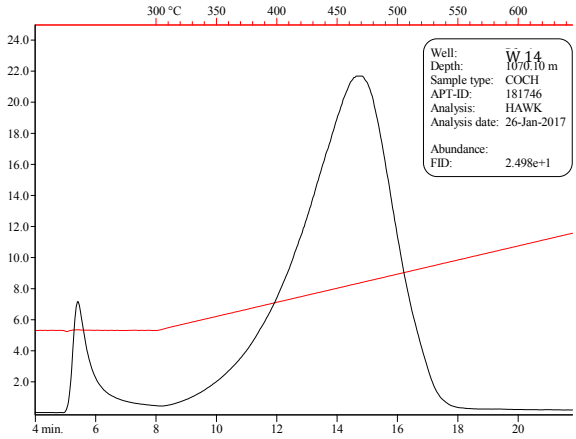
300 °C 350 400 450 500 550 600
Well: W 14
Depth: 1070.10 m
Sample type: COCH
APT-ID: 181746
Analysis: HAWK
Analysis date: 26-Jan-2017
Abundance:
FID: 2.498e+1
4 min. 6 8 10 12 14 16 18 20

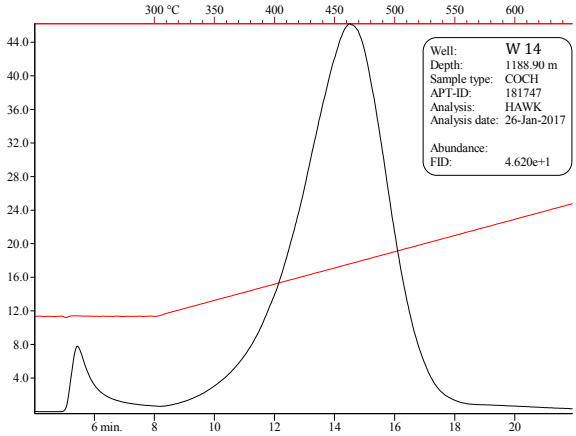
300 °C 350 400 450 500 550 600
Well: W 14
Depth: 1188.90 m
Sample type: COCH
APT-ID: 181747
Analysis: HAWK
Analysis date: 26-Jan-2017
Abundance:
FID: 4.620e+1
6 min. 8 10 12 14 16 18 20

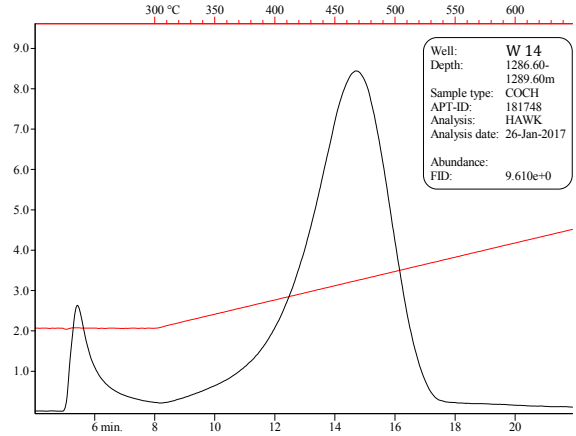
300 °C 350 400 450 500 550 600
Well: W 14
Depth: 1286.60-1289.60m
Sample type: COCH
APT-ID: 181748
Analysis: HAWK
Analysis date: 26-Jan-2017
Abundance:
FID: 9.610e+0
6 min. 8 10 12 14 16 18 20

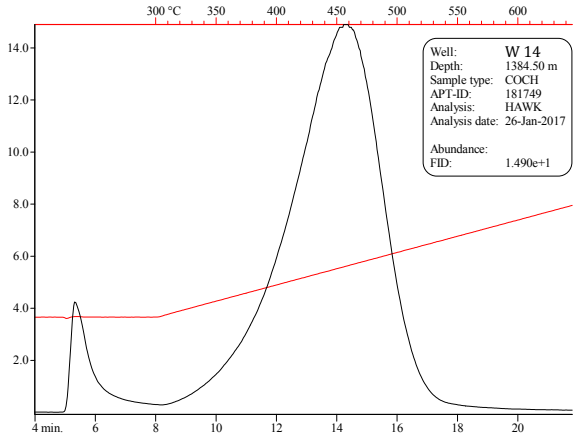
300 °C 350 400 450 500 550 600
Well: W 14
Depth: 1384.50 m
Sample type: COCH
APT-ID: 181749
Analysis: HAWK
Analysis date: 26-Jan-2017
Abundance:
FID: 1.490e+1
4 min. 6 8 10 12 14 16 18 20

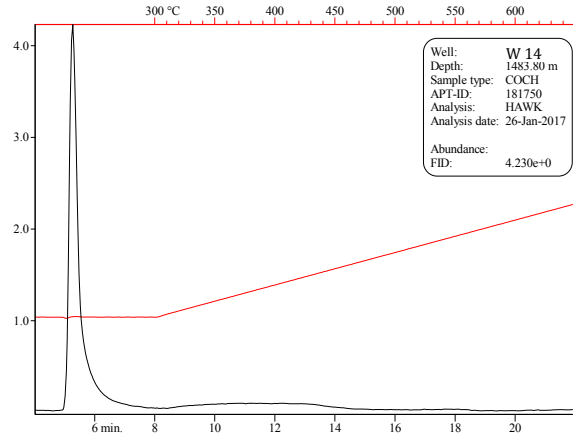
300 °C 350 400 450 500 550 600
Well: W 14
Depth: 1483.80 m
Sample type: COCH
APT-ID: 181750
Analysis: HAWK
Analysis date: 26-Jan-2017
Abundance:
FID: 4.230e+0
6 min. 8 10 12 14 16 18 20

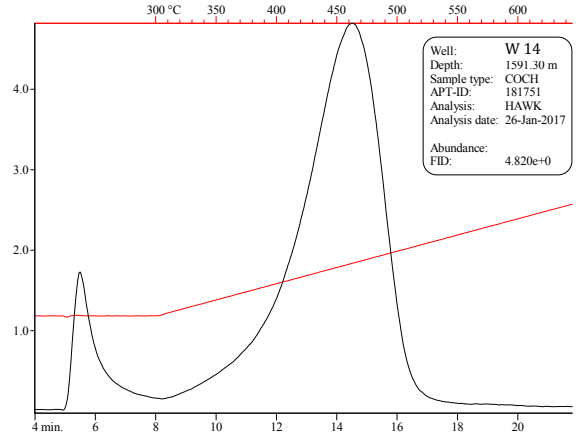
300 °C 350 400 450 500 550 600
Well: W 14
Depth: 1591.30 m
Sample type: COCH
APT-ID: 181751
Analysis: HAWK
Analysis date: 26-Jan-2017
Abundance:
FID: 4.820e+0
4 min. 6 8 10 12 14 16 18 20

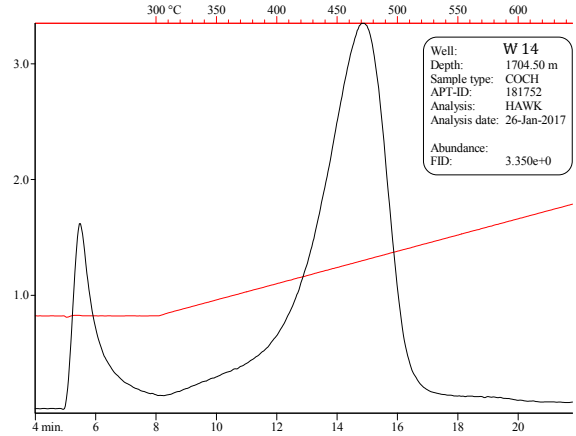
300 °C 350 400 450 500 550 600
Well: W 14
Depth: 1704.50 m
Sample type: COCH
APT-ID: 181752
Analysis: HAWK
Analysis date: 26-Jan-2017
Abundance:
FID: 3.350e+0
4 min. 6 8 10 12 14 16 18 20

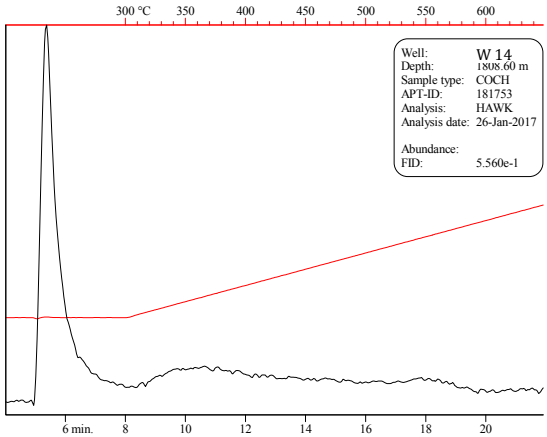
300 °C 350 400 450 500 550 600
Well: W 14
Depth: 1808.60 m
Sample type: COCH
APT-ID: 181753
Analysis: HAWK
Analysis date: 26-Jan-2017
Abundance:
FID: 5.560e-1
6 min. 8 10 12 14 16 18 20

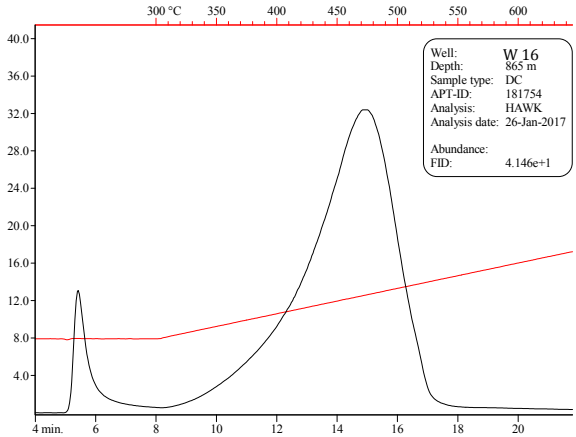
300 °C 350 400 450 500 550 600
40.0 36.0 32.0 28.0 24.0 20.0 16.0 12.0 8.0 4.0
Well: W 16
Depth: 865 m
Sample type: DC
APT-ID: 181754
Analysis: HAWK
Analysis date: 26-Jan-2017
Abundance:
FID: 4.146e+1
4 min. 6 8 10 12 14 16 18 20

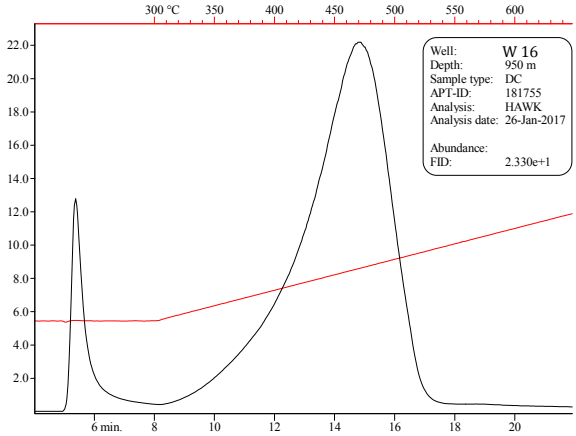
300 °C 350 400 450 500 550 600
22.0 20.0 18.0 16.0 14.0 12.0 10.0 8.0 6.0 4.0 2.0
Well: W 16
Depth: 950 m
Sample type: DC
APT-ID: 181755
Analysis: HAWK
Analysis date: 26-Jan-2017
Abundance:
FID: 2.330e+1
6 min. 8 10 12 14 16 18 20

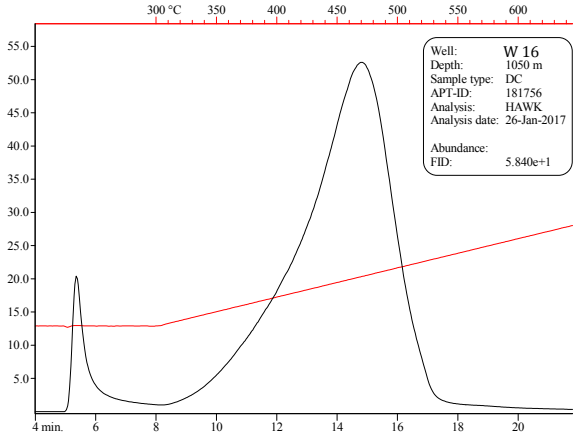
300 °C 350 400 450 500 550 600
55.0 50.0 45.0 40.0 35.0 30.0 25.0 20.0 15.0 10.0 5.0
Well: W 16
Depth: 1050 m
Sample type: DC
APT-ID: 181756
Analysis: HAWK
Analysis date: 26-Jan-2017
Abundance:
FID: 5.840e+1
4 min. 6 8 10 12 14 16 18 20

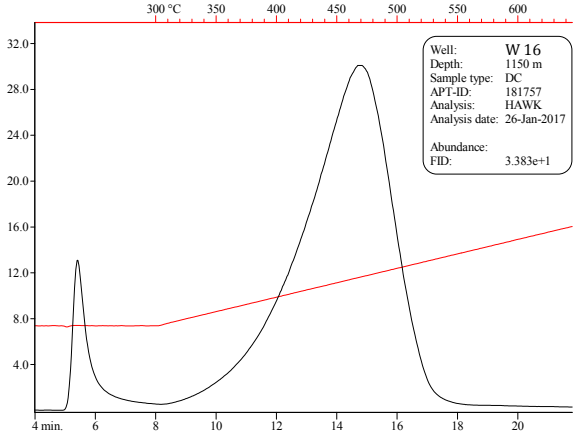
300 °C 350 400 450 500 550 600
32.0 28.0 24.0 20.0 16.0 12.0 8.0 4.0
Well: W 16
Depth: 1150 m
Sample type: DC
APT-ID: 181757
Analysis: HAWK
Analysis date: 26-Jan-2017
Abundance:
FID: 3.383e+1
4 min. 6 8 10 12 14 16 18 20

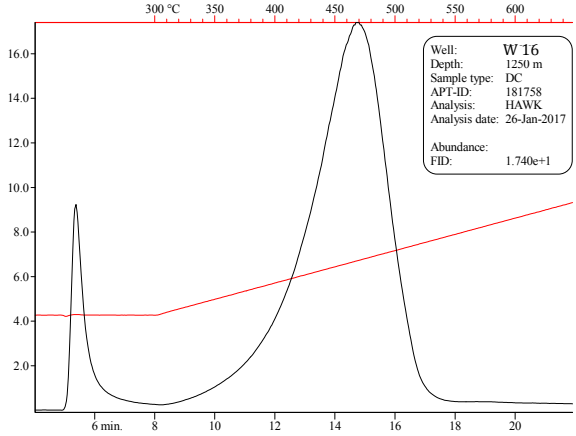
300 °C 350 400 450 500 550 600
16.0 14.0 12.0 10.0 8.0 6.0 4.0 2.0
Well: W 16
Depth: 1250 m
Sample type: DC
APT-ID: 181758
Analysis: HAWK
Analysis date: 26-Jan-2017
Abundance:
FID: 1.740e+1
6 min. 8 10 12 14 16 18 20

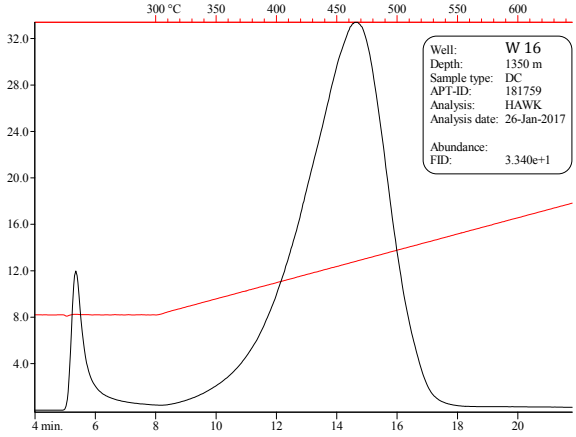
300 °C 350 400 450 500 550 600
32.0 28.0 24.0 20.0 16.0 12.0 8.0 4.0
Well: W 16
Depth: 1350 m
Sample type: DC
APT-ID: 181759
Analysis: HAWK
Analysis date: 26-Jan-2017
Abundance:
FID: 3.340e+1
4 min. 6 8 10 12 14 16 18 20

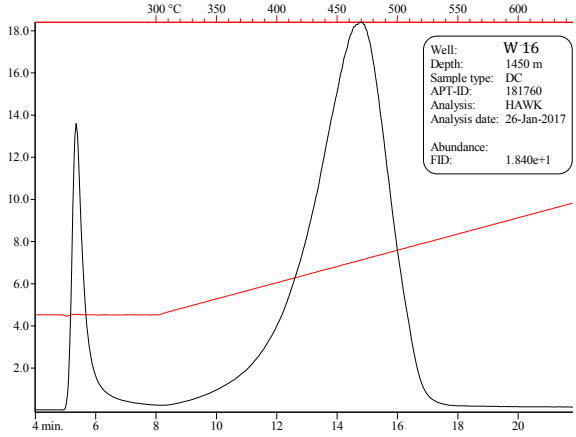
300 °C 350 400 450 500 550 600
18.0 16.0 14.0 12.0 10.0 8.0 6.0 4.0 2.0
Well: W 16
Depth: 1450 m
Sample type: DC
APT-ID: 181760
Analysis: HAWK
Analysis date: 26-Jan-2017
Abundance:
FID: 1.840e+1
4 min. 6 8 10 12 14 16 18 20

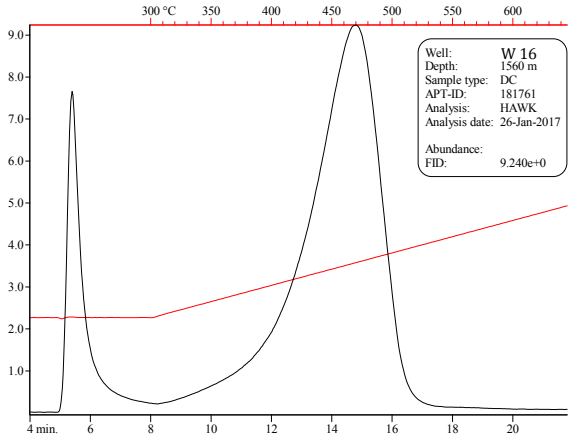
300 °C 350 400 450 500 550 600
Well: W 16
Depth: 1560 m
Sample type: DC
APT-ID: 181761
Analysis: HAWK
Analysis date: 26-Jan-2017
Abundance:
FID: 9.240e+0
4 min. 6 8 10 12 14 16 18 20

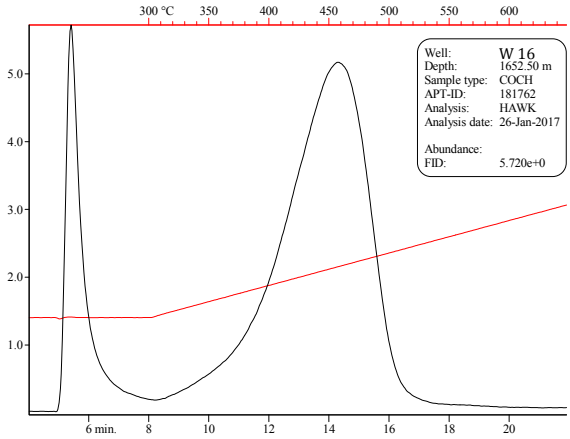
300 °C 350 400 450 500 550 600
Well: W 16
Depth: 1652.50 m
Sample type: COCH
APT-ID: 181762
Analysis: HAWK
Analysis date: 26-Jan-2017
Abundance:
FID: 5.720e+0
6 min. 8 10 12 14 16 18 20

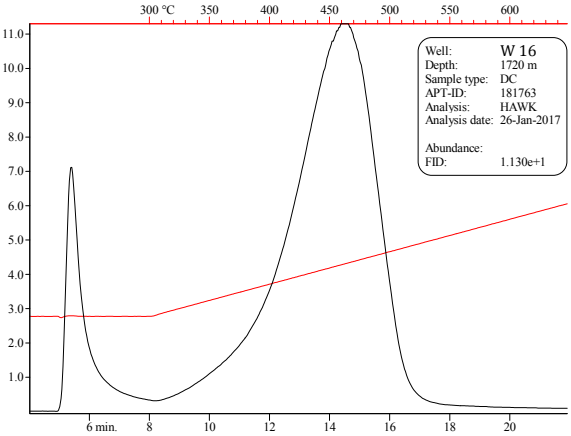
300 °C 350 400 450 500 550 600
Well: W 16
Depth: 1720 m
Sample type: DC
APT-ID: 181763
Analysis: HAWK
Analysis date: 26-Jan-2017
Abundance:
FID: 1.130e+1
6 min. 8 10 12 14 16 18 20

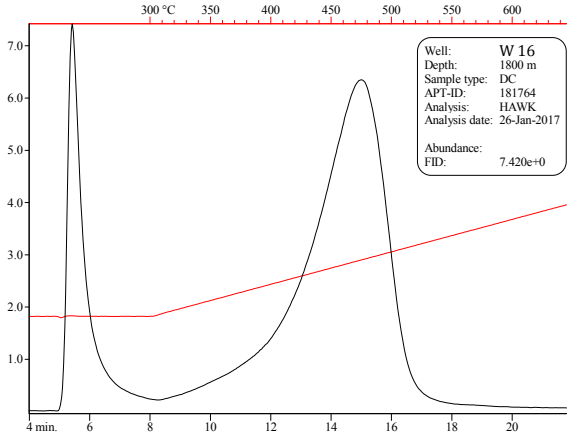
300 °C 350 400 450 500 550 600
Well: W 16
Depth: 1800 m
Sample type: DC
APT-ID: 181764
Analysis: HAWK
Analysis date: 26-Jan-2017
Abundance:
FID: 7.420e+0
4 min. 6 8 10 12 14 16 18 20

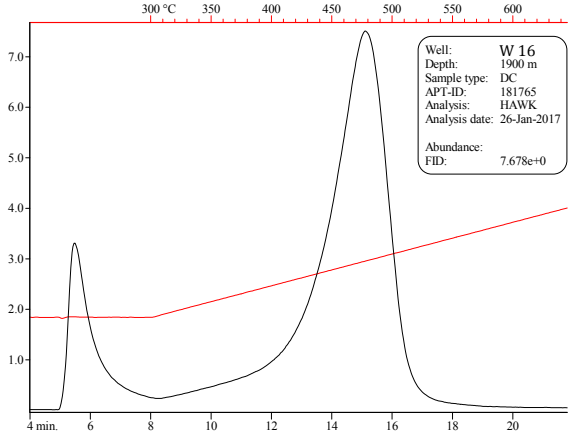
300 °C 350 400 450 500 550 600
Well: W 16
Depth: 1900 m
Sample type: DC
APT-ID: 181765
Analysis: HAWK
Analysis date: 26-Jan-2017
Abundance:
FID: 7.678e+0
4 min. 6 8 10 12 14 16 18 20

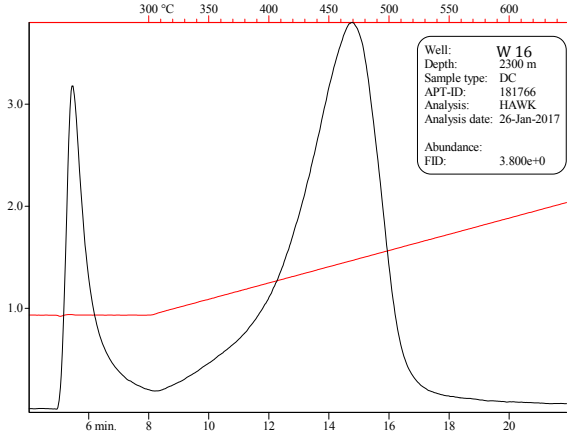
300 °C 350 400 450 500 550 600
Well: W 16
Depth: 2300 m
Sample type: DC
APT-ID: 181766
Analysis: HAWK
Analysis date: 26-Jan-2017
Abundance:
FID: 3.800e+0
6 min. 8 10 12 14 16 18 20

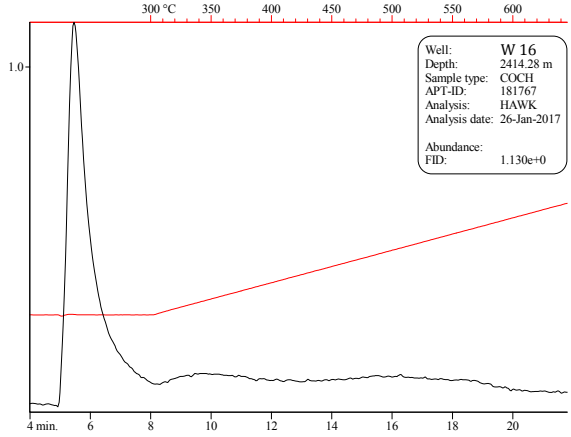
300 °C 350 400 450 500 550 600
Well: W 16
Depth: 2414.28 m
Sample type: COCH
APT-ID: 181767
Analysis: HAWK
Analysis date: 26-Jan-2017
Abundance:
FID: 1.130e+0
4 min. 6 8 10 12 14 16 18 20

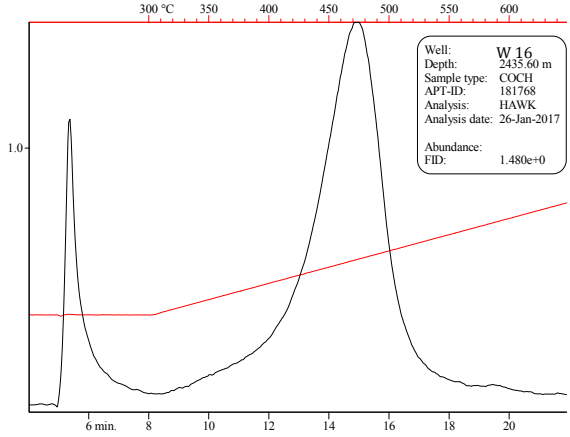
300 °C 350 400 450 500 550 600
Well: W 16
Depth: 2435.60 m
Sample type: COCH
APT-ID: 181768
Analysis: HAWK
Analysis date: 26-Jan-2017
Abundance:
FID: 1.480e+0
6 min. 8 10 12 14 16 18 20

Well	Depth (TVD)	Formation	N [%]	C_{total} [%]	S [%]	C_{org} [%]
W1	650.0	UHy	0.29	8.92	1.66	4.16
W1	750.0	UHy	0.26	7.52	1.60	3.77
W1	850.0	UHy	0.23	6.52	1.86	2.76
W1	950.0	UHy	0.26	6.96	2.08	3.51
W1	1050.0	UHy	0.23	5.55	2.53	3.25
W1	1150.0	UHy	0.22	5.82	3.08	3.24
W1	1250.0	UHy	0.18	5.21	2.58	2.58
W1	1300.0	UHy	0.20	5.90	2.03	2.17
W1	1370.0	Cor	0.19	4.65	2.46	2.12
W1	1400.0	Cor	0.18	5.43	2.22	2.01
W1	1430.0	Cor	0.20	5.16	2.41	2.01
W1	1500.0	Cer	0.22	5.57	2.00	2.18
W1	1600.0	Cer	0.22	5.43	1.13	1.47
W1	1700.0	Cer	0.15	4.58	0.35	1.21
W1	2070.0	FS (RpC)	0.30	4.06	0.38	1.75
W1	2080.0	FS (RpC)	0.28	4.11	1.58	2.95
W1	2100.0	FM (RpC)	0.57	4.79	1.77	3.39
W1	2120.0	FM (RpC)	0.30	5.46	2.02	3.55
W1	2140.0	FM (RpC)	0.25	4.90	2.18	2.93
W1	2160.0	FM (RpC)	0.19	2.75	0.55	1.30
W1	2300.0	PE	0.11	1.31	0.30	0.64
W2	391.4	UHy	0.14	8.49	1.87	4.63
W2	449.8	UHy	0.16	3.27	3.03	3.04
W2	510.4	UHy	0.12	3.50	2.66	2.19
W2	556.0	UHy	0.11	5.76	2.64	2.61
W2	650.8	UHy	0.09	2.43	3.45	1.77
W2	674.8	UHy	0.07	3.04	3.83	2.53
W2	709.3	UHy	0.09	1.80	3.35	1.68
W2	755.9	UHy	0.08	3.32	3.98	2.52
W2	801.0	UHy	0.07	1.74	3.04	0.82
W3	1727.3	RpC	0.10	1.88	5.71	0.46
W3	1727.7	RpC	0.08	1.37	0.84	0.48
W3	1728.3	RpC	0.05	3.34	0.34	0.74
W3	1728.7	RpC	0.07	2.08	0.22	0.43
W3	1729.3	RpC	0.08	1.30	0.39	0.45
W3	1729.7	RpC	0.06	2.20	0.37	0.45
W5	1566.0	RpC	0.18	3.62	1.59	3.04
W5	1567.5	RpC	0.16	5.61	2.58	3.32
W5	1568.5	RpC	0.17	4.46	2.33	2.95
W5	1569.5	RpC	0.16	4.19	3.00	3.13
W5	1570.5	RpC	0.18	4.70	3.18	3.67
W5	1571.5	RpC	0.17	4.09	2.57	3.23
W5	1572.7	RpC	0.21	4.45	2.71	4.26
W5	1573.7	RpC	0.17	4.55	3.56	3.25
W5	1577.0	RpC	0.10	1.75	1.87	0.63
W5	1579.0	RpC	0.11	1.22	0.66	0.87
W5	1581.0	RpC	0.10	1.49	0.86	0.70
W7	760.0	UHy	0.11	7.50	1.94	2.63
W7	838.0	UHy	0.15	5.93	2.56	2.87
W7	920.0	UHy	0.15	6.67	2.02	2.94
W7	997.0	UHy	0.12	5.91	2.05	2.73
W7	1097.0	UHy	0.10	6.26	1.94	1.85
W7	1173.0	UHy	0.09	5.74	2.54	1.79
W7	1257.0	Cer	0.06	5.04	1.16	0.50
W7	1330.0	BN	0.11	4.05	2.29	1.99
W7	1435.0	BN	0.06	4.21	0.18	0.51
W7(2.)	1080.0	UHy	0.10	8.01	0.88	2.24
W7(2.)	1165.0	LHy	0.07	8.80	1.56	1.73
W7(2.)	1250.0	Cer	0.06	7.83	1.71	0.98
W7(2.)	1334.0	BN & CyM & ME	0.05	4.27	0.83	0.41
W7(2.)	1396.0	BN & CyM & ME	0.11	2.60	0.96	0.60
W7(2.)	1460.0	BN & CyM & ME	0.07	3.92	0.23	0.48
W7(2.)	1550.0	BN & CyM & ME	0.07	4.22	0.21	0.53
W7(2.)	1647.0	RpC	0.15	3.09	2.42	1.87
W7a	1070.0	UHy	0.16	6.17	1.09	3.57
W7a	1110.0	UHy	0.11	4.82	2.48	1.52
W7a	1125.0	UHy	0.09	5.68	2.21	1.99
W7a	1135.0	UHy	0.11	5.12	2.90	2.48
W7a	1155.0	LHy	0.10	5.18	2.82	2.18
W7a	1163.0	LHy	0.10	5.28	3.14	2.46
W7a	1167.0	LHy	0.10	5.76	3.17	2.54
W7a	1172.0	LHy	0.07	5.38	2.47	1.44
W7a	1191.0	LHy	0.07	5.30	2.55	1.14
W7a	1200.0	LHy	0.08	5.88	2.59	1.99
W7a	1210.0	LHy	0.08	5.44	2.37	1.47
W7a	1220.0	LHy	0.07	6.20	1.97	1.20
W7a	1288.0	Cer	0.08	5.06	1.59	0.89
W7a	1418.0	CyM & ME	0.07	3.76	0.80	0.47
W7a	1537.0	CyM & ME	0.06	4.19	0.10	0.44
W7a	1557.0	CyM & ME	0.06	4.19	0.06	0.69
W7a	1596.0	CyM & ME	0.06	4.48	0.11	0.46

Well	Depth (MD)	Formation	N [%]	C_{total} [%]	S [%]	C_{org} [%]
W7a	1600.0	FS (RpC)	0.07	3.72	0.14	0.52
W7a	1606.0	FS (RpC)	0.10	3.20	0.42	0.68
W7a	1610.0	FS (RpC)	0.17	2.66	1.42	1.81
W7a	1616.0	FM (RpC)	0.18	4.19	2.73	2.98
W7a	1621.0	FM (RpC)	0.16	4.01	1.85	2.59
W7a	1628.0	FM (RpC)	0.16	4.45	2.04	2.76
W7a	1633.0	PE	0.13	4.20	1.70	2.05
W7a	1635.0	PE	0.16	4.24	2.36	2.80
W7a	1637.0	PE	0.15	4.25	2.10	2.54
W7a	1641.0	PE	0.14	4.68	2.64	2.33
W7a	1643.0	PE	0.14	4.81	2.50	2.44
W7a	1646.0	PE	0.09	3.25	0.71	0.84
W7a	1650.0	PE	0.16	3.99	2.10	2.59
W7a	1650.0	PE	0.12	3.60	1.69	1.73
W7a	1657.0	PE	0.14	3.76	1.90	2.18
W8	875.0	UHy	0.13	8.63	1.38	3.14
W8	915.0	UHy	0.10	10.22	0.60	4.59
W8	1353.5	LHy	0.11	3.36	3.14	1.33
W8	1405.0	LHy	0.10	7.29	1.89	1.99
W8	1430.0	LHy	0.10	7.58	1.76	2.49
W8	1450.0	LHy	0.12	4.12	2.98	2.14
W8	1475.0	Cor	0.12	5.11	3.17	2.43
W8	1525.0	Cor	0.10	3.46	2.77	1.71
W8	1555.0	Cor	0.09	4.25	3.11	1.53
W8	1575.0	Cor	0.11	3.14	2.89	1.48
W8	1600.0	Cor	0.11	4.24	2.84	2.05
W8	1624.0	Cer	0.11	4.50	2.63	2.15
W8	1650.0	Cer	0.10	4.14	2.24	1.53
W8	1674.0	Cer	0.08	5.00	1.89	1.30
W8	1700.0	Cer	0.09	5.00	2.28	1.34
W8	1714.0	Cer	0.08	4.82	2.65	1.16
W8	1756.0	Cer	0.09	5.44	2.59	1.71
W8	1795.0	Cer	0.09	6.02	1.96	1.90
W9	845.0	UHy	0.14	4.28	2.11	2.37
W9	920.0	UHy	0.13	6.77	2.29	2.97
W9	994.0	UHy	0.14	7.98	1.76	3.32
W9	992.0	UHy	0.14	7.98	1.76	3.32
W9	1065.0	UHy	0.18	6.05	2.25	2.90
W9	1125.0	UHy	0.20	4.61	2.89	3.37
W9	1155.0	UHy	0.11	8.51	0.50	1.94
W9	1175.0	UHy	0.16	7.37	2.25	3.45
W9	1183.0	UHy	0.15	6.30	2.44	2.87
W9	1192.0	UHy	0.10	8.44	0.70	2.18
W9	1200.0	LHy	0.14	6.41	2.36	2.62
W9	1214.0	LHy	0.07	9.09	0.54	1.69
W9	1225.0	LHy	0.13	5.62	2.15	1.57
W9	1236.0	LHy	0.14	5.89	1.89	2.08
W9	1250.0	LHy	0.13	6.24	2.85	2.55
W9	1266.0	LHy	0.12	5.16	2.93	2.02
W9	1284.0	LHy	0.09	5.99	3.61	1.50
W9	1308.0	LHy	0.12	4.85	3.77	1.78
W9	1320.0	LHy	0.13	4.71	3.10	2.23
W9	1342.0	LHy	0.11	6.47	1.15	1.99
W9	1354.0	LHy	0.09	6.72	1.19	2.05
W9	1362.0	LHy	0.10	6.37	1.13	2.09
W9	1377.0	CyM & ME	0.06	4.45	0.75	0.60
W9	1405.0	CyM & ME	0.07	4.39	0.74	0.71
W9	1483.0	FS (RpC)	0.12	2.94	0.49	0.95
W9	1489.0	FS (RpC)	0.18	2.84	0.47	1.71
W9	1496.0	FS (RpC)	0.16	3.61	0.60	2.06
W9	1504.0	FM (RpC)	0.18	4.30	0.72	2.69
W9	1525.0	FM (RpC)	0.12	3.71	0.62	0.99
W9	1527.0	FM (RpC)	0.18	3.74	0.62	2.11
W9	1534.0	UPE	0.17	3.48	0.59	1.89
W9	1544.0	UPE	0.18	3.20	0.54	1.63
W9	1546.0	MPE	0.21	3.94	0.65	2.12
W9	1554.0	MPE	0.27	4.28	1.35	2.30
W9	1563.0	LPE	0.15	4.07	1.26	1.58
W9	1570.0	LPE	0.28	4.57	1.16	2.40
W10	784.0	UHy	0.13	6.32	1.59	2.58
W10	815.0	UHy	0.17	6.68	1.95	3.98
W10	895.0	UHy	0.13	6.55	1.63	2.73
W10	930.0	UHy	0.11	7.07	2.01	2.45
W10	1045.0	UHy	0.13	7.57	2.16	2.92
W10	1125.0	UHy	0.11	7.41	1.96	2.14
W10	1215.0	UHy	0.20	5.56	2.81	3.75
W10	1260.0	UHy	0.14	5.94	2.45	2.99
W10	1285.0	LHy	0.09	8.80	0.76	2.49
W10	1325.0	LHy	0.14	5.94	3.08	3.14
W10	1357.0	LHy	0.12	4.95	2.55	2.15
W10	1375.0	LHy	0.19	6.34	3.23	3.93
W10	1430.0	LHy	0.13	4.99	3.51	2.67
W10	1462.0	LHy	0.12	5.37	3.73	2.49

Well	Probe	Formation	N [%]	C_{total} [%]	S [%]	C_{org} [%] (Phosphorsäure)
W10	1495.0	LHy	0.04	9.23	0.44	1.03
W10	1527.0	LHy	0.07	7.19	2.80	1.36
W10	1555.0	LHy	0.11	6.20	3.00	1.80
W10	1565.0	Cor	0.11	6.43	3.35	2.35
W10	1575.0	Cor	0.09	5.20	3.21	1.25
W10	1600.0	Cor	0.10	5.79	3.46	2.13
W10	1615.0	Cor	0.10	5.23	3.20	1.59
W10	1534.0	Cor	0.10	6.40	2.94	2.14
W10	1650.0	Cor	0.10	5.10	3.17	1.51
W10	1665.0	Cor	0.10	5.23	3.24	1.65
W10	1685.0	Cor	0.09	6.03	2.24	1.28
W10	1730.0	Cer	0.08	5.46	3.43	1.04
W10	1748.0	Cer	0.09	4.91	1.99	0.96
W10	1780.0	BN	0.06	6.23	0.74	0.50
W10	1865.0	BN	0.08	3.72	0.66	0.50
W10	1955.0	CyM & ME	0.06	4.06	0.24	0.46
W10	2035.0	CyM & ME	0.05	4.48	0.17	0.46
W10	2110.0	CyM & ME	0.07	4.01	0.31	0.51
W10	2120.0	CyM & ME	0.07	4.18	0.17	0.52
W10	2134.0	FS (RpC)	0.17	3.05	2.30	1.78
W10	2140.0	FM (RpC)	0.16	4.07	2.19	2.37
W10	2150.0	FM (RpC)	0.15	4.52	2.62	2.83
W10	2165.0	FM (RpC)	0.10	2.27	0.79	0.98
W10	2174.0	FM (RpC)	0.08	3.33	0.86	0.66
W10	2252.0	MPE	0.06	5.36	0.04	0.34
W10	2256.0	MPE	0.04	4.76	0.28	0.43
W10	2260.0	MPE	0.06	4.38	0.09	0.37
W10	2308.0	LPE	0.13	3.29	0.33	0.67
W10	2320.0	LPE	0.10	2.69	0.48	0.65
W10	2326.0	LPE	0.15	3.12	0.34	0.97
W10	2342.0	LPE	0.08	2.11	0.38	1.88
W10	2350.0	LPE	0.04	0.74	0.14	0.65
W10	2353.0	LPE	0.09	1.15	0.14	1.14
W12	914.4	UHy	0.12	2.87	2.61	2.07
W12	1042.0	UHy	0.13	3.54	2.53	2.24
W12	1236.2	LHy	0.16	3.65	2.43	2.98
W12	1426.2	Cor	0.10	2.95	0.43	1.01
W12	1634.3	Cer	0.06	7.14	1.41	0.96
W13	1799.0	PE	0.07	1.29	0.12	0.14
W13	1828.8	PE	0.13	3.21	1.61	1.85
W14	738.4	UHy	0.21	4.62	1.76	4.25
W14	855.9	UHy	0.13	5.60	2.11	2.20
W14	962.9	UHy	0.13	5.57	1.89	2.48
W14	1070.1	UHy	0.15	5.03	2.07	2.23
W14	1124.1	UHy	0.17	5.36	2.18	3.51
W14	1168.5	UHy	0.21	3.14	2.33	3.14
W14	1188.9	UHy	0.16	3.91	3.08	3.30
W14	1264.7	LHy	0.33	4.84	2.91	4.84
W14	1289.6	LHy	0.12	3.34	2.05	1.47
W14	1315.9	LHy	0.15	1.79	2.47	1.57
W14	1354.0	LHy	0.11	2.71	2.31	1.51
W14	1384.5	LHy	0.16	2.22	3.22	2.22
W14	1423.5	LHy	0.13	2.37	2.49	1.60
W14	1446.5	Cor	0.01	8.79	0.13	1.07
W14	1483.8	Cor	0.03	3.11	1.70	0.75
W14	1523.1	Cor	0.10	1.97	2.91	1.25
W14	1566.5	Cor	0.08	2.46	2.52	0.71
W14	1591.3	Cor	0.09	3.06	2.46	0.98
W14	1631.8	Cer	0.09	5.35	1.53	1.15
W14	1704.5	Cer	0.09	3.74	1.19	0.81
W14	1749.3	Cer	0.07	5.66	1.32	0.46
W14	1808.6	Cer	0.06	3.68	0.08	0.23
W14	2196.6	PE	0.17	4.80	3.14	4.16
W16	865.0	UHy	0.11	8.82	0.46	2.43
W16	900.0	UHy	0.14	6.04	1.52	3.46
W16	950.0	UHy	0.09	8.64	0.71	2.60
W16	1000.0	UHy	0.06	9.42	0.70	2.05
W16	1050.0	UHy	0.10	9.14	1.61	3.47
W16	1100.0	UHy	0.11	7.75	1.78	2.19
W16	1150.0	UHy	0.12	6.83	1.72	2.98
W16	1200.0	UHy	0.11	5.95	2.17	2.46
W16	1250.0	LHy	0.10	8.41	1.43	2.27
W16	1300.0	LHy	0.09	8.39	0.58	1.49
W16	1350.0	LHy	0.12	6.61	2.04	2.51
W16	1400.0	LHy	0.10	3.61	3.17	2.12
W16	1450.0	LHy	0.12	5.73	1.98	1.90
W16	1502.5	LHy	0.09	6.64	1.64	1.57
W16	1560.0	LHy	0.09	6.33	1.84	1.16
W16	1597.5	Cor	0.09	5.65	1.96	1.26
W16	1652.5	Cor	0.09	5.19	2.37	1.17
W16	1700.0	Cor	0.10	3.73	2.92	1.25
W16	1720.0	Cor	0.08	4.32	3.14	1.32

Well	Probe	Formation	N [%]	C_{total} [%]	S [%]	C_{org} [%] (Phosphorsäure)
W16	1750.0	Cer	0.09	4.07	2.59	1.17
W16	1800.0	Cer	0.08	4.76	1.36	0.94
W16	1850.0	Cer	0.08	5.02	1.93	0.88
W16	1900.0	Cer	0.07	5.22	1.45	0.86
W16	2300.0	FS (RpC)	0.08	3.78	1.41	0.75
W16	2414.3	PE	0.05	2.78	0.01	0.30
W16	2428.3	PE	0.06	1.66	0.01	0.32
W16	2435.6	PE	0.06	1.89	1.49	0.64
W17	674.3	UHy	0.19	4.43	1.58	4.05
W17	676.8	UHy	0.13	5.06	1.31	2.69
W17	749.5	UHy	0.11	5.32	2.35	2.89
W17	750.8	UHy	0.09	6.55	1.98	2.27
W19	1504.6	Cer	0.10	4.20	0.89	1.48
W19	1509.6	Cer	0.10	4.00	0.92	1.05
W19	1927.0	PE	0.08	0.47	0.12	0.47
W19	1927.2	PE	0.10	0.94	3.20	0.88
W19	1927.6	PE	0.10	1.45	1.34	1.43
W19	1927.8	PE	0.23	6.77	2.41	5.97
W19	1928.2	PE	0.20	5.96	1.74	5.85
W23	1136.5	Cor	0.04	9.15	0.56	1.16
W23	1245.0	Cor	0.09	3.73	3.02	1.66
W23	1350.0	Cer	0.06	6.49	2.93	1.56
W27	1915.5	UPE	0.08	0.64	0.42	0.65
W27	1919.1	UPE	0.06	0.19	0.03	0.19
W29	1265.0	PE	0.05	0.26	0.04	0.26
W31	2687.9	MPE	0.06	3.98	0.12	0.51
W31	2752.5	MPE	0.02	4.12	0.09	0.17
W31	2767.0	LPE	0.08	0.62	0.13	0.51
W31	2768.0	LPE	0.09	0.53	1.01	0.53
W31	2768.4	LPE	0.09	1.13	0.40	0.95

W35	2513.7	CyM	0.07	0.65	0.01	0.24
W35	2623.0	LPE	0.09	0.51	0.04	0.51
W35	2625.0	LPE	0.06	0.48	0.05	0.48

Well	Depth (TVD)	Formation	VR	Std Dev	# of measurements	SCI
W1	350.0	UT II	0.21	0.03	18	1.50
W1	450.0	UT II	0.64	0.09	37	1.50
W1	560.0	UT I	0.54	0.06	47	2.00
W1	650.0	UHy	0.61	0.09	40	2.50
W1	700.0	UHy	0.73	0.09	45	2.00
W1	750.0	UHy				2.00
W1	800.0	UHy	0.67	0.07	59	2.50
W1	850.0	UHy				2.00
W1	900.0	UHy	0.65	0.65	32	2.00
W1	950.0	UHy				3.50
W1	1000.0	UHy	0.63	0.07	85	2.50
W1	1050.0	UHy				2.50
W1	1100.0	UHy	0.62	0.08	66	2.00
W1	1150.0	UHy				2.00
W1	1200.0	LHy	0.65	0.08	71	2.50
W1	1250.0	LHy				2.50
W1	1300.0	LHy	0.64	0.09	92	2.50
W1	1370.0	Cor				2.00
W1	1400.0	Cor	0.71	0.07	60	2.00
W1	1430.0	Cor				2.50
W1	1500.0	Cer	0.71	0.08	38	2.50
W1	1600.0	Cer				2.50
W1	1700.0	Cer	0.73	0.05	80	3.00
W1	1900.0	CyM	0.76	0.1	85	2.50
W1	2000.0	ME	0.62	0.09	97	4.00
W1	2070.0	FS (RpC)				3.50
W1	2080.0	FS (RpC)				3.50
W1	2100.0	FM (RpC)	0.61	0.08	77	3.50
W1	2120.0	FM (RpC)				3.00
W1	2140.0	FM (RpC)				3.00
W1	2160.0	FM (RpC)				4.00
W1	2166.0	FM (RpC)	0.65	0.05	15	4.00
W1	2210.0	PE				2.50
W1	2300.0	MPE	0.65	0.06	43	2.50
W2	308.0	UT II	0.42	0.07	12	1.50
W2	351.8	UT I				1.50
W2	391.4	UHy				1.50
W2	398.8	UHy	0.43	0.05	58	1.50
W2	449.0	UHy	0.54	0.08	47	1.50
W2	503.3	UHy				1.50
W2	510.4	UHy	0.61	0.09	100	1.50
W2	556.0	Hy				1.75
W2	561.9	Hy	0.64	0.09	80	1.75
W2	596.3	Hy				
W2	650.8	Hy	0.61	0.07	37	1.50
W2	670.5	Hy				1.50
W2	671.0	Hy				1.50
W2	673.0	Hy				1.50
W2	709.3	Hy				2.50
W2	747.7	Hy				2.00
W2	755.9	Hy	0.59	0.10	47	2.00
W2	801.0	Hy				2.50
W2	805.2	Hy	0.78	0.10	39	2.50
W3	1729.3	FM (RpC)	0.58	0.09	90	
W3	1734.2	FM (RpC)	0.50	0.08	8	
W3	1748.5	PE	0.57	0.09	59	
W5	1566.0	RpC	0.53	0.08	80	
W6	1841.0	PE	0.63	0.09	68	
W7	488.0	UT II	0.29	0.18	5	2.50
W7	555.0	UT II	0.24	0.11	3	2.75
W7	675.0	UHy	0.56	0.14	59	2.00
W7	762.0	UHy	0.57	0.14	52	2.00
W7	838.0	UHy	0.61	0.12	60	2.25
W7	921.0	UHy	0.6	0.13	56	2.00
W7	997.0	UHy	0.47	0.12	59	2.50
W7	1072.0	UHy				2.50
W7	1098.0	UHy	0.55	0.10	43	2.25
W7	1174.0	UHy	0.64	0.11	62	2.25
W7	1259.0	Cer	0.46	0.15	59	4.00
W7	1330.0	BN	0.63	0.12	43	2.50
W7	1435.0	BN	0.57	0.14	52	2.50
W7(2.)	1080.0	UHy	0.55	0.10	54	2.25
W7(2.)	1164.0	LHy	0.56	0.10	50	2.50
W7(2.)	1250.0	Cer	0.57	0.08	57	2.50
W7(2.)	1332.0	BN	0.57	0.10	49	2.50
W7(2.)	1396.0	BNB/CyM/ME	0.63	0.09	25	2.50
W7(2.)	1460.0	BNB/CyM/ME	0.59	0.12	43	2.25
W7(2.)	1550.0	ME	0.52	0.10	55	3.00
W7(2.)	1648.0	RpC	0.58	0.08	23	2.75

Well	Depth (MD)	Formation	VR	Std Dev	# of measurements	SCI
W7a	1070.0	UHy				2.25
W7a	1107.0	UHy				2.25
W7a	1126.0	UHy				2.50
W7a	1135.0	UHy				2.25
W7a	1154.0	LHy				2.25
W7a	1162.0	LHy				2.25
W7a	1167.0	LHy				2.25
W7a	1172.0	LHy				2.25
W7a	1191.0	LHy				2.50
W7a	1200.0	LHy				2.25
W7a	1210.0	LHy				2.25
W7a	1220.0	LHy				2.25
W7a	1288.0	Cer				2.25
W7a	1418.0	CyM				2.50
W7a	1536.0	ME				2.50
W7a	1557.0	ME				2.75
W7a	1595.0	ME				2.75
W7a	1602.0	RpC				2.75
W7a	1608.0	RpC				3.00
W7a	1612.0	RpC				2.75
W7a	1618.0	RpC				2.75
W7a	1621.0	RpC				2.50
W7a	1627.0	RpC				2.50
W7a	1631.0	RpC				2.75
W7a	1633.0	PE				2.50
W7a	1636.0	PE				2.50
W7a	1641.0	PE				2.50
W7a	1644.0	PE				2.75
W7a	1647.0	PE				2.50
W7a	1651.0	PE				2.25
W7a	1653.0	PE				2.50
W7a	1657.0	PE				2.50
W8	605.0	UT II				1.75
W8	610.0	UT II	0.29	0.04	67	1.75
W8	675.0	UT I	0.32	0.04	57	2.00
W8	765.0	UHy				2.50
W8	775.0	UHy	0.50	0.07	24	2.50
W8	825.0	UHy				2.50
W8	875.0	UHy	0.59	0.07	27	2.00
W8	915.0	UHy				2.00
W8	985.0	UHy	0.66	0.08	52	2.00
W8	1020.0	UHy	0.63	0.07	57	3.00
W8	1353.4	LHy	0.64	0.10	33	2.50
W8	1395.0	LHy	0.63	0.08	60	2.50
W8	1405.0	LHy				2.50
W8	1430.0	LHy				2.50
W8	1450.0	LHy				2.50
W8	1475.0	Cor	0.62	0.10	57	3.00
W8	1505.0	Cor				2.50
W8	1525.0	Cor				2.50
W8	1555.0	Cor				2.50
W8	1575.0	Cor	0.62	0.10	60	2.50
W8	1600.0	Cor				2.50
W8	1603.6	Cor				2.25
W8	1624.0	Cer				2.50
W8	1650.0	Cer	0.65	0.07	50	2.50
W8	1674.0	Cer				2.25
W8	1700.0	Cer				2.50
W8	1714.0	Cer				2.50
W8	1756.0	Cer	0.64	0.09	62	3.00
W8	1764.7	Cer				3.00
W8	1795.0	Cer				3.00
W8	1820.0	Cer				3.00
W8	1850.0	BN	0.60	0.09	62	2.50
W8	1875.0	BN				2.50
W8	1905.0	BN				2.50
W8	1930.0	BN				2.25
W8	1950.0	BN	0.64	0.07	54	2.50
W8	1975.0	BN				2.50
W8	1980.0	CyM & ME				2.50
W8	2025.0	CyM & ME	0.64	0.06	53	2.50
W8	2050.0	CyM & ME				2.50
W9	385.0	UT II				2.00
W9	490.0	UT II				
W9	545.0	UT II	0.37	0.06	16	2.25
W9	630.0	UT I	0.29	0.10	9	2.75
W9	740.0	UT I	0.31	0.06	59	3.00
W9	838.0	UHy	0.42	0.16	58	2.50
W9	920.0	UHy	0.53	0.14	54	2.00
W9	992.0	UHy	0.49			2.50
W9	1064.0	UHy	0.53			2.00
W9	1124.0	UHy	0.45			2.75
W9	1155.0	UHy				2.00
W9	1170.0	UHy				2.75
W9	1183.0	UHy	0.46			2.50
W9	1192.0	UHy				2.25

Well	Probe	Formation	VR	Std Dev	# of measurements	SCI
W9	1201.0	LHy				2.25
W9	1214.0	LHy				2.25
W9	1225.0	LHy				3.25
W9	1231.0	LHy				3.00
W9	1248.0	LHy	0.46			2.25
W9	1268.0	LHy				2.25
W9	1285.0	LHy				2.50
W9	1308.0	LHy	0.64			2.25
W9	1322.0	LHy				1.75
W9	1342.0	LHy				2.00
W9	1353.0	LHy				2.75
W9	1362.0	CyM & ME	0.61			2.00
W9	1377.0	CyM & ME				2.00
W9	1406.0	CyM & ME	0.37			2.00
W9	1482.0	RpC	0.4			2.75
W9	1489.0	RpC				2.75
W9	1496.0	RpC				2.75
W9	1502.0	RpC				2.50
W9	1525.0	RpC				2.00
W9	1527.0	UPE				
W9	1529.0	UPE				
W9	1544.0	UPE				2.25
W9	1546.0	MPE				2.25
W9	1554.0	MPE				2.50
W9	1563.0	LPE				2.50
W9	1570.0	LPE	0.51			2.50
W10	480.0	UT II	0.27	0.05	11	
W10	557.0	UT II	0.2	0.04	32	2.25
W10	658.0	UT I	0.48	0.11	50	2.00
W10	709.0	UT I	0.44	0.11	17	
W10	758.0	UT I	0.63	0.15	41	3.00
W10	783.0	UHy				
W10	815.0	UHy	0.6	0.17	40	2.25
W10	845.0	UHy				
W10	895.0	UHy	0.57	0.13	51	1.25
W10	903.0	UHy				
W10	967.0	UHy	0.55	0.12	24	2.25
W10	1045.0	UHy	0.74	0.17	35	2.00
W10	1125.0	UHy	0.67	0.11	28	3.00
W10	1212.0	UHy	0.53	0.11	36	3.00
W10	1260.0	UHy				2.75
W10	1285.0	LHy	0.6	0.13	62	2.75
W10	1325.0	LHy				2.50
W10	1357.0	LHy	0.54	0.11	30	3.00
W10	1373.0	LHy				2.75
W10	1430.0	LHy	0.61	0.12	43	3.75
W10	1461.0	LHy				2.75
W10	1494.0	LHy				2.75
W10	1526.0	LHy	0.62	0.14	54	2.75
W10	1555.0	LHy				2.50
W10	1564.0	Cor				2.25
W10	1576.0	Cor				2.75
W10	1600.0	Cor				2.50
W10	1616.0	Cor				2.50
W10	1634.0	Cor				2.25
W10	1649.0	Cor				2.75
W10	1665.0	Cor				2.25
W10	1686.0	Cor	0.62	0.13	46	2.50
W10	1731.0	Cer				2.75
W10	1747.0	Cer				2.75
W10	1780.0	Cer				2.50
W10	1865.0	BN	0.55	0.12	45	2.50
W10	1955.0	CyM	0.54	0.13	16	2.75
W10	2037.0	ME				3.00
W10	2110.0	ME				3.25
W10	2119.0	RpC				2.75
W10	2128.0	RpC	0.53			3.00
W10	2132.0	RpC				
W10	2142.0	RpC				2.75
W10	2155.0	RpC				2.50
W10	2165.0	RpC				2.50
W10	2172.0	RpC				2.75
W10	2248.0	UPE				3.00
W10	2252.0	UPE				2.50
W10	2256.0	UPE				3.25
W10	2259.0	UPE				
W10	2307.0	MPE				2.75
W10	2320.0	LPE				
W10	2327.0	LPE				
W10	2338.0	LPE	0.32	0.11	61	2.00
W10	2342.0	LPE				2.75
W10	2346.0	LPE				1.75
W10	2350.0	LPE				1.75
W10	2350.0	LPE				
W11	1714	Eocene?	0.38	0.05	38	
W11	1723	Eocene?	0.37	0.07	6	
W11	1764	Eocene?	0.42	0.07	16	

Well	Probe	Formation	VR	Std Dev	# of measurements	SCI
W12	604.4	UT I	0.30	0.03	68	2.00
W12	609.4	UT I				2.00
W12	671.2	UT I	0.51	0.07	64	2.00
W12	676.2	UT I				2.00
W12	797.5	UHy	0.65	0.09	66	2,5
W12	875.2	UHy	0.71	0.09	65	2.50
W12	914.4	UHy	0.73	0.09	63	2.50
W12	1040.0	HyB				2.50
W12	1042.0	HyB				2.50
W12	1042.5	HyB				2.50
W12	1236.2	LHy	0.59	0.11	65	2.50
W12	1426.2	Cor	0.63	0.08	67	3.00
W12	1428.0	Cor				3.00
W12	1429.0	Cor				3.00
W12	1634.3	Cer	0.69	0.09	34	3.25
W12	1841.2	BN				3.00
W13	509	UT I	0.39	0.06	21	
W13	551	UT I	0.29	0.04	54	
W13	1831	PE	0.61	0.08	66	
W14	655.0	UT I				2.00
W14	657.5	UT I	0.49	0.09	46	2.50
W14	738.4	UHy	0.51	0.09	46	2.50
W14	805.0	UHy	0.64	0.13	48	2.50
W14	855.0	UHy	0.67	0.08	48	2.00
W14	910.0	UHy	0.60	0.10	70	2.50
W14	962.9	UHy	0.64	0.08	60	2.00
W14	1016.0	UHy	0.58	0.07	46	2.50
W14	1022.7	UHy				2.50
W14	1070.0	UHy	0.62	0.08	86	2.50
W14	1124.0	Hy				3.00
W14	1163.0	Hy	0.58	0.08	63	3.00
W14	1164.0	Hy				3.00
W14	1165.0	Hy				3.00
W14	1167.8	Hy				3.50
W14	1188.9	Hy				3.50
W14	1189.0	Hy				3.00
W14	1193.0	Hy				3.00
W14	1199.3	Hy				3.50
W14	1265.0	Hy	0.62	0.07	65	3.00
W14	1271.6	LHy				3.00
W14	1289.6	LHy				3.00
W14	1300.0	LHy				3.00
W14	1312.9	LHy				3.50
W14	1347.8	LHy	0.60	0.08	80	3.50
W14	1351.0	LHy				3.00
W14	1384.5	LHy				
W14	1418.8	LHy	0.64	0.11	60	3.50
W14	1446.5	Cor	0.66	0.13	76	2.50
W14	1448.0	Cor				2.50
W14	1449.0	Cor				3.50
W14	1483.8	Cor				
W14	1523.1	Cor				3.00
W14	1526.0	Cor				2.50
W14	1566.4	Cor	0.67	0.11	67	3.00
W14	1567.0	Cor				2.50
W14	1569.0	Cor				3.00
W14	1591.3	Cor				3.00
W14	1631.8	Cer	0.63	0.08	60	3.00
W14	1637.6	Cer				3.50
W14	1672.0	Cer				4.00
W14	1704.5	Cer				3.00
W14	1749.0	Cer	0.69	0.10	41	3.00
W14	1754.9	Cer				3.00
W14	1780.8	Cer	0.64	0.08	68	3.00
W14	1808.6	Cer				3.00
W14	1945.8	BN	0.64	0.10	59	3.50
W14	2019.0	CyM & ME				3.50
W14	2064.3	CyM & ME	0.60	0.10	68	3.50
W14	2104.2	CyM & ME	0.66	0.12	45	2.50
W14	2152.9	RpC				3.50
W14	2196.6	PE	0.72	0.10	63	3.50
W14	2197.0	PE				3.00
W16	410.0	UT II				1.50
W16	575.0	UT II	0.18	0.05	86	1.50
W16	592.5	UT II				1.50
W16	705.0	UT I	0.36	0.09	39	2.00
W16	808.0	UT I	0.37	0.10	67	2.00
W16	865.0	UHy				2.50
W16	900.9	UHy	0.57	0.12	56	2.50
W16	950.0	UHy				2.50
W16	1000.0	UHy	0.59	0.08	50	2.50
W16	1050.0	UHy				2.50
W16	1100.0	UHy	0.59	0.09	100	2.50
W16	1150.0	UHy				2.50
W16	1200.0	UHy	0.62	0.10	55	2.50
W16	1250.0	UHy				2.25

Well	Probe	Formation	VR	Std Dev	# of measurements	SCI
W16	1300.0	LHy	0.64	0.08	62	2.50
W16	1350.0	LHy				2.50
W16	1400.0	LHy	0.69	0.1	75	3.00
W16	1450.0	LHy				3.00
W16	1502.0	LHy	0.66	0.09	89	3.00
W16	1560.0	LHy				3.00
W16	1597.5	Cor	0.68	0.1	39	3.00
W16	1652.5	Cor				2.50
W16	1700.0	Cor	0.68	0.1	94	3.00
W16	1720.0	Cor				3.00
W16	1750.0	Cer				2.50
W16	1800.0	Cer	0.7	0.11	60	3.00
W16	1850.0	Cer				3.00
W16	1900.0	Cer	0.72	0.1	71	3.00
W16	2000.0	BN	0.75	0.1	51	3.00
W16	2055.0	BN				2.50
W16	2100.0	BN	0.82	0.12	80	3.00
W16	2150.0	CyM & ME				3.00
W16	2200.0	CyM & ME	0.77	0.13	58	3.00
W16	2250.0	CyM & ME				3.00
W16	2300.0	RpC	0.67	0.1	69	3.00
W16	2350.0	PE				3.50
W16	2398.4	PE				5.50
W16	2414.3	PE				
W16	2425.3	PE				4.50
W16	2425.7	PE				4.50
W16	2431.0	PE				4.50
W16	2435.6	PE	0.72	0.08	29	4.50
W16	2438.0	PE				4.00
W16	2444.9	PE				4.00
W16	2440.7	PE				4.00
W18	2399	PE	0.54	0.06	60	
W19	1504.6	Cer	0.63	0.07	100	
W19	1710.4	CyM	0.64	0.08	67	
W19	1927.3	PE	0.63	0.07	44	
W21	1455.3	CyM & ME	0.56	0.07	56	
W21	1587.5	CyM & ME	0.55	0.1	60	
W23	1136.5	Cor	0.6	0.08	45	
W23	1245	Cor	0.61	0.1	44	
W23	1350	Cer	0.52	0.1	56	
W23	1642.3	Cer	0.53	0.1	88	
W23	1773.6	CyM & ME	0.63	0.11	100	
W23	1812.6	CyM & ME	0.57	0.12	100	
W23	1955	PE	0.57	0.11	37	
W25	1705	PE	0.58	0.1	50	
W25	1796	PE	0.56	0.13	8	
W27	1917	PE	0.52	0.08	49	
W29	853.1	Cer	0.62	0.1	68	
W29	1001.2	CyM	0.56	0.08	95	
W29	1121.1	CyM & ME	0.55	0.09	31	
W29	1267	RpC	0.6	0.09	48	
W31	2767	PE	0.76	0.08	57	
W31	2768.4	PE	0.74	0.09	45	
W33	2442.5	PE	0.7	0.1	43	
W33	2562.7	PE	0.72	0.1	43	
W35	2314	CyM & ME	0.73	0.08	42	
W35	2623.3	PE	0.81	0.09	49	

Supplementary VR Data	Well	Probe	Formation	VR	Std Dev	# of measurements
Lampe (2001)	W 29	200.0	UT II	0.16	0.07	30
	W 29	410.0	UT II	0.22	0.28	40
	W 29	500.0	UT I	0.52	0.25	7
	W 29	630.0	Hy-Cor	0.44	0.25	5
	W 29	806.0	Hy-Cor	0.5	0.33	36
	W 29	980.0	CyM-ME	0.6	0.29	46
	W 29	998.0	CyM-ME	0.6	0.34	40
	W 29	1121.2	CyM-ME	0.36	0.19	30
	W 29	1224.0	RpC	0.87	0.35	135
	W 29	1272.0	PB	0.56	0.23	22
	W 29	1374.6	PB	0.63	0.31	3
Lampe (2001)	W 31	160.0	Q	0.24	0.04	40
	W 31	350.0	UT II	0.23	0.04	41
	W 31	500.0	UT II	0.24	0.04	20
	W 31	700.0	JT1	0.21	0.08	6
	W 31	875.0	JT1	0.33	0.07	13
	W 31	915.0	UHy	0.47	0.18	38
	W 31	990.0	UHy	0.58	0.21	23
	W 31	1155.0	UHy	0.54	0.20	23
	W 31	1230.0	UHy	0.57	0.27	19
	W 31	1340.0	UHy	0.51	0.25	35
	W 31	1580.0	UHy	0.59	0.22	46
	W 31	1675.0	LHy	0.63	0.26	50
	W 31	1790.0	Cor	0.68	0.22	33
Rückheim (1989)	W 31	2767.9	PE	0.75	0.04	20
	W 31	2768.4	PE	0.77	0.07	49
Lampe (2001)	W 33	2105.0	Cer	0.67	0.26	10
	W 33	2220.0	CyM-ME	0.61	0.27	35
	W 33	2285.0	CyM-ME	0.63	0.18	27
	W 33	2380.0	RpC	0.69	0.23	22
Rückheim (1989)	W 33	2430.0	PE	0.72	0.07	31
Lampe (2001)	W 33	2441.3	PE	0.72	0.34	52
Rückheim (1989)	W 33	2443.0	PE	0.72	0.03	46
Lampe (2001)	W 33	2453.4	PE	0.61	0.08	55
Rückheim (1989)	W 33	2562.0	PE	0.75	0.06	20
	W 33	2562.0	PE	0.75	0.06	20
Lampe (2001) (Wintershall Holding GmbH)	W 16	2360	UPE	0.68		
	W 16	2390	UPE	0.74		
	W 16	2440	MPE	0.79		
Rückheim (1989)	W 35	2476	PE	0.76	0.02	54
	W 35	2543.8	PE	0.78	0.04	49
Rückheim (1989)	W 19	1928.2	PE	0.64	0.05	58
Rückheim (1989)	W 11	1711.6	Eocene?	0.33	0.09	23
	W 11	1714	Eocene?	0.39	0.07	29

Well	Layer	Top (m TVD)	Base (m TVD)	Thickness (m)	Depo. From (ma)	Depo to (ma)	Eroded from (ma)	Eroded to (Ma)	Lithology
W1	Q	0.0	100.0	100.00	1.60	0			Sandstone
W1	UT II	100.0	540.0	440.00	5.30	1.60			Sandstone
W1	Erodion UT I	540.0	540.0	0.00	10.00	9.00	9	5.3	Sandstone
W1	Depos UT I	540.0	540.0	0.00	16.20	10.00			Sandstone
W1	UT I	540.0	645.0	105.00	18.30	16.20			Sandstone
W1	(Upper) Uhy	645.0	910.0	265.00	20.00	18.30			Shale calc
W1	(Lower) Uhy	910.0	1150.0	240.00	22.20	20.00			Shale calc
W1	LHy	1150.0	1350.0	200.00	23.90	22.20			Marl
W1	Cor	1350.0	1460.0	110.00	24.50	23.90			Shale evap
W1	Cer	1460.0	1710.0	250.00	26.40	24.50			Shale calc
W1	BN	1710.0	1890.0	180.00	28.70	26.40			Marl
W1	CyM & ME	1890.0	2055.0	165.00	29.90	28.70			Shale calc
W1	RpC	2055.0	2177.0	122.00	31.00	29.90			Shale
W1	UPE	2177.0	2230.0	53.00	32.50	31.00			Sandstone (clay rich)
W1	MPE	2230.0	2280.0	50.00	33.10	32.50			Shale calc
W1	LPE	2280.0	2390.00	110.00	36.00	33.10			Sandstone (clay rich)
						36.00			
W 10	Q	0.0	130.0	130.00	1.60	0			Sandstone
W 10	UT II	130.0	632.0	502.00	5.30	1.60			Sandstone
W 10	Erodion UT I	632.0	632.0	0.00	10.00	9.00	9	5.3	Sandstone
W 10	Depos UT I	632.0	632.0	0.00	16.20	10.00			Sandstone
W 10	UT I	632.0	770.0	138.00	18.30	16.20			Sandstone
W 10	UHyB (upper)	770.0	1280.0	510.00	20.00	18.30			Shale calc
W 10	LHy	1280.0	1560.0	280.00	23.90	20.00			Marl
W 10	Cor	1560.0	1690.0	130.00	24.50	23.90			Shale evap
W 10	Cer	1690.0	1813.0	123.00	26.40	24.50			Shale calc
W 10	BN	1813.0	1897.0	84.00	28.70	26.40			Marl
W 10	CyM & ME	1897.0	2118.0	221.00	29.90	28.70			Shale calc
W 10	RpC	2118.0	2173.0	55.00	31.00	29.90			Shale
W 10	UPE	2173.0	2221.0	48.00	32.50	31.00			Sandstone (clay rich)
W 10	MPE	2221.0	2260.0	39.00	33.10	32.50			Shale calc
W 10	LPE	2260.0	2365.0	105.00	36.00	33.10			Sandstone (clay rich)
						36.00			
W 16	Q	0.0	150.0	150.00	1.60	0			Sandstone
W 16	UT II	150.0	679.0	529.00	5.30	1.60			Sandstone
W 16	Erodion UT I	679.0	679.0	0.00	10.00	5.30	9	5.3	Sandstone
W 16	Depos UT I	679.0	679.0	0.00	16.20	10.00			Sandstone
W 16	UT I	679.0	832.0	153.00	18.30	16.20			Sandstone
W 16	Hy & Cor	832.0	1745.0	913.00	20.00	18.30			Shale calc
W 16	Cer	1745.0	1916.0	171.00	26.40	20.00			Shale calc
W 16	BN	1916.0	2105.0	189.00	28.70	26.40			Marl
W 16	CyM & ME	2105.0	2295.0	190.00	29.90	28.70			Shale calc
W 16	RpC	2295.0	2335.0	40.00	31.00	29.90			Shale
W 16	UPE	2335.0	2406.0	71.00	32.50	31.00			Sandstone (clay rich)
W 16	MPE & LPE	2406.0	2470.0	64.00	33.10	32.50			Shale calc
						33.10			

Acknowledgements

There are many people whom I would like to thank for the role they played, be it academic or otherwise, in making this project possible.
Many thanks to my supervisors Prof. Dr. Wolfgang Stinnesbeck and Prof. Dr. Thilo Bechstädt, for their kind support, expertise and supervision during the project. I also thank Dr. Carsten Reinhold (Rhein Petroleum GmbH) and Dr. Hartmut Jäger (GeoResources STC) for their expert contribution, insightful comments, and many fruitful discussions, which encouraged me to widen my research from various perspectives.
Many thanks also to Prof. Dr. Margot Isenbeck-Schröter and Prof. Dr. Mario Trieloff for being members of my examination panel.

I gratefully acknowledge Rhein Petroleum GmbH for the financial sponsoring of the study, as well as for access to subsurface data and rock samples, and for the permission to present the results. Thank you also to GeoResources STC (Steinbeis-TransferCentre) for cooperation.

Many thanks to DEA Deutsche Erdöl AG, Hamburg, and EMPG Exxon Mobil Productions Germany, Hannover, as well as to ÜWG Überlandwerk Groß-Gerau GmbH, Groß-Gerau, for access to subsurface data and rock samples, and for the permission to present the results. I also acknowledge the GeoForschungszentrum Potsdam for the permission to use the DEKORP 9N seismic profile.

Further, this study benefited from many scientific discussions with the subsurface team at Rhein Petroleum GmbH: Dr. Michael Schwarz, Dr. Dietfried Bruss and Bart Heesbeen.

I acknowledge my colleagues from the GeoResources STC team: Thomas Reutner and Sven Brysch for the microscopic introduction, Seija Beckmann for supporting me with the preparation of samples, Georg Miernik and Till Drews for their technical support. Many thanks also to Dr. Axel Emmerich for the introduction into basin modelling.

My sincere thanks to my family and to Florian for their encouragement and moral support.

Eidesstattliche Versicherung gemäß §8 der Promotionsordnung der Naturwissenschaftlich-Mathematischen Gesamtfakultät der Universität Heidelberg

1. Bei der eingereichten Dissertation zu dem Thema

Evolution of Palaeoenvironment, Kerogen Composition and Thermal History in the Cenozoic of the Northern Upper Rhine Graben, SW-Germany

handelt es sich um eine eigenständig erbrachte Leistung.

2. Ich habe nur die angegebenen Quellen und Hilfsmittel benutzt und mich keiner unzulässigen Hilfe Dritter bedient. Insbesondere habe ich wörtlich oder sinngemäß aus anderen Werken übernommene Inhalte als solche kenntlich gemacht.

3. Die Arbeit oder Teile davon habe ich bislang nicht an einer Hochschule des In- oder Auslands als Bestandteil einer Prüfungs- oder Qualifikationsleistung vorgelegt.

4. Die Richtigkeit der vorstehenden Erklärungen bestätige ich.

5. Die Bedeutung der eidesstattlichen Versicherung und die strafrechtlichen Folgen einer unrichtigen oder unvollständigen eidesstattlichen Versicherung sind mir bekannt.

Ich versichere an Eides statt, dass ich nach bestem Wissen die reine Wahrheit erklärt und nichts verschwiegen habe.

_____ _____

Ort und Datum Unterschrift